

GC
57
U5
N6E5
1976
V.12

*See back
of cover*

*See CRPT
for Kadish J*

Volume 12. Geology

Principal Investigators' Reports
for the Year Ending March 1976

U. S. DEPARTMENT OF COMMERCE
National Oceanic and Atmospheric Administration



U. S. DEPARTMENT OF INTERIOR
Bureau of Land Management

April 1976

Annual Reports from Principal Investigators

- Volume:
1. Marine Mammals
 2. Marine Birds
 3. Marine Birds
 4. Marine Birds
 5. Fish, Plankton, Benthos, Littoral
 6. Fish, Plankton, Benthos, Littoral
 7. Fish, Plankton, Benthos, Littoral
 8. Effects of Contaminants
 9. Chemistry and Microbiology
 10. Chemistry and Microbiology
 11. Physical Oceanography and Meteorology
 12. Geology
 13. Geology
 14. Ice

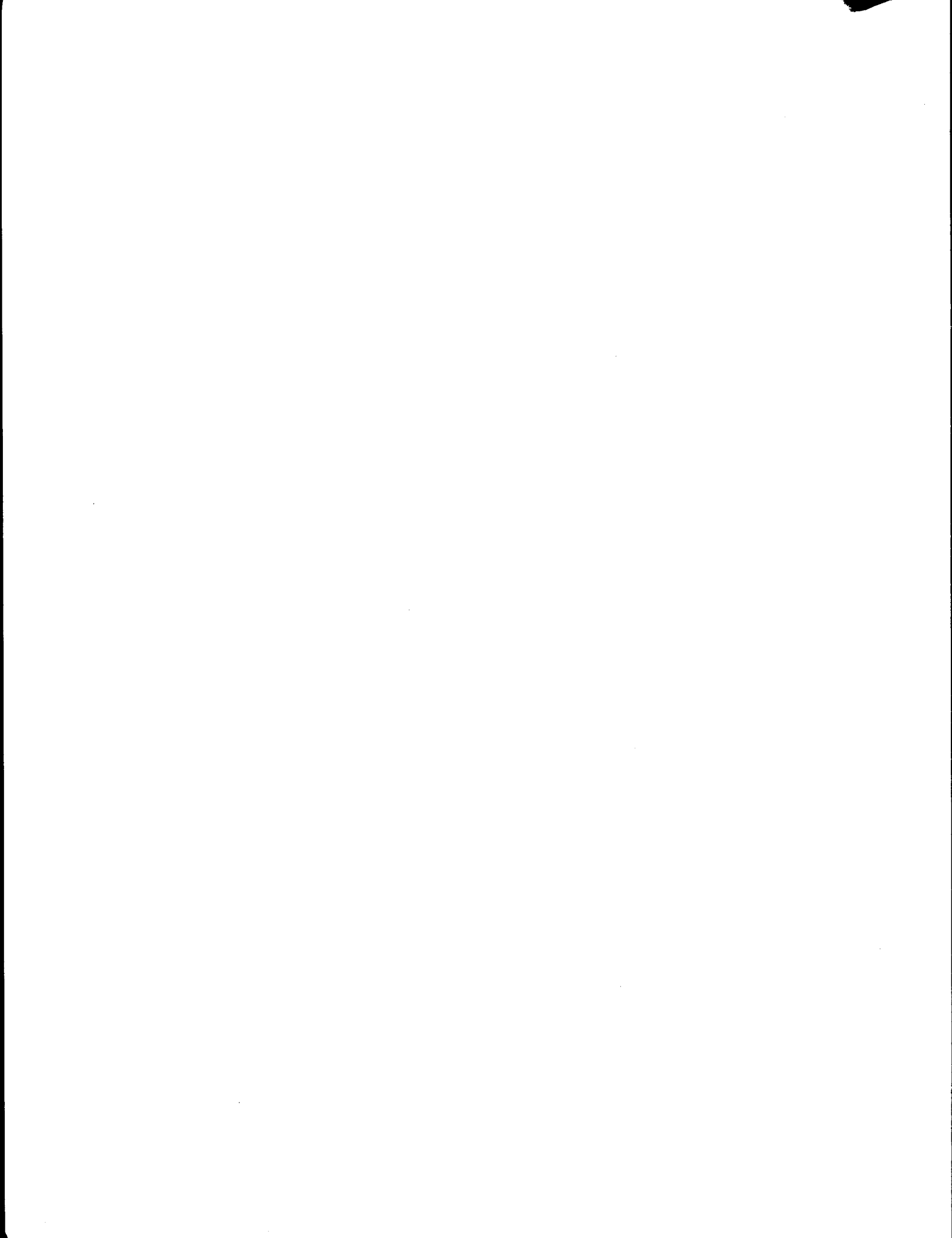
GC
57
US
N6E5
1976
V. 12

Environmental Assessment of the Alaskan Continental Shelf

Volume 12. Geology

*Fourth quarter and annual reports for the reporting period ending March 1976,
from Principal Investigators participating in a multi-year program of environmental
assessment related to petroleum development on the Alaskan Continental Shelf.
The program is directed by the National Oceanic and Atmospheric Administration
under the sponsorship of the Bureau of Land Management.*

ENVIRONMENTAL RESEARCH LABORATORIES / Boulder, Colorado / 1976



CONTENTS

| <u>Research Unit</u> | <u>Proposer</u> | <u>Title</u> | <u>Page</u> |
|----------------------|--|--|--|
| 16 | John Davies et al. Lamont-Doherty Geolo. Obs. Columbia U. | Seismotectonic Study of the Seismic and Volcanic Hazards in Pribilof Islands - Eastern Aleutian Islands Region of the Bering Sea | 1 |
| 59 | Jon C. Boothroyd Dept. of Geology U. of Rhode Island Mark S. Cable Raymond A. Levey Dept. of Geology U. of S. Carolina | Coastal Morphology and Sedimen- tation, Gulf Coast of Alaska (Glacial Sedimentation) | 87 ✓ |
| 99 | P. Jan Cannon Dept. of Geology U. of Alaska | The Environmental Geology and Geomorphology of the Gulf of Alaska Coastal Plain | 373 ✓ |
| 105 | P. Sellmann CRREL | Delineation and Engineering Character- istics of Permafrost beneath the Beaufort Sea | 391 - 408 |
| 152/ 154 | Richard A. Feely Joel D. Cline PMEL/NOAA | Distribution, Composition and Transport of Suspended Particulate Matter in the Gulf of Alaska and Southeastern Bering Shelf | 467 <i>CRREL pp</i> <i>(mis-bound)</i> <i>Includes pp. 409-</i> <i>484</i> |
| 204 | Peter Barnes et al. USGS | Offshore Permafrost Studies, Beaufort Sea | 485 |
| 205 | Peter Barnes Erk Reimnitz David Drake USGS | Marine Environmental Problems in the Ice Covered Beaufort Sea Shelf and Coastal Regions | 512 |

RU#16

LAMONT-DOHERTY GEOLOGICAL OBSERVATORY
OF COLUMBIA UNIVERSITY

PALISADES, NEW YORK

A SEISMOTECTONIC STUDY OF SEISMIC AND VOLCANIC
HAZARDS IN THE PRIBILOF ISLANDS - EASTERN ALEUTIAN ISLANDS REGION
OF THE BERING SEA

FOURTH QUARTER/ANNUAL REPORT

April 1, 1975 - March 31, 1976

J.N. Davies, L. House, K.H. Jacob

R. Bilham, V.F. Cormier and J. Kienle

Prepared jointly for the

National Oceanic and Atmospheric Administration

under contract No. 03-5-022-70

and the

U.S. Energy Research and Development Administration

under contract No. ERDA(11-1)3134

PREFACE

This report describes work done under NOAA contract number 03-5-022-70 entitled "Seismotectonic Analysis of the Seismic and Volcanic Hazards in the Pribilof Islands - Eastern Aleutian Islands Region of the Bering Sea". It was originally prepared under the title "A Comprehensive Study of the Seismotectonics of the Aleutian Arc", and was presented to the U.S. Energy Research and Development Administration (ERDA) as an annual progress report on work carried out under contract number ERDA(11-1) 3134 during the period March 1, 1975 - February 29, 1976. Because the seismic and geodetic work done under the present NOAA contract was, by design, completely complementary to that done under the above ERDA contract all of the work done is presented in this one report which is intended to satisfy the reporting requirements of both agencies. An effort has been made throughout the report to note which portions of the work were specifically supported by NOAA.

This complementary arrangement exists because at the time NOAA's need for a hazards analysis in the Bering Sea area arose, the ERDA seismotectonic study was well under way. It was proposed that NOAA provide funds and logistic support to allow a reorganization of the existing seismic network and an expansion of the geodetic leveling program. This supplementary support has strongly improved the hazards analysis. It has also provided additional manpower which allows a more rapid analysis of the data than would otherwise have been possible.

All of the results discussed in the Data Analysis section of this report are relevant to the evaluation of the seismic or volcanic hazards in the eastern Aleutians. The historic seismicity map for 1965-1975, the most recent data set available, shows that the Shumagin seismic gap (Sanak Island to Kodiak Island) continues to exist as a region with presently low seismicity. The local network data reveal that most of the earthquakes which are occurring in the Shumagin gap

are contained within a northward dipping Benioff zone which is well defined between the depths of 30 and 50 kilometers. The likelihood of a large earthquake occurring in the gap in the near future is discussed in an appendix prepared especially for this NOAA version of the report. The conclusions of that appendix is that it is almost a certainty that an earthquake larger than or equal to magnitude seven will occur within the next 20 years and that the probability that this event might be larger than or equal to magnitude eight is significant.

Seismological and geodetic research performed during the past contract year has increased our understanding of the seismotectonics of the eastern Aleutian Island Arc. While generally aimed at producing a coherent theory for the evaluation of the entire arc, our research has focused on the Shumagin Islands seismic gap, a region within which a major earthquake is expected in the not too distant future. To collect basic seismological data and to investigate certain earthquake prediction techniques we maintain 19 short period and 3 long period seismograph stations, 2 strong motion accelerographs and a pair of strainmeters. To investigate possible regional tilting due to strain accumulation within the seismic gap we have made limited geodetic leveling measurements. We have expanded the baseline and increased the resolution of these tilt measurements with the installation of two remote tide gauges. In this report we present (1) historic seismicity maps of the Shumagin seismic gap vicinity which show the relatively low level of seismic activity in the gap, a possible offset in the Benioff zone, and a few events associated with the Bering shelf continental margin south of the Pribilof Islands; (2) a seismicity map and hypocenter cross-sections based on data from the local Shumagin Islands seismic network which show a very well developed Benioff zone beneath the Shumagin Islands; (3) studies of the focal mechanisms of April 6, 1974 Shumagin Islands earthquake and the February 2, 1975 Near Islands earthquakes which respectively show thrust faulting perpendicular to the arc and right-lateral strike-slip faulting oblique to the arc along the slip direction inferred from the relative motion of the plates; (4) the first strong motion accelerograph data from the eastern Aleutians, which show accelerations consistent with those observed for earthquakes in California; (5) this year's geodetic leveling results which when compared with those from 1972 indicate

that regional tilting due to tectonic strain accumulation, if it is occurring, is less than 1.9 microradians per year; and (6) seismic observations of two Strombolian eruptive cycles of Pavlof Volcano which reveal monochromatic wave trains which are identical one to the next suggesting a common source region and a harmonic source function or very efficient filtering of the body waves by the pyroclastic layers of the volcano.

TABLE OF CONTENTS

| | |
|--|----|
| Abstract | 1 |
| Table of Contents | 3 |
| Introduction | 4 |
| Field and Instrumental Work | 5 |
| Reorganization, installation and maintenance of the seismograph network | 5 |
| Maintenance and calibration of long period seismographs | 9 |
| Geodetic instrumentation (R. Bilham) | 10 |
| Geodetic leveling | 20 |
| Strong motion accelerograph maintenance | 20 |
| Preliminary design and fabrication of Pavlof seismic array | 20 |
| Personnel | 21 |
| Acknowledgements | 22 |
| Data Analysis | 24 |
| Historic seismicity maps | 24 |
| Shumagin Island seismicity from local stations | 26 |
| Shumagin Islands focal mechanism | 28 |
| Near Islands focal mechanism (V.F. Cormier) | 30 |
| Strong motion data | 32 |
| Geodetic measurements | 34 |
| Seismic monitoring of Pavlof Volcano (J. Kienle) | 38 |
| Conclusion | 41 |
| Percentages of Time Devoted by Principal Investigators | 42 |
| References | 43 |
| Figures | 45 |
| Tables | 65 |
| Appendix | 70 |

INTRODUCTION

This report summarizes progress on work and research carried out by Lamont-Doherty Geological Observatory (L-DGO) personnel under Contract ERDA(11-1) 3134, "A Comprehensive Study of the Seismotectonics of the Aleutian Arc", for the period March 1, 1975 to February 29, 1976. Parts of this work were performed in cooperation with Drs. H. Pulpan and J. Kienle of the Geophysical Institute of the University of Alaska (UA). Portions of the work carried out primarily for this contract received additional support from a new contract with the National Oceanic and Atmospheric Administration (NOAA) entitled "Seismotectonic Analysis of the Seismic and Volcanic Hazards in the Pribilof Islands - Eastern Aleutian Islands Region of the Bering Sea." This NOAA contract (see work statement in Appendix I) supported additional work complementary to the ERDA work which is summarized in this report because of its direct relevance to the goals of the ERDA contract. Finally, this report summarizes the initial progress on work carried out under an expansion of scope to the ERDA contract entitled "Search for a Magma Chamber under Pavlof Volcano".

Both the expansions to the basic seismotectonic study supported by NOAA and the ERDA expansion of scope arise out of the growing recognition of the acuteness of the national energy situation. The seismic and volcanic hazards analysis (NOAA) is part of the Outer Continental Shelf Energy Program (OSCEP) and will help evaluate the environmental risks to and from the exploration for oil on the outer continental shelves. The geothermal work on Pavlof volcano is part of ERDA's mandated program to evaluate alternative energy sources.

It is somewhat fortuitous that these more applied needs arise at a turning point in our research program. After several years of intensive field work we

now have a seismic network which can provide some of the basic data for these hazards and geothermal evaluations. In the following section we will describe the field and instrumental work which have been carried out during the past year. Following that we will discuss our recent results and plans for the coming year.

FIELD AND INSTRUMENTAL WORK

Reorganization, installation and maintenance of the seismographic network.

During this past field season we accomplished a major reorganization of the seismographic network. This reorganization included the relocation of remote seismic stations, the establishment of a VHF telemetry link from Port Moller, through the mountains of the Alaska Peninsula to Sand Point on Popof Island and the expansion of the data recording centers at Sand Point, Dutch Harbor and Saint Paul. The reasons for this reorganization were threefold: (1) We faced rising costs on the White Alice Communications System (WACS) for our data link from Driftwood Bay to Homer and its eventual (one to five years) phase out. (2) The addition of stations on Kodiak Island by the University of Alaska required an additional develocorder thus allowing the possibility to relocate the previously shared L-DGO develocorder from Homer to Sand Point and (3) By moving the L-DGO develocorder to Sand Point all of the Cold Bay and Shumagin Island stations could be recorded on a single 16 mm film, eliminating the costly and time consuming data reduction of two different kinds of records (tape and film). The Sand Point location minimized the telemetry requirements necessary to accomplish this consolidation of the data recording.

Figure 1 shows the locations of seismograph stations in the eastern Aleutians. Some of the station parameters for the current L-DGO stations shown in this figure

are given in Table 1. The remote stations are all battery (air cell) powered and connected via VHF telemetry links to the recording sites at Dutch Harbor or Sand Point. Most of these stations were serviced from the NOAA ship Surveyor with the aid of the ship based Jet Ranger helicopter. Table 2 summarizes the stations visited and tasks accomplished from the Surveyor. The remaining stations were serviced from locally chartered fishing boats or small aircraft.

A GeoSpace HS-10/B 1 Hz seismometer was installed in the long period vault at Saint Paul. This instrument is recorded on a Helicorder in the Weather Bureau along with the long period instrument. The single short period seismograph will not, of course, allow location of earthquakes, but is intended to measure the general seismicity level of the Saint Paul area. The equipment for this installation was purchased with NOAA funds.

The seismic stations at the White Alice Communications Systems (WACS) sites of Driftwood Bay (DWB) and Cape Sarichef (CPS) were removed because of the high cost of the WACS telemetry link, the scheduled (1976) phase out of the CPS site and the relatively poor seismometer locations available close to the WACS sites. The seismometers and amplifiers/VCO's from these sites were incorporated in the remote installations at Makushin Valley (MKV) and Dolgoi Island (DOL). The removal of CPS and the Akutan Island (AKN) receiver there necessitated the relocation of AKN to ARV so that it could be telemetered to MKV where it is repeated into Dutch Harbor. Both AKV and MKV are intended to monitor volcanic activity as well as the tectonic earthquakes. Due to logistic constraints MKV is located too far away from Makushin to record small volcanic tremors but certainly will record any major eruptive activity. These two remote stations are recorded at Dutch Harbor on Helicorders purchased with NOAA funds. They and the local horizontal and vertical instruments which are recorded on a dual channel Auto-

corder, comprise the Dutch Harbor array. This tripartite array is minimally sufficient for independently locating local earthquakes and has an accurate enough time base so that data from this array can be used in conjunction with other data to locate larger regional events.

The new station on Dolgoi Island (DOL) is telemetered to Deer Island (DRR) as is the Sanak Island station (SNK). The data from DOL, SNK and DRR are mixed and transmitted to the Cold Bay WACS site, CDB. The stations at Baldy Mountain (BAL) and False Pass (FPS) are also transmitted to Cold Bay. These five stations DOL, DRR, SNK, BAL and FPS, comprise the Cold Bay subarray of the Shumagin Islands array. Data from the Cold Bay subarray are transmitted via a WACS voice circuit from Cold Bay to Port Moller (PMA) and then to Sand Point on a L-DGO installed and NOAA funded VHF link.

The University of Alaska station, PVS, which was located in the saddle between Mt Pavlof and Pavlof's Sister was removed because the site proved unsatisfactory. The L-DGO station at Black Hills (BLH) was not gotten operational due to logistic constraints. We originally intended to tap the amplifier output from the NOAA station at Port Moller (PMA) and transmit that data to Sand Point to provide the basis for a direct comparison of our timing and magnitude determinations with those of NOAA at the Palmer Observatory. Although this was not accomplished this summer we hope to complete this hook-up in the near future.

All of the original eight remote Shumagin Island seismic stations, PVV, WUN, CNB, NGI, SQH, BKJ, IVF and SGB, were serviced and operational by the end of the summer except CNB which is operational but not being recorded because its receiver at NGI failed. The vertical seismometer at Sand Point was replaced by a GeoSpace HS-10/B identical to the seismometer installed at Saint Paul.

This seismometer has a calibration coil, so complete system responses from the seismometer through the amplifier/filters to the recorder could be (and were) calibrated.

The original eight remote Shumagin Island stations, the three component local station at Sand Point and the five Cold Bay stations are all recorded on the Develocorder at Sand Point. The Develocorder was installed in parallel with the 14 channel tape recorder so that the tape recorder can be used as a back up in case of failure of the Develocorder. A redundant timing system was set up. The top and the bottom trace of the Develocorder records the BCD time code from a Sprengnether TS200 chronometer. The minute mark from a Sprengnether TS100 (primary time for the long period records) is superimposed on one of the seismic traces. For convenience of reading the records the Develocorder internal date-time group is recorded on the margin of the records.

The accuracy of the comparison of station time to WWV was improved at Sand Point, Dutch Harbor and Saint Paul by the installation of a semi-automatic time calibrator. This L-DGO built device, when manually switched on, provides WWV minute-tone-activated relay closures which are recorded, along with the minute marks from the TS100, on a single channel strip chart recorder. These strip charts form a convenient and permanent record of the time calibration for each recording site (SDP, DUT and SNP).

In summary, L-DGO now maintains 19 short period seismograph stations in the eastern Aleutians, 13 of which are recorded on a Develocorder at Sand Point. The time calibration has been upgraded at all three recording sites so that absolute arrival times can be read to better than a tenth of a second at any of these stations.

This will improve our ability to locate larger regional events and to compute travel times. The main purpose in maintaining these stations is to obtain detailed seismicity data for the Shumagin gap region of the eastern Aleutian arc. Some of the stations are situated close to active volcanos so they can monitor both the regional seismicity and local volcanic activity.

Maintenance and Calibration of Long Period Seismographs.

At each of the recording sites, SDP, DUT and SNP, there is a long period vertical seismograph. In addition, at SDP there is an orthogonal set of horizontal instruments. All of the seismometers are set to 20 sec natural period. The signals are amplified and filtered using L-DGO built equipment which has a cut-off period of 100 seconds. All of these signals are recorded on Helicorders with superimposed minute marks from a Sprengnether TS100 chronometer.

The L-DGO amplifiers originally had basic gains (before attenuation) of 60 db. This high a gain turned out to be unnecessary at these Aleutian sites and contributed somewhat to an instability in the zero position. Therefore we reduced the gain of all amplifiers from 60 db to 40 db. 40 db.

Following the modification to the amplifiers a complete calibration was carried out. The seismometers were reset to a 20 second natural period. Then each component (seismometer, amplifier, filter and Helicorder) was individually calibrated to assure its proper operation. Finally the entire system response was calibrated by driving the seismometer calibration coils at various periods over the range 5-200 seconds while recording the output on the Helicorder. Magnification was computed based on direct observation of the boom deflection using an optical comparator.

Geodetic Instrumentation, Shumagin Islands, August 1975 (R. Bilham)

As part of the program to monitor surface deformation and bulk changes of elasticity in the Shumagin Islands of the Aleutian Arc two mean sea level indicators and two wire strainmeters were installed during August 1975. The following account describes the justification for, construction and installation of the instruments.

The Shumagin Islands are within an area in which a major earthquake is expected in the not too distant future. On the global seismic map this area appears as a relative absence of seismicity in the otherwise continuous seismicity associated with the Benioff zone along the Aleutian Arc. This condition often precedes major seismicity.

In order to study whether surface deformation occurs as part of the mechanism of any future earthquake we have instigated various long term projects which attempt to monitor manifestations of regional strain. Some earthquake mechanism models suggest surface elevation may precede an earthquake (dilatancy) whereas other theories indicate that the underthrusting slab may drag the overthrusting lithospheric plate downward. The parameters we have chosen to monitor in the Shumagins are surface tilt and strain. The earth tilt measurements are achieved by two independent methods, geodetic levelling on an annual basis (described in later sections) and the comparison of continuous records of mean sea level measured on different islands. The mean-sea-level indicators (MSLI) are newly conceived devices and the prototypes will be described in detail. The wire strainmeters are not new and are described less fully. The strainmeters are installed so as to monitor changes in load tide strain amplitude on Popof Island which may be an indicator of changes of elasticity beneath the Island such as are predicted in dilatancy-diffusion models. They are not good indi-

cators of secular strain rates unless a significant change of strain rate should occur. That is, the instrumental stability is sufficient to detect transient events (strain rate $>10^{-7}$ /day) but not sufficient to detect strain accumulation of less than 10^{-6} per year.

The MSLI is an instrument for recording mean sealevel. It differs from a conventional tide gauge in that it has a long time constant (>20 hours) and therefore damps the unwanted sea tides significantly. The present design will operate for 18 months on internal dry batteries with a maximum measurement precision of 1 mm. Samples are taken once per minute on a pressure sensitive analog chart and the device both calibrates itself and stays on scale automatically.

The MSLI takes two men two days to install by hand. An instrument costs \$500 in parts (1973) and is estimated to cost a further \$500 to emplace in an average remote site when travel (hire of boat) and per diem costs are included.

Principle of Operation. In common with normal tide gauges the MSLI uses a buoyant float as a reference for the height of the sea surface. The float is connected by a stainless steel wire to a measuring device positioned some distance above the high water mark. The connection to the sea is through a capillary tube in order to remove rapid variations of sea level. By this means it is possible to attenuate the amplitudes of the tides relative to longer period (monthly) variations which allows greater measurement precision using inexpensive transducers and analog chart recorders of limited dynamic range.

The mathematics of the hydraulically filtered tide gauge have been described in Groves 1965 and Filloux and Groves 1960. The time constant of the syphon is given by

$$\tau = 8\nu l \alpha^2 / r^4 g$$

where ν is the kinematic viscosity of sea water ($.01 \text{ cm}^2 \text{ s}^{-1}$), l is the length of the entry tube, α the inside radius of the standpipe and r the inside radius of the entry tube. Thus using a 6 cm radius standpipe and a 150 m long 3 mm radius entry tube we achieve a time constant of approximately 1 hour and by inserting a 1 m long 0.3 mm radius capillary in the hydraulic path the time constant can be increased to 100 hours. In the Aleutians, where the sea level variation is approximately 4 m, we chose a 30 hour time constant capillary (.4 mm radius) which led to an attenuation factor of approximately .013. The resulting 5 cm tide was arranged to record as approximately 1/2 chart width by selecting a 10 cm circumference measurement pulley. The resolution of the record in this instance is 2% of full scale chart width (2mm). The chart width is 6 cm so that the one millimetre of chart corresponds to 1.7 mm of change of elevation of mean sea level.

Measurement (Figure 3). The system uses a low-friction 100 k continuous-rotation potentiometer with 0.1% linearity to measure the motion of the float. One 1.5V cell provides a voltage source for the potentiometer at a drain of approximately $1 \mu\text{A}$. A programmable $\mu\text{A}776$ amplifier set to operate at approximately $2 \mu\text{A}$ quiescent drain converts the variable potentiometer voltage into a current source feeding $10 \mu\text{A}$ galvanometer of the recorder. The total current consumption varies from $2 \mu\text{A}$ to $12 \mu\text{A}$ depending on the potentiometer setting. Two AAA-type alkaline cells are sufficient for 18 months operation.

If required it would be possible to transmit the transducer output to a remote recording location using FM coded VHF telemetry. The VCO in this application need be of merely moderate stability since the transducer provides regular calibration and datum.

Recording. The recorder motor is rated at 6V, 24mA. In this application it is operated at 2.8V for two seconds every 60 seconds. The power is supplied from a single Lithium D-Cell, with a rated capacity of 10AH. The switching system adopted is the prototype involves a commercial clock movement (Endura, \$6) with a 60 second sweep hand onto which is fitted a pill shaped magnet (1/4" diameter, 1/8" thick, N-S faces). Each minute this sweeps past a reed relay whose fixed position is adjusted to give the required 2 second contact closure. The clock is operated from a separate battery (1.5V Alkaline D). The batteries chosen are sufficient to operate the recorder and clock for 18 months.

Chart speed can be adjusted by using interchangeable gear boxes. The normal operating time is chosen to be 13 months which gives a chart speed of approximately 5 cm/day.

Calibration and Timing. The electronic calibration depends on the state of the batteries since it is difficult to regulate the low voltage ($\pm 1.5V$) in the measurement system without wasting power. However, the system automatically calibrates itself as long as the mean level measured oscillates over more than one chart width. For example the sea tides are never removed totally nor are they exactly centered on the chart. Thus as the potentiometer rotates from maximum to minimum or vice versa a record of amplifier calibration is produced. The daily tides are used to time the record since they are not themselves of interest and can be read to one hour.

Subsequent digitisation of MSLI records leads to automatic compensation for calibration changes and tidal delay during computer processing.

Temperature Effects. The complete electronic package has been tested between -10° and $+25^{\circ}\text{C}$ with no effect on the mechanical operation and only 2% change in the fullscale indicated value. However, the present mechanical design will freeze at 0°C since the standpipe uses sea water. It would be possible to introduce oil into the system to enable it to operate at subzero temperatures without major changes to the standard instrument.

Mechanical Construction. The base of the standpipe is embedded inland 50 cm below mean sea level in a block of concrete. Bolted to the top of the pipe is the recording, measuring package. The recorder, electronics and batteries are all enclosed in a hermetically sealed PVC tube (Figure 2). The design is such that during flood conditions, such as could be caused by a high-tide storm or a tsunami, water will be forced up the outside of the tube creating increased air pressure inside the tube. This back pressure is designed to prevent flooding of the recorder compartment in the event of failure of the O-ring seal. The entire system can thus be flooded to a depth of several meters without damage. This was considered to be a necessary design feature in view of the destruction of the Alaskan tide gauges by the tsunami immediately following the 1964 earthquake. The standpipe is installed slightly inland from the coast and is more than 80% buried which further prevents mechanical damage.

The float is a 4" diameter glass jar, weighted inside with steel embedded in wax (to give it buoyant stability) and sealed hermetically. It is held by a 0.4 mm diameter corrosion resistant stainless steel wire with a breaking strength of 10 Kg weight. The counterbalance weight is a 100 gm lead weight.

The mechanical construction material, except for the Aluminum alloy standpipe, is entirely 1/2" P.V.C. which has good mechanical strength and does not corrode. The measurement system is held to the standpipe by three bolts and is designed to be replaced annually by a spare unit. This enables rapid inspection in the field and allows careful overhaul of the apparatus in a more favourable environment.

The entry tube is transparent PVC tubing with a 1/4" internal diameter and a 1/2" external diameter. It is tough and resilient. Air bubbles are easily visible in the tube if it is in air or under water. The entry orifice to the system consists of a 5 cm copper tube approximately 30 cm long, held by an heavy framework approximately 1 m above the sea floor. The copper tube discourages barnacle growth and produces a poisonous environment in the entry tube which prevents bacteriological fouling. It points downward so that sediment accumulation cannot occur.

Long Term Stability. The stability is dependent on the standpipe position, the buoyance of the glass float and frictional effects in the pulley potentiometer. The latter is very low in friction compared to the forces exerted by the float and stainless steel wire (which is wrapped 1 1/2 times around the pulley). The glass float may become heavier if bacterial growth occurs and annual inspection will be required to identify such effects. Mercuric chloride in dilute solution in the standpipe may prevent organic growth.

The standpipe position is geodetically surveyed to a nearby solid rock outcrop. Long term settling of the standpipe will be monitored to a precision of 0.2 mm.

The electronic package is self calibrating and long term gain changes are recoverable in subsequent processing.

Installation (see Figure 4). The site for a mean sea level indicator is chosen with care. The most important requirement is that the entry tube should be well protected as it passes through the intertidal zone. This usually requires a sheltered sandy beach or a storm beach with a surge channel.

The base of the standpipe has to be buried to a depth greater than the lowest expected mean sea level and has to be long enough to emerge above the high water mark. In the Shumagin Islands the tidal range can exceed 4 m so that a 3.3 m standpipe was adopted. The excavation was carried out by hand to a depth of 3 m at low tide. The resulting hole measured 1.5 m x 1 m in area and took two men four hours to dig in gravel, sand and soil. Two hundred-pound bags of concrete were mixed with water repellent liquid ("antihydro") and local sand to provide a firm 40 cm deep foundation for the base of the standpipe. The remainder of the hole was filled immediately with the excavated material before the turn of the tide.

The entry tube was buried to a depth of 50 cm under the beach. Since this also had to be done at low tide it was completed on the following day. Ideally this occasion is the lowest low-tide of the month as it was in the case of the August 1975 installation. The tube is more dense than sea water and naturally sinks when offshore. The greatest difficulty arises in burying the tube as it passes under water from the beach. Large boulders were placed upon it to prevent movement and appeared to be adequate in the sheltered bays chosen.

Water was pumped into the system from the seaward end by an electric im-

pellier pump. This introduced cavitation and future installations will utilize a slow speed hand pump to prevent the production of bubbles. The final adjustment of the syphon was accomplished by operating the valves around the capillary tube. All bubbles were removed by vibration and bleeding the system.

The final operation was to sink the entry port for the syphon at the extreme end of the entry tube. The entry port is placed some distance from the shore (150 m - 250 m) to prevent biological fouling, sedimentation or physical damage. In each of the Shumagin installations the water depth was 10-20 m. The framework used to hold the entry port was in each case a disused king crab pot framework, weighing more than 100 kg.

Shumagin Islands - Location of MSLI. The two instruments were installed at Pirates Cove, Popof Island and Eagle Harbor, Nagai Island. The two installations are separated by a distance of 32 km (Figure 5). Since they have a resolution of 1.7 mm per mm of chart we can resolve tilts manifest as vertical motions of the islands approximately 5 parts in 10^8 . The "noise" associated with the measurements is related to seasonal changes in wind direction and sea currents, precipitation and atmospheric pressure changes. We intend to learn more about the noise by installing additional instruments in the coming 1976 field season. In particular we will install instruments on the south facing shores of the two islands already instrumented and extend the baseline of the measurements to the extreme south of the area (Chernabera Island) and to the mainland. The additional five instruments planned will give a 100 km baseline at right angles to the strike of the Benioff zone and the multiplicity of instruments will enable us to estimate the noise present in sea-level measurements in the Shumagin Islands.

Strainmeters. The surface strain measured some distance from a surface load can be calibrated using standard rock-mechanics techniques. The magnitude of the strain is proportional to the size of the load and the rigidity of the material beneath the source and instrument. By placing the strainmeter n km from a coastline it is possible to monitor the rigidity of the surface rocks to a depth of approximately $\frac{n}{3}$ km. The original intention was to install three wire-strainmeters near the center of Unga Island, the largest of the Shumagin Group which would allow us to sample the upper 3 km of the crust. However, it was not possible to get installation equipment onto the island and instead two instruments were installed near the only road in existence in the Shumagins on the Island of Popof.

The site is far from ideal in that it is less than 2 km to the nearest coastline. However, we may be able to reduce the effects of the closest load tide by using data from the Sand Point Coast and Geodetic Survey Tide Gauge. This tide gauge is located within 1.5 km of the strainmeter installation and we are obtaining continuous strip charts of the data. In addition we have some control over the regional tidal loading pattern since the mean sea level indicator data can be converted back to unattenuated tidal magnitudes knowing the MSLI characteristics. We hope that the quality of the strain data will be sufficient to observe 10% changes in thirty-day tidal strain analyses.

The study of body-tide admittance is fundamentally more useful since it allows greater penetration with regard to elasticity measurements. However, the predicted body-strain tide is approximately three times smaller than the load strain tide according to our initial measurements of the total strain tide

in the Shumagins. Thus changes in the strain load tide are expected to mask the smaller changes expected in the body tide (Beaumont and Berger, 1975). It is too early to know whether the measurements are of sufficiently low noise to enable resolution of tidal amplitudes to the accuracy that would enable us to examine the body-tide tidal admittance.

Two wire strainmeters were installed on a weathered gabbro sub-surface rock two meters beneath the surface of the tundra. The length of each instrument is approximately 12 m and their azimuths are 0° and 90° geographically.

The wire strainmeter is described elsewhere (King and Bilham, 1975). Its stability is poor compared to laser strainmeters ($<10^{-6}$ /year) but it is cheaper and is simple to install. The recording system consists of zero suppression electronics and automatic drift correction to maintain instrument operation. The recorder is a strip-chart pressure sensitive Esterline-Angus which samples alternate instruments. Timing is provided by an Accutron clock which interrupts the analog record and indicates the amount of long-period drift on the record every twenty-four hours. The chart speed is 5 cm/day and a data point is recorded once per minute.

Caustic soda batteries (11 x 1.2 volt) provide sufficient power for a year's operation which corresponds to the chart recorder capability. The electronics and strainmeters are hermetically sealed and are buried totally. Two small tubes supply fresh air to the batteries which are installed in a sub-surface brick enclosure at one end of one of the wire strainmeters.

Geodetic Leveling

The level lines and dry tilt figures (see Figure 5) which were established at Sand Point and Squaw Harbor in 1972 were all reoccupied during this field season. Specially made portable turning points for the rods and a more redundant observational technique than was employed during the past two years allowed substantial improvement in accuracy over the measurements made in 1973 and 1974 and slight improvement over those made in 1972. The results of these measurements will be discussed under the data analysis heading.

Strong Motion Accelerograph Maintenance

L-DGO operates two strong motion accelerographs; one at Dutch Harbor and one at Sand Point. New batteries and film were installed in each of these instruments and the traces were rezeroed. We recovered one record of a seismic event from the Sand Point instrument. This record and two previous ones are discussed under the data analysis heading.

Preliminary Design and Fabrication of Pavlof Seismic Array.

Work has begun on the design and fabrication of the seismic array to be deployed around Pavlof Volcano next summer. The general system design has been completed and research into the question of which specific pieces of equipment best meet the design requirements is underway. Two of the three L-DGO "OAS" tape recorders earmarked for use with this project have been refurbished and work on the third should be completed soon. A prototype timing system which will superimpose 12 hour, hour and minute marks on one of the seismic traces of each of the tape recorders is complete and is now undergoing reliability testing. We have selected a 4 channel 1/4" tape playback unit which meets our specifications and will soon begin testing this unit. So far the work on this seismic

array is on schedule and we are confident that it will be deployed around Pavlof as planned.

Personnel

The above described fieldwork was carried out by five persons from L-DGO; Drs. John Davies and Roger Bilham, graduate students Leigh House and Stuart Nishenko; and technician Laszlo Skinta. Dr. Davies was responsible for overall planning, maintenance and modification of the short period seismograph network, the long period seismograph stations and the strong motion accelerographs and the geodetic leveling. He was assisted in all of the above by Mr. Skinta. Dr. Bilham was in charge of the design, fabrication and installation of the strainmeters and the mean sea level indicators. Mr. House and Mr. Nishenko assisted with the maintenance and modification of the short period network, the geodetic leveling and the installation of the strainmeters and mean sea level indicators.

This field work was jointly supported by ERDA and NOAA. The equipment and supply charges were easily allocatable to the appropriate contract. However, since the travel to, from and within the Aleutians was pursuant to the goals of both contracts and not always separable, an attempt was made to keep the travel and per diem charges roughly equal. The actual percentage distribution of these charges by contract for each person and for the total amount spent is given in the following table:

| <u>Person</u> | <u>ERDA (11-1)3134</u> | <u>NOAA 03-5-022-70</u> |
|---------------|------------------------|-------------------------|
| Davies | 77% | 23% |
| Bilham | 36 | 64 |
| House | 82 | 18 |

| <u>Person</u> | <u>ERDA (11-1)3134</u> | <u>NOAA 03-5-022-70</u> |
|---------------|------------------------|-------------------------|
| Nishenko | 39% | 61% |
| Skinta | 53 | 47 |
| Total | 56 | 44 |

Acknowledgements. It is impossible to carry out a field program of this type without help from many people. We were indeed fortunate to receive support from almost every quarter: the NOAA ship Surveyor, ITT site personnel, the U. S. Air Force at Cold Bay, U. S. National Marine Fisheries, National Weather Service, U. S. Army, U. S. Coast Guard, U. S. Fish and Wildlife, bush pilots at Sand Point and King Cove, the Wakefield, Peter Pan and New England Fish Co. cannery personnel at Squaw Harbor, Sand Point, Port Moller and False Pass, the seismic station operators and many private persons who provided a skiff, a cup of coffee, information, a hot meal or who helped with the backpacking to one or more of the remote seismic stations.

Space does not allow a detailed acknowledgement to all of those referred to above. Special mention and thanks are extended to the following: Captain MacDonald, the officers and crew of the NOAA ship "Surveyor" provided the major logistic support for servicing the remote seismic stations. NOAA helicopter pilot Don Winters deserves commendation for his skillful flying in the always marginal Aleutian weather. Sand Point school principal George Kimball and teachers Bob Cochran and Kevin Daley cooperated and assisted with the modification of the recording center there. Sand Point bush pilot Charlie Barnes flew us many places during this and past summers, often under very adverse conditions. It appears likely that he will carry out his oft-threatened plans for retirement this year. His advise and skill will be missed. Sand Point station operator Connie Griffy and her husband Chuck gave much help above and

beyond the station routine, including providing the use of their skiff for most of the summer. The ITT White Alice site personnel at Port Moller, Cold Bay, Cape Sarichef and Driftwood Bay were uniformly helpful in assisting with our work at these sites. In particular Bob Williams and Hank Ickes of the Cold Bay site spent many off duty hours hiking to remote sites. At Saint Paul the National Marine Fisheries people provided very comfortable rooms, the U. S. Coast Guard allowed us to share their kitchen and the Weather Service provided transportation and assistance with the installation of our equipment in their observatory. At Dutch Harbor the station operator, Charlie Brown, provided room and board, the U. S. Army personnel and Bob Nelson of the Fish and Game helped with the transportation to and installation of the Makushin Valley station. The Kodiak U. S. Coast Guard provided transportation from Kodiak to Cold Bay on Labor Day weekend when all public flights were either full or cancelled, thus saving several days of field time. One of the rewards of the work in the Aleutians has been the cooperation, hospitality and friendship of the people who live there. This is perhaps best exemplified by the people of Ivanof Bay who, upon seeing us dropped off the airstrip, invited us in for coffee and arranged for skiffs to take us to and from our remote seismic station. We are grateful to many such people who live and work in the eastern Aleutians.

DATA ANALYSIS

Historic Seismicity Maps. The historic seismicity for the region of the eastern Aleutians surrounding the Shumagin Islands is shown in Figures 6, 7 and 8. The first figure shows all of the epicenters available from 1902 through February 1975. The data for these figures is taken from the World Wide Standard Seismograph Network (WWSSN). The triangular symbols which mark the epicenters are both color and size coded: black, green and red correspond to the depth intervals 0-30, 30-60, and greater than 60 respectively; small medium and large correspond to the magnitude ranges 0-3, 3-5, and greater than 5, respectively.

This data was divided into pre- and post-1965 sets which are shown in figures 7 and 8. This division at 1965 is somewhat arbitrary: the purpose is simply to look at recent subsets of the data which may be better located than the earlier subset due to an increase in the number of seismographic stations in the eastern Aleutians. There is a diffuse character to the pre-1965 set which indicates more scatter in the locations than is shown for the post-65 group. This is especially evident if one compares the locations of the deepest events (shown in red) which more clearly show the expected alignment along the northern edge of the arc in the post-65 figure.

The most obvious feature of the seismicity shown in these figures, again most clearly seen in Figure 8, is the gap or relatively low level of activity between 162° and 154° west longitude. This is one of the seismic gaps discussed by Kelleher (1970) and Sykes (1971). On the basis of the space-time progression of the 1949, 1958 and 1964 Aleutian-Alaska earthquakes, Kelleher has suggested that this Shumagin Islands gap may be the location of a major ($m_g > 7.8$) earthquake in the period 1974-1980. Sykes notes that much of this region broke in

1938 and suggests, therefore, that the Shumagin gap has a slightly lower potential for a major earthquake than those gaps which have not had a major event for more than 70 years. However, he also notes that the aftershock zone of the 1938 event is not well defined so it is possible that the western 200 to 300 kilometers of this gap did not break in 1938. Sykes further comments that in any case a recurrence time of 35 years may be reasonable and on that basis it is possible that the 1938 region may have accumulated enough strain energy to be the source of a major earthquake. If this is the case than the low level of seismic activity in the Shumagin gap is due to the overthrusting plate being "locked" with the subducting Pacific lithosphere. Another possibility is that in this region underthrusting occurs primarily aseismically by fault creep and, hence, fewer earthquakes occur. This seems less likely though since there have been two major events in the Shumagin vicinity since 1900.

A second striking feature of these maps is the en echelon offset in the deep events (red triangles) shown in Figure 8. It is possible that this offset is due to a systematic mislocation of these events. However, the geographic coincidence of the offset with the Shumagin Islands and an unusual earthquake whose focal mechanism indicates a fault plane transverse to the arc suggests that it is tectonically significant.

A third feature, which again is best defined in the post-65 data shown in Figure 8, is the smaller group of events which appear to be related to the Bering-shelf continental margin which is indicated by the 100 fathom contour line which strikes out of the figure to the northwest. It has been suggested (Minster et al., 1974) that there is a Bering subplate. These events may be caused by relative motion along the western boundary of this subplate. It is also possible that they result from a differential stress at the continental margin which is caused by erosion of the continental material and its deposition

onto the Aleutian floor.

Finally there are a number of smaller scale features revealed by these regional maps. For example there are concentrations of events at 169.5° , 167° , 163° and 160.5° W. These concentrations deserve more detailed study to evaluate their tectonic significance.

Shumagin Island Seismicity from Local Stations

The seismicity in the vicinity of the Shumagin Islands for the first year of data collection, August 1973 through July 1974 is shown in Figure 9. The epicenters are marked by numbers which give the depth to the hypocenter in kilometers. The figure is oriented such that the volcanic axis is horizontal. Unimak Island, the western tip of the Alaska peninsula and the Shumagin Islands are outlined. The 100 and 3000 fathom isobaths are shown. The dashed rectangles labeled W, C and E show the surface projection of the volumes containing the hypocenters shown in cross-section in Figures 10, 11 and 12 respectively.

The seismicity map (Figure 9) shows only the best locations obtained; approximately 135 events are plotted. The concentration of events at 55° N and 160° W is the April 6, 1974 earthquake sequence; 3 main events ($m_g = 6.0$, 4.3 and 5.7) and about 30 aftershocks. A focal mechanism for the largest event of this sequence is presented later in this report. There are no striking lineations seen on this map. There are some interesting voids or "mini gaps" which will be interesting to watch as more data becomes available. Examples of these mini gaps are the region around Pavlof Volcano (PVV) and the areas southeast of Nagai Island (NGI) and Ivanof Bay (IVF).

The cross-sections shown in Figures 10, 11 and 12 are projections onto planes normal to the volcanic axis of the hypocenters contained in the respective

volumns as described above. This axis is labeled "volcano line" in the figures. The three letter station codes mark the locations of the stations used in locating the events shown. All of these stations except two are within the center dashed rectangle shown in Figure 9. The other two, PVV and IVF, are in the western and eastern dashed rectangle respectively. Consequently, the locations for the center section, Figure 11, are much better than those for the adjacent western and eastern sections.

The center section reveals a well defined Benioff zone which dips at approximately 30° from about 30 km below the outer Shumagin Islands to 100 km beneath the volcanic arc. The western section shows a clear Benioff zone but, the hypocenters are not contained in as narrow a zone as those in the center section. This scatter may be real but, it is most likely due to the station distribution which is concentrated over the center section. The hypocenter section. This scatter may be real but, it is most likely due to the station distribution which is concentrated over the center section. The hypocenters shown in the eastern section also clearly show a Benioff zone. Again, the lack of definition here is probably due to the small number of stations in this area. Both the seismicity map based on the local data (Figure 9) and the regional map based on the WWSSN data (Figure 9) show very few epicenters in the vicinity of the eastern section. Near this section in Figure 8 there is an area about 50 km wide and extending clear across the arc from north to south which does not contain a single epicenter. This area is part of a region of very low seismicity which extends from the eastern edge of the Shumagin Islands to the western end of the 1964 aftershock zone and coincides exactly with the well-defined portion of the 1938 aftershock zone. This contrast in seismicity between the western and eastern parts of the Shumagin gap may indicate that these two parts are mechanically decoupled from each other along a transverse boundary which passes through the

Shumagin Islands. The Shumagin Islands focal mechanism described in the next section is consistent with this interpretation.

Shumagin Island focal mechanism

The April 6, 1974 earthquake sequence was described above. The aftershock zone for this sequence is shown in the Shumagin seismicity map (Figure 9) and the center hypocenter cross-section (Figure 11). A lower hemisphere, stereographic plot of the first motions at 35 seismic stations for the largest shock ($m_b = 6.0$) is shown in Figure 13. Compressions are given with solid symbols; dilatations with open symbols. First motions at the WWSSN long period stations are plotted as circles, those at the local L-DGO short period stations as squares, and those at the Palmer Observatory short period stations as triangles. There are only two exceptional first motions which is quite good for a plot such as this which mixes short and long period observations.

The focal mechanism implied by this plot is thrust faulting in response to nearly horizontal compression parallel to the strike of the arc. The parameters of the two possible fault planes are: (1) strike N16°W and dip 49° at S74°W or (2) strike N68°W and dip 56° at N22°E. The principal axes parameters are: P, plunge 6° at N74°E; T, plunge 61° at S36°E and; B, plunge 29° at N47°W. The above parameters are constrained by the data within limits of approximately plus or minus 10° in dip or plunge and 5° in strike.

This focal mechanism is unusual and not explainable in terms of simple subduction of the oceanic lithosphere (see e.g. Stauder, 1968). It is consistent with the idea of segmentation of the subducted slab as suggested by Stoiber and Carr (1972) for central America, VanWormer, Davies and Gedney (1974) for central Alaska, and Stauder and Mualchin (1976) for the Kurile-Kamchatka region. The idea is that there exists transverse faults in the downgoing slab which can mechanically decouple adjacent

segments allowing the independent release of tectonic stress. This segmentation is manifested by the rectilinear shape of the aftershock zones, abrupt changes in strike and dip of a Benioff zone, and by cyclic changes along an arc in the chemistry, distribution and activity of volcanos. Several of these features are present in the Shumagin Island region. The 1938 aftershock zone, the present difference in seismicity between the eastern and western portions of the gap and the offset in the trend of the deep earthquakes have been discussed above. There is a 15-20° bend in the trend line for the volcanos east and west of the Shumagin Islands. Several of the volcanoes immediately to the west are presently active; none immediately to the east are. Finally, of course, there is the transverse orientation of the fault planes shown in Figure 13. All of these observations suggest a transverse boundary in the Shumagin vicinity. The offset of the deep seismicity and location of the April 6, 1974 earthquakes relative to the Shumagin Islands (considered as a transverse topographic high) suggest that the plane dipping to the northeast is probably the actual fault plane. The plunge and strike of the B axis is identical with that of the Benioff zone which implies that in the frame of the dipping slab the fault plane is almost exactly transverse to the trend of the arc. All of the observations presented above suggest that the Pacific plate is segmented along a transverse fault which runs just to the west of the Shumagin Islands and dips under them. The geometrical constraints of thrusting two adjacent segments of a spherical cap of oceanic lithosphere down into the mantle requires compression between these slabs. This is the source of the compression shown by the horizontal P axis in Figure 13.

NEAR ISLANDS FOCAL MECHANISMS (V.F. Cormier)

On February 2, 1975 a series of shallow focus earthquakes occurred along the northern margin of the Aleutian Ridge in the Near Islands region (Figure 14). The U.S. Geological Survey assigned to the mainshock a surface wave magnitude of 7.6 and a body wave magnitude of 6.1. Shemya Island sustained extensive damage from the mainshock, consistent with a maximum modified Mercalli intensity IX, with extensive cracking and fissuring to runways and roads, ground slumping, and sand-fountaining (Person, 1975).

Focal mechanism solutions were determined for the mainshock and a foreshock with body wave magnitude 5.9 (GS) using P wave first motions and S wave polarizations (Figure 15). For both earthquakes one nodal plane strikes $N49^{\circ}E$ and dips $74^{\circ}SE$; the other nodal plane strikes $N44^{\circ}E$ and dips $74^{\circ}NW$. The large strike-slip component of the focal solutions is similar to that of focal solutions of shallow focus earthquakes occurring along the northern margin of the Aleutian Ridge to the west in the Commander Islands (Cormier, 1975). The locations and focal solutions therefore suggest that the tectonic regime observed along the Commander Islands must extend as far as $174.5^{\circ}E$.

If the NE striking nodal planes are chosen as the fault planes, the fault motion is largely left-lateral strike-slip with a small component of vertical motion such that the western side of the Aleutian Ridge is uplifted relative to the eastern. If the NW striking nodal planes are chosen as the fault plane, the motion is largely right-lateral strike-slip with a small component of vertical motion such that the Aleutian Ridge is uplifted relative to the Bowers Basin. The slip vector resulting from this latter choice parallels the

local trend of the Aleutian Ridge and is consistent with relative motion between the Pacific and North American plates in the Near Islands. The apparent ESE extension of the aftershock zone along the northern margin of the Aleutian Ridge (Figure 14) and the trend of recent faults on Attu Island (Gates et al., 1971) are also consistent with this choice.

Strong Motion Data. The Kinematics SMA-1 accelerometer of Sand Point has been triggered by earthquakes 3 times since it was installed in September, 1971. The Dutch Harbor instrument has yet to be triggered by an earthquake. Copies of the 3 Sand Point records are shown in Figures 16, 17 and 18. The upper trace on each record gives time marks at half second intervals. The next three traces labeled L, V and T record the longitudinal, vertical and transverse components, respectively. The SMA-1 is oriented such that up on the record corresponds to up on the vertical component, N30°E on the transverse component at N120°E on the longitudinal component. The earthquake parameters, maximum acceleration and distance to the hypocenter which correspond to each record are given in the respective figure captions.

The identification of the specific earthquakes recorded is based on inference since there is not absolute time on the records. The records shown in Figures 16 and 17 were first identified with the two largest events of the April 6, 1974 Shumagin Islands earthquake sequence because these were the largest events to occur in the vicinity of Sand Point in the interval between the calibrations of the instrument in the summers of 1973 and 1974. Further, if the S-minus-trigger-time is equated with the S-P time, this inferred S-P time is consistent with the hypocentral distance to within a tenth of a second. Lastly, the order of the amplitudes is consistent. The three largest events in the earthquake sequence occurred in the order: 5.7, 4.3, 6.0. Based on acceleration versus distance data from California (Page et al., 1972) and the trigger threshold of the Sand Point SMA-1 the 5.7 and 6.0 events would be expected to trigger the SMA-1 and the 4.3 would not. Assuming a similar failure mechanism the 5.7 event would be expected to cause slightly smaller accelerations at Sand Point than the 6.0 event. Both of the above expectations

are consistent with the observed records. All of the above observations together make a strong circumstantial case for identifying these records with the April 6 earthquakes.

The record shown in Figure 18 was written in a two week period between observations of the SMA-1 by the L-DGO field party. During this period there was one felt earthquake near Sand Point. This earthquake is assumed to have triggered the record shown in Figure 18. Unfortunately, the majority of the Shumagin Island network was not operational at this time so a good location of this event cannot be obtained. The S-P time observed at two of the local stations are consistent with the location given by the U.S.G.S. from the WWSSN data; however, there remains uncertainties in the location of as much as 50 kilometers.

These three records are the first accelerograph data available for the eastern Aleutian-Alaskan Peninsula region. In comparison to peak horizontal acceleration data for California given by Page (1972), the Alaskan data tend to show slightly higher accelerations for a given distance and magnitude. However, this is a very preliminary observation based on a comparison of three data points with a data set which shows a scatter of almost an order of magnitude and which is almost certainly not complete. Much more data is clearly required before reliable estimates of expected ground motion can be made for the eastern Aleutian-Alaska Peninsula region.

GEODETIC MEASUREMENTS

In 1972 a "dry tilt" figure and a level line were each established at Sand Point and Squaw Harbor to monitor regional tilting which might exist due to tectonic strain accumulation in the Shumagin Gap. A dry tilt figure is a small two dimensional array of benchmarks spaced approximately 100 meters apart. A level line is a linear array of benchmarks. In this case the level lines essentially consist of just two reference points about 1 kilometer apart and oriented NW-SE; perpendicular to the trend of the Aleutian arc. Changes in the relative heights of the benchmarks are measured using a Zeiss Ni-2 automatic level.

Sand Point dry tilt figure. The configuration of the Sand Point dry tilt figure is shown in Figure 19. The benchmarks are brass caps cemented into large concrete blocks which were once the base for a radio communications tower built during World War II. Benchmark D is mounted in a smaller block which was noticed during the 1975 field season to be loose. All of the measurements to this bench mark should be discounted.

Reduced data from observations of the Sand Point dry tilt figure during the years 1972-1975 are given in Table 3. The column headings A-B, A-C, etc. refer to the pair of benchmarks whose relative height is given below. The order and sign convention adopted is that a positive (negative) value means the second benchmark in the pair is higher (lower) than the first. The values given in the first four rows of this table are the means of 4 to 6 independent measurements. The error limits quoted are the 1-sigma standard deviations about the means which imply a 56% confidence level. In 1975 relative heights were measured between B and C and E and D so that the closing error on loops ABC and AED could be evaluated. In both cases the closing error (e.g. sum of A-B, B-C and C-A) was less than the 1-sigma standard deviation associated with the sum. This gives confidence that significant systematic errors are not

present and that the error limits given are reasonable.

The lower 3 lines of the table summarize a calculation of the tilt rate(s) implied by the data presented in the first 4 rows. The line labeled "75-72" gives the difference between the 1975 and the 1972 relative heights. This change in relative height is divided by the distance between the benchmarks, given in the next row, and by 3 years to obtain the tilt rate expressed in microradians per year in the last row.

These tilt rates are large, have large errors associated with them, and are inconsistent with simple planar tilting. The long term (tens of years) average regional tilt rates observed in Japan (Fitch and Scholz, 1971; Shimazaki, 1974) were on the order of 0.5 microradian per year. The rates observed here are 1-2 orders of magnitude larger. The resolution of the present measurements at the 98% confidence level ($3 \times \sigma$) implied by the errors associated with these rates is about 5.0 microradians per year. This means a minimum of ten years measurements would be required before tilt rates similar to those in Japan could be observed. Of course, the much larger tilts of 50-500 microradians which might accompany a major earthquake (Plafker, 1972) would be easily resolvable.

That the "tilts" here presented are inconsistent with a simple planar model can easily be seen by considering the values for the benchmark pairs A-C and A-E. Since the three benchmarks E, A and C roughly lie on a north-south line (Figure 19) the tilt rates observed for planar regional tilting at A-E should be equal and of opposite sign to that observed for A-C. The values observed are of opposite sign, but the magnitude of A-E is significantly three times greater than at A-C. Further, if the relative heights for a given benchmark pair are plotted against time it is found that the changes from year to year do not progress in any systematic way. Therefore these changes and the implied "tilts" cannot be ascribed to simple regional tilting and are probably

due to quasi-random individual motions of the benchmarks caused, perhaps, by frost heaving. This suggestion is consistent with the observation that the two very large changes in relative height (A-D; A-E) are upward, assuming that the three benchmarks with little or no significant relative motion (A, B, C) are fixed.

Squaw Harbor dry tilt figure. The Squaw Harbor dry tilt figure consists of a triangular array of three benchmarks cemented into bedrock outcrops. Reduced data and a tilt-rate calculation for this figure are given in Table 4. The format is the same as specified for Table 3. Data are only given for 1972 and 1975 because no measurements were made in 1973 and 1974. Independent measurement of the pair B-C was made in 1975 to evaluate the closing error as described above for Sand Point. In this case the closing error is slightly larger than the 2-sigma error limits; small enough to assure that the error limits given are reasonable. Because of the large error associated with the C-A value for 1972, a tilt rate is only computed for the benchmark pair A-B. This rate, 1.8 ± 0.7 microradians, is contained within the 98% confidence level error limits ($3 \times \text{sigma}$) and is therefore not significantly different from zero. Notice that the error limits in this case are half those given for the Sand Point rates. This may be due to the intermediate distance between the benchmarks or to good weather conditions. In any case, this indicates that it might be possible to obtain better resolution using the dry tilt technique than was indicated by the Sand Point data.

Level line data for Sand Point and Squaw Harbor. In 1972 and 1975 both the Sand Point and Squaw Harbor level lines were measured. Both lines were run twice so that the closing errors could be evaluated. For both lines the closing error was less than the sum of the 3-sigma error limits associated with each measurement; that is, within the 98% confidence limits the two measurements of each line were identical. Therefore, in Table 5 the means of these measurements are presented for each line for each year. The column headings C-S and

B-K refer to the benchmarks at the northwest and southeast ends, respectively, for each of the lines. Benchmark C is also part of the dry tilt figure at Sand Point. It is one of the three which showed the least relative motion within the dry tilt figure. Benchmark S is an isolated brass cap cemented into a fractured bedrock outcrop, hence its stability cannot be evaluated. The Squaw Harbor level line has a pair of benchmarks at each end. From 1972 to 1975 the change in relative height for both pairs was less than 0.1 millimeter with 1-sigma error limits of about 0.1 millimeters. This lack of significant relative motion supports confidence in the stability of the benchmarks. The last three rows of the table give a calculation of the tilt rate implied by the level line data. In both cases the rate computed is less than the 2-sigma error limits and is therefore not significantly different from zero.

With the exception of some of the Sand Point dry tilt figure observations, all of the leveling measurements reveal no significant change between the 1972 and 1975. It was shown that the relative motion which was observed at Sand Point was probably not due to regional tilting. These measurements imply that if regional tilting is occurring, it is proceeding at less than 1.9 microradians per year. The newly installed tide gauges (MSLI's) should improve our resolution by 1-2 orders of magnitude. It would then be possible to observe in a years time regional tilting similar to that seen in Japan.

Seismic Monitoring of Pavlof Volcano (J. Keinle)

Pavlof is a stratovolcano near the tip of the Alaska Peninsula which erupts frequently. It is one of the more active -- if not the most active -- Aleutian volcano. Because of the high probability of observing an eruption the University of Alaska included the volcano as a site in its general program to study forerunning phenomena to eruptions, specifically seismic fore-runners. A University of Alaska Helicorder was therefore installed at the recording side of the L-DGO regional network which is designed to study the seismotectonics of the Aleutian arc in the Shumagin Island region (this contract). This Helicorder for the volcano station was purchased under NSF grant GA 40753. In general Lamont-Doherty Geological Observatory personnel maintains the station while University of Alaska personnel have participated substantially in the initial effort to install the Shumagin array.

The Pavlof station is located about 7 kilometers southeast of the summit of the volcano and went into operation on October 15, 1973. Unfortunately the station has only functioned for 65% of its lifetime. The failures were partly due to vandalism and bear problems and partly due to electronic failure. On the other hand we have been able to observe in two years of operation two Strombolian eruption cycles, one in November, 1973 -- one month after we turned the station on -- and one which began on September 13, 1975, and is continuing at this writing. Unfortunately, Murphy's law holds and the station failed promptly on October 20, 1975.

1973 eruption: Contrary to what we anticipated based on observations on other instrumented volcanoes in Kamchatka, Japan and Hawaii where seismic forerunners to eruptions are common, the November 13, 1973 Pavlof eruption began quite unexpectedly with the onset of continuous harmonic tremor at about 03 GMT. The tremor amplitude built from noise level to about 19 mm peak to peak in 11 hours (Figure 20) and then remained constant until 10 hours later the tremor suddenly stopped. Visual observations suggest that the tremor was associated with lava fountaining up to a height of some 100 meters at the summit. The fountain was clearly visible against the background of dense black clouds of ash which were emitted almost continuously during this period. Fourier power spectra of the tremor showed a characteristic frequency of 1.8 Hz with satellite peaks at 1.3, 2.0 and 2.3 Hz.

No marked increase in microearthquake activity signalled the eruption in 1973 and also the current eruption, which began just as suddenly on September 13, 1975. Seismic events for the month prior to the November 13, 1973 eruption occurred at a constant daily rate of 44 ± 10 and were all of remarkably similar magnitude. There were two more active days with 107 events registered on November 8, 1973 and 65 on November 11, 1973. Very puzzling, however, was the very intense microearthquake activity following the eruption with more than 1000 events per day registered during the first three days, declining exponentially to 543 events per day on November 19, 171 by November 21, 56 by November 24, 3 by November 28 and 1 by November 30, a rate admittedly well below the level prior to the eruption. Perhaps a larger record prior to the eruption would have shown a gradual building to the average rate of a few tens of events per day.

It is not clear at this point with only one station to work with where the microearthquakes occurred or whether indeed the seismic events were earthquakes, i.e. events caused by brittle fracture. There is also a

question of whether the seismic wave trains represent largely surface waves or body waves, dispersion, however, is visually not obvious. The nearly identical wave trains of these events and their monochromatic nature (Figure 21) suggest (1) a common source region and (2) a harmonic source function (e.g. a vibrating magma column) or very efficient filtering of body waves from brittle fracture events in the pyroclastic mantling layers of the volcano. Events of similar appearance were recorded following individual bursts of tremor associated with the current eruption cycle. Some of these events had a strong late high frequency phase which is clearly the signature of an air blast sweeping over the seismometer, i.e. these events represent summit explosions. Some of these are so strong that fishing boats 10 to 15 kilometers away in Pavlof Bay have reported being rocked by them. Peculiar, however, is the fact that we have not observed a single late high frequency phase amongst the thousands of events following the November 1973 eruption suggesting that they might represent true brittle fracture events or vibrations associated with fast and "noisy" magma withdrawal. By implication then magma intrusion prior to the eruption seems to have been a quiet - in terms of seismicity - and possibly very slow process. An attempt to shed some light on these problems was made in early November when we tried to place two portable tape recording stations near the eruption site in an effort to try to distinguish whether filtering or source effects are shaping the characteristic low frequency wave trains. We failed to even get near the mountain because of extreme and adverse weather and storm conditions.

Without additional stations on the flanks of Pavlof we will obviously not be able to understand the details of wave propagation in a composite volcano such as Pavlof but the one station alone clearly provided much data relating to the problem of seismicity related to eruptive activity.

CONCLUSION

The national energy situation has led to two expansions in the scope of our seismotectonic research program. Additional support under the present contract will allow a seismic investigation of the geothermal potential of Pavlof Volcano during the next field season. A new research contract with the National Oceanic and Atmospheric Administration provides additional logistic and manpower support to expedite the seismic and volcanic hazards evaluation to aid in a Bureau of Land Management analysis of the environmental impact of oil exploration on the outer continental shelves of Alaska.

During the past field season we have carried out a major reorganization of the short period network which included expansions of the recording centers at Sand Point, Dutch Harbor and Saint Paul. This reorganization, in part required by changes in the White Alice Communications System, is designed to reduce telemetry costs and stream-line the data reduction. We have also increased our geodetic study of possible tectonic strain accumulation in the Shumagin gap with the addition of a pair of strain meters at Sand Point designed to measure tidal admittance evidence of dilation and two remote tide gauges to monitor changes in land elevation with respect to mean sealevel.

In this report we have presented (1) historic seismicity maps of the Shumagin seismic gap vicinity which show the relatively low level of seismic activity in the gap, a possible offset in the Benioff zone, and a few events associated with the Bering shelf continental margin south of the Pribilof Islands; (2) a seismicity map and hypocenter cross-sections based on data from the local Shumagin Islands seismic network which show a very well developed Benioff zone beneath the Shumagin Islands; (3) studies of the focal mechanisms of the April 6, 1974 Shumagin Islands earthquake and the February 2, 1975 Near Islands earthquakes which respectively show thrust faulting perpendicular

to the arc and right-lateral strike-slip faulting oblique to the arc along the slip direction inferred from the relative motion of the plates; (4) the first strong motion accelerograph data from the eastern Aleutians, which show accelerations consistent with those observed for earthquakes in California; (5) this year's geodetic leveling results which when compared with those from 1972 indicate that regional tilting due to tectonic strain accumulation, if it is occurring, is less than 1.9 microradians per year; and (6) seismic observations of two Strombolian eruptive cycles of Pavlof Volcano which reveal monochromatic wave trains which are identical one to the next suggesting a common source region and a harmonic source function or very efficient filtering of the body waves by the pyroclastic layers of the volcano.

During the next year we will continue to collect and analyze data as summarized above along with evaluating the new data expected from our expanded geodetic work and the dense seismic network on Pavlof volcano. We will emphasize synthesis of this data with other geochemical, geological and geophysical data into a coherent theory for the evolution of the Aleutian arc.

PERCENTAGE OF TIME DEVOATED BY PRINCIPAL INVESTIGATORS

| | |
|--------------------|-----|
| Dr. Lynn R. Sykes | 5% |
| Dr. Klaus H. Jacob | 33% |

REFERENCES

- Beaumont, C., and J. Berger (1974). Earthquake prediction: modification of the earth tide tilts and strains by dilatancy, Geophys. Jour. Roy. astr. Soc., 39, 111-121.
- Chase, T.E., A.W. Menard and J. Mammerickx (1971). Bathymetry of the north Pacific (charts 1 and 2 of 10): La Jolla, Institute of Marine Research, California University, San Diego.
- Cormier, V.F. (1975). Tectonics near the junction of the Aleutian and Kurile-Kamchatka arcs and a mechanism for middle Tertiary magmatism in the Kamchatka Basin, Geophys. Soc. of Am. Bull., 86, 443-453.
- Filloux, J., and G. Groves (1960). A seasonal mean sea level indicator, Deep-Sea Research, 7, 52-61.
- Gates, O., H.A. Powers, R.E. Wilcox and J.P. Schater (1971). Geology of the Near Islands, Alaska, Geol. Surv. Bull., 1028-u.
- Groves, G. (1965). Observation of sea level at remote islands, Proc. of the Symp. on Tidal Instrumentation and Prediction of Tides, Paris (May), Publication-scientifique No. 27 de l'A.I.O.P., Unesco.
- Kanamori, H. and D.L. Anderson (1975). Theoretical basis of some empirical relations in seismology, Bull. Seis. Soc. Am., 65, 5, 1073-1096.
- Kelleher, John A. (1970). Space-time seismicity of the Alaska-Aleutian Seismic Zone, Jour. of Geophys. Res., 75, 29, 5745-5256.
- King, G., and R. Bilham (1976). A geophysical wire strainmeter, submitted to Bull. Seis. Soc. of Am.
- Minster, B., T. Jordan, P. Molnar and E. Haines (1974). Numerical modelling of instantaneous plate tectonic, Geophys. Jour. Roy. astr. Soc., 36, 541-576.
- Page, R.A., D.M. Boore, W.B. Joyner, and H.W. Coultner. (1972). Ground motion values for use in the seismic design of the Trans-Alaska Pipeline System, U.S. Geol. Surv., Circular No. 672.

- Person, W.I. (1975). Seismological Notes, January-February 1975, Bull. Seis. Soc. Am., 65, 5, 1517.
- Stauder, W. (1968). Tensional character of earthquake foci beneath the Aleutian trench with relation to sea-floor spreading, Jour. Geophys. Res., 73, 24, 7693-.
- Stauder, W., and L. Mualchin (1976). Fault motion in the larger earthquakes of the Kurile-Kamchatka Arc and of the Kurile-Hokkaido Corner, Jour. Geophys. Res., 81, 2, 297-308.
- Stoiber, R.E. and M.J. Carr (1972). Quaternary volcanics and tectonic segmentation of Central America, Bull. Volcanologique, 37, 3, 304-.
- Sykes, L.R. (1971). Aftershock zones of great earthquakes, seismicity gaps, earthquake prediction for Alaska and the Aleutians, Jour. Geophys. Res., 76, 36, 8021-8041.
- VanWormer, J.D., J. Davies and L. Gedney (1974). Seismicity and plate tectonics in south central Alaska, Bull. Seis. Soc. Amer., 64, 5, 1467-1475.

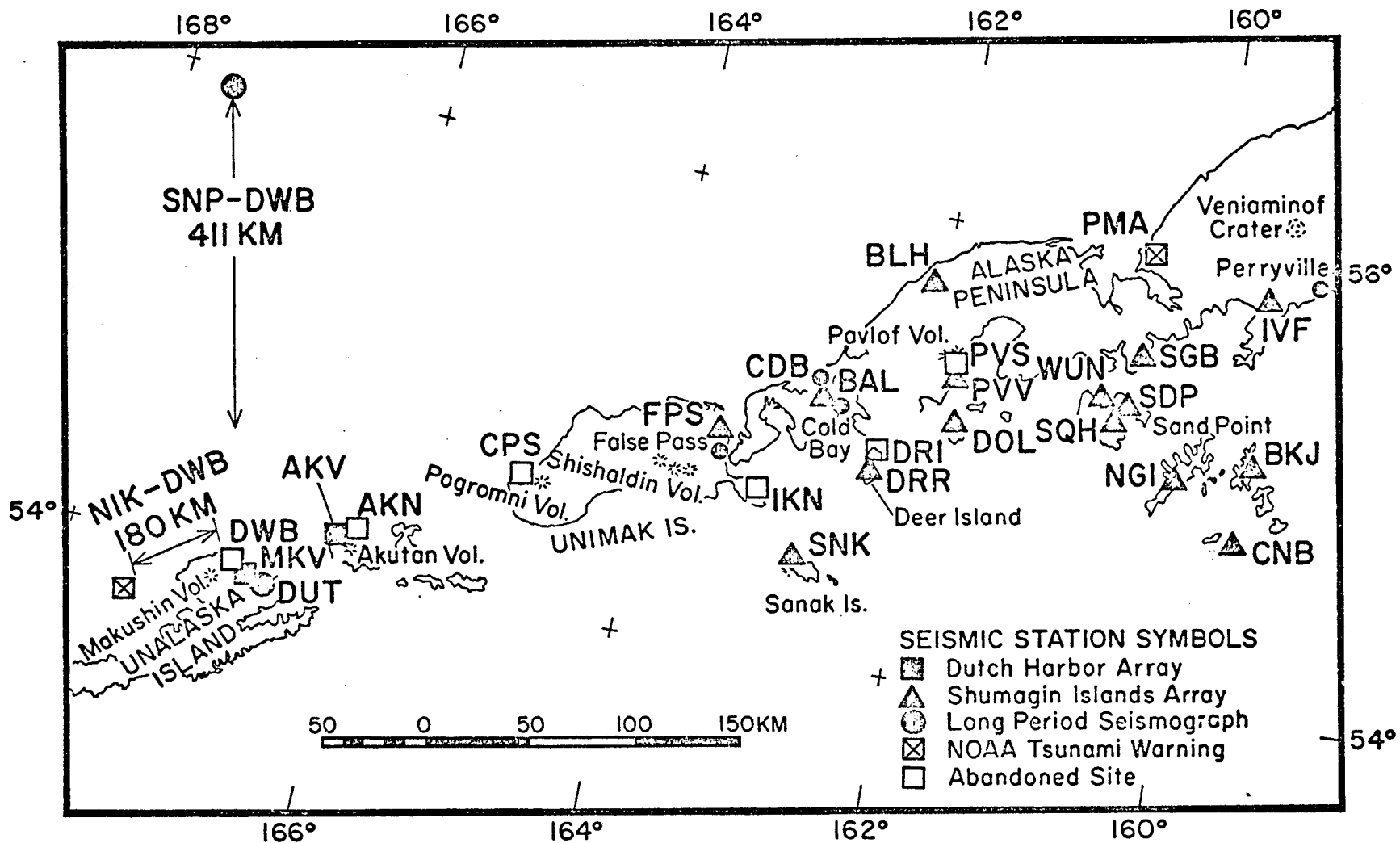


Figure 1: Eastern Aleutian Seismograph Stations. The Saint Paul station (SNP) has an SPV and an LPV seismometer. At Dutch Harbor (DUT) are recorded two remote SPV and the local SPV, SPH, and LPV seismometers. At Sand Point (SDP) are recorded 14 remote SPV and the local SPV, SPN, SPE, LPV, LPN and LPE seismometers. The NOAA stations are recorded at Palmer, Alaska.

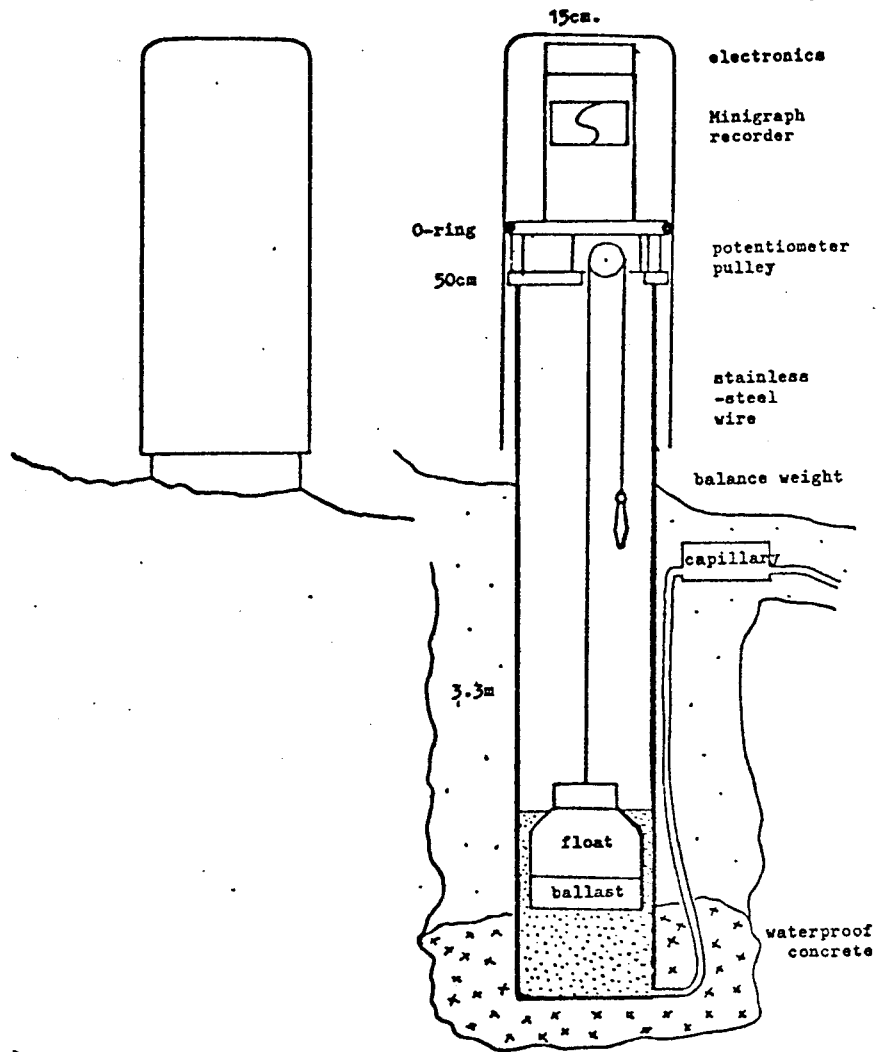


Figure 2: Mean Sea Level Indicator (MSLI) Schematic. This self contained, highly damped, remote tide gauge will operate unattended for a year. The recorder is activated (see Figure 3) once each minute. The tides themselves are used for timing and calibration is obtained when the recorder shifts from one edge of the chart paper to the other to avoid going off scale.

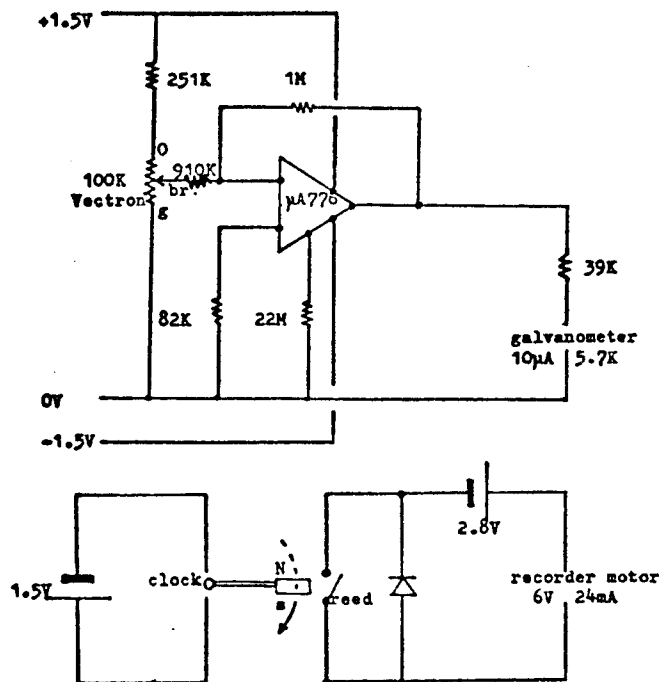


Figure 3: MSLI Recording Electronics. The Vectron, a 100 k continuous rotation potentiometer is connected by a stainless steel wire to the float (Figure 2). The Minigraph recorder is activated each minute as the magnet attached to the second hand of the clock sweeps by the reed switch. Two alkaline AAA-cells, an alkaline D-cell and a Lithium D-cell (10 AH) are sufficient to power this recording system for 18 months.

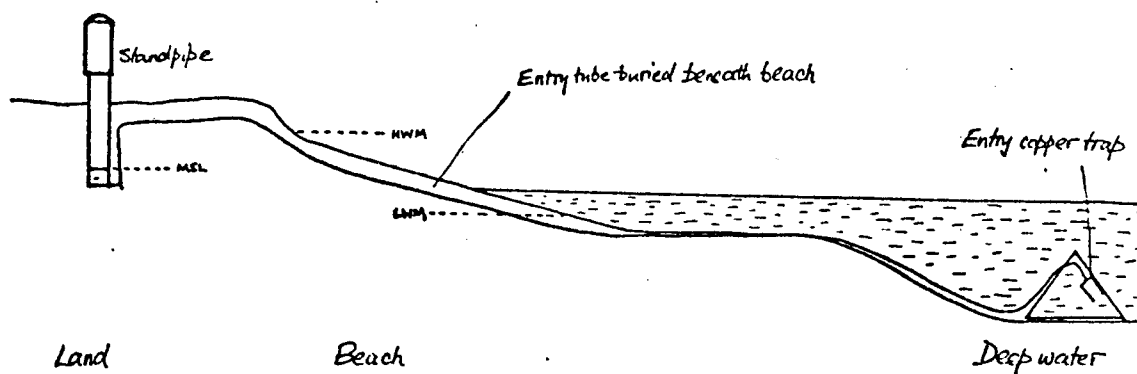


Figure 4: Syphon Arrangement of MSLI. The MSLI standpipe is located just above the highest water mark. Its base is dug in to below the lowest expected water level in the pipe. The deep water end of the syphon is anchored below the lowest expected sea level.

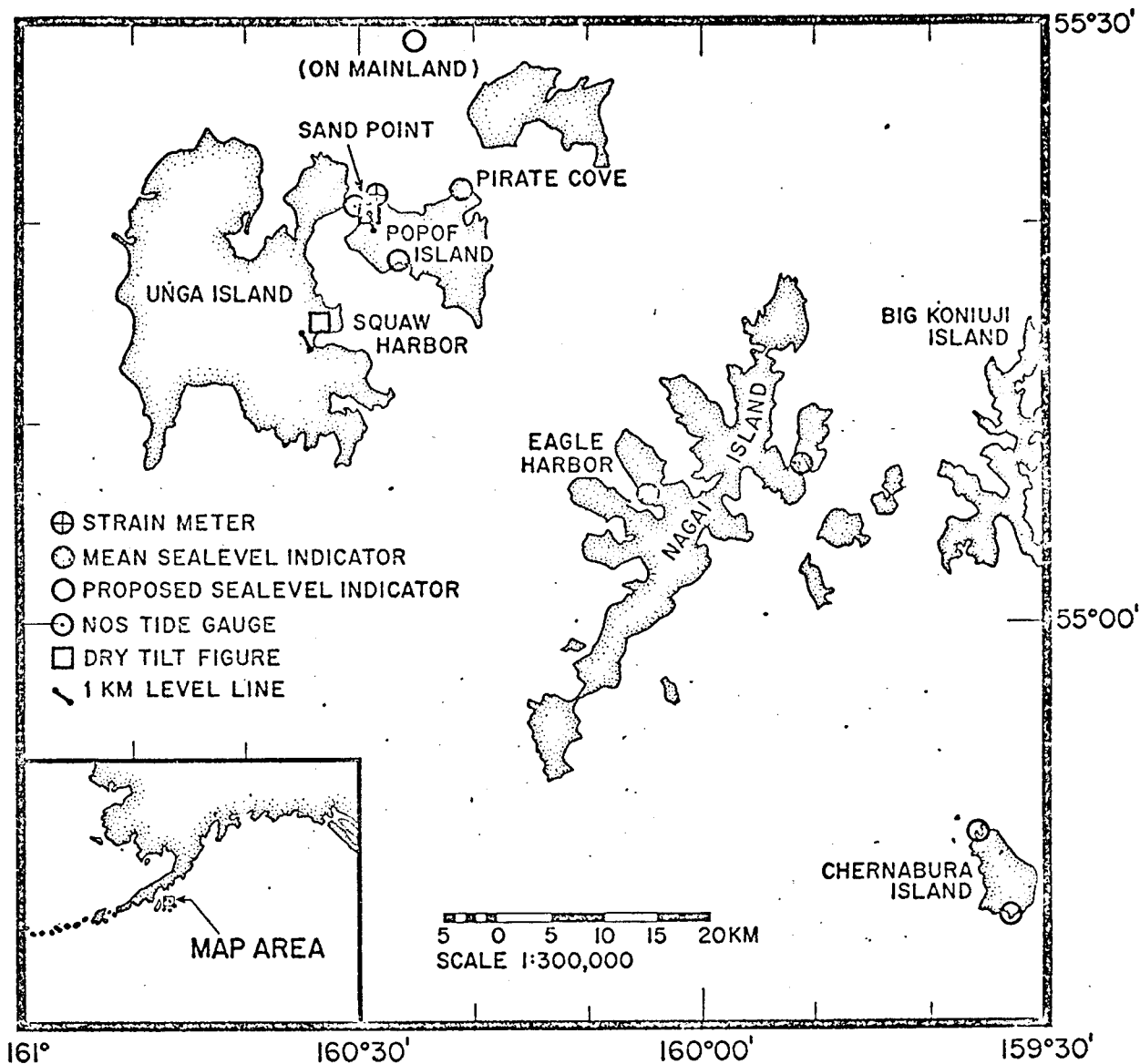


Figure 5: Geodetic Measurement Sites in the Shumagin Gap. An orthogonal pair of strainmeters at Sand Point and two MSLI's, one each at Pirate Cove and Eagle Harbor, were installed this year. Five additional MSLI's will be installed next year; one on the mainland, one each on Popof and Nagai Islands and two on Chernabura Island. Also indicated are the National Ocean Survey standard tide gauge at Sand Point and the dry tilt figures and level lines at Sand Point and Squaw Harbor.

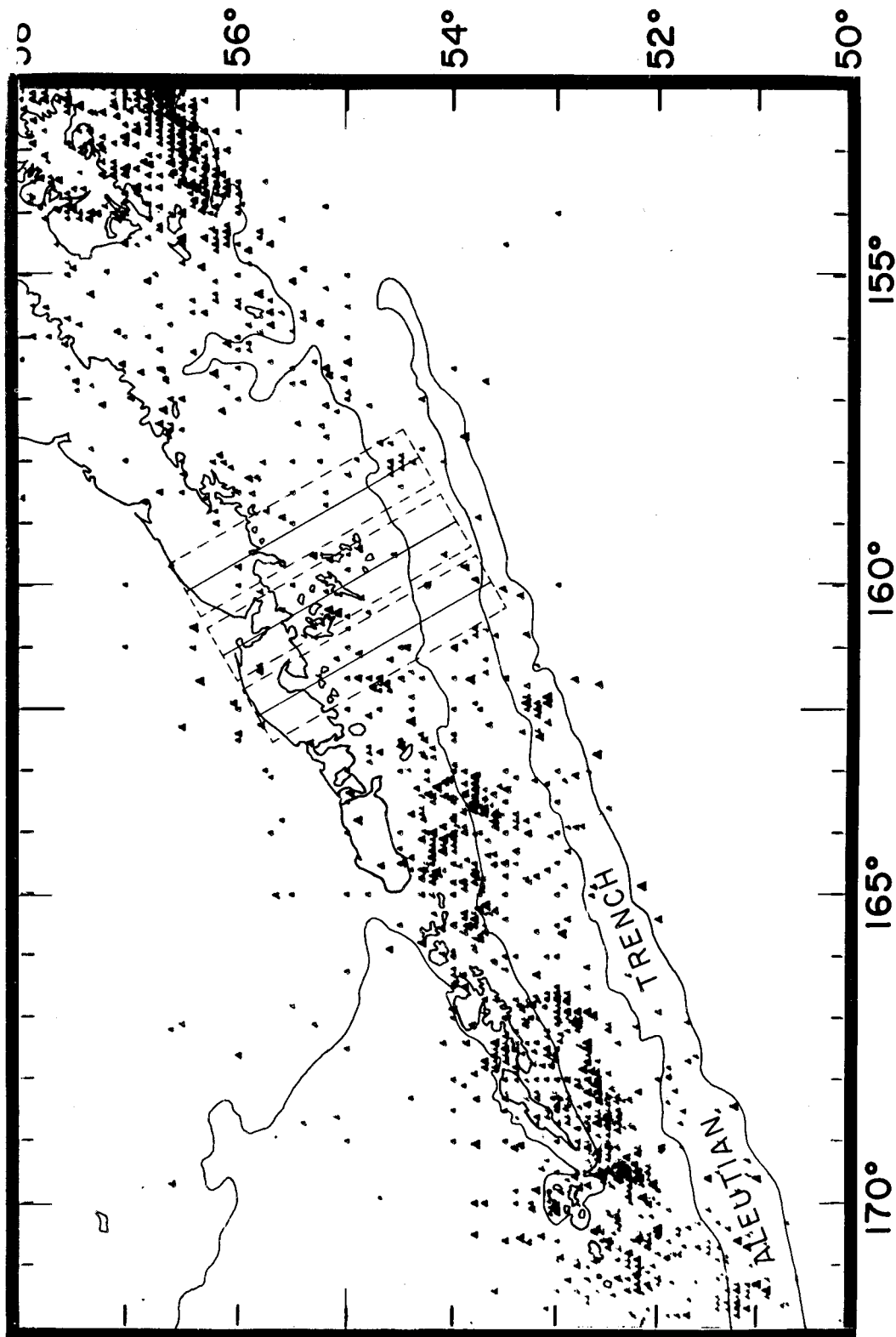


Figure 6: Historic seismicity in the Shumagin Gap Vicinity, 1902-1975. The triangles represent epicenters located from WSSN data. Black, green and red triangles correspond to hypocenter depths of 0-30, 30-60 and greater than 60 kilometers, respectively. Small medium and large triangles correspond to events with magnitudes of 0-3, 3-5, and greater than 5, respectively.

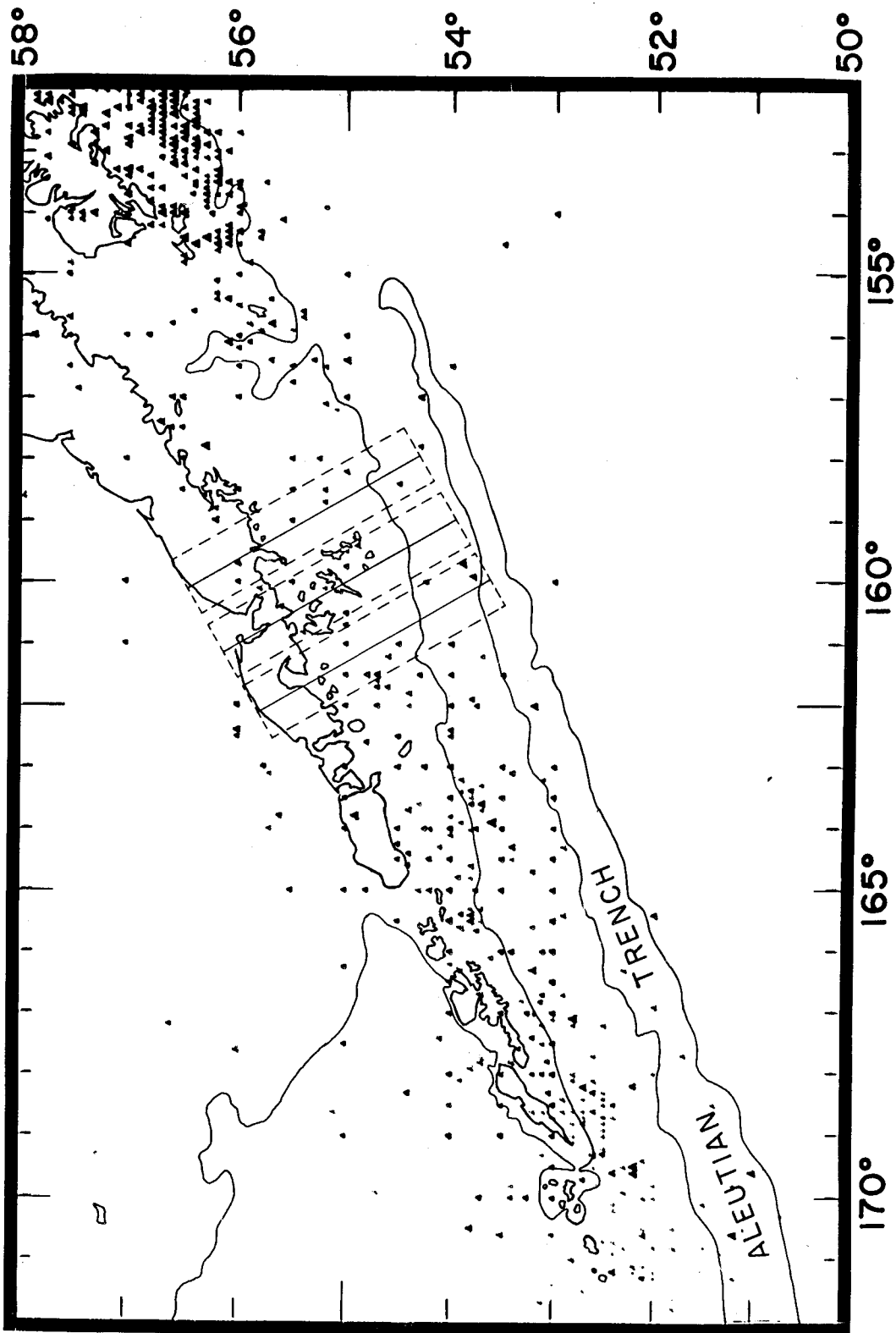


Figure 7: Historic seismicity in the Shumagin Gap Vicinity, 1902-1964. Symbols are the same as in Figure 6.

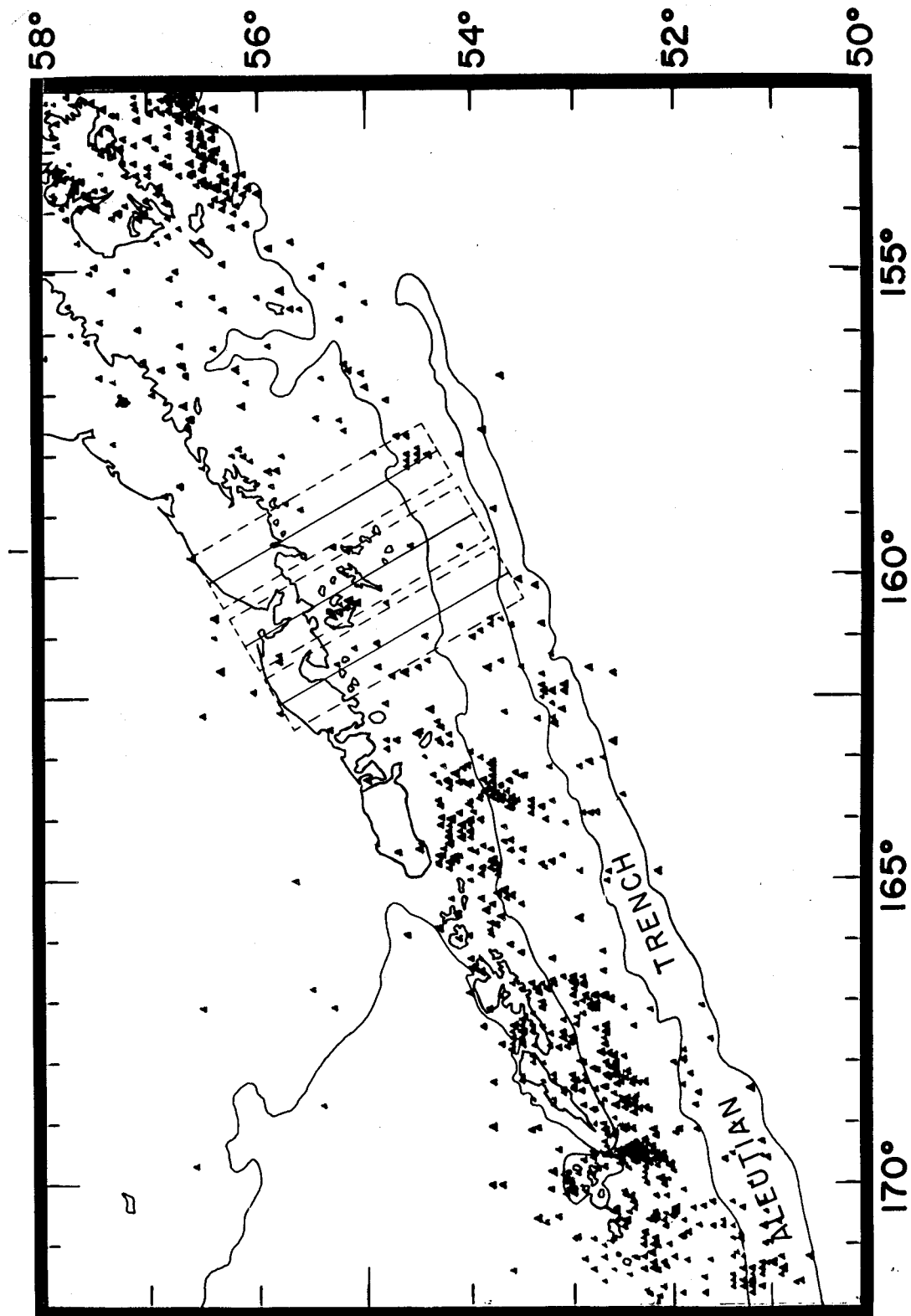


Figure 8: Historic seismicity in the Shumagin Gap Vicinity, 1965-1975. Symbols are the same as in Figure 6.

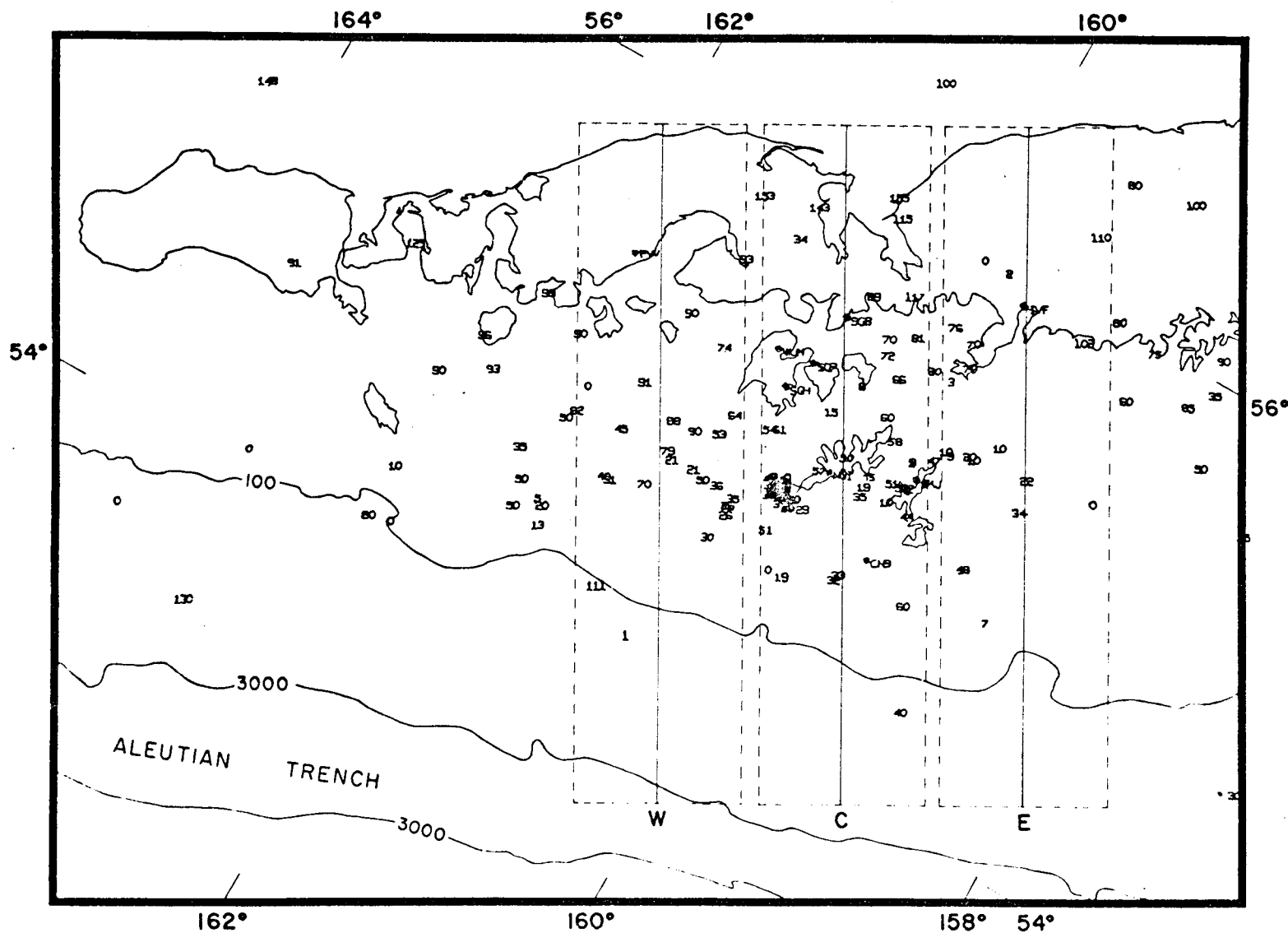


Figure 9: Shumagin Islands Seismicity, August 1973–July 1974. Epicenters located by the local L-DGO network are marked by numbers which correspond to the depth in kilometers of their respective hypocenters. Unimak Island, the southwest tip of the Alaska Peninsula and the Shumagin Islands are outlined. The 100 and 3000 fathom isobaths are shown, the latter delineates the Aleutian Trench. The dashed boxes show the location of the hypocenters shown in cross-section in Figures 10, 11 and 12.

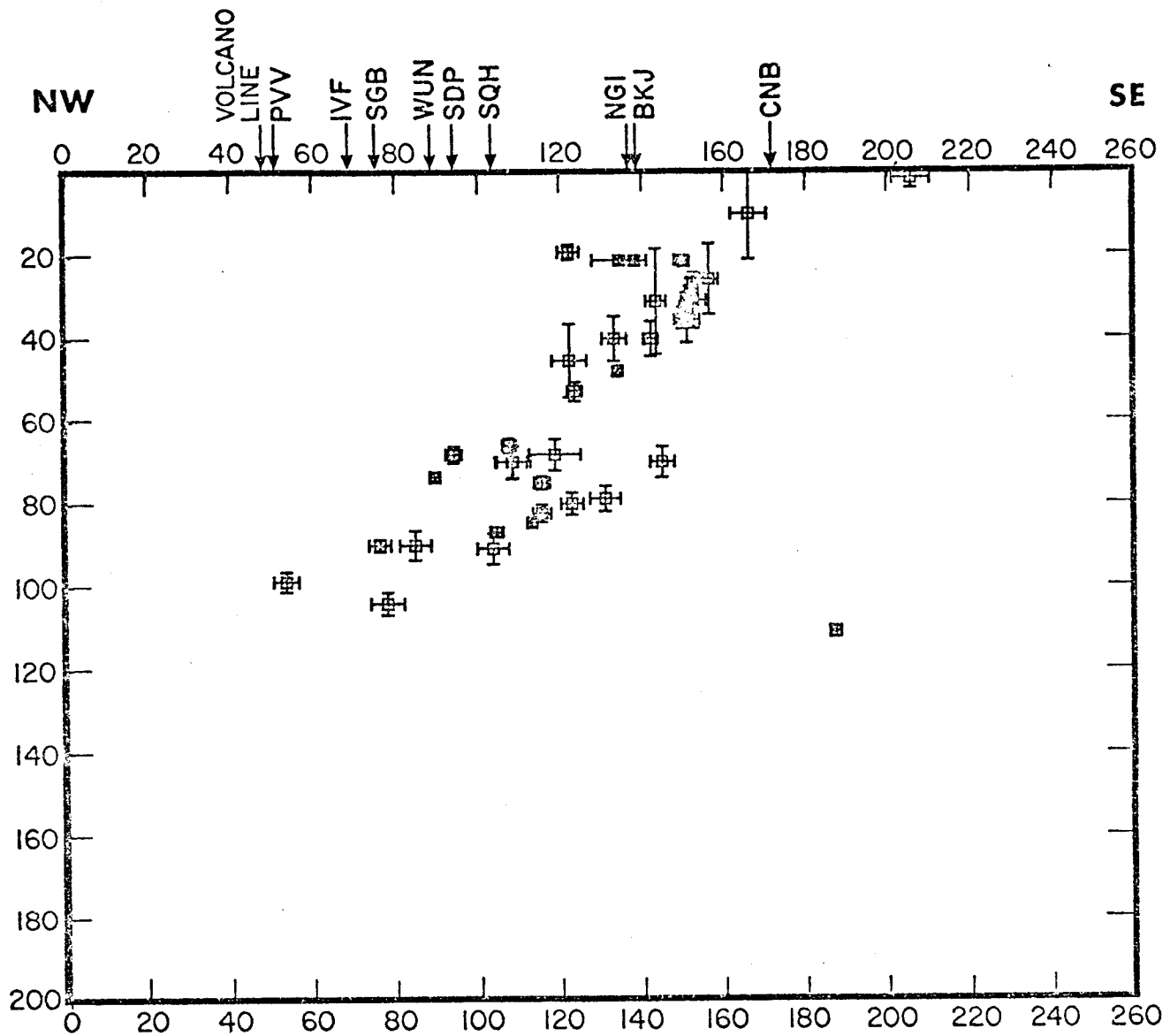


Figure 10: Western Hypocenter Cross-section. The location of this section is shown in Figure 9 by the dashed box labeled W. This view, to the northeast along the axis of the arc, shows the Benioff zone dipping to the northwest. Distances and depths are given in kilometers with no vertical exaggeration. The projected position of the volcano axis and the stations used in locating these hypocenters are shown along the top of the figure. The trench axis would plot 10 kilometers off of this figure to the southeast at 270.

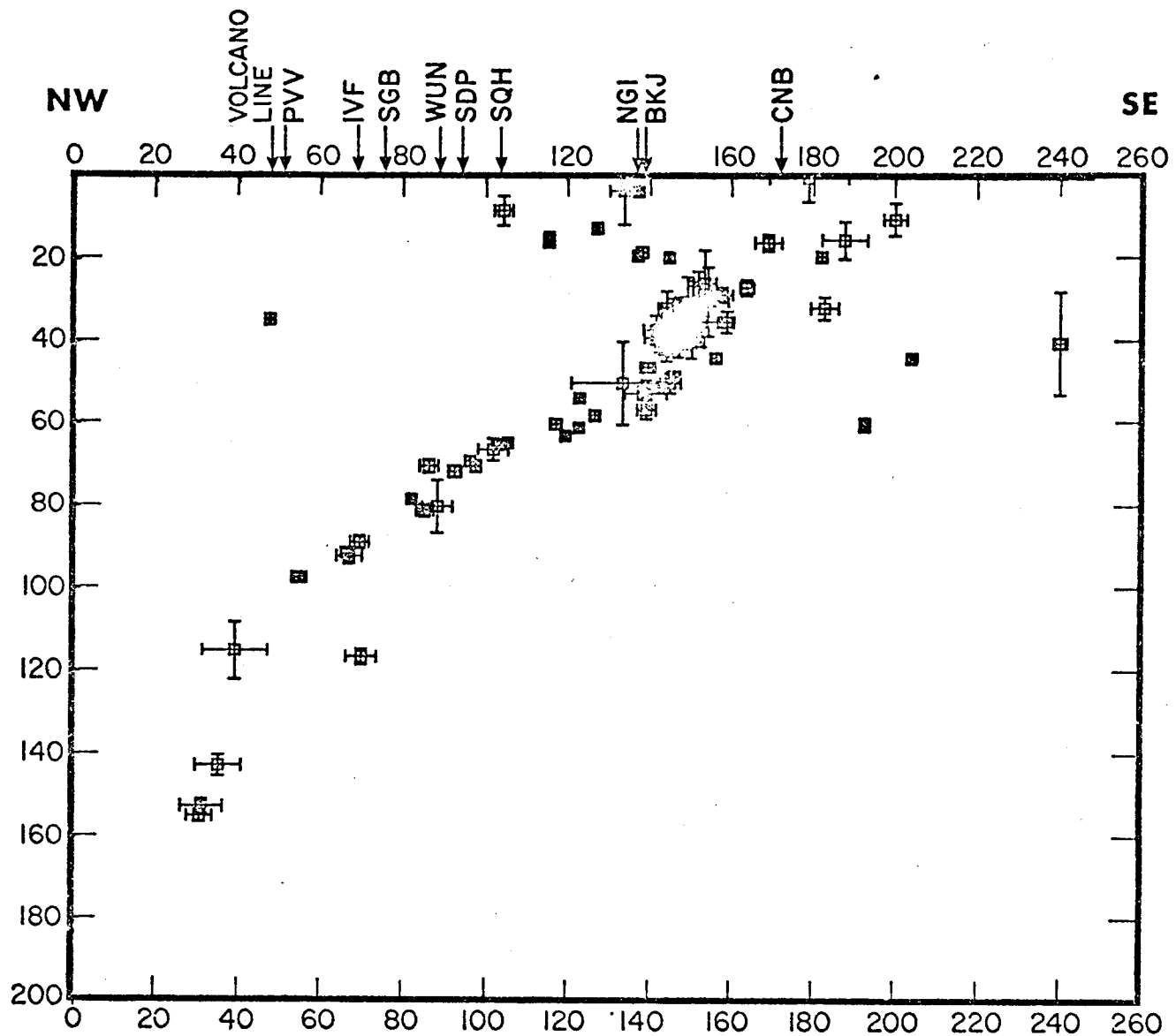


Figure 11: Central Hypocenter Cross-section. The location of this section is shown in Figure 9 by the dashed box labeled C. Other details are the same as for Figure 10, except that the trench axis would plot 25 kilometers to the southeast at 285.

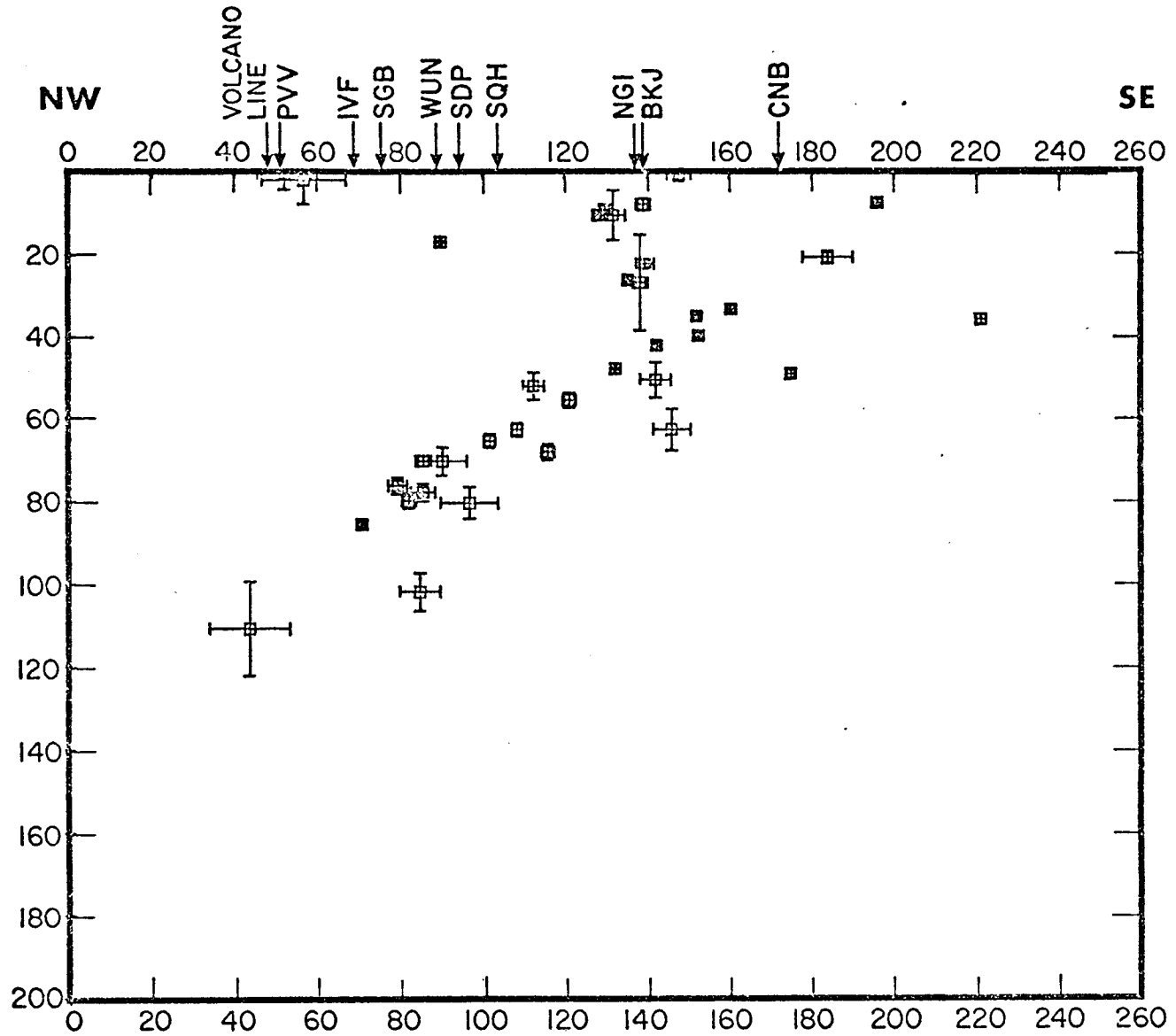


Figure 12: Eastern Hypocenter Cross-section. The location of this section is shown in Figure 9 by the dashed box labeled E. Other details are the same as for Figure 10, except that the trench axis would plot 35 kilometers to the southeast at 295.

SHUMAGIN ISLANDS APRIL 6, 1974

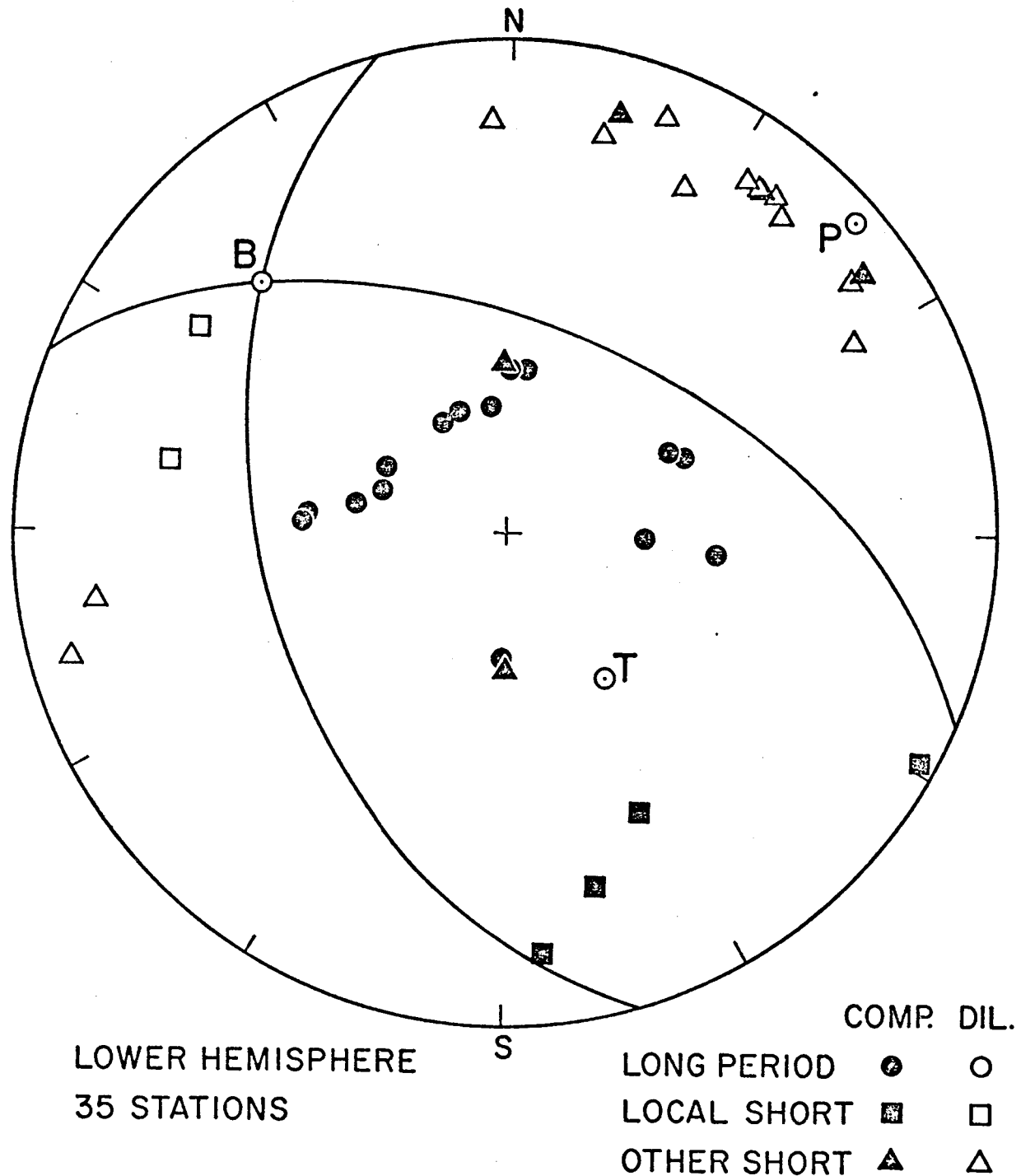


Figure 13: Fault Plane Data for the Shumagin Islands Earthquake ($m_b = 6.0$, GS) of April 6, 1974. The first motions at 35 stations are given in an equal area, lower hemisphere focal projection. The solid symbols correspond to compressive arrivals; open symbols to dilatational arrivals. The arrivals marked by circles were read from the WSSN long period records; those marked by squares from the local L-DGO short period records; and those by triangles from the Plamer Tsunami Warning Observatory records. The compression, tension and null axes are respectively labeled P, T and B.

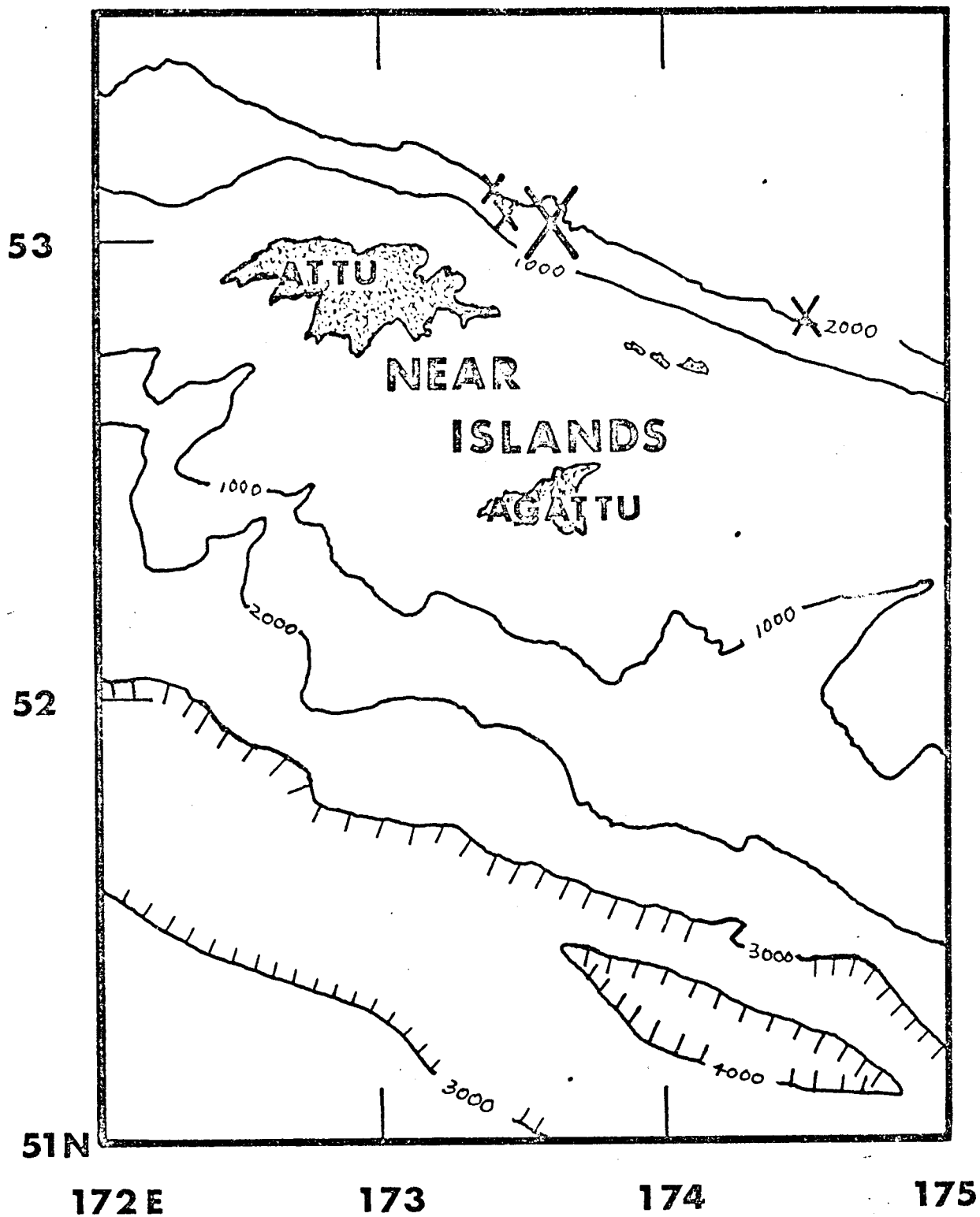


Figure 14: Mainshock (large X) and aftershocks (smaller x's) located by U.S.G.S. using 15 or more stations. Shemya Island is the eastern most of the three smaller isalnds north of Agattu. Bathymetry in fathoms is from Chase et al. (1971).

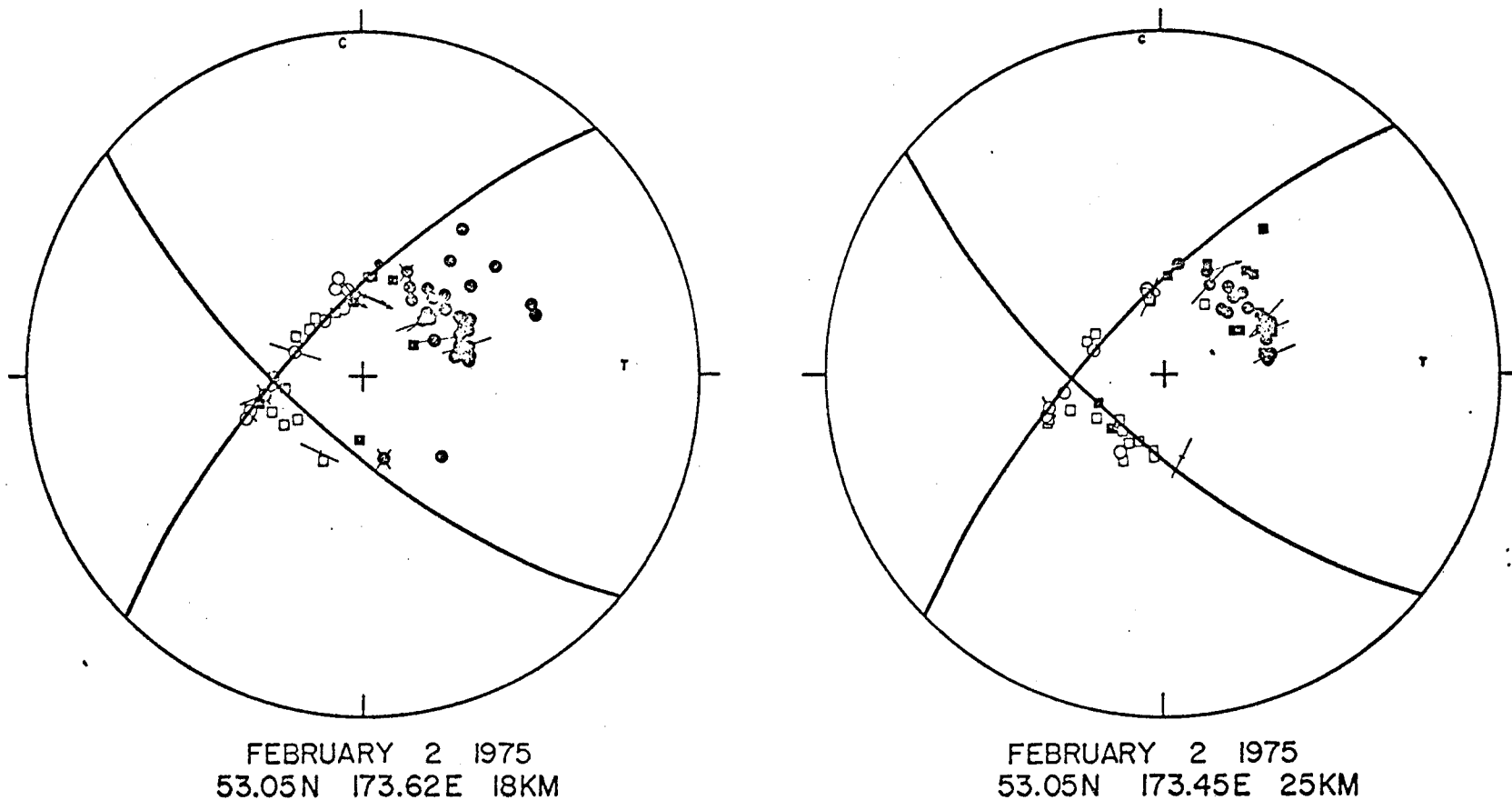
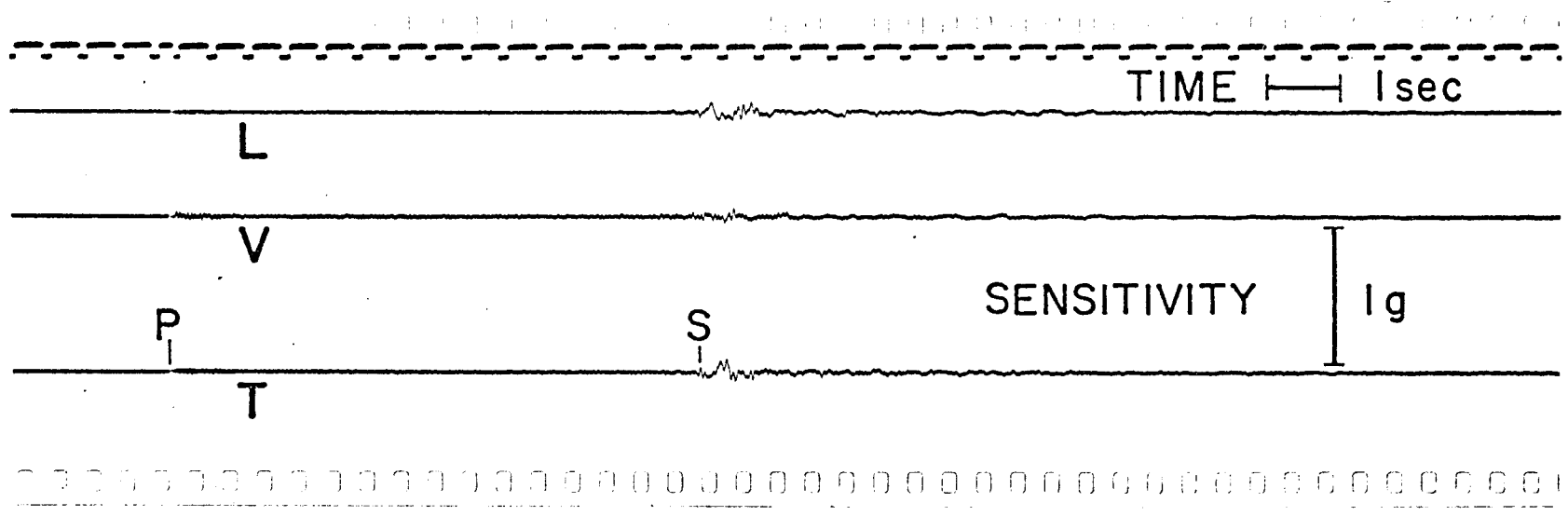
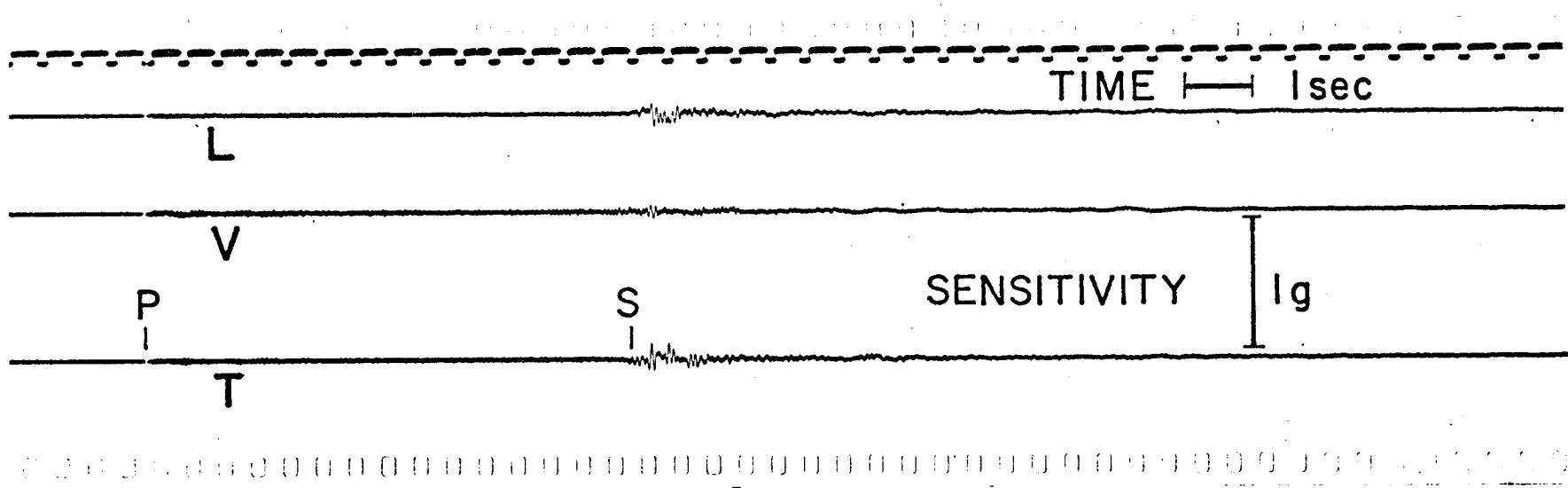


Figure 15: Fault plane solution data for the mainshock (53.05N, 173.62E, 18 km depth) and a foreshock (53.05N, 173.45E, 25 km depth). Focal projection plots are equal-area, lower hemisphere projections. Solid circle = compressional first motion read from station record. Solid square = compression reported from station bulletin. Open circle = dilatation read from station record. Open squares = dilatation reported from station bulletin. Lines drawn through these symbols indicate direction of S-wave polarization determined from horizontal component seismograms from stations from which first motion are plotted. An arrow is drawn whenever a clear impulsive onset of an S wave on both components could resolve the 180° ambiguity in polarization direction. C = position of axis of compression. T = axis of tension.



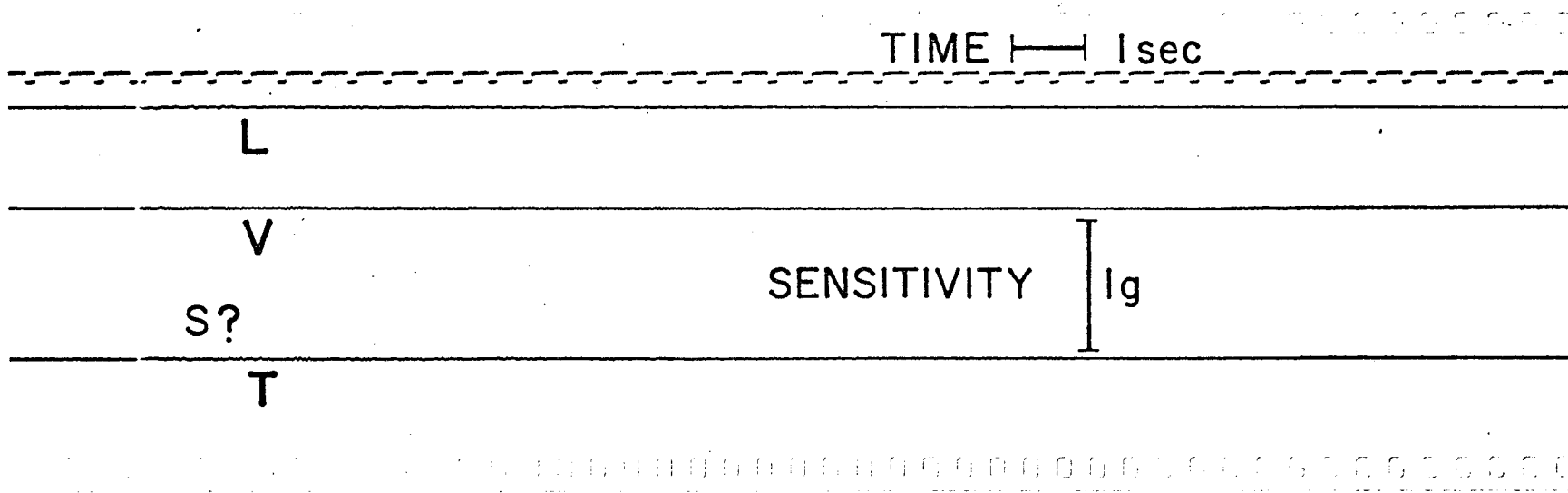
62

Figure 16: Accelerogram from Sand Point SMA-1. Record from earthquake of 0153 April 6, 1974: epicenter, 54°52.06'N and 160°17.49'W; depth, 37.km; magnitude, 5.7 m_b GS; maximum zero-to-peak horizontal acceleration, L 0.07g, T 0.09g, distance to hypocenter, 64 km. Earthquake parameters are from the L-DGO Shumagin Islands network.



63

Figure 17: Accelerogram from Sand Point SMA-1. Record from earthquake of 0356 April 6, 1974: epicenter, 54°54.33'N and 160°17.71'W' depth, 40 km; magnitude, 6.0 m_b GS; maximum zero-to-peak horizontal acceleration, L 0.10g, T 0.12g; distance to hypocenter, 65 km. Earthquake parameters are from the L-DGO Shumagin Islands network.



64

Figure 18: Accelerogram from Sand Point SMA-1. Record from earthquake of 1040 July 25, 1975: epicenter 54.9°N and 160.4°W; depth, 56 km; magnitude, 5.7 m_b GS; maximum zero-to-peak horizontal acceleration, T 0.02g; distance to hypocenter, 76 km. Earthquake parameters are from the WSSN.

SAND POINT DRY TILT FIGURE

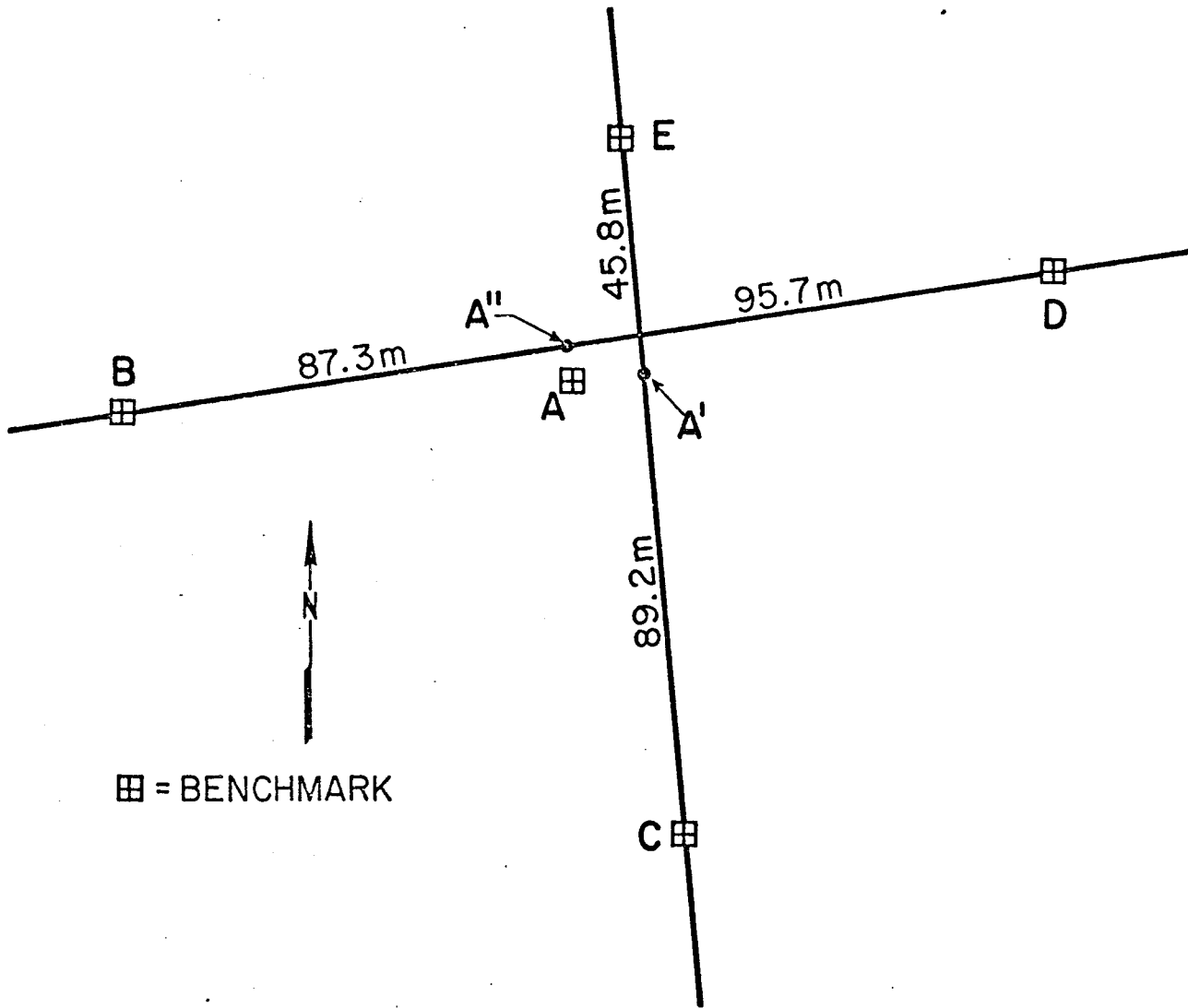


Figure 19: Sand Point Dry Tilt Figure. Benchmarks are brass caps cemented into concrete piers. Relative heights are measured with a Zeiss Ni-Z² automatic level.

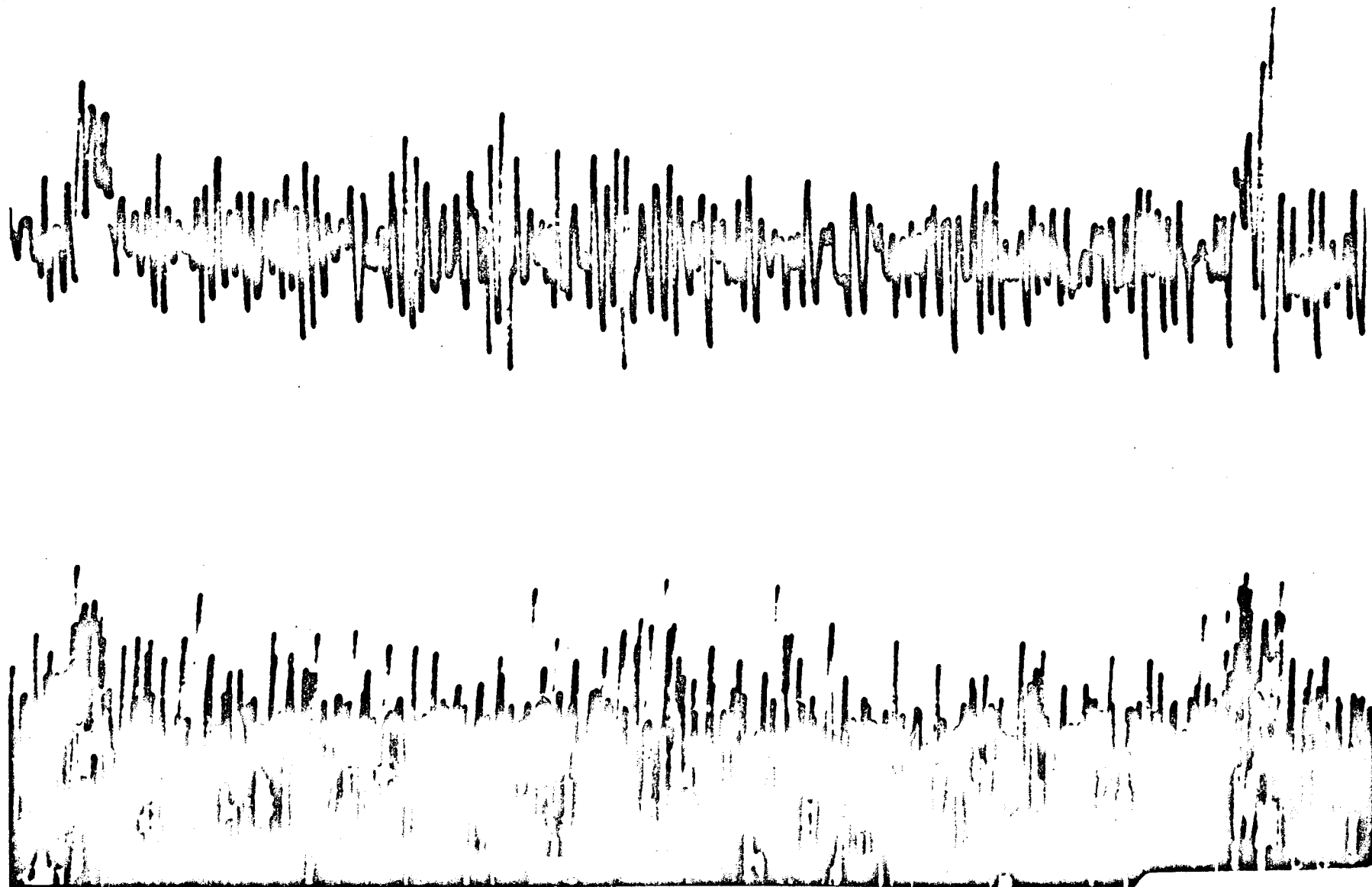
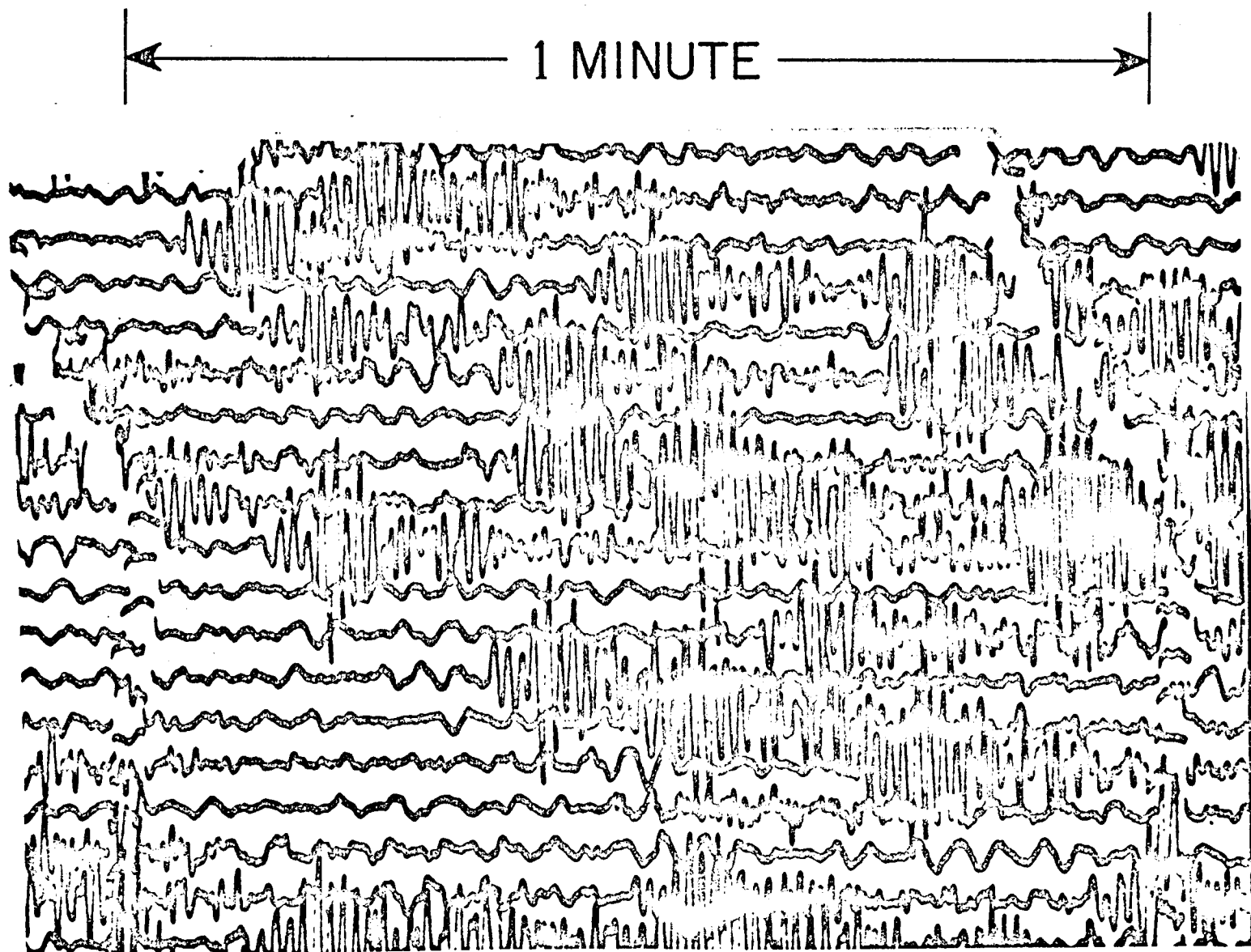


Figure 20: Helicorder record from Pavlof Volcano Station. This is a sample of the harmonic tremor which was produced during the eruption of November 13, 1973. The characteristic frequency of this tremor is 1.8 Hz.



67

Figure 21: Helicorder record from Pavlof Volcano station. This sample shows typical microearthquakes which precede and follow the eruptions. Note the nearly identical wave trains and their monochromatic nature.

TABLE I

Lamont-Doherty Aleutian Seismic Stations October 1975

| STATION | CODE | COMPONENT | N. LAT | W. LONG | ELEV. (m) | STATUS |
|--------------------|------|-----------|-----------|------------|-----------|-----------------|
| Saint Paul | SNP | SPZ | 57°9.28' | 170°13.09' | 5 | operational |
| Saint Paul | SNP | LPZ | 57°9.28' | 170°13.09' | 5 | operational |
| Dutch Harbor | DUT | SPZ | 53°53.43' | 166°32.32' | 60 | operational |
| Dutch Harbor | DUT | SPH | 53°53.43' | 166°32.32' | 60 | operational |
| Dutch Harbor | DUT | LPZ | 53°53.43' | 166°32.32' | 60 | operational |
| Makushin Valley | MKV | SPZ | 53°56.02' | 166°39.50' | 275 | operational |
| Akutan Volcano | AKV | SPZ | 54°07.82' | 166°04.02' | 240 | operational |
| Sand Point | SDP | SPZ | 55°20.48' | 160°29.82' | 30 | operational |
| Sand Point | SDP | SPN | 55°20.48' | 160°29.82' | 30 | operational |
| Sand Point | SDP | SPE | 55°20.48' | 160°29.82' | 30 | operational |
| Sand Point | SDP | LPZ | 55°20.48' | 160°29.82' | 30 | operational |
| Sand Point | SDP | LPN | 55°20.48' | 160°29.82' | 30 | operational |
| Sand Point | SDP | LPE | 55°20.48' | 160°29.82' | 30 | operational |
| San Diego Bay | SGB | SPZ | 55°32.75' | 160°27.23' | 275 | operational |
| Ivanof Bay | IVF | SPZ | 55°53.76' | 159°31.80' | 275 | operational |
| Big Koniuji Island | BKJ | SPZ | 55°09.64' | 159°33.92' | 240 | operational |
| West Unga Island | WUN | SPZ | 55°19.87' | 160°43.13' | 150 | operational |
| Pavlof Volcano | PVV | SPZ | 55°22.85' | 161°48.45' | 180 | operational |
| Squaw Harbor | SQH | SPZ | 55°12.65' | 160°34.55' | 360 | operational |
| Nagai Island | NGI | SPZ | 55°02.36' | 160°04.14' | 240 | operational |
| Chernabura Island | CNB | SPZ | 54°49.18' | 159°35.30' | 90 | NGI revr out |
| False Pass | FPS | SPZ | 54°56.70' | 163°25.86' | 120 | operational |
| Sanak Island | SNK | SPZ | 54°28.50' | 162°47.25' | 230 | operational |
| Deer Island | DRR | SPZ | 54°55.42' | 162°16.94' | 380 | operational |
| Dolgoi Island | DOL | SPZ | 55°05.80' | 161°45.50' | 275 | operational |
| Baldy Mountain | BAL | SPZ | 55°11.94' | 162°47.55' | 230 | operational |
| Black Hills | BLH | SPZ | 55°40.67' | 162°05.67' | 275 | no batt., rcvr. |

TABLE II

LAMONT-DOHERTY SEISMIC STATIONS SERVICED FROM SURVEYOR

| <u>DATE</u> | <u>STATION</u> | <u>CODE</u> | <u>TASK</u> |
|-------------|--------------------|-------------|--|
| 7-23-75 | Herendeen Bay | HNB | Installed VHF repeater station |
| 7-26-75 | Driftwood Bay | DWB | Removed White Alice seismic sta |
| | Makushin Valley | MKV | Installed seismic repeater sta. |
| 7-27-75 | Akutan Island | AKN | Removed seismic station |
| | Akutan Volcano | AKV | Installed seismic station |
| 7-28-75 | Cape Sarichef | CPS | Removed White Alice seismic sta |
| 7-29-75 | Sanak Island | SNK | Serviced seismic station |
| | Deer Island | DRI | Serviced seismic repeater sta. (incomplete) |
| | Dolgoi Island | DOL | Installed seismic station |
| 7-30-75 | San Diego Bay | SGB | Serviced seismic repeater sta. |
| 8-23-75 | Makushin Valley | MKV | Serviced seismic repeater sta. |
| 8-24-75 | Deer Island | DRI | Serviced seismic repeater sta. |
| 8-25-75 | Pavlof Sister | PVS | Removed seismic station |
| | Pavlof Volcano | PVV | Serviced seismic station |
| | Balboa Bay | BBB | Installed VHF repeater station |
| | West Unga | WUN | Serviced seismic repeater sta. |
| | Squaw Harbor | SQH | Left batteries |
| 8-26-75 | Chernabura Island | CNB | Serviced seismic station |
| | Nagai Island | NGI | Serviced seismic repeater sta. |
| | Big Koniuji Island | BKJ | Serviced seismic station |
| | Squaw Harbor | SQH | Serviced seismic repeater sta. |

TABLE 3

SAND POINT DRY TILT FIGURE

RELATIVE HEIGHT DATA FOR 1972-1975
(all values in decimeters)

| Benchmark pair | A-B | A-C | A-D* | A-E |
|----------------|------------------------|-------------------------|------------------------|------------------------|
| 1972 | - 2.383 \pm 0.003 | - 10.688 \pm 0.004 | - 1.925 \pm 0.001 | + 3.223 \pm 0.001 |
| 1973 | - 2.376 \pm 0.003 | - 10.694 \pm 0.003 | - 1.925 \pm 0.003 | + 3.239 \pm 0.001 |
| 1974 | - 2.384 \pm 0.002 | - 10.704 \pm 0.002 | - 1.794 \pm 0.002 | + 3.265 \pm 0.002 |
| 1975* | - 2.390 \pm 0.003 | - 10.704 \pm 0.001 | - 1.804 \pm 0.003 | + 3.251 \pm 0.002 |
| ----- | | | | |
| 75-72 | - 0.007 \pm 0.004 | - 0.016 \pm 0.004 | + 0.121 \pm 0.003 | + 0.028 \pm 0.002 |
| Distance | 878 \pm 10 | 899 \pm 10 | 957 \pm 10 | 478 \pm 10 |
| μ rad/yr | - 2.7 \pm 1.6 | -5.9 \pm 1.7 | + 42 \pm 1.3 | + 20 \pm 1.4 |

*Benchmark D was noticed to be loose while making the 1975 measurements.

TABLE 4

SQUAW HARBOR DRY TILT FIGURE

RELATIVE HEIGHT DATA FOR 1972 and 1975*
 (all values in decimeters)

| Benchmark pair | A-B | B-C | C-A |
|----------------|------------------------------|------------------------------|-----------------------------|
| 1972 | + 14.6009 <u>±</u> 0.0012 | | - 3.5893 <u>±</u> 0.0462 |
| 1975 | + 14.5975 <u>±</u> 0.0006 | - 11.0370 <u>±</u> 0.0012 | - 3.5641 <u>±</u> 0.0011 |
| ----- | | | |
| 75-72 | - 0.0034 <u>±</u> 0.0013 | | - 0.0252 <u>±</u> 0.0462 |
| Distance | 680 <u>±</u> 10 | | |
| μ rad/yr | -1.8 <u>±</u> 0.7 | | |

* No measurements were taken in 1973 nor 1974.

TABLE 5

LEVEL LINE DATA FOR 1972 AND 1975
(all values in decimeters)

| Benchmark pair | SAND POINT C-S | SQUAW HARBOR B-K |
|----------------|------------------------------|------------------------------|
| 1972 | + 31.0045 <u>±</u> 0.0104 | + 12.2245 <u>±</u> 0.0062 |
| 1975 | + 30.9870 <u>±</u> 0.0083 | + 12.2390 <u>±</u> 0.0044 |
| ----- | | |
| 75-72 | - 0.0175 <u>±</u> 0.0133 | + 0.0145 <u>±</u> 0.0076 |
| Length | 11,000 <u>±</u> 500 | 6,500 <u>±</u> 500 |
| μ rad/yr | - 0.53 <u>±</u> 0.40 | + 0.74 <u>±</u> 0.46 |

Appendix 1
NOAA WORK STATEMENT (Research Unit #16)

- I. TITLE: Seismotectonic analysis of the seismic and volcanic hazards in the Pribilof Islands - Eastern Aleutian Islands region of the Bering Sea.
- II. PRINCIPAL INVESTIGATOR: John Davies
Lamont-Doherty Geological Observatory
Columbia University
Palisades, New York 10964
- III. GEOGRAPHICAL AREA AND INCLUSIVE DATES:
Bering Sea: Pribilof Islands, Eastern Aleutian Arc
May 15, 1975 - June 30, 1975
July 1, 1975 - September 30, 1976

IV. COST SUMMARY:

| <u>FY 1975</u> | <u>FY 1976</u> |
|----------------|----------------|
| \$52,349 | \$71,793 |

V. PROPOSED RESEARCH:

- A. We propose a detailed seismotectonic study of the Pribilof Islands - Eastern Arc region. This study includes an analysis of the present seismicity of the region to identify active fault zones and other regions of high seismic risk, an evaluation of the deformation of the Shumagin Islands, seismic gap zone, and the seismic activity of Makushin, Akutan, and Pavlof volcanos. The primary emphasis is therefore on task D-5.

There is presently only a limited quantity of data available from a small seismic network which has been operated in the Shumagin Islands region. Other than this data there is no other data available with which to perform detailed seismicity studies in the proposed study area. It will be possible to make preliminary identifications of active zones by September 30, 1976. The amount of deformation within the Shumagin gap zone and its significance in terms of the possibility of a major earthquake may be difficult to access within this short time span; however, the effort should be begun. The present activity of Akutan, Makushin, and Pavlof volcanos will be known. These studies, with the exception of the geodetic measurements, are similar and complementary to seismic and volcanic hazards work proposed by the University of Alaska and the USGS in the Gulf of Alaska. They will be coordinated with these other studies. The marine geophysical work of the USGS may identify structures offshore which can be correlated with active faults or zones seen in the seismicity studies here proposed.

- B. We propose to reorganize and augment the present seismic network which we presently operate in this region under ERDA support. We will add a short period seismograph in the Pribilof Islands. We will relocate two stations in the Dutch Harbor vicinity so that Makushin and Akutan volcanos can be monitored. We will purchase and install telemetry equipment which will allow all of the stations in the Cold Bay - Shumagin Islands area to be recorded on a single Develocuder. The data from all of these seismic stations will be used to more precisely locate earthquake hypocenters than is possible with the World Wide Standard Seismographic Network. The data from stations located on or near volcanos will be used to determine the present level of activity of these volcanos.

We will increase the frequency and the redundancy of our geodetic leveling measurements in the Shumagin Islands region. These leveling data will allow us to begin to access the tectonic strains accumulation in the Shumagin seismic gap. This information is important because it will aid our interpretation and evaluation of the potential for a major earthquake in the gap.

VI. INFORMATION PRODUCTS:

We will produce earthquake catalogs, seismicity maps and hypocenter cross sections. These will be analyzed to identify active faults or other high seismic risk areas. We will produce seismic frequency plots for Makushin Akutan, and Pavlof volcanos. We will analyze the geodetic leveling data in terms of tectonic strain accumulation in this Shumagin seismic gap.

VII. DATA OR SAMPLE EXCHANGE INTERFACES:

The primary data required of other investigators by this study will be arrival time information in the form of phase cards from the Senedi-Kodiak network of the University of Alaska. This data exchange has been discussed and will best proceed on an informal basis. We will require the services of NGSDC to provide WWSSN film chips, perhaps Russian stations for occasional events which are large enough to allow world wide first motion study. We may also require plots of historic seismicity maps for the study region as an aid to interpretations of the detailed seismicity maps which we will produce. We may also require their plotting services for data produced by this study.

It is suggested that data inventories be provided to general data banks, rather than individual events data since it would be wasteful to include this specialized data in a general data bank.

VIII. SAMPLE ARCHIVAL REQUIREMENTS:

Lamont-Doherty will archive the original seismograms and films accrued in their seismic archive.

IX. SCHEDULE:

Seismic data will be continuously recorded. Films and seismograms will be mailed weekly from field sites to Lamont where they will be routinely read. Analysis of the data will depend upon acquisition rate, but probably will be carried out toward the end of the funding period, i.e. Fall of 1976.

X. EQUIPMENT:

See budget and logistic list.

XI. LOGISTICS REQUIREMENT:

Helicopter time (about 2 hours per day)

1. Port Moller - 2 days
2. Shumagin Islands - 5 days
3. Cold Bay - 6 days
4. Cape Senichef - 1 day
5. Dutch Harbor - 3 days

XII. COST:

See attached list.

APPENDIX II

ESTIMATES OF REPEAT TIMES FOR MAJOR AND GREAT EARTHQUAKES IN THE SHUMAGIN SEISMIC GAP

On maps of worldwide seismicity an obvious and striking feature in the Aleutian region is the relative lack of events in the vicinity of the Shumagin Islands. This 600 kilometer long region of relatively sparse activity between Sanak Island (longitude 162.5°W) and Kodiak Island (longitude 154.5°W) is here referred to as the Shumagin seismic gap. This gap is bounded on the west by the aftershock zone of the March 9, 1957 Andreanof-Fox Islands earthquake ($m = 8.2$) and on the east by the aftershock zone of the March 28, 1964 Prince William Sound earthquake ($m = 8.5$).

Following Kelleher (1970) and Sykes (1971) the use of the term "gap" implies that this is a region in which no great earthquake has recently occurred and hence is accumulating strain which is likely to be released in the not too distant future by a great earthquake or a series of major earthquakes or both. The possibility that the lack of activity used to define the Shumagin gap is due to aseismic creep cannot be dismissed but is unlikely since this region did produce a great earthquake in 1938 ($m = 8.7$).

In the following paragraphs we will consider four methods for calculating occurrence rates for large earthquakes in the Aleutian arc. We will then normalize these rates in terms of repeat times for events of magnitude 7 and larger and 7.8 and larger, respectively, in the Shumagin gap.

Occurrence rates. Sykes (1971) has compiled a summary of the available data for all shallow earthquakes of magnitude greater than or equal to seven which have occurred in the Aleutian arc for the period 1920-1970, and greater than or equal to 7.8 for 1900-1970. Data for this and the following section are taken from Sykes' compilation. The simplest estimate of repeat times is to count the number of events larger than or equal to a given threshold

value which have occurred within the Shumagin gap and divide the period of time for which the count was made by the number of large events. In the Shumagin gap six events with $m \geq 7$ occurred between 1920 and 1970 which implies a repeat time of eight years. Similarly 2 events with $m \geq 7.8$ occurred between 1900 and 1970 which implies a 35 year repeat time for this magnitude threshold. These estimates are obviously based on very few data. We can utilize a larger data set and indirectly estimate these times if we assume that the occurrence rate is the same for all regions of the Aleutian arc and count the number of events which have occurred in the whole arc and prorate this number to the Shumagin gap by multiplying by the ratio of the length of the gap to the length of the arc. Then the repeat time for events with magnitude larger than or equal to seven for the Shumagin gap can be estimated as follows:

$$T_r(m \geq 7) = T_s / N_g(m \geq 7)$$

where

T_r is the repeat time for the gap

T_s is the sample time for the arc data set

N_g is the prorated number of events for the gap

with

$$N_g(m \geq 7) = N_g(m \geq 7) \frac{L_g}{L_a}$$

where

N_g is the number of events counted for the arc

L_g is the length of the gap

L_a is the length of the arc

For the available record in the Aleutian arc we find:

$$N_g(m \geq 7) = 22 \times \frac{600}{3600} = 3.67$$

and

$$T_r(m \geq 7) = 50 \div 3.67 = 14 \text{ years}$$

Similarly we can calculate:

$$N_g(m \geq 7.9) = 7 \times \frac{600}{3600} = 1.17$$

and

$$T_r(m \geq 7.9) = 70/1.17 = 60 \text{ years}$$

We can guess at the error limits for the latter estimate by making extreme value calculations. We will assume that $N_a(m \geq 7.9) = 7 \pm 1$ and $L_g = 300$ to 1200 , which are the observed limits of the length of Aleutian aftershock zones for earthquakes with $m \geq 7.9$. Then the

$$\text{minimum } N_g(M \geq 7.9) = 6 \times \frac{300}{3600} = 0.50, \text{ and the}$$

$$\text{maximum } N_g(m \geq 7.9) = 8 \times \frac{1200}{3600} = 2.67; \text{ so the}$$

$$\text{minimum } T_r(m \geq 7.9) = 60/2.67 = 26 \text{ years, and the}$$

$$\text{maximum } T_r(m \geq 7.9) = 70/0.50 = 140 \text{ years.}$$

Historic Recurrence Intervals. There are a few events with $m \geq 7.9$ whose epicenter falls within the aftershock zone of a subsequent earthquake of $m \geq 7.9$. If we assume that these are instances of great earthquakes breaking the same fault zone then the time interval between them may be used to estimate the recurrence time for future earthquakes. For the Aleutians we have:

Rat Islands: 1965-1907 = 58 years

Andreanof Islands: 1957-1905 = 52 years

Fox Islands: 1957-1929 = 28 years

Shumagin Islands: 1938-(1903)* = (35) years; *questionable depth of 100 km

Prince William Sound: 1964-(<1900) = >64

From this limited sample we obtain for events with $m \geq 7.9$ a minimum recurrence interval of 28 years, a median time of 52 years, and a maximum estimate in excess of 64 years.

b-Value from WSSN Data. Many earthquake data sets have been observed to be describable by the relation:

$$\log N = A - bM$$

where N is the cumulative number of events with magnitude greater than or equal to M . The slope of the relation is called the b -value. If this slope can be established on the basis of a large number of smaller events from a limited time sample, it can be extrapolated to estimate the repeat times for larger events. The largest data set available and appropriate was thought to be all of the events which had been reported for the Aleutians since June, 1963, when magnitudes began to be consistently assigned to most events. However, it was found that this data set was not distributed as expected. That is, the number of events with magnitudes larger than M did not increase monotonically with decreasing M . This may have been due to the presence of two major aftershock sequences in the data. Therefore the data set was limited to those events located between the aftershock regions of the 1964 Prince William Sound earthquake and the 1965 Rat Island earthquake ($180^\circ = 155^\circ\text{W}$ longitude). While this data set is much better distributed than the previous one, the plot of $\log N$ vs. M does not obviously exhibit a straight line portion from which to determine the b -value (Figure A-1). Utsu's maximum likelihood method was used to compute b for threshold magnitudes in decreasing steps of $0.2M$. These b -values monotonically increase with increasing magnitude but change least rapidly, corresponding to the flattest portion of the curve, near $m = 4.6$. From general experience it is felt that 4.6 is probably slightly lower than the detection threshold for WWSSN in the Aleutian region. Therefore a plot of $\log (N_i - N_{i+1})$ vs. M (Figure A-2) was made to help determine the detection threshold. The quantity N_i is the number of events in the i th $0.2M$ magnitude interval, so the difference is a measure of the rate of increase of events with decreasing magnitude. The straight line portion of this plot between $m = 5.0$ and $m = 6.0$ shows that the rate of increase is exponential in this range and begins to fall off below $m = 5.0$ which is therefore close to the detection threshold. The drop-off above $m = 6.0$ implies that the sample time

interval of 11.75 years is too short to record an adequate number of higher magnitude events. This deficiency in the higher magnitude range results in the increase of the b-value computed with increasing threshold magnitude. Therefore it is necessary to use the minimum reasonable threshold in computing the b-value. Since there is no drop-off evident at $m = 5.0$ we assume that the detection threshold is slightly lower than this and pick $m = 4.8$ as the threshold value. Utsu's method then yields $b = 1.23 \pm 0.07$ where the error limits are for the 95% confidence level. However, for thresholds of 4.6 and 5.0 we have $b = 1.43$ and 1.09 respectively so we adopt as our estimate $b = 1.2 \pm 0.2$ which covers the whole range of what we consider are reasonable values.

We can now compute repeat times for the Shumagin gap, $T_r(m)$, as follows:

$$T_r(m) = \frac{T_s \times 10^{bm}}{N(M^*) \times 10^{bm}} \frac{L_s}{L_g}$$

where

T_s is the sample time interval = 11.75 years

b is v-value = 1.2 ± 0.2

m is the magnitude threshold of interest

$N(M^*)$ is the number of events with $m \geq M^*$

M^* is the detection threshold used in computing b

L_s is the length of the sample region = 1400 km

L_g is the length of the gap = 600 km.

For $m = 7$ and $b = 1.0, 1.2$ or 1.4 we obtain repeat times, $T_r(7) = 3, 10$ and 26 years respectively. Similarly we find $T_r(7.8) = 22, 87$ and 350 years.

Slip Rates. The following discussion is not intended to estimate repeat times (because of the many assumptions necessary to do so) rather it is to demonstrate the plausibility of those given above on the basis of plate tectonic arguments. The source of the strain energy released by earthquakes in the Aleutians is the relative motion of the Pacific and American plates. In the

eastern Aleutians the convergence rate is about 7cm/year. If we consider a single fault surface which repeatedly fails in a pure stick-slip mode (i.e. we don't consider creep at all) due to this convergence rate we can compute the "repeat times" for events of various magnitudes from certain relations and data given by Kanamori and Anderson (1975). For this type of discontinuous shear displacement we can write the displacement, $D = M_0/\mu S$ where M_0 is the seismic moment, μ is the elastic rigidity of the medium and S is the surface area of the fault. From this relation we obtain the displacement as a function of magnitude by finding M_0 and S for the given magnitudes from plots of M_0 vs. M_S and S vs. M_S given by Kanamori and Anderson (1975). Then the "repeat time" is just this displacement divided by the convergence rate, V :

$$T_r(M_S) = D(M_S)/V.$$

There is, of course, scatter in the plots of M_0 vs. M_S and S vs. M_S ; to account for this we compute extreme value estimates of the repeat times by combining the extreme values for M_0 and S in a worst-case manner. Following the procedure outlined above we obtain:

$$T_r(7) = 0.2, 12, 27 \text{ years and}$$

$$T_r(8) = 3.6, 80, 1200 \text{ years}$$

where the middle times are computed from the median values of $D(M_S)$ and the short and long times are from the extreme values of $D(M_S)$. It should be emphasized that these "repeat times" are not directly comparable to those computed in previous sections because they assume that all of the strain energy available is released by a single magnitude class whereas the previous estimates are made for earthquakes of a given magnitude and larger. Also these "repeat times" do not reflect any attempt to allow for creep nor to estimate how many such fault surfaces might exist in the Shumagin gap. For example, if we take the stick-slip contact zone between the Pacific and American plates to be a region 600 x 300 kilometers for the Shumagin gap we could accommodate 180 fault surfaces large enough to

produce a magnitude 7 earthquake. If all of the relative motion along this zone produced such earthquakes there would be 15 events per year with magnitude seven in the Shumagin gap. Similarly, we could estimate 1.5 events per year with magnitude eight. Besides the unphysical nature of our assumptions, these absurdly high occurrence rates suggest that there is potentially a large amount of strain energy continuously available, and that it is not unreasonable to expect earthquakes to occur in the future with repeat times of the order of those estimated in previous sections on the basis of the short historic record available.

Summary and Conclusions. The repeat times estimated by the various methods discussed above are summarized in Table A-1. For an event with magnitude greater than or equal to seven the estimated repeat times range between 8 and 14 years with extreme values of 3 to 26 years suggested by the b-value computation. Since the last event with magnitude greater than or equal to seven and located within the Shumagin gap occurred in 1964, these results suggest that another event of at least magnitude seven is likely to occur between 1967 and 1990 with the most probable time falling between 1972 and 1978.

TABLE A-1

ESTIMATES FOR REPEAT TIMES OF LARGE EARTHQUAKES IN THE SHUMAGIN GAP (YEARS)

| Method | Magnitude ≥ 7.0 | | | Magnitude ≥ 7.9 | | |
|---|----------------------|------|------|----------------------|------|------|
| | min. | mid. | max. | min. | mid. | max. |
| Occurrence Rate (gap) | - | 8 | - | - | (35) | - |
| Occurrence Rate (arc) | - | 14 | - | 26 | 60 | 140 |
| Recurrence Interval (arc) | - | - | - | 28 | 52 | >64 |
| b-value (mid-arc) | 3 | 10 | 26 | 22 | 87 | 350 |
| ----- | | | | | | |
| Plate Tectonic Convergence Rate (If relieved on a single fault) | 0.2 | 12 | 27 | 3.6 | 80 | 1200 |

For events with magnitude greater than or equal to 7.9 the estimated repeat times range between 60 and 87 years with extremes of 26 and 350 years. The last event with $m \geq 7.9$ in the Shumagin gap occurred in 1938; therefore these extremes suggest that it is likely that a great earthquake ($m \geq 7.9$) will happen between 1964 and 2288 with the most probable time falling between 1998 and 2025.

These predictions based on repeat times are shown in Figure A-3 along with the times of earthquakes which have occurred in the Shumagin gap. Also shown is the 20-year time frame which might be associated with exploration for oil on the continental shelf in the vicinity of the Shumagin gap. It can be seen from this figure that an event of magnitude seven or larger is almost a certainty within this time frame and that it is not unlikely that a great earthquake could occur. Also shown is the time interval, 1974-1980, within which Kelleher (1970) has predicted a major earthquake in the Shumagin gap. This prediction is based on extrapolation from the linear progression observed on a space-time seismicity plot including the 1949 Queen Charlotte Island earthquake, the 1958 southeast Alaska earthquake, and the 1964 Prince William Sound earthquake. Given this prediction and the 35 year interval between previous great ($m \geq 7.9$) earthquakes in the Shumagin gap, the probability for the occurrence of a great earthquake must be regarded as significant within the 20 year time interval 1976-1996.

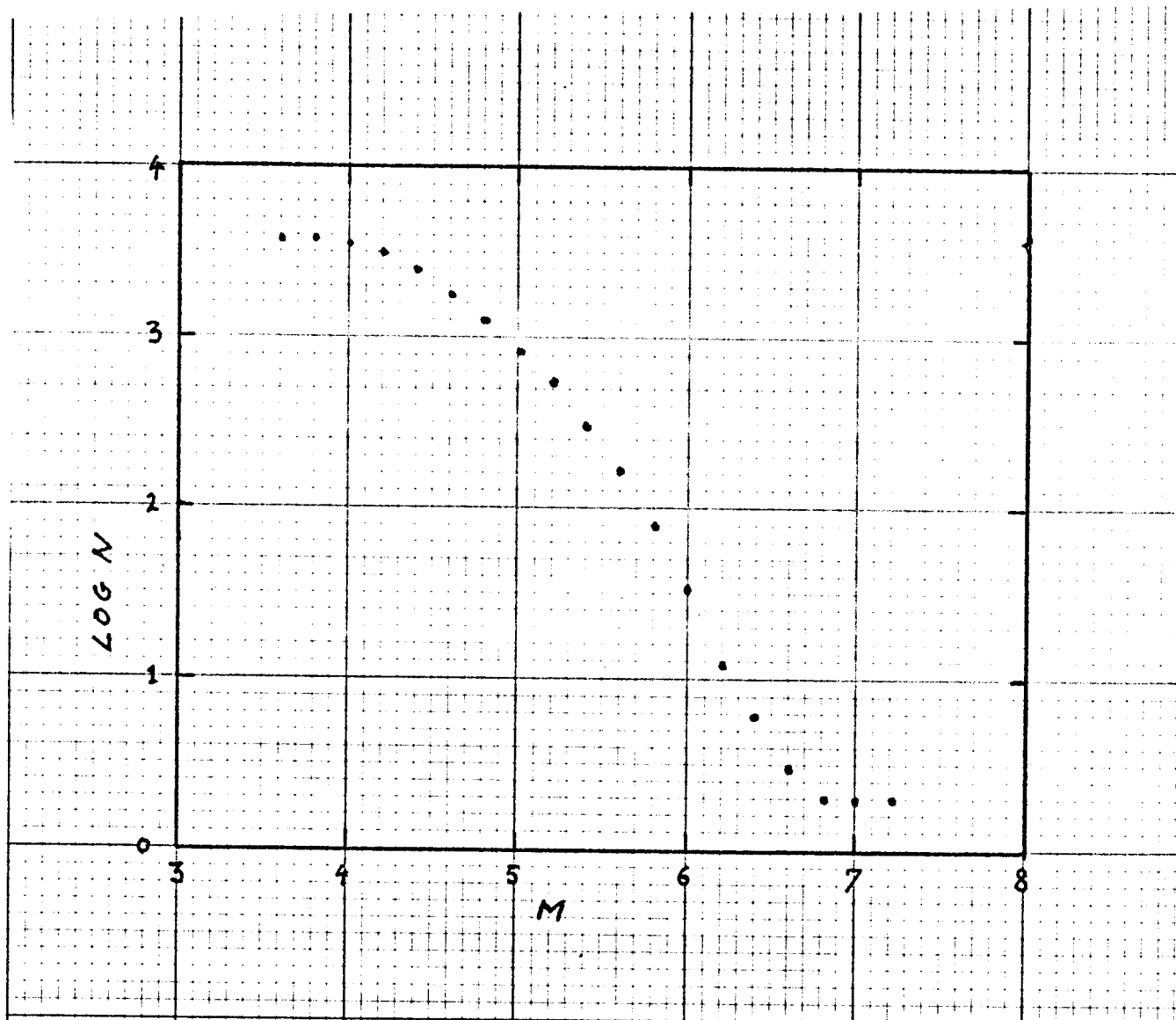


Figure A-1: b-value plot for the Aleutian arc between 180° and 155°W longitude and the time period from June 1963 to March 1975. Utsu's method yields $b = 1.43$, 1.23 , and 1.09 respectively for threshold magnitudes of $m = 5.0$, 4.8 , and 4.6 .

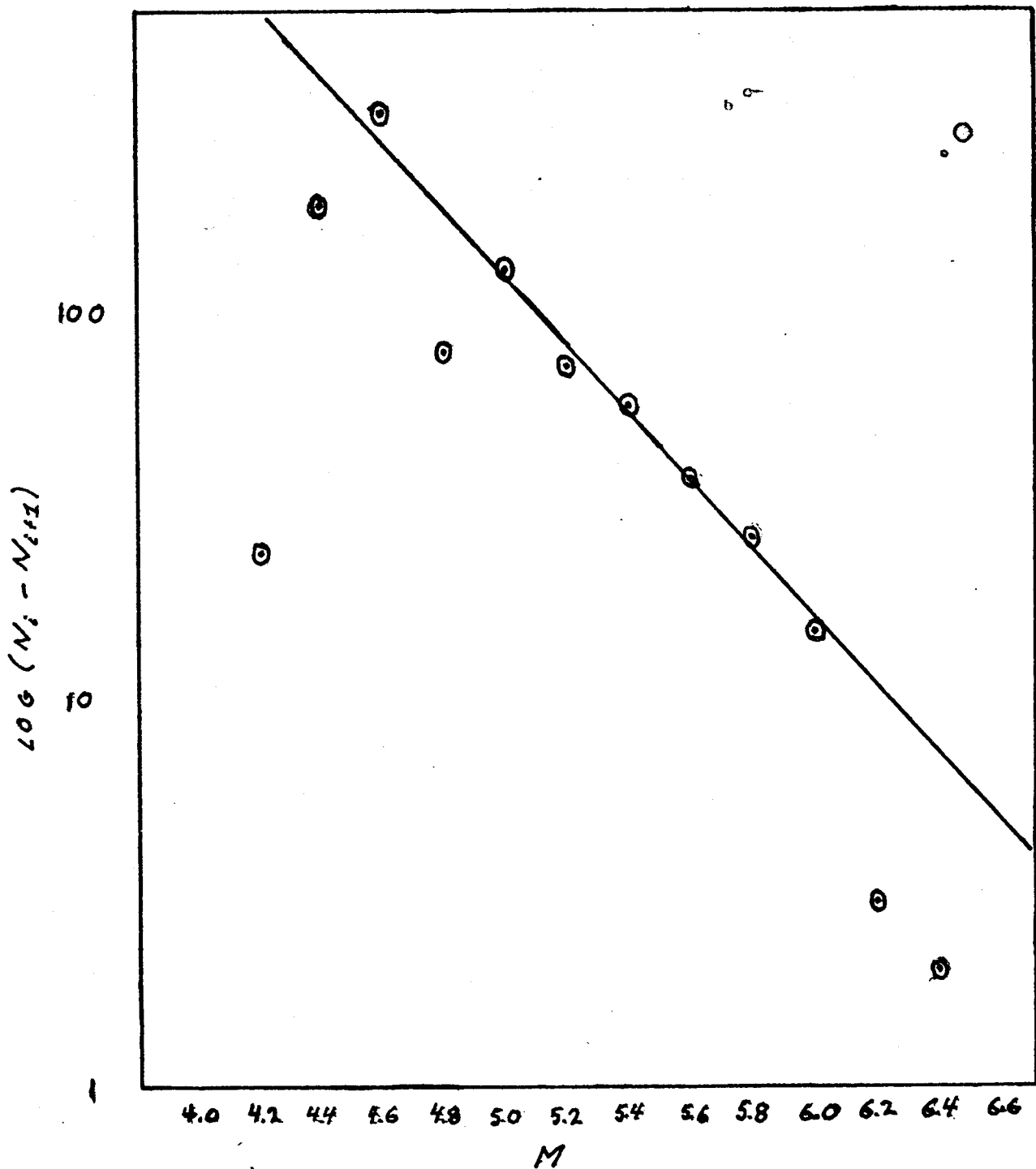


Figure A-2: Accumulation rate plot for data shown in figure A-1. The quantity $(N_i - N_{i+1})$ is the difference between the number of events in successive 0.2M magnitude intervals. The straight line, or exponential, portion of the plot corresponds to the magnitude range for which the data set is complete.

PREDICTIONS BASED ON
REPEAT TIMES FOR MAJOR AND GREAT EARTHQUAKES
IN THE SHUMAGIN GAP

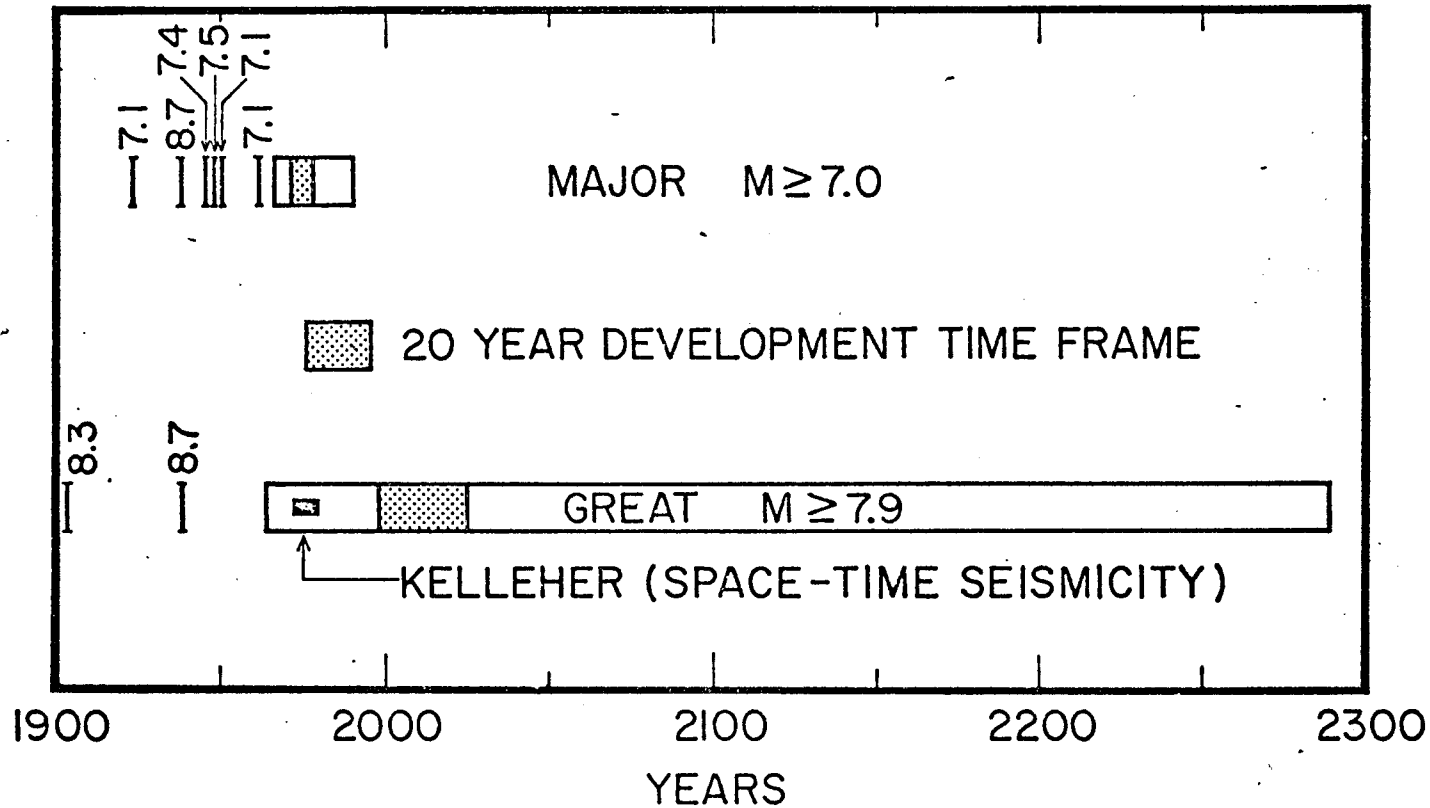


Figure A-3: Shown in the top row are the times of occurrence of previous major ($m \geq 7.0$) earthquakes and the range of times predicted by the various methods used to estimate repeat times. The open box represents the range of extreme values and the shaded portion represents the range of median values. The bottom row shows the same thing for great ($m \geq 7.9$) earthquakes. Also shown here by the solid box is the prediction of Kelleher (1970). The middle row shows the time frame of the next 20 years during which exploration for oil might take place on the continental shelf near the Shumagin Islands.

ANNUAL REPORT

Contract No. 03-5-022082

Research Unit RU 59

July 1, 1975 - April 1976

84 pages

COASTAL MORPHOLOGY AND SEDIMENTATION, GULF COAST OF ALASKA

(GLACIAL SEDIMENTATION)

Jon C. Boothroyd, Ph.D.
(co-principal investigator)

Department of Geology
University of Rhode Island
Kingston, R.I. 02881

Mark S. Cable
Raymond A. Levey

Department of Geology
University of South Carolina
Columbia, S.C. 29208

April 1, 1976

TABLE OF CONTENTS

| | <u>Page</u> |
|--|-------------|
| I. Summary of objectives, conclusions and implications with respect to OCS oil and gas development . . . | 1 |
| II. Introduction | 4 |
| A. General nature and scope of study | 4 |
| B. Specific objectives | 4 |
| C. Relevance to problems of petroleum development | 5 |
| III. Current state of knowledge | 6 |
| IV. Study area | 7 |
| V. Sources, methods and rationale of data collection | 8 |
| VI. Results. | 11 |
| VII. Discussion | 12 |
| VIII. Conclusions | 18 |
| IX. Needs for further study | 20 |
| Acknowledgments | 22 |
| References cited | 23 |
| Figures | 25 |
| Explanatory texts: | 64 |
| Location map | 65 |
| Preliminary bathymetric chart | 67 |
| Environmental geologic map | 69 |
| Geologic hazards and processes map | 75 |
| Bottom profiles | 81 |
| Appendices | 82 |

Enclosures:

Location map

Preliminary bathymetric chart

Environmental geologic map

Geologic hazards and processes map

Bottom profiles

I. Summary of objectives, conclusions and implications with respect to OCS oil and gas development.

This project is charged with:

- 1) identifying and evaluating glacial sedimentary processes and products in the Icy Bay area, including both present and past activity.
- 2) examination of nearshore bottom morphology in Icy Bay, for evidence of mode of formation, and importance of presently-active processes.
- 3) evaluating the effect of the various geologic processes on man's activities in specific areas within, and along the shore of, Icy Bay.

Man's activities in Icy Bay, as they relate to OCS oil and gas development,

- 1) Ship anchorages
- 2) Shore facilities including:
 - a) personnel quarters
 - b) supply depots
 - c) construction and repair facilities
 - d) oil storage

The geologic processes and products specifically identified as potentially hazardous to the above activities are:

- 1) glacier-burst floods
- 2) glacier surges
- 3) buried ice blocks and stagnant ice masses

- 4) unstable ground (onshore and subtidal)
- 5) coastal erosion
- 6) drift ice from calving glaciers

In addition, the overall nearshore-bottom morphology of the Bay (deep water vs. shallow water) places a limiting factor on use of certain areas within the Bay.

The following conclusions pertain to the feasibility of locating shore facilities along Icy Bay, in combination with suitable ship anchorages. They must be viewed as tentative interpretations at this time. The conclusions are:

- 1) Use of Icy Bay north of Kichyatt Point is not feasible because of: heavy drift ice; active glaciers; steep bedrock cliffs; and stagnant ice masses and active flowtill on the foreland areas.
- 2) New Yahtse, Caetani, and Kettlehold Deltas are not suitable for shore facilities due to: potential glacier-burst flooding; ground subsidence due to melting of buried ice blocks; and potential delta-front slumping and slope failure.
- 3) All other areas may be considered for potential onshore sites.
- 4) Known hazardous shallow-water areas are east of Gull Island, and south of Moraine Island, including the entrance to Riou Bay.
- 5) A definite deep water area exists off the Icy Bay Lumber Company dock.
- 6) Seal Camp Harbor is excellent for smaller vessels, but has an entrance depth of 11 meters and limited turning room for large vessels.
- 7) Best all-round potential sites for shore facilities with anchor-

ages identified so far are:

- a) Icy Cape Foreland adjacent to the Icy Bay Lumber Foreland adjacent to the Icy Bay Lumber Company dock. A drawback is that this is an area of high wave-energy.
- b) Lower Chaix Hills area.
- c) An anchorage west and northwest of Gull Island, with a causeway to mainland shore facilities.

The dispersal pattern of oil spills within the Bay is unknown and requires further field study.

II. Introduction

A. General nature and scope of study

The major emphasis of the project falls under Task D4, to evaluate present rates of change in coastal morphology, with particular emphasis on the possible impact of man-induced changes. Further, the purpose of the study is to: 1) locate areas where the coastal environment is likely to be changed by man's activities and evaluate the effect of these changes, if any; and 2) evaluate effect of various geologic processes on man's activities in specific areas along the coast in the study area.

B. Specific Objectives

This part of the project is charged with identifying and evaluating glacial sedimentary processes and products, including both present and past activity. In addition, nearshore bottom morphology is to be examined for evidence of mode of formation and importance of presently-active processes.

The specific objectives are:

- 1) Determine the absolute and relative importance of active braided streams in the study area, as sediment providers to the coastal zone.
- 2) Delineation of areas underlain by glacial sediments; map the sediment type; and determine relative ground stability.
- 3) Location of areas probably underlain by buried ice and magnitude of ground subsidence likely to result.
- 4) Determine areas likely to be threatened by glacier-burst floods and locate possible flood channels.

- 5) Examination of the margin of the Malaspina ice sheet to determine which, if any, portions of the glacier are surging.
- 6) Determine the general configuration and slope of outwash delta (fan delta) fronts and the location of slumps.

Two additional objectives not outlined in the work statement but deemed important on the basis of field observations are:

- 7) Determination of nearshore bottom morphology on the east side of Icy Bay and correlation with onshore geology.
- 8) Location and movement patterns of drift ice in Icy Bay.

C. Relevance to problems of petroleum development

Problems concerning petroleum development as it states to this part of the project are:

- 1) Feasibility of the use of Icy Bay for:
 - a) a ship anchorage
 - b) shore facilities (personnel quarters; supply depots; construction and repair; oil storage)
- 2) Direction and rate of transport of oil from a spill near or within Icy Bay.

III. Current state of knowledge

Scientific observation began in the vicinity of the present Icy Bay and West Malaspina Foreland with the voyages of discovery of Vancouver in 1794. These and other early expeditions are excellently summarized by Post and Plafker (in preparation). A summary of the Recent history of glaciation and ice retreat in the Malaspina district accompanies the map by Plafker and Miller (1958). Other useful maps are by Miller (1971), 1961, 1957); Plafker and Miller (1957); and Post and Mayo (1971).

Ground investigation of surficial processes and deposits in the vicinity of the eastern margin of Icy Bay has been mainly of a reconnaissance nature; early work has been concentrated around and on the eastern margin of the Malaspina Glacier (Gilbert, 1904; Sharp, 1951, 1953, 1958; Tarr, 1909; Tarr and Butler, 1909; Tarr and Martin, 1906; Washburn, 1935). Later work around the eastern margin of the Malaspina includes work on patterns of glacial deposits (Hartshorn, 1952); Glacial Lake Malaspina (Gustavson, 1972, 1974, 1975); and glacial outwash fans (Gustavson, 1974). Investigations along and near Icy Bay include an excellent report by Russell (1893) of the Old Yahtse River, Chaix Hills region; surficial mapping of Icy Cape Foreland by Miller (1971); and various sample-collecting trips (Plafker and Miller, 1958; Post and Plafker, in preparation).

Prior work by our group was on beaches along the entire Malaspina, Icy Cape Forelands (Hayes and others, 1973); and on outwash-fan sedimentation (Boothroyd and Ashley, 1975; included in the appendix).

IV. Study Area

The area of study for this part of the project is on the northeast Gulf coast of Alaska from Sitkagi Bluffs to about 10 km west of Icy Cape, including specifically the margin of Icy Bay. Field work concentrated on the east margin of the Bay, offshore and onshore; and on the West Malaspina Foreland as far east as Yana Stream. Figure 1 and 2 and accompanying maps give general locations and specific localities.

V. Sources, methods and rationale of data collection.

Data collected during the field season (June 6 to August 19, 1975) were designed to meet each of the specific objectives. Please refer to maps for specific localities.

1) Active streams.

A theodolite survey of New Yahtse River was carried out to determine the longitudinal profile. Stations were occupied every 300-400 meters. Fifteen stations were occupied with surface velocity measured; surface suspended sediment sample obtained; and maximum clast size on bar surfaces measured. The size of the fountain source of New Yahtse River was measured so that discharge could be determined by the velocity-head method. This measurement was made at maximum melt-water discharge.

2) Glacial sediment type and ground stability.

A ground check of most of the West Malaspina Foreland was carried out on foot and by trail motorcycle. Seismic-line roads cut in the late 1950's and early 1960's proved useful. Spot landings by Cessna 180 fixed-wing aircraft also aided in access to some areas. Shore sites were readily accessible by Zodiac rubber boat.

Oblique color aerial photographs (35 mm) were taken through the summer from various altitudes ranging from 30 to 3300 meters. Ground photographs were also obtained (2000 total, air and ground).

3) Buried ice and ground subsidence.

Aerial reconnaissance was carried out of possible buried ice localities that were previously identified on vertical aerial photographs (1957). Many sites were visited on the ground and stagnant ice masses documented. More deeply-buried blocks were postulated from ground cracking and sag ponds.

4) Glacier-burst floods.

Status of ice-marginal lakes and ice-marginal channels were checked by aerial survey and compared with past aerial photography and Landsat imagery. Oblique aerial photography by Austin Post (U.S.G.S Tacoma) proved particularly useful. Changes in ice-marginal drainage to new drainage-ways was ground checked where possible to determine further likely changes in the drainage. Local air-taxi pilots were interviewed in regard to recent, unusual flood flows. This led to the investigation of the Oily Lake flood.

5) Glacier surges.

An aerial survey was made of the margin of the Malaspina, Tyndall, Yahtse and Guyot glaciers. Low oblique aerial photos were taken of the Malaspina margin at an altitude of 3300 meters to compare with, and update older photos and maps. Variations in position of the ice margin in comparison to older photos was noted and photographed in detail (aerial).

6) Delta front morphology.

70 kilometers of high-resolution bottom profiles (24 individual profiles) were run with a Bludworth EM-130SS profiler mounted in a 5 meter, Zodiac rubber boat. Seven of these profiles were run from the New Yahtse and Kettlehole deltas. Most profiles were run from shore point to shore point. The others were begun at a shore point and run on a compass bearing. All profiles were run at a constant boat speed; chart speed was varied for resolution purposes. Horizontal scale was checked by the measured line-timing method. Primary coverage was on the east side of Icy Bay. Equipment failure and transportation problems precluded coverage of deltas in Yakutat Bay.

7) Nearshore bottom morphology.

Profiling method, and tracklines are described in 6) above. Priority was given to those areas most likely to be considered for ship anchorages, and secondly, hazardous shoal areas.

8) Drift ice in Icy Bay.

Bay-ice location and density was checked at least twice daily during the summer field season. An aerial photo survey of bay ice as flown seven times during the summer. Manuvering in various ice conditions was done to test the feasibility of working and transporting personnel through drift ice.

VI. Results

The major information products included in this report are a series of large-scale maps and charts accompanied by photographs that illustrate specific features on those maps. The maps and charts are:

- 1) Location map for the West Malaspina Foreland and Icy Bay area.
(scale: 1:63,360).
- 2) Geologic hazards and processes map of the West Malaspina Foreland and Icy Bay area (scale: 1:63,360).
- 3) Preliminary bathymetric chart of Icy Bay (scale: 1:40,000; adopted from NOS chart 16741).
- 4) Environmental map of the east margin of Icy Bay (scale: 1:10,475).

An explanatory text accompanies each map giving results and discussion pertinent to that map. Interpretative figure captions are provided for each photograph. The three maps, the chart, and the photographs are to be used together to verify and cross-check results.

Also included are copies of the bottom profiles at a reduced scale. Interpretation of these profiles is incomplete at this time but results thus far are given in an explanatory text included with the profiles.

An appendix is included containing the following items.

- 1) Table of weather data and drift-ice observations collected during the summer field season.
- 2) Reprint of a paper (Boothroyd and Ashley, 1975) discussing outwash fan sedimentation on the northeast Gulf of Alaska, including Yana Stream on the West Malaspina Foreland.

VII. Discussion

Topics pertinent to each map or chart, and illustrated by the figures, have been discussed either in the explanatory texts accompanying each map, or in the figure captions. A summary of this discussion, including the relationship of the map and figures to one another, is presented in outline form below. The explanatory framework of the geologic hazards and processes map is followed, and the depositional systems and zones discussed in conjunction with the environmental geologic map are considered where appropriate. The effect of the possible use of Icy Bay for petroleum development is given.

Glacier-burst floods

- 1) Oily Lake discharge into Yana Stream, Shoal Bay Lakes, and Seward Lake (Figs. 3, 4, and 19). Would not affect Icy Bay.
- 2) Oily Lake discharge (?) into the New Yahtse fluvial-deltaic system (FAny) via a small fountain (south of New Yahtse fountain) and ice-block ponds (LPi) (Figs. 3 and 4). Postulated minor flooding only.

Zone affected: Fluvial-fan delta and moraine complex (New Yahtse River area).

Specific environment affected: New Yahtse fluvial system (FAny_{C,1}); New Yahtse Delta (BSo, BSag, and ITf).

Flooding would probably be similar to maximum summer discharge.

- 3) Agassiz Lakes discharge via the Caetani ice-marginal drainage (FM ca) into the New Yahtse system (FAny); overflow drains into the Caetani proflacial system (Fic) (Figs. 3, 4, 9, 10, 11, and

12). Major flooding is possible.

Zone affected: Fluvial-fan delta and moraine complex (New Yahtse River area).

Specific environments affected: New Yahtse fluvial system (FAny_{C,1,2,2.5} and 3 (?)); New Yahtse Delta (BSo, BSag, ITf); Kettlehole Delta (BSo, BSag, ITf); Caetani River fluvial system (FIc₁ and 2); and Caetani Delta (BSag, ITf)

Major damage by inundation, or channel shifting and lateral erosion, would occur to structures constructed on much of the New Yahtse and Caetani fluvial-deltaic systems. Kettlehole Delta would be relatively unaffected although the site of the 1975 summer field station would be flooded.

Glacier Surges

- 1) Agassiz lobe (GIa) in the vicinity of Chaix Hills airstrip (Figs. 3, 4, and 9). Magnitude of possible surges is unknown.

Zone affected: Fluvial-fan delta and moraine complex (New Yahtse River area).

Specific environments affected: Active ice (GIa) and adjacent sinkhole-pocked ice (GIs); stagnant ice blocks (SIb, SIv); and probably the younger moraine complex (TFa, Ta, LPa). A surge could block the Caetani and New Yahtse drainage and cause temporary ice-dammed lakes.

There have been no recorded surges of this margin, thus effects are difficult to assess.

- 2) Tyndall, Yahtse, and Guyot Glaciers, upper Icy Bay (Figs. 3, 4, and 7). Magnitude of possible surges is unknown.

Area affected: Upper Icy Bay.

The major hazard created by a surge of any of these galciers would be the creation of a large mass of drift ice that would be a danger to shipping.

Buried ice blocks and stagnant ice masses

- 1) Large stagnant ice masses (Figs. 3, 4, 7, 8, and 9).

Areas affected: Yahtse Foreland; and area east of Kageet Point.

Zone affected: Fluvial-fan delta and moraine complex (New Yahtse area)

Specific environment affected: Stagnant ice (SIB, SIV) and developing lakes (LPA).

There is no active danger; the area near blocks should simply be avoided for construction or storage sites.

- 2) Buried ice blocks (Figs. 8, 9, 10, 11, and 12).

Zones affected: Fluvial-fan delta and moraine complex (New Yahtse area); and Old Yahtse River fluvial-deltaic system.

Specific environments affected: New Yahtse fluvial system (FAny₄ (includes LPI), 3 and 2.5 (includes LPI, LPb, and LPI?)); Kettlehole fluvial system (FIK₃ (includes LPb); upper Old Yahtse River (FLoy_C, LPb).

Active ground subsidence makes the affected areas unfit for permanent structures.

Unstable ground

- 1) Active flowtill (Figs. 3, 4, 7, 8, 9, 10, 11, and 12).

Areas affected: entire Yahtse Foreland; most of area between

Kageet Point and Chaix Stream.

Zones affected: Till plains (Chaix Hills); and fluvial-fan delta and moraine complex (New Yahtse Delta area)

Specific environments affected: flowtill (Tfi) of till plain (?); flowtill (Tfa) near Malaspina Glacier between the Caetani and New Yahtse River.

This terrain is unsuitable for use unless it can be stabilized by draining and filling. The till plain area is probably stabilized in most part, but zones of instability could remain. A further cautionary note: All till complexes north and west of the Kettlehole Delta, and the apex of Old Yahtse River, could contain buried ice blocks or active flow-till. Ground cover prevents a more accurate assessment and not all areas were field checked.

- 2) Delta-front slumps (Figs. 3, 4, 10 and 12; bottom profiles 1, 2, 10, 11, 19, 20, 21, and 22).

Zone affected: Fluvial-fan delta and moraine complex (New Yahtse area).

Specific environments affected: a catastrophic failure could cause subsidence or removal of the immediate fluvial surface (e.g., FAny₁), as well as the intertidal (ITf), and the beach-spit system (BSa). Catastrophic slumping is an extremely likely occurrence in the event of a severe earthquake (magnitude ?).

Coastal Erosion

- 1) Point Riou and Riou spit (Figs. 3, 4, 16, 17, and 18).

Zone affected: Point Riou moraine and fan complex; and Riou Spit.

Specific environments affected: Eroding cliff in Point Riou basal and ablation till complex (Tpr); developing erosional platform (ITg/ITb); and active outwash (BSag), receding Riou Spit.

There is no immediate danger to activities in Icy Bay. The main problem is sediment transport along the spit to the vicinity of Moraine Reef, effectively sealing off Riou Bay.

- 2) Icy Cape Foreland (Figs. 3, 4, 5, and 6).

Area affected: Icy Cape, eroding beach and till cliffs. There is no immediate danger to man's activities on the Icy Cape Foreland.

Drift Ice

- 1) Ice stream position (Figs. 3, 4, 7, and 8).

Areas affected: upper Bay (heavy ice); mid Bay (moderate ice); lower Bay (scattered ice).

An aperiodic but a major hazard. Fishing boats and large craft avoid the main ice stream in Icy Bay.

- 2) Grounded ice accumulation and dispersed drift ice (Figs. 3, 4, 5, 6, 8, 10, 12, and 14).

Areas affected: Gull Island and associated shoals; the Bay north of Caetani Delta; beach south of Icy Bay Lumber Company dock.

Specific environments affected: Gull Island beaches (BSab), and northern intertidal shoals (ITm).

Dispersed drift ice is scattered at times over most of the Bay but appears to be of nuisance value only. Heavy accumulations of grounded ice could pose problems for docking facilities.

General:

1) Bedrock (Figs. 3, 4, 5, 6, 7, and 8).

Locations near the margin of the Bay: Adjacent to Icy Bay Lumber Company dock; Kichyatt Point; Tsaa Fiord; Taan Fiord; and lower Chaix Hills. Bedrock crops out almost continuously along the Bay north of Kichyatt and Kageet Points, but mostly as steep faces.

Building sites located on bedrock would afford the most secure protection against ground failure during earthquakes.

2) Deep-water areas. (Figs. 3, 4, 6, 8, 10, 12; profiles 1, 2, 6, 10, 11, 13, 14, 15, 19, 20, 21, 22, and 23).

Locations: Off Icy Bay Lumber Company dock; in front of Caetani, New Yahtse, and northeast of Kettlehole Deltas.

3) Shallow-water areas (Figs. 3, 4, 12, and 16; profiles 3, 4, 6, 7, 9, 23, and 24).

Locations: East of Gull Island; entrance to Riou Bay; and directly off Point Riou and Icy Cape.

4) Present Harbor (Figs. 3, 4, 12, 13, 14; profile 8).

Location: Seal Camp Harbor.

VIII. Conclusions

The following statements pertain to the feasibility of locating shore facilities along the Icy Bay, combined with suitable ship anchorages. They must be deemed tentative and subject to change with further data interpretation. The conclusions thus far are:

- 1) Use of the Bay north of Kichyatt and Kageet Points for any activities is not feasible because of:
 - a. heavy drift ice
 - b. active glaciers
 - c. steep bedrock cliffs
 - d. forelands are underlain by stagnant-ice masses and subject to active flowtill processes.
- 2) Caetani, New Yahtse, Kettlehole Deltas are not suitable for shore facilities. Problems are:
 - a. potential glacier-burst flooding.
 - b. ground subsidence due to melting of buried ice blocks.
 - c. delta-front slope slumping and slope failure.
- 3) All other areas may be considered for potential onshore sites.
- 4) Shallow-water areas unsuitable for most vessels with a draft deeper than several meters are located:
 - a. east of Gull Island
 - b. south of Moraine Island including the entrance to Riou Bay.
- 5) A definite deep water area is located offshore of the Icy Bay Lumber Company dock. But this area is subject to high wave energy.
- 6) The present Seal Camp Harbor is excellent for fishing boat-sized vessels, but is small and has an entrance depth of 11 meters at M.L.L.W.

7) Best, all-round potential sites, providing an anchorage plus sites for shore facilities are:

a. Icy Cape Foreland adjacent to the Icy Bay Lumber Company dock.

Positive features are: deep water; adjacent to bedrock terraces; relatively stable glacial sediment. The negative aspect is that high-wave energy impinges on the dock.

b. Lower Chaix Hills area:

Positive: bedrock terrace and relatively deep water anchorage.

Negative: glacial sediment may be unstable (till plain); moderate drift-ice accumulation area.

c. Gull Island; with a connecting causeway running across the shoals to the mainland sites.

Positive: relatively deep water; low-wave energy.

Negative: no bedrock nearby; aperiodic, scattered to moderate drift-ice accumulation; and substantial development needed to create a dock facility.

IX. Needs for further study

Further study of Icy Bay should be initiated to: 1) complete some aspects of the work begun with this project; 2) answer questions raised by this study; and 3) provide additional detailed information on potential sites for shore facilities identified by the present study.

Specific tasks that should be undertaken are:

- 1) Continuation and completion of high-resolution bottom profiling to acquire detailed knowledge of the bottom morphology over the entire Bay.
- 2) High resolution (Uniboom) sub-bottom profiling to delineate type, extent, and thickness of bay sediments; especially the basal till horizon, and large slump blocks off the deltas and elsewhere. These units would be tied to onshore geology.
- 3) Study of the wind and tidal-current pattern in Icy Bay by occupying a series of 13-25 hour hydrographic stations, and the placement of wind recorders at onshore sites around the Bay. In this manner, the movement pattern of drift ice, and dispersal of oil from spills could be determined.
- 4) Detailed environmental and engineering geology of the most likely sites for shore facilities as identified in this report (Icy Cape Foreland, lower Chaix Hills, and Gull Island complex); and of other potential sites suggested by others.
- 5) A visit should be made to Icy Bay to assess winter-storm condition particularly in the area of Icy Bay Lumber Company dock, and at Gull Island. In addition, a wave recorder should be placed at the end of the dock.

A project similar to that already carried out in Icy Bay should be initiated for the eastern margin of Yakutat Bay from Knight Island to Ocean Cape, including offshore studies in Yakutat Bay, and onshore studies of the Yakutat Foreland. The specific objectives would be the same as those for the present project.

ACKNOWLEDGMENTS

I would like to thank Ray Levey, and particularly Mark Cable, for independent work and able assistance in the field, and for their help in map compilation. Chris Rubey and Steve Wilson also assisted in the field.

This report would not have been possible without the effort of many persons at the University of Rhode Island. They are: Steven Gautie, map compilation and drafting; Karen Barrett, photo work; Jon Barrett, drafting; Susan Morrow and Terry Tonon, manuscript typing; and the engineering Machine Shop (E.C. Bachelder, Head), map reproduction.

I wish to particularly acknowledge the support of Austin Post, who has generously provided unlimited access to unpublished maps and other material.

REFERENCES CITED

- Boothroyd, J.C., in press, Sandur plains, northeast Gulf of Alaska: A model for alluvial - fan delta sedimentation in cold-temperate environments: in Recent and Ancient depositional environments in Alaska, Alaska Geological Society Symposium Volume.
- _____, and Ashley, G.M., 1975, Processes, bar morphology, and sedimentary structures on braided outwash fans, northeastern Gulf of Alaska: p. 193-222, in McDonald, B.C., and Jopling, A.V., eds., Glaciofluvial and glaciolacustrine sedimentation, Soc. Econ. Paleontologists and Mineralogists, Spec. Pub. 23, 320 p.
- Brooks, Alfred H., 1916, Mineral resources of Alaska: U.S. Geol. Survey Bull. 662, 469 p.
- Gilbert, G.K., 1904, Glaciers and glaciation (of Alaska): Harriman Alaska Expedition, v. 3, New York, Doubleday, Page Co.
- Gustavson, Thomas C., 1972, Sedimentation and physical limnology in proglacial Malaspina Lake, Alaska: Dept. of Geol., Univ. of Mass., Amherst; Tech. Rept. No. 5-CRC, 48 p.
- _____, 1974, Sedimentation on gravel outwash fans, Malaspina Glacier Foreland, Alaska: Jour. Sed. Petrology, v. 44, p. 374-389.
- _____, 1975, Sedimentation and physical limnology in proglacial Malaspina Lake, southeastern Alaska: p. 249-263, in McDonald, B.C., and Jopling, R.V., eds., Glaciofluvial and glaciolacustrine sedimentation, Soc. Econ. Paleontologists and Mineralogists, Spec. Pub. 23, 320 p.
- Hartshorn, J.H., 1952, Superglacial and proglacial geology of the Malaspina Glacier, Alaska, and its bearing on glacial features of New England (abs.): Geol. Soc. Am. Bull., v. 63, p. 1259-1260.
- Hayes, M.O., Owens, E.H., Hubbard, D.K., and Abele, R.W., 1973, The investigation of form and process in the coastal zone: p. 11-41, in Coates, D.R., ed., Coastal geomorphology, third annual proceedings volume, Geomorphology Symposia Series, Binghamton, N.Y., 404 p.
- Miller, Don J., 1957, Geology of the southeastern part of the Robinson Mountains, Yakataga district, Alaska: U.S. Geol. Survey Oil and Gas Inv. Map OM-187.
- _____, 1961, Geology of the Malaspina district, Gulf of Alaska Tertiary province, Alaska: U.S. Geol. Survey open-file report, 2 sheets.
- _____, 1971, Geologic map of the Yakataga district, Gulf of Alaska Tertiary Province, Alaska: U.S. Geol. Survey Misc. Geol. Inv. Map I-610.

- Plafker, George, 1967, Geologic map of the Gulf of Alaska Tertiary Province, Alaska: U.S. Geol. Survey Misc. Geol. Inv. Map I-484.
- _____, and Miller, Don J., 1958, Glacial features and surficial deposits of the Malaspina district, Alaska: U.S. Geol. Survey Misc. Geol. Inv. Map I-271.
- Post, Austin, and Plafker, George, in preparation, Nonsynchronous Neoglacial advances and retreats of the Hubbard, Guyot, and Malaspina Glaciers, Alaska: U.S. Geol. Survey Prof. Paper.
- _____, and La Chapelle, E.R., 1971, Glacier ice: Univ. of Washington Press, Seattle, 110 p.
- _____, and Mayo, L.R., 1971, Glacier dammed lakes and outburst floods in Alaska: U.S. Geological Survey Hydr. Atlas No. 455.
- Russell, I.C., 1893, Second expedition to Mount St. Elias in 1891: U.S. Geol. Survey 13th Ann. Rept., pt. 2, p. 1-91.
- Sharp, R.P., 1951, Accumulation and ablation on the Seward-Malaspina Glacier system, Canada-Alaska: Geol. Soc. Am. Bull., v. 62, p. 725-743.
- _____, 1953, Deformation of bore hole in Malaspina Glacier, Alaska: Geol. Soc. Am. Bull., v. 64, p. 97-100.
- _____, 1958, The latest major advance of Malaspina Glacier, Alaska: Geog. Rev., v. 48, p. 16-26.
- Tarr, R.S., 1909, The Yakutat Bay region, Alaska, Physiography and glacial geology: U.S. Geol. Survey Prof. Paper 64, pt. 1, p. 11-144.
- _____, and Butler, B.S., 1909, The Yakutat Bay region, Alaska, areal geology: U.S. Geol. Survey Prof. Paper 64, pt. 2, p. 145-170.
- _____, and Martin, Lawrence, 1906, Recent changes of level in the Yakutat Bay region, Alaska: Geol. Soc. Am. Bull., v. 17, p. 29-64.
- Washburn, Bradford, 1935, Morainic bandings of Malaspina and other Alaskan glaciers: Geol. Soc. Am. Bull., v. 46, p. 1879-1890.



FIGURES

Figure 1. General location map of the northeast Gulf of Alaska between Cordova and Yakutat.

Numbers refer to selected active, or recently active, glacial-outwash fans. Numbers 5, 6, and 7 refer to Old Yahtse River, Yana Stream, and Fountain Stream respectively. They are located on the West Malaspina Foreland.

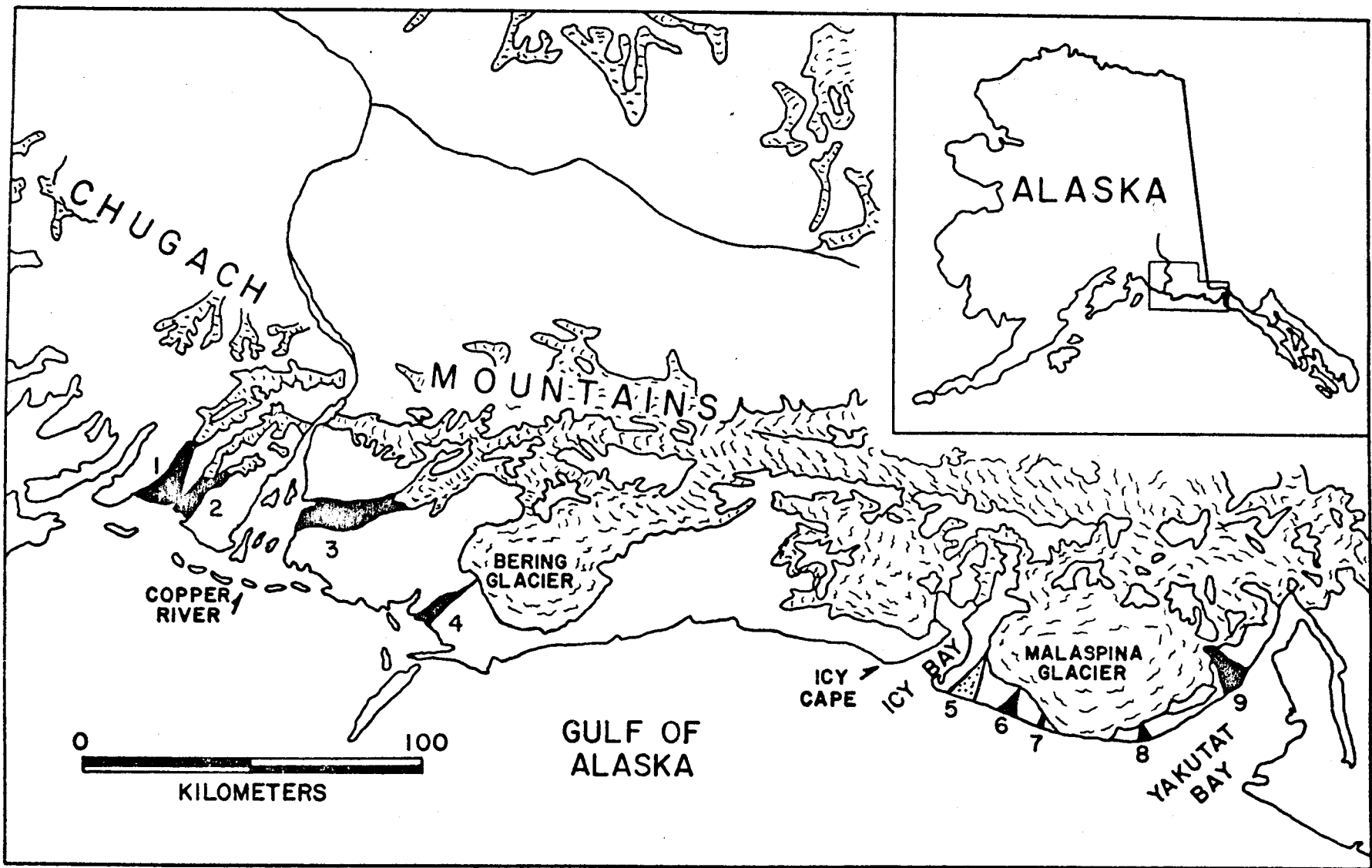


Figure 2. Preliminary facies map of the West Malaspina Foreland with major emphasis on glacial-outwash fans (sandurs). This map was prepared before summer, 1975 field work along Icy Bay, and thus should be used for general orientation and interpretation only. It is included as a figure in Boothroyd (in press), a paper concerning regional distribution and variation of outwash fans.

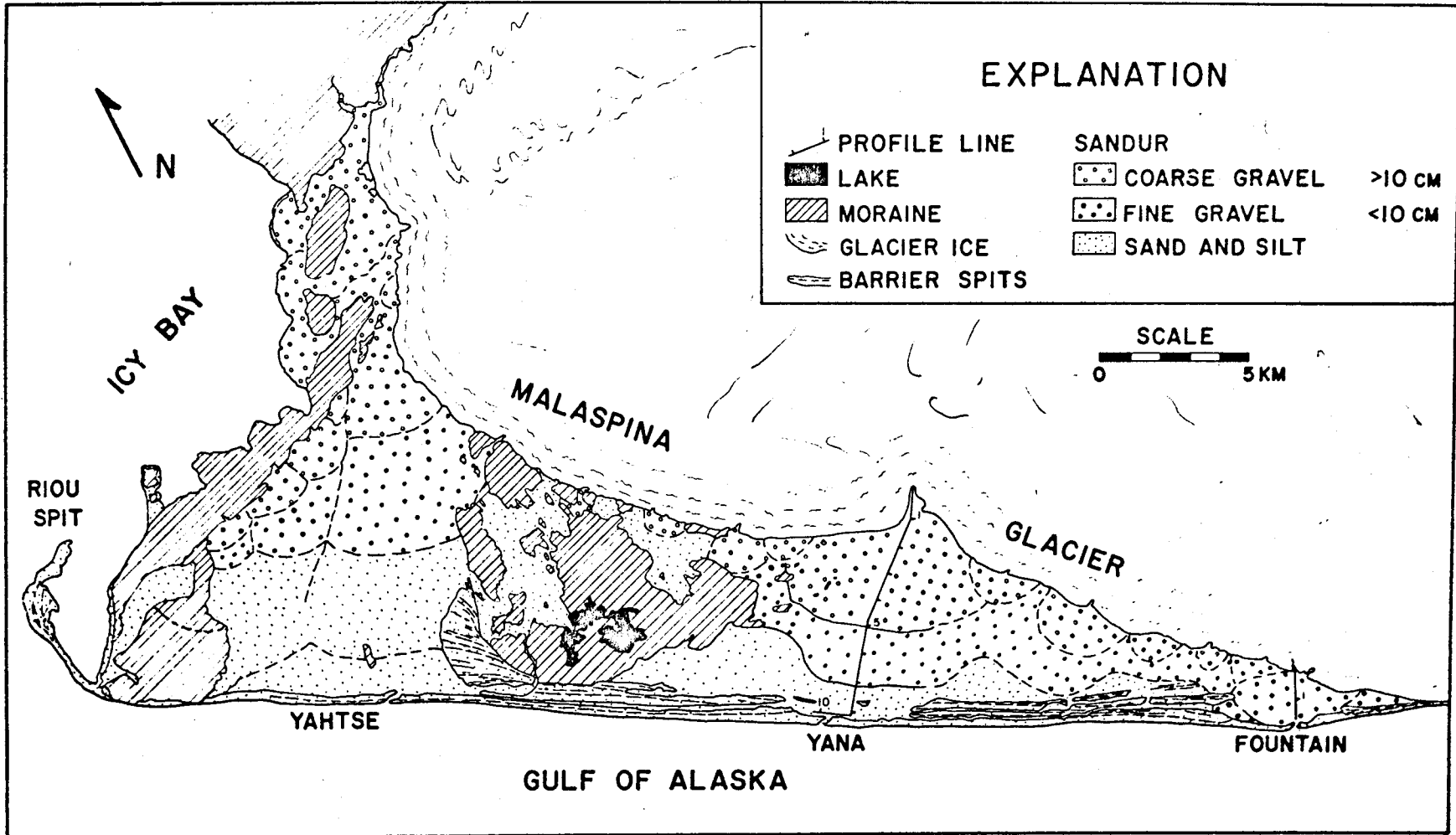


Figure 3. Landsat band 5 image of Malaspina Glacier, Icy Bay area. Ice from the Guyot and Yahtse Glaciers fills the upper half of the Bay, with an ice stream projecting down the center of the lower Bay. This is the most common location for the ice stream when it occurs in the lower Bay. Active outwash streams, sediment-laden lakes and lagoons, and sediment plumes in the Bay and Gulf of Alaska proper are light-colored. Flood-tidal currents are deflecting the sediment plume from the active Yahtse River, up the Bay. These tidal currents also deflect the ice stream and cause some of the observed swirl patterns.

Oily Lake, at the base of the Samovar Hills, was empty at the time this image was obtained; it had partially refilled when observed in July, 1975. The lake emptied through a postulated subglacial drainage system that extends beneath the medial moraine that divides the Agassiz and Seward lobes of Malaspina Glacier. This drainage emerges at Yana Stream and at a smaller reactivated stream 3 km to the west. Flood waters have flowed into some of the Shoal Bay lakes as well as down Yana Stream and into the Gulf. This appears to be the preferred route for breakout floods (jökulhlaups) from Oily Lake.

Inactive streams such as old Yahtse River appear darker; vegetated moraines on the Malaspina Glacier, as well as older ground and end moraine appear still darker. Areas on the Icy Cape Foreland clearcut by the Icy Bay Lumber Company appear as lighter patches.

Image taken July 1, 1974; Scene ID: 81708200355A000.

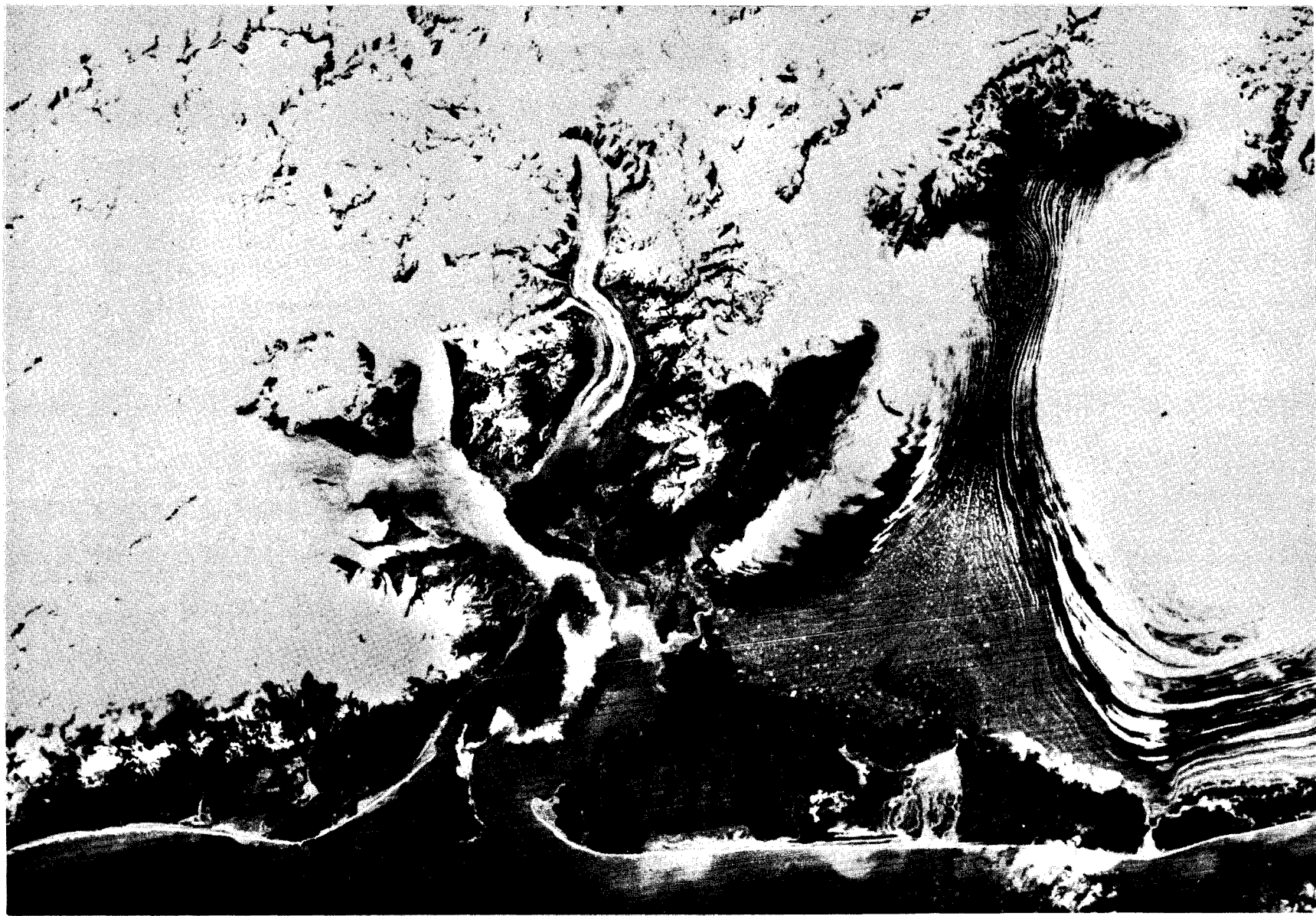


Figure 4. Landsat band 7 image of Malaspina Glacier, Icy Bay area taken at the same time (July 1, 1974) as Figure 3. Vegetation appears white at this wavelength, especially that on the Malaspina Glacier itself. Water with a low suspended-sediment concentration is a lighter shade. The grayish splotch is the lower center of Old Yahtse River is groundwater discharge into open marshlands.

A stagnant ice mass, just northeast of Kageet Point, and the entire Yahtse Foreland show dark gray, indicating wet and unstable surface conditions.

The erosional terraces cut in bedrock on Icy Cape Foreland (Miller, 1971) show quite clearly.

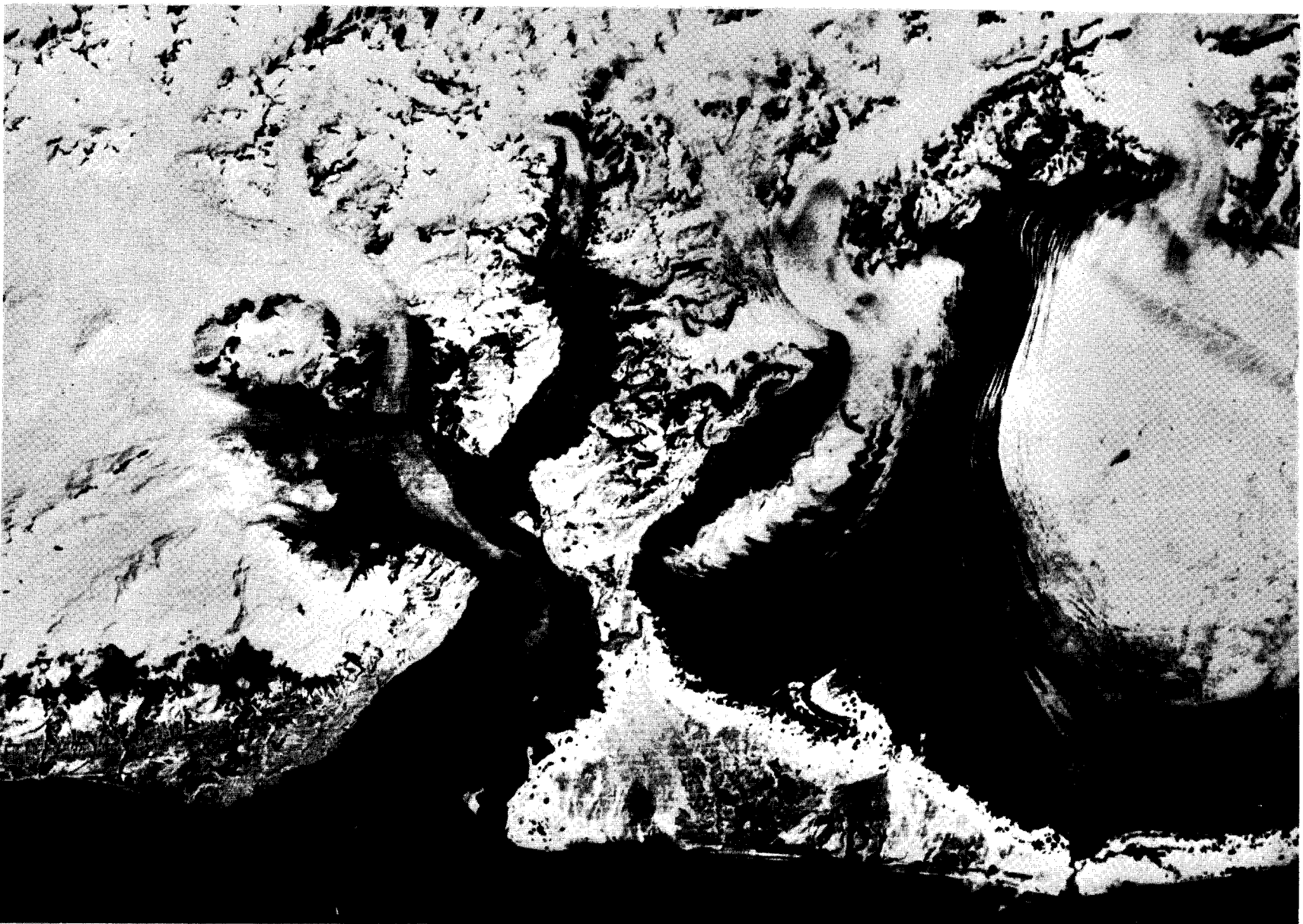


Figure 5. East portion of Icy Cape Foreland adjacent to Icy Bay. Icy Bay airstrip is in the center of the photograph. The Foreland is the site of an active logging operation by Icy Bay Lumber Company. Their dock is at the top center, at the base of the Robinson Mountains. This side of the Bay is open to storm waves from the southeast and thus is an area of high-wave energy.

Photograph taken August 16, 1975.



Figure 6. Beach-spit shoreline in the vicinity of the Icy Bay Lumber Company dock facility.

Dock proper is at top right; supply barge and tug are lying off the end of the dock. Bedrock terrace had been quarried for riprap in an attempt to hold barge used at the outer dock in place during winter storms. The attempt has been somewhat unsuccessful according to local sources (Jerry Wells, personal communication). Sediment transport in the beach zone is up the Bay toward the dock area, resulting in multiple beam-ridge accretion at the bottom left of the photo.

Grounded ice was transported to the beach by wave action from an ice stream in the center of the lower Bay. When ice does penetrate into the lower bay it usually ends up in this area. Some of the deepest depths (70+ m) in the lower Bay occur just off the dock.

Photo taken July 2, 1975.

127



Figure 7. Upper Icy Bay and surrounding icefields. Clockwise from the left, the features are: Kichyatt Point, a bedrock spur; Taan Fiord; an unnamed bedrock plateau; widest single terminus of the Guyot Glacier; Guyot Hills; terminus of the Yahtse Glacier; Yahtse Foreland with rise of Karr Hills behind; Tsaa Fiord; and Kageet Point on the right.

The Yahtse Glacier flows from the upper left and behind Guyot Hills on its way to the Icy Bay.

Ice in the upper Bay was this density approximately 75% of the time during the summer of 1975. Swirling pattern is formed by curving ice streams during alternate flood and ebb-tidal current transport.

Photo taken July 2, 1975.

129

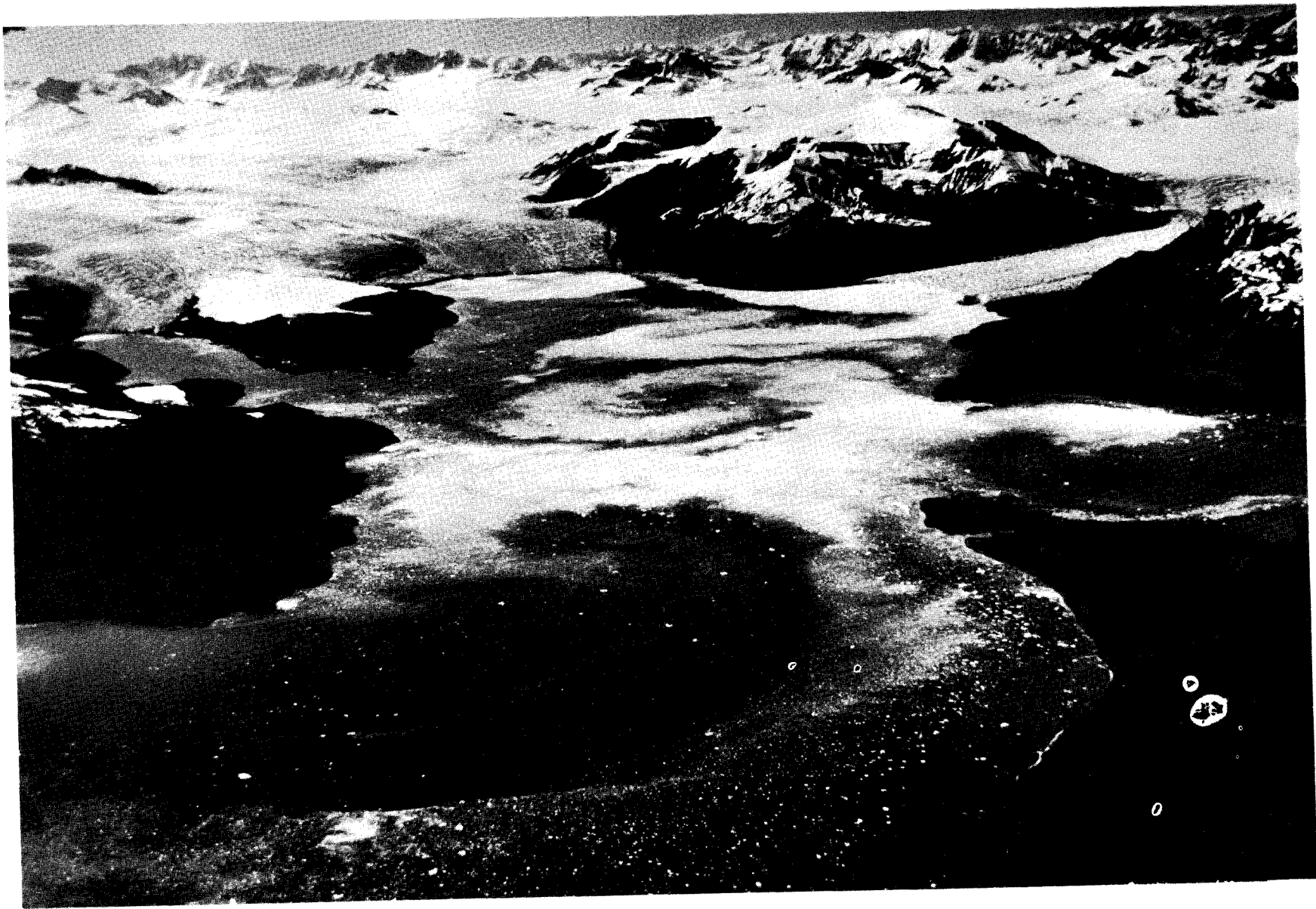


Figure 8. Area underlain by till and bedrock on the east side of Icy Bay north of Caetani Delta.

Taan Fiord shows at the top center, just above Kageet Point, an end moraine complex underlain in part by stagnant ice. The terrain steps down from a spur of the Chaix Hills (top right) to a flat bedrock plateau thinly veneered by ground moraine. The next lower level is a till surface composed of ablation moraine that has undergone mass movement (flowtill) and end moraine. This area may have been unstable in 1957 and possibly underlain by some stagnant ice blocks, but appears stable now (1975). Caetani Delta and associated outwash is just visible at the bottom of the photograph. The road running through the center of the photo was used for oil exploration in the 1950's and 60's. It extends to Chaix Hills airstrip.

Ice is commonly carried by wind or tidal currents into adjacent waters when ice streams project into the central Bay. This photograph represents a fairly typical ice configuration. Scattered soundings indicate up to 40 meters depth of water close to shore, but no detailed bottom profiles were obtained.

Photo taken July 2, 1975.

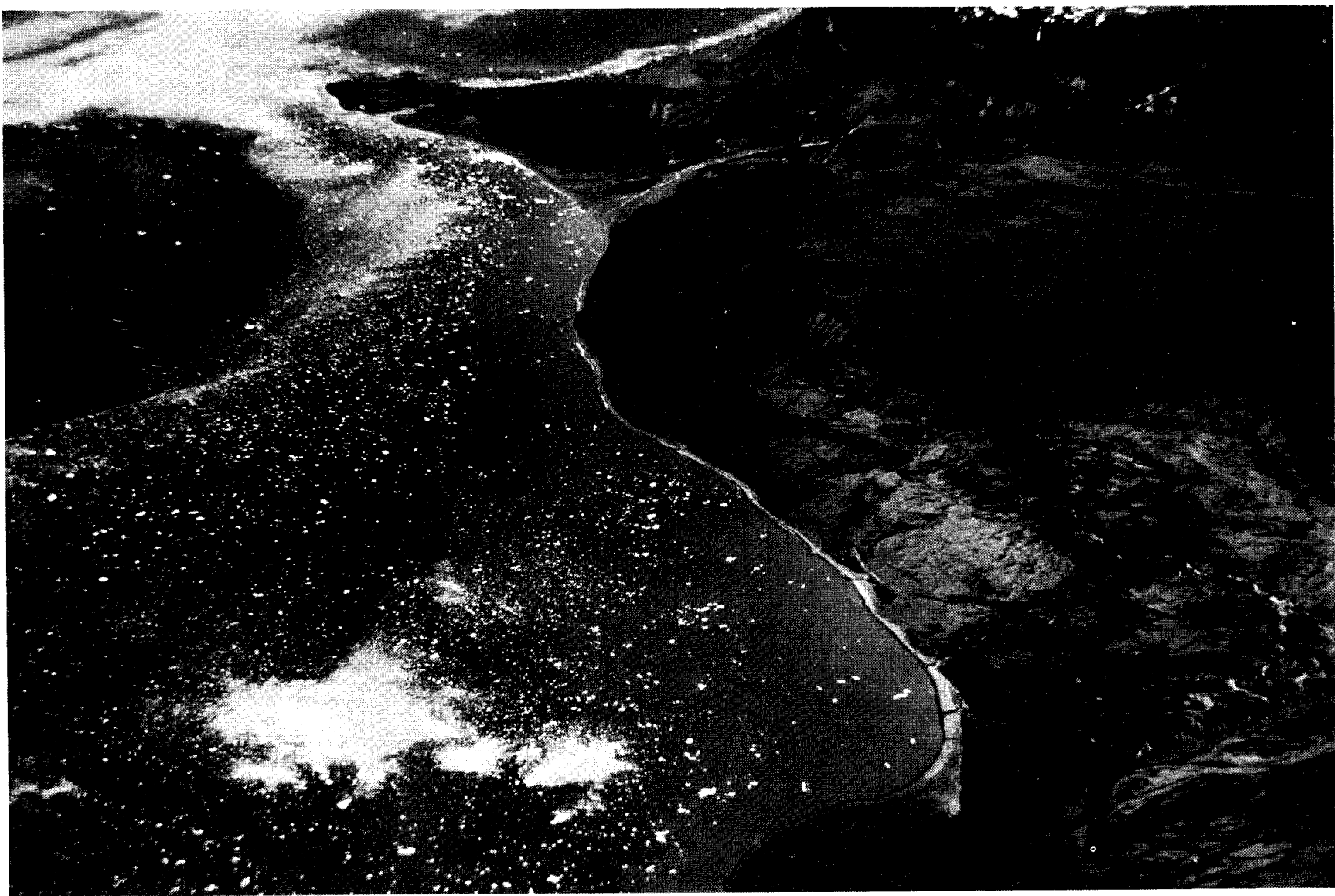
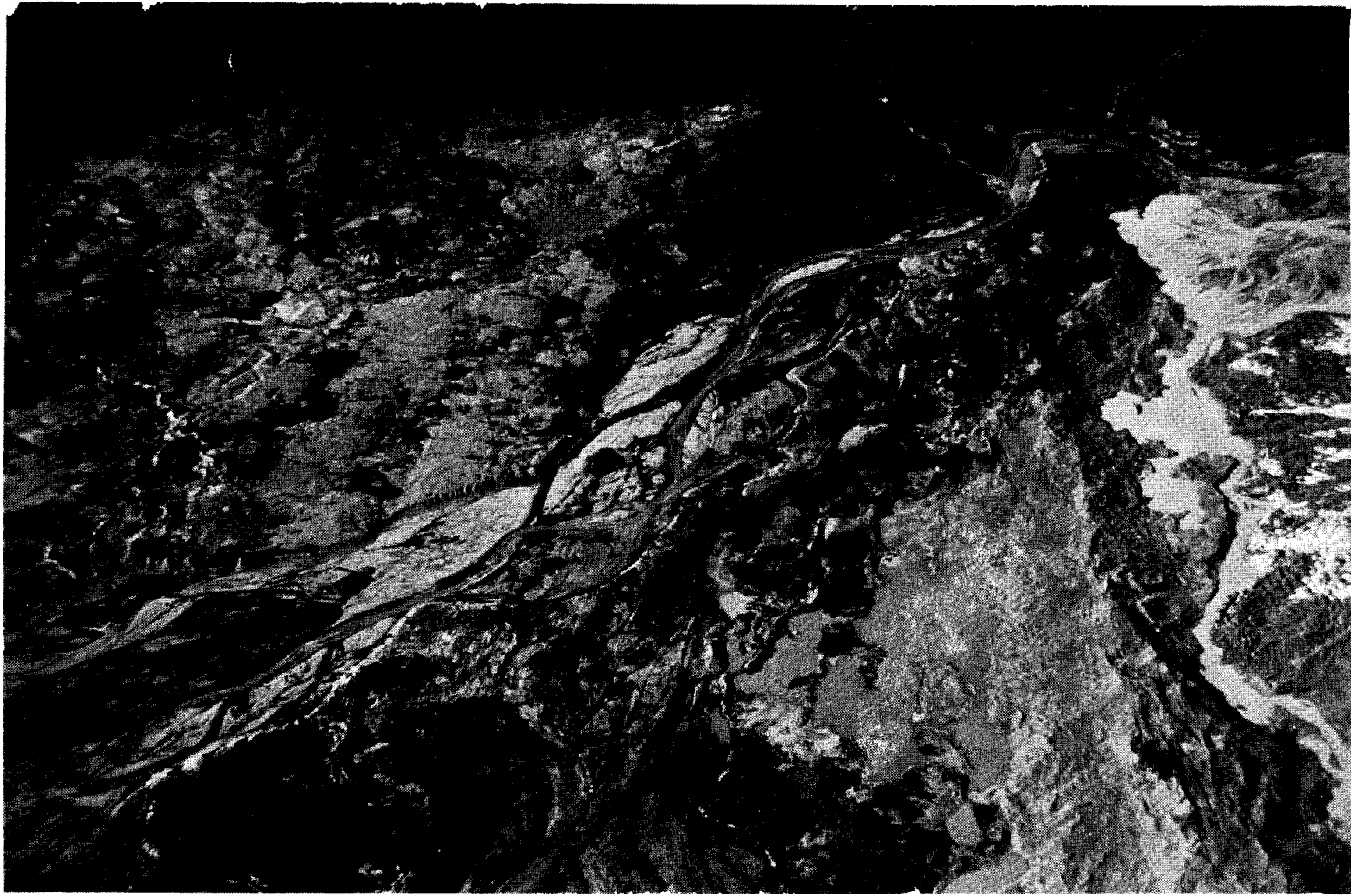


Figure 9. Extreme northwest corner of the West Malaspina Foreland. Agassiz lobe of Malaspina Glacier is along the right side of the photo. Chaix Hills airstrip is in the upper right corner. Present ice-marginal drainage is fed behind a stagnant ice mass and into the New Yahtse River (New Yahtse River not visible in this photo). Breakout floods (jökulhlaups) from the Agassiz Lakes and other ice-marginal lakes would follow this drainage-way. Any overflow would reoccupy the abandoned Caetani River that extends from the top right to bottom left. Till area at the upper left is discussed in Figure 3.

Photo taken July 2, 1975.

133



134

Figure 10. Fan-delta systems on the east side of Icy Bay. From top left to lower right are Kettle-hole Delta, named for the origin of the lagoon in middle of the delta; New Yahtse Delta, the only active delta of the three; and Caetani Delta, abandoned except for small overflow discharge during the height of the meltwater-runoff season. The high, darker, heavily vegetated areas are underlain by till. The lighter, less vegetated areas with the braided pattern are abandoned outwash channels floored with coarse gravel (average clast size greater than 10 cm long axis).

Arrows indicate areas of extensive ground cracking and/or subsidence due to melting of buried ice. This process was active between 1957 and 1975, and is still active in the area at the left center of the photo.

New Yahtse stream is at maximum discharge for the summer melt season. Scattered bay ice is a common occurrence at this locality.

Photo taken July 2, 1975.

135



Figure 11. Cracks, in longitudinal bars composed of coarse outwash gravel, located on the south side of the delta of New Yahtse River. The area is inactive and slightly elevated over the active-stream area at the upper left. The cracks occur in a reticulate pattern, are 2-3 meters wide and not more than a meter deep. They appear old and are areas for preferential growths of shrubs, while the gravel surface is moss-covered. These cracks are not visible on 1957 vertical aerial photography (scale 1:41,900) but may be too small to show at this scale. They are interpreted to be the result of melting of buried ice. It is not known if the process is still active at this locality but ground subsidence did occur between 1957 and 1975 on the adjacent Kettle Hole delta.

Photograph measured about 400 meters across at center. Taken July 10, 1975.

137

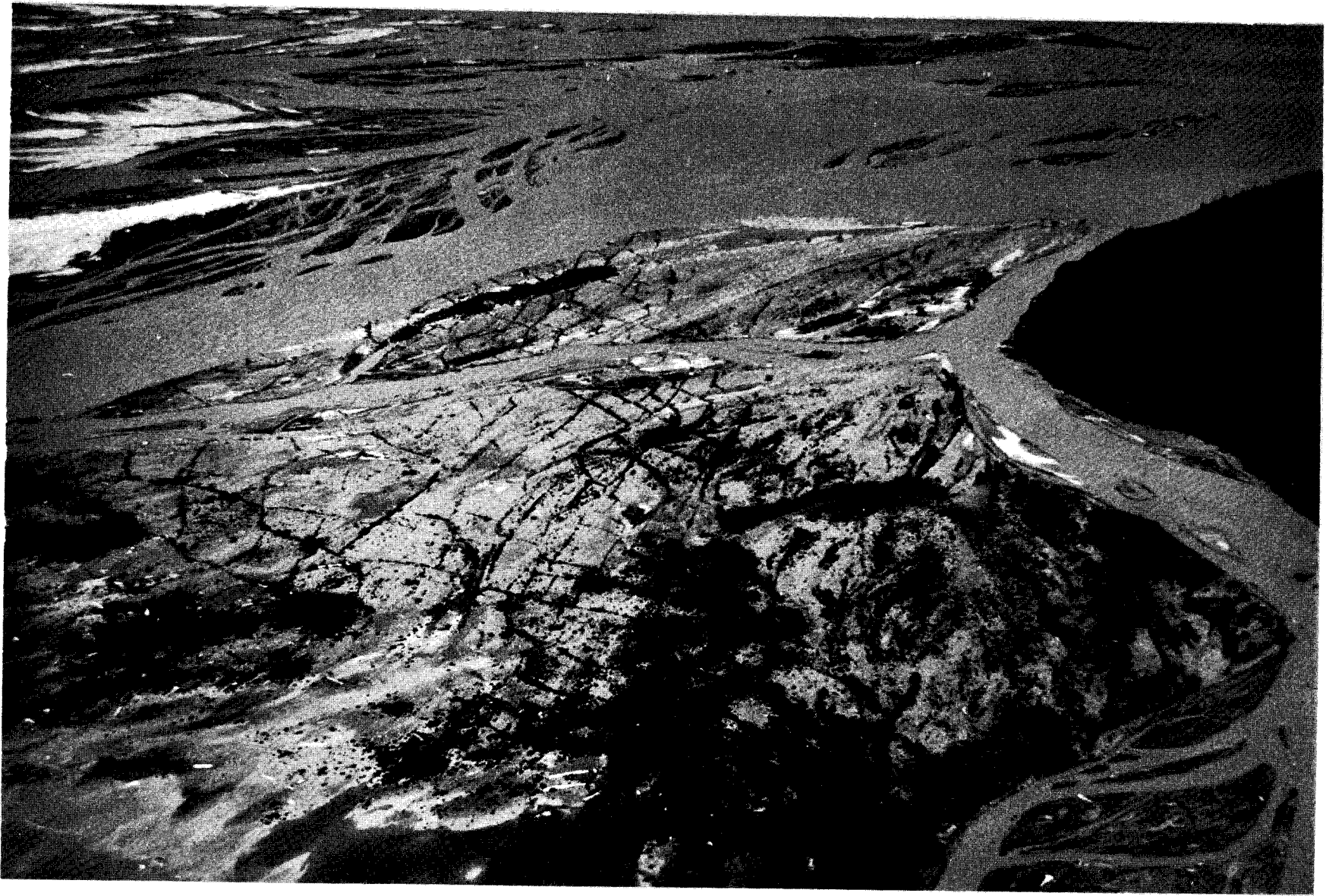


Figure 12. View southwest of central and lower east margin of Icy Bay. Features beginning the top of the photo and proceeding along the bay margin are: Riou spit, enclosing Riou Bay; Moraine Island, actually joined to the mainland by beach-ridge progradation, forming a neck-like protuberance; Seal Camp Harbor, the small, rectangular bay used as a harbor of refuge; various small headlands; Kettlehold Delta, an abandoned fan delta; and New Yahtse Delta, an active fan delta that receives almost all of the meltwater drainage that flows from the Malaspina Glacier margin into Icy Bay. Gull Island is in the right center of the photo. The darker, heavily vegetated terrain is a complex of older moraine and ice-marginal fluvial material deposited along the margin of the former glacial lobe that filled Icy Bay until 1904 (Plafker and Miller, 1958). The ice terminus had receded to the vicinity of Gull Island by 1916 and north of the New Yahtse Delta by 1926 (Post and Plafker, in preparation).

The bay water between Gull Island and the small headlands is shallow with a maximum water depth of 5 meters at lower low water. Water depth off the deltas drops off rapidly to about 50 meters. Scattered drift ice is a common occurrence off the deltas; large accumulations become grounded on the shoals near Gull Island when ice streams penetrate into the lower Bay.

Photo taken July 2, 1975 at about mid-tide.



Figure 13. Seal Camp Harbor on the lower east margin of Icy Bay. Moraine Island is on the right; the low hills and ponds beyond the Harbor are underlain by till; and at the top of the photo are small outwash fans formed when glacial ice occupied Icy Bay. This small bay is used as a harbor of refuge by fishing boats and tugs during storm conditions in the open Gulf of Alaska. It is also used as a base of operation for seismic crews operating in and around Icy Bay; by crab boats; and formerly by seal harvesters. A temporary camp was occupied during the summer of 1975 was on the left (north) side of the Harbor.

The entrance is 600 meters wide, a bottom profile (profile 8) shows a maximum water depth of 13 meters at lower low water. This photo was taken at mid to 3/4 to high tide when the wave-cut platforms off both points flanking the harbor were submerged. Compact basal till is exposed at low tide on the platform beneath the bluffs on Moraine Island.

Photo taken July 2, 1975.



Figure 14. North side of Seal Camp Harbor, with sandy beach at right and wave-cut platform at top of the photo. This platform is illustrated in Figure 15. Abandoned buildings of a former seal-hunters camp are visible in the trees. The large king-crab boat at the left is 11- feet long; the smaller fishing boats are about 50 feet in length. Drift ice rarely occurs inside the Harbor.

Photo taken at low tide on June 21, 1975.

143

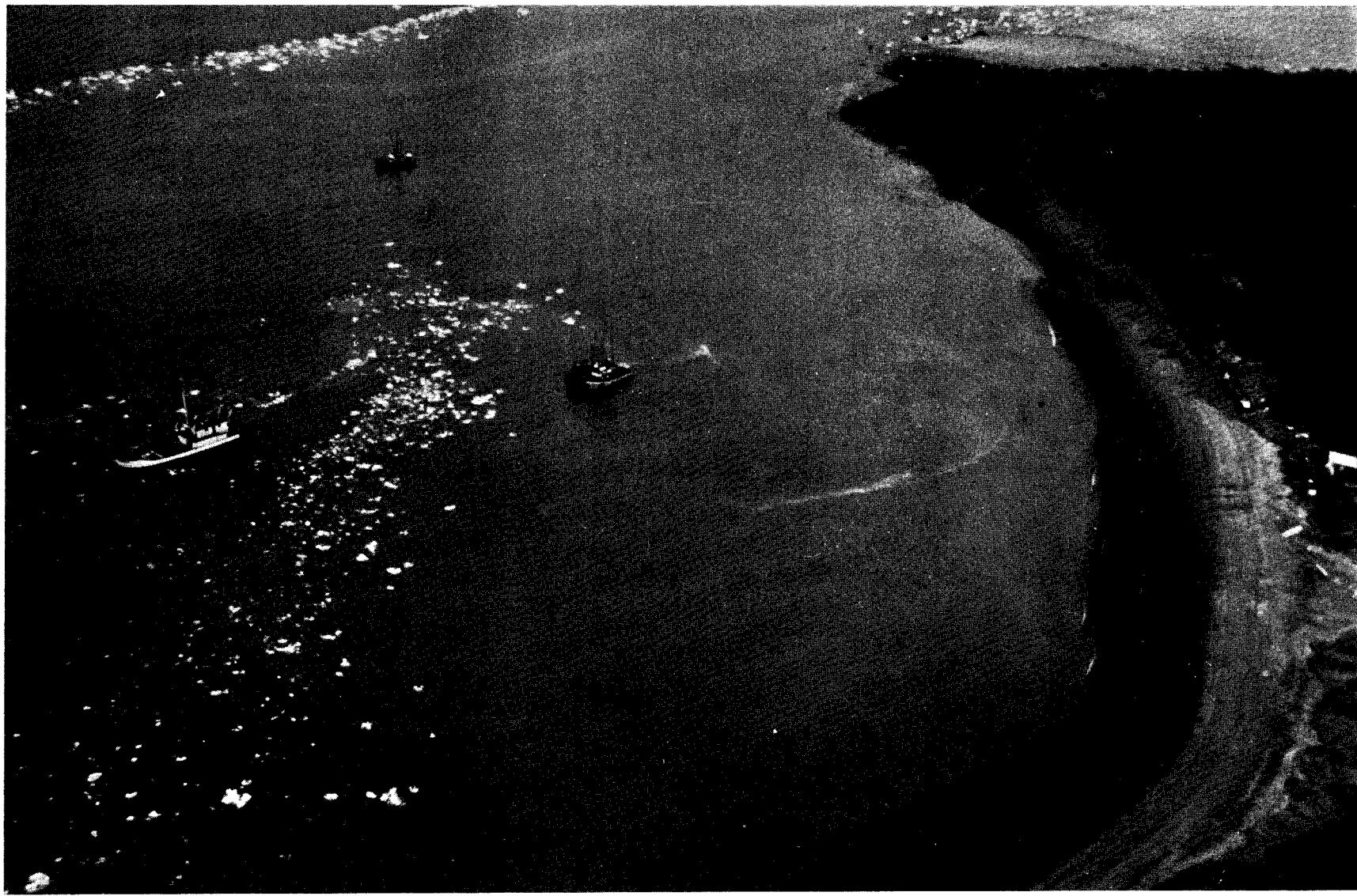


Figure 15. Wave-cut platform and bluffs at the headland on the north side of Seal Camp Harbor.

The eroding bluff is cut in ice-contact fluvial material; large angular ablation-till boulders are scattered over the platform pavement. These ablation-till boulders occur ubiquitously in intertidal, shallow subtidal, and possible deeper subtidal zones near on-shore morainal, and ice-contact, deposits along the east margin of the bay.

Photo taken July 17, 1975.



Figure 16. Riou spit and the southwest margin of the West Malaspina Foreland. Point Riou, where the spit is attached to the Foreland, is at the right center of the photo. The heavily vegetated area beyond the spit is underlain by till and old alluvial fans; the area beyond that is the abandoned Old Yahtse River that was active for some time after the visits of I.C. Russell in 1891 (Russell, 1893). Old Yahtse River is postulated to be the location of the Icy Bay explored by Vancouver in 1794 (Russell, 1894; Plafker and Miller, 1958; Post and Plafker, in preparation). Recurved spits that were built into the old Icy Bay are just visible under the clouds at the top of the photo.

Riou spit is at the end of the drift system that extends from Sitkagi Bluffs. Additional material is being eroded from the till bluffs along Point Riou. Erosion amounts to about 15 meters/year for a total of 250 meters since 1957. The lagoon (Riou Bay) enclosed by Riou spit is less than 2 meters in depth at the entrance on the left, and thus appears unsuitable for an anchorage.

Photo taken July 8, 1975.

147



Figure 17. Cliff cut in basal till just east of Point Riou on the West Malaspina Foreland outer coast. This basal till crops out at or near sealevel at several localities along the east margin of the Bay. It may underly large portions of the wave-cut and shallow subtidal platforms on the east side of Icy Bay.

Photo taken August 9, 1975 at low tide.

149



150

Figure 18. Wave-cut platform of basal till at Point Riou on the outer coast of the West Malaspina Foreland. Felled trees are the result of rapid erosion that has averaged about 15 meters per year from 1957 to 1975, for a total of 250 meters. The platform is scattered with boulders, the larger ones eroded from overlying ablation till, the smaller from the basal till. Waves are breaking on swash bars migrating across the offshore, subtidal extension of the till platform. This basal till is the most resistant to erosion of any glacial deposits exposed along Icy Bay.

Photo taken at low tide on August 10, 1975.

151



Figure 19. View east along the outer coast (Gulf of Alaska) of the West Malaspina Foreland. Features from the top are : Malaspina Glacier (white area at left); dark protuberance of the shoreline is the Fountain Stream fan delta; linear forms are older vegetated barrier spits; light area is Yana Stream; more vegetated barrier spits; left of spits (inland) is a till area with small lakes (Shoal Bay Lakes); bulbous vegetated mass just below and to right of lakes is a complex of recurved spits built into the former Icy Bay of Vancouver; next is Old Yahtse River sediment that has filled the former Icy Bay; and at the bottom, a till complex. Spruce Island is the dark spot in the middle of Old Yahtse River. A white debris line is just visible, extending from Spruce Island toward the bottom of the photo. This marks the landward margin of significant storm-surge flooding. The active barrier spits are unvegetated and are subject to overwash during winter storms (particularly in the Old Yahtse River area). Lagoon outlets shift constantly; these are the summer, 1975 positions.

Photo taken at mid-tide, July 2, 1975.

153



EXPLANATORY TEXTS

TEXT TO ACCOMPANY LOCATION MAP OF ICY BAY AND WEST MALASPINA FORELAND
AREA, NORTHEAST GULF OF ALASKA

The base for this map, and the geologic hazards and processes map, are unpublished 1:63,360 scale topographic maps on a stable base obtained from Austin Post (U.S.G.S., Tacoma, Wash.). Other sources used for control are listed on the map. Provisional names for locations not identified on published maps or on Post's maps are placed in quotes.

The morainal pattern on the Malaspina Glacier is that recorded on 1948-1957 aerial photographs. Continued ice movement has, of course, modified the detail but has not changed the overall pattern. Likewise, the position of sinkhole ponds on the ice changes constantly; but the overall pattern remains similar to that shown on the map. Detail of the ice margin of the Malaspina in the Chaix Hills airstrip-New Yahtse fountain area reflects 1972-1975 ice positions; Seward Lake detail is from July 1, 1974, Landsat imagery.

Icy Bay, north of Kichyatt Point has been remapped by Austin Post (Post and Plafker, in preparation) using aerial photography taken by him and available from the World Data Center, Glaciology, U.S.G.S., Tacoma, Washington. The 1972 shoreline position is shown. Particularly important are the location of various glacier termini. The shoreline of the remainder of Icy Bay generally reflects the mean high water position of 1957, with some modification of the outer part of Riou Spit to a 1975 configuration. Along the outer coast (Gulf of Alaska) the summer, 1975 outlets of the braided-stream systems are plotted. These outlets shift constantly.

Major lakes and ponds on moraine and proflacial deposits are shown; some very small ponds were deleted. Active braided-stream channels also

shift constantly; representative position are shown. The portions of the outwash fans likely to be flooded by extreme high water are delineated by dotted lines. This dot pattern also encompasses some lagoonal areas. Margins of formerly-active fans are shown by dashed lines. Other now-vegetated fans are located between Fountain and Yana Streams and on the Icy Cape Foreland between Big and Little Rivers. These fans are not differentiated from till and bedrock on the map.

Active beach-spit systems are immediately adjacent to the shoreline; older, vegetated systems are shown with beach-ridge trends indicated by dashed lines. Particularly interesting is the large recurved-spit complex built into the former Icy Bay of Vancouver (now the Old Yahtse River).

Till and bedrock are undifferentiated on this map. Also included are various small, fluvial kame and esker deposits.

The larger airstrips are graded gravel or sand (local deposits); the smaller landing areas are available smooth, open areas. The improved strips are capable of handling aircraft at least as large as Twin Otters; the other strips are usable only by Cessna 180 or smaller-sized planes with experienced pilots. Much of the sandy intertidal beachface also can be used for landings.

Photograph locations are shown; viewing areas are within the polygons. Viewing direction is shown by the small arrows; figure numbers are tilted to reflect these directions. The geologic hazards and processes map falls within the dashed lines enclosing the east margin of Icy Bay.

TEXT TO ACCOMPANY PRELIMINARY BATHYMETRIC CHART OF ICY BAY, NORTHEAST
GULF OF ALASKA

This chart is adapted directly from the latest edition of N.O.S. chart 16741, June 1974. Depths are recomputed to meters and contoured where density of data points is great enough. Contours interval is 20 meters except in shallow depths where supplemental 2, 5, 10, and 15 meter contours are added where feasible. Some shore features are modified in vicinity of the deltas along eastern Icy Bay. Names of various geologic and cultural features have been added. Provisional names are used for features not identified on published maps. Bottom-profile track lines are shown and identified by number, with an arrow indicating running direction. Each map and chart is subject to continual modification and updating as work progresses. This chart has an early draft of redefined detail on the New Yahtse and Kettlehole Deltas.

Contouring at the mouth of Icy Bay enhances the large arcuate shoal. This shoal is interpreted to be an end moraine deposited by the Icy Bay lobe of the Guyot Glacier during its last maximum Neoglacial advance (Plafker and Miller, 1958; Miller, 1971; Post and Plafker, in preparation). The shallowest water depths (5, 10, and 15 m contours) represent the probable terminus of the Guyot as viewed by Russell in 1891 (Russell, 1893). The 2 meter contour near Pt. Riou encloses an erosional platform, cut by waves in basal till of the 'clay bluffs'.

Depths in the Bay increase rapidly north of the arcuate ridge; paucity of data does not allow contouring. Interpretation of the bottom profiles is incomplete but they indicate a deep channel on the west side of the Bay and several shallower terraces on the east side of the Bay (see

bottom profiles for amplification). Particularly shallow, is the area east of Gull Island bounded by profiles 7 and 24. Maximum depths at lower low water are less than 5 meters with many shoals exposed at low tide. Another shallow area blocks the entrance to Riou Bay (labeled on location Map); water depth is generally less than 2 meters with large ablation-till boulders scattered about (i.e., Moraine Reef). No profiles were run in Riou Bay.

Seal Camp Harbor, used as a harbor of refuge by fishing boats and as a base for seismic operations in summer 1975, has a maximum depth of 11 meters MLLW across the entrance (Profile 8). By contrast, water depth off the New Yahtse and northern Kettlehole Deltas increases rapidly to 40-50 meters. Deep water is also present north of Caetani Delta, although supporting data are scanty.

In summary, deepest water (up to 70 m) in lower Icy Bay is on the west side, particularly near the Icy Bay Lumber Company dock. Deep water (40-50 m) also occurs off the New Yahtse and northern Kettlehole Deltas (probably Caetani Delta also), and north of Caetani Delta. Almost impassable waters exist east of Gull Island and at the entrance to Riou Bay. Seal Camp Harbor is deep enough (11 maximum) to accommodate moderate-draft ships but is rather cramped for maneuvering.

TEXT TO ACCOMPANY THE ENVIRONMENTAL GEOLOGIC MAP, EAST MARGIN OF ICY BAY,
NORTHEAST GULF OF ALASKA

The base for this map is an uncontrolled photomosaic (2 photos) using vertical aerial photographs taken July 30, 1957. They were enlarged to a scale of 1:10,475, and detail was mapped directly off the photographs. Stereo pairs of the same view, at a scale of 1:41,900, were also used for the initial interpretation. Oblique aerial, and ground, photos taken during the summer of 1975 were used for additional interpretation and to document changes that had occurred since 1957. The shoreline configuration, particularly Point Riou, Riou spit, and the entire intertidal zone was adapted from N.O.S. chart 16741, June, 1974 edition. The end of Riou spit, Kettlehole Delta, and New Yahtse Delta have been further redrafted to conform to 1975 shoreline detail.

The area was mapped in part and field-checked during the summer of 1975, but since this check predated the generation of much of the map from aerial photos, some questions concerning map detail raised by laboratory study are unanswered in this report. Particularly puzzling is the till complex and fans in the vicinity of Point Riou.

The eastern margin of Icy Bay south of Kageet Point can be divided into a number of zones based on various combinations of depositional processes. These processes may be active at present, or have been active in the past. Each process, or combination of processes, can be assigned to a unique depositional system or combination of depositional systems. The deposits or products resulting from the process can also be assigned to a depositional system or environment. The map explanation is organized into a depositional systems framework.

As stated above, the map area may be divided into zones based on a technique similar to that outlined by Hayes and others (1973). The zones from north to south, are:

- 1) Bedrock hills, veneered with till.
- 2) Till plain. Flowtill was dominant in this zone.
- 3) Active and abandoned braided-stream and fan delta systems dissecting a moraine complex.
- 4) Large moraine system with associated ice-marginal fluvial deposits. Gull Island is included. End moraine is important.
- 5) Point Riou moraine and fan complex.
- 6) Riou spit; a beach-spit system.
- 7) Large outwash fan - fan delta system (Old Yahtse River), including the marginal fans on the western boundary of the major system.

Bedrock hills (Chaix Hills area)

This zone extends from Taan Fiord south into the map area to the old road leading to Chaix Hills airstrip. It is lowest portion of the Chaix Hills. The bedrock (BXt), Yakataga Formation of Tertiary age (Plafker, 1967), is veneered with till. The area is heavily vegetated and the till appears stable. This area was not field checked.

Till plain (Chaix Hills area)

The plain is bounded on the north by the Chaix Hills and on the south and east by the Caetani River fluvial-deltaic system. The till apron extending toward Kageet Point, between the bedrock hill and Icy Bay, is included.

Flowtill (Tfi) underlies a large portion of the area, and is most-

ly inactive at the present time. Limited activity usually takes the form of slow downslope creep. The basal till (Tb) exhibits greater stability. End moraine (Tem) is identified on the basis of hilly topography.

The beach system (BSag) is a simple gravel berm subject to overwash during severe storms.

Fluvial-fan delta and moraine complex (New Yahtse River area)

This zone encompasses the Caetani, New Yahtse, and Kettlehole fluvial deltaic systems and various morainal bodies. New Yahtse River is the only active fluvial system; it receives meltwater from a fountain source as well as ice-marginal drainage from the Caetani River system. Changes in the Malaspina Glacier margin due to ice stagnation and disintegration allowed the Caetani drainage to be rerouted into New Yahtse River, sometime between 1969 and 1975. This resulted in the Caetani proglacial channel system and delta being abandoned except for very high flood flows.

Both abandoned and active fluvial-deltaic systems lie between dissected higher till topography, and are also incised into their own older fluvial sequences. This is illustrated by the New Yahtse River. Oldest deposits of the sequence (FAny₄) are highest, and are covered by dense cottonwood and young spruce vegetation. Each successively younger unit is successively lower and has a corresponding less dense vegetation cover. The active fan (FAny₁) and channel (FAny_c) system is shifting slowly and cutting into older outwash and till deposits. The Caetani River has a similar age succession.

The Kettlehole fluvial-deltaic system is also abandoned and is covered by moderate to dense alder and cottonwood growth (FIk). The

abandoned channel (FIu) that intersects the New Yahtse River on the north side may correlate with Kettlehole outwash, but this is not certain. Both of these fluvial surfaces are higher (+6 m) than present active streams, and thus would not be affected by glacier-burst floods.

However, both the New Yahtse and Kettlehole systems have buried-ice localities, with presently-active ground cracking and formation of ponds (LPi) by ground subsidence.

Shoreline systems consist of low gravel spits (BSag), subject to storm overwash, with wide, intertidal, gravel platforms (ITf) seaward of the spits. The gravel platform is an erosional wave-modified terrace on the inactive Kettlehole Delta, but is composed of swash-modified fluvial, longitudinal bars on the active New Yahtse Delta. A grassy area (BSo) subject to overwash is present behind the Kettlehole Delta spits.

The moraine system near the Malaspina Glacier is dominated by large ice masses (SIb and SIV), and active flowtill areas (Tfa), underlain by ice blocks. Lakes (LPa) are developing in this terrain. Separated from this complex by the abandoned fluvial channel (FIu) is an older moraine system that is a combination of basal (Tb) and ablation (Ta) till, as well as end moraine topography (Tem). This linear body probably extended through the present New Yahtse River area and connected with the end moraine south of the river. Vegetation consists of dense cottonwood and young spruce.

Moraine and associated ice-marginal fluvial systems (Seal Camp Harbor area)

The main body in this complex is an elongate till ridge that extends northeast to southwest from east of Kettlehole Delta to Riou Bay. Most

prominent are the low hills of the end moraine (Tem), marking the latest Neoglacial advance of the Icy Bay lobe of the Guyot Glacier (Plafker and Miller, 1958). Extensive bodies of ablation till (Ta) flank the end moraine hills. This till complex includes Gull Island, and the intertidal shoals between Gull Island and the mainland.

Associated with the till are isolated bodies of ice-marginal fluvial sediment (FMu) probably formed when the Icy Bay lobe began retreating from its last maximum advance.

Shoreline systems include both small sandy (BSa_s) and gravel (BSag) berms and sandy, vegetated overwash (BSo). Overwash deposits tie 'Moraine Island' to the mainland. An intertidal gravel platform (ITg) is important in this area. It is a wave-cut erosional feature that is particularly well-defined at the entrance to Seal Camp Harbor, and as shoals east of Gull Island.

Point Riou moraine and fan complex (Pt. Riou area)

This zone is difficult to interpret. It extends south, from the morainal ridge of the last zone, to the Gulf of Alaska. Plafker and Miller (1958) interpret the area as dunes (?), but cliffs along the coast are basal till, overlain by some fluvial sediment; but mainly overlain by till-like material formed into a conspicuous northwest-southeast linear pattern of unknown origin (Tpr). Some fluvial systems are also included in this zone, but interpretation is not yet complete so no further comment will be made at this time.

The shoreline is characterized by an eroding till cliff flanked in a seaward direction by an erosional, till platform. A sandy berm is present in places.

Riou Spit

This large spit is the western terminus of the longshore-drift system that reaches back to Sitkagi Bluffs and Fountain Stream. The bulbous portion is a series of grassy dune ridges (BSv) and unvegetated, multiple berm-ridges (BSa₅). The connection to Point Riou is receding rapidly into Riou Bay due to berm erosion and active overwash during winter storms.

Old Yahtse River fluvial-deltaic system

Old Yahtse River, and included marginal fans, is bounded on the northeast by the Malaspina Glacier and on the west by the long morainal ridge of the Seal Camp Harbor area. This system is unique in that it is the only fluvial system in the map area that does not, or did not, discharge into Icy Bay. The crest of the morainal ridge marks a drainage divide. The small fountain at the apex of the Old Yahtse fan marks the drainage divide at that location. Meltwater from this fountain flows into the New Yahtse River.

The upper Old Yahtse is a sloping gravel plain (Floy) with pronounced bar and channel topography. It is well drained and covered with dense cottonwood and young spruce growth. Average maximum clast size at the New Yahtse Airstrip is about 15 cm.

TEXT TO ACCOMPANY THE GEOLOGIC HAZARDS AND PROCESSES MAP, ICY BAY AND
WEST MALASPINA FORELAND AREA, NORTHEAST GULF OF ALASKA

The base is the same as that used for the Location Map, refer to the text that accompanies that map for further explanation, concerning this type of information.

This map represents an interpretive summary of data presented on the other maps, in the figures, and in the main body of the report. The geologic hazards and processes deemed important for consideration are:

- 1) Glacier-burst floods (jökulhlaups)
- 2) Glacier surges
- 3) Buried ice blocks and stagnant ice masses
- 4) Unstable ground (onshore and subtidal)
- 5) Coastal erosion
- 6) Drift ice from actively calving glaciers

Glacier-burst floods

The solid arrows indicate subglacial and ice-marginal drainage-ways that can carry floodwater from emptying ice-marginal lakes. Post and Mayo (1971) present data on glacier-burst flooding that includes the West Malaspina Foreland. The interpretations given here differ slightly from theirs.

The flood waters from Oily Lake drain subglacially beneath the large medial moraine that forms the boundary between the Agassiz and Seward lobes of the Malaspina Glacier. The major discharge emerges at the fountain of Yana Stream, and through a tunnel 7 km west of the Yana.

Other points where Oily Lake flood water emerges are: 5 km west of Yana Stream, and probably at the deltas in Seward Lake. Landsat imagery taken July 1, 1974 shows Oily Lake almost empty, but it had begun to refill in July 1975.

Proglacial drainage-ways for Oily Lake water are down Yana Stream and into the Shoal Bay Lakes. Flood water from the Shoal Bay area escapes back into Yana Stream, or if discharge is large enough, into the stream just east of the old recurved spit complex. Old Yahtse lagoon would probably not be flooded because high discharges tend to breach the active barrier-spit immediately in front of the flooded area (based on observations in Iceland).

Many of the Shoal Bay lakes can be seen to be clouded with suspended sediment on the Landsat images, (July, 1974) and they remained that way through the summer of 1975.

Flood water from Seward Lake drains down Fountain Stream. A possible subglacial channel for Oily Lake water is beneath the lower Agassiz lobe to a small fountain 2 km south of New Yahtse fountain, and from there into the New Yahtse system.

Drainage from the Agassiz Lakes is postulated to follow a subglacial path around the corner of the Chaix Hills and into the marginal Caetani River system. Flow is diverted along the Malaspina Glacier and into the New Yahtse River. Overflow would reoccupy the proglacial Caetani River. Kettlehole Delta would not be flooded because the New Yahtse channel is incised (+6 m) below the abandoned Kettlehole fluvial-channel system.

Glacier Surges

The western Malaspina Glacier is characterized by a passive to stag-

nant, disintegrating ice margin that is debris-covered and may be vegetated. The only exception is in the vicinity of the Chaix Hills airstrip. Here, the margin of the Agassiz lobe shows a history of fluctuation (oblique aerial photography, Post, 1963, 1964, 1969, 1972; Boothroyd, 1975). The margin was stagnant and disintegrating in 1969 but had advanced and developed a steep terminus by 1972. This terminus was debris-free and steeply sloping when visited in 1975. However, this advance is not a surge.

The Icy Bay lobe of the Guyot Glacier has undergone a number of catastrophic advances and retreats during Neoglacial time that are excellently detailed by Post and Plafker (in preparation). The position of the terminus at the height of the last Neoglacial advance (1904), lay on the shoals at the mouth of Icy Bay. Retreat began soon after and the margin had receded to Gull Island by 1916 (Brooks and others, 1916) and to Kichyatt Point by 1938 (Post and Lachapelle, 1971). The ice margin was at Kageet Point in 1957 (vertical aerial photos) and thereafter separated into the 3 component glaciers, Tyndall, Yahtse, and Guyot. The ice-margin shown on the map represents the 1972 position as mapped by Post.

All three ice sheets are still receding. A readvance is possible, but it probably would not be nearly as rapid as the retreat. Short-term surges are possible, but a very large volume of ice would be required to push the margin south of Kageet Point.

Buried ice blocks and stagnant ice masses

Large stagnant ice masses presently exist on the Yahtse Foreland; east of Kageet Point; and along the Malaspina Glacier margin between Caetani and New Yahtse River. The ice is debris-covered and appears as

hilly, hummocky topography.

Ground cracking and subsidence has recently occurred on the Kettlehole and New Yahtse Deltas. It is occurring at present at the junction of the New Yahtse and Kettlehole fluvial channels, and between the small fountain (2 km south of New Yahtse) and the New Yahtse River. This process is the result of melting of buried ice blocks. Ground subsidence due to melting of buried ice is distinguished from flow-till activity, on, and around, stagnant ice masses, by a greater intensity of the latter process.

Unstable Ground

This category includes mass movement of flowtill, either in the form of creep or debris-flow; and catastrophic slumping of fan-delta fronts.

Presently-active flowtill processes occur on most of the Yahtse Foreland; around the stagnant ice mass east of Kageet Point; and around the lakes in front of the Malaspina margin, between New Yahtse and Caetani Rivers.

The steep fronts of the northern part of Kettlehole Delta, New Yahtse Delta, and Caetani Delta may be subject to catastrophic slope failure as a normal depositional process.

Possible slump blocks can be seen on the bottom profiles run off the deltas. The entire delta front could fail during a severe earthquake, similar to what occurred at Valdez during the 1964 earthquake.

An additional aspect of ground stability, not evaluated in this report is the relative stability, or instability, of unconsolidated sediment over the entire West Malaspina Foreland during a severe earthquake.

Eyewitnesses reported ground cracking and sand fountaining at the Old Yahtse River during the 1958 Lituya Bay earthquake. This earthquake could be a possible explanation for the ground cracking on the New Yahtse Delta. These cracks appear quite similar to some observed on the Valdez River Delta that did result from ground shaking in 1964.

Coastal erosion

Coastal erosion, particularly on the outer coast, is not a specific topic of this part of the study but is included because of its effect on the character of the terrain around Point Riou. The shoreline as of 1957 map was transferred from the base map, the 1975 shoreline was compiled from the 1974 N.O.S. chart and 1975 field observations. During this interval (1957-1975) the bluffs at Point Riou receded about 15 meters/year for a total of over 250 meters.

An extensive erosional-till platform has been developed and it extends into the shallow subtidal zone.

Drift ice

The major source of ice in Icy Bay is from Yahtse Glacier and from Guyot terminus adjacent the Guyot Hills. Lesser amounts are contributed by Tyndall Glacier and the Guyot lobes ending in Tsaa Fiord. The largest iceberg observed during the summer of 1975 measured 50 by 50 by 6 meters (projecting above the sea surface). Most bergs are much smaller, averaging about 10 by 10 by 2 meters and smaller. Small ice chunks (1 by 1 meter), that float just at the water surface are ubiquitous adjacent to ice streams, and are a hazard to small boats.

The ice-stream position shown on the map is typical and approximates

that seen on July 1, 1974 Landsat imagery. Selected Landsat images taken during various seasons in 1972, 1973, and 1974, show a similar ice configuration. Observations during the summer of 1975 (aerial and ground) indicate that heavy ice is the rule in the upper Bay. Ice is carried into the mid and lower Bay at intervals of uncertain periodicity, but about every 7-12 days. Tidal currents, as well as wind, appear to play an important role in the ice movement.

Once in the mid and lower Bay, ice is dispersed from the main stream to 3 major locations. In decreasing order of importance, these are: 1) Gull Island; 2) north of Caetani Delta; and 3) the beach south of Icy Bay Lumber Company dock. The ice then breaks up and melts within several days.

General

Various features such as, the location of bedrock adjacent to the Bay margin, the general character of the Foreland around Seal Camp Harbor, and known deep and shallow-water areas in the Bay, are indicated on the map.

EXPLANATORY TEXT TO ACCOMPANY THE BOTTOM PROFILES

These profiles were obtained using a Bludworth EM-130SS bottom profiler mounted on a 5 meter Zodiac rubber boat. Tracklines are shown on the preliminary bathymetric map. All profiles were run at constant boat speed; chart speed was varied for different profiles for resolution purposes. Mean lower low water and mean high water lines on each diagram were calculated from standard tide tables. No tide gauge records were available. The xerox reproduction has introduced a slight distortion in some profiles. Actual data reduction is done using the original profiles.

Analysis of the profiles is incomplete, thus discussion will be limited to a few comments on various bottom morphologies or geographic areas.

Deep-water areas: Profiles 1, 2, 6, 10, 11, 13, 14, 15, 19, 20, 21, 22, and 23).

Locations: Off Icy Bay Lumber Company dock; in front of Caetani, New Yahtse, and northeast of Kettlehole Deltas.

Shallow-water areas: Profiles 3, 4, 6, 7, 9, 23, and 24).

Locations: East of Gull Island; entrance to Riou Bay; directly off Point Riou and Icy Cape.

Present Harbor: Profile 8).

Location: Seal Camp Harbor.

APPENDICES

APPENDIX I.

Weather data and drift-ice observations

| Date | Time | Wind (m/sec) | | Temp °C | Hum | Pres MB | Precipitation (mm) | | | Cloud Cover (Elev M) | | | Vis. Km | Conditions | Bay Ice | | | Remarks | |
|---------------|------------------|--------------|-----|------------|-----|------------|--------------------|------------------|---------------------|----------------------|----------------|----------------|------------|------------|---|-----------------------------|-----|--|---------------------|
| | | Speed | Dir | | | | 06 ⁰⁰ | 20 ⁰⁰ | Tot Past 24 Hrs. | Low Elev % | Med. Elev % | High Elev % | | | Intensity | Location U M L | | | |
| 15 June | 08 ⁰⁰ | Calm | | -- | --- | -- | | N | N | 200m | OC | | | .4-7 | Drifting Fog | Heavy | x x | Ice Grounded East Side of Bay | |
| | 20 ⁰⁰ | 2.5 | 265 | -- | --- | -- | N | | | 450 | SC | 1800 | Br .4 | | Bright Sun Over Bay | | | | |
| 16 | 08 ⁰⁰ | 1.5 | 000 | -- | --- | -- | | N | N | | | 900 | OC | | >25 | Blue Sky Over Guyot Glacier | Mod | x | No New Ice East Bay |
| | 20 ⁰⁰ | 2.5 | 270 | -- | --- | -- | N | | | 600 | OC | | | >25 | OC Over Bay & Malaspina Glac. | | | Mountains Clear | |
| 17 | 08 ⁰⁰ | 3.5 | 350 | -- | --- | -- | | N | N | 600 | OC | | | >25 | Top of Mt. St. Elias Clear | Heavy | x | Some Ice West Side of Bay | |
| | 20 ⁰⁰ | 2.5 | 270 | -- | --- | -- | N | | | 600 | Br .6 | 2400 | SC | >25 | | Light | x | Grounded Ice | |
| 18 174 | 08 ⁰⁰ | 2.5 | 340 | 11.0 | 87 | 1017.5 | | N | N | 200 | OC | | | 8 | Fog | Heavy | x | Ice Moving Down Bay | |
| | 20 ⁰⁰ | 2.5 | 270 | 10.5 | 94 | 1010 | N | | | Clear | | | | >25 | 600 OC, BR Malaspina Glac. & Icy Cape | | | | |
| 19 | 08 ⁰⁰ | 1.0 | 350 | 8.0 | 100 | 1011 | | 1.3 | 1.3 | 450 | OC | | | 8 | Fog, L-M Rain | | | | |
| | 20 ⁰⁰ | 2.5-3.5 | 240 | 7.5 | 100 | 1011 | 3.0 | | | 200 | OC .9 | 900 | .9 | <1.5 | Fog, L Rain | Heavy | x | Isolated Lq. Bergs Off Kettle Hole & Yahtse | |
| 20 | 08 ⁰⁰ | 1.0 | 065 | 6.8 | 93 | 1010 | | 0.6 | 3.6 | 300 | OC | | | 12 | L Rain | | | | |
| | 20 ⁰⁰ | 2.5 | 010 | 6.0 | 90 | 1012.5 | 6.9 | | | 300 | SC | 1500 | OC | 20-25 | VL Rain | Heavy | x | Ice Streaming Down Center of Bay | |
| 21 | 08 ⁰⁰ | 0-1.5 | 315 | 7.0 | 84 | 1013.5 | | N | 6.9 | 600 | SC .1 | | | >25 | Lenticular Cloud Mt St Elias & Mt. Cook | Heavy | x x | Ice Choked Middle & West Side | |
| | 20 ⁰⁰ | Calm | | 9.5 | 86 | 1015 | N | | | 300 | SC | 900 | OC | | Fog Over Bay VL Rain | | | *Aerial Photos, Bay Ice 10 ⁰⁰ -11 ⁰⁰ | |

| Date | Time | Wind (m/sec) | | Temp °C | Hum | Pres MB | Precipitation (mm) | | | Cloud Cover (Elev M) | | | Vis. Km | Conditions | Bay Ice | | | Remarks |
|---------|------------------|--------------|-----|------------|-----|------------|--------------------|------------------|---------------------|----------------------|------|--------------|------------|------------|--------------------------------|--------------|-----|--|
| | | Speed | Dir | | | | 08 ⁰⁰ | 20 ⁰⁰ | Tot Past 24 Hrs. | Low Elev | % | Med. Elev | | | % | High Elev | % | |
| 22 June | 08 ⁰⁰ | Calm | | 7.5 | 89 | 1012.5 | 0.2 | 0.2 | | | 1100 | OC | | >25 | | | | |
| | 20 ⁰⁰ | 1.5 | 350 | 9.0 | 78 | 1013 | N | | | | 1100 | OC | | >25 | | | | |
| 23 | 08 ⁰⁰ | 2.5-3.5 | 060 | 6.8 | 90 | 1007.5 | 4.8 | 4.8 | | | 900 | OC | | 3-12 | L Rain Showers | Heavy | x x | Grounded Ice East Side of Bay |
| | 20 ⁰⁰ | 2.5-4.5 | 040 | 7.5 | 84 | 1002 | 1.8 | | | | 900 | OC | | 5-15 | L Rain Showers & Fog | Mod | x | Isolated Lg Bergs |
| 24 | 08 ⁰⁰ | 2.5-4.5 | 035 | 7.8 | 86 | 1002 | 6.8 | 8.6 | | | 1100 | OC | | 5-12 | L-M Rain Showers | | | |
| | 20 ⁰⁰ | 1.0 | 040 | 10.0 | 80 | 1005.5 | 1.3 | | | 900 | SC | 1800 | OC | — | | Mod | x | Lg Grounded Bergs Bird Is. & Shoals |
| 25 | 08 ⁰⁰ | 0.5 | 000 | 7.5 | 85 | 1008 | N | 1.3 | | | 1400 | BR | .4 | >40 | | | | |
| | 20 ⁰⁰ | 2.5 | 020 | 10.0 | 97 | 1012 | 2.4 | | | <100 | OC | | | .5-1.0 | Fog & M Rain | | | *Bay Ice Photos Bird Is. |
| 26 | 08 ⁰⁰ | 1.0 | 000 | 7.0 | 95 | 1013 | 3.3 | 5.7 | | 200 | BR | 450 | OC | 5 | Fog & L Rain | | | |
| | 20 ⁰⁰ | 0.5 | 240 | 11.8 | 80 | 1011.5 | N | | | 450 | SC | 1200 | SC | >40 | 450 OC Over Malaspina Glac. | | | |
| 27 | 08 ⁰⁰ | 1.5 | 350 | 8.5 | 83 | 1010 | N | N | | 600 | SC | | +6000 SC | | | Light | x | Little Ice in Lower Bay |
| | 20 ⁰⁰ | Calm | | 11.2 | 86 | 1011 | N | | | 300 | SC | | +6000 SC | >40 | +Good Cirrus Inc, L Fog on Bay | | | |
| 28 | 08 ⁰⁰ | 1.5 | 005 | 8.5 | 83 | 1012.5 | N | N | | 30 | OC | | | <0.5 | Heavy Fog | | | |
| | 09 ³⁰ | | | | | | | | | 300 | OC | | | 8 | Fog Lifting | | | |
| | 16 ⁰⁰ | | | | | | | | | | | | +6000 BR | >40 | Cirrus Only | | | |
| | 20 ⁰⁰ | 0.5 | 000 | 11.0 | 88 | 1013 | N | | | 60 | OC | | | 3 | Heavy Fog | Light | x | No New Ice in Middle Bay Isolated Lg Bergs |

| Date | Time | Wind (m/sec) | | Temp °C | Hum | Pres MB | Precipitation (mm) | | | Cloud Cover (Elev M) | | | Vis. Km | Conditions | Bay Ice | | | Remarks |
|---------|------------------|--------------|-----|---------|------|---------|--------------------|------------------|------------------|----------------------|-----------|-----------|---------|------------|------------------------------|----------|-------|------------------------------|
| | | Speed | Dir | | | | 08 ⁰⁰ | 20 ⁰⁰ | Tot Past 24 Hrs. | Low Elev | Med. Elev | High Elev | | | Intensity | Location | U M L | |
| 29 June | 08 ⁰⁰ | 1.5 | 050 | 8.8 | 80 | 1015 | | N | N | 600 | OC | | | 15-20 | | | | |
| | 20 ⁰⁰ | 1.5 | 080 | 12.5 | 77 | 1017 | N | | | | | 900 | Br | | | | | *Aerial Photos Bay Ice, 1500 |
| 30 | 08 ⁰⁰ | 2.5 | 100 | 8.9 | 93 | 1012.5 | | 6.5 | 6.5 | 60-150 | OC | | | 1-3 | L-M Rain Showers | | | |
| | 20 ⁰⁰ | 3.5 | 050 | 7.7 | 97 | 1010 | 29.7 | | | 150 | OC | | | 3 | M-H Rain | | | |
| 1 July | 08 ⁰⁰ | 2.5-3.5 | 060 | 9.0 | 94 | 1008 | | 42.3 | 72.0 | 150 | OC | | | 3 | L Rain Showers | | | |
| | 20 ⁰⁰ | 4.5-5.5 | 055 | 8.9 | 90 | 1009 | 12.7 | | | | | | | — | | | | |
| 2 | 08 ⁰⁰ | 0.5-1.5 | 000 | 8.0 | 89.5 | 1012 | | 0.3 | 13.0 | 450 | SC .1 | | | >25 | | | | |
| | | | | | | | | | | 900 | SC .4 | 1700 | OC | | | | | |
| | 10 ³⁰ | | | | | | | | | | | 1700 | BR | | | | | |
| | 20 ⁰⁰ | | | 11.1 | 73 | 1011 | N | | | Clear | | | | >40 | | Heavy | x | *Aerial Photos Bay Ice |
| 3 | 08 ⁰⁰ | 1.5-2.5 | 055 | 10.8 | 74 | 1012 | | N | N | 450 | SC | 1500 | OC | | | M-L | x | Ice Back Up Bay |
| | 20 ⁰⁰ | 0.5-1.5 | 055 | 11.0 | 96 | 1012 | 17.0 | | | <100 | OC | | | 1-3 | M-H Rain Showers; Began 1600 | | | |
| 4 | 08 ⁰⁰ | 0.5-1 | 105 | 8.2 | 96.5 | 1017 | | 6.1 | 23.1 | 450 | SC | 750 | OC | | L Rain Showers | | | |
| | 20 ⁰⁰ | | | | | | | | | 450 | OC | | | 3-8 | Mod Rain Showers | | | |
| 5 | 08 ⁰⁰ | | | 6.0 | 94 | 1022.5 | | | 5.8 | | | | | — | | | | |
| | 20 ⁰⁰ | 0.5 | 000 | 11.0 | 75 | 1023 | N | | | Clear | | | | 40 | 450 SC Over Malaspina Glac. | | | |

176

| Date | Time | Wind (m/sec) | | Temp °C | Hum | Pres MB | Precipitation (mm) | | | Cloud Cover (Elev M) | | | | Vis. Km | Conditions | Bay Intensity | Ice Location U M L | Remarks |
|--------|------------------|--------------|-----|---------|-----|---------|--------------------|------------------|---------------------|----------------------|-----------|-----------|-----------|---------|---|---------------|-----------------------|--|
| | | Speed | Dir | | | | 08 ⁰⁰ | 20 ⁰⁰ | Tot Past 24 Hrs. | Low Elev | Med. Elev | High Elev | Low % | | | | | |
| 6 July | 08 ⁰⁰ | Calm | | 9.5 | 90 | 1023 | | N | N | < 30 | OC | | | 2-30 | Ground Fog Broken Tops 300 | | | |
| | 20 ⁰⁰ | Calm | | 10.5 | 92 | 1022 | N | | | < 30 | OC | | | < 0.5 | Heavy Fog | | | |
| 7 | 08 ⁰⁰ | 0.5 | 305 | 9.4 | 92 | 1018 | | N | N | | | +6000 | Br .5 | > 40 | Some Ground Fog in Bay | Light | x x | Little Ice In Bay |
| | 20 ⁰⁰ | Calm | | 13.0 | 58 | 1012.5 | N | | | | | +6000 | SC .2 | > 40 | Some Ground Fog In Bay SC Cirrus | | | |
| 8 | 08 ⁰⁰ | Calm | | 10.5 | 80 | 1010 | | N | N | | | +6000 | SC | > 40 | Cirrus Some Haze | Heavy | x | Tongue of Ice Bngng to Move Down West Bay |
| | 20 ⁰⁰ | 2.0-3.5 | 020 | 19.8 | 48 | 1012.5 | N | | | | | +6000 | SC | > 40 | Lenticular Cloud Mt. Augus- ta, Fog Mouth of Bay | Heavy | x x | Ice Moving Dn Bay with Ebb Tide to Bird Island |
| 9 | 08 ⁰⁰ | 1.0 | 240 | 12.0 | 82 | 1015 | | N | N | | | 3600 | SC .4 | > 40 | Cirrocumulus Top Mt. St. Elias in Clouds | Heavy | x x | *Ice Photos from Bird Is. Ice Grounded at Lum- ber Co Dock & Bird Is. H Wind & Tide Moved Ice Spring Tide |
| | 20 ⁰⁰ | 3.5 | 015 | 14.0 | 61 | 1013 | N | | | | | 3000 | SC .3 | > 40 | Cirrocumulus | | | |
| 10 | 08 ⁰⁰ | 0.5 | 350 | 12.0 | 67 | 1012 | | N | N | Clear | | | | > 40 | | | | *Aerial Photos of Bay Ice |
| | 20 ⁰⁰ | 2.0 | 020 | 15.0 | 59 | 1013 | N | | | | | +6000 | SC <.1 | > 40 | | | | |
| 11 | 08 ⁰⁰ | 2.5 | 040 | 10.5 | 82 | 1015 | | N | N | 750 | OC | | | > 30 | Clear Over High Mountains | | | |
| | 20 ⁰⁰ | 0.5-1.5 | 070 | 9.1 | 97 | 1017 | 1.8 | | | 450 | OC | | | 8 | L Rain and Fog, Rain Began 1530 | | | |
| 12 | 08 ⁰⁰ | Calm | | 7.5 | 90 | 1015 | | N | 1.8 | 300 | SC | 1800 | Br .7 | 30 | Cloud Deck Over Malaspina Glac. | | | |
| | 20 ⁰⁰ | 1.5 | 290 | 10.0 | 80 | 1010 | N | | | 300 | OC | | | G | Fog, Rain Be- ginning | | | |

177

| Date | Time | Wind (m/sec) | | Temp °C | Hum | Pres MB | Precipitation (mm) | | | Cloud Cover (Elev M) | | | Vis. Km | Conditions | Bay Ice | | Remarks | | | |
|---------|------------------|-----------------|-----|------------|-----|------------|--------------------|------------------|---------------------|----------------------|-----------|--------------|------------|------------|--|-------------------|---------------------------|-------|----------------------------------|--|
| | | Speed | Dir | | | | 08 ⁰⁰ | 20 ⁰⁰ | Tot Past 24 Hrs. | Low Elev | Med. % | High Elev | | | Intensity | Location U M L | | | | |
| 13 July | 08 ⁰⁰ | Calm | | 8.5 | 94 | 1009 | | 21.2 | 21.2 | 600 | BR | | | >40 | H Rain Past 12 Hrs Storm Breaking Up | | | | | |
| | 20 ⁰⁰ | Calm | | 13.8 | 70 | 1009 | N | | | | | 3000 | Br .6 | 30 | | | | | | |
| 14 | 08 ⁰⁰ | 0.5 | 345 | 10.5 | 80 | 1005 | N | N | | | 1500 | Br .8 | | 30 | | Heavy | x | x | | |
| | 20 ⁰⁰ | | | 10.0 | 73 | 1002 | N | | | | | | | 30 | | M-L | | x | | |
| 15 | 08 ⁰⁰ | | | 8.0 | 97 | 1001 | | 12.5 | 12.5 | 750 | OC | | | 25 | | | | | | |
| | 20 ⁰⁰ | 3.5-4.5 | 100 | 12.0 | 88 | 1001 | 9.1 | | | 750 | OC | | | < 8 | M Rain Showers Strong Wind at Night, 8 | | | | | |
| 16 | 08 ⁰⁰ | 1.5-2.5 | 040 | 10.0 | 93 | 1001 | | 6.4 | 15.5 | 850 | OC | | | 12 | L Rain | | | | | |
| | 20 ⁰⁰ | 0.5 | 005 | 10.0 | 95 | 1002 | 0.5 | | | | | 1800 | OC | >25 | | Heavy | x | | Heavy Ice Upper Third of Bay | |
| 17 | 08 ⁰⁰ | Calm | | 9.0 | 90 | 1002 | | N | 0.5 | | | 1800 | Br .8 | +3000 | Br | >25 | OC Over Bay | Heavy | x | Some Lg Bergs Near Bird Is, Most In Upper 1/3 of Bay |
| | 20 ⁰⁰ | 0.5 | 000 | 12.2 | 71 | 1002.5 | N | | | | | 1800 | SC | +6000 | SC | — | Fog @ 300 Forming Rapidly | Heavy | | x |
| 18 | 08 ⁰⁰ | 1.5-2.5 | 035 | 10.0 | 83 | 1002 | | N | N | | | | | 30 | Fog Mouth of Bay | Heavy | | x | Much Ice Mid Bay Around Bird Is. | |
| | 20 ⁰⁰ | Calm | | 14.0 | 81 | 1004.5 | N | | | | | 1100 | SC | 1600 | OC | 30 | VL Rain | | | |
| 19 | 08 ⁰⁰ | Calm | | 9.5 | 92 | 1005 | | 5.8 | 5.8 | 300 | SC | 1100 | SC | 1800 | OC | | | | | |
| | 20 ⁰⁰ | 2.5 | 000 | 10.0 | 95 | 1008.5 | 2.0 | | | | | 1100 | OC | | | 1-8 | Mod Rain Showers and Fog | | | x |

178

| Date | Time | Wind (m/sec) | | Temp °C | Hum | Pres MB | Precipitation (mm) | | | Cloud Cover (Elev M) | | | Vis. Km | Conditions | Bay Ice | | Remarks | | | |
|---------|------------------|--------------|-----|---------|------|---------|--------------------|------------------|------------------|----------------------|--------|-------------|---------|------------|----------------------------|----------------|-------------------------|--|---|----------------------|
| | | Speed | Dir | | | | 08 ⁰⁰ | 20 ⁰⁰ | Tot Past 24 Hrs. | Low Elev | Med. % | High Elev % | | | Intensity | Location U M L | | | | |
| 20 July | 08 ⁰⁰ | 1.0 | 000 | 8.0 | 89 | 1009 | | 1.0 | 3.0 | 300 | SC | 1100 | OC | — | | | | | | |
| | 20 ⁰⁰ | | | | | | 0.25 | | | 800 | OC | | | — | Showers at Base of Mts. | | | | | |
| 21 | 08 ⁰⁰ | 1.0 | 000 | 7.5 | 91 | 1007.5 | | 0.55 | 0.8 | 400 | SC | 1100 | OC | 25 | | | | | | |
| | 20 ⁰⁰ | 1.0 | 000 | 10.0 | 85 | 1012 | 2.5 | | | 600 | BR | 1200 | OC | 25 | Scattered M Rain Showers | | | | | |
| 22 | 08 ⁰⁰ | 1.5-2.5 | 020 | 8.0 | 82.5 | 1012 | | 2.6 | 5.1 | 300 | SC | 900 | Br .8 | | | Mod | x | Some Lg Bergs In Mid Bay | | |
| | 20 ⁰⁰ | | 020 | 13.0 | 59 | 1010 | N | | | | | 6000 | SC | >30 | | Heavy | x | Ice Tongue Bgng to Move Dn Bay Opposite Kichyatt Point | | |
| 23 | 08 ⁰⁰ | 1.5-2.5 | 000 | 10.2 | 68 | 1001 | | 0.5 | 0.5 | | | 2000 | OC | | L Rain Showers | | | Aerial Photos of Bay Ice | | |
| | 20 ⁰⁰ | 2.4-3.5 | 060 | 11.0 | 98 | 1000 | 11.2 | | | 300 | OC | | | 3-12 | M-H Rain Showers & Fog | Mod | x | Lg Bergs In Mid Bay | | |
| 24 | 08 ⁰⁰ | 2.5-3.5 | 080 | 9.0 | 86 | 1002.5 | | 5.6 | 16.8 | | | 1100 | SC | 1800 | OC | 15 | L Rain Showers | Light | x | Few Lg Bergs Mid Bay |
| | 20 ⁰⁰ | 2.5 | 040 | 10.0 | 85 | 1002 | 1.5 | | | | | 1100 | OC | | 12 | L Rain Showers | | | | |
| 25 | 08 ⁰⁰ | 2.5-3.5 | 060 | 10.0 | 80 | 1003 | | 0.5 | 2.0 | | | 1100 | Br .5 | 1800 | OC | | L-M Rain Shrs Scattered | Light | x | Few Lg Bergs Mid Bay |
| | 20 ⁰⁰ | 1.0 | 050 | 10.0 | 78 | 1005 | 1.0 | | | | | 1100 | Br .8 | 1800 | OC | | L Rain Showers | | | |
| 26 | 08 ⁰⁰ | Calm | | 11.0 | 76 | 1002 | | 0.3 | 1.3 | Clear | | | | >40 | 600 SC Over Malaspina Glac | Light | x | Few Lg Bergs Mid Bay | | |
| | 20 ⁰⁰ | 1.0 | 020 | 13.0 | 66 | 1003 | N | | | | | 2700 | Br .5 | >25 | | Heavy | x x | Ice at Kichyatt Pt; SC Bergs Mid Bay | | |

6.7.9

| Date | Time | Wind (m/sec) | | Temp °C | Hum % | Pres MB | Precipitation (mm) | | | Cloud Cover (Elev M) | | | Vis. Km | Conditions | Bay Intensity | Ice Location U M L | Remarks | | | |
|---------|------------------|--------------|-----|---------|-------|---------|--------------------|------------------|------------------|----------------------|----|-----------|---------|------------|----------------------------|---------------------------------------|--|--|---|----------------------------------|
| | | Speed | Dir | | | | 08 ⁰⁰ | 20 ⁰⁰ | Tot Past 24 Hrs. | Low Elev | % | Med. Elev | | | | | | % | High Elev | % |
| 27 July | 08 ⁰⁰ | | | 9.0 | 86 | 1005 | | N | N | 900 | Br | .5 | | | >25 | 200 SC near Chaix Hills | Heavy | x | Ice Tongue Just Past Kichyatt Point | |
| | 20 ⁰⁰ | Calm | | 9.3 | 94 | 1007.5 | 0.4 | | | 300 | OC | | | 15 | L Rain & Fog | | | | | |
| 28 | 08 ⁰⁰ | Calm | | 9.0 | 85 | 1009 | | 0.6 | 1.0 | 900 | OC | | | 30 | 100 BR Over Malaspina Glac | Heavy | x | Ice Tongue to Icy Bay Lumber Co Dock, West Bay | | |
| | 20 ⁰⁰ | Calm | | 9.8 | 83 | 1010 | 0.25 | | | 300 | OC | | | 25 | | Heavy | x | Ice Tongue turning to ward Kettle Hole Delta, East Side of Bay | | |
| 29 | 08 ⁰⁰ | 1.0 | 000 | 11.1 | 78 | 1013 | | N | 0.25 | | | 1500 | Br | .9 | | 30 | | Heavy | x | Ice Drifting to East Side of Bay |
| | 20 ⁰⁰ | 2.5 | 040 | 11.0 | 80 | 1012 | N | | | 900 | OC | | | 30 | | | | | | |
| 30 | 08 ⁰⁰ | 4.5-6.0 | 070 | 9.0 | 90 | 1007.5 | | 7.4 | 7.4 | 100 | OC | | | 3 | M Rain & Fog | Heavy | x | Ice Spreading Over Entire Mid Bay | | |
| | 20 ⁰⁰ | | | 10.0 | 97 | 1010 | 8.4 | | | 100 | OC | | | 2-3 | M Rain & Fog | Heavy | x x | Dense Ice of Yahtze & Caetani Deltas | | |
| 31 | 08 ⁰⁰ | 1.5-2.5 | 020 | 8.0 | 93 | 1011 | | 17.5 | 25.9 | 300 | SC | 900 | OC | | 8-12 | L Rain Shows | | | | |
| | 20 ⁰⁰ | 1.0 | 020 | 10.0 | 95 | 1015 | 5.3 | | | | | 1200 | OC | | 15 | L Rain & Fog | | | | |
| 1 Aug | 08 ⁰⁰ | 1.0 | 000 | 8.0 | 95 | 1015 | | 0.5 | 5.8 | | | 1800 | OC | | 25 | 900 SC Over Icy Cape | Light | x x | Little Ice In Bay | |
| | 20 ⁰⁰ | | | 11.4 | 76 | 1015 | N | | | | | | | +6000 | SC | >30 | Snow Plume Mt St Elias Good SC Over Icy Cape | Light | x x | Almost No Ice In Bay |
| 2 | 08 ⁰⁰ | 1.0 | 020 | 8.3 | 80 | 1015 | | N | N | 900 | SC | .1 | | | >25 | Sc Near Mtns | Heavy | x | Much Ice Yahtse Glac to Kickyatt Point | |
| | 20 ⁰⁰ | Calm | | 12.5 | 72 | 1014 | N | | | | | Clear | | | >30 | 300 SC Over Icy Cape & Malaspina Glac | Heavy | x x | Ice Tongue into Mid Bay *Aerial Photos of Bay Ice | |

180

| Date | Time | Wind (m/sec) | | Temp °C | Hum | Pres MB | Precipitation (mm) | | | Cloud Cover (Elev M) | | | Vis. Km | Conditions | Bay Intensity | Ice Location U M L | Remarks |
|-------|------|--------------|-----|---------|------|---------|--------------------|------|------------------|----------------------|-------------|-------------|---------|---------------------------------------|---------------|--------------------|---|
| | | Speed | Dir | | | | 0800 | 2000 | Tot Past 24 Hrs. | Low Elev % | Med. Elev % | High Elev % | | | | | |
| 3 Aug | 0800 | Calm | | 8.0 | 88 | 1012.5 | | N | N | Clear | | | >25 | 600 SC Over Icy Cape & Malaspina Glac | | | |
| | 2000 | 0.5-1.0 | 000 | 14.5 | 62 | 1011 | N | | | | +6000 SC | | >25 | | Heavy | x | Ice Tongue Curled up to Yahtse Delta *Aerial Photos of Bay Ice |
| 4 | 0800 | Calm | | 11.5 | 66 | 1004 | | N | N | Clear | | | >40 | | Heavy | x x | Bay Choked with Ice |
| | 2000 | 2.5 | 015 | 13.0 | 59 | 1002 | N | | | Clear | | | >40 | | | | |
| 5 | 0800 | Calm | | 11.2 | 65 | 1000 | | N | N | | 5200 SC | 6000 OC | | Cloud Cover Overspread @ 0400 | | | |
| | 2000 | 1.5 | 045 | 11.0 | 86 | 1000 | 0.8 | | | 600 SC | 1500 OC | | 12-15 | L Rain Shrs Began @ 1300 | | | |
| 6 | 0800 | Calm | | 7.0 | 90 | 1001 | | 1.0 | 1.8 | Clear | | | >40 | Clouds Off-shore | Mod | x | Lg Bergs Near Deltas Main Pack Thinning |
| | 2000 | Calm | | 11.5 | 68 | 1002 | N | | | | 6000 | | >25 | Fog Patches | Heavy | x x | Giant Berg from Glac near Quoyot Hills |
| 7 | 0800 | 1.5-2.5 | 050 | 9.0 | 90 | 1003.5 | | T | T | 600 SC | 1500 BR | 2400 BR | 25 | | Light | x | Ice Gone from Mid Bay Back to Upper Bay? |
| | 2000 | 2.5-3.0 | 050 | 11.0 | 92.5 | 1007.5 | 1.3 | | | | 1100 Br .9 | | 15 | L Rain Shrs., Scattered | | | |
| 8 | 0800 | 2.5 | 050 | 9.0 | 91 | 1008.5 | | 0.7 | 2.0 | 750 OC | | | 11 | | | | |
| | 2000 | 2.5 | 050 | 10.0 | 91 | 1008 | 3.6 | | | | 1100 OC | | 12 | L Rain Shrs. | | | |
| 9 | 0800 | 1.0 | 020 | 8.0 | 96 | 1007 | | 6.1 | 9.7 | | 1200 OC | | 25 | VL Rain Shrs | | | |
| | 2000 | 1.0 | 020 | 9.2 | 78 | 1005.5 | 0.25 | | | | 1500 Br .7 | | 30 | | Mod | x x | Narrow Ice Tongue Past Bird Is close to Is. |

181

| Date | Time | Wind (m/sec) | | Temp °C | Hum | Pres MB | Precipitation (mm) | | | Cloud Cover (Elev. M) | | | Vis. KM | Conditions | Bay Ice Intensity Location | Remarks | |
|--------|------------------|-----------------|-----|------------|-----|------------|--------------------------------------|--------------------------------------|---------------------|-----------------------|--------------|--------------|------------|------------|-------------------------------|--|---------------------------------------|
| | | Speed | Dir | | | | 08 ⁰⁰ 20 ⁰⁰ | 20 ⁰⁰ 08 ⁰⁰ | Tot Past 24 Hrs. | Low Elev | Med. Elev | High Elev | | | | | % |
| 10 Aug | 08 ⁰⁰ | Calm | | 7.0 | 93 | 1008.5 | | N | 0.25 | 900 | Br .8 | +1800 | OC | | 25 | 450 SC Near Chaix Hills | Giant Berg Aground on Yahtse Delta |
| | 20 ⁰⁰ | 0.5 | 000 | 9.8 | 81 | 1011 | | N | | 600 | SC | 1500 | Br .8 | | | | |
| 11 | 08 ⁰⁰ | 1.5 | 040 | 7.0 | 95 | 1015 | | | 3.6 3.6 | 100 | OC | | | 2 | Mod Rain & Fog | Giant Berg Still Aground | |
| | 20 ⁰⁰ | 1.5 | 045 | | | | | | 11.9 | | | 1100 | BR | 25 | Rain Ended @ 1800 | Giant Berg Broken into Smaller Berg | |

NOTE: BIRD ISLAND = GULL ISLAND

SC - SCATTERED
BR - BROKEN
OC - OVERCAST

U - UPPER
M - MID
L - LOWER

APPENDIX II

Reprint:

Boothroyd, Jon C., and Ashley, Gail M., 1975, Processes, bar morphology, and sedimentary structures on braided outwash fans, northeast Gulf of Alaska: p. 193-222 in McDonald, B.C. and Jopling, A. V. ed., Glaciofluvial and glaciolacustrine sedimentation, Soc. Econ. Paleontologists and Mineralogists Spec. Pub. No. 23, 320 pp.

PROCESSES, BAR MORPHOLOGY, AND SEDIMENTARY STRUCTURES ON BRAIDED OUTWASH FANS, NORTHEASTERN GULF OF ALASKA¹

JON C. BOOTHROYD² AND GAIL M. ASHLEY³

Department of Geology and Geography, University of Massachusetts, Amherst

ABSTRACT

The Scott and Yana outwash fans on the northeastern Gulf of Alaska exhibit a succession of facies from glacier terminus to tidewater that are each characterized by differences of gradient, clast size, bar morphology, and sedimentary structures. The upper fan has steep gradients (as much as 17.6 m/km), large maximum clast size (>10 cm), and longitudinal bars. The midfan has gentler gradients (2 to 6 m/km), clast size ranging from less than 10 cm to sand, and predominantly longitudinal bars. The lower fan, a sand area, has gradients less than 2m/km, longitudinal and linguoid bars in braided reaches, and point and lateral bars in meandering reaches.

The longitudinal bars of the upper fan consist mainly of well imbricated, poorly sorted gravel that have clast long-axes oriented transverse to the flow direction. Bars are often covered with transverse ribs, here interpreted as an upper flow regime bedform, and perhaps as relict antidunes. The midfan area is characterized by a decrease in gravel, with a corresponding increase in sand. Sand is deposited as flat upper regime beds interbedded with gravel and as lower regime megaripples in channels forming trough cross-beds. The longitudinal bars of the lower fan show planar cross-beds formed by migration of the bar slipface topped by flat beds on the bar-surface and low-angle ripple-drift cross-lamination. Linguoid bars exhibit large-scale planar to tangential cross-beds topped by ripple-drift cross-lamination. Point and lateral bars are characterized by large-scale planar to trough cross-beds caused by migration of the bar surface and bar slipface. Overbank deposits of silty sand ripple-drift cross-lamination and draped lamination increase in importance downfan.

Stream regimen is governed by early summer flooding. Measurements taken during a rising stage and a declining stage indicate gravel movement in channels on the upper fan (bars were mostly emergent), but little gravel movement on the midfan. Megaripple migration in midfan channels and linguoid-bar migration on the lower fan continue at low flow stages.

INTRODUCTION

The Scott and Yana outwash fans are located on the northeastern Gulf of Alaska, the Scott on the western side of the Copper River Delta, and the Yana on the West Malaspina Foreland (fig. 1). These two fans are within the area delineated as a glacial outwash plain shoreline by Hayes and others (1972), and were chosen for study because they represent a contrast in distal fan margins, even though they appear similar in their proximal areas. This paper is a part of a broader study of outwash plain and shoreline environments of the Gulf of Alaska depositional basin, and is an extension of a report on coarse-grained sedimentation on the Scott outwash fan (Boothroyd, 1972). The present study compares and contrasts environments of deposition of the coarse and fine-grained facies of both fans.

GENERAL MORPHOLOGY AND FACIES DISTRIBUTION

Previous work in the Platte River by Smith (1970) allows the identification of proximal-distal environments on the basis of grain size and bar morphology, among other parameters.

Rust (1972a, p. 221) stated that the Donjek River is proximal, as are the glacial braided streams studied by Krigström (1962) and Fahnestock (1963), whereas the lower Brahmaputra River (Coleman, 1969) and the Tana River (Collinson, 1970) are distal. The Scott and Yana outwash fans contain both proximal and distal facies that are similar to those described by Fahnestock (1969) for the Slims River.

Scott Outwash Fan

The Scott outwash fan extends 25 km to tidewater from the Scott Glacier terminus, ending in intertidal mudflats behind barrier islands of the Copper River Delta (fig. 2A). Sediments of the fan partially fill the valley formerly occupied by the Scott Glacier. The Heney Range (fig. 3A) forms the western boundary of the fan; to the east, Scott outwash sediments merge with those of the Sheridan outwash fan (fig. 2A). The facies map (fig. 2A) shows coarse gravel (>10 cm long axis) extending 8 km from the glacier terminus, grading to finer gravel, and then to sand 16 km from the ice front. Extensive vegetation is present from the fine-gravel area

¹ Manuscript received June 15, 1973.

² Present address: Department of Geology, University of South Carolina, Columbia, SC 29208.

³ Present address: Department of Geological Sciences, University of British Columbia, Vancouver.

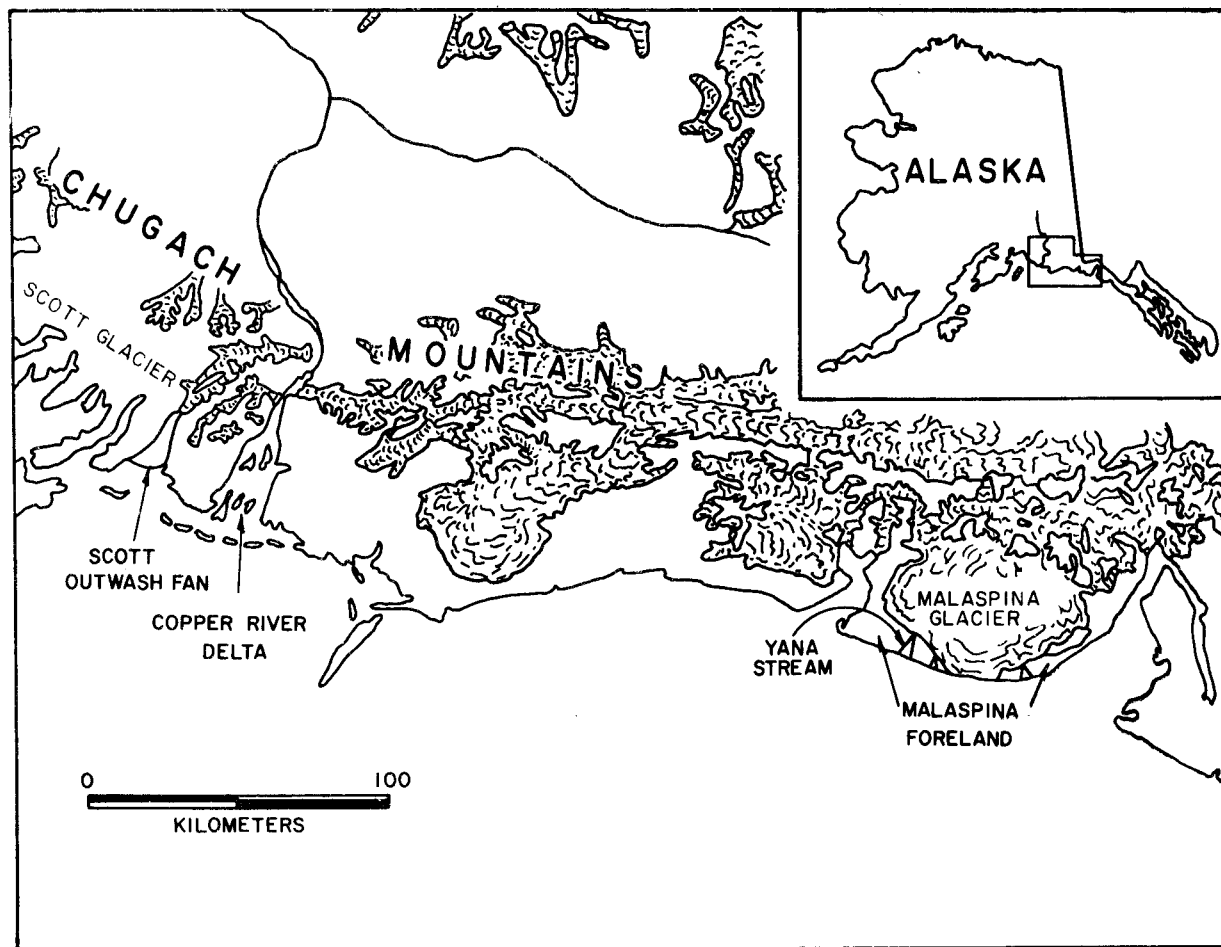


FIG. 1.—Location map of the Scott and Yana outwash fans on the northeastern Gulf of Alaska.

seaward, with active streams occupying only 10 percent of the fan area. Streams on the lower 4 to 5 km of the fan are meandering, not braided, and flow is confined between natural levees. The streams flow through an extensive marsh area for the last 3 km.

Yana Outwash Fan

The Yana outwash fan extends 8.5 km seaward from the Malaspina Glacier and ends at a barrier spit (fig. 3B). The facies map (fig. 2B) shows a distribution pattern similar to that of the Scott: an unvegetated coarse-gravel area that grades to fine gravel, where vegetation is well established in interstream areas, followed by a sand facies. No marsh is present, however, and each facies is compressed longitudinally in comparison to the Scott fan. One major difference contributing to this variation in distal fan margins is that the Scott fan terminates in a protected area behind extensive barrier islands, whereas the Yana fronts on an open coast with a strong drift component. This active longshore drift moves much of the sand toward the west,

and the stream itself turns and flows parallel to and behind the spit, finally discharging into the sea 15 km west of the main body of the fan. Both of these fans may be termed fan deltas in the terminology of McGowen (1970, p. 1) who states that "fan deltas are alluvial fans grading into an adjacent body of water."

STREAM HYDROLOGY

Seasonal Discharge

Discharge on the Scott and Yana fans is controlled by seasonal weather variations over the ablation zones of the Scott and Malaspina Glaciers respectively, and to a lesser extent by local rainfall in the immediate drainage area. Discharge is very low in the winter, rises rapidly in late May and early June to a flood peak in late June, and subsides slowly to a low level again in the fall. This pattern is similar to that of the Donjek (Rust, 1972a, p. 223; Williams and Rust, 1969, p. 649). Short-term fluctuations in discharge also may result from summer temperature variations. Prolonged warm weather causes

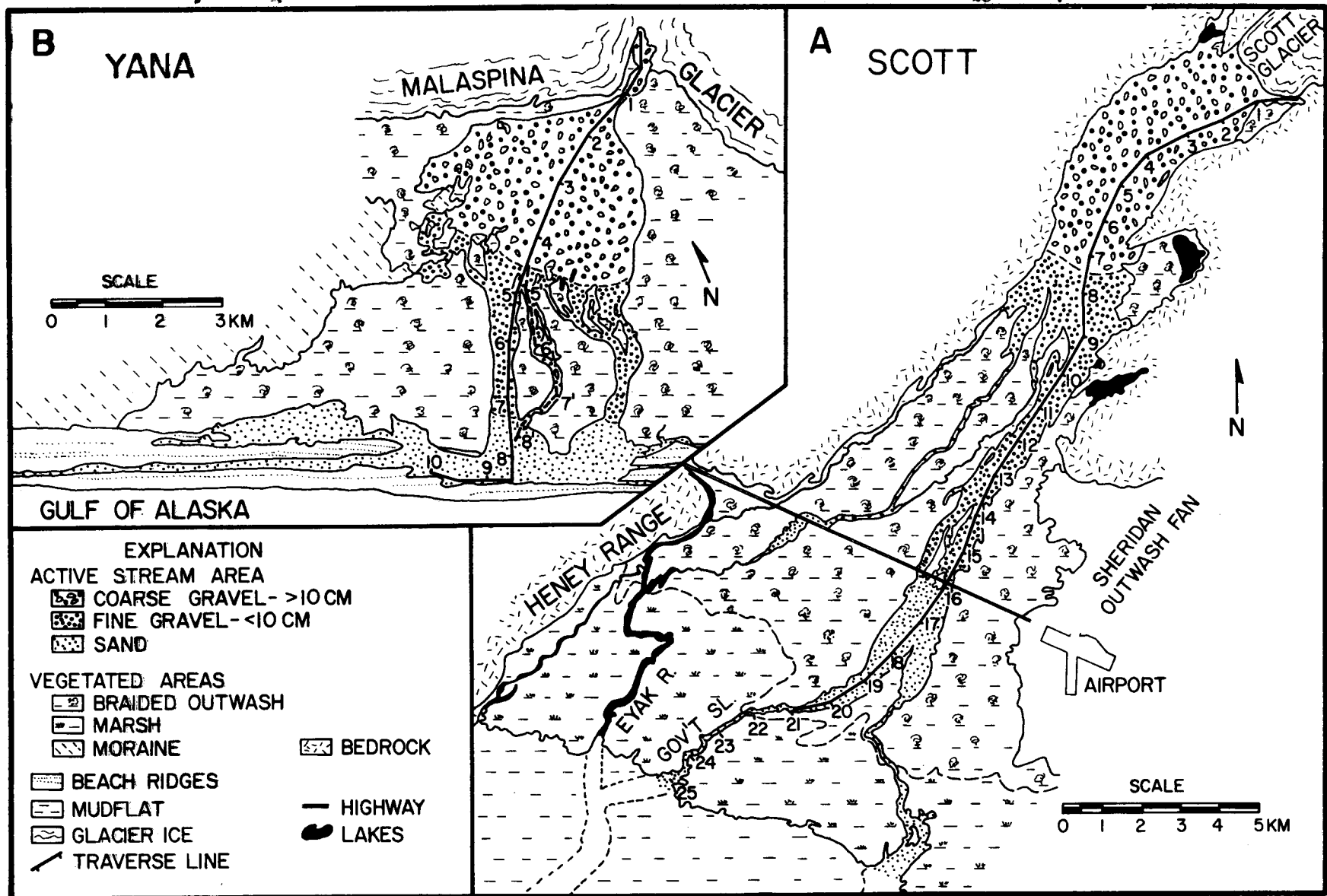


FIG. 2.—Distribution of facies on the outwash fans, with largest clast size plotted for the unvegetated areas. Sample and theodolite traverses are shown by the solid lines. Numbers are distance in km from source. A, Scott outwash fan. B, Yana outwash fan. Dashed line shows the traverse to measure stream parameters (fig. 6) where it varies from the theodolite and sample traverse.

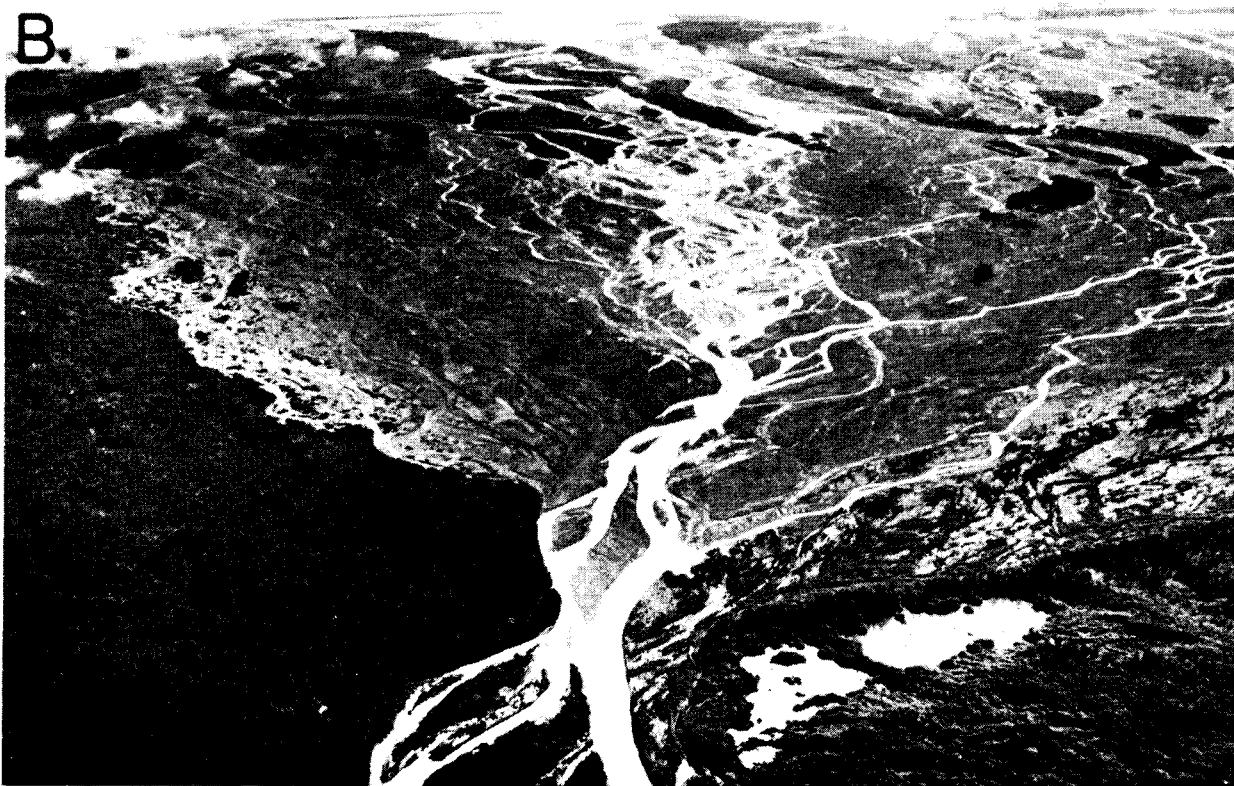


FIG. 3.—Aerial views of the outwash fans. A, Scott outwash fan. The view is upstream toward Scott Glacier terminus. Distance from the lower midfan at the bottom of the photograph to the glacier terminus is about 13 km. Photograph was taken during 1970 peak flow. B, Yana outwash fan. View is downfan. The barrier beach is just visible at the top of the photograph.

a corresponding increase in meltwater discharge. There was no detectable diurnal variation in runoff.

Discharge values were not obtained for either stream system; however, field observations of flow variations and stream height on the Scott were similar to discharge variations recorded at Power Creek (fig. 4), a stream that drains several small glaciers in the mountains just west of the Scott Glacier. Hence the Power Creek record (fig. 4) can be used to show seasonal trends and minor fluctuations caused by short-term weather changes.

Flow Conditions

Velocity and depth of flow in channels were

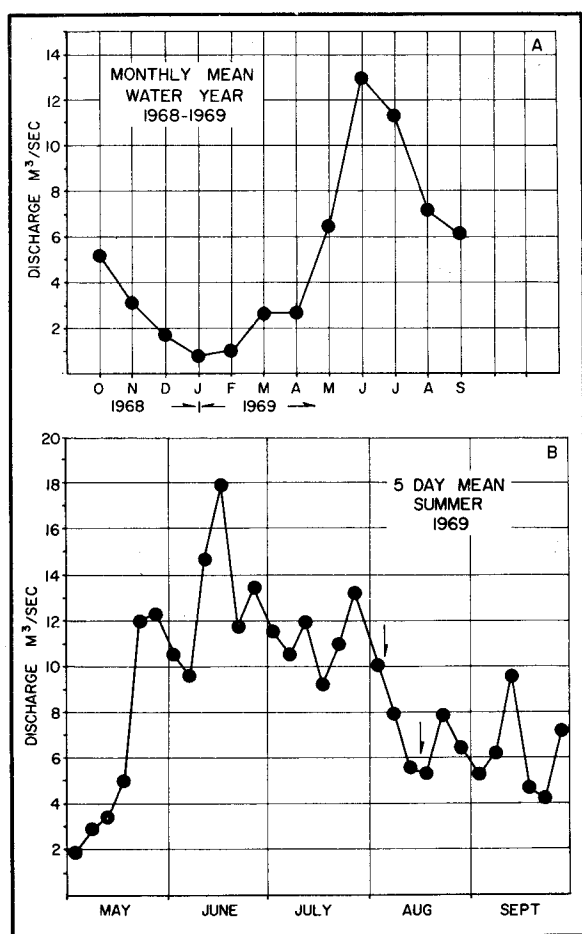


FIG. 4.—Power Creek discharge curves. A, Mean monthly discharge for the water year 1968-69. A pronounced flood peak occurred in early summer. B, Mean discharge averaged over 5-day periods for the summer of 1969. Minor fluctuations are caused by local rainfall and temperature variation over the ablation zone of the glacier. Data on flow parameters for the Scott were obtained on two consecutive days within the time period delineated by the arrows (Source: U.S. Geological Survey, 1969, Surface Water Records for Alaska, 1969, p. 69).

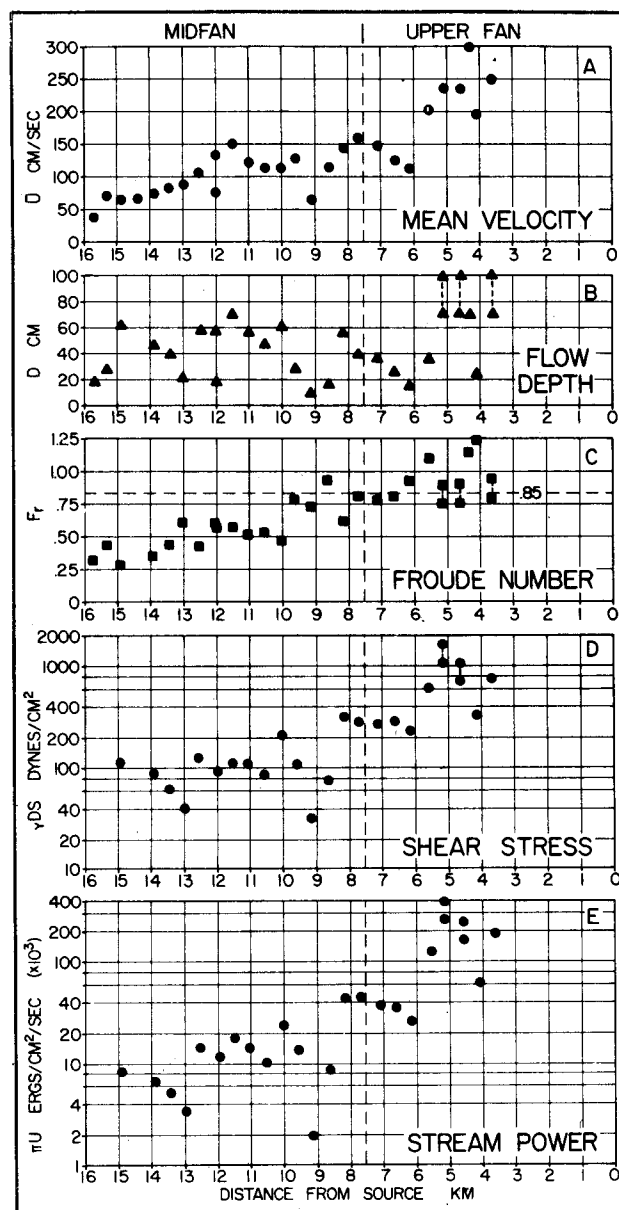


FIG. 5.—Flow parameters for the Scott outwash fan. Velocity (A) and depth (B) readings were obtained during a falling flood stage (see fig. 4b) along the profile line shown in Figure 2A. Readings were made in the channel closest to the profile line.

recorded at twenty-seven localities along the profile line (fig. 2A) on the mid and upper Scott fan (fig. 5). Readings were taken in the channels nearest a profile station, and thus they do not illustrate either precise variations or a downstream trend within a single channel. They do indicate velocities and depths typical of the various areas of the fan. The data were obtained on two consecutive days during falling stages within the general time period shown between the arrows on Figure 4.

Field work on the lower Scott fan was done in late May and early June of 1971 (during an

extremely late spring) before the flood season began; thus, no velocity-depth measurements were possible. Velocity, temperature readings, and suspended-sediment samples were taken at approximately 500-m intervals in the main stream of the Yana (fig. 2B) during a rising flood stage in late June (fig. 6). All velocity measurements were of surface velocities later adjusted to average velocity ($= 0.9 \times$ surface velocity; Helley, 1969, p. 10).

Flow conditions undergo a marked change from the upper to lower fan areas. Mean velocities greater than 200 centimeters per second have been recorded for channels 5 km downstream from the glacier termini. Values then fall rather rapidly on the Yana, but less so on the Scott, with increasing distance from the sources. Suspended-sediment concentration rises to a maximum coinciding with the region of maximum velocity on the Yana fan, then decreases to a minimum at the distal fan margin (fig. 6).

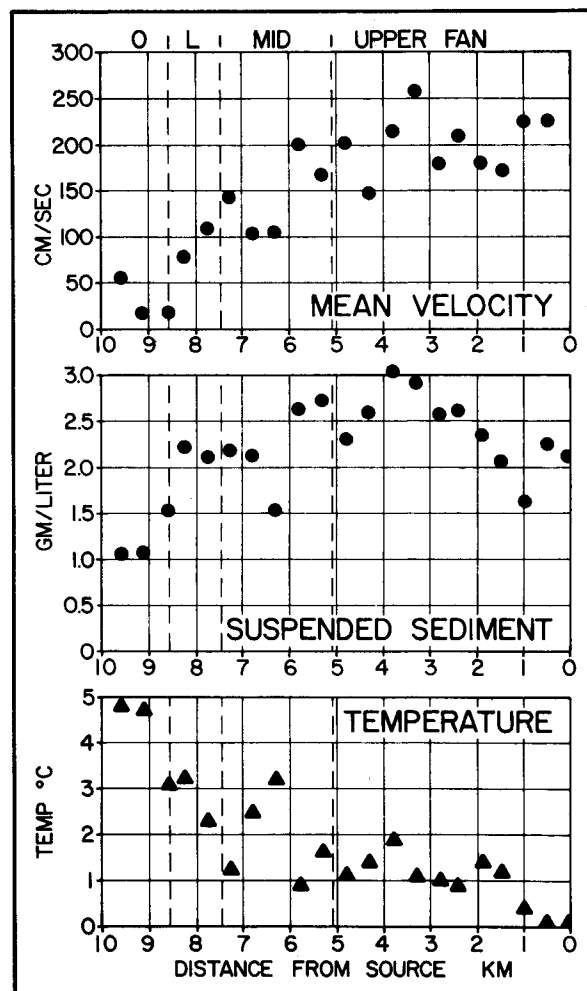


FIG. 6.—Flow parameters for the Yana outwash fan. Data were obtained from the main channel during a rising flood stage. This sample line is shown in Figure 2B.

Temperature is directly proportional to distance from the source.

The different areas or zones of the outwash fans are defined for this discussion on the basis of grain size; on the upper fan largest clasts are greater than 10-cm long axis; on the midfan the clasts are less than 10 cm, decreasing to sand size material; on the lower fan the sediment consists of sand only.

UPPER FAN

Stream Sources

The stream systems on both fans begin at a point source. Scott Stream issues from a large subglacial tunnel at the extreme eastern side of the glacier terminus, close to the bedrock valley wall (fig. 2A). The major source of melt water was formerly near the center of the terminus, but shifted to its present position sometime between 1959 and 1964, as interpreted from aerial photographs. This abandoned segment now exists as a terrace 2 m above the present active outwash surface near the glacier. The abandoned surface merges with the present level of active streams some 4 km from the glacier terminus.

Yana Stream begins at a fountain (fig. 7), the result of water emerging under hydrostatic head at the terminus of the Malaspina Glacier near the junction of the Seward and Agassiz lobes (fig. 2B). Utilizing photographs taken during a visit to the fountain, supplemented by aerial photographs taken within a few days of the visit, the fountain is estimated to be 6 to 10 m wide and 1.5 m high. Using the method described by Fahnestock (1969, p. 162) for obtaining the velocity of the vertical jet, an estimated discharge can be calculated from the following equations:

$$U = \sqrt{2gh}$$

$$Q = AU$$

where

u = velocity of flow

h = height of the fountain

g = acceleration due to gravity

Q = flow discharge

$A = \pi d^2 =$ cross-sectional area of the circular fountain

The estimated discharge ranges from 150 to 425 cubic meters per second, depending on the width value used. Observation of width and depth of channels and measurement of flow velocity in the channels indicate that the lower discharge figure may be more nearly correct.

Water flows away from the point source in

one or two incised channels and then fans into a braided channel pattern several kilometers out on the fan (fig. 3B). One or more dominant channels are visible throughout most of the length of the fans; Rust (1972, p. 223) noted the same pattern on the Donjek. This feature is better displayed on the Yana than on the Scott fan. These channels are best seen at low water as they become somewhat obscured during flood stage. However, the channels can still be discerned because they are areas of higher flow velocities and commonly contain antidune surface-wave forms.

Slope and Clast Size

The upper fan is a coarse gravel (long axis > 10 cm) area characterized by steep gradients as much as 17.6 m/km on the Scott, but only 7.6 m/km at the steepest point on the Yana (fig. 8B). Largest clast size is greater than 30 cm for both fans (fig. 8C).

Gradients on the fan surfaces were measured by theodolite leveling, with elevation readings being obtained on the high points of bar surfaces every 150 to 300 m. Twenty km of continuous profile line were obtained for the Scott and 4.3 km for the Yana fan. Clast size was measured at approximately 500-m intervals along the profile line. The largest clasts tended to form a linear band in the high-stage flow direction on the highest part of the bar surfaces. The ten largest clasts within a 2-m line along the linear concentration were selected, the long (L) axes measured, and a mean calculated for that station.

Clast size measurements were not carried to the stream sources on either fan, but it was observed that the largest clasts do not decrease greatly in size in the first 4 to 5 km from the source. Clast size then decreases markedly from over 30 cm to under 10 cm in just 5 km (fig. 8). The rapid decrease in clast size begins approximately at the point where the stream systems change from incised to braided.

Flow velocity, discussed in detail elsewhere, shows a marked decrease downfan from approximately the same point on both fans. It appears that flow strength (any parameter that measures the ability of the stream to transport sediment) is great enough to transport large clasts from the stream source to a point some kilometers out on the fan, but decreasing flow strength then results in a marked size reduction in clasts and a slight increase in gradient. This increase in gradient is followed by a significant decrease further downfan. Fahnestock (1969, p. 165) stated that slope appears to be inversely related to the efficiency of sediment transport or

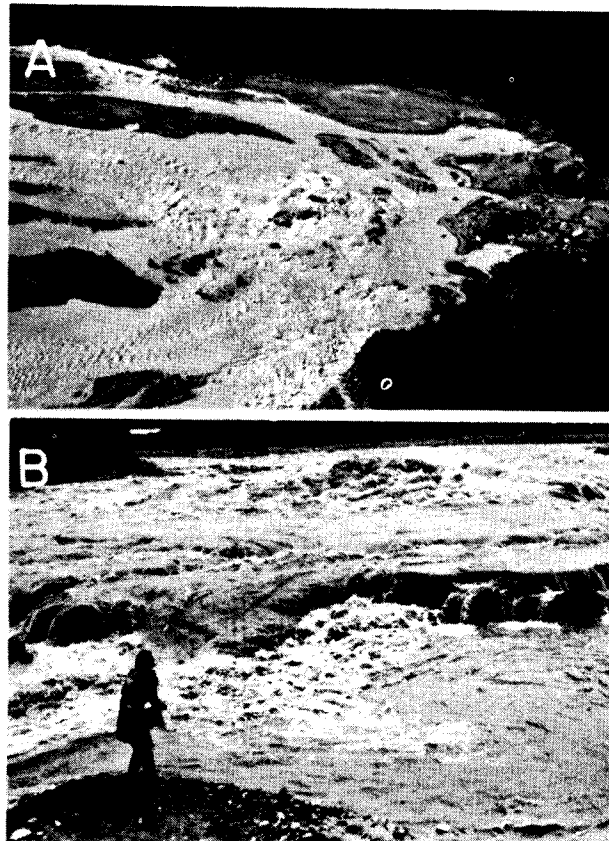


FIG. 7.—Fountain source of Yana Stream. A, Aerial view taken during a rising flow stage. The width of the main body of the fountain is estimated at 6 to 10 m. Antidunes are common in the channels leading from the fountain. The dark areas at the top and lower right of the photo are alders growing on the Malaspina Glacier. B, Ground view of the fountain. Water is cascading over dirty ice formed by melt water that froze during the previous winter.

to flow strength.

The gradient of the upper fan of both the Scott and Yana streams is greater than that of the upper Donjek (Rust, 1972a, p. 225), the upper Knik (Bradley and others, 1972, p. 1267), and the upper Slims River (Fahnestock, 1969, p. 167), but less than the gradient of the upper reaches of White River (Fahnestock, 1963, p. 26) and the Bow and Peyto outwash plains (McDonald and Banerjee, 1971, p. 1285). Plots of slope (gradient) *versus* clast size for various proximal proglacial braided streams are shown in Figure 9. Slope is roughly proportional to clast size, but the reason for deviations such as those between values of the upper Scott and Yana are unclear. It could perhaps be related to the characteristically greater discharge of Yana Stream.

Gravel Shape and Orientation

Boulders, cobbles, and pebbles on the Scott

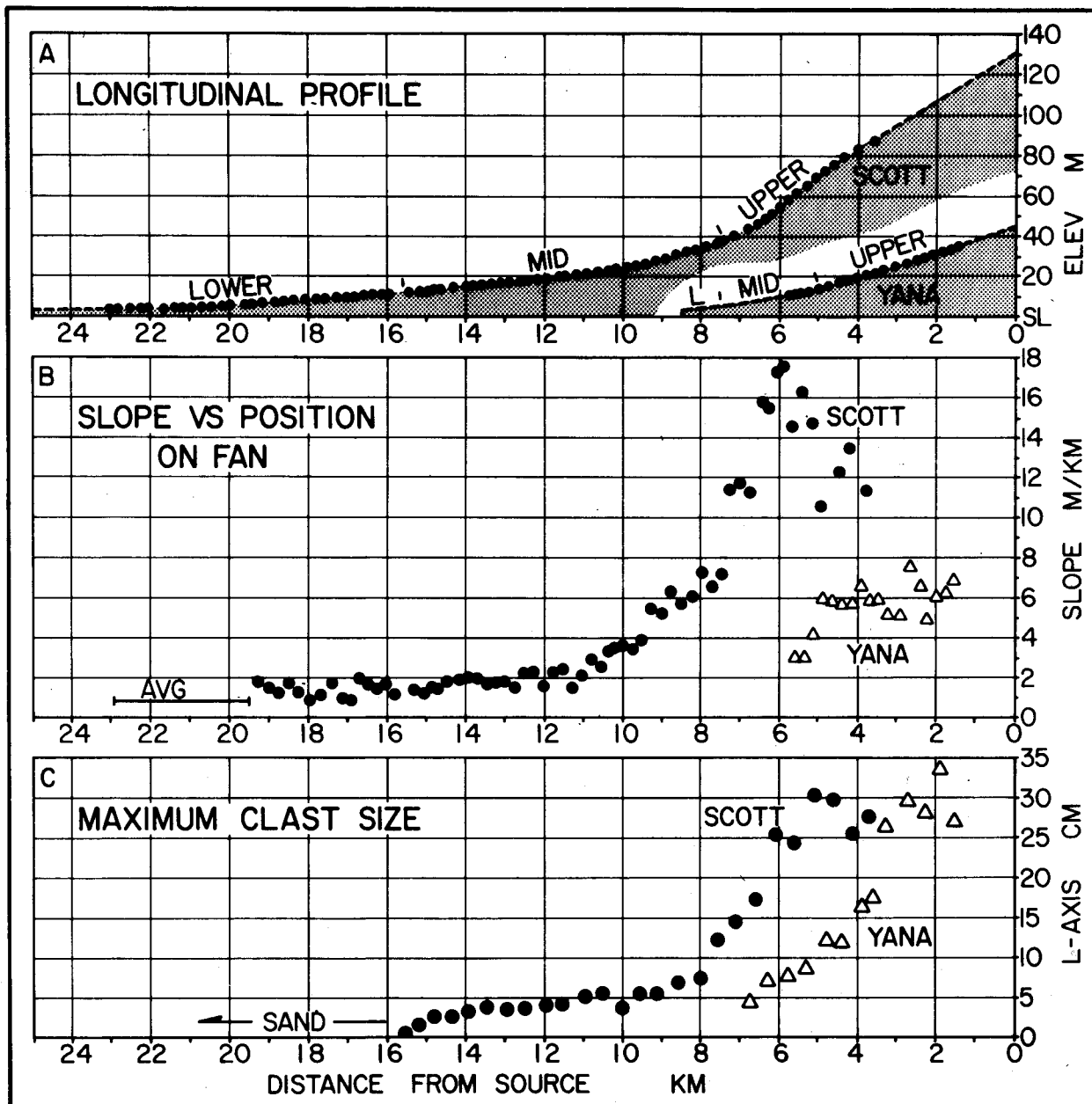


FIG. 8.—Slope and clast size parameters. A, Longitudinal profiles. Large dots represent elevations obtained every 100-150 m; dashed lines indicate interpretation from maps. B, Slope (gradient) versus position on the fans. Symbols represent slope values plotted at the midpoint between two elevation readings. C, Maximum clast size (average of 10 largest long-axes) versus position on the fans.

outwash fan are predominantly composed of Orca Group (Eocene) litharenite rocks (Plafker, 1967) with perhaps 5 to 10 percent quartz diorite clasts mixed in. Gravel on the Yana outwash is polymict with a mixture of granitic, ultramafic, and Tertiary litharenite rocks.

Clasts on the bar surfaces and in shallow channels are well imbricated with the *LI* plane dipping upstream, where *I* is intermediate axis. Upstream dip of imbricated clasts is considered by most workers (Krumbein, 1939; Lane and Carlson, 1954; Schlee, 1957; Doeglas, 1962;

Ore, 1964; Rust, 1972b) to be a good current-direction indicator. No detailed measurements such as those of Rust (1972b) were carried out, but readings were obtained to define flow directions across bar surfaces, and to delineate current direction independently when determining the orientation of other sedimentary structures.

The long axes of the clasts are strongly oriented transverse to flow direction, similar to those documented by Rust (1972b). Measurements were made on oriented vertical photo-

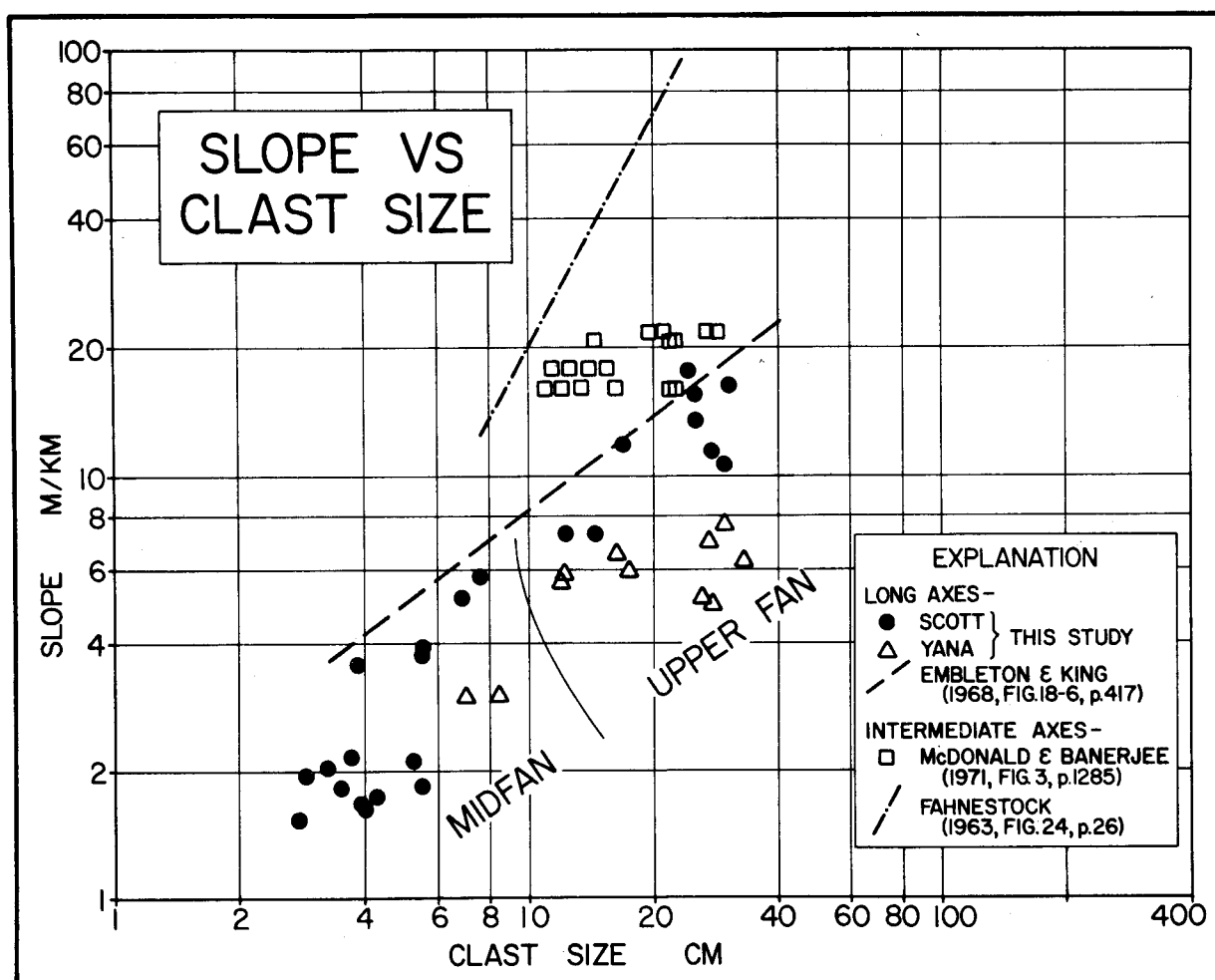


Fig. 9.—Slope (gradient) *versus* clast size. There is a rough correlation of slope and clast size. Data of Fahnestock (1963) and McDonald and Banerjee (1971) presumably would plot further to the right on the diagram if long axes were recorded.

graphs taken at four localities along the profile on the Scott fan (fig. 2A). The photographs are of 50 by 80-cm areas on the central axes of longitudinal bars. The long axes of 25 to 50 clasts were measured, beginning with the largest clast and using only those clasts for which the long and intermediate axes were readily discernible. The mean and range of long axes measured are: station 5.5, mean 4.55 cm, range 3 to 37 cm; station 6.5, mean 6.7 cm, range 4 to 17 cm; station 8, mean 5.78 cm, range 4 to 9.5 cm; and station 11, mean 3.55 cm, range 2.5 to 7 cm.

The summary data for long-axis orientation measured at each station and the total for the four stations are shown in Figure 10A. These data illustrate general orientation of clast long-axes at given points on bar surfaces along the longitudinal profile of the fan and do not take into account the variability across bar surfaces or within channels. Johansson (1963, p. 89), in flume studies of pebble orientation, found that

pebbles that moved as "contact" load took up a transverse orientation, whereas saltating pebbles assumed a more haphazard orientation. Observations on both fans did indicate that at any locality the larger clast sizes showed a better transverse orientation.

Clast shape or form was measured at two of the orientation stations on the Scott to obtain an indication of what shapes contributed to the transverse orientation of the long axes. Samples measured were originally collected for grain-size analysis at, or very close to, the photography locations. The three axes of every clast with an *L*-axis greater than 3 cm were measured and the results plotted (fig. 10B) on Folk form triangles (Sned and Folk, 1958, p. 123).

On the Folk form diagrams, the clasts plot as primarily bladed, showing strong compact-bladed and elongate components. The average configuration can be described as a "fat brick." These shape data are in good agreement with

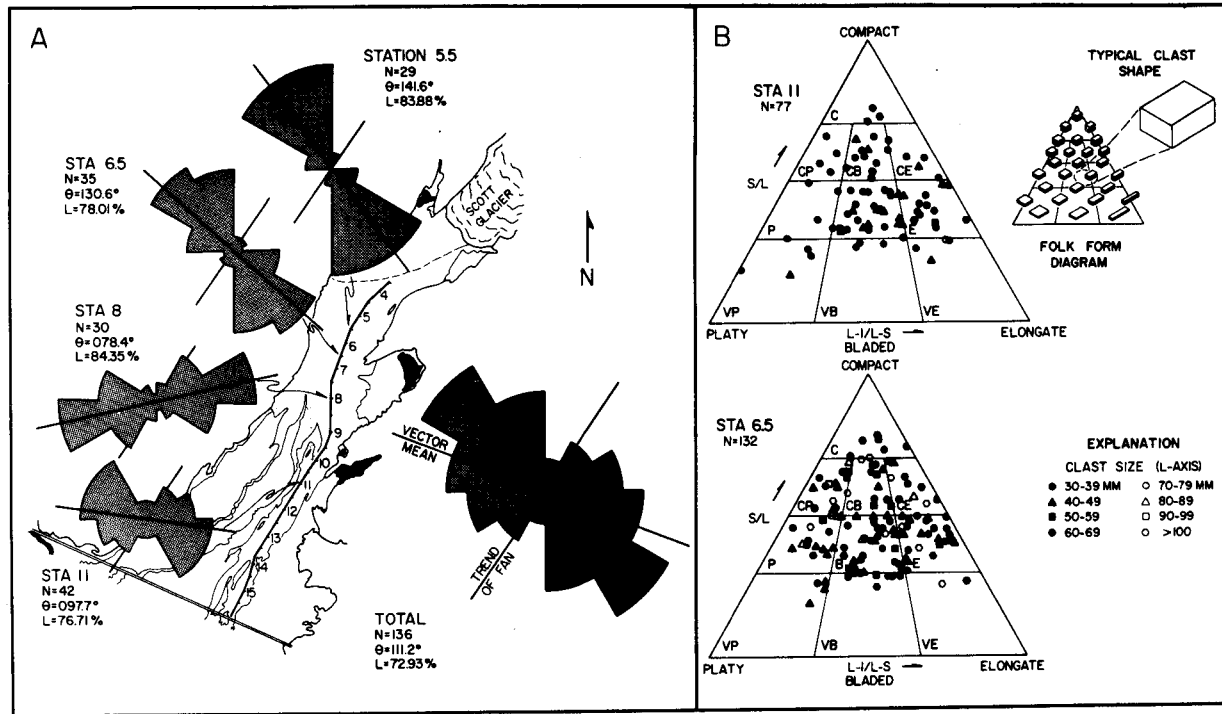


FIG. 10.—A, Clast long-axis orientation, Scott outwash fan. Clasts were measured in a 50- by 80-cm area on the higher points of bar surfaces at several stations along the profile line. Station 8 represents a location where the stream system is oriented about 60° from the main trend of the fan. B, Clast form, Scott outwash fan. Measurements were made for samples collected at two of the orientation stations indicated in (A). The typical shape is bladed to elongate.

those obtained by Sneed and Folk (1958, p. 143) for quartz and chert pebbles of the Colorado River in Texas and also with those of Dobkins and Folk (1970, p. 1186) for basalt clasts in rivers on Tahiti-Nui. Greatly elongated clasts probably are not necessary for development of a good transverse orientation pattern.

Bar Morphology

Bar morphology changes systematically in a downfan direction from coarse-gravel longitudinal bars with low bed relief to finer gravel longitudinal bars with somewhat higher bed relief, and then to a combination of sandy longitudinal and linguoid bars. The longitudinal bars of the upper fan are diamond-shaped in plan with a slightly higher central axis and little to no slipface development on their downstream margins (fig. 11A). They occur mainly in interstream areas between incised erosional channels and are rarely subject to flooding. These bars appear to consist of a thin sheet of coarse, poorly-sorted, well-imbricated gravel with the coarsest material concentrated along the central axis. Relief of the bars appears to be not much greater than the size of the largest clasts (30 cm).

Observations suggest that the form of the

bars on the upper fan surface is transitional from forms of low bed relief to longitudinal bars of higher bed relief that are elongate in the downcurrent direction, and which appear to be similar to the "spool-bars" of Krigström (1962, p. 332) and to the longitudinal bars of Rust (1972a, p. 232), Williams and Rust (1969, p. 667), and Smith (1970, p. 2994). They are rhomboid in plan, with the longitudinal axes ranging from 30 to 100 m in length (fig. 12). Coarsest material is concentrated on the upstream apex of the bar, with a large decrease in grain size down the bar parallel to the flow direction. Poorly to moderately developed sandy slipfaces may occur at the downstream margins. Bar relief is generally greater than that of the upper fan bars, and shallow channels usually dissect the bar surface. Most midfan longitudinal bars have one or more erosional edges caused by shifting channels around other accreting bars and by channel incision as flood waters recede. It may be difficult or impossible to discern the original dimensions of the bar.

Figure 13 illustrates the differences in longitudinal bar morphology between the upper and midfan areas of the Scott. Table 1 summarizes various characteristics of longitudinal bars as well as other bar types found on the outwash

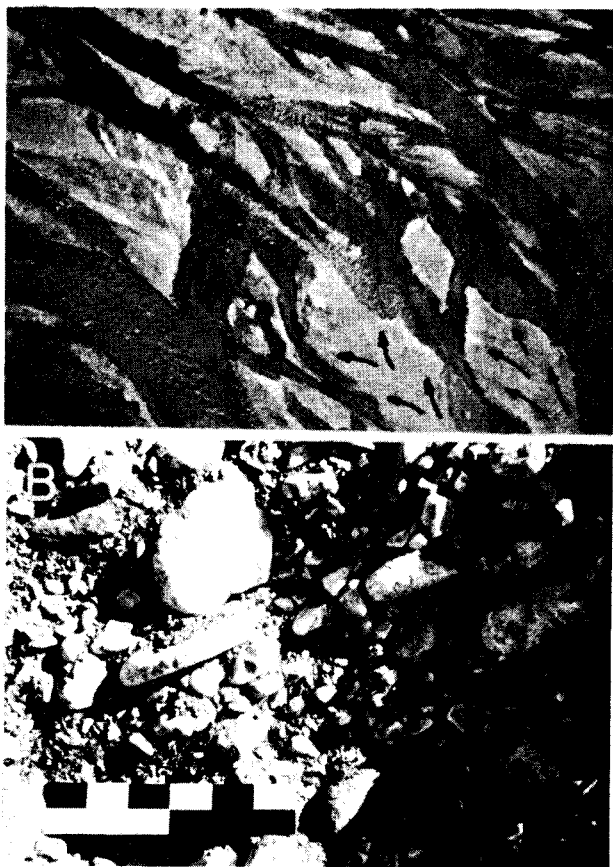


FIG. 11.—Longitudinal bar morphology, flow pattern, and internal structure. A, Aerial view of bars on the upper Scott fan taken during a declining flow stage (late summer). Flow is confined to relatively straight erosional channels and is from lower right to upper left. Dashed lines outline bar forms and arrows trace direction of flow across the bar surfaces as indicated by lineations and ground checks of imbrication dip directions. Note antidunes in the deep channels and transverse ribs (marked by a "T" in the exposed shallow channels. Compare with upper fan sketch in Figure 13. B, Natural cut in a bar on the upper Scott fan (near station 4). The gravel is poorly sorted and generally lacks bedding. The excellent imbrication of the clasts is readily apparent. Flow was from left to right; scale is 30 cm long.

fans. These characteristics will be discussed in the following pages.

Differences in morphology between the two longitudinal bar variations evidently are related to differences in clast size and to differences in flow strength across the bar. Large clasts composing the upper fan bars are less subject to transport and tend to accrete as thin sheets where transported by rare, very high flood flows. Longitudinal bars composed of smaller grain sizes may grow and be modified at lower intensity flows.

Gravel Fabric and Sedimentary Structures

Cuts in upper fan longitudinal bars show

poorly sorted coarse gravel with rather crude bedding (fig. 11B). On close inspection, excellent clast imbrication is also apparent. Some bars contain interbeds of flat-bedded sand. These two facies are similar to facies G and D of Williams and Rust (1969, p. 668, fig. 20) or facies 6 of Rust (1972a, p. 232).

Sand is rare in the upper fan area, except as a matrix in the gravel and as the minor interbeds mentioned above. However, during falling stages of flow, megaripples (bedforms with 60 cm to 6 m spacings; Boothroyd, 1969, p. 426) may form in channels (fig. 14). The megaripple trains exist as discontinuous sandy lenses a few tens of centimeters thick and 5 to 20 m in length. Individual megaripples have spacings of 1 to 3 m. Cross-beds are tangential in longitudinal section and curving or trough-shaped in horizontal cuts (fig. 14B).

Transverse Ribs

Linear stripes of pebbles, cobbles, and boulders (long axes from 1.5 to > 45 cm) occur in groups on bar surfaces and in shallow channels on the upper midfan and upper fan areas. The stripes are oriented transversely to the current flow, as determined from imbrication measurements of clasts taken independently of the stripes (fig. 15). The clasts making up the stripes are themselves imbricated and show a strong upstream dip. These stripes are particularly well displayed on longitudinal bars on the upper fan of the Yana (fig. 12A). McDonald and Banerjee (1970, 1971) have described the same structure, which they have named *transverse ribs*, from the Peyto outwash plain, North Saskatchewan River and No-See-Um Creek in Alberta.

One hundred and twenty nine measurements of transverse ribs at twenty-five localities on both outwash fans indicate a range of spacings from 6 cm to 2 m, with a concentration of spacings from 40 to 70 cm (fig. 16). Ribs with larger spacings tend to be made up of clasts of larger mean size, whereas those with smaller spacings have smaller clasts, although there is some overlap in the smaller size ranges (fig. 16). Transverse ribs within the range of spacings measured may occur at any position on the upper fan and upper midfan. There is no systematic decrease in spacings in a downfan direction. However, because of the grain size-spacing correlation, maximum transverse-rib spacings will be smaller in the midfan areas than on the upper fan.

Transverse ribs were not observed in the process of formation or migration, but laboratory studies by Fahnestock and Haushild (1962, p. 1433) found that rolling clasts tended to stop

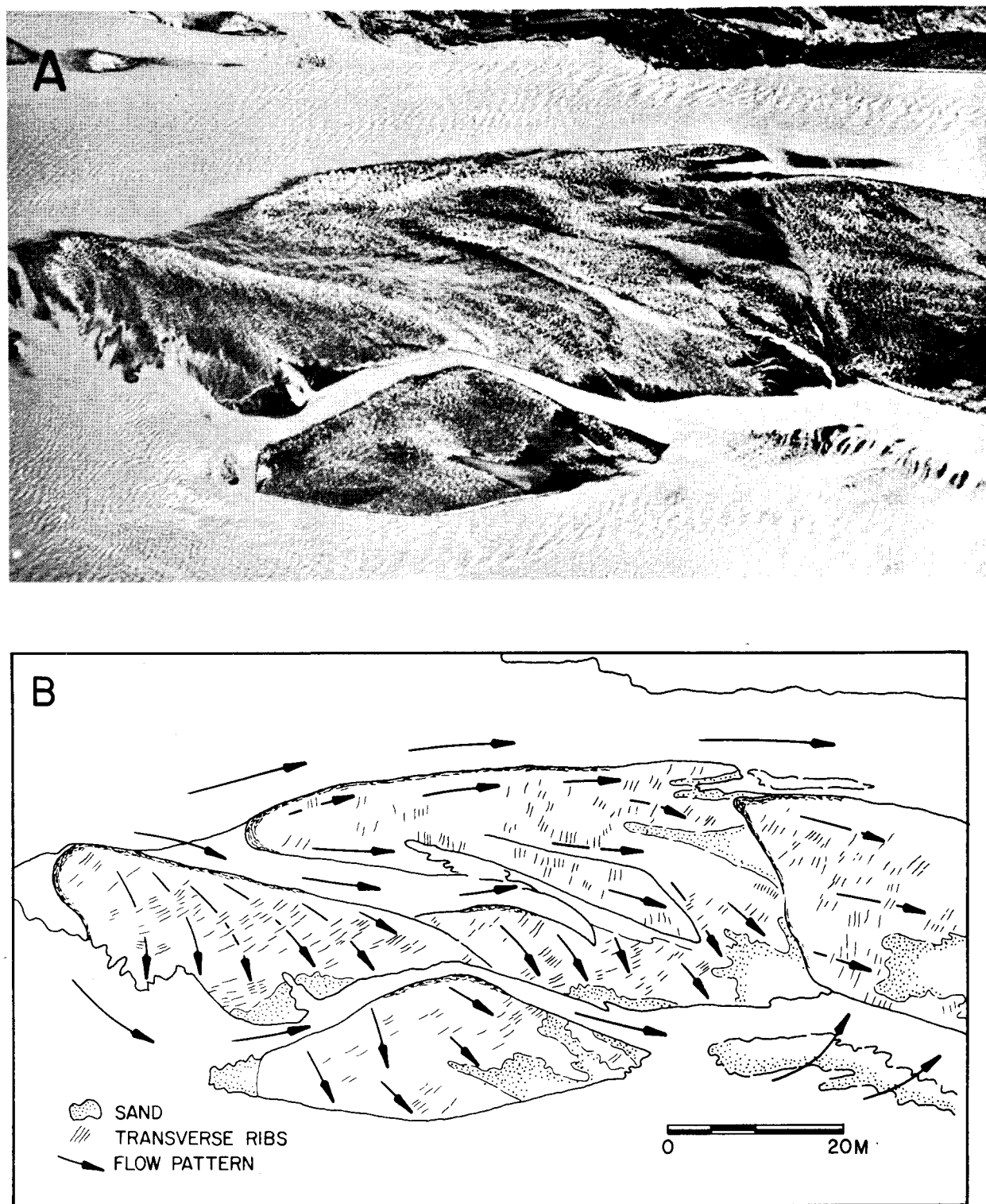


FIG. 12.—Longitudinal bar morphology and flow pattern. A, Aerial view of several longitudinal bars on the upper Yana fan taken during a rising flow stage (early summer). Flow is from left to right; scale is given on the diagram. B, Diagram of bar boundaries and flow pattern made from an overlay of the photograph above. Transverse ribs are extremely common on the bar surfaces and reflect the flow pattern across the bars. Some sand is present around the downstream margins of the bars.

TABLE 1.—BAR CHARACTERISTICS

| Bar type | Longitudinal | | | Linguoid | Point and lateral | |
|-----------------------------------|--|--|--|--|---|--|
| Location of Fan | Upper | Mid | Lower | Lower | Mid | Lower |
| Slope (m/km) | 10-18 (Scott) 5-8 (Yana) | 2-8 3-4 | <2 | <2 | 2-8 | ≈1 |
| Mean max. clast size | 10-30 cm (Scott) 10-35 cm (Yana) | 4 mm-10 cm | 2-4 mm | 2-4 mm | 5-10 cm | 2-4 mm |
| Position with respect to channels | Between incised channels | Transition from between channels to within channels (low stage) | Within low-stage channels | Flooring low-stage channels | Within low-stage channels on curves | Within channels, channels occur between cohesive banks |
| Morphology | Low bed relief; 30 cm or less Diamond shaped, 20-50 m (long axis) Erosional edges (U) Slipfaces (R) | Bed relief >30 cm. Diamond shaped, 30-100 m (long axis) Erosional edges (C) Sand-wedge slipfaces (C) | Bed relief >30 cm. Diamond shaped, 20-50 m (long axis) Erosional edges (C). Slipfaces (A) | Spoon shaped, lobate, 10-50 m (long axis) Repetitive well-developed slipfaces, commonly multilobate (A) | Bed relief; >30 cm. 30-100 m long Sandwedge slipfaces, oriented to inside of curve (C) | Bed relief 50 cm-1 mm. 75-125 m long Slipfaces always present, oriented toward outside of bend |
| Sedimentary structures and fabric | Coarse imbricate gravel Sand lenses with flat bedding (R) | Fine imbricate gravel Sand lenses with flat bedding (C-A) Planar tangential large-scale cross-beds (U-C) | Planar cross-beds (C) Flat beds (A) Type A ripple-drift cross-lamination (U) | Planar-tangential cross-beds (C) Type A and B ripple-drift cross-lamination (A) | Fine imbricate gravel Flat bedded sand lenses (C) Planar tangential cross-beds (C) | Planar-tangential large-scale cross-beds (C) Large-scale trough cross-beds (A) Small-scale trough X-lamination (C) |
| Time of initial movement | Rare high floods | Maximum annual flooding | Moderate flow | Low-flow stages | Moderate flow | Moderate flow |

A—abundant, B—common, U—uncommon, R—rare.

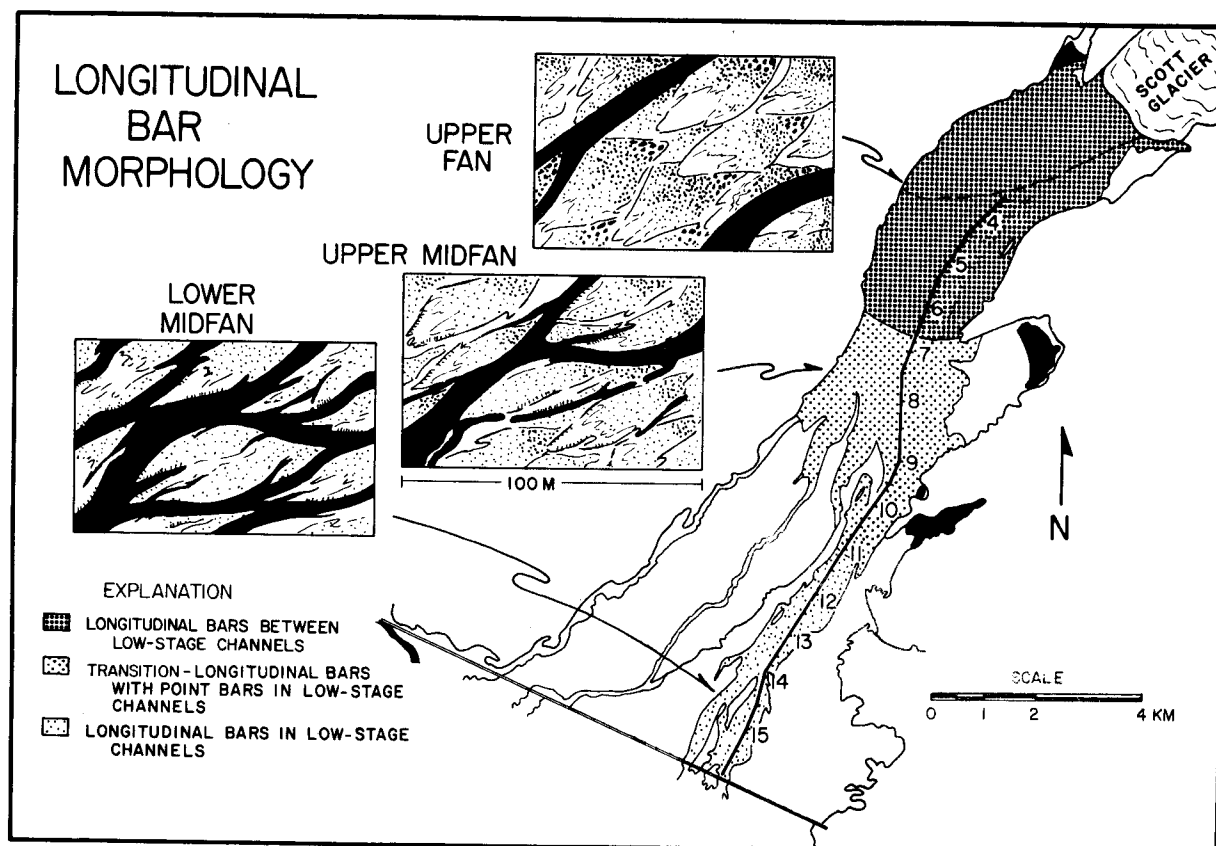


FIG. 13.—Variation in bar morphology and channel pattern for gravel longitudinal bars. Sketches were drawn from aerial photographs.

and imbricate under antidune breaking waves. B. C. McDonald (written comm.) reports the formation of transverse ribs in a flume by an upstream migrating hydraulic jump. These two laboratory studies indicate that transverse ribs certainly are formed under upper flow regime conditions, either under near-critical to super-critical antidune breaking waves, or by super-critical flow events resulting in hydraulic jumps.

MIDFAN

In contrast to the unvegetated upper outwash fan, the midfan is heavily vegetated, with active braided streams confined to approximately 10 percent of the surface area (figs. 2 and 3). Vegetation first becomes established on the highest bar surfaces and tends to trap finer sediment, mainly fine to medium sand with some silt. This process builds vegetated areas into islands standing above the general stream level. The islands generally have elevated margins populated by alders (*Alnus sinuata*), whereas the surrounding lower interior basins contain freshwater marsh grass (*Calamagrostis*).

Slope and Clast Size

In the midfan area maximum clast size decreases from 10 cm to sand-sized material.

This decrease occurs in a distance of 8 km on the Scott fan, but the same diminution in clast size is compressed into approximately 2.5 to 3 km on the Yana fan (fig. 8C). The main stream of the Yana, flowing between highly vegetated, semicohesive banks, actually transports some fine gravel to less than one km from the back beach (fig. 2B). This somewhat anomalous deposit exists as a tongue of gravel protruding into an area of sand.

The gradient declines from 6 m/km to about 2 m/km on the Scott, whereas the Yana shows a decrease from 4 m/km to an unsurveyed value of certainly less than 3 m/km. The trend of the gradient for the Scott in Figure 8B shows a break about 10 km from the source, which suggests that the midfan region can be divided into two additional subenvironments. The clast-size plot for the Scott (fig. 8C) also reflects this division. This subdivision is discussed at length in Boothroyd (1972) and thus will not be discussed here. The slope and clast sizes of the midfan areas of the Scott and Yana fans correspond with those of the intermediate zone of the Slims River (Fahnestock, 1969, p. 168).

Bar Morphology

The most abundant bar forms in the midfan area are longitudinal bars. Longitudinal bars in

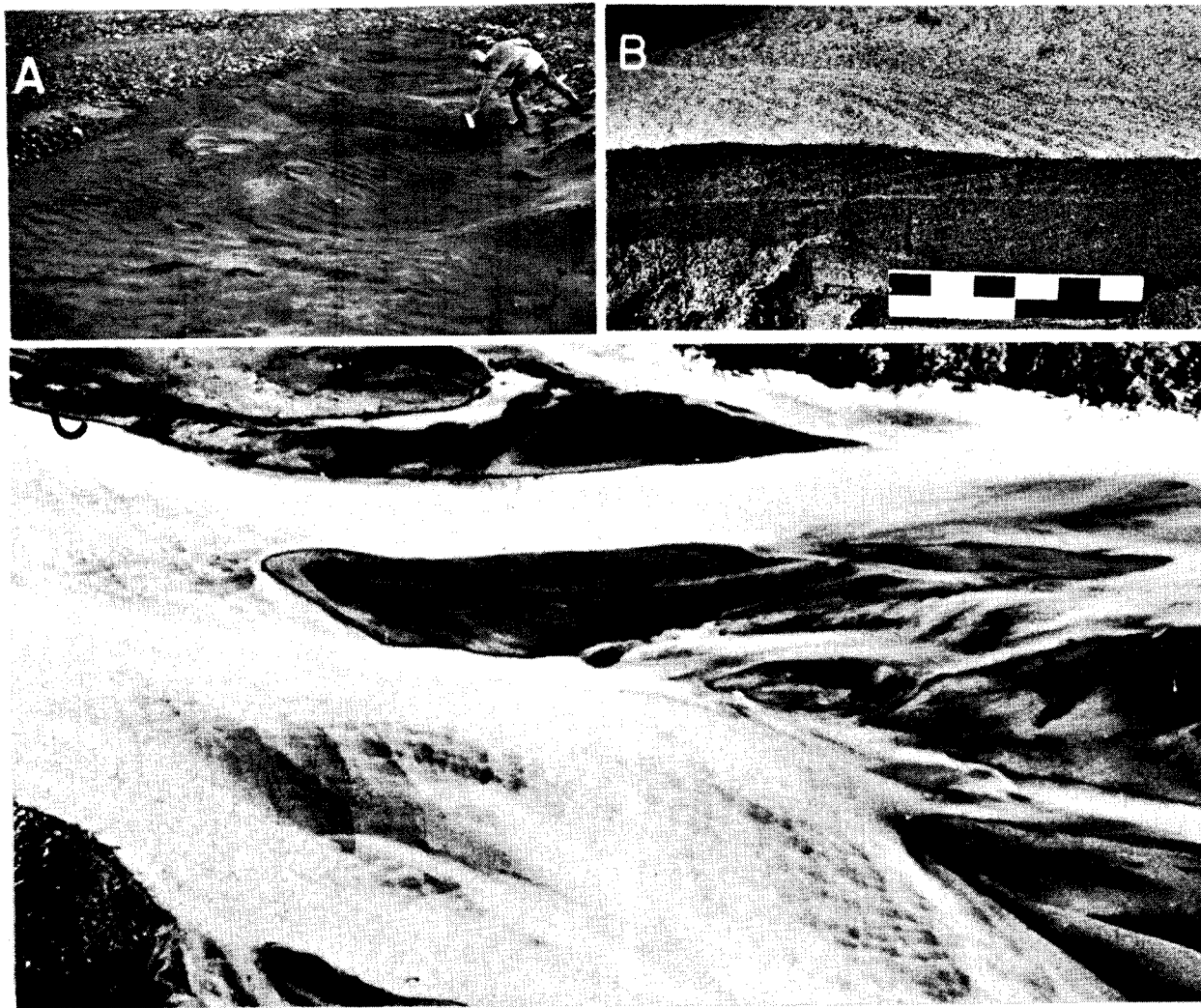


FIG. 14.—Megaripple occurrence and internal structure. A, Short megaripple train deposited in an erosional channel on the upper Yana fan. Flow was from the top to bottom of the photograph; spacing of megaripples ranges from 1 to 3 m. B, Trench in one of the megaripples shown in A. Two sets of cross-beds, tangential in longitudinal section and curving or trough in horizontal section, are shown. Flow was from right to left; scale is 30 cm long. C, Aerial view of megaripples in a channel on the Scott midfan. Flow is from left to right. Photograph taken during a declining flow stage.

the coarser gravel portions of the fan are situated between shallow channels that are active only at flood stage. As grain size decreases downstream, the bars tend to be located in channels that are active at lower flow stages. Sandy slipfaces are poorly to moderately developed at the downstream margins of the coarser gravel bars, but are better developed where grain size is finer. Many slipfaces are of the sand-wedge type reported by Rust (1972a, p. 228, his fig. 4) that are deposited as water level and velocity decrease from high flood stage (fig. 17). Other sandy slipfaces appear to result from continuous transport across the bar surface (avalanche deposition over the bar crest) during flood stage and they continue to grow as the bar remains active during lower flows. Flow patterns reconstructed from pebble imbrication and minor

sedimentary structures indicate that bar-surface deposition and slipface development occurred simultaneously. Some of these distal midfan longitudinal bars were still active during the declining late-summer flow of 1969.

Another bar type—the point bar—is also prevalent in the midfan area. These bars develop in curved channels during lower stages of flow and thus are subjected to active sedimentation over a longer period of time than are the longitudinal bars that occur in the same geographic area. Slipfaces are well developed and commonly may be built into a secondary channel or slough, with the resulting azimuth of cross-bed dip at a large angle to the main channel axis. These point bars are especially prevalent on the upper midfan area of the Scott and are similar in plan to “river curve spurs”

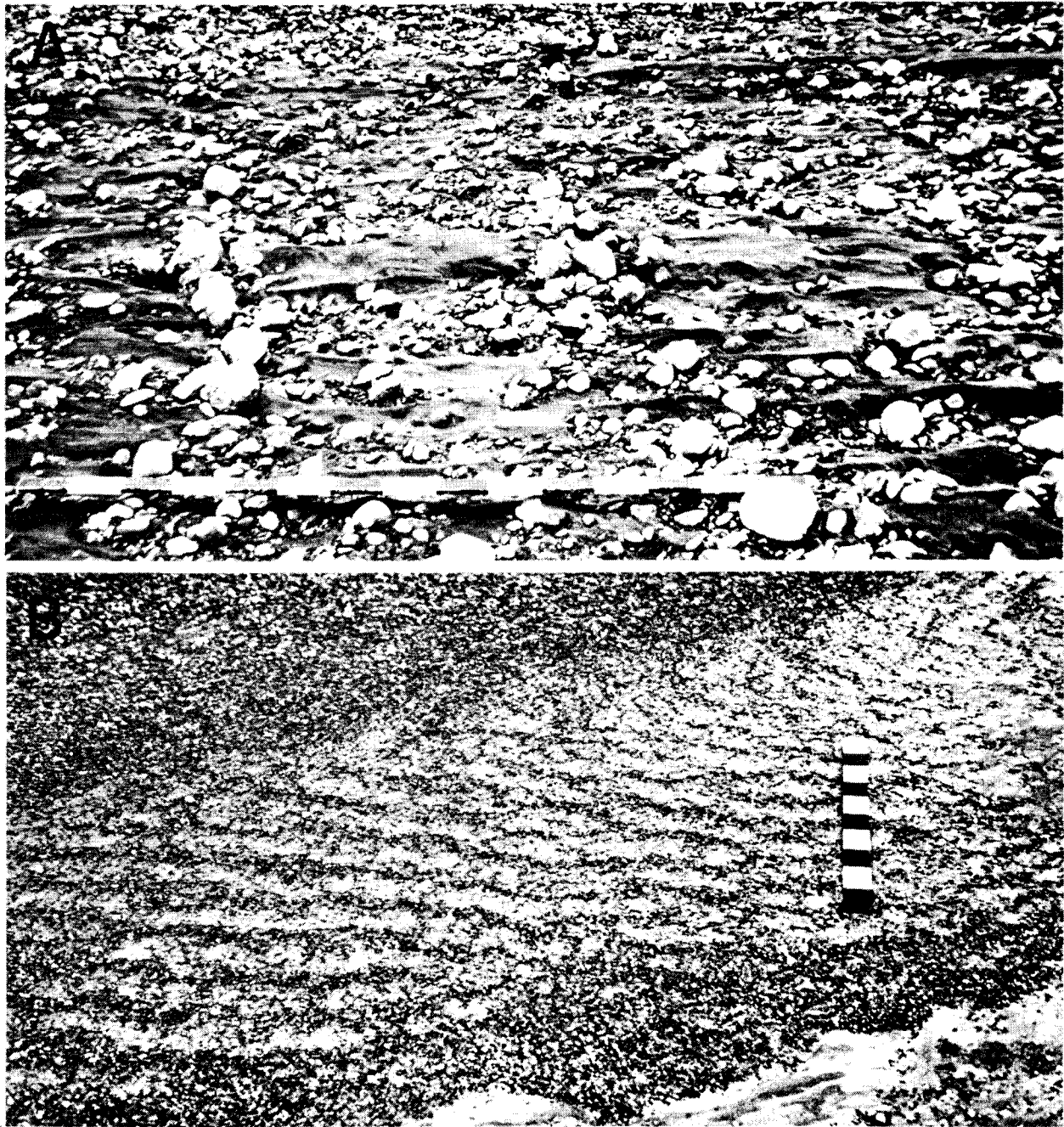


FIG. 15.—Transverse ribs. A, Ribs with large spacing (55 cm) and large clast size (6 cm) on the surface of a longitudinal bar on the Scott midfan. Clasts making up the individual ribs or stripes are well imbricated and occur on a gravel bed. Sand was deposited during declining flow as sand shadows and lineations. Flow was from left to right, increments on the scale are 10 cm. B, Ribs with small spacing (15 cm) and clast size (2 cm) on a longitudinal bar on the upper Yana fan. Flow was toward the bottom of the photograph, increments on the scale are 10 cm.

of Krigström (1962, his fig. 9, p. 338).

Bedforms and Sedimentary Structures

Figure 17B shows the morphology and internal structure of a lobate sand wedge deposited at the margin of a longitudinal bar. Cross-bedding varied from tangential to planar as the wedge developed due to a decrease in the

depth-ratio (increase in the depth of the basin being filled; see Jopling, 1965, p. 779). Reactivation surfaces (Collinson, 1970, p. 52) are common and often are enhanced by a silt drape (fig. 17B).

Sand is present on the bar surfaces, especially in low areas, and in the shallow channels that dissect the surfaces. Most sand on the upper

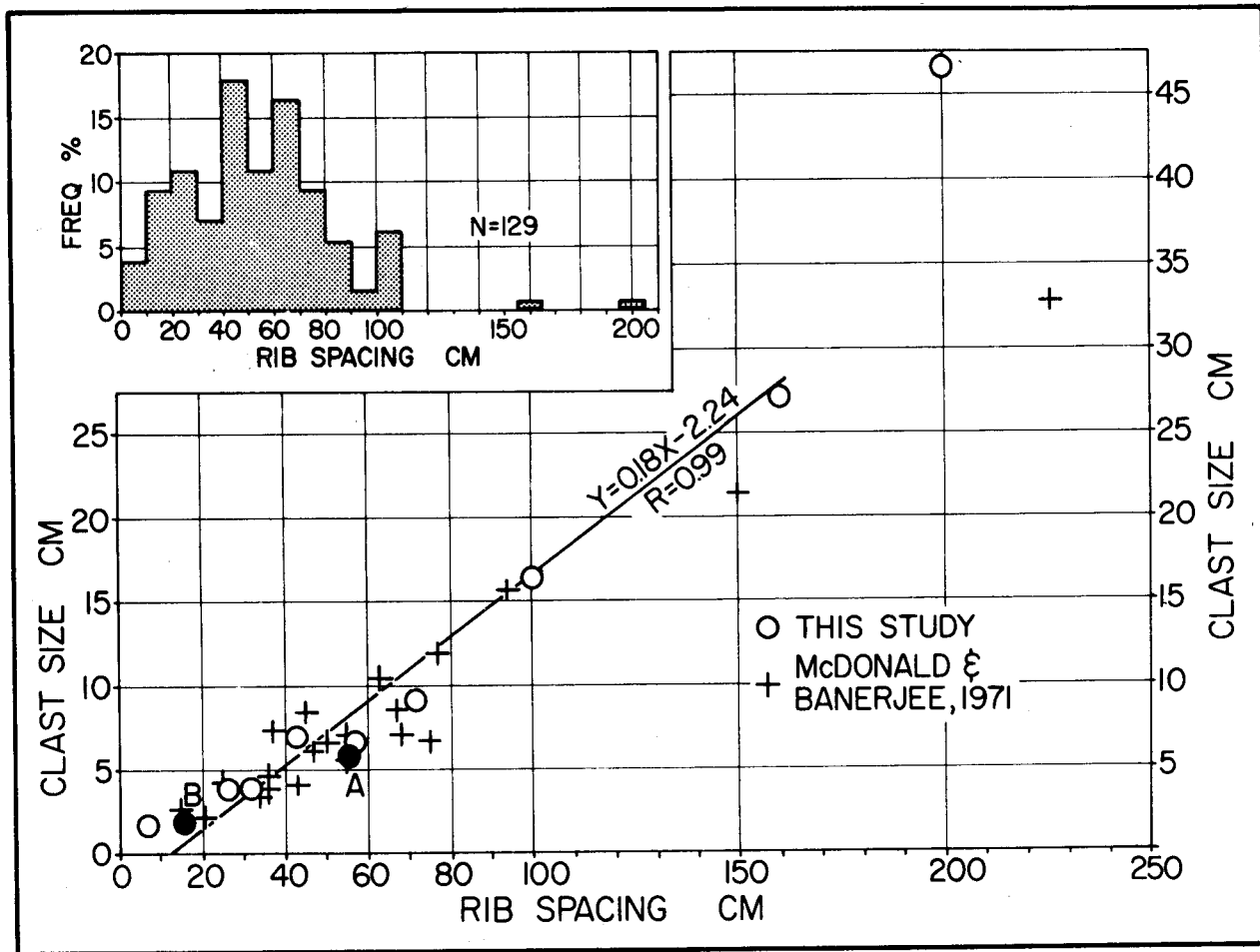


FIG. 16.—Clast size versus spacing of transverse ribs. The ribs shown in Figure 15 A and B are labeled (A and B) on the diagram. The inset is a histogram of rib spacings measured on both fans.

midfan consists of thin lenses of flat or plane beds, although most of the surfaces of the lenses are covered by a veneer of linear to cusped ripples that are in turn mantled by a silt drape. Small-scale trough cross-bedding formed by cusped ripple migration is more important on bars on the lower than on the upper midfan. Ripple-drift cross-lamination is rare on the upper midfan and is uncommon on bar surfaces on the lower midfan. Some type A ripple-drift cross-lamination (no stoss side preservation; Jopling and Walker, 1968, p. 973) may be present in trenches on bar surfaces on the lower midfan. Fine sand and silty sand may be deposited as overbank material in splay-like deposits across vegetated islands (fig. 18A). This sand is in the form of ripple-drift cross-lamination and is commonly overlain by a veneer of silt and clay.

LOWER FAN

A lower fan sand facies is extensively developed in the distal portions of the Scott outwash fan. Gravel disappears from bar surfaces

16 km from the glacier terminus. The area of active sedimentation at the present time is a sand plain up to 2 km wide that is almost completely submerged during high flow stage (fig. 2A). This area is similar to the downstream zone of the Slims River (Fahnestock, 1969, p. 168). The active depositional area bifurcates and each segment narrows to a meandering reach at kilometer 21 on the longitudinal profile. The terminal 2 to 3 km of the fan are mantled by thin salt-marsh vegetation. This marsh is now brackish to fresh, the result of 2 m of uplift sustained in the March 1964 earthquake (Reimnitz, 1966). The lower fan terminates behind a large expanse of intertidal mudflats 25 km from the glacier front.

The Yana fan, by contrast, has a distal sand facies that begins some 7.5 km from the source and ends within a kilometer behind an active sand spit (fig. 2B). The stream waters are deflected westward to flow behind a series of active and inactive spits before discharging into the Gulf of Alaska. Aerial photographs taken in 1948 indicate that the spit was breached at

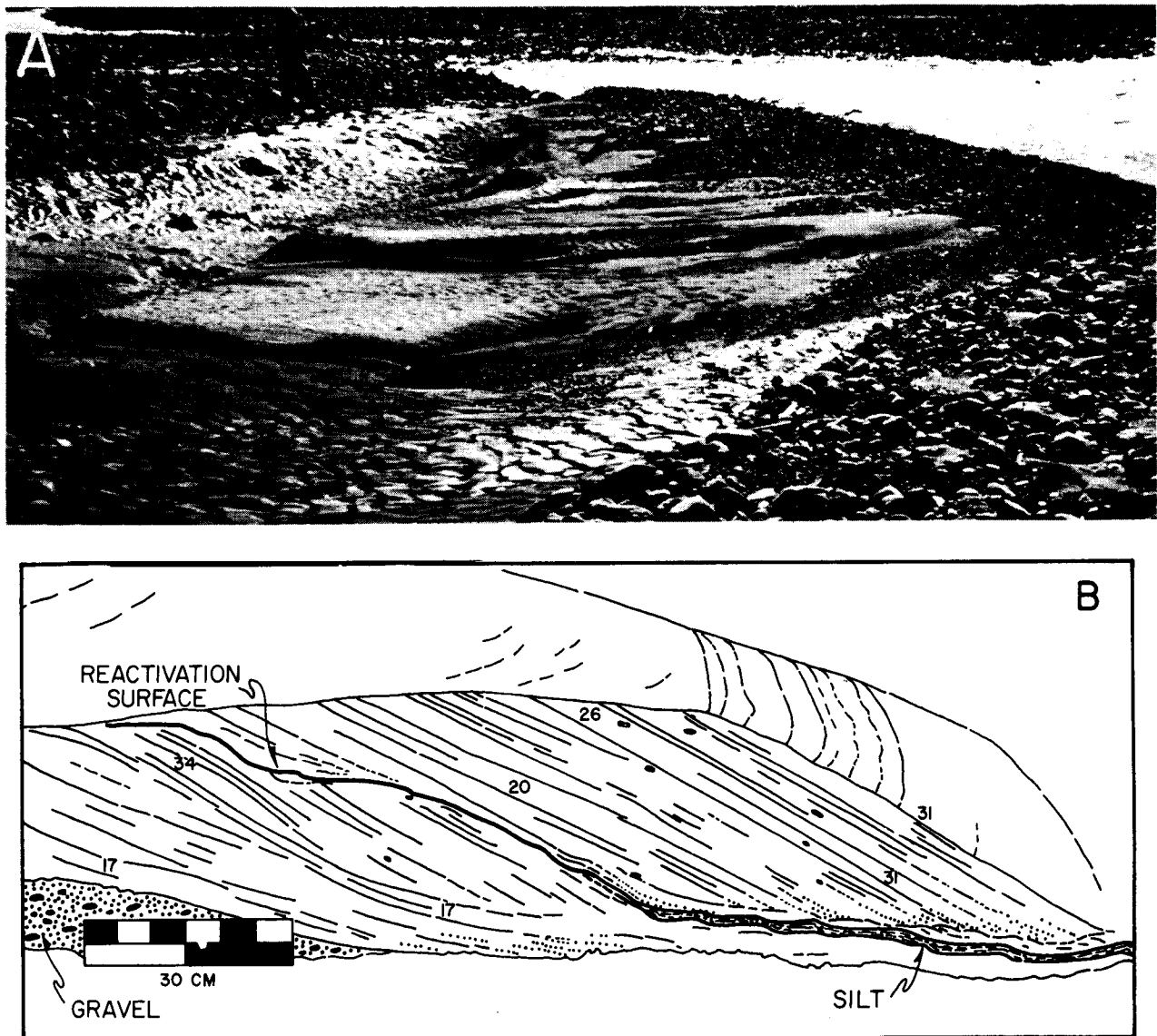


FIG. 17.—Morphology and internal structure slipfaces of coarse-grained longitudinal bars. A, Sand-wedge type of lobate slipface deposited at a bar margin on the upper Scott fan. Main body of the bar is now largely removed. Arrow points to location of trench shown in 13B. B, Sketch of a trench in one of the lobes of the sand wedge shown in A. Reactivation surface is mantled by a silt drape. Numbers indicate cross-bed dips in degrees.

that time and the Yana stream system discharged directly into the sea in front of the main body of the fan. Since that time this outlet has closed and a large pond now forms around the distal fan margin during peak flooding.

Slope and Grain Size

Slope decreases from approximately 2 m/km on the Scott lower midfan to values grouped around 1.5 m/km on the braided portion of the lower fan (fig. 8B). There is a further decrease to an average slope of 0.76 m/km in

the meandering reach. By comparison, a reach in the downstream zone of the Slims River has a slope of 0.85 m/km (Fahnestock, 1969, p. 168), whereas the Platte River ranges from about 2 m/km to 1 m/km (Smith, 1970, p. 2996). Slope values were not obtained for the lower Yana fan. Maximum grain size varies from coarse to medium sand. Detailed laboratory analyses are not complete, but field observations indicate that medium sand is present on bar surfaces and that it makes up the cross-bedding observed in trenches throughout the entire lower fan to the intertidal mudflats.

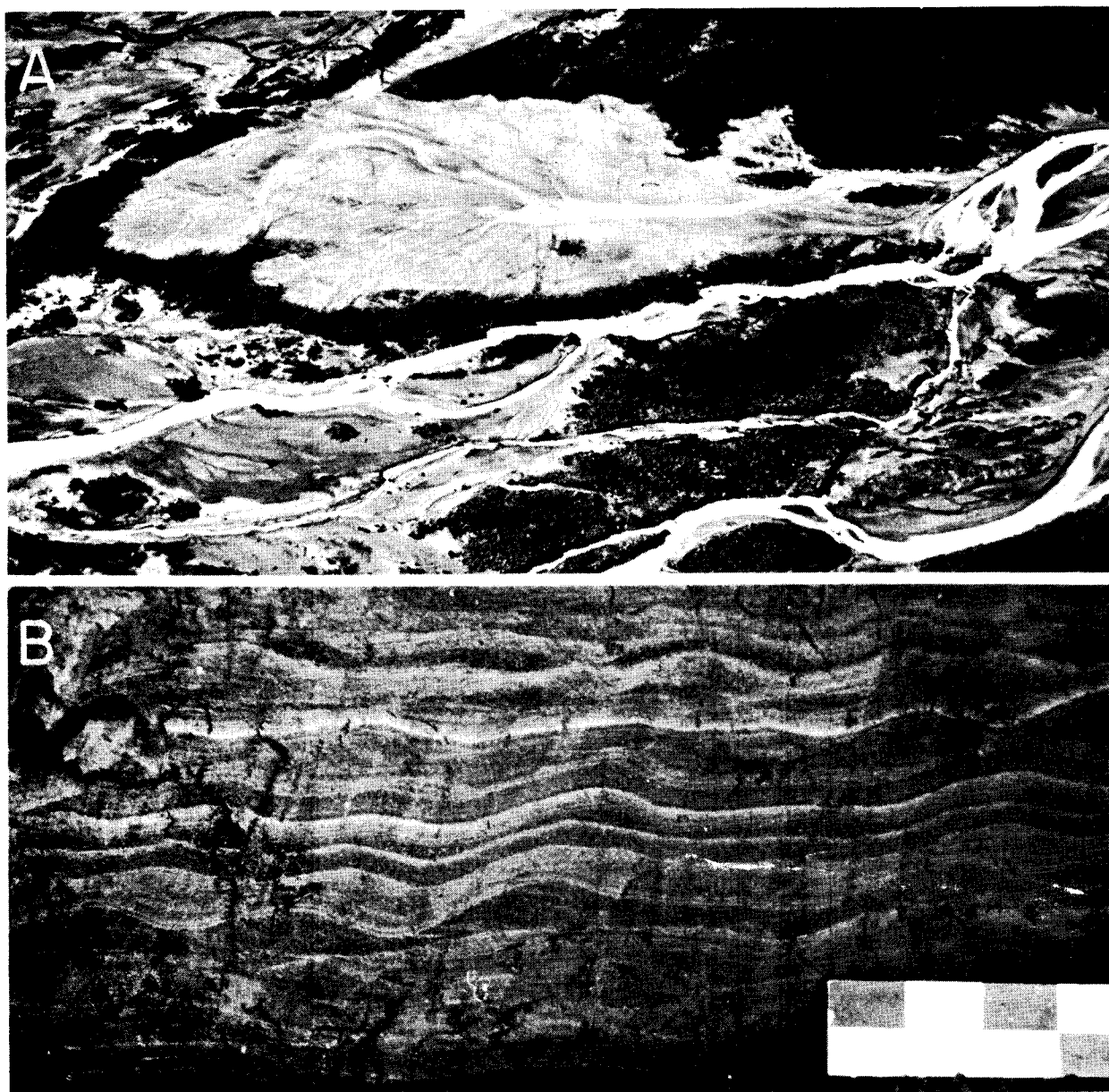


FIG. 18.—Overbank depositional forms and internal structure. A, Splay-like deposit on the Yana midfan. Sand, overlain by silt and clay was deposited during high-flood stage over grass and small alders on an elevated island. Length of the deposit is about 50 to 75 m. B, Overbank levee silty ripple-drift cross-lamination and silt and clay drape laminations on the lower Scott fan. Flow was from left to right; scale increments are 5 cm.

Bar Morphology

Braided reach.—Bars in the braided reach of the Scott fan are a combination of longitudinal and linguoid types (fig. 19). Longitudinal bars are 20 to 50 m in length and appear to be a few tens of centimeters thick. Their surfaces are generally higher topographically than are those of linguoid bars. This relationship is similar to that shown by Williams (1971, his

plate IV, p. 16) for longitudinal and linguoid bars.

Linguoid bars are repetitive spoon-shaped forms 10 to 50 m in length that have well-developed slipfaces on their downstream margins. This terminology for the description of bars follows that of Collinson (1970), and Williams (1971), who describe similar features in the Tana River, Norway, and ephemeral streams in interior Australia, respectively.

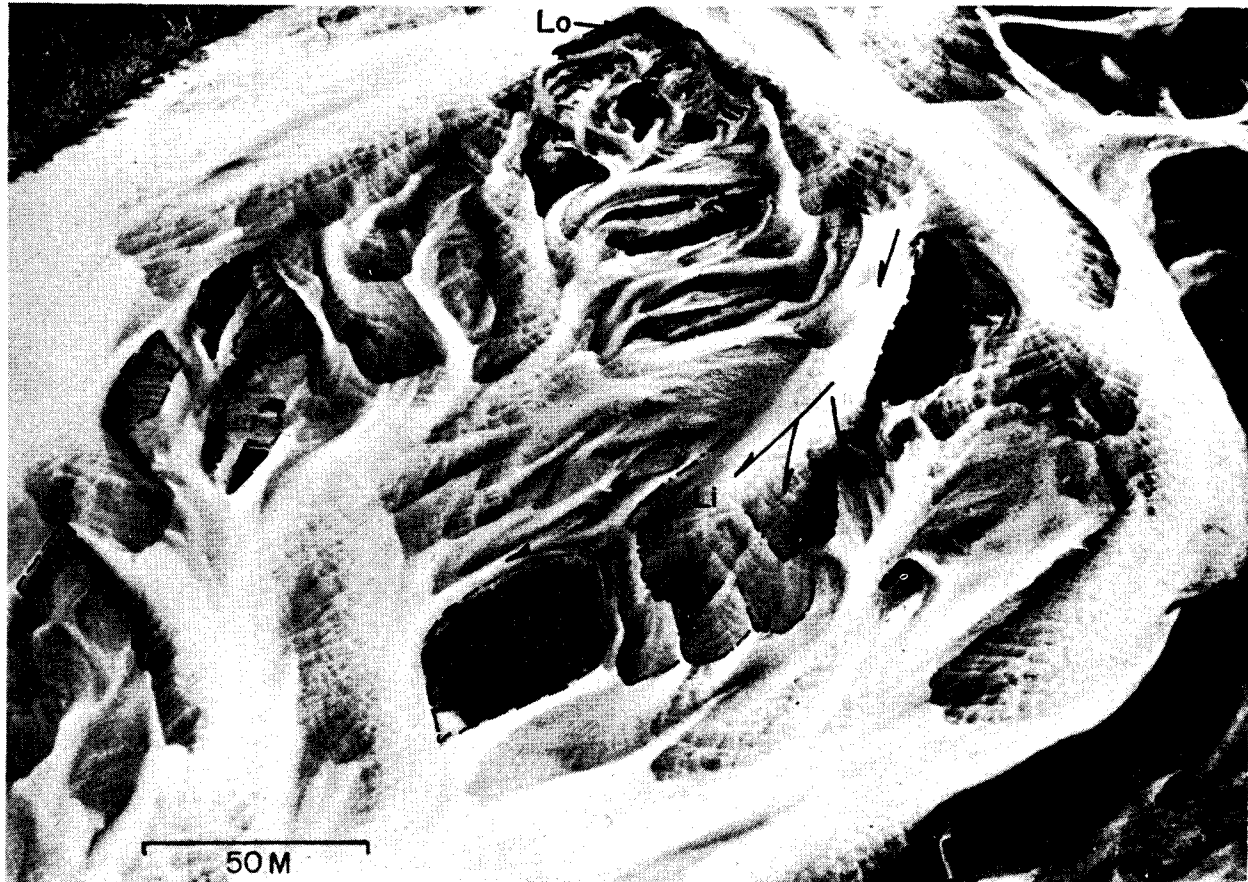


FIG. 19.—Linguoid bar morphology and flow pattern. Aerial view of a complex of longitudinal and linguoid bars on the lower Scott fan. Photograph was taken during a rising flood stage. View is looking upstream. Linguoid bars (*Li* and *dash-dot* outline) are attached to, and growing away from, eroded remnants of longitudinal bars (*Lo* and *dashed* outline). The linguoid bars are repetitive and most slipfaces are multilobate. Arrows show representative flow pattern.

Linguoid bars observed by the writers are also similar to transverse bars described by Smith (1970, 1971, 1972) from the Platte River. Smith (1972, p. 625) suggests that linguoid bars are merely transverse bars that assume symmetrical, lobate, repetitive forms at high flow. These forms then become distorted and modified through time. The writers prefer, however, to retain the term *linguoid* to describe those lobate bars that have a larger longitudinal dimension relative to width, regardless of later modification of slipfaces.

As mentioned above, linguoid bars occur lower in channels than longitudinal bars. Figure 19, representing conditions during a rising flood stage on the lower Scott, shows lobate slipfaces of linguoid bars attached to, and actively growing away from eroding remnants of longitudinal bars whose surfaces are emergent. It is assumed that both bar forms are present and active at high flows when most bar surfaces

are submerged. Linguoid bars continue active migration at lower flow stages when longitudinal bars are no longer active and are being dissected.

Meandering reach.—Point and lateral bars are found in the lower portion of the Scott fan where flow is confined between cohesive banks in a channel 40 to 80 m wide (fig. 20). Lateral bars exist where the channel becomes temporarily straight but where the thalweg continues to meander. These bars are 75- to 125-m long with the distal end of the upstream bar opposite the apex of the next bar downstream. Bar relief is variable between 50 and 100 cm. Some bar surfaces are more than 2 m above the bottom of scour pools in the channels. Bar surfaces are usually a few centimeters lower than the active levee. A slipface is present along the downstream half of the bar margin. Often this slipface is oriented perpendicular to the channel axis (fig. 20).



FIG. 20—Aerial view of two point bars and a levee system on the lower Scott fan (near station 21) taken during extreme low water. Downstream is to the right. Dashed lines separate various labeled depositional environments. Dashed-dot line (arrow) indicates the bar slipface. Active overbank sedimentation is destroying alders on portions of the levee. Marsh is brackish to fresh since the 1964 earthquake. Scour pools in the channels have a silt-clay drape deposited during low-water stages.

Bedforms and Sedimentary Structures

Trenches were dug at 500-meter intervals along the longitudinal profile of the lower Scott fan during an extreme low water stage (early June, 1971). Several trenches were dug at each locality in bar slipfaces, on the top surfaces of bars, and in overbank deposits. Most trenches were L-shaped and included a horizontal cut. Attempts to trench in the lower channels were generally unsuccessful due to the thixotropic nature of the sediment. Trench localities were correlated with bar morphology by low-level aerial photographs obtained during extreme low water, and at a time several weeks later during a rising flow stage related to annual flooding.

The active stream system of the Yana was at flood stage when visited in 1971; therefore, examination of internal structures of bars in the presently active area was impossible. However, trenches were dug into an adjacent abandoned sandy surface that aerial photographs taken in 1948 show to be an active depositional

area. The presently active streams are incised about 1 m below this surface.

Slipface migration of longitudinal bars produces large-scale planar to somewhat tangential cross-bedding (fig. 21). Cross-bed sets are 10 to 30 cm in height with dip angles ranging from 15 degrees to over 30 degrees. The planar cross-beds are usually overlain by flat beds or by type A ripple-drift cross-lamination usually less than 10 cm in total thickness and of the same mean grain size as the large-scale cross-beds (fig. 21B and C). Flat beds and ripple-drift cross-lamination commonly are interbedded with one another, indicating fluctuations in intensity of flow across the bar surface. A few trenches revealed large-scale trough cross-bedding formed by megaripple migration. Occasionally a planar cross-bed set composed of medium sand was overlain by ripple-drift cross-lamination consisting of poorly sorted silty sand, indicating an abrupt decrease in flow strength. Multiple planar cross-bed sets of the thickness shown by Williams (1971, fig. 11,

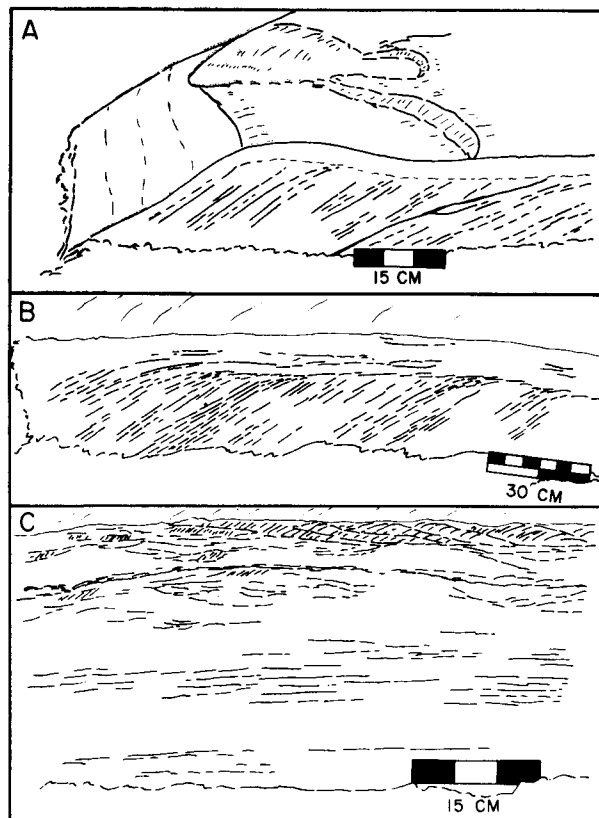


FIG. 21.—Internal structure of sandy longitudinal bars. A, Slipface morphology and planar cross-bedding. Large cusped ripples cover the bar surface but ripple cross-bedding is indistinct. Reactivation surface is mantled by a silt drape. B, Large-scale planar cross-beds formed by bar-slipface migration overlie flat beds. The bar crest is preserved in portions of the trench. C, Flat beds overlain by type A ripple-drift cross-lamination. Some type B ripple-drift cross-lamination is present at the top 5 cm of the trench. All trenches are in bars on the lower Scott fan.

p. 26) were not observed on the Scott fan.

Linguoid bars on the lower Scott fan have a bedform distribution pattern similar to that of transverse bars of Smith (1971, fig. 8, p. 3416). Megaripples (dunes) in the deeper central area (bar mouth) give way to diminished dunes of larger spacing and decreased height in shallower flow depths just upstream of the lobate bar crest. Migration of the bar slipface is accomplished by avalanching of sand carried to the crestline by migration of these diminished dunes. It is common for the bar crestline to assume a complex, multilobate shape.

A trench cut into an abandoned terrace on the lower Yana revealed a sequence of sedimentary structures interpreted as the result of deposition by a linguoid bar (fig. 22). In longitudinal section, a solitary planar to slightly tangential cross-bed set, 15 to 20 cm thick and

formed by migration of the slipface overlies indistinct ripple-drift cross-lamination. The contact is erosional. The planar foresets in turn are succeeded by as much as 50 cm of sandy type A ripple-drift cross-lamination that exhibits a low angle of climb (5 to 10 degrees). The top surface is an eolian deflation surface. Contact relations suggest that the planar foresets and overlying ripple-drift cross-lamination (deposition on the bar-surface) belong to one continuous depositional cycle with minor fluctuations in velocity or aggradation rate. A decrease in velocity allowed the ripple-drift cross-lamination to mantle the bar slipface (fig. 22A and B) which was then reactivated by an increase in flow velocity. In transverse section the multilobate nature of the bar slipface is apparent (fig. 22A).

Trough cross-beds, the result of megaripple migration, are extremely uncommon in sandy longitudinal and linguoid bar deposits, although these bedforms are readily apparent on active bar surfaces observed during low and rising flow stages. However, several sequences of sedimentary structures, interpreted here as deposition resulting in vertical accretion of a linguoid bar, do contain a single trough cross-bed set (fig. 23). The trench revealed several sequences of sandy ripple-drift cross-lamination succeeded by silty ripple-drift cross-lamination that was overlain by a silt-clay drape. The trough cross-bed set is at the base of 30 cm of type A ripple-drift cross-lamination. The sandy type A ripple-drift cross-lamination is succeeded upward by silty type B ripple-drift cross-lamination in a sequence that is quite common on the braided lower fan.

Cross-bedding in point bars and lateral bars is a combination of large-scale trough cross-bedding formed by megaripple migration on bar surfaces, and large-scale planar to tangential cross-bedding, the result of migration bar of slipfaces (fig. 24). Trough cross-bed sets 15 to 30 cm thick are interbedded with the bar foresets. Figure 24 illustrates that the bar slipface has migrated over a silty wedge of channel-bottom sediments. Two stages of migration of bar slipfaces, apparent in the photograph, are separated by the silty ripple-drift cross-lamination of the channel wedge. Figure 24A illustrates megaripple migration across the bar surfaces and active migration of part of the point-bar slipface.

Overbank deposits on the lower fan consist of silty ripple-drift cross-lamination, draped lamination (Gustavson and others, this vol.), and silt and clay laminations. Total thickness of the deposits is commonly 30 to 50 cm, but oc-

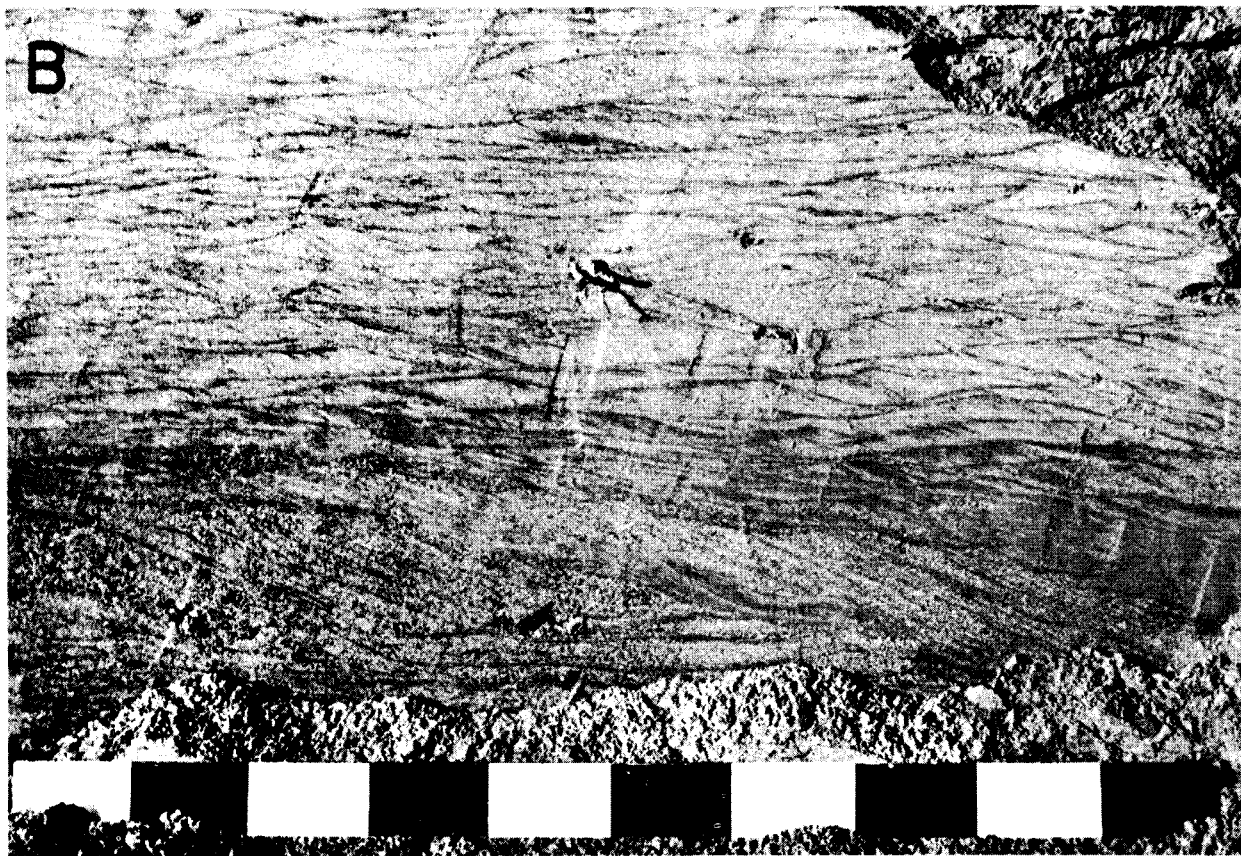
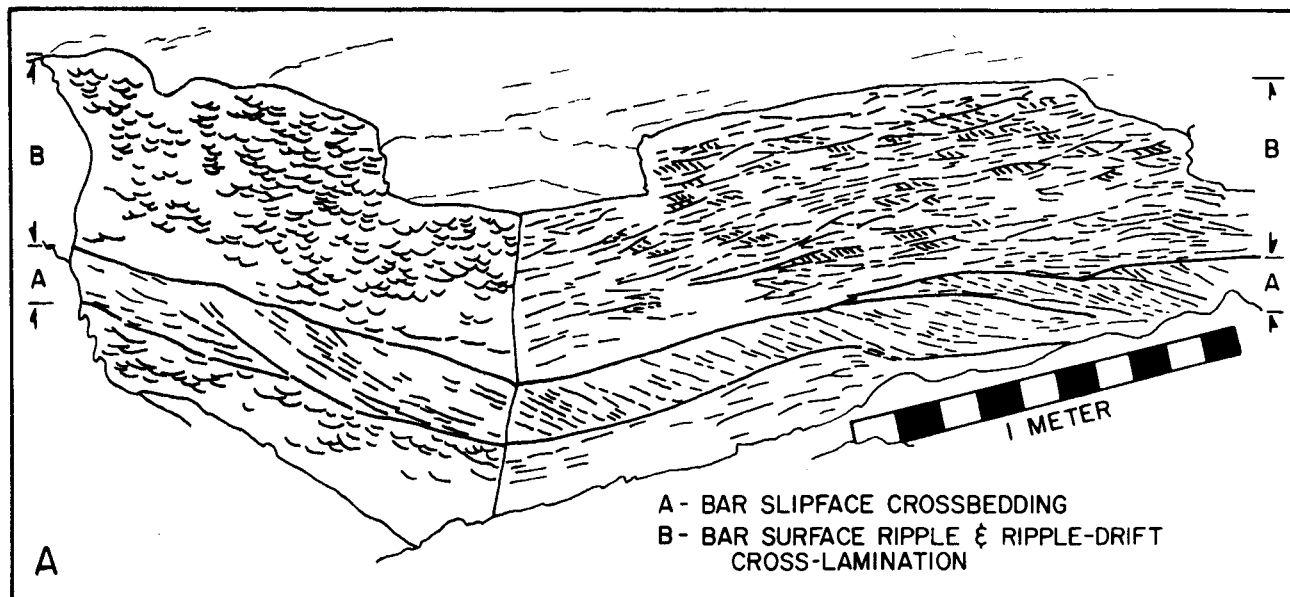


FIG. 22.—Internal structure of a linguoid bar. A, Sketch made from a longitudinal and transverse cut revealing type A ripple-drift cross-lamination overlain by large-scale tangential cross-beds, in turn overlain by type A ripple-drift. Large-scale cross-beds formed by slipface migration, ripple-drift cross-lamination by bar surface accretion. Flow was from left to right. B, Closeup of section of trench just above scale in B. Large-scale cross-beds are mantled by ripple-drift cross-lamination indicating a decrease in flow velocity. The slipface was later reactivated. Scale increments are 10 cm.

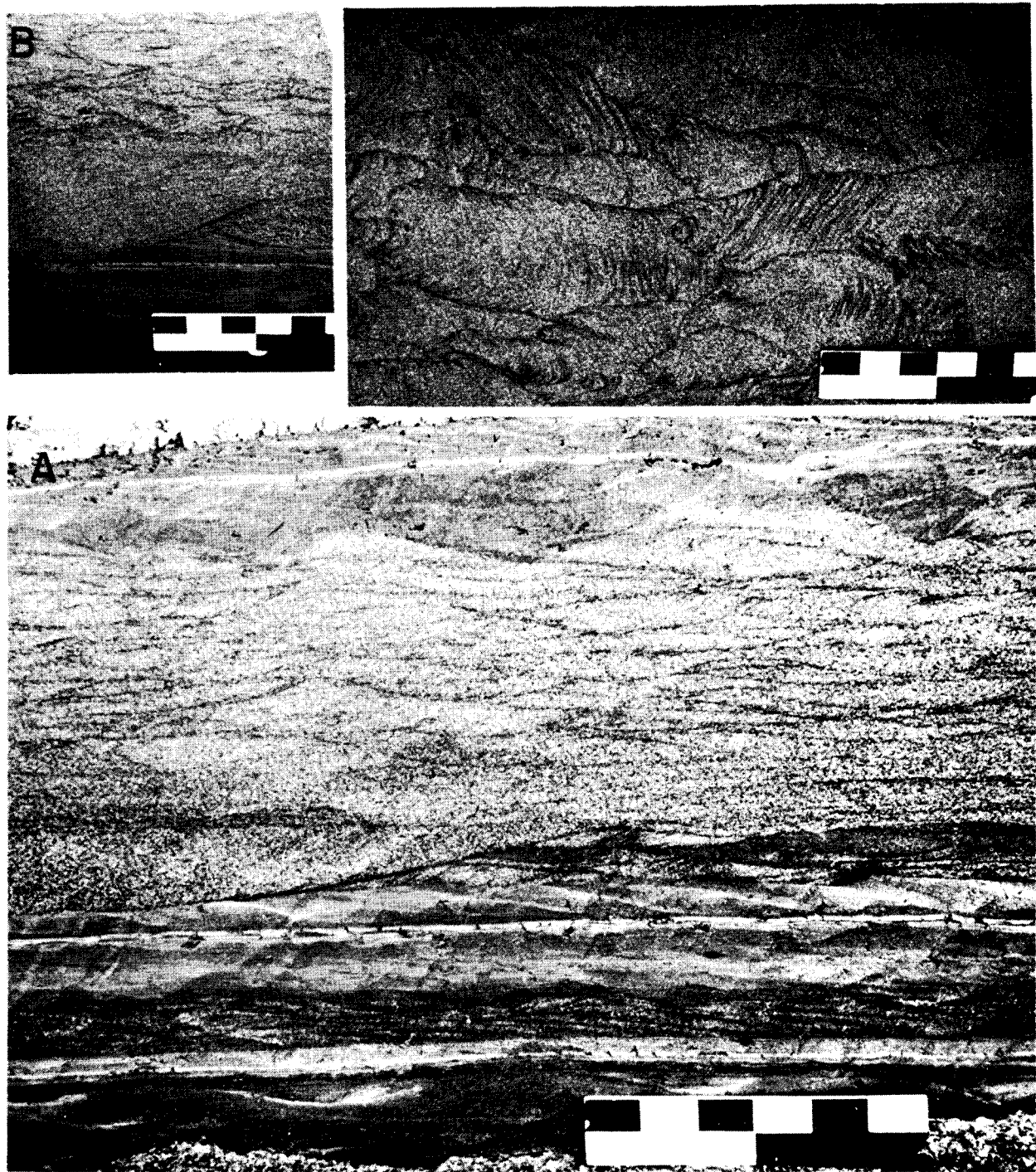


FIG. 23.—Linguoid bar internal structure. All views are from a trench on the lower Yana fan. A, Longitudinal section. Several sequences of ripple-drift cross-lamination are visible. A large-scale tangential cross-bed set is visible at left center. Flow was from right to left. B, Transverse section. The large-scale trough cross-beds resulted from megaripple migration. C, Horizontal section through type A ripple-drift cross-lamination in the upper part of the trench. Flow was from right to left. Scale is 30 cm in all photographs.

asionally varies up to 1 m (fig. 18B). Silt on overbank surfaces, other than silt drapes, becomes widespread at about kilometer 18 on the Scott fan. Relief of vegetated islands (above the channel bottom) becomes greater as one pro-

ceeds downstream. Islands on the proximal portion of the lower fan are more subject to flooding at intermediate flood flows, whereas those on the distal parts of the lower fan are flooded only at highest flood flows.

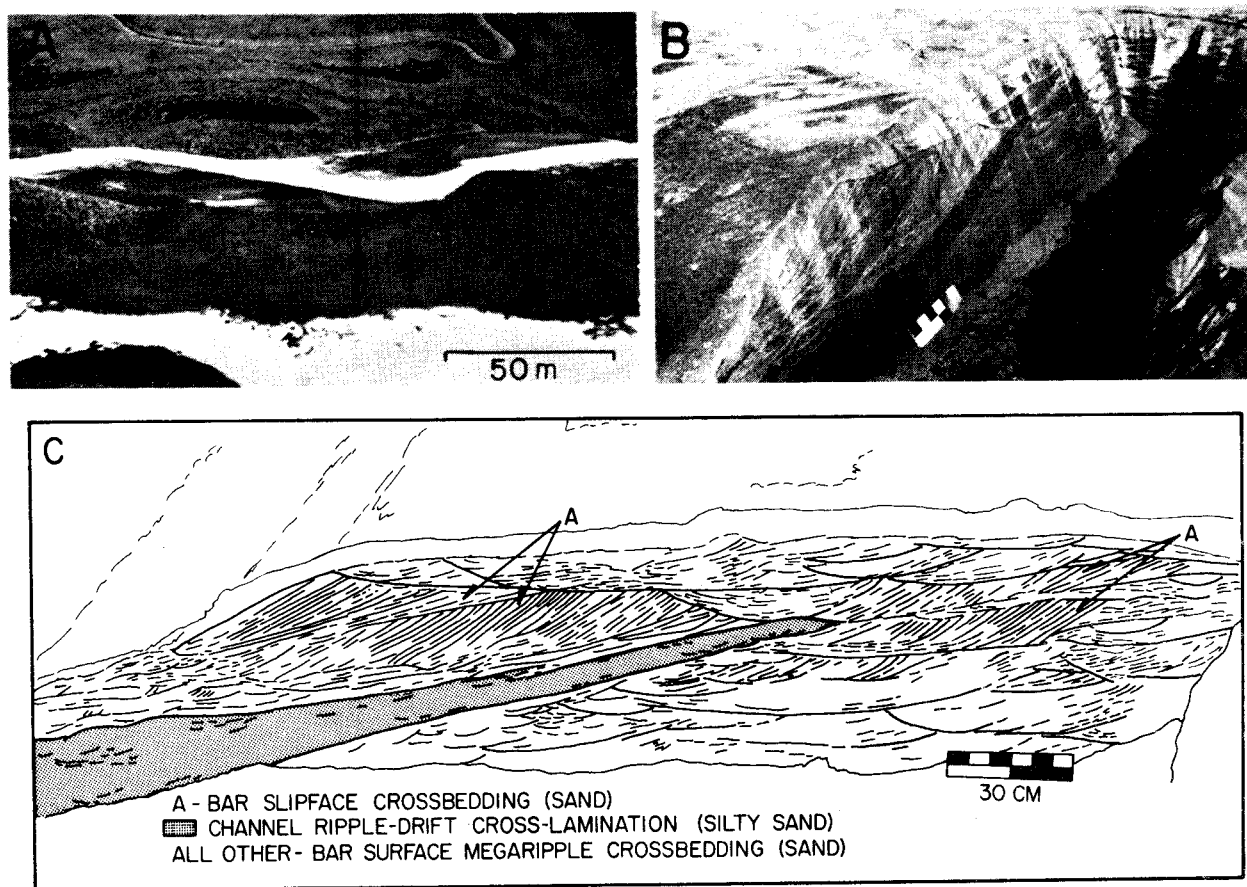


FIG. 24.—Surface morphology and internal structure of point bars. A, Aerial view taken during flood stage. Megaripples are active on the bar surface. There is an active slipface along portions of the bar margin. Flow is from left to right. B, Large-scale trough cross-beds overlain by silty wedge of channel-bottom sediments. Bar slipface has prograded over this wedge. Scale is 30 cm. C, Sketch made from photograph composite of trench shown in A. Several cycles of bar-slipface migration are apparent.

SUMMARY OF FACIES AND SEDIMENTARY STRUCTURES

Figure 25 summarizes the downstream variation in facies and sedimentary structures and gives typical stratigraphic columns for the upper fan (A), upper midfan (B), lower midfan (C), braided lower fan (D), and meandering lower fan (E). A comparison of Figure 25 with Table 1 ties the various facies to the appropriate bar types.

The upper fan (A) is mainly a coarse-gravel facies consisting of well-imbricated pebbles, cobbles, and boulders similar to facies 6 of Rust (1972, p. 232). The upper midfan (B), and to a certain extent the distal upper fan, is also a gravel facies, but with decreasing size of the largest clasts. This gravel is interbedded with flat beds and large-scale trough cross-beds of sand resulting from megaripple migration in low-stage channels. Sand-wedge deposition (Rust, 1972) is important in this area. The percent of sand versus gravel increases down-

stream, as illustrated by the column for the lower midfan (C). Large-scale festoon cross-beds have also increased in abundance.

The braided facies of the lower fan (D) exhibits planar cross-beds (slipface migration of longitudinal and linguoid bars) and abundant ripple-drift cross-lamination (bar-surface deposition), as well as some flat beds (longitudinal bar-surface deposition). Bar-slipface cross-bedding is similar to that shown for similar features by Smith (1971, 1972), Collinson (1970), and Williams (1971). The meandering facies of the lower fan (E) shows abundant large-scale trough cross-beds (megaripple migration on point-bar surfaces) and planar to tangential cross-beds resulting from migration of the bar slipface.

Overbank deposits are absent on the upper fan (A) but decrease in importance downfan. Grain size of the overbank silty ripple-drift cross-lamination and draped lamination decreases downfan.

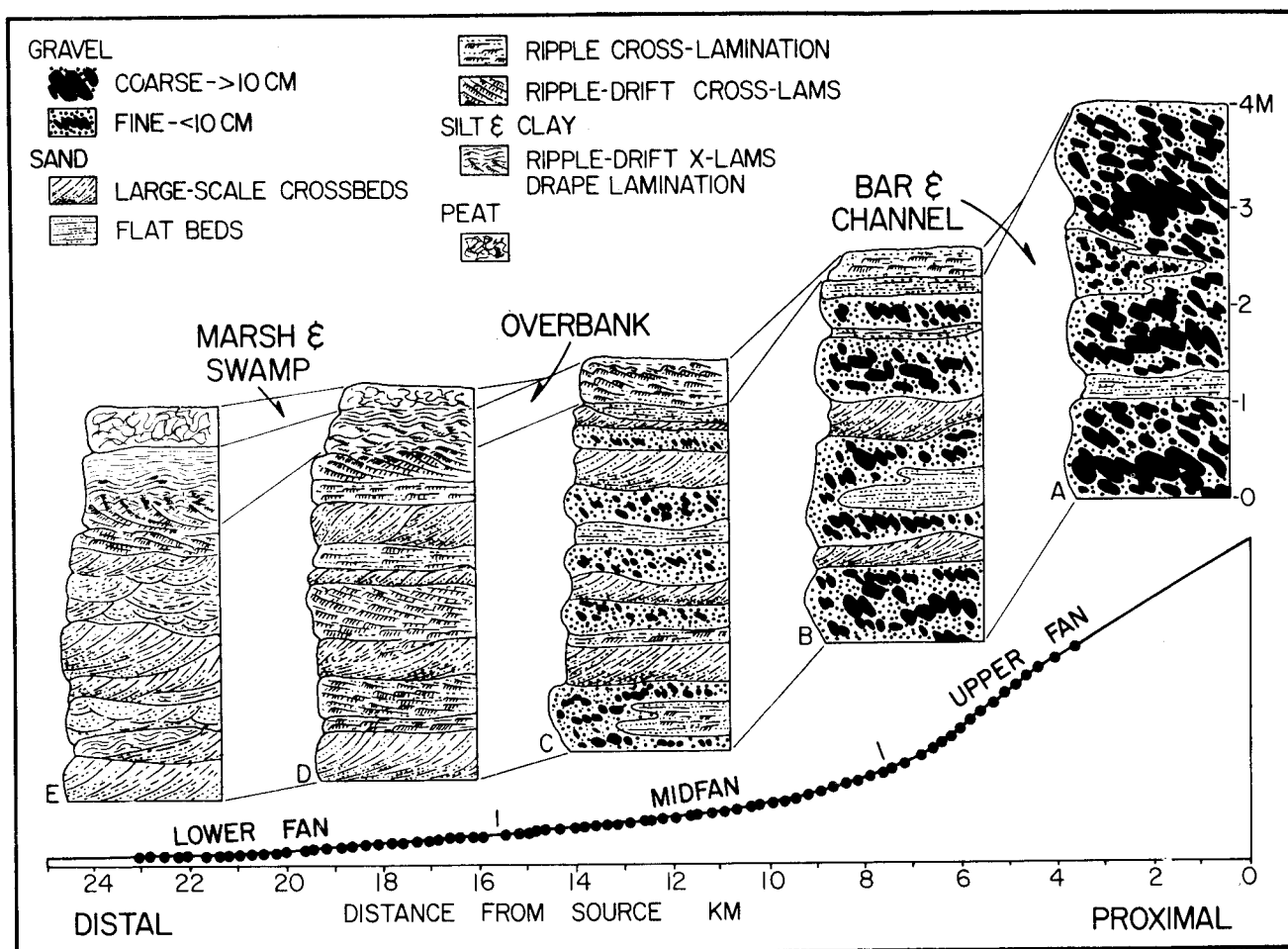


FIG. 25.—Downstream variation in facies and sedimentary structures. Bar and channel sequences do not fine upward, but are capped by a finer overbank facies that becomes more important in a downfan direction.

FLOW PROCESSES AND DEPOSITIONAL MECHANISMS

Measurements of mean velocity in channels on both the Scott and Yana fans (fig. 5A, 6A) indicate that velocity values vary around 200 centimeters per second for the upper fan, then decrease sharply about 6 km from the stream sources. An examination of flow-depth measurements obtained for Scott channels (fig. 5B) shows that depth follows no general trend, although flow in incised channels of the upper fan is deeper than for other areas.

Calculations of Froude number (F_r), boundary shear stress (τ_o), and stream power ($\tau_o \bar{U}$) were made using velocity, depth, and slope parameters obtained for the Scott fan (fig. 5C, D, E). Froude number:

$$F_r = \frac{\bar{U}}{\sqrt{gD}} \quad \begin{array}{l} \bar{U} = \text{mean velocity} \\ D = \text{flow depth} \end{array}$$

the ratio of inertia force to gravity force, is used to define the subcritical-supercritical flow boundary ($F_r = 1$) (Simons and others, 1965, p. 40;

Allen, 1970, p. 126). Froude number can also be used to predict the type of bedform in subcritical flow under shallow flow conditions (< 2 m) when used in conjunction with data of Guy and others (1966).

Boundary shear stress:

$$\tau_o = \gamma DS \quad \begin{array}{l} \gamma = \rho g = \text{specific weight of the fluid} \\ S = \text{slope} \end{array}$$

was calculated using a fluid density (ρ) of 1.0013 grams per milliliter (water temperature = 4.0°C; suspended sediment = 2.0 grams per liter, mid-point value from fig. 6). Stream power ($\tau_o \bar{U}$), defined as shear stress times mean velocity, has been used by Simons and others (1965), Allen (1970, p. 79), and Smith (1971, p. 3411) to illustrate changes in bed configuration.

Upper and Middle Fan

Water is confined to incised channels on the upper fan except at the highest flood stages. Extreme floods were not observed on any visits

to either fan. Floodwaters may spread from the main channel across bar surfaces during rising flood stages at any location downstream from the point where the channel pattern changes from incised to braided (fig. 3). For any given flood stage, there is successively greater areal flooding of bar surfaces in the downstream direction.

Observations and measurements indicate that both shear stress (τ) and mean velocity (u), and hence stream power, are greater for flow in deeper channels than over nearby bar surfaces (fig. 26). Therefore, larger size clasts can be transported in the channels than on an adjacent bar surface, or, conversely, critical shear stress (τ_c) and a critical "erosion" velocity would be exceeded sooner in the channel than on the bar surface. The geometry of the upper fan bars adjacent to channels (fig. 26) suggests that coarse gravel is transported up out of the channel and onto a bar surface as the main flow swings by, or bifurcates around, adjacent bars. This mechanism allows for the transport of coarse gravel in incised channels

several kilometers away from the stream source. A locus of deposition then occurs in the area of abrupt decrease in velocity and slope (fig. 8).

A comparison of shear stress values for the upper Scott fan (fig. 5D) with those obtained by Fahnestock (1963, p. 31) for bed-load transport in the White River shows a general agreement in magnitude of shear stress for similar size ranges of clasts (that is, assuming clast sizes in the Scott channels are similar to the largest on adjacent bar surfaces). This suggests that significant gravel transport is occurring in channels even during declining flows after the maximum flood stage. Actual observation of bed-load transport was impossible due to the high suspended-sediment content of the water.

Rust (1972, p. 243) suggests that longitudinal bars accrete by deposition of planar sheets of gravel on their surfaces, and that this process may lead to an upstream migration of the bar form. The depositional mechanism outlined above for bars on the Scott fan suggests that accretion of coarse clasts occurs on the up-

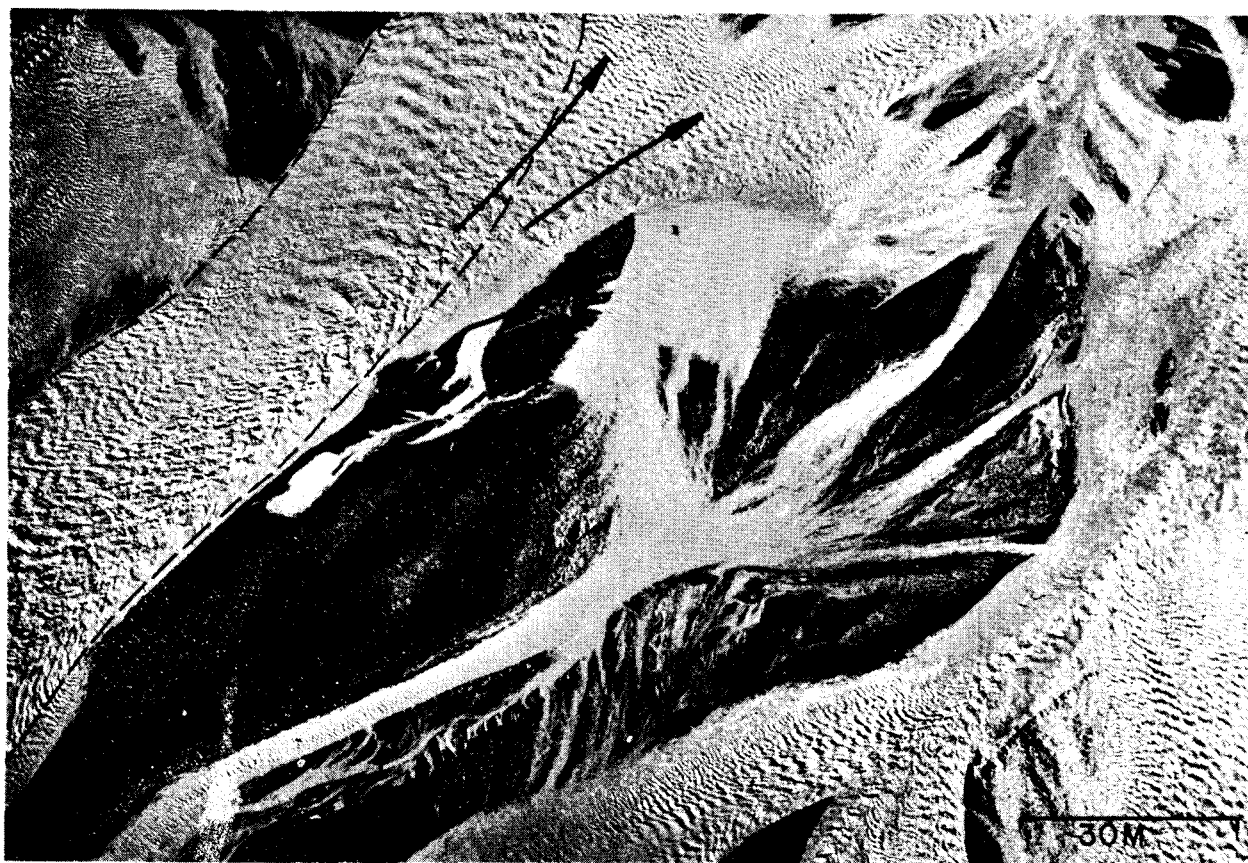


FIG. 26.—Bar and channel flow pattern. Aerial view of flow during flood stage on the upper Yana fan. Dashed line outlines a deeply incised erosional channel. Larger antidunes are in the deeper portions of the channel where stream power is greatest. Smaller antidunes are present in the shallower parts of the channel and over the bar surface at top center. Arrows indicate flow of water out of channel and across bar surface. (T) indicates transverse ribs.

stream apex of the bar, but that finer clasts are transported and deposited across the bar surface. This would lead to down-bar fining and account for the surface morphology of the low-relief, longitudinal bars of the upper fan (fig. 12). Bedding planes are obscure in cuts in coarse material (fig. 11B), but are essentially horizontal where observed.

Antidunes or in-phase waves can form under subcritical flow conditions (Williams, 1967, p. 213; Southard, 1971, p. 908) at $F_r \approx 0.85$ or less. Observation and measurements on both fans show that in-phase waves are common in the major channels and on submerged bar surfaces in the upper midfan and upper fan areas (fig. 5C, 26). The ubiquitous occurrence of antidune water-wave forms as shown in Figure 26, particularly on bar surfaces together with the evidence presented by Fahnestock and Hauschild (1962), suggests that they are important in the formation of transverse ribs.

Calculated shear stress values indicate little or no gravel transport in Scott midfan channels (fig. 5D) when compared with Fahnestock's values (1963, p. 31) for similar clast size. Observation of the channels during this declining flow stage also indicates no gravel movement on the upper midfan. On the distal midfan, channels were floored with medium to coarse sand with megaripple or flat-bed configuration.

Stream power calculations (fig. 5E) when compared with compilations of Allen (1970, p. 79) and the field data of Smith (1971, p. 3411), also indicate plane or flat bed or higher regime bedforms for the upper midfan, whereas calculations for the lower midfan show a megaripple bed configuration. Froude number calculations for the midfan (fig. 5C) show most values below 0.60. This is in the range of megaripples (dunes) to transition forms, according to the data of Guy and others (1966) for medium to coarse sand sizes.

Lower Fan

Longitudinal bar migration occurs at moderate to high-stage flooding and was not observed during visits to the fans. The presence of abundant flat beds and low-angle (< 5 degrees) type A ripple-drift cross-lamination (fig. 21) suggests higher intensity flow across longitu-

dinal bar surfaces than across linguoid bars. Longitudinal bar growth appears to have been largely by slipface migration.

Linguoid bar migration occurs at all but the lowest flow stages. Migration of linguoid or transverse bars has been thoroughly discussed by Smith (1971, 1972). On the outwaash fans these bars seem to have grown by slipface migration and vertical accretion of ripple-drift cross-lamination deposited partially from suspension (figs. 22 and 23). A puzzling question is the common occurrence of megaripples on linguoid-bar surfaces at low flows (fig. 22), as opposed to their lack of widespread preservation in the internal structure of the bars. One answer might be that they are equilibrium bedforms at both high and low flows, contributing sediment to the bar slipface but not often themselves being preserved. Abundant trough cross-bed sets are preserved, however, in lower fan point bars and lateral bars (fig. 24).

ACKNOWLEDGMENTS

Funds for this research were provided by the Office of Naval Research, Geography Branch (contract N00014-67-A-0230-0001; M. O. Hayes, principal investigator), and by the Department of Geology and Geography, University of Massachusetts.

We would like to thank J. H. Hartshorn, N. D. Smith, and Peter Lewis for their critical review of the manuscript and T. C. Gustavson, Noel Waechter, and N. D. Smith for their interest in discussing outwash-fan sedimentation. J. H. Hartshorn also gave access to unpublished maps and rare aerial photographs that aided materially in facies interpretation. Dennis Wilkins, E. G. Rhodes, R. L. Henry, and S. C. Farrell provided valuable assistance in the field.

We would also like to thank Wallace Watts and other members of the United States Forest Service (Cordova), the personnel of Alaska Division of Fish and Game (Cordova), Sid Nalley and other personnel of the FAA Flight Service Station (Cordova), and Richard Nichols and John Davis of Gulf Air Taxi (Yakutat). Particular recognition is given to pilot John Davis, whose landings on gravel bars made possible much of the field work on Yana Stream.

REFERENCES

- ALLEN, J. R. L., 1970, *Physical processes of sedimentation*: American Elsevier Publishing Co., New York. 248 p.
- BOOTHROYD, J. C., 1972, *Coarse-grained sedimentation on a braided outwash fan, northeast Gulf of Alaska*: Technical Report No. 6-CRD, Coastal Research Division, Univ. of South Carolina, Columbia, S.C. 127 p.

- , 1969, Hydraulic conditions controlling the formation of estuarine bedforms: p. 417-427 in M. O. Hayes (ed.), Coastal Research Group, Coastal environments of northeastern Massachusetts and New Hampshire, Eastern Section, Field Trip Guidebook, 462 p.
- , AND ASHLEY, G. M., 1972, Bedforms and sedimentary structures of braided outwash streams, Northeast Gulf of Alaska: Geol. Soc. America Annual Meeting, N.E. Section, Program Abstract, v. 4, No. 1, p. 3.
- BRADLEY, W. C., FAHNESTOCK, R. K., AND ROWEKAMP, T. T., 1972, Coarse sediment transport by flood flows on Knik River, Alaska: Geol. Soc. America Bull., v. 83, p. 1261-1284.
- COLEMAN, J. M., 1969, Brahmaputra River: channel process and sedimentation: Sedimentary Geology, v. 3, p. 129-239.
- COLLINSON, J. D., 1970, Bedforms of the Tana River, Norway: Geografiska Annaler, v. 52A, p. 31-56.
- DOBKINS, J. E., JR., AND FOLK, R. L., 1970, Shape development on Tahiti-Nui: Jour. Sed. Petrology, v. 40, p. 1167-1203.
- EMBLETON, CLIFFORD, AND KING, C. A. M., 1968, Glacial and periglacial geomorphology: St. Martin's Press, New York, 608 p.
- FAHNESTOCK, R. K., 1969, Morphology of the Slims River: p. 161-172 in Bushnell, V. C., and Ragle, R. H., eds., Scientific results, Icefield Ranges Research Project, Am. Geog. Soc. and Arctic Inst. North America, v. 1.
- FAHNESTOCK, R. K., 1963, Morphology and hydrology of a glacial stream—White River, Mount Rainier, Washington: U.S. Geol. Survey Prof. Paper 422-A, p. 1-70.
- FAHNESTOCK, R. K., AND HAUSHILD, W. L., 1962, Flume studies of the transport of pebbles and cobbles on a sand bed: Geol. Soc. America Bull., v. 73, p. 1431-1436.
- GUY, H. P., SIMONS, D. B., AND RICHARDSON, E. V., 1966, Summary of alluvial channel data from flume experiments: U.S. Geol. Survey Prof. Paper 462-I, 96 p.
- HAYES, M. O., HOBBS, C. H., HENRY, R., HAGUE, P., AND RAFFALDI, F., 1972, Coastal sedimentation in a tectonically active geosynclinal basin: the glacial-outwash plain shoreline of the northeastern Gulf of Alaska (abs.): Am. Assoc. Petroleum Geologists Bull., v. 56, p. 624.
- HELLEY, E. J., 1969, Field measurement of the initiation of large bed particle motion in Blue Creek near Klamath, California: U.S. Geol. Survey Prof. Paper 562-G, p. G1-G19.
- JOHANSSON, C. E., 1962, Orientation of pebbles in running water: A laboratory study; Geografiska Annaler, v. 45, p. 85-111.
- JOPLING, A. V., 1965, Hydraulic factors controlling the shape of laminae in laboratory deltas: Jour. Sed. Petrology, v. 35, p. 777-791.
- , AND WALKER, R. G., 1968, Morphology and origin of ripple-drift cross-lamination, with examples from the Pleistocene of Massachusetts: *ibid.*, v. 38, p. 971-984.
- KRIGSTRÖM, A., 1962, Geomorphological studies of sandur plains and their braided rivers in Iceland: Geografiska Annaler, v. 44, p. 328-346.
- KRUMBEIN, W. C., 1939, Preferred orientation of pebbles in sedimentary deposits: Jour. Geology, v. 47, p. 673-706.
- LANE, E. W., AND CARLSON, E. J., 1954, Some observations on the effect of particle shape on the movement of coarse sediments: Am. Geophys. Union Trans., v. 35, p. 453-462.
- LEOPOLD, L. B., AND WOLMAN, M. G., 1957, River channel patterns: braided, meandering and straight: U.S. Geol. Survey Prof. Paper 282-B, p. 39-85.
- MCDONALD, B. C., AND BANERJEE, INDRANIL, 1970, Sedimentology studies on the outwash plain below Peyto Glacier, Alberta: Geol. Survey Canada, Report of Activities, Paper 70-1, Pt. A, p. 199.
- , 1971, Sediments and bedforms on a braided outwash plain: Canadian Jour. Earth Sci., v. 8, p. 1282-1301.
- MCGOWEN, J. H., 1970, Gum Hollow fan delta, Nueces Bay, Texas: Report of Inv. No. 69, Bureau of Econ. Geology, Univ. of Texas, 91 p.
- ORE, H. T., 1964, Some criteria for recognition of braided stream deposits: Wyoming Univ. Geology Contr., v. 3, p. 1-14.
- PLAFKER, G., 1967, Geologic map of the Gulf of Alaska Tertiary Province, Alaska: U.S. Geol. Survey Misc. Geol. Inv. Map I-484.
- REIMNITZ, E., 1966, Late Quaternary history and sedimentation of the Copper River Delta and vicinity, Alaska: Unpub. Ph.D. dissertation, Univ. of Calif. at San Diego, 160 p.
- RUST, B. R., 1972a, Structure and process in a braided river: Sedimentology, v. 18, p. 221-245.
- RUST, B. R., 1972b, Pebble orientation in fluvial sediments: Jour. Sed. Petrology, v. 42, p. 384-388.
- SCHLEE, J., 1957, Fluvial gravel fabric: *ibid.*, v. 27, p. 162-176.
- SCOTT, K. M., AND GRAVLEE, G. C., JR., 1968, Flood surge on the Rubicon River, California—hydrology, hydraulics and boulder transport: U.S. Geol. Survey Prof. Paper 422-M, 40 p.
- SIMONS, D. B., RICHARDSON, E. V., AND NORDIN, C. F., JR., 1965, Sedimentary structures generated by flow in alluvial channels: p. 34-52 in Middleton, G. V., ed., Primary sedimentary structures and their hydrodynamic interpretation: Soc. Econ. Paleontologists and Mineralogists, Spec. Pub. 12, 265 p.
- SMITH, N. D., 1972, Some sedimentological aspects of planar cross-stratification in a sandy braided river: Jour. Sed. Petrology, v. 42, p. 624-634.
- SMITH, N. D., 1971, Transverse bars and braiding in the lower Platte River, Nebraska: Geol. Soc. America Bull., v. 82, p. 3407-3420.
- SMITH, N. D., 1970, The braided stream depositional environment: Comparison of the Platte River with some Silurian clastic rocks, North-Central Appalachians: *ibid.*, v. 81, p. 2993-3014.
- SNEED, E. D., AND FOLK, R. L., 1958, Pebbles in the lower Colorado River, Texas—A study in particle morphogenesis: Jour. Geology, v. 66, p. 114-150.

- SOUTHARD, J. B., 1971, Representation of bed configuration in depth-velocity-size diagrams: *Jour. Sed. Petrology*, v. 41, p. 903-915.
- U.S. GEOLOGICAL SURVEY, 1969, Surface water records for Alaska, 1969: *Water Resources Data for Alaska*, Pt. 1.
- WILLIAMS, G. E., 1971, Flood deposits of the sand-bed ephemeral streams of central Australia: *Sedimentology*, v. 17, p. 1-40.
- WILLIAMS, G. P., 1967, Flume experiments on the transport of a coarse sand: *U.S. Geol. Survey Prof. Paper 562-B*, 31 p.
- WILLIAMS, P. F., AND RUST, B. R., 1969, The sedimentology of a braided river: *Jour. Sed. Petrology*, v. 39, p. 649-679.

A reprint from
GLACIOFLUVIAL AND GLACIOLACUSTRINE SEDIMENTATION
Society of Economic Paleontologists and Mineralogists
Special Publication No. 23
1975

RO# 59

Coastal Research Division
Department of Geology
University of South Carolina
Columbia, South Carolina 29208

Technical Report No. 9-CRD

COASTAL DYNAMICS AND SEDIMENT TRANSPORTATION,
NORTHEAST GULF OF ALASKA

Dag Nummedal

Michael F. Stephen

May 1976

Technical Report obtained under Contract No.
03-5-022-82, The Environmental Research Laboratory,
National Oceanic and Atmospheric Administration,
Boulder, Colorado. Reproduction in whole or in part is
permitted for any purpose of the United States Government.
Distribution of this document is unlimited.

Bibliographic reference

- Nummedal, D., and M. F. Stephen, 1976, Coastal dynamics and sediment transportation, northeast Gulf of Alaska; Tech. Rept. No. 9-CRD, University of South Carolina, 148 p.

ABSTRACT

Analysis of the climatology and physical oceanography of the northeast Gulf of Alaska provides a predictive model for wave height and longshore sediment transportation along the coastline between Yakutat and Cape Suckling. The relationships between the offshore wave climate, the bathymetrically controlled patterns of refraction and the resulting shoreline variability in physical processes have been emphasized.

Field observations of coastal morphology, sediment dispersal trends and breaker parameter variability were made in July and August of 1975. Despite the absence of any major storm episodes during the field season, the observed processes correlate well with the sediment distribution in all environments except on high-level storm berms and washover terraces at the east Malaspina Foreland where occasional storms induce a sediment transport direction opposite to that of the dominant conditions.

The wave climate model and field observations demonstrate a general westward transport of sediment on the exposed beaches of the northeast Gulf of Alaska. Reversals of this trend are observed on the west side of Icy Bay and Yakutat Bay where the net transport direction is towards the northeast, i.e., towards the head of the bays.

The annual average gross longshore sediment transport rate was determined to be about 6.5 million cubic meters. The annual net sediment flux ranges from about 5.8 million cubic meters to the west between Cape Yakataga and Icy Cape, to about 170,000 cubic meters to the east between Sitkagi Bluffs and the western shores of Yakutat Bay.

TABLE OF CONTENTS

| | <u>Page</u> |
|---|-------------|
| ABSTRACT | i |
| LIST OF FIGURES. | iv |
| LIST OF TABLES | vii |
| LIST OF SYMBOLS. | viii |
| ACKNOWLEDGEMENTS | ix |
| INTRODUCTION | 1 |
| SUMMARY OF WAVE CLIMATE. | 18 |
| North Pacific Cyclones. | 18 |
| Gulf of Alaska Coastal Wind Regimes | 19 |
| Wave Energy Flux Distribution | 38 |
| WAVE REFRACTION. | 47 |
| Principles and Bathymetry | 47 |
| Discussion of Refraction Diagrams | 49 |
| Wave Height Distribution. | 61 |
| SEDIMENT TRANSPORT | 67 |
| Sediment Transport Computation Methods. | 67 |
| Results of SSMO Computations. | 68 |
| Transport Rates Based on Observed Wave Conditions | 74 |
| OBSERVED COASTAL PROCESSES | 74 |
| General | 74 |
| Regional Process Network. | 76 |
| Time-series Process Measurements. | 80 |
| Special Studies | 117 |
| Summary of Process Variability. | 137 |

| | <u>Page</u> |
|----------------------|-------------|
| CONCLUSIONS. | 144 |
| REFERENCES | 147 |

LIST OF FIGURES

| <u>Figure</u> | <u>Page</u> |
|---|-------------|
| 1. ERTS-image mosaic of the northeast coast of the Gulf of Alaska . . . | 3 |
| 2. Oblique aerial photo looking west across Icy Cape. | 5 |
| 3. Oblique aerial photo of Claybluff Point and the west side of Icy Bay. | 7 |
| 4. Oblique aerial photo of the east side of Icy Bay. Riou Spit in the foreground | 9 |
| 5. Oblique aerial photo of the west Malaspina Foreland, looking east. Riou Spit is in the foreground | 11 |
| 6. Oblique aerial photo of the west Malaspina Foreland. | 13 |
| 7. Oblique aerial view of the east Malaspina Foreland, looking west . | 15 |
| 8. Oblique aerial view of Grand Wash Stream on the west side of Yakutat Bay. | 17 |
| 9. Principal frontal zones in winter. | 21 |
| 10. Cyclone tracks across the North Pacific in January, 1973 | 23 |
| 11. Cyclone tracks across the North Pacific in July, 1972. | 25 |
| 12. A. Percentage frequency of cyclone centers in winter. | 27 |
| B. Percentage frequency of cyclone centers in summer. | 27 |
| 13. Wind frequency distribution in the Gulf of Alaska. | 29 |
| 14. Synoptic chart for January 9, 1973 | 31 |
| 15. Synoptic chart for January 17, 1973. | 33 |
| 16. Synoptic chart for July 25, 1972 | 35 |
| 17. Synoptic chart for July 11, 1972 | 37 |
| 18. Wave energy flux distribution in the Gulf of Alaska derived from SSMO-data. | 43 |
| 19. Resultant wave energy flux and sediment transportation in the Gulf of Alaska | 45 |
| 20. Refraction diagram for eight-second waves out of the south | 51 |

| <u>Figure</u> | <u>Page</u> |
|---|-------------|
| 21. Refraction diagram for twelve-second waves out of the southwest. . . | 53 |
| 22. Refraction diagram for twelve-second waves out of the south. . . . | 55 |
| 23. Refraction diagram for twelve-second waves out of the southeast. . . | 57 |
| 24. Refraction diagram for sixteen-second waves out of the south . . . | 59 |
| 25. Predicted wave height distribution along the northeast coast of the Gulf of Alaska | 65 |
| 26. Sediment transport rate diagram. | 73 |
| 27. Nearshore wave parameter variability | 79 |
| 28. Location map for process zonals and special study sites. | 83 |
| 29. Process variables at the Old Yahtse zonal site | 85 |
| 30. Tidal curve for Sitka, Alaska, for the period of July 21 to August 22, 1975. | 87 |
| 31. Oblique aerial view of the Old Yahtse process zonal site | 89 |
| 32. Beach profiles at the Old Yahtse process zonal site. | 91 |
| 33. Claybluff Point process variables. | 95 |
| 34. Oblique aerial view of Claybluff Point | 97 |
| 35. Beach profiles at Claybluff Point. | 99 |
| 36. Process variables at the Shipwreck zonal site. | 101 |
| 37. Beach profiles at the Shipwreck zonal site | 103 |
| 38. Process variables at the Train-barge Wreck zonal site. | 107 |
| 39. Train-barge Wreck. | 109 |
| 40. Beach profiles at the Train-barge Wreck zonal site | 111 |
| 41. Process variables at Riou Spit | 113 |
| 42. Oblique aerial view of Riou Spit | 115 |
| 43. Location of fathometer tracks in Icy Bay | 119 |
| 44. Riou Spit fathometer profiles no. 1-4. | 121 |

| <u>Figure</u> | <u>Page</u> |
|--|-------------|
| 45. Riou Spit fathometer profiles no. 5-7. | 123 |
| 46. Riou Spit beach profiles | 125 |
| 47. Photo of Riou Spit erosion scarp | 127 |
| 48. Process variables at Alder Stream. | 129 |
| 49. Morphology of Chirp Island | 133 |
| 50. Oblique air photo of Chirp Island. | 135 |
| 51. Cliffs at Point Riou at low tide | 139 |
| 52. Waves reflecting from Point Riou at high tide. | 141 |
| 53. Summary diagram of sediment transport directions | 143 |

LIST OF TABLES

| <u>Table</u> | <u>Page</u> |
|---|-------------|
| 1. Deep water wave energy flux values for the Gulf of Alaska | 46 |
| 2. Refraction coefficients at 25 meter water depth for eight, twelve and sixteen-second waves in the north-central Gulf of Alaska. . . . | 62 |
| 3. Orientation of shoreline and wave crests for four segments of the northeast coast of the Gulf of Alaska | 69 |
| 4. Longshore sediment transport rates on the northeast coast of the Gulf of Alaska. | 70 |
| 5. Sediment transport rates for observed unidirectional waves. | 75 |
| 6. Chirp Island littoral processes | 131 |

LIST OF SYMBOLS

| | |
|-----------|---|
| b | spacing of wave orthogonals |
| C | phase velocity of a progressive wave |
| E | wave energy density |
| g | acceleration of gravity |
| H | wave height |
| K_r | refraction coefficient |
| K_s | shoaling coefficient |
| n | ratio between group velocity and phase velocity of a progressive wave |
| P | wave energy flux |
| P_l | longshore component of wave energy flux |
| $P_{i,m}$ | probability of occurrence of wave height H_i , traveling in direction m |
| Q | rate of longshore transport of sediment |
| Q_g | gross transport rate |
| Q_l | rate of transport to the left |
| Q_n | net transport rate |
| Q_r | rate of transport to the right |
| $r_{i,j}$ | probability of occurrence of wave height H_i and period T_j |
| T | wave period |
| α | angle of wave crest relative to shore |
| ρ | density of water |
| | subscript o refers to deep water conditions |
| | subscript b refers to breaker conditions |

ACKNOWLEDGEMENTS

The authors are indebted to Miles O. Hayes for valuable advice and assistance. Chris Ruby and Steve Wilson rendered outstanding services in the field.

Financial support was granted by the National Oceanic and Atmospheric Administration, Contract No. 03-5-022-82, Miles O. Hayes, Principal Investigator.

INTRODUCTION

This represents an annual report to the National Oceanic and Atmospheric Administration, Environmental Research Laboratories, for contract no. 03-5-022-82, Miles O. Hayes, Principal Investigator.

The main objective of the project was to evaluate the geological aspects of coastal environments of the northeast Gulf of Alaska between Dry Bay and Cape Yakataga (Fig. 1). The study and the report preparations were divided into three parts: (1) coastal dynamics and sediment transportation, (2) morphology and sedimentology of the coastal zone, and (3) environmental geology of the Icy Bay region and the west Malaspina Foreland.

This report on coastal dynamics and sediment transportation emphasizes the relationship between offshore wave climate in the Gulf of Alaska, the bathymetrically controlled patterns of wave refraction across the steep Alaskan continental shelf and the resulting shoreline variability in wave energy, longshore current regime, morphology and sediment transportation rates.

Detailed field observations between Cape Yakataga and Yakutat Bay during July and August of 1975 form the basis for the analysis of characteristics of shoreline variability. Ship wave observations (SSMO-data), surface synoptic meteorological charts and bathymetric charts of the northeast Gulf provide the data needed for determination of physical oceanographic conditions related to shoreline geology.

As an introduction to the study area, Figures 1 through 8 provide a LANDSAT-satellite view and seven high-altitude oblique air photos of the coastal zone from Cape Yakataga to Yakutat Bay.

Figure 1. LANDSAT -mosaic of the coastal region of the northeast Gulf of Alaska from Dry Bay to Cape Yakataga. The numbered arrows refer to the location and direction of view of high-altitude oblique aerial photographs presented in Figures 2 through 8.

227

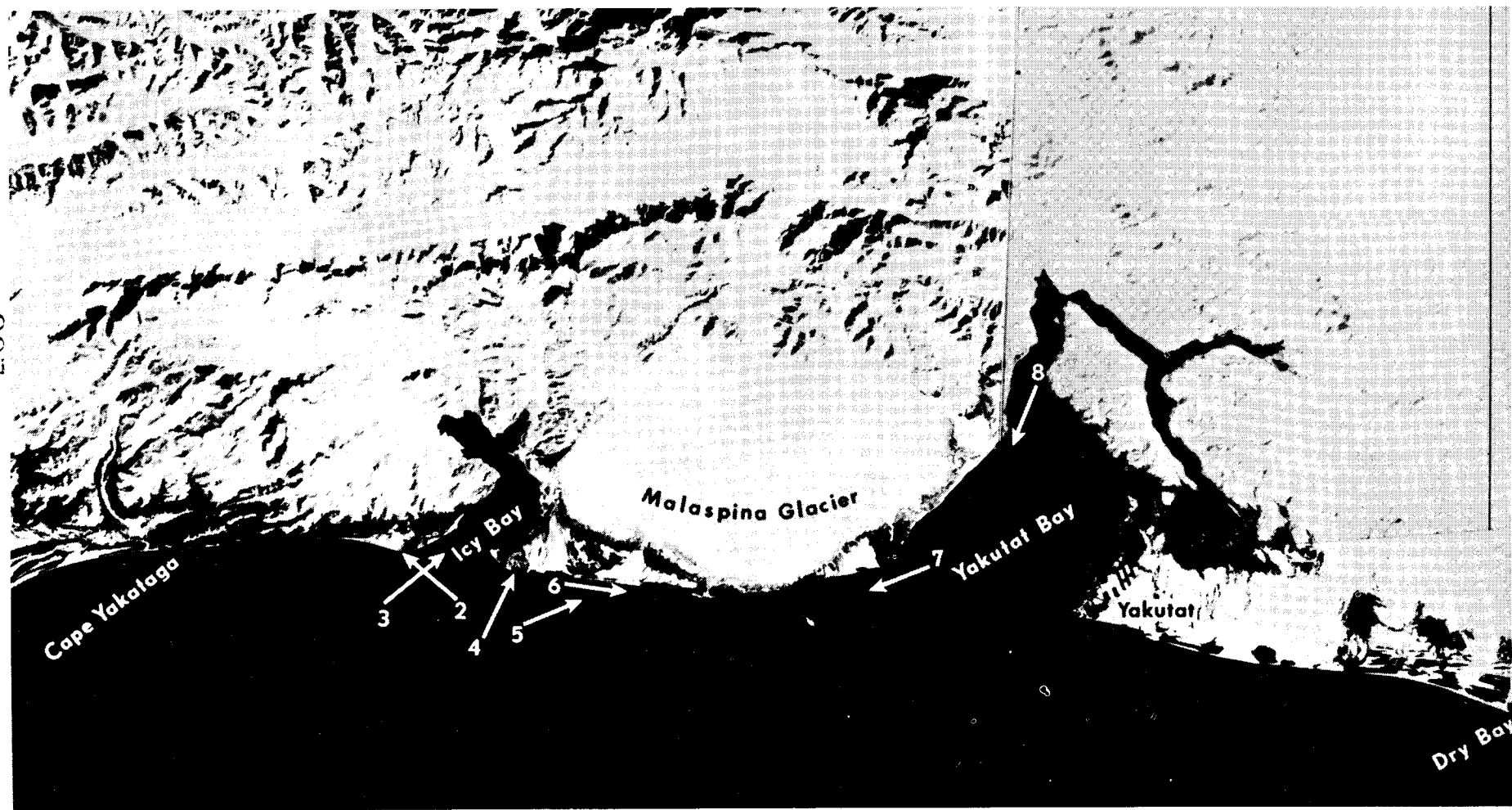


Figure 2. Oblique air photo of the coast from Icy Cape (foreground) to Cape Yakataga (background). The photo was taken on August 4, 1975, from 9000 ft. For location of photo, see Figure 1. The largest waves observed during the field season were at Icy Cape. Processes and geomorphology indicate a net westward sediment transport between Icy Cape and Cape Yakataga, and a northeastward transport into Icy Bay.



Figure 3. Oblique air photo of Claybluff Point (center) and the west side of Icy Bay. The Tyndall Glacier and the Karr Hills are in the background. The photo was taken on August 4, 1975, from 9000 ft. The amount of ice seen in the central part of Icy Bay is typical of summer conditions. Sediment transport on the shoreline in the foreground is consistently into the bay.



Figure 4. Oblique aerial view towards the north on the east side of Icy Bay. Riou Spit is in the foreground; Chirp Island is in center background. The photo was taken on August 4, 1975, from an altitude of about 8000 ft.

Riou Spit has grown to its present size (about 8 km long) since the retreat of the ice margin from this site about 75 years ago. This demonstrates a rapid westward transport of sediment into the bay from Point Riou and beaches further east.

233



Figure 5. Oblique aerial view of the west Malaspina Foreland, looking east. Riou Spit is in the foreground, Point Riou is the first vegetated cliff, the Old Yahtse and Yana streams form the two wide outwash plains further east, and Fountain Stream forms the cusped delta in the background. The photo was taken on August 4, 1975, from an altitude of 8000 ft. Nearshore sediment plumes demonstrate high meltwater discharge.

235



Figure 6. Oblique aerial view to the east of the western Malaspina Foreland. The area extends from Point Riou (lower left) to Fountain Stream (upper right). The Malaspina Glacier is in the upper left corner of the photograph. The photo was taken on August 4, 1975, from 8000 ft.

The barrier-spits off the Old Yahtse and Yana outwash plains are both oriented westward in agreement with measured and computed direction of sediment transport. Note the suspended sediment plumes and the peculiar "sediment stringers" in the foreground.



Figure 7. Oblique aerial view of the east Malaspina Foreland, looking west. Manby Point is in the foreground; Sitkagi Bluffs, Fountain Stream, and part of the Malaspina Glacier are visible in the background. The photo was taken on August 4, 1975, from an altitude of 8000 ft.

The barrier spits off the Manby and Alder stream outwash plains (center) demonstrate a net long-term transport of coarse sediments to the east.



Figure 8. Oblique aerial view to the south of the prograding beach ridge plain of the Grand Wash River (Kwik Stream). The photo was taken on August 4, 1975, from an altitude of about 3000 ft.

Kwik Stream, draining the eastern Malaspina Glacier, carries large volumes of sediment into the low energy inner part of Yakutat Bay, hence the rapid progradation. Note the suspended sediment plumes and the northeastward orientation of the barrier spits.

241



SUMMARY OF WAVE CLIMATE

North Pacific Cyclones

The principal frontal zones of the northern hemisphere winter are shown in Figure 9. Two Pacific polar fronts and one Pacific arctic front are generally present. Normally, the front near Asia is the stronger and generates a majority of the storms which travel into the Gulf of Alaska. Storm tracks derived from inspection of northern hemisphere surface synoptic charts (NOAA, National Climatic Center, 1973) illustrate this well (Fig. 10, storm track no. 13). The Pacific arctic front can also be responsible for local storm generation within the Gulf of Alaska as illustrated by Figure 10, tracks no. 7, 15, and 18. The steep temperature gradients at the Alaska and St. Elias Ranges in winter, which separate the mild maritime climate from the cold continental interior (Alaska Regional Profiles, 1975, vol. 1, p. 7), prevent the cyclones from penetrating inland, and low pressure centers which enter the central Gulf of Alaska have a tendency to remain there until they dissipate. This combination of locally-generated cyclones on the Pacific arctic front and decaying traveling cyclones arriving from the west generates in the Gulf of Alaska the highest winter cyclone frequency in the northern hemisphere (Petterssen, 1969, p. 227; Fig. 12A).

The reduction in intensity of latitudinal pressure differences in summer causes a breakdown of the zonal current with consequent decrease in frontal cyclogenetic activity. The cyclones that do occur are weak but surprisingly long lived. A typical travel pattern is illustrated in Figure 11 by storm tracks no. 3, 4, and 5. Most of the summer storm activity is located in the western Gulf of Alaska and to the south of the

outer Aleutian Islands. Even there, the summer cyclone frequency is not any higher than many other places in the northern hemisphere (Petterssen, 1969, p. 229; Fig. 12B).

Winter cyclones of the North Pacific frequently have central pressures of less than 950 mb. This is the same pressure reduction as that generally associated with Caribbean hurricanes. In summer very few North Pacific cyclones have central pressures much less than 1000 mb.

Gulf of Alaska Coastal Wind Regime

Summary of Synoptic Meteorological Observations (U. S. Naval Weather Service Command, 1970), hereafter referred to as SSMO data, were used to derive wind frequency distributions for data squares in the coastal area of the Gulf of Alaska from Unimak to Vancouver Island (Fig. 13). The average wind regime for the Gulf of Alaska over a seven year period from 1963 to 1970 demonstrates that both dominant and prevailing winds are aligned with the general trend of the shoreline (Fig. 13). The dominant winds blow out of the southeast in the Queen Charlotte and Sitka data squares, out of the east and southeast in Cordova, out of both east and west in Seward, and dominantly out of the west off the Alaska Peninsula.

This wind pattern, which in turn controls coastal sedimentation dynamics, can be explained by the storm track patterns of Figures 10 and 11 and synoptic charts for selected typical storms (Figs. 14-17). The strong easterly and southeasterly winds on the central and eastern coasts are generally caused by cyclones moving into the Gulf south of the Aleutians. Interior high pressure centers create a strong pressure gradient along the coast, strengthening the southeasterly wind components of the

Figure 9. Principal frontal zones of the northern hemisphere in winter. The western Pacific polar front and the Pacific arctic front are areas of generation for cyclones traveling into the central Gulf of Alaska. Data are from Petterssen (1969, p. 222).

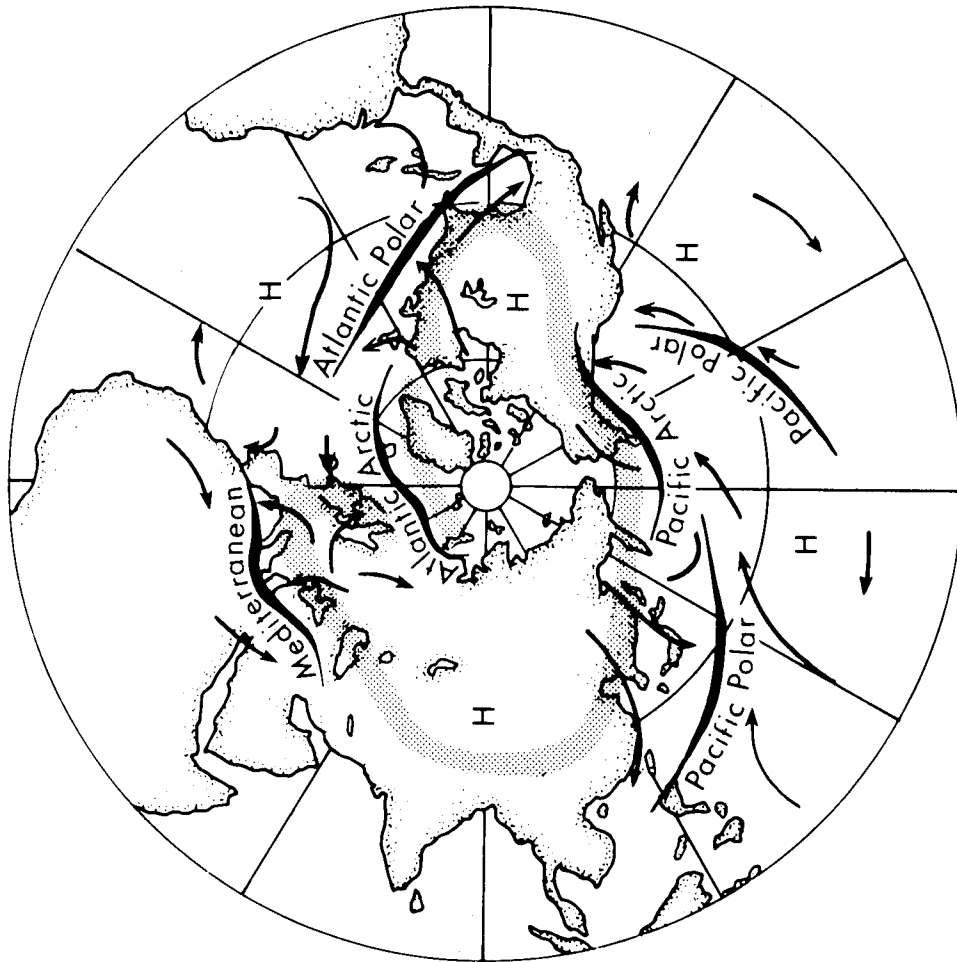


Figure 10. Cyclone tracks across the North Pacific in January, 1973. The map was derived by visual inspection of Northern Hemisphere Surface Synoptic Charts (NOAA, National Climatic Center, 1973). All storms occurring in one month were mapped. The time interval between two consecutive tick-marks is 6h. The number indicates the starting point of each track. Letter designations, e.g., 12b, 12c, refer to secondary cyclones formed in the wake of the primary one, e.g., no. 12. Note the general eastward migration pattern and the clustering of tracks in the north central Gulf of Alaska, caused by the steep temperature-induced pressure barrier at the high coastal mountain ranges.

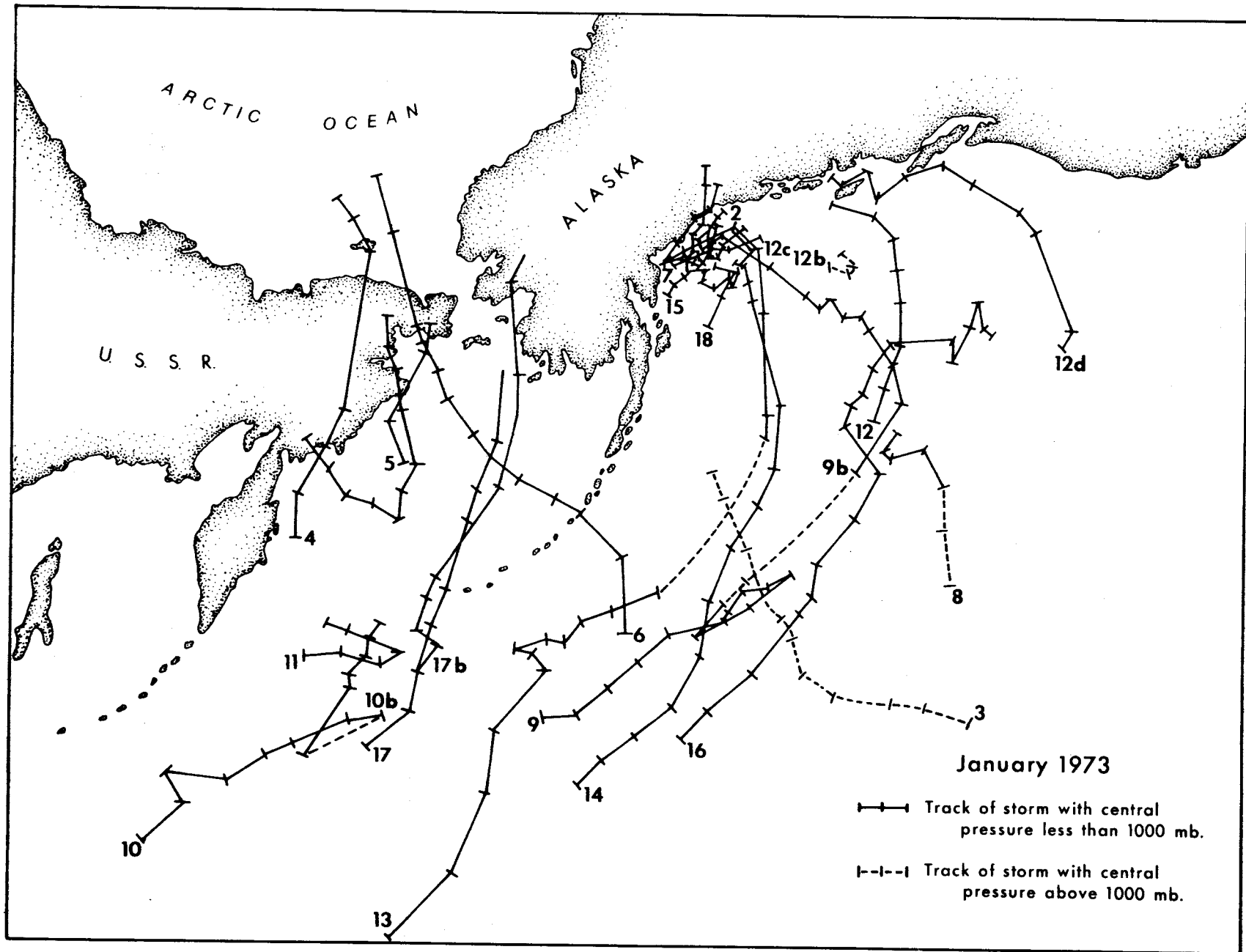


Figure 11. Cyclone tracks across the North Pacific in July, 1972.
For explanation of symbols, see Figure 10. The main storm activity in summer is concentrated to the south and west of the Aleutian Islands, with only a few weak cyclones migrating into the Gulf of Alaska.

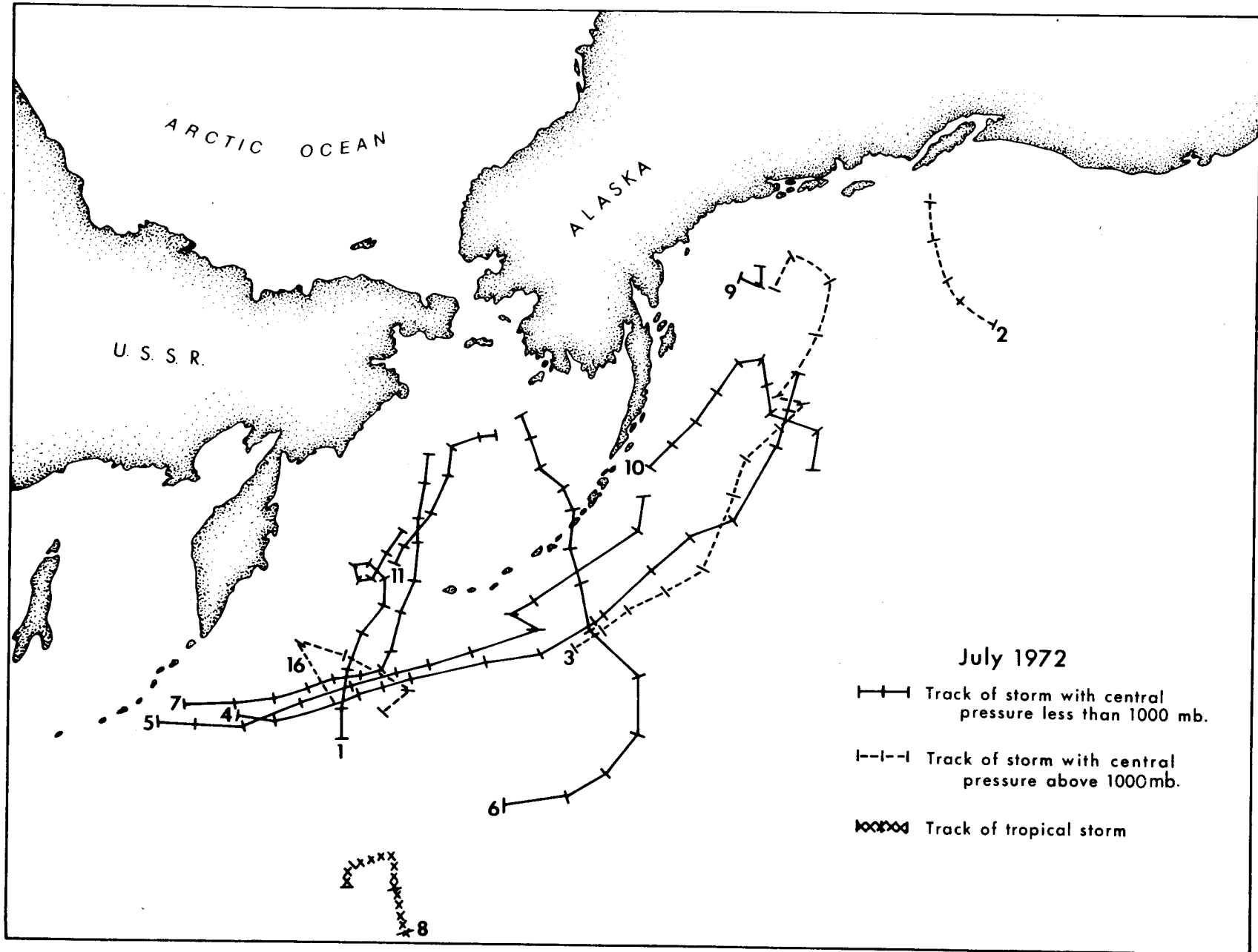


Figure 12A. Percentage frequency of cyclone centers in winter. The frequencies refer to areas of 100,000 km². Note the regional maximum in the central Gulf of Alaska. Data are from Petterssen (1969, p. 227).

Figure 12B. Percentage frequency of cyclone centers in summer. Units are as above. Note the reduction in northern latitude frequencies and the development of subtropical intense lows. Data are from Petterseen (1969, p. 229).

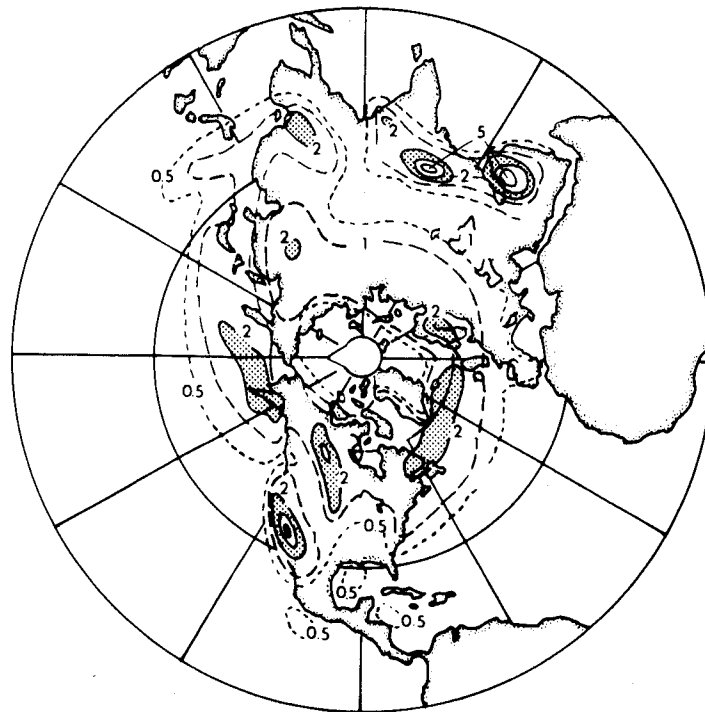
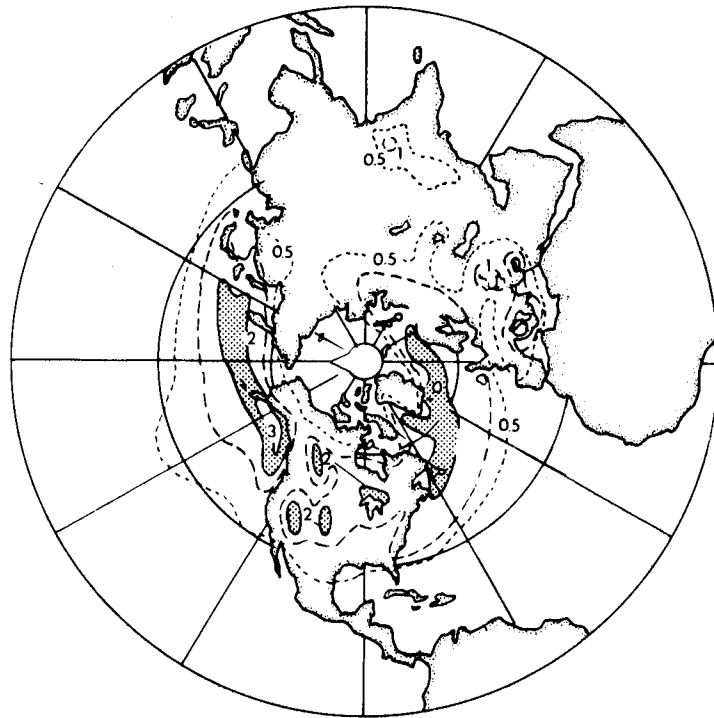


Figure 13. Wind frequency distributions for coastal data squares in the Gulf of Alaska. The diagrams are based on wind observations presented in Summary of Synoptic Meteorological Observations (U. S. Naval Weather Service Command, 1970). The dominant and prevailing winds are generally aligned parallel to the shoreline because of the temperature-induced pressure gradient along the coastal mountains. On the northeast coast of the Gulf, the dominant winds blow towards the northwest; on the northwest coast they blow towards the east and northeast.

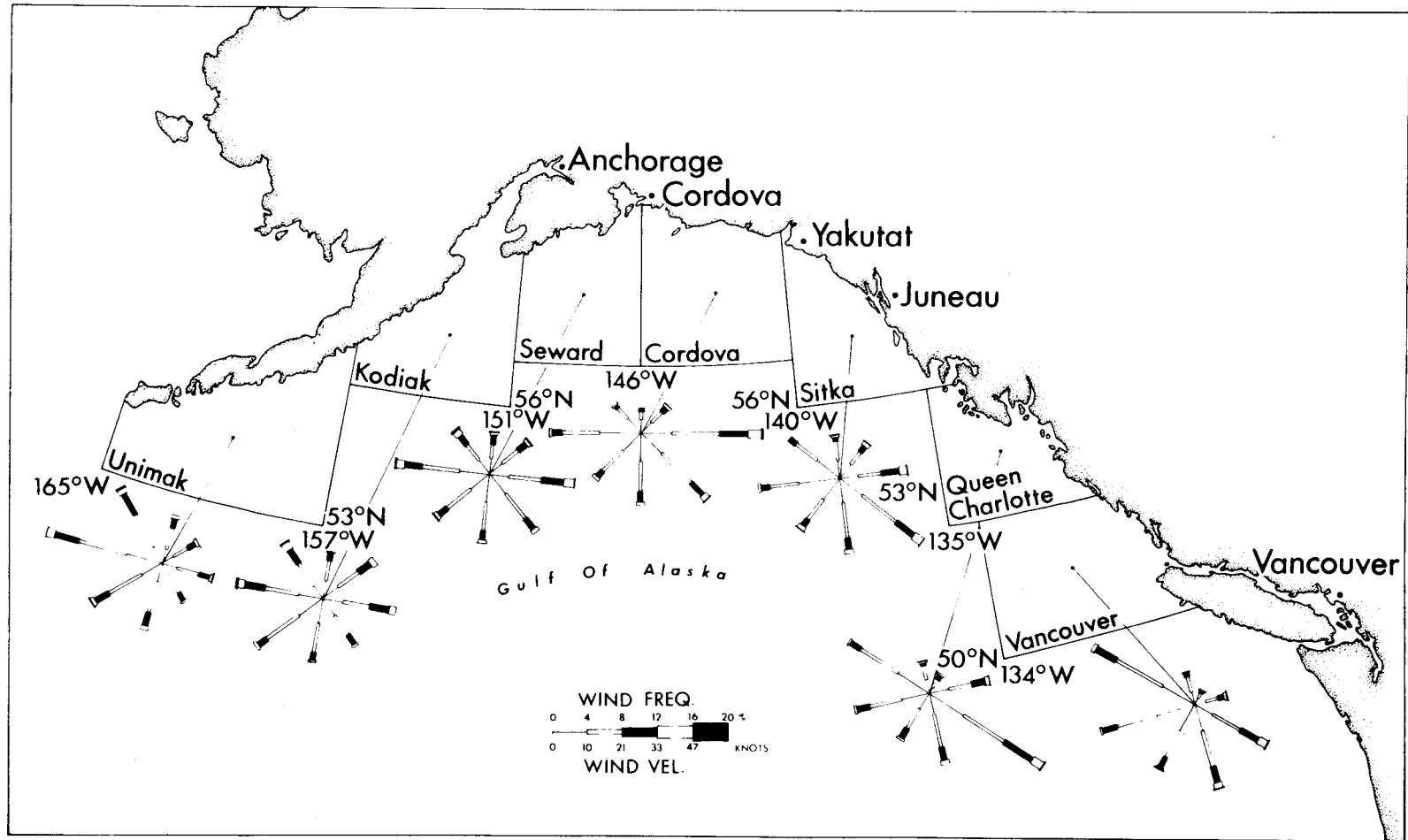


Figure 14. Synoptic chart for the North Pacific at 1200 Z on January 9, 1973. Isobar interval is 4 mb. A strong cyclone (central pressure 976 mb) is located south of the Aleutians. The southeasterly wind components along the coast of southeast Alaska are strengthened by the steep Cordilleran pressure gradient. Data are from Northern Hemisphere Surface Synoptic Charts (NOAA, National Climatic Center, 1973).

255

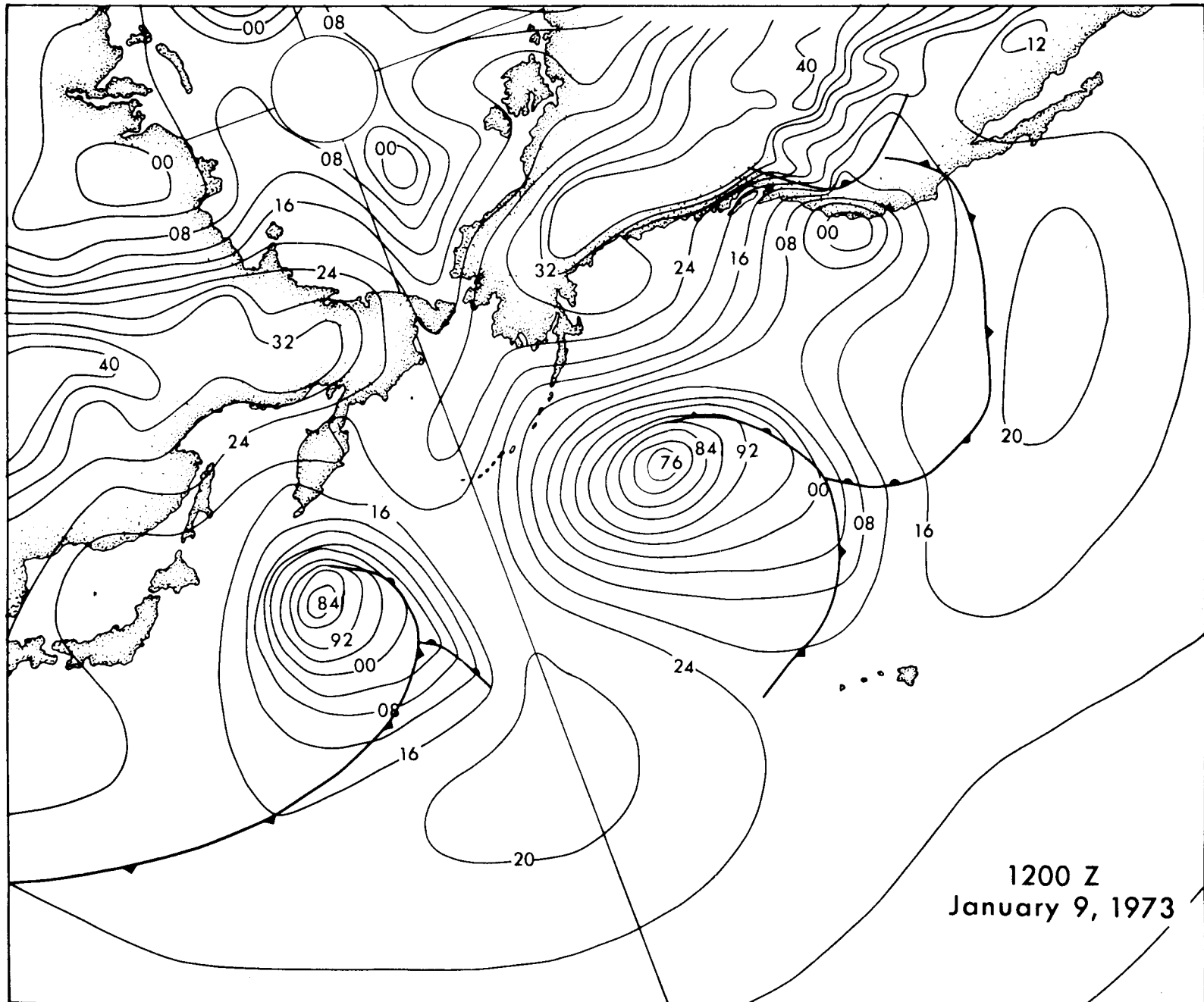
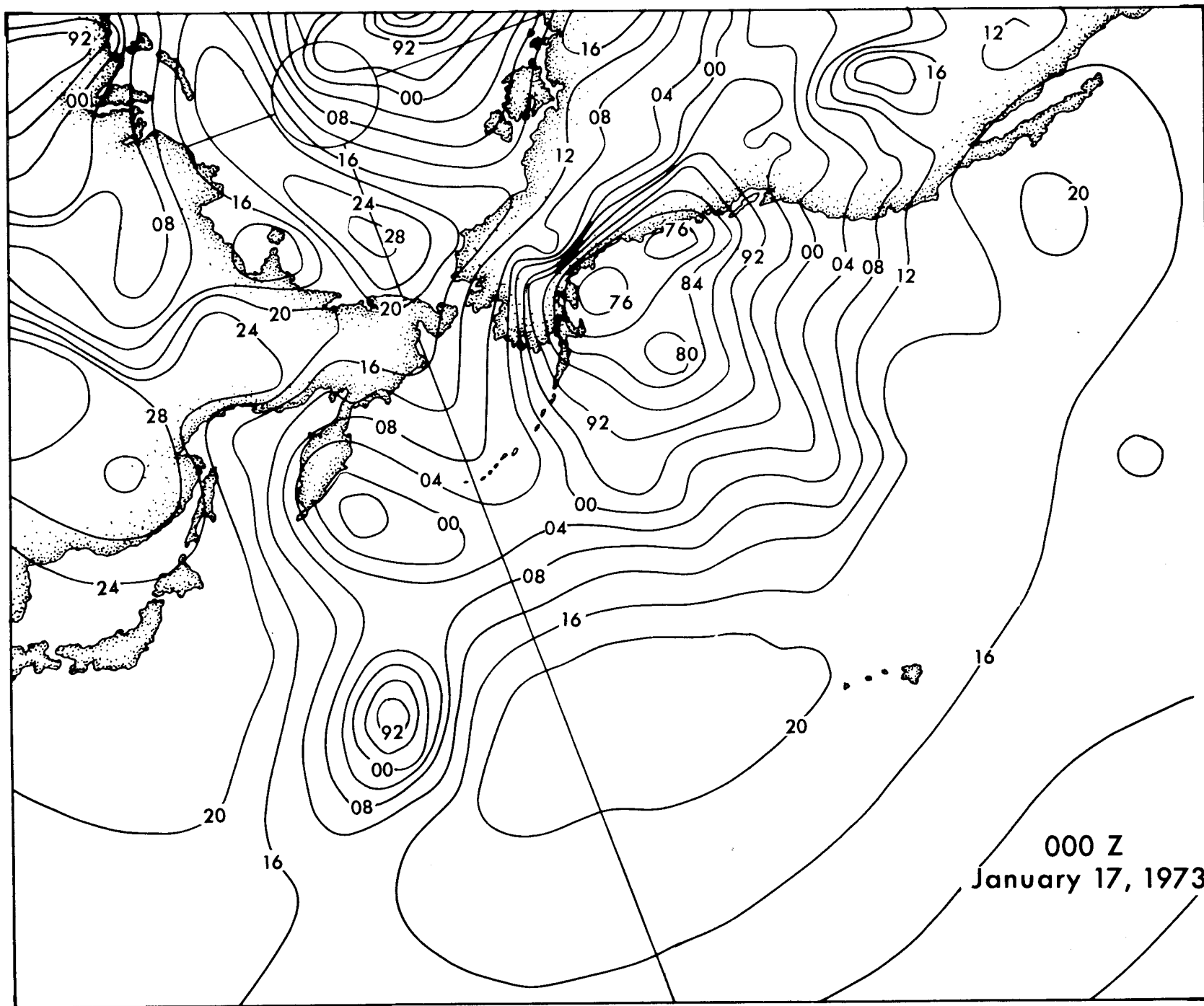


Figure 15. Synoptic chart of the North Pacific at 0000 Z, January 17, 1973. Isobar interval is 4 mb. In this winter situation an eastward traveling cyclone has just broken into three secondary cyclones scattered through the Gulf of Alaska. The pressure gradient at the Alaska Range is very steep, generating strong easterly winds on the north-central Gulf coast. Data are from Northern Hemisphere Surface Synoptic Charts (NOAA, National Climatic Center, 1973).

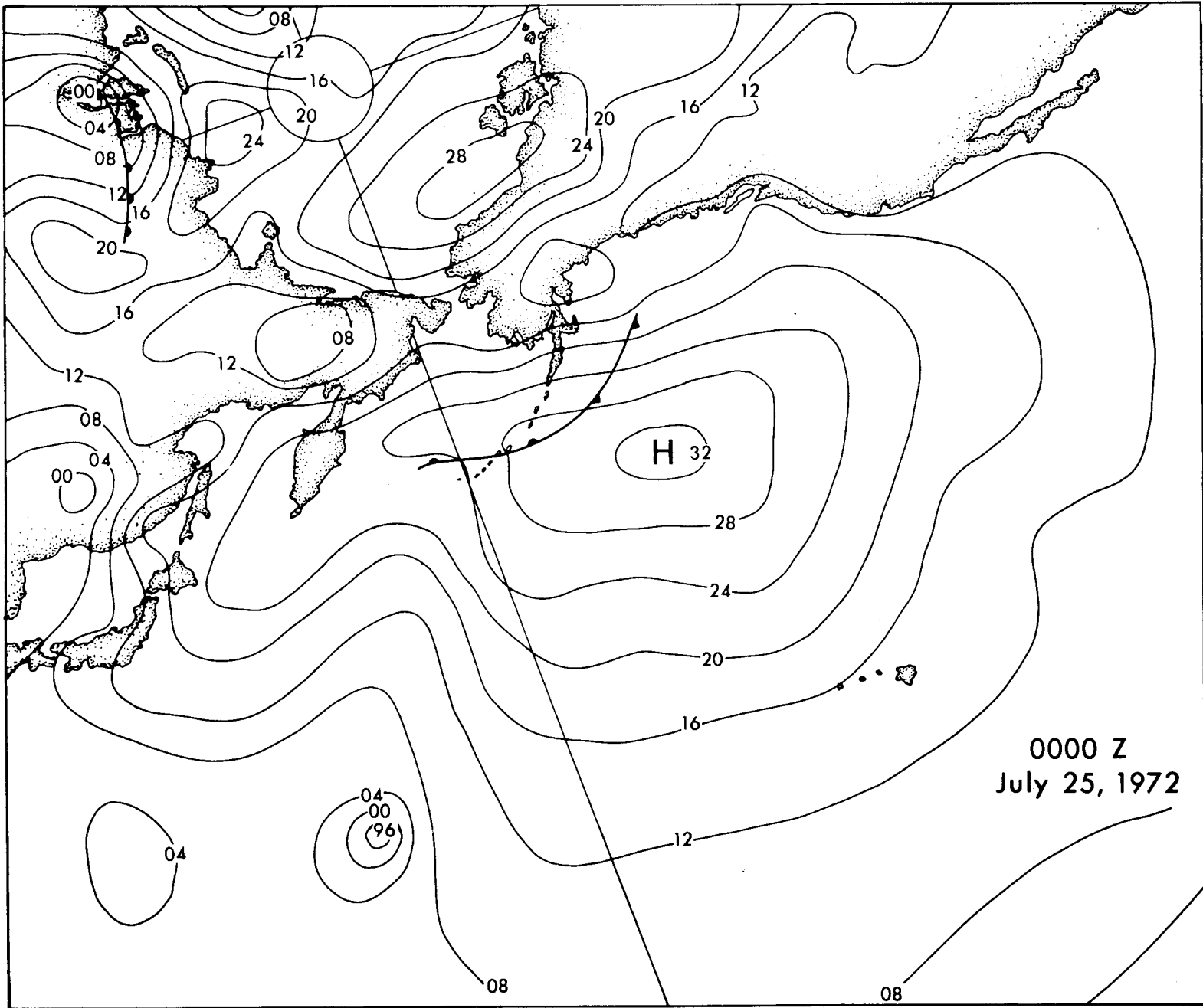
257



000 Z
January 17, 1973

Figure 16. Synoptic chart for the North Pacific at 0000 Z, July 25, 1972. Isobar interval is 4 mb. The North Pacific high, here centered mid-way between Hawaii and Alaska, directly controls the circulation in the Gulf, causing gentle westerly winds along the south-central Alaskan coast. Data from Northern Hemisphere Surface Synoptic Charts (NOAA, National Climatic Center, 1973).

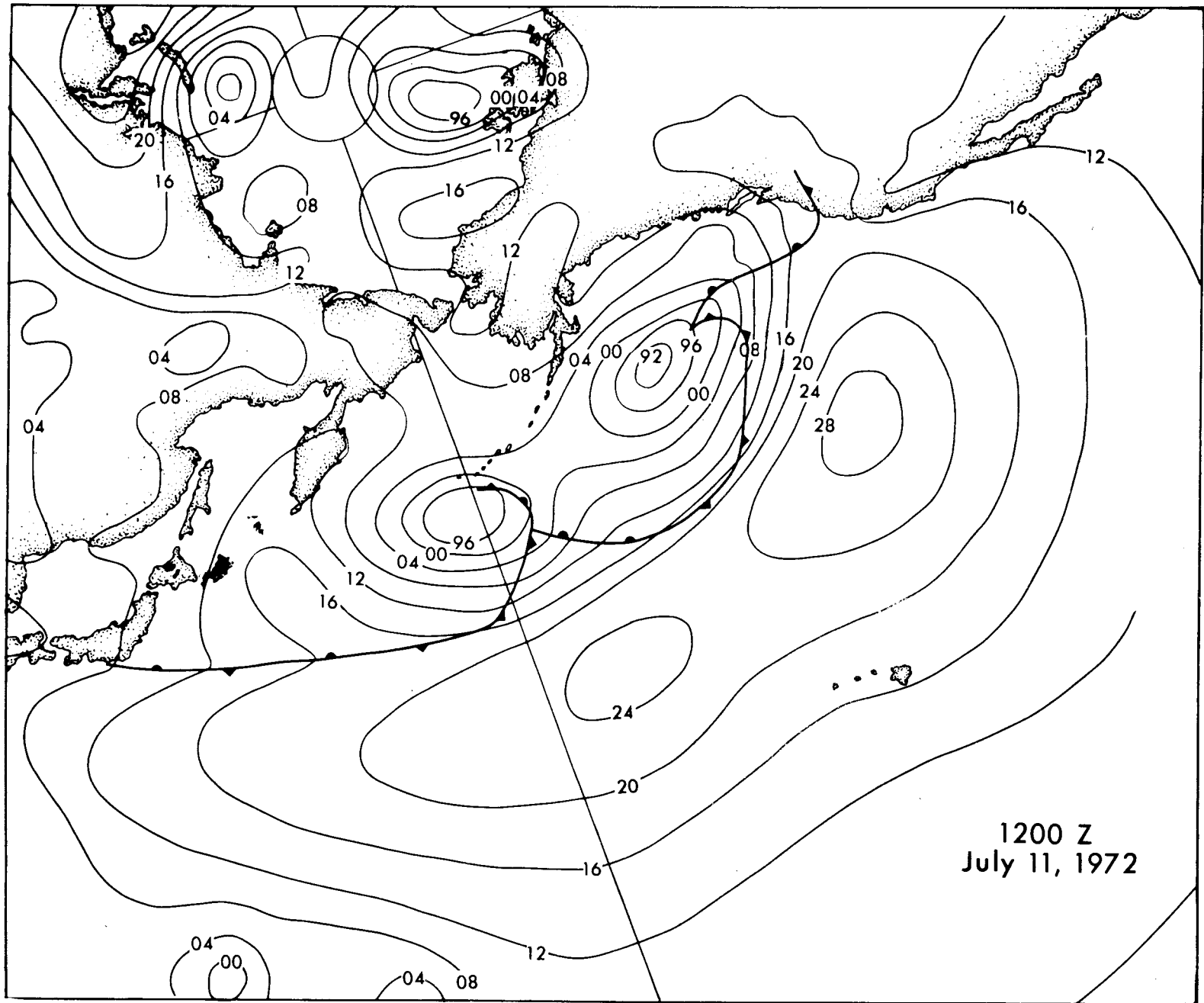
259



0000 Z
July 25, 1972

Figure 17. Synoptic chart for the North Pacific at 1200 Z, July 11, 1972. Isobar interval is 4 mb. An elongated North Pacific high pressure center controls the path of travel of two smaller cyclones to the north. Both cyclones will generate moderate southeasterly waves along the south-central coast of Alaska. Data from Northern Hemisphere Surface Synoptic Charts (NOAA, National Climatic Center, 1973).

261



cyclone (Fig. 14). Frequently, the cyclones stagnate or disperse into a cluster of two or more secondary low pressure centers within the Gulf. This situation, illustrated in Figure 15, also generates strong southeasterly coastal winds. Because of the oceanic conditions on both sides of the Alaska Peninsula and the Aleutians, the winds there are much weaker than those on the east side of the circulation system, and they blow generally out of the north, becoming offshore winds on the Gulf side.

The strong westerly winds in the Unimak and Kodiak data squares are caused by cyclones following the other major storm track belt, that across the Bering Sea into northwest Alaska. These storms are illustrated by tracks no. 6 and 17 in Figure 10.

In summer, the Gulf of Alaska is influenced by a strong North Pacific high pressure center which at times controls the winds directly (Fig. 16). At other times the high pressure system exerts constraints on the path of travel of migrating cyclones (Fig. 17), indirectly controlling the wind regime within the Gulf. The smaller size of summer cyclones in the Gulf of Alaska causes great variability in coastal wind regime. The predominant pattern, however, is that of southeasterly winds in the eastern Gulf and northerly and northwesterly winds in the western Gulf. As in winter, many cyclones do travel up the Bering Sea (Fig. 11, tracks no. 1, 6, and 11), causing westerly winds in the Aleutians.

Wave Energy Flux Distribution

The wind frequency diagrams of Figure 13 present a qualitative picture of the regional variability in physical processes of coastal sedimentation. In order to attain a quantitative estimate of littoral transport rates, the wind frequency distribution must be combined with observed wave heights

and periods (also presented in SSMO tables) to compute the wave energy flux, a quantity directly related to longshore sediment transport rates (Coastal Engineering Research Center, 1973, p. 4-101). In utilizing the SSMO data for computations of wave energy flux distributions, the following assumptions are made: 1) the direction of propagation of the observed waves corresponds to the measured local wind direction; 2) waves are propagating in one direction only, at one period, in any specific time interval; 3) all recorded observations were made in deep water. This first assumption is critical and is generally more justifiable on the west coast where the weather systems move onshore than on the east coast where they move offshore. Because of the reduction of data prior to presentation in the SSMO tables, directions are given by an eight point compass rose, i.e., 45° sectors.

The wave energy flux for a given sea state is defined as total wave energy per unit area of the sea surface times the velocity of propagation of this energy, i.e., the group velocity. For deep water wave conditions this becomes:

$$P_o = 9.58 \cdot 10^9 \cdot H^2 \cdot T \quad (1)$$

where all parameters are in metric units. P_o is wave energy flux in units of ergs/m \cdot sec. H is wave height in meters, and T is wave period in seconds. The following procedure was followed in computing the mean annual wave energy flux.

Let the probability of occurrence of a wave with height H_i , travelling in direction m , be denoted by $p_{i,m}$ (where m is a directional indicator representing N, NE, ...NW). The distribution is normalized such that:

$$\sum_m \sum_i p_{i,m} = 1 \quad (2)$$

Let the probability of occurrence of wave height H_i and period T_i be $r_{i,j}$. This distribution is normalized for each H such that:

$$\sum_j r_{i,j} = 1 \quad (3)$$

The contribution to the mean annual wave energy flux for deep water from each direction (m) can then be expressed as

$$P_o(m) = 9.58 \cdot 10^9 \sum_i \sum_j H_i^2 \cdot T_j \cdot r_{i,j} \cdot p_i \quad (4)$$

Deep water wave energy flux values for each of the eight compass directions were computed according to equation 4 from SSMO tabulated $p_{i,m}$'s and $r_{i,j}$'s. The results of the energy flux computations are presented graphically in Figures 18 and 19, and in tabular form in Table 1.

The energy flux diagrams of Figure 18 reflect the wind frequency distributions of Figure 13 and the available fetch lengths. Dominant southeasterly energy flux is observed at Queen Charlotte and Sitka, directly reflecting the strong winds parallel to this coastline. The onshore and offshore energy flux components are relatively small, reflecting the scarcity of westerly winds and the short fetch available for easterlies. In the north-central Gulf of Alaska, the two directions of dominant energy flux are parallel to shore with the westerly and onshore components increasing in significance towards the west.

The resultant energy flux vector (Fig. 19) for each data square points north at Queen Charlotte and Sitka, northwest at Cordova, and northeast at Seward. This indicates a convergence of wave energy towards Montague Island and Prince William sound. Farther west, in the Kodiak and Unimak data squares, the resultant energy flux vectors point offshore in a general

eastward direction (Fig. 19) because of the large westerly and northwesterly components.

The direction of the resultant wave energy flux vector should correspond to the direction of net coarse sediment transport on an adjacent exposed beach not subject to topographically controlled local reversals. The SSMO data predict a net long-term transport towards the northwest along the North American coast from Vancouver to Cordova and, where beaches are present, a northeast transport direction from the Aleutians to the entrance of Prince William Sound.

The small arrows in Figure 19 indicate directions of littoral sediment transport determined from coastal geomorphic features like spits, headland and inlet offsets, and crescentic bays. The detailed littoral sediment transport pattern is much more complicated than indicated here because of local bathymetrically controlled reversals. The figure does demonstrate, however, a good correlation between the long-term transport direction on an open coast and the resultant regional wave energy flux distribution. The pattern presented in Figure 19 gives more detail but is in general agreement with that deduced by Silvester (1974, p. 92) from geomorphology alone.

Compared to annual wave energy flux values computed elsewhere in the world, the ones for the Gulf of Alaska are high but not the highest. Nummedal (1975) computed SSMO derived wave energy flux values for the south coast of Iceland ranging up to $13.5 \cdot 10^{10}$ ergs/m \cdot sec from the east. Unpublished computations for the North Sea give values up to $10 \cdot 10^{10}$ ergs/m \cdot sec. Brown (1975) computed the mean annual wave energy flux off South Carolina to have a maximum of $3.5 \cdot 10^{10}$ ergs/m \cdot sec out of the northeast.

Typical Gulf of Alaska figures range up to $7.4 \cdot 10^{10}$ ergs/m \cdot sec out of the east at Cordova (Table 1) indicating a moderate storm wave environment.

Figure 18. Wave energy flux distribution for the coastal areas of the Gulf of Alaska. The computations are based on deep water wave observations presented in Summary of Synoptic Meteorological Observations (U. S. Naval Weather Service Command, 1970). The wave energy flux is highest out of the southeast for the Vancouver, Queen Charlotte, and Sitka data squares, out of the east at Cordova, and out of the west at Seward, Kodiak, and Unimak. This pattern corresponds closely to that of the winds presented in Figure 13.

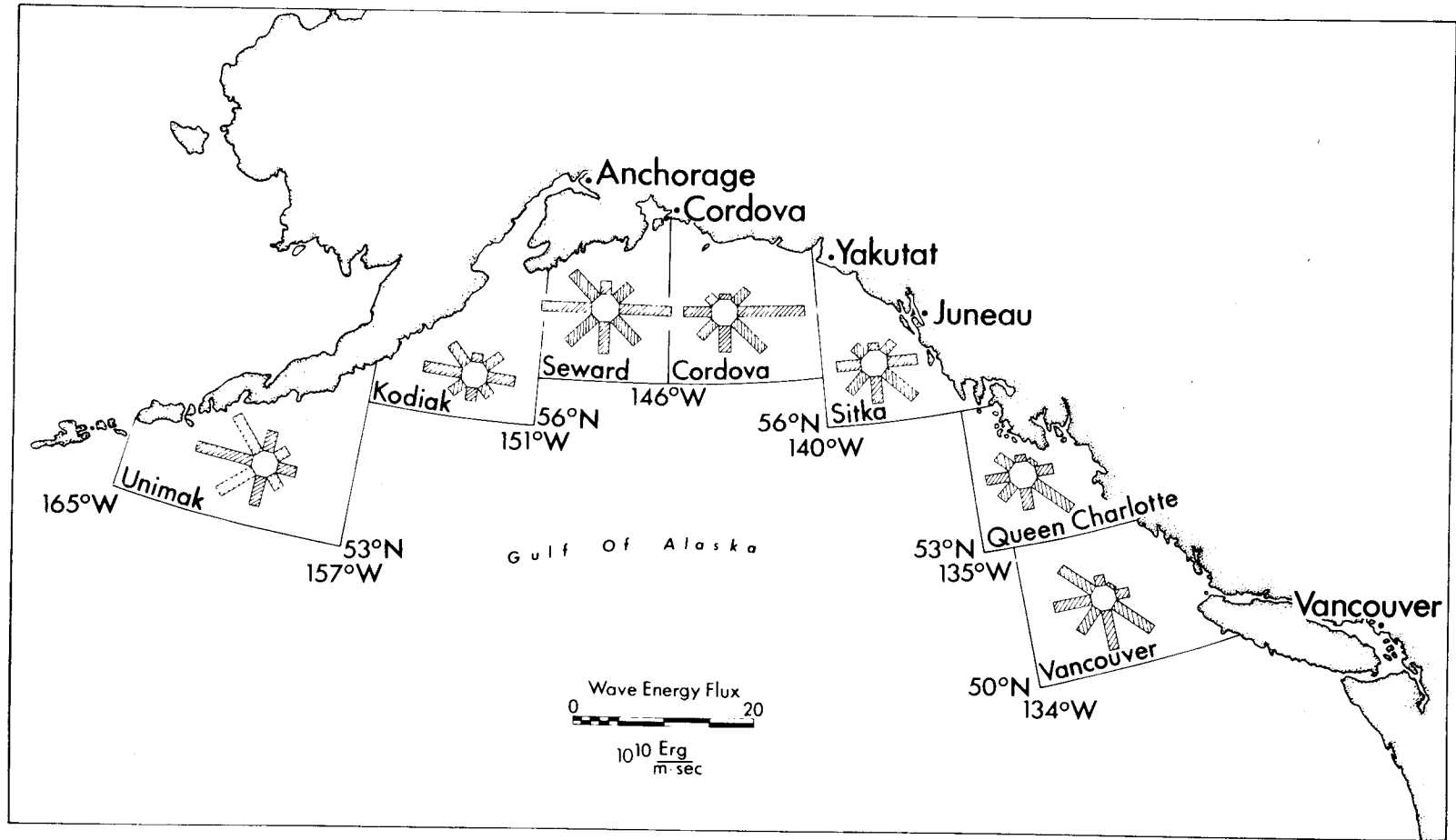


Figure 19. Direction of longshore sediment transportation based on large scale coastal geomorphic features and resultant wave energy flux distribution for the coastal areas of the Gulf of Alaska. Large scale coastal features used in establishing long-term transport directions include spits, offsets, and crescentic embayments. The resultant wave energy flux is determined by vectorial addition of the distributions presented in Figure 18. Note the convergence of wave energy flux towards Prince William Sound.

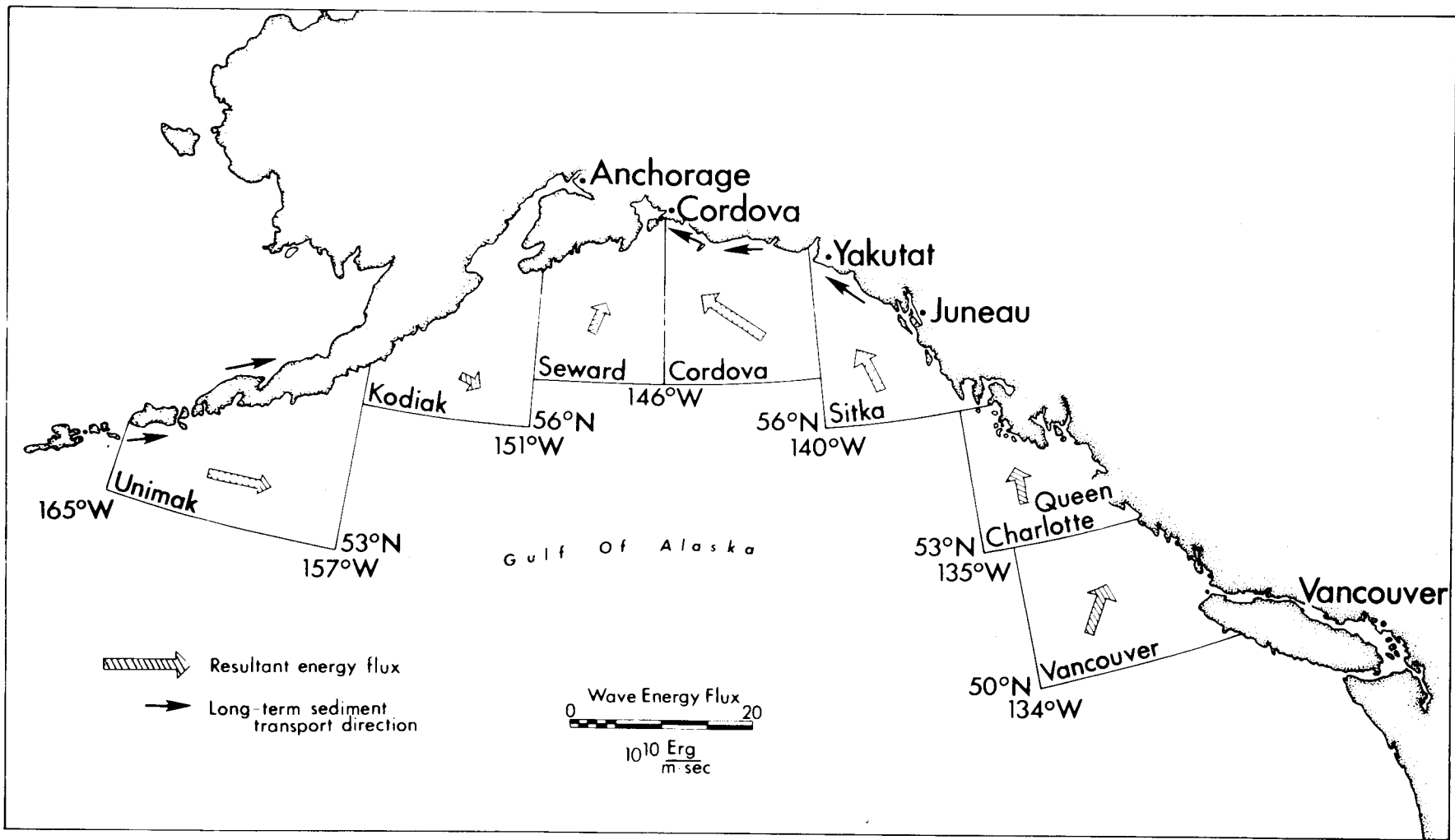


TABLE 1

Deep Water Wave Energy Flux Values for Gulf of Alaska SSMO Squares

Wave energy flux in units of $10^{10} \frac{\text{ergs}}{\text{m} \cdot \text{sec}}$

| Data Square | Direction | | | | | | | |
|-----------------|-----------|------|------|------|------|------|------|------|
| | N | NE | E | SE | S | SW | W | NW |
| Vancouver | 1.12 | .39 | 1.45 | 5.01 | 4.44 | 3.07 | 4.21 | 4.37 |
| Queen Charlotte | .83 | .55 | 1.84 | 5.00 | 2.44 | 2.05 | 2.66 | 2.08 |
| Sitka | .71 | 1.60 | 3.18 | 4.45 | 2.94 | 2.72 | 2.72 | 1.40 |
| Cordova | .54 | 2.04 | 7.42 | 4.66 | 2.86 | 2.54 | 3.00 | 1.10 |
| Seward | 1.49 | 2.23 | 5.70 | 3.76 | 3.54 | 4.09 | 5.44 | 3.78 |
| Kodiak | 1.02 | 2.27 | 3.06 | 1.43 | 1.56 | 1.69 | 4.37 | 2.68 |
| Unimak | 2.30 | 1.64 | 2.23 | 1.78 | 3.25 | 4.53 | 6.46 | 5.28 |

This is in agreement with the world-wide distribution of wave climate presented by Davies (1973).

In comparing the Alaska wave energy flux values to other places in the world, the reliability of SSMO data comes into question. In an evaluation by the Coastal Engineering Research Center (CERC, 1973) SSMO-derived wave height data were found to correspond well to hindcast data, except for very high waves, where the SSMO frequencies tend to be less than the hindcast ones. This discrepancy is probably a direct result of the tendency for a fair-weather bias on the part of shipboard observations. This bias tends to be most severe in areas visited by only a few ships on a seasonal basis. In areas where SSMO wave height data are found to be good, e.g., the east coast of the U. S. (CERC, 1973), the North Sea (Quale, 1975, personal communication), and Iceland (Nummedal, 1975), there are typically from a few thousand to more than 20 thousand observations per degree square. In contrast, a degree square in the central Gulf of Alaska has only a few hundred observations (U. S. Naval Weather Service Command, Surface Marine Environmental Data Survey Charts). Probably few of these record the major winter storms.

There is reason to expect that the wave energy fluxes in Table 1, computed from SSMO data, give a lower limit of the actual annual wave energy flux values for the central Gulf of Alaska.

WAVE REFRACTION

Principles and Bathymetry

Wave trains moving landward across the continental shelf in a depth of water less than about one half the deep water wavelength will travel

with a phase velocity which depends on the depth (Eagelson and Dean, 1966). Consequently, when waves move at an angle to the depth contours, different parts of the wave crest will move at different speeds, causing the direction of wave propagation to change, i.e., the wave is refracted.

Wave refraction diagrams have been constructed for the shelf of the northeast Gulf of Alaska between Cape Suckling and Yakutat in order to relate the offshore wave climate, as recorded in SSMO data, to observed nearshore wave conditions and sediment transportation.

The most recent bathymetric chart of the area is that by Molnia and Carlson (1975). This bathymetry was used to produce five refraction diagrams (Figs. 20-24) for wave conditions judged to be typical for the Gulf of Alaska. The diagrams are constructed by hand according to the refraction principles of geometrical optics as recommended in the Shore Protection Manual (Coastal Engineering Research Center, 1973, p. 2-65). Basically, the method utilizes Snell's law which states that when waves traverse a velocity discontinuity (contour) the direction of propagation changes according to the relation:

$$\frac{\sin \alpha_1}{\sin \alpha_2} = \frac{C_1}{C_2} \quad (5)$$

where α_1 and α_2 represent the angles between the perpendicular to the contour and the wave orthogonal on the deep and shallow side, respectively. C_1 and C_2 are the velocities of wave propagation in deep and shallow water. Depth is generally decreasing as a continuous function in a landward direction. This continuous function is transformed into a step function in order to utilize eq. 5 in the refraction analysis; the step interval is determined either by the available bathymetry or practical considerations about the needed refraction accuracy. For the Gulf of Alaska the 25 meter

contour interval of Molnia and Carlson's (1975) map was used. Because significant refraction occurs landward of 25 meters depth, the wave orthogonals in Figures 20 through 24 are carried only half-way across this last bathymetric interval.

Discussion of Refraction Diagrams

Eight-second waves are typical of summer conditions in the Gulf during the absence of major storms. According to the SSMO tables, eight-second waves occur in the Cordova data square 9.4 per cent of the time. Multiple simultaneous fetch areas commonly generate complex deep water wave trains. Differential refraction of separate components of the wave spectrum adds further to the multidirectional approach of waves at the shoreline. The pattern of unidirectional (south) monochromatic (8 sec) waves with simultaneous existence over an area about 30,000 square kilometers as shown in Figure 20, therefore, is greatly simplified from natural conditions. The nearshore wave variability predicted from a simple refraction diagram like Figure 20 is more a measure of average conditions along the shore contributed by eight-second waves than a picture of instantaneous lateral variability for any given sea state.

The continental shelf off south-central Alaska is narrow and steep. Southeast of Cape Suckling the width to the 200 m contour is only 7 km, giving an average slope of 28 meters per kilometer. Where the shelf is the widest, off Icy Bay, the 200 m contour is 70 km offshore, giving an average slope of 2.8 meters per kilometer. Because of this steepness, refraction of the short eight-second waves is first noticed 10 to 20 km offshore, and only minor reorientation of the wave crests takes place before they run ashore. The most noticeable effect on the eight-second waves is the focusing of energy towards the entrance of Icy Bay due to

Figure 20. Refraction diagram for eight-second waves out of the south in the north-central Gulf of Alaska. The bathymetry is based on a map by Molnia and Carlson (1975). Contour interval is 25 meters, except at the entrance to Icy Bay. This large contour interval prevents the extension of the wave orthogonals all the way to the shoreline because of significant shallow water refraction.

The steep and narrow shelf produces insignificant refraction for these short period waves.

275

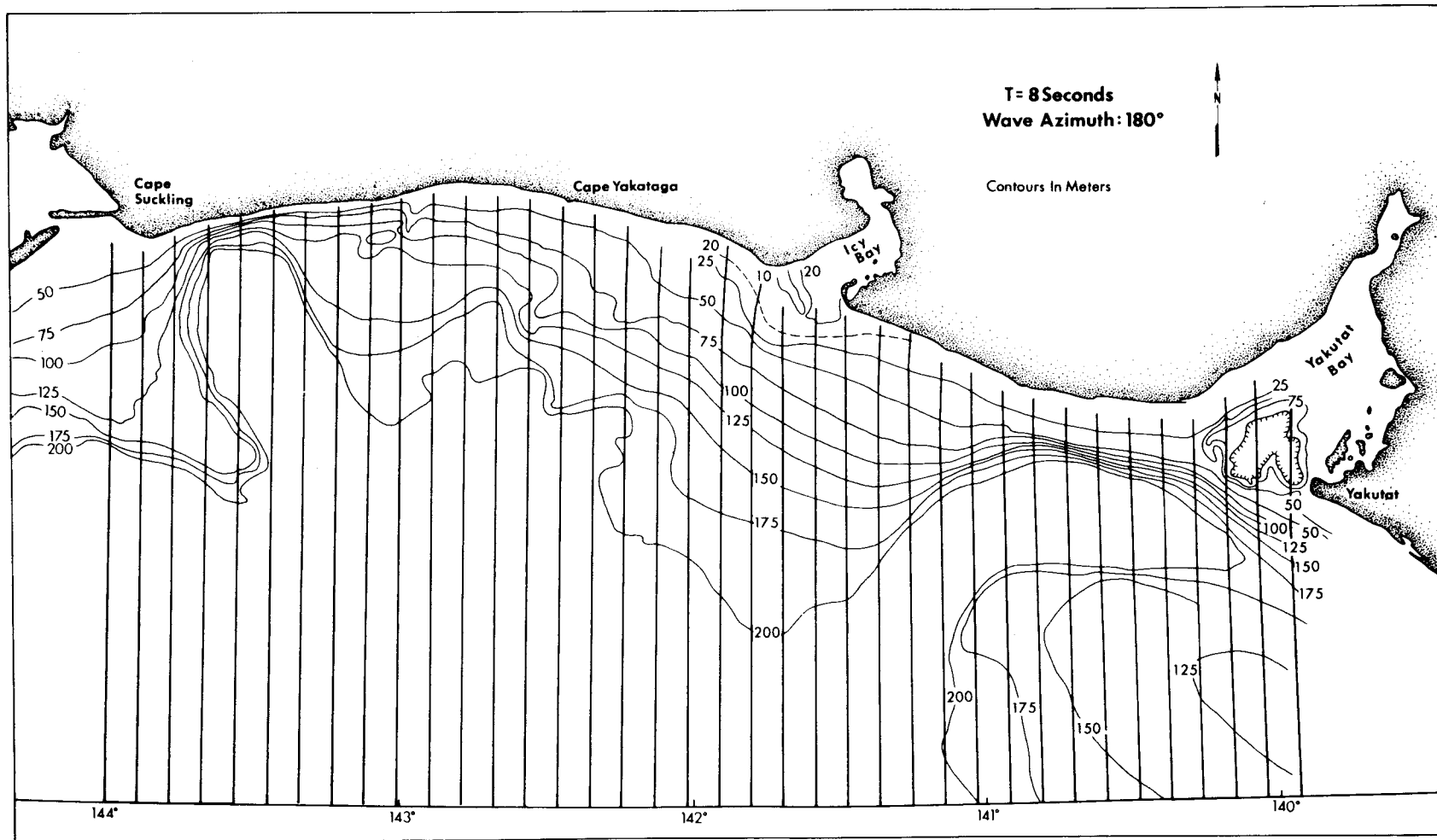


Figure 21. Refraction diagram for twelve-second waves out of the southwest in the north-central Gulf of Alaska. For explanation, see Figure 20.

There is a significant concentration of wave energy at the entrance to Icy Bay and a reduction in energy in Yakutat Bay because of the different entrance bathymetry in the two bays. Along the exposed shoreline west of Icy Bay and along the Malaspina Foreland the energy density is relatively constant.

277

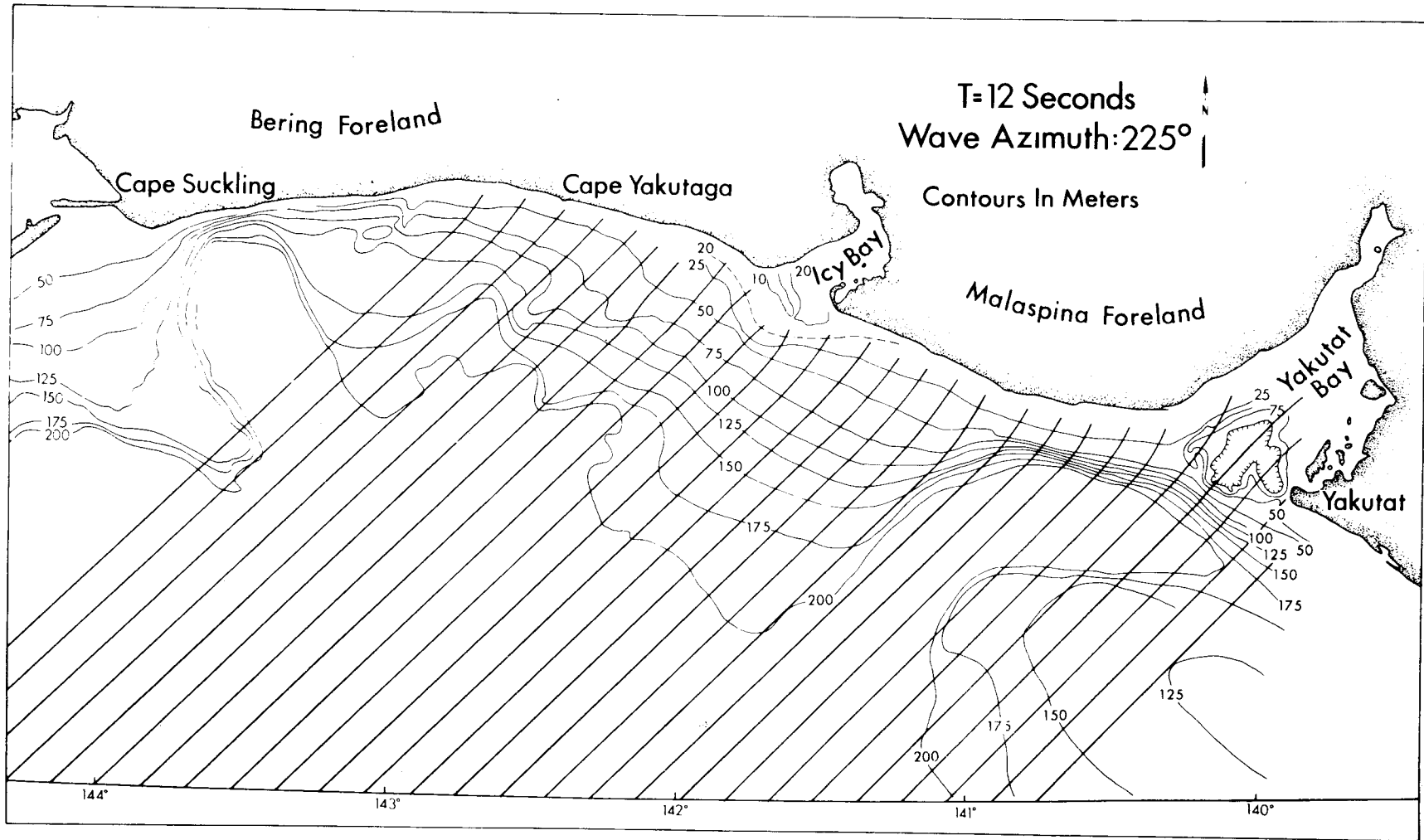


Figure 22. Refraction diagram for twelve-second waves out of the south in the north-central Gulf of Alaska. For explanation, see Figure 20.

Note the convergence of wave orthogonals towards Icy Bay and divergence into Yakutat Bay. Along the remainder of the shoreline these waves are subject only to minor refraction because of the general alignment of the bathymetric contours and the incoming wave crests.

279

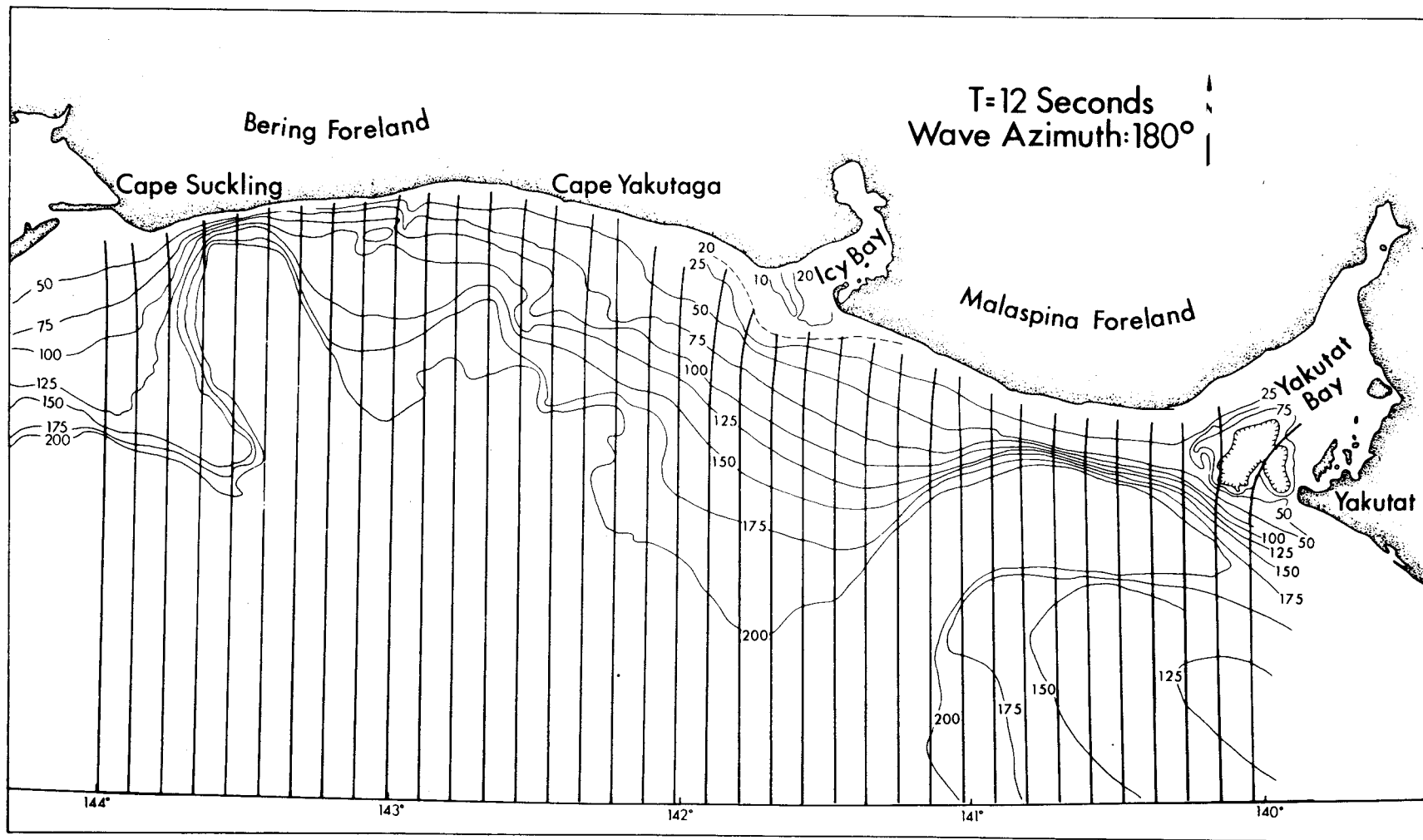


Figure 23. Refraction diagram for twelve-second waves out of the southeast in the north-central Gulf of Alaska. For explanation see Figure 20.

Because of the general alignment of the bathymetric contours, southeasterly waves propagate less energy per meter of beach to the shore east of Cape Yakataga than do south and southwesterly waves (Figs. 22 and 21). The effect of the bathymetric high at the Icy Bay entrance is to disperse the wave energy in the region between the Bay entrance and Cape Yakataga.

281

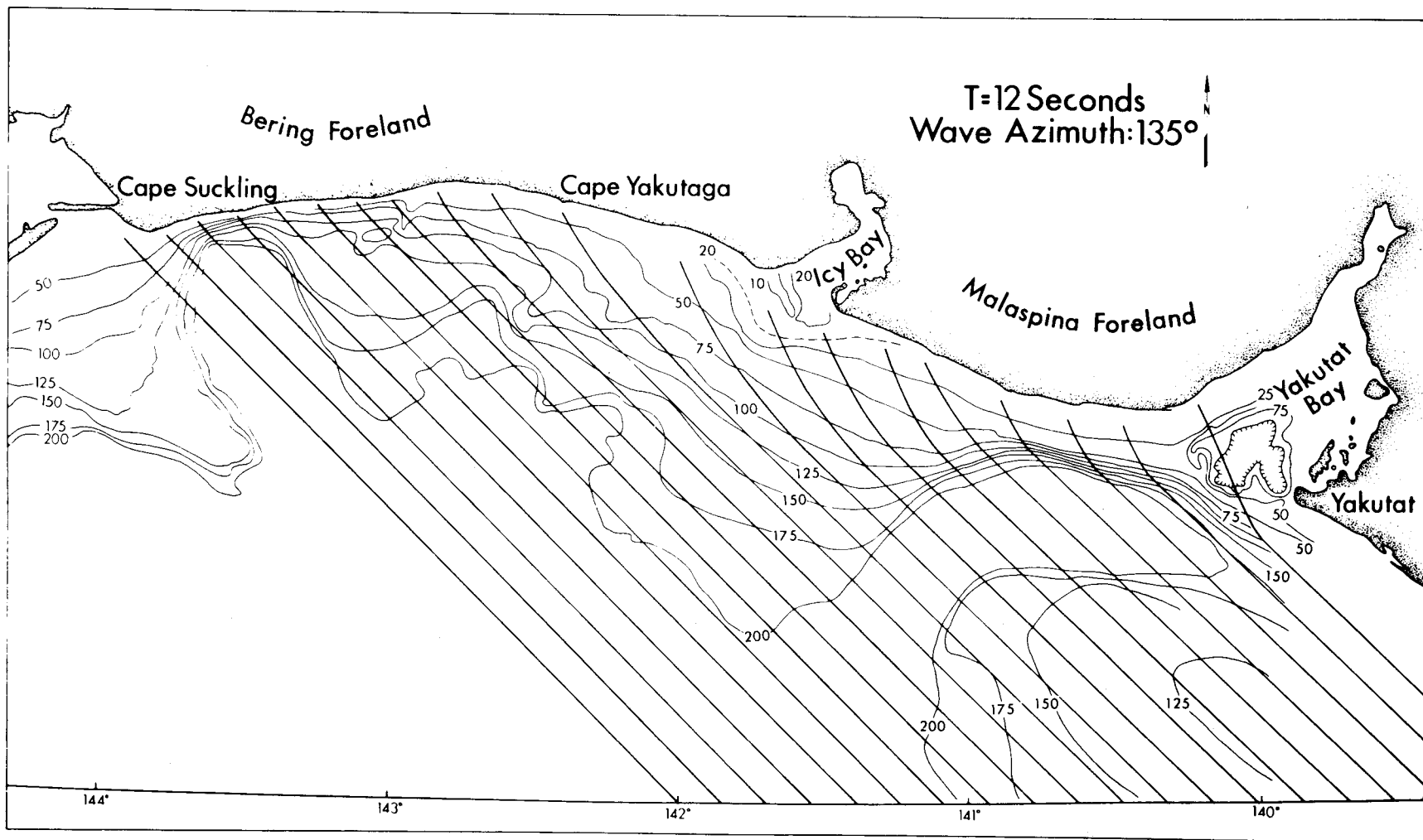
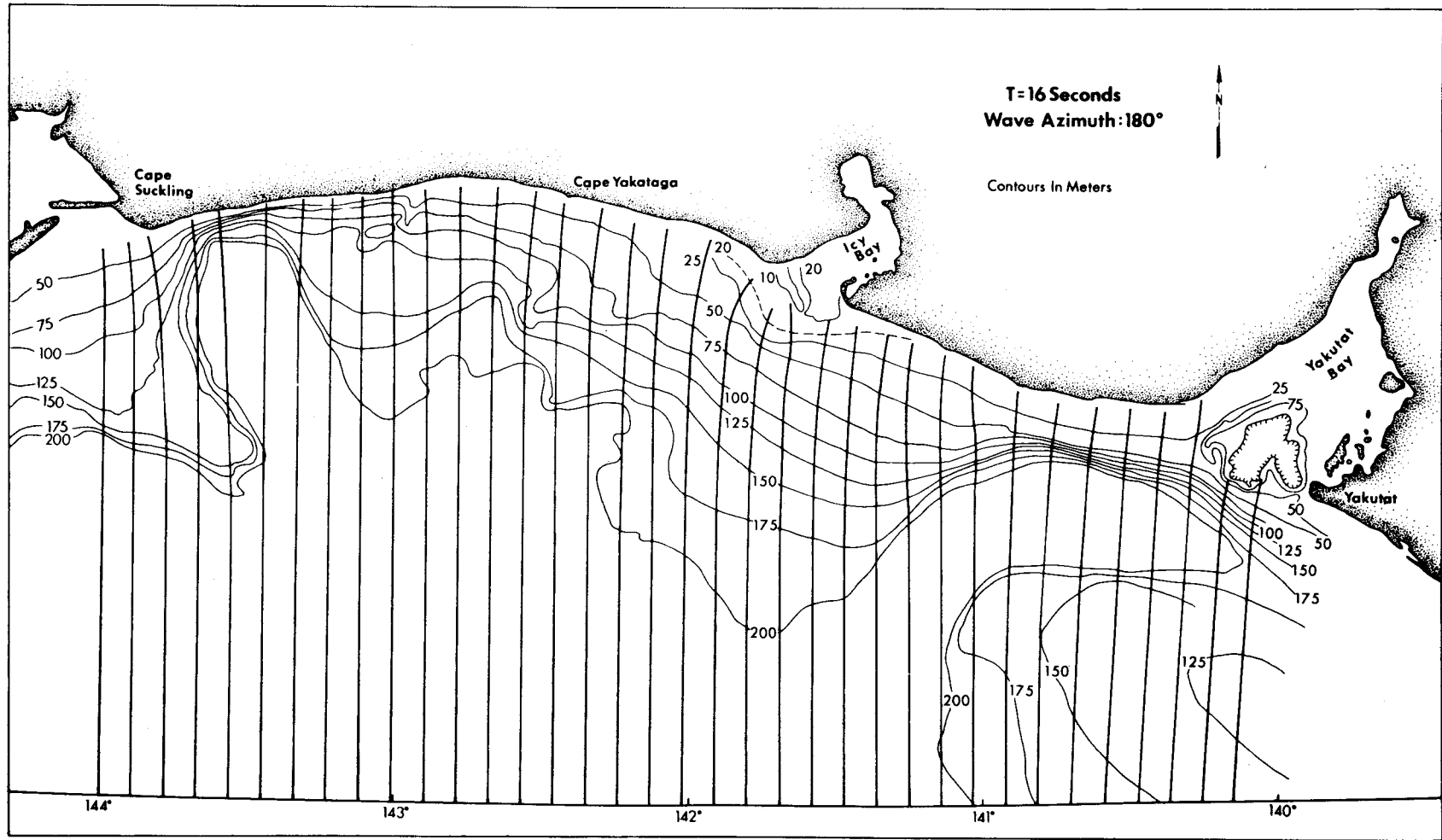


Figure 24. Refraction diagram for sixteen-second waves out of the south in the north-central Gulf of Alaska. For explanation, see Figure 20.

Generally, the pattern of lateral variability in nearshore wave energy corresponds to that for twelve-second waves from the south, but the variations are greater because the whole shelf influences the refraction of these long period waves. Wave energy concentrations are observed at Point Riou, the east Malaspina Foreland, the moraine off Icy Bay, and the Bering Foreland (see Fig. 25 for location names).

283



shoaling by submerged Neoglacial moraines. For southwesterly and southeasterly waves the pattern is much the same except for lower energy per meter of beach caused by the oblique wave approach.

Twelve-second waves are typical for major winter storms (according to preliminary wave hindcasting) and distant swells arriving at the Gulf. According to the SSMO tables, twelve-second waves occur in the Cordova data square 1.3 per cent of the time. With a deep water wavelength of 250 meters, twelve-second waves are significantly refracted in water less than 125 meters deep. The offshore distance to the 125 meter contour varies from about 3 to 40 km. The refraction pattern is a lot more complex than that for the eight-second waves. For south (Fig. 22) and southwesterly (Fig. 21) wave approaches, there is a significant concentration of wave energy at the Icy Bay entrance, and a divergence of wave orthogonals with consequent reduction in wave energy at the entrance to Yakutat Bay. The energy flux along the remainder of the exposed shoreline is relatively constant, but slight variations, reflected in the predicted wave height distributions (Fig. 25), are observed. For a given offshore wave energy density, southeasterly waves propagate less energy to the shore east of Cape Yakataga than do waves from the south and southwest (Fig. 23). Also, the effect of the moraine off Icy Bay is such as to disperse the wave energy, placing the Cape Yakataga-Icy Bay shoreline in a "shadow" zone. Wave energies are also uniformly low on the Malaspina Foreland. The narrow shelf and change in orientation of the coast west of Yakataga make this the most exposed segment of the shore for southeasterly waves.

A refraction diagram for sixteen-second waves was included to illustrate the extent and pattern of refraction for the most extreme storm and

swell conditions. Sixteen-second waves are not listed as a separate category in the SSMO tables. With a deep water wavelength of 430 meters, sixteen-second waves will start to refract significantly at the 200 meter depth contour. The whole shelf controls the refraction pattern. Essentially, the pattern illustrated in Figure 24 for waves out of the south corresponds to that for shorter period waves (e.g., 12 sec waves in Fig. 22) with a very pronounced convergence of orthogonals towards the entrance to Icy Bay and a divergence at Yakutat Bay. The lateral wave energy variability, however, is greater the longer the wave period.

For use in computations below, Table 2 lists wave refraction coefficients computed from Figures 20 through 24. The refraction coefficient, K_R , is defined as:

$$K_R = (b_0/b)^{1/2} \quad (6)$$

where b_0 is the spacing of two adjacent wave orthogonals in deep water and b is the spacing between the same two orthogonals at the desired shallow water depth. Table 2 lists refraction coefficients for each orthogonal interval starting with the one farthest west, computed for a shallow water depth of 25 meters.

Wave Height Distribution

The wave refraction diagrams (Figs. 20-24) provide the information necessary for a prediction of shallow water wave heights for known deep water conditions. The computations are based on the following line of reasoning.

Specific wave energy, i.e., total wave energy per unit area of sea surface, can be expressed as:

$$E = \frac{\rho g H^2}{8} \quad (7)$$

TABLE 2

Refraction coefficients at 25 m water depth for 8, 12 and 16 sec waves in the north-central Gulf of Alaska. The coefficients refer to Figures 20 through 24 and are listed for each orthogonal interval beginning with the one farthest west.

| Period (sec) | 8 | | 12 | | 16 |
|--------------|-------|-------|-------|-------|-------|
| Direction | S | SW | S | SE | S |
| | .988 | .898 | 1.066 | .981 | 1.091 |
| | .973 | .913 | .945 | .981 | 1.235 |
| | .992 | .925 | .913 | .973 | .833 |
| | .981 | .955 | .973 | .952 | 1.091 |
| | 1.012 | 1.102 | 1.000 | .928 | .811 |
| | .977 | 1.091 | .988 | .973 | .928 |
| | .992 | .952 | .973 | 1.043 | 1.043 |
| | 1.029 | .938 | 1.000 | .895 | 1.043 |
| | .992 | .945 | .962 | .838 | 1.000 |
| | .977 | 1.147 | 1.047 | .807 | .981 |
| | 1.012 | .952 | 1.043 | .640 | .952 |
| | 1.008 | .913 | 1.008 | .696 | .928 |
| | .981 | .996 | .945 | .857 | .898 |
| | 1.000 | 1.066 | 1.000 | .791 | .913 |
| | .988 | .988 | .919 | 1.004 | .962 |
| | .973 | 1.004 | 1.118 | .781 | 1.000 |
| | 1.043 | .850 | .907 | .762 | .843 |
| | .938 | .973 | 1.021 | .801 | .754 |
| | .898 | 1.025 | .870 | .633 | .754 |
| | 1.091 | .945 | .962 | | .913 |
| | .981 | .981 | 1.043 | | 1.066 |
| | 1.021 | .843 | .981 | | .945 |
| | .962 | .762 | 1.000 | | 1.021 |
| | 1.021 | 1.029 | 1.004 | | 1.043 |
| | 1.000 | .981 | 1.043 | | 1.091 |
| | 1.025 | .969 | .962 | | .945 |
| | 1.004 | | 1.118 | | 1.021 |
| | 1.021 | | 1.000 | | .833 |
| | .988 | | 1.043 | | .870 |
| | 1.038 | | .945 | | .913 |
| | .996 | | 1.000 | | .945 |
| | .981 | | 1.038 | | .981 |
| | 1.021 | | .945 | | .962 |
| | .981 | | 1.043 | | |
| | 1.021 | | .928 | | |
| | .962 | | .611 | | |

(see Egelson and Dean, 1966, p. 54) where ρ is water density, g is the acceleration of gravity and H is wave height. Two assumptions are made: (1) for waves advancing toward shore no energy flows laterally along the crest; i.e., the energy flux between two wave orthogonals of the refraction diagram remains constant; (2) seaward of the breaker zone there is no energy loss due to bottom friction or internal turbulence. Based on these assumptions one can equate the wave energy flux between two adjacent orthogonals in deep and shallow water. The deep water wave energy flux is:

$$P = \frac{1}{2} \cdot b_o \cdot E_o \cdot C_o \quad (8)$$

where subscript o refers to deep water; b is the spacing of the orthogonals and C is the wave phase velocity. In shallow water the energy flux is:

$$P = n \cdot b \cdot E \cdot C \quad (9)$$

where n is the coefficient relating group velocity to phase velocity for transitional water depths (for details see: Coastal Engineering Research Center, 1973, v. 1, p. 2-25 and 2-66). Equating the deep water to the shallow water energy flux yields:

$$\frac{E}{E_o} = \frac{1}{2} \cdot \frac{1}{n} \cdot \frac{b_o}{b} \cdot \frac{C_o}{C} \quad (10)$$

Substituting H for E according to equation 7 gives:

$$\frac{H}{H_o} = \left(\frac{1}{2} \cdot \frac{1}{n} \cdot \frac{C_o}{C} \cdot \frac{b_o}{b} \right)^{\frac{1}{2}} \quad (11)$$

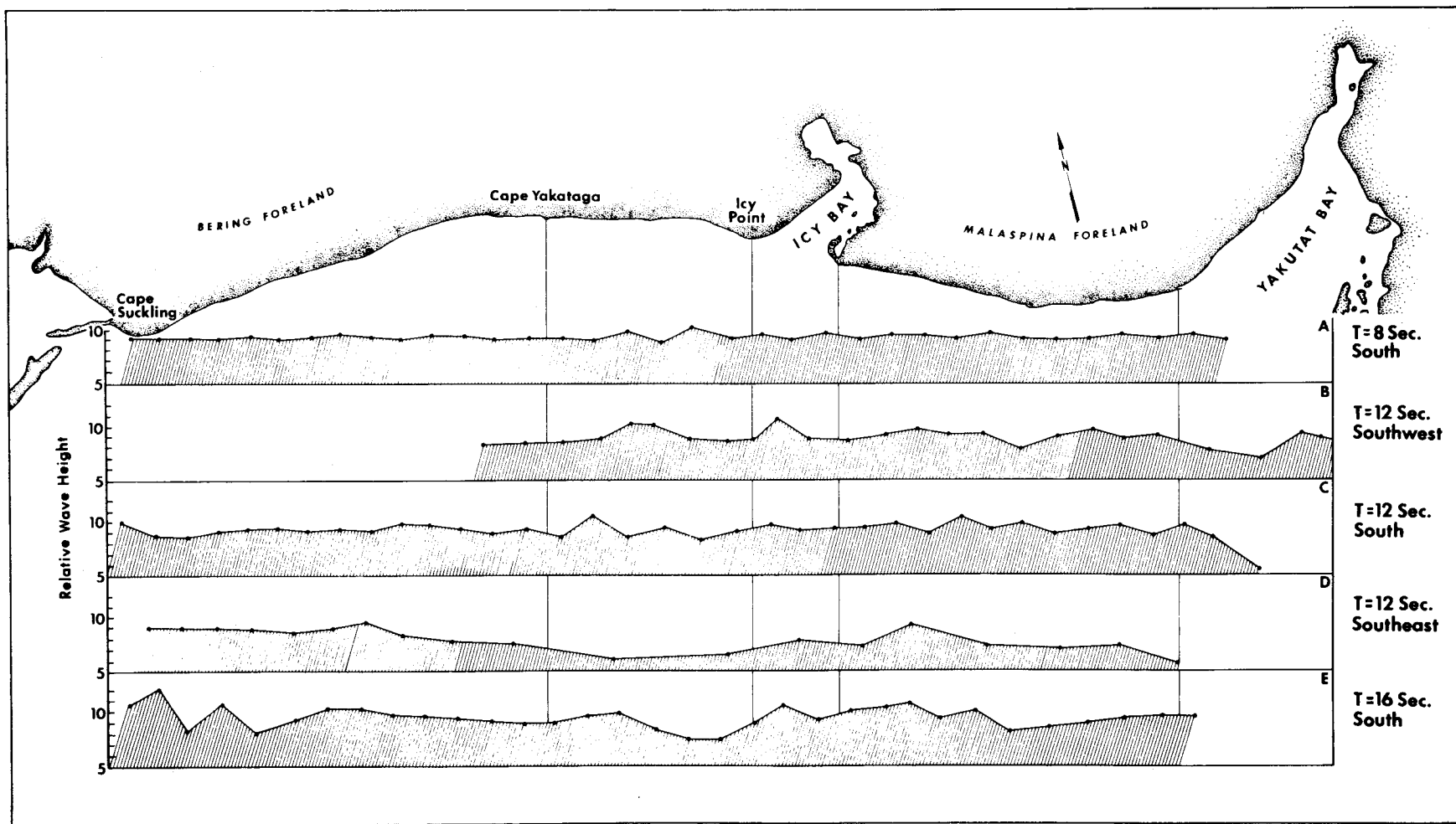
The term $\left(\frac{1}{2} \cdot \frac{1}{n} \cdot \frac{C_o}{C} \right)^{\frac{1}{2}}$ is known as the shoaling coefficient, K_s , and $(b_o/b)^{\frac{1}{2}}$ is known as the refraction coefficient, K_r . Thus:

$$\frac{H}{H_o} = K_s \cdot K_r \quad (12)$$

when energy losses are ignored. Equation 12 is used to predict wave height distribution along the northeast coast of the Gulf of Alaska for the

Figure 25. Predicted wave height distributions for the north-central coast of the Gulf of Alaska. Predictions are based on wave refraction diagrams (Figs. 20-24) according to a method outlined in the text. The wave height is given in relative units from 0 to 10 for a deep water wave height of 10. For example, a 10-foot deep water wave off Cape Suckling approaching from the southeast with a period of twelve seconds will be 9 feet high in 25 meters of water off the Cape (graph D). A similar wave approaching from the south with a sixteen-second period will be 12 feet high at the same point (graph E).

The pattern of wave height variability depends on period and approach direction. Typically, however, the waves are large near Cape Suckling, maintain the deep water wave height along the Bering Foreland, decrease in height west of Icy Point, increase again at the entrance to Icy Bay, are high along the west Malaspina Foreland, and drop off dramatically in height into Yakutat Bay.



25 meter depth contour. K_s is a function of depth and wave period only and is tabulated in the Shore Protection Manual (Coastal Engineering Research Center, 1973, v. III, Table C-1). The refraction coefficient has been computed for each orthogonal interval of the refraction diagrams (Table 2). The resulting wave height distribution is plotted in Figure 25. The wave height is given in relative units from 0 to 10, for a deep water wave height of 10. For example, a 10 foot high deep water wave approaching Cape Suckling from the southeast with a period of twelve seconds will be 9 feet high in 25 meters of water off the cape. A similar wave approaching from the south with a sixteen-second period will be 12 feet high at the same point.

Eight-second waves show little variability along the shoreline because of the insignificant refraction. There is a slight increase in wave height immediately west of Icy Bay, however. Southerly waves show the same variability pattern for twelve- and sixteen-second periods. The variation is larger, however, for the longer period waves. Typically, these waves are large near Cape Suckling, maintain about the deep water wave height along the Bering Foreland, decrease near Icy Point, increase again at the entrance to Icy Bay, are high along the west Malaspina Foreland, and drop off dramatically in height into Yakutat Bay. The pattern is similar for southwesterly and southeasterly waves. Because of the general trend of this segment of the shoreline, waves out of the southeast are the ones subject to most refraction, as demonstrated by the generally small wave heights in Figure 25D. This pattern of wave height variability should be compared to the observed wave heights for the summer of 1975, presented in Figure 27.

SEDIMENT TRANSPORT

Sediment Transport Computation Methods

Longshore sediment transportation rates for the northeast coast of the Gulf of Alaska were computed both from the SSMO-derived annual wave energy flux distribution and the coastal process data collected in the field during the summer of 1975. A brief presentation of methods is appropriate.

If the deep water wave energy flux from a given direction is P , the longshore component of that flux can be shown to be P_1 , where:

$$P_1 = P \cdot \sin \alpha_b \cdot \cos \alpha_o \quad (13)$$

(for derivation see Walton, 1972). α_b and α_o are the angles between the shoreline and the crests of the breaking wave and deep water wave, respectively. Equation 13 properly accounts for refraction and shoaling but assumes a friction-percolation coefficient of unity. In this equation the angle α_o is determined by selection of the shoreline orientation. Determination of α_b is based on constructed refraction diagrams which properly account for the shelf bathymetry. For simplicity the refraction diagrams constructed for twelve-second waves (Figs. 21-23) were used, assuming the breaker angle to be independent of wave period for the wave conditions which dominate the longshore sediment transport. Only southwest, south and southeast wave approaches contribute to the longshore energy flux along this section of shoreline. The annual sediment transport rate is found from the following equation (the metric equivalent of eq. 4-40 in Coastal Engineering Research Center, 1973):

$$Q = 1.28 \cdot 10^{-4} \cdot P_1 \quad (14)$$

where Q is cubic meters of sediment per year and P_1 is the mean annual longshore energy flux measured in ergs/s·m. Two longshore transport rates

are computed as both are important in the assessment of coastal sedimentation problems. The gross longshore transport rate, Q_g , is defined as the sum of the amounts of littoral sediment transported to the right and to the left past a point on the shoreline:

$$Q_g = Q_r + Q_l \quad (15)$$

The net longshore transport rate, Q_n , is defined as the difference between the amounts moving left and right:

$$Q_n = Q_r - Q_l \quad (16)$$

In calculating longshore sediment transport rate from observed shoreline processes one can use a form of eq. 13 which does not require knowledge of the deep water wave approach angle, α_o . It can be shown that (Coastal Engineering Research Center, 1973, p. 4-98):

$$P_l \approx 2.69 \cdot 10^{10} \cdot H_b^{5/2} \cdot \sin 2\alpha_b \quad (17)$$

where H_b is breaker height in meters and P_l is longshore energy flux in ergs/m·s.

Results of SSMO Computations

The shoreline between Yakutat Bay and Cape Suckling was subdivided into four segments for the purpose of sediment transport computation (Fig. 26). Each segment was approximated by a straight line. α_o is directly computed for each of the segments for three deep water wave approach directions. α_b is measured from wave refraction diagrams presented in Figures 21 through 23. All these data are summarized in Table 3.

The contribution to the annual sediment transport rate for waves out of the three approach directions considered is computed from data in Tables 1 and 3 by equations 13 and 14. Results are listed in Table 4. The total gross and net transport rates, calculated according to eqs. 15 and 16, are

TABLE 3

Orientation of shoreline and incoming wave crests
for four segments of the northeast coast of the Gulf of Alaska.
A map is presented in Figure 26.

| Segment | 1 | 2 | 3 | 4 |
|----------------------------|-----|-----|-----|-----|
| Shoreline azimuth | 98 | 117 | 103 | 78 |
| α_o Southeast waves | 37 | 18 | 32 | 57 |
| South waves | 82 | 63 | 77 | 102 |
| Southwest waves | 127 | 108 | 122 | 147 |
| α_b Southeast waves | 69 | 65 | 50 | 75 |
| South waves | 98 | 84 | 73 | 100 |
| Southwest waves | 123 | 109 | 97 | 110 |

TABLE 4

Longshore sediment transport rates on the northeast coast of the Gulf of Alaska, based on SSMO data for the time period 1963-1970. Positive sign indicates transport to the right (west); negative sign indicates transport to the left (east).

| Wave Approach Direction | Longshore Energy Flux (P_1)* $10^{10} \frac{\text{ergs}}{\text{s}\cdot\text{m}}$ | Sediment transport rate in $10^6 \text{ m}^3/\text{yr}$ for shoreline segment | | | |
|-------------------------|---|---|------|-------|-------|
| | | 1 | 2 | 3 | 4 |
| Southeast | 4.66 | 4.45 | 5.14 | 3.87 | 3.14 |
| South | 2.86 | .50 | 1.65 | .79 | -.75 |
| Southwest | 2.54 | -1.64 | -.95 | -1.71 | -2.56 |
| Gross Transport Rate | | 6.59 | 7.73 | 6.37 | 6.45 |
| Net Transport Rate | | 3.31 | 5.84 | 2.95 | -.17 |

*For the Cordova SSMO data square

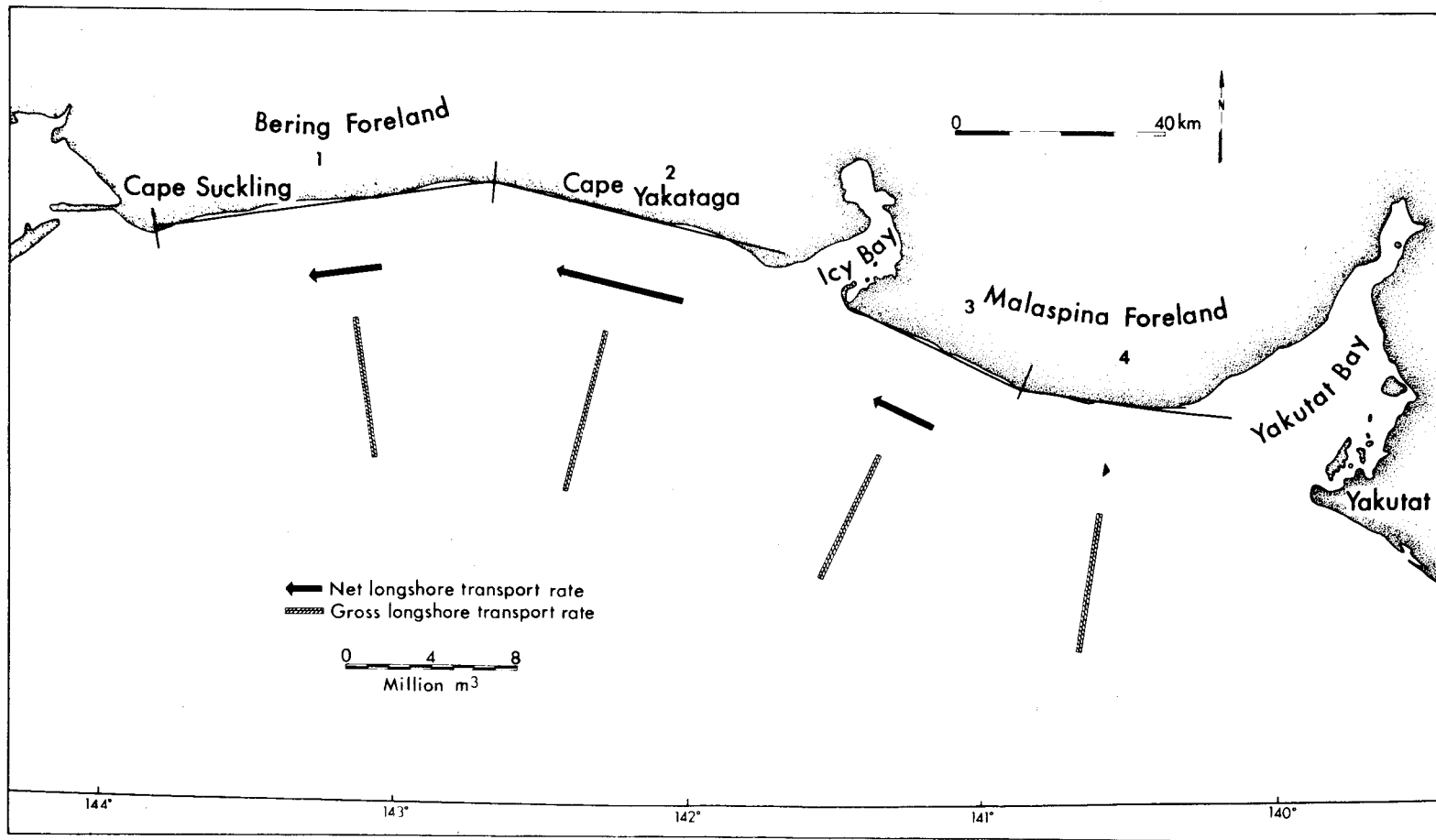
presented in Table 4 and Figure 26.

The results indicate that southeasterly waves are responsible for the dominant sediment transportation along this coast. This is to be expected in light of the cyclone patterns shown in Figures 10, 14 and 15, which indicate strong southeasterly winds associated with low pressure centers commonly located for long periods of time within the central Gulf of Alaska region. The gross transport rates are higher than what is reported anywhere else along the shores of the United States (Wiegel, 1964), and very similar to rates determined for the south coast of Iceland (Nummedal, 1975). It is interesting in this respect to note the similarity in setting of these two coasts with respect to cyclone track frequencies in the North Pacific and the North Atlantic (Fig. 12A).

The net transport is uniformly westward on the exposed shorelines between Cape Suckling and the central Malaspina Foreland, a predicted pattern which agrees well both with the large-scale transport pattern in the Gulf of Alaska (Fig. 19) and local geomorphology and process observations (Fig. 53). The presence of Yakutat Bay makes the shoreline east of the central Malaspina Foreland trend to the northeast, thus inducing a local reversal in transport direction. The net transport rate to the east in segment 4, however, is less than 3 percent of the gross rate, indicating the existence of a delicate balance. Slight changes in wave climate from one year to the next might displace the nodal point at the central Malaspina Foreland a distance of many kilometers. Further into Yakutat Bay the shoreline trends more to the north, and the predicted transport direction is towards the head of the bay, in accord with morphology and process observations (Fig. 53).

Figure 26. Summary diagram of computed longshore sediment transportation rates along the northeast coast of the Gulf of Alaska. Computations are based on local SSMO data and wave refraction diagrams. See text for the method.

A gross longshore transport rate of about 6.5 million cubic meters per year characterizes this shoreline. The net transport rate is highly dependent on the local shoreline orientation and is found to range from 170,000 m³/yr to the east on the east Malaspina Foreland (segment 4) to a high of 5.8 mill. m³/yr to the west along the shoreline between Icy Point and Cape Yakataga.



Transport Rates Based on Observed Wave Conditions

Table 5 presents littoral wave parameters for three stations on the Malaspina Foreland, observed in July and August of 1975 (for location see Fig. 28). Equations 17 and 14 are used to determine the longshore transport rate for any given observation. For a range in wave height of .7 to 2.8 meters, the sediment transport rate changes more than 2 orders of magnitude, clearly demonstrating the significance of major storm waves. Ranges of a few hundred thousand to about 40 million cubic meters per year for the observed range of conditions are reasonable in light of an annual average over a 7 year period of about 6.5 million m³.

OBSERVED COASTAL PROCESSES

General

Field studies of littoral sedimentation processes were undertaken in July and August of 1975. The area covered extends from Cape Yakataga to Yakutat Bay (Fig. 1). It is recognized that the observed processes generally describe summer "fair weather" conditions and are not representative of long time periods. According to SSMO tables for the Cordova data square, the range in wave heights observed (up to 2.8 meters) covers about 75% of the annual height-frequency distribution.

Summer process observations involved both a regional process network and a set of time-series measurements at specific sites. The regional process network involved nearly simultaneous measurements for constant wave conditions at 10 stations distributed over 150 km of shoreline. The time-series measurements (process zonals) involved detailed observations at one station over a 48-hour period. At each zonal site, meteorological and

TABLE 5

Sediment transport rate (Q) for observed unidirectional waves.

| Date | Time | H_b (m) | T(s) | α_b (deg.) | Q(m ³ /yr) |
|---------------------------|------|-----------|------|-------------------|-----------------------|
| <u>Riou Spit</u> | | | | | |
| July 24 | 1600 | 2.30 | 9.0 | 30 | $2.50 \cdot 10^7$ |
| | 1700 | 2.80 | 10.2 | 31 | $4.16 \cdot 10^7$ |
| July 25 | 1300 | 2.00 | 10.0 | 15 | $1.05 \cdot 10^7$ |
| | 1500 | 1.90 | 10.0 | 25 | $1.36 \cdot 10^7$ |
| July 26 | 1430 | .80 | 10.0 | 10 | $7.00 \cdot 10^5$ |
| <u>Alder Stream, AS-1</u> | | | | | |
| July 28 | 1400 | .90 | 7.5 | 6 | $5.72 \cdot 10^5$ |
| | 1500 | .80 | 7.5 | 5 | $3.56 \cdot 10^5$ |
| | 1600 | .70 | 8.0 | 5 | $2.56 \cdot 10^5$ |
| | 1700 | .70 | 8.0 | 5 | $2.56 \cdot 10^5$ |
| | 1800 | .80 | 8.0 | 5 | $3.57 \cdot 10^5$ |
| | 1900 | 1.00 | 8.0 | 8 | $9.85 \cdot 10^5$ |
| <u>Shipwreck, SW-1</u> | | | | | |
| August 13 | 1500 | 1.60 | 8.0 | 8 | $3.20 \cdot 10^6$ |
| | 1700 | 1.30 | 9.0 | 5 | $1.20 \cdot 10^6$ |
| | 1900 | 1.10 | 8.0 | 6 | $9.45 \cdot 10^5$ |
| August 14 | 0700 | 1.60 | 9.0 | 7 | $2.81 \cdot 10^6$ |
| | 0900 | 1.70 | 9.5 | 11 | $5.08 \cdot 10^6$ |
| | 1100 | 1.50 | 9.0 | 14 | $4.63 \cdot 10^6$ |
| | 1300 | 1.50 | 10.0 | 15 | $3.42 \cdot 10^6$ |
| | 1500 | 1.65 | 9.5 | 18 | $7.35 \cdot 10^6$ |
| | 1700 | 1.75 | 9.5 | 8 | $4.00 \cdot 10^6$ |
| | 1900 | 1.80 | 9.5 | 5 | $2.71 \cdot 10^6$ |
| | 2100 | 1.40 | 9.0 | 10 | $2.84 \cdot 10^6$ |

littoral processes and beach morphological variability were monitored. Each zonal site was selected as representative of a shoreline segment based on similar shoreline orientation and morphology (Hayes, et al., 1973).

Regional Process Network

Regional process variability was determined by multiple observations over the entire study area during a single low tide period (about 5 hours) with constant wave conditions. The field crew moved from station to station by plane, landing on the beaches during low tide. The selection of periods of uniform offshore wave conditions permits regional differences in near-shore wave characteristics to be attributed to effects of beach slope, shoaling, refraction, and shoreline orientation.

Processes observed on three different dates are summarized in Figure 27. On July 23, 1975, the dominant wave approach was out of the SSE. Stations monitored around Icy Bay documented littoral parameters consistent with local geomorphology.

At Icy Cape, on the western side of Icy Bay (Fig. 2), the approaching wave crests were subparallel to the beach, resulting in highly variable longshore current directions and velocities. The largest waves observed were at this station (Fig. 27). Two-meter waves were striking the beach face, and 2.5 to 3 meter waves were breaking about 150 m offshore.

West of Icy Cape, a combination of 1 meter spilling and plunging waves was striking the beach at a 10 degree angle, open to the west. Littoral transport was consistently to the west. Multiple offshore bars and an extremely wide surf zone characterized the site.

East of Icy Cape, moving towards Claybluff Point (Fig. 3), the wave height systematically decreased. In contrast, breaker angle increased from 0° at Icy Cape to 2° at an intermediate station and 8° at Claybluff Point

The breaker angle opened to the east. Longshore currents were strong and moved consistently eastward into Icy Bay. Breaker type changed from spilling to plunging as a result of gradual steepening of the beach face into the bay. Observed significant wave period for 23 July was 9.5-10.0 seconds.

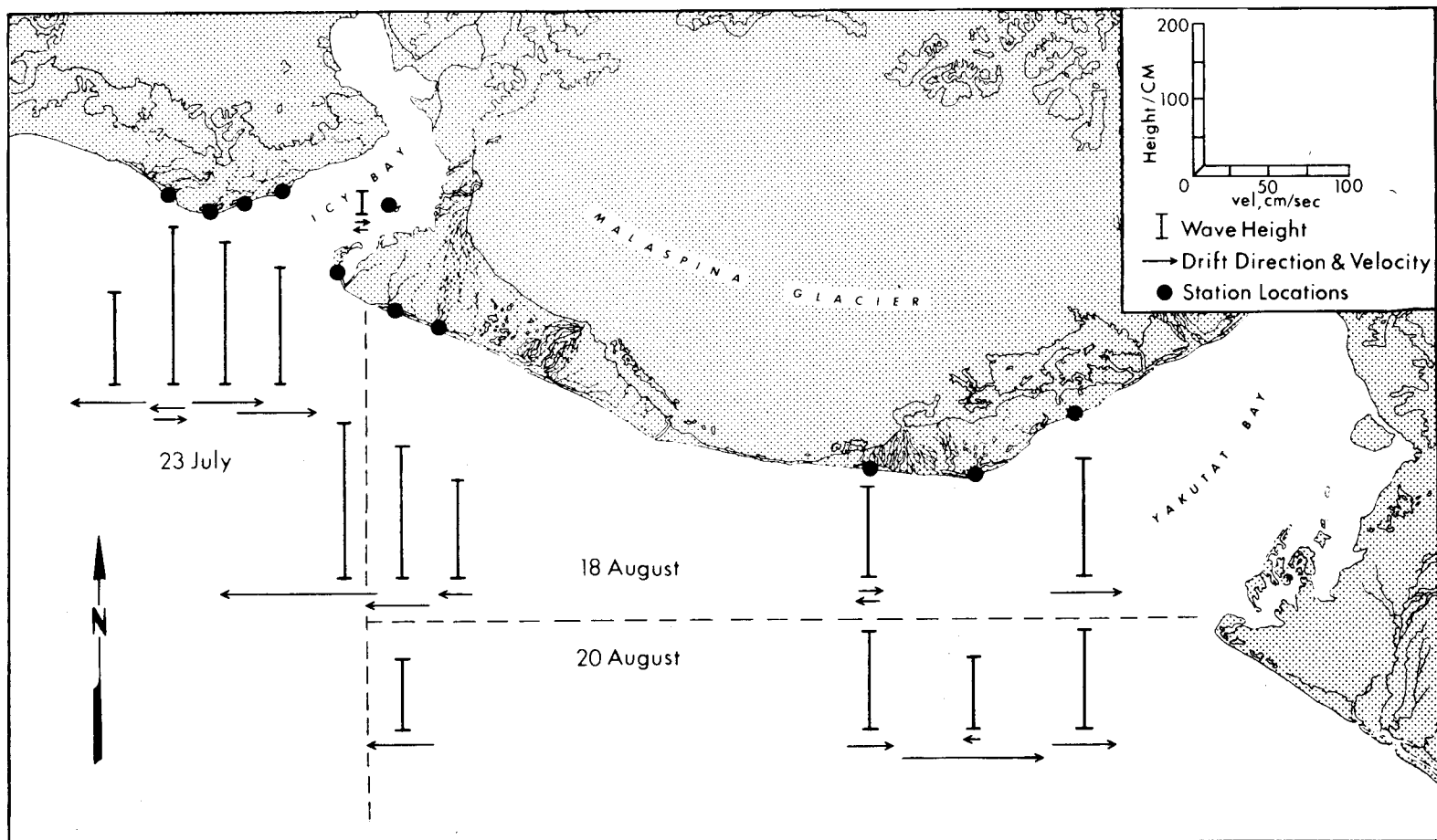
Wave refraction diagrams (Figs. 20, 22 and 23) for eight and twelve second waves approaching from the south and southeast show that the submerged moraine at the mouth of Icy Bay causes refraction and a general convergence of wave orthogonals at Icy Cape and a divergence of orthogonals further west. This pattern of wave energy flux variability agrees well with observed changes in wave height and current direction. Process variability near Icy Cape is concluded to be controlled by offshore bathymetry and shoreline orientation.

The morphology of Riou Spit, at the eastern side of the Icy Bay entrance (Figs. 4 and 5), demonstrates westward sediment transport into Icy Bay. Observed processes correlate well with this morphology. Breakers observed on July 23 at Riou Spit were more than 200 cm high with a 15 to 18 degree breaker angle open to the west. Littoral currents were strong, in excess of 150 cm/sec in a westward direction (Fig. 27).

In contrast to the high wave energy on the outer coast, observations at Chirp Island, located well inside Icy Bay (Fig. 4), illustrate the sheltered nature of eastern Icy Bay. Maximum observed wave heights were 30-40 cm.

On August 18 and August 20, 1975, the beaches on the Malaspina Foreland were under the influence of two wave trains approaching from the south and southeast. Observations along the western margin of the foreland (Fig. 5)

Figure 27. Wave height and longshore currents observed at process network stations on 23 July, 18 August, and 20 August, 1975. Measurements were made on days of regionally uniform offshore wave conditions. Variations in nearshore wave parameters reflect the effects of shoreline orientation, refraction, shoaling and beach slope.



indicate dominant transport direction towards the west. In the vicinity of Point Riou, wave heights varied between .9 and 1.2 meters with the breaker angles ranging between 0 and 4 degrees, open to the west. Ridge-and-runnel systems were well developed in this area throughout the study period. Local refraction and interference between the two wave trains caused highly variable current readings. Spilling waves generated long-shore currents to the west ranging in speed from .2 to .7 m/sec.

Wave heights in the vicinity of Manby Point on the eastern margin of the foreland (Fig. 7) are strongly controlled by bathymetry. Wave orthogonals for southeast and southwest waves show strong divergence in the vicinity of Manby Point (Figs. 21 and 23). This relates well to the wave height distribution recorded along this shoreline on August 20 (Fig. 27).

Observed waves inside Yakutat Bay (Fig. 27) were consistently larger than those at Manby Point. Plunging breakers with an 8 to 10 degree breaker angle, open into the bay, were dominant. Littoral currents were consistently to the east.

The results of the process network study are summarized in Figure 53, which demonstrates that the resultant longshore currents in the summer season are oriented to the west between Icy Cape and Yakataga, to the northeast on the west bank of Icy Bay, to the west along the western Malaspina Foreland, in a variable direction but mostly to the east along the eastern Malaspina Foreland, and to the northeast on the west bank of Yakutat Bay.

Time-Series Process Measurements

Five process zonal sites were established at locations representative of different shoreline segments. The choice of each shoreline segment

was based on uniform morphology and orientation. A process zonal consisted of 48-hour monitoring of the following parameters at two-hour intervals: wind speed, wind direction, significant breaker height, breaker angle, longshore current velocity, and significant wave period. The instantaneous beach response to these processes was determined by measurement of beach profiles at successive low tides during the zonal study. Beach profiles were referred to a temporary base line running parallel to the beach. Profile A was the westernmost profile at each zonal site, and B, C, D, E, and F were spaced 50 m apart towards the east along the baseline. The profiles were measured perpendicularly to the beach. The process zonals serve to characterize wave processes at sites typical of larger shoreline segments and allow computation of local longshore wave energy flux and sediment transport rate at the time of study.

Old Yahtse River, OY-1 Process Zonal--Beach processes were observed at the Old Yahtse River station (OY-1) on the western front of the Malaspina Foreland from August 1 to 3, 1975 (Fig. 28). The weather was clear and the winds remained fairly light or calm during the study (Fig. 29). Breaker height and period generally decreased during the observation interval from 1.3 m waves of 10 second periods on August 1 to 60 cm waves of 7 to 8 second periods on August 3. Longshore current velocities and breaker angle showed less distinct trends (Fig. 29). On August 1 and 2, 80 percent of the breaker crests were parallel to the beach, while 20 percent were inclined either east or west at angles up to 6 degrees. This complexity is largely due to the presence of a well developed ridge-and-runnel system, causing local refraction of the waves. Observed current velocities fluctuated both east (left) and west (right) in response to the shifts in breaker angle.

Figure 28. Location of process zonals and special study sites in Icy Bay and on the Malaspina Foreland. The study sites were concentrated around Icy Bay and on the east Malaspina Foreland because of the rapid lateral variability in processes at those locations.

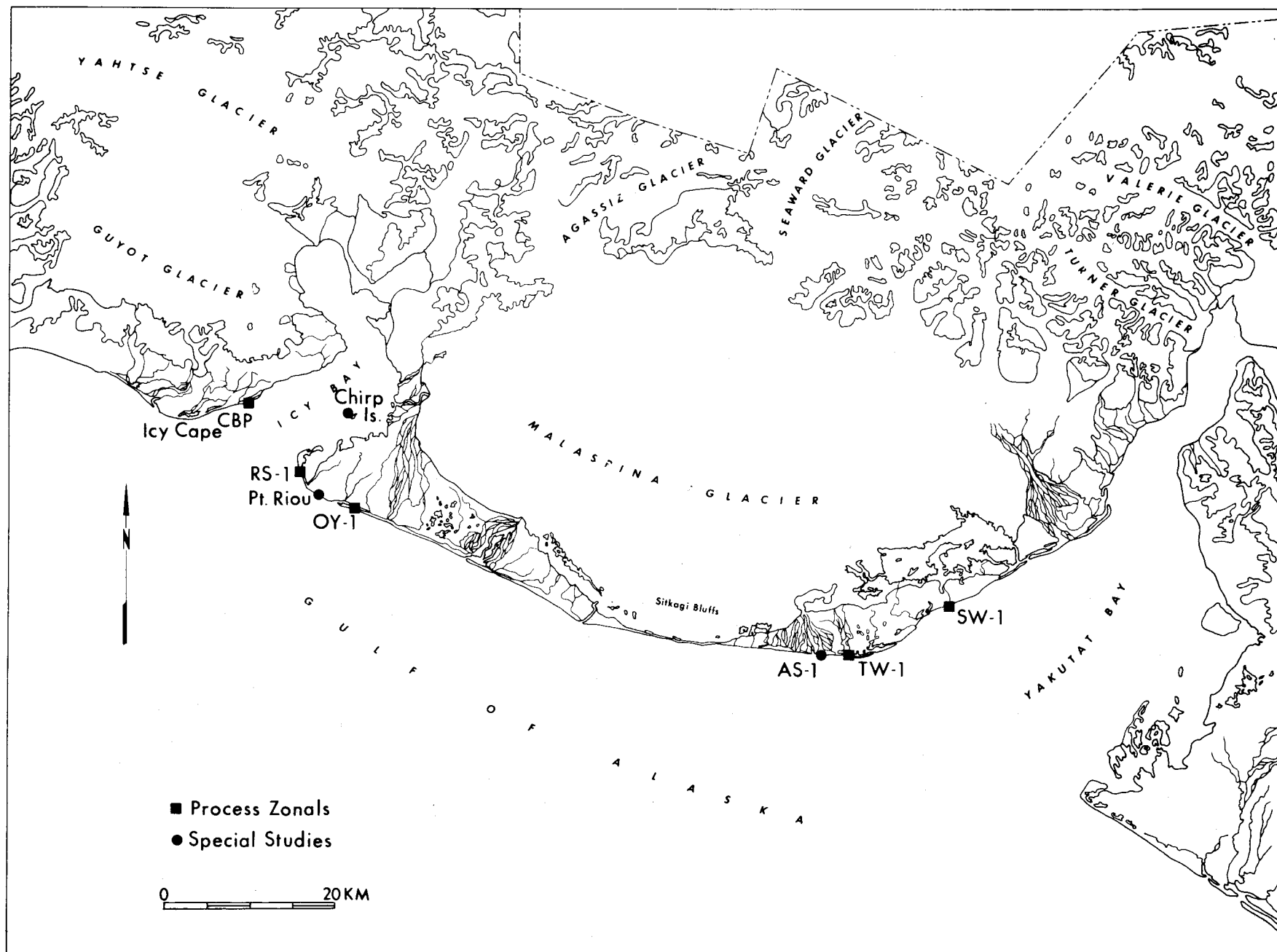


Figure 29. Beach process variables measured at two hour intervals at the Old Yahtse process zonal, OY-1, from August 1 to August 3, 1975. Left currents are to the east; right currents are to the west. Left breaker angles open to the east; right angles open to the west.

A general decrease in wave energy occurred during the study period. Tide-dependent refraction over nearshore bars caused westward oriented currents at low tide and eastward currents at high tide. See tide curve in Figure 30.

PROCESS VARIABLES AT OY-1, AUGUST 1-3, 1975

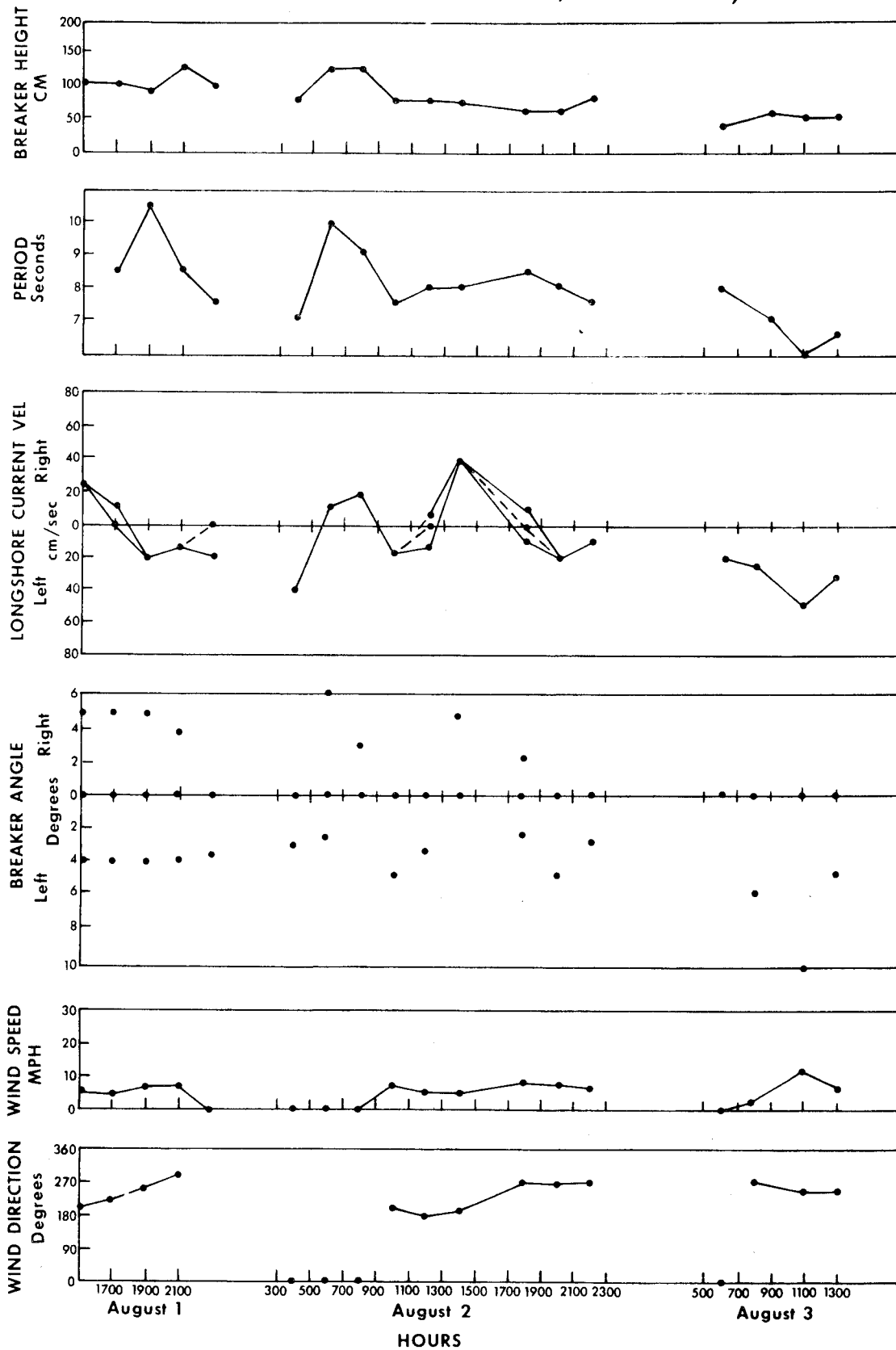


Figure 30. Tide curves for Sitka, Alaska, for the period July 21 to August 22, 1975. A strong diurnal inequality is present, especially at neap tide. The actual tidal phase at Icy Bay and Yakutat Bay precedes that at Sitka by about forty minutes. From: National Oceanic and Atmospheric Administration, Tide Tables, West Coast of North and South America, 1975.

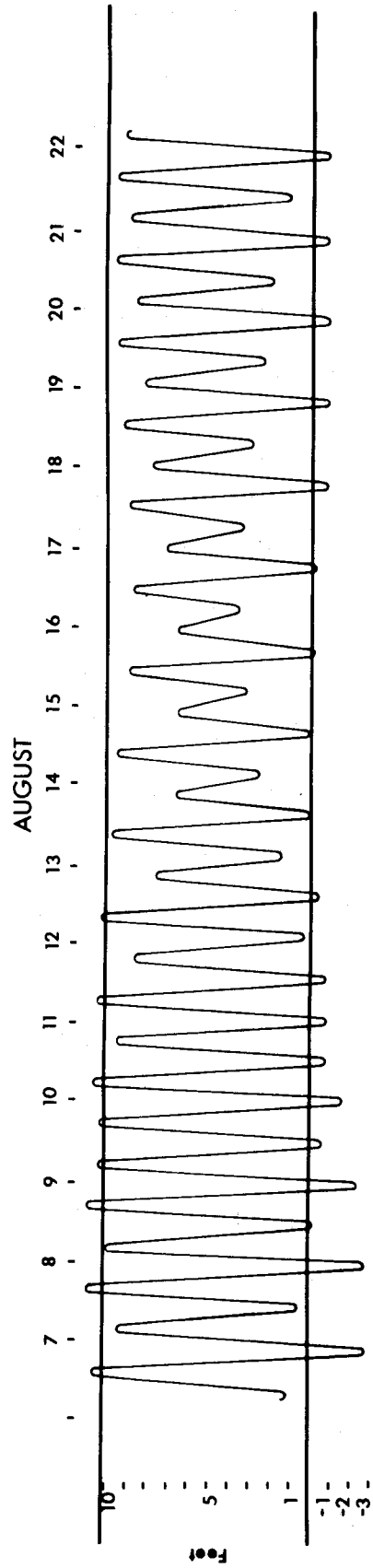
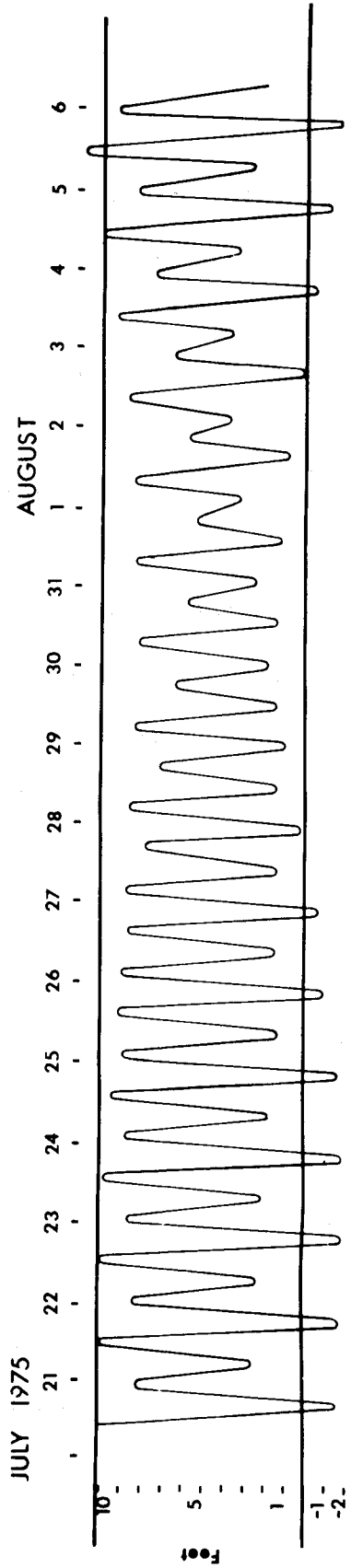


Figure 31. Oblique aerial view to the east of the seaward margin of the Old Yahtse outwash with process zonal site OY-1. The photo was taken on August 4, 1975. The stream in the upper part of the photo is the Old Yahtse, and the trees in the foreground form part of the eastern end of Point Riou. Note the logs on the overwash terrace to the west of OY-1.



313

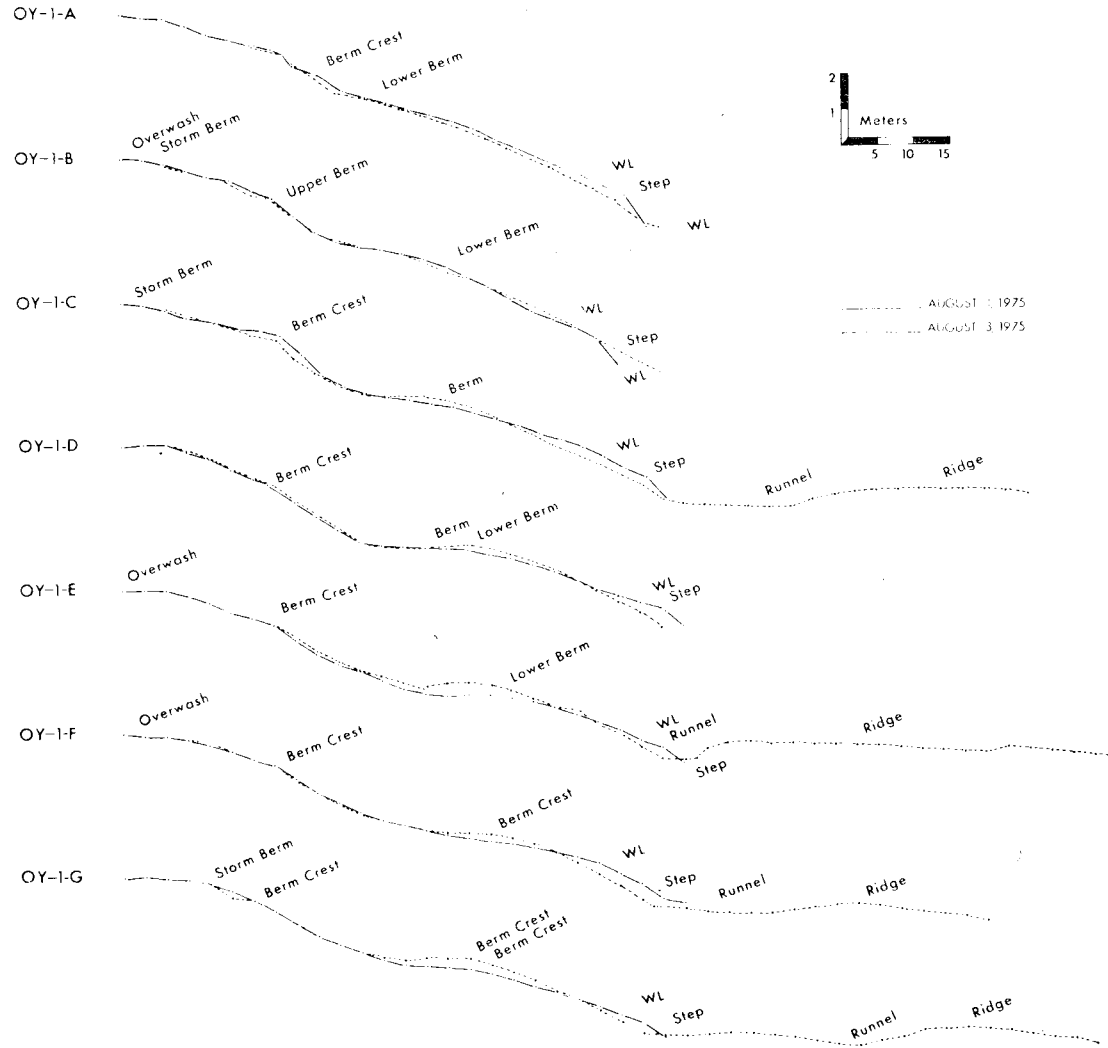
Figure 32. Consecutive beach profiles at process zonal site Old Yahtse, OY-1, on August 1 and 3, 1975. Profile A refers to the westernmost survey of the site; the other profiles are spaced 50 meters apart towards the east. The profiles are characteristic of the accretionary phase of the barrier spits at the terminus of the Old Yahtse and Yana outwash plains (see Figs. 6 and 31).

The berm accreted during the 48 hours of observation, causing the formation of a berm runnel, the steepening of the beach face, and the development of a low-tide step at the foot of the beach. Intertidal and shallow subtidal ridge-and-runnel systems were well developed. The high-level storm berm remained essentially unmodified, except for slight aeolian reworking, during the observation period.

The refraction controlled breaker angle is tide-dependent, causing a dominant westward littoral current at low tide and a dominant eastward current at high tide (Figs. 29 and 30). Surf zone suspended sediment samples obtained by holding a one liter plastic jar in the breaker showed concentrations of 5, 56, 65, 25, and 9 grams/liter. All OY-1 beach profiles are short and have typical depositional forms with well developed multiple berms and large ridge-and-runnel systems (Figs. 31 and 32). Profiles C, E, F, and G illustrate the growth of the lower berm and the consequent steepening of the beach face between August 1 and 3, attesting to the constructional nature of the small spilling waves.

Claybluff Point, CBP Process Zonal--Beach processes were observed at Claybluff Point on the western side of Icy Bay (Figs. 3 and 28) on August 11, 1975. Wave heights and periods recorded at this station were the lowest for all the process zonals (Fig. 33). Ocean waves arriving at Claybluff Point have been subject to significant energy dissipation across the Icy Bay entrance moraine. Because of the local shoreline orientation, the breaker angle for oceanic waves opens to the north. Northerly orographic winds off the icecap often produce significant waves out of the north, progressing in opposition to the oceanic swell. On August 11, a combination of persistent northerly winds and small oceanic swell produced rapidly shifting current velocities and breaker angles. The morphology of Claybluff Point (Figs. 3 and 34) demonstrates significant sediment transport into Icy Bay. The long-term sediment transportation, therefore, is controlled by the oceanic rather than local bay waves. Waves observed at Claybluff Point on July 23 (Fig. 27) were more representative of the dominant conditions than those observed on August 11. The process measurements were terminated ahead of schedule because of the ice problems.

CONSECUTIVE BEACH PROFILES, OY-1 PROCESS ZONAL



Beach profiles measured at the CBP process zonal on August 11 were not repeated because of the ice. However, it can be seen in Figures 34 and 35 that the beach was in a depositional phase. Each profile consisted of a high storm berm with logs deposited on the washover terrace. Seaward of the storm berm was a very large active berm and berm-runnel system. The beach face was very steep and reflected the dominance of plunging waves on this section of shoreline.

The importance of floating icebergs in Icy Bay cannot be overemphasized. During the summer large volumes of ice calf off the Tyndall and Yahtse glaciers at the head of Icy Bay. Northerly winds, wind generated waves, and tidal currents commonly move the icebergs to the outer reaches of the bay. Many of these icebergs are tens and probably hundreds of feet across. During the night of August 11 a large volume of this drift ice was carried onto the beach at Claybluff Point (Fig. 34). A band of icebergs over 100 m wide formed a natural rampart, preventing waves from striking the beach face. The drifting ice would present a significant hazard to shipping if Icy Bay were developed as a port facility.

Shipwreck Station, SW-1 Process Zonal--The SW-1 process zonal was located on the west side of Yakutat Bay, about 10 km northeast of Manby Point (Fig. 28). As shown in Figure 36, winds remained very light or calm during the observation period of August 12 through 14, 1975. Wave height decreased gradually from about 1.7 to 1.1 meters, accompanied by a reduction in period from 9 to 7.5 seconds.

The recorded variations in breaker angle and longshore current velocity indicate an interesting tide-dependent trend. At high tide, at 0600 hours on August 13 (Fig. 30), the breaker angle was 7 degrees and the longshore current flowed northeast at 50 cm/sec. At low tide, at 1400 hours on

Figure 33. Process variables measured at two hour intervals on August 11, 1975, at Claybluff Point. During the night of August 11, the beach became covered with icebergs, preventing waves from striking the beach. Longshore currents to the left go into the bay; those to the right go seaward. The variations in current direction and breaker angle reflect the opposing trends of oceanic waves, progressing to the left, and locally generated bay waves, progressing to the right.

CLAY BLUFF POINT PROCESS VARIABLES, AUGUST 11-12, 1975

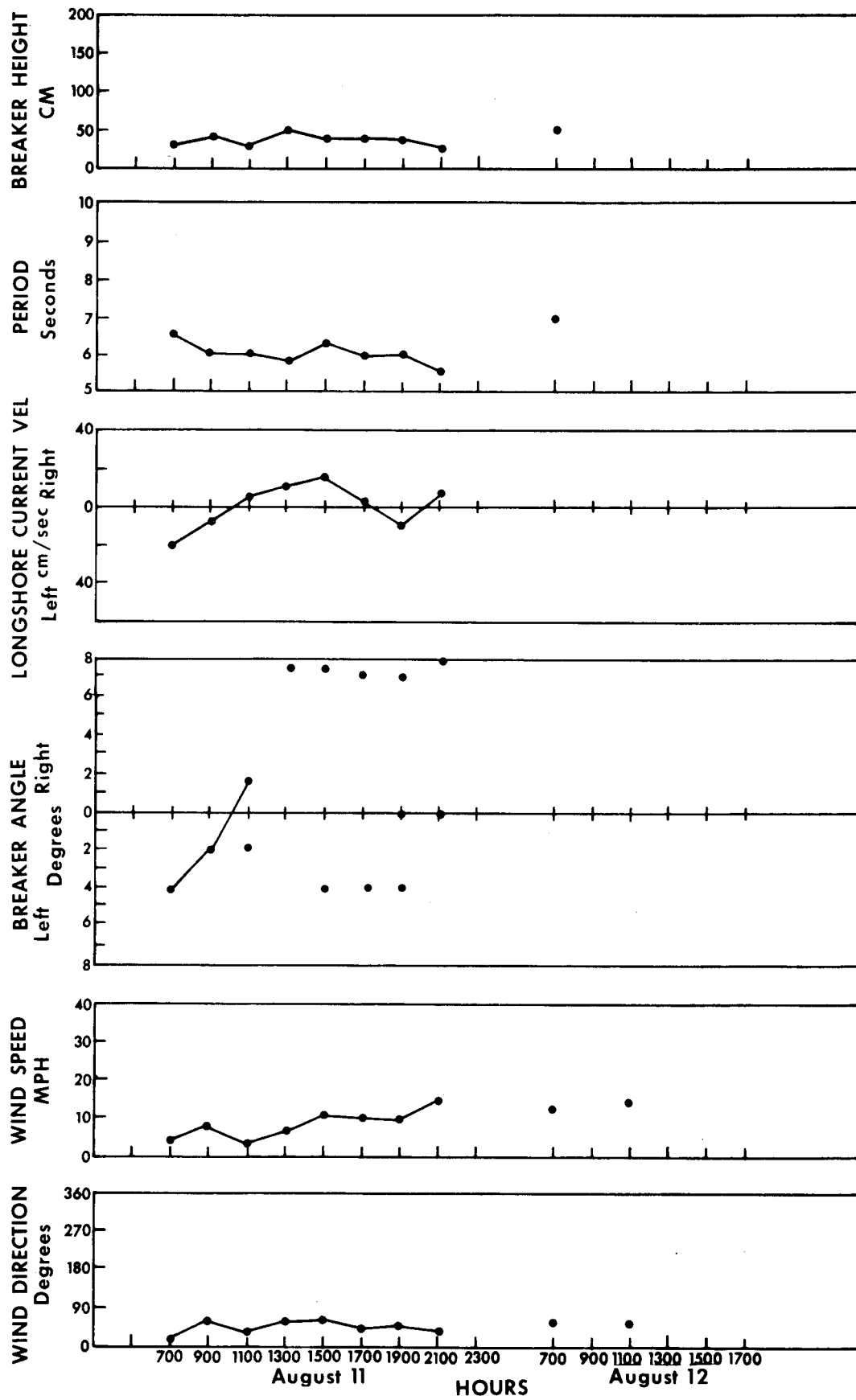


Figure 34. Aerial view of Claybluff Point. The photo was taken on August 12, 1975, from 1000 ft. During the night of August 11, strong orographic winds out of the north blew these icebergs out of Icy Bay and onto the beach. This 100 m wide swath of icebergs effectively protected the beach from wave attack and curtailed the CBP process zonal observations.



321

Figure 35. Beach profiles measured on August 11, 1975, at the Claybluff Point process zonal. These profiles demonstrate a depositional beach with well developed storm berms, berms, and berm-runnels. A is the westernmost profile; the others are spaced 50 m apart into the bay.

BEACH PROFILES, CBP PROCESS ZONAL, AUGUST 11, 1975

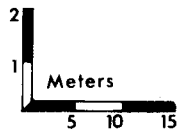
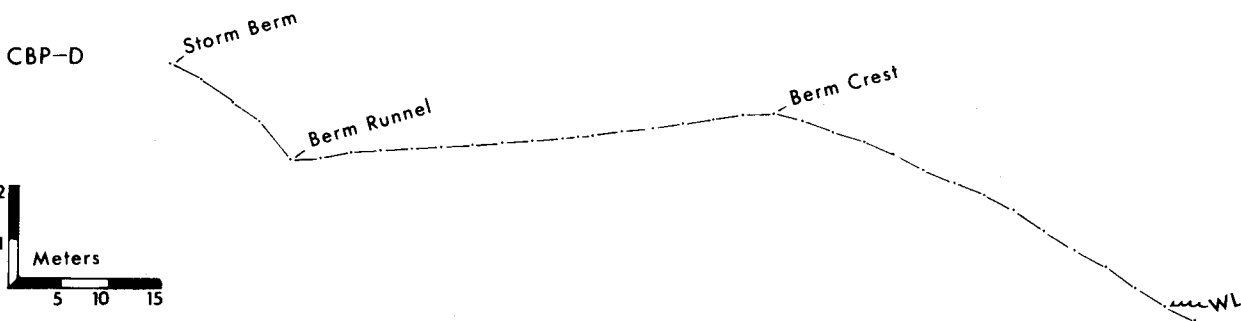
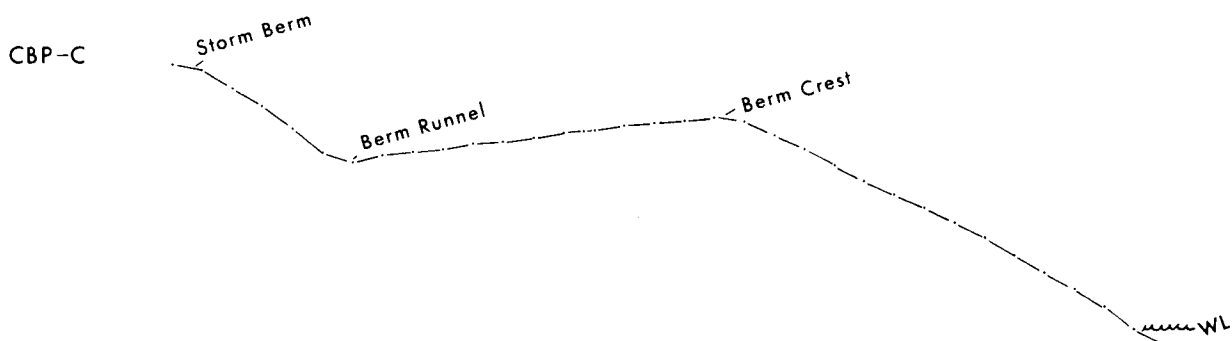
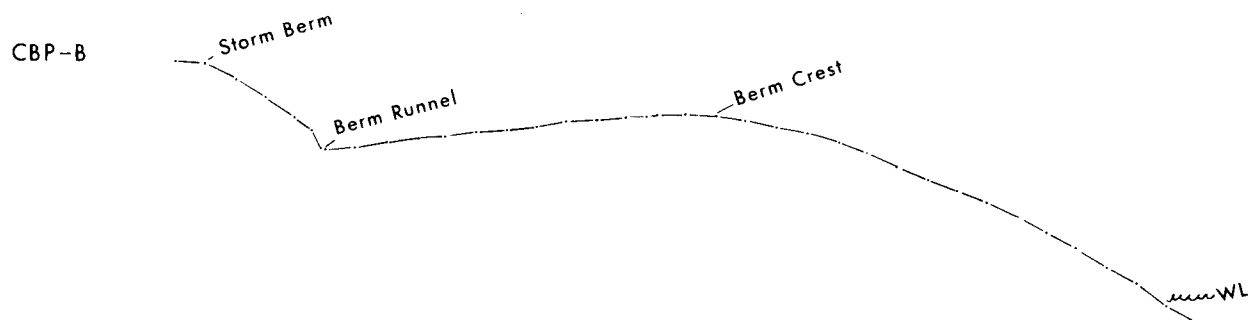
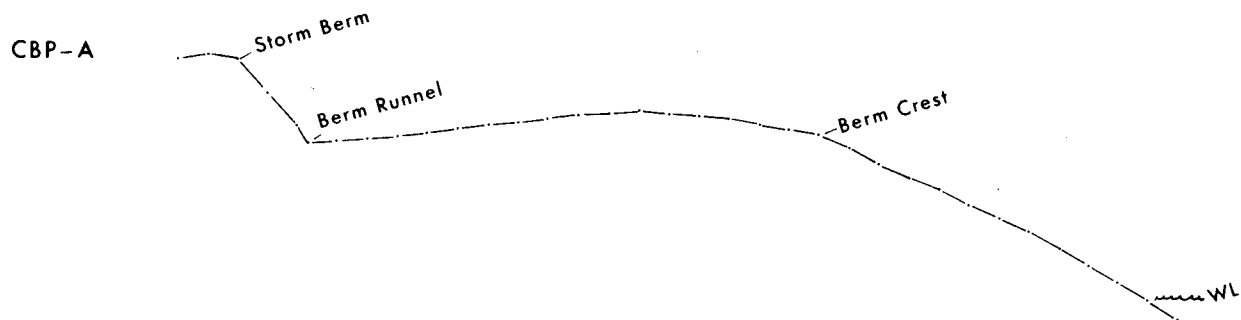


Figure 36. Littoral process variables measured at two hour intervals during day-time occupancy of the Shipwreck process zonal (SW-1) from August 12 to 14, 1975. Longshore currents flow consistently to the northeast (left) into Yakutat Bay. A slight decrease in wave energy occurred during the observation period.

PROCESS VARIABLES, SW-1, AUGUST 12-14, 1975

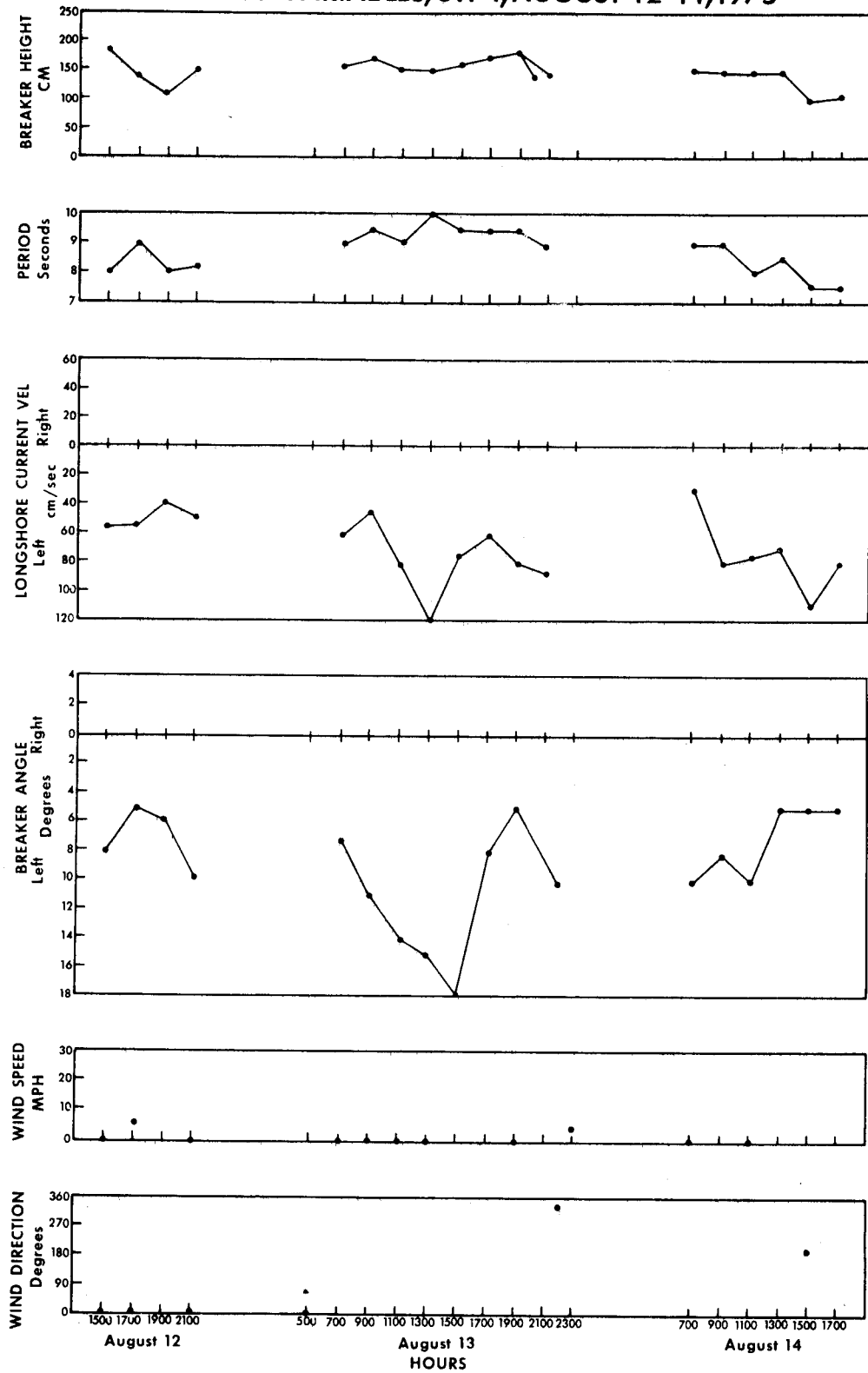
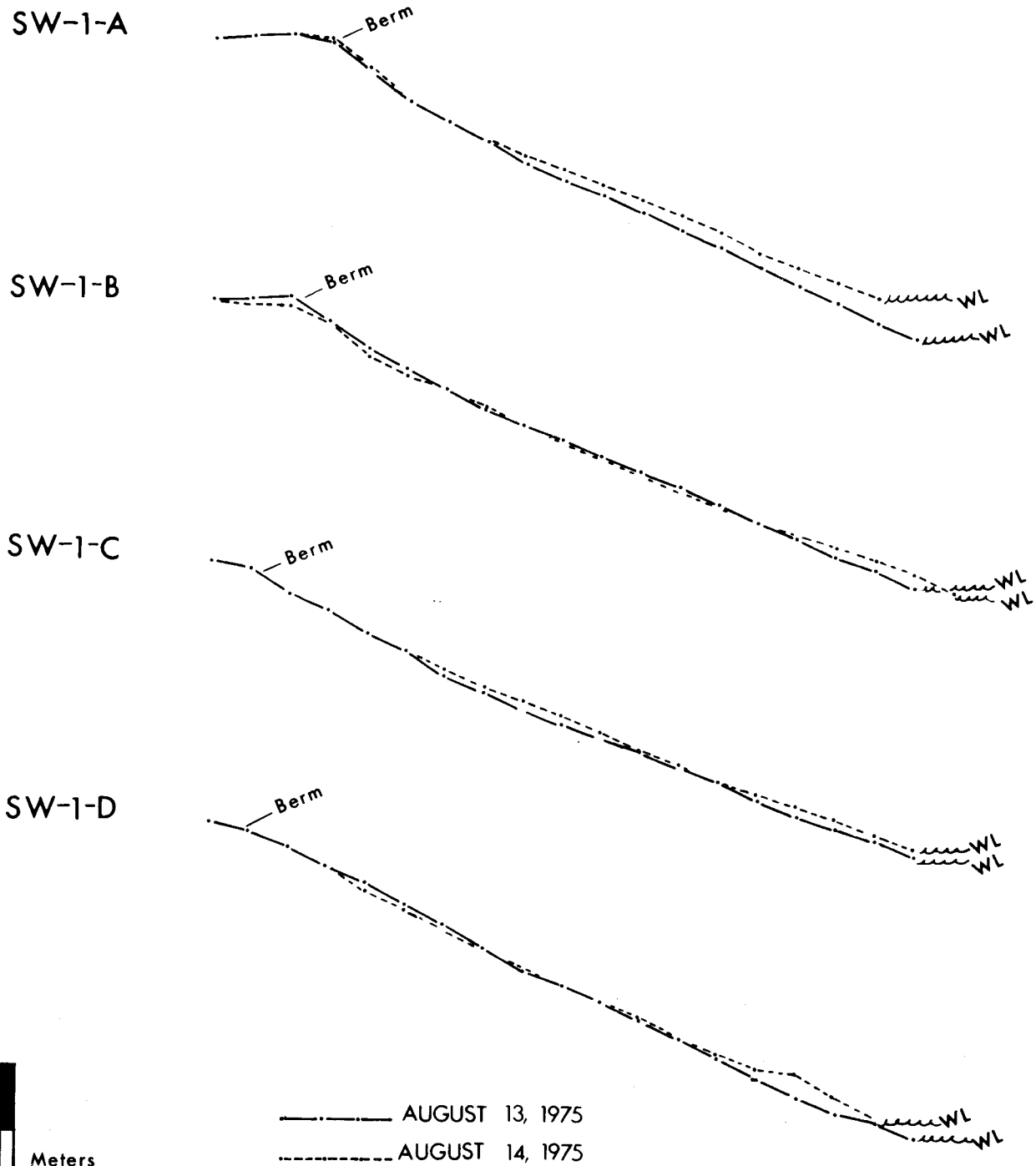


Figure 37. Profiles of the beach at the SW-1 process zonal on August 13 and 14, 1975. A is the westernmost profile; the others are spaced 50 meters apart to the east. Note the generally steep beach face and the development of the small berm at SW-1-D by August 14th.

CONSECUTIVE BEACH PROFILES, SW-1 PROCESS ZONAL



August 13, the breaker angle had increased to 18 degrees and the current velocity to 120 cm/sec. This variation might be related to increased refraction over the nearshore bar at low water, causing an increase in breaker angle and the longshore component of the wave energy flux.

Surf zone suspended sediment samples obtained by holding a jar in the uprushing bore of plunging waves recorded the following concentrations: 67 g/l, 71 g/l, 92 g/l and 147 g/l. The suspended sediment included coarse sand and pebbles, some of which were tossed two meters into the air at wave breaking. The concentrations recorded at SW-1 and station OY-1 are orders of magnitude higher than those typical of breaking waves on the east coast of the U. S. (T. Kana, personal communication, 1976), indicating very high rates of longshore sediment transportation for the Alaskan littoral zone.

Beach profiles surveyed at SW-1 on August 13 and 14, 1975, show a steep beach face and a well developed berm (Fig. 37). Profiles SW-1-A and SW-1-C had the largest overall accretion. Profile SW-1-D had developed a small berm on the lower beach face by August 14th.

Train-Barge Wreck, TW-1 Process Zonal--At the train-barge wreck (Fig. 28) littoral processes were observed at 2-hour intervals during daylight hours from August 14 through 16, 1975. A small storm, causing an increase in breaker height from 1.5 to 2 meters, passed through the area in the afternoon of August 15. Prior to the storm the littoral currents were flowing eastward (left) in response to the breaking of incoming swell. A combination of long-period swell and shorter period local sea during the storm passage produced rather variable current readings. The resultant longshore current, however, was oriented to the west (Fig. 38).

The coastal morphology of the area (Fig. 7) demonstrates a long-term net sediment movement to the east. For example, the Alder Stream barrier spits build eastward, and gravel, derived from Sitkagi Bluffs, dominates the beaches more than 15 km to the east. However, timber from a wrecked barge is dispersed westward on the storm berms and overwash terraces.

One might therefore conclude, from combined process and sedimentary evidence, that the long-term net sediment movement is to the east as a result of persistent swell and occasional storms from the west. Periodic transport reversals occur, however, in response to strong southeasterly storms.

Figure 39 illustrates some of the wreckage observed near process zonal TW-1. A railroad barge with box cars and tank cars was driven ashore by a storm during the winter of 1970. The wreckage is distributed over a large area of storm berm and overwash terrace. Steel plates, 3/4-inch thick, have been rolled, twisted and broken. The storm waves which occasionally hit this beach are enormous and must be considered a severe hazard which warrant special attention in the design of shorefast structures.

Profiles (Fig. 40) measured at low tide on August 15 and 16 demonstrate the narrow, steep beaches and well developed berms characteristic of the Manby Point area. Landward migration and a slight erosion of the berm crest is observed (TW-1-D), probably as a result of the small storm.

Riou Spit, RS-3 Process Zonal--Littoral processes on the seaward side of Riou Spit at RS-3 (Figs. 4 and 42) were monitored from July 24 to July 26, 1975. An offshore storm caused a rapid increase in wave height from 1.4 to 2.8 meters during the first two hours of station occupancy (Fig. 41). The wave period was about 10 seconds and the longshore current

Figure 38. Littoral process variables measured at two-hour intervals during day-time occupancy of the train-barge wreck (TW-1) process zonal from August 14 to 16, 1975. The zonal was located between Alder Stream and Manby Point (see Figs. 7 and 28). Swell-generated longshore currents normally flow eastward, while storm-generated currents observed on August 15 were oriented towards the west (left).

PROCESS VARIABLES, TW-1, AUGUST 14-16, 1975

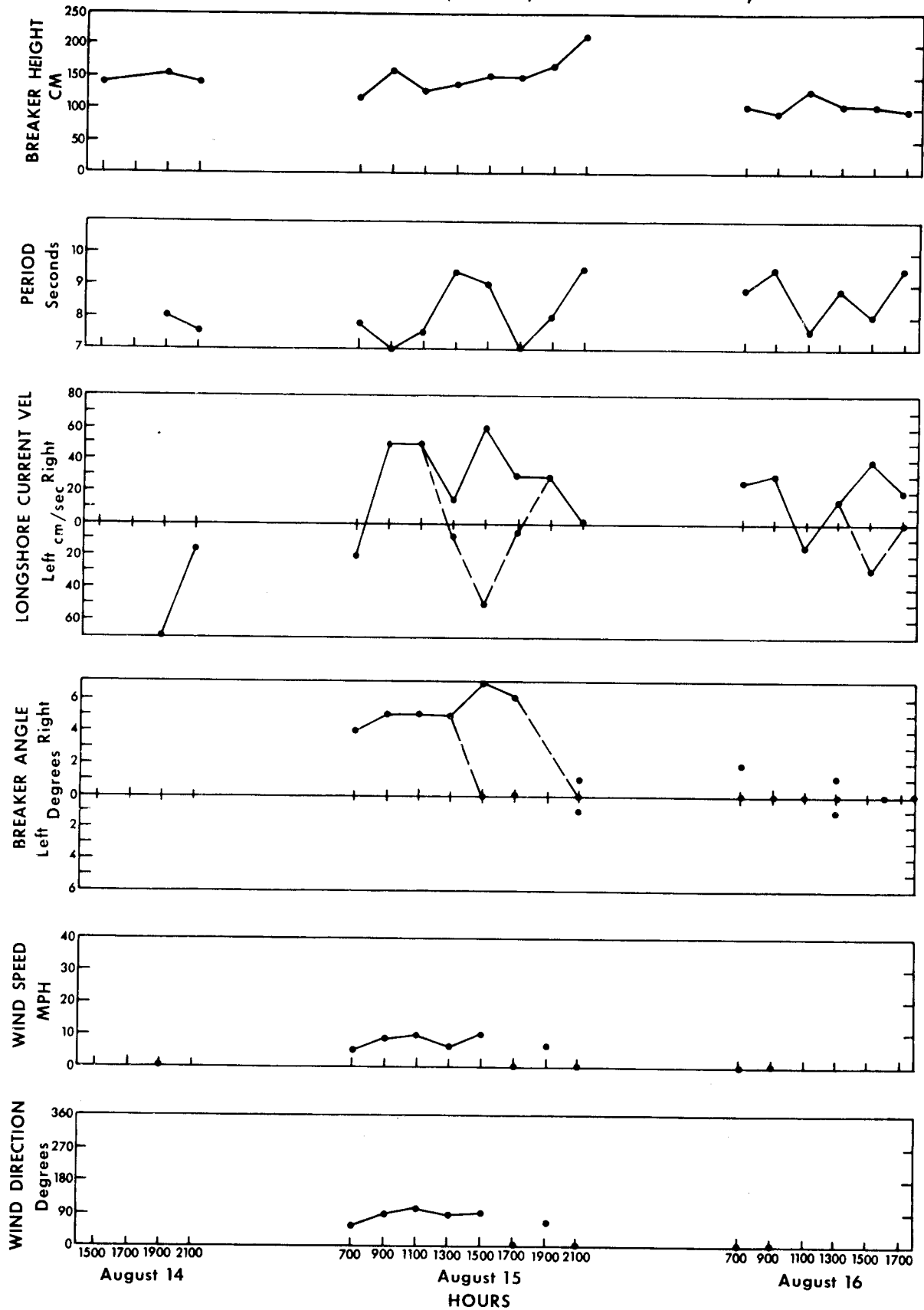


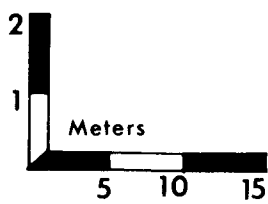
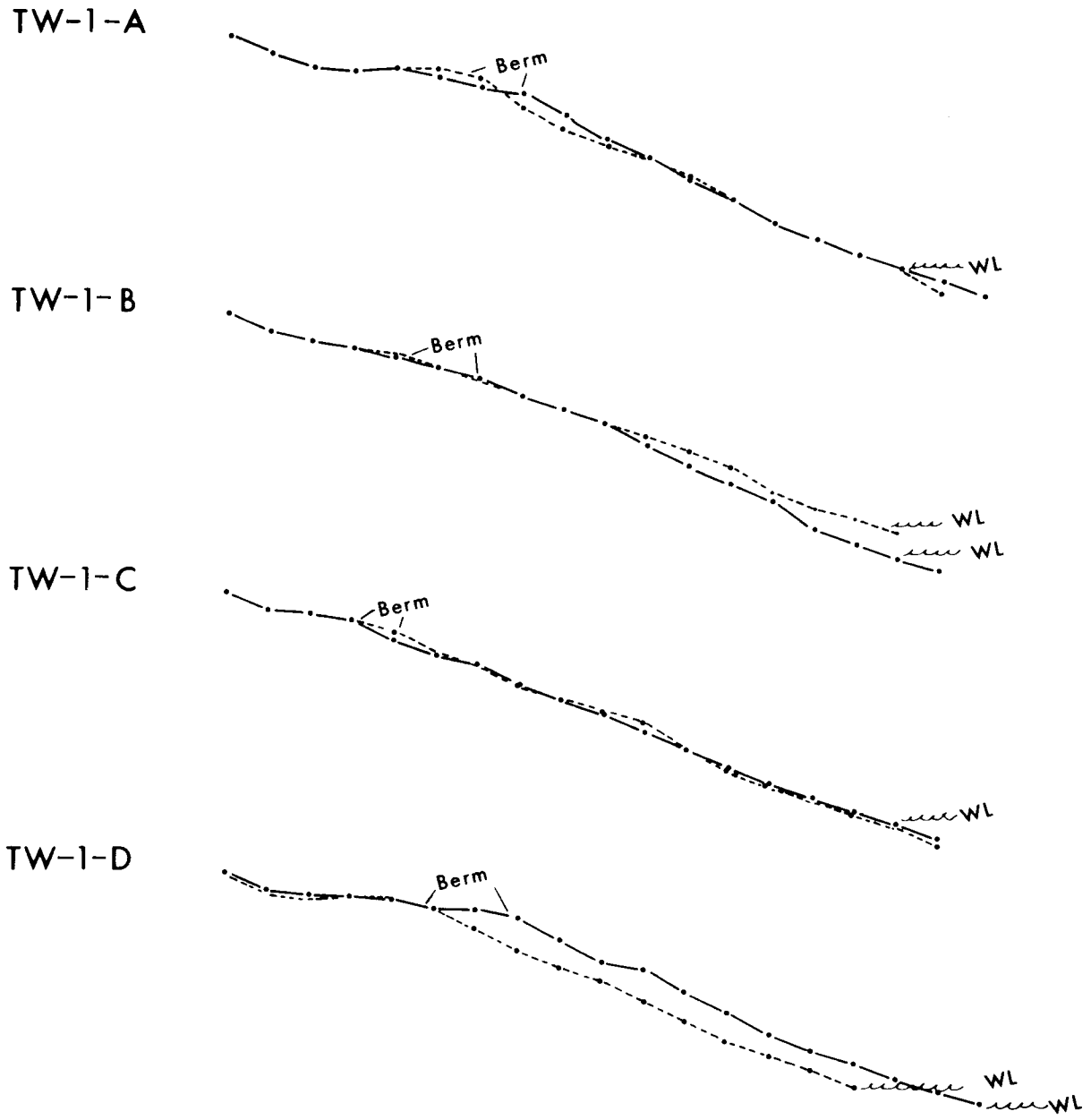
Figure 39. A train barge was driven ashore in a storm during the winter of 1970, leaving box and tank cars scattered over the berm and overwash terrace. 3/4-inch steel plates have been twisted, rolled and broken by the waves. The extreme winter storms that occasionally hit this area must be properly assessed prior to the initiation of coastal construction activities.

333



Figure 40. Beach profiles at the TW-1 process zonal on August 15 and 16, 1975. A is the westernmost profile; the others are spaced 50 meters apart towards the east. Note the steep, narrow beach, characteristic of the Manby Point area, and the erosion and landward migration of the berm crest at TW-1-D.

CONSECUTIVE BEACH PROFILES, TW-1 PROCESS ZONAL



—•—•—•— AUGUST 15, 1975
- - -•- - -•- - - AUGUST 16, 1975

Figure 41. Littoral process variables measured at two-hour intervals during day-time occupancy of the Riou Spit process zonal from July 24 to July 26, 1975. For location of the zonal site see Figures 28 and 42. A small offshore storm on July 24 generated peak breaker heights of about 2.8 meters. The longshore current was consistently westward during the study period.

RIOU SPIT PROCESS VARIABLES, JULY 24-26, 1975

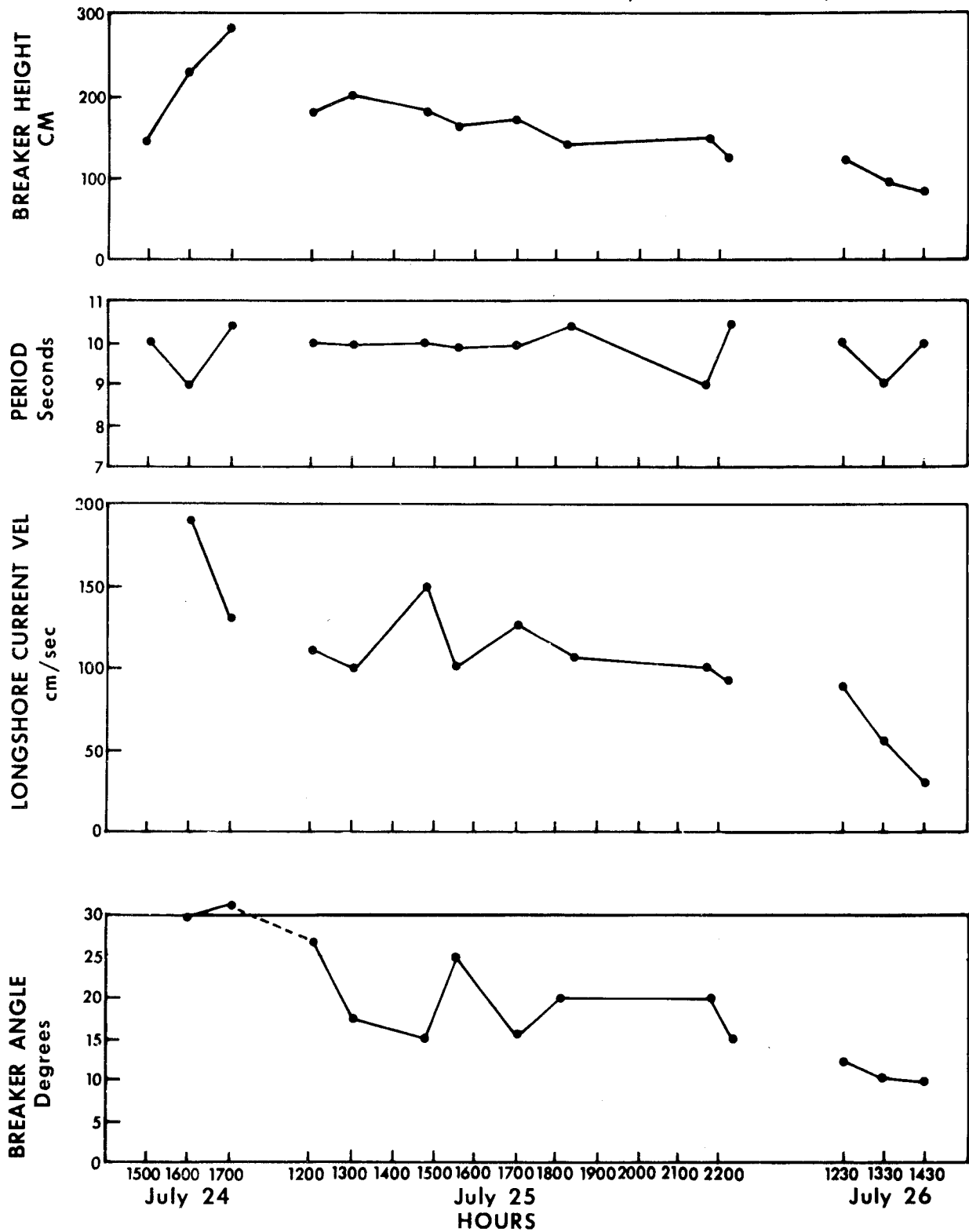


Figure 42. Oblique aerial view of Riou Spit. The photo was taken on August 4, 1975, from about 8000 feet. The site designations refer to beach profiles presented in Figure 46. Note the transgressive morphology of the neck and the wide progradational morphology at RS-1. Suspended sediment outlines current gyres both seaward (foreground) and landward (center) of the spit.

339



velocity reached a maximum value of almost 200 cm/sec during the storm. During the remainder of the study period, a steady decline in wave energy was observed.

To characterize the nearshore environment on the seaward side of Riou Spit, seven fathometer profiles were run for a distance of a few hundred meters. The locations are shown in Figure 43; the traces in Figures 44 and 45.

The variations in bathymetry around the spit follow a clearly defined pattern. Fathometer profile no. 1 (Fig. 44) demonstrates the gently sloping nearshore zone of the spit neck with a well developed bar about 150 meters offshore. Further west, profile no. 2 shows that the bar has moved closer to shore. The bar crest is shallower and the shoreward face steeper than at profile 1. This same bar can be visually traced by a line of breaking waves past Point Riou east to the Old Yahtse River section of the shoreline (Fig. 31). There is reason to believe that the bar is indicative of sediment transportation from the Yana and Old Yahtse shores onto Riou Spit.

Further west, off Riou Spit, the bar disappears and the nearshore profile steepens (traces 3 and 4) in response to a change in shoreline orientation (Figs. 42 and 43). Profile 5 (Fig. 45) illustrates a 600 m wide shallow subaqueous platform, gradually disappearing as the steep southwest-facing depositional end of the spit is approached (profiles 6 and 7). Gravel does not bypass this zone; however, sand is transported on the beach and on the low tide terrace further into Icy Bay to form the bulbous recurved end of the spit. The most rapid rates of accretion are observed at this location. The Riou Spit beach profiles (Fig. 46) show an

interesting relationship to the offshore bathymetry. The spit neck beach profiles (RS-3, RS-3-A) are short and rather steep compared to the near-shore fathometer profiles (nos. 1 and 2), indicating that sediment is bypassing the beaches on the nearshore bar system. Further west, at the curved portion of the spit, the beach profiles are long with well developed berms and washover terraces (RS-1 and RS-2), whereas the adjoining nearshore zone is very steep (fathometer profiles no. 5, 6, and 7). This suggests the westward building of a subaqueous gravel platform overlain by sandy beach face and berm deposits.

The RS-3 and RS-3-A beach profiles document the effects of the erosional wave conditions at the Riou Spit neck on July 25th and 26th. Erosion at RS-3 had eliminated the high berm and initiated a new ridge-and-runnel system at the lower beach face (Fig. 46). Figure 47 illustrates the typical beach morphology at RS-3-A.

Special Studies

In addition to the regional process network and time-series measurements at specific zonal sites, special studies were made in areas of unique character. Special studies at Point Riou and Alder Stream on the Malaspina Foreland (Fig. 28) and at Chirp Island in Icy Bay are reported below.

Alder Stream, AS-1--Measurements of littoral process parameters at hourly intervals during daylight from 1300 hours on July 27 through 2200 hours on July 28 are shown in Figure 48. The most interesting aspect of the process variability at Alder Stream is the interference of two apparent incoming wave trains. On July 27th many waves were striking the beach at low angles either to the east or west, causing a rather confused picture of longshore currents (Fig. 48). A large percentage of the waves arrived

Figure 43. Location map of fathometer profiles in the eastern part of Icy Bay. Profiles off Riou Spit, discussed in the text, are numbered 1 through 7 towards the west. The other profiles will be discussed elsewhere.

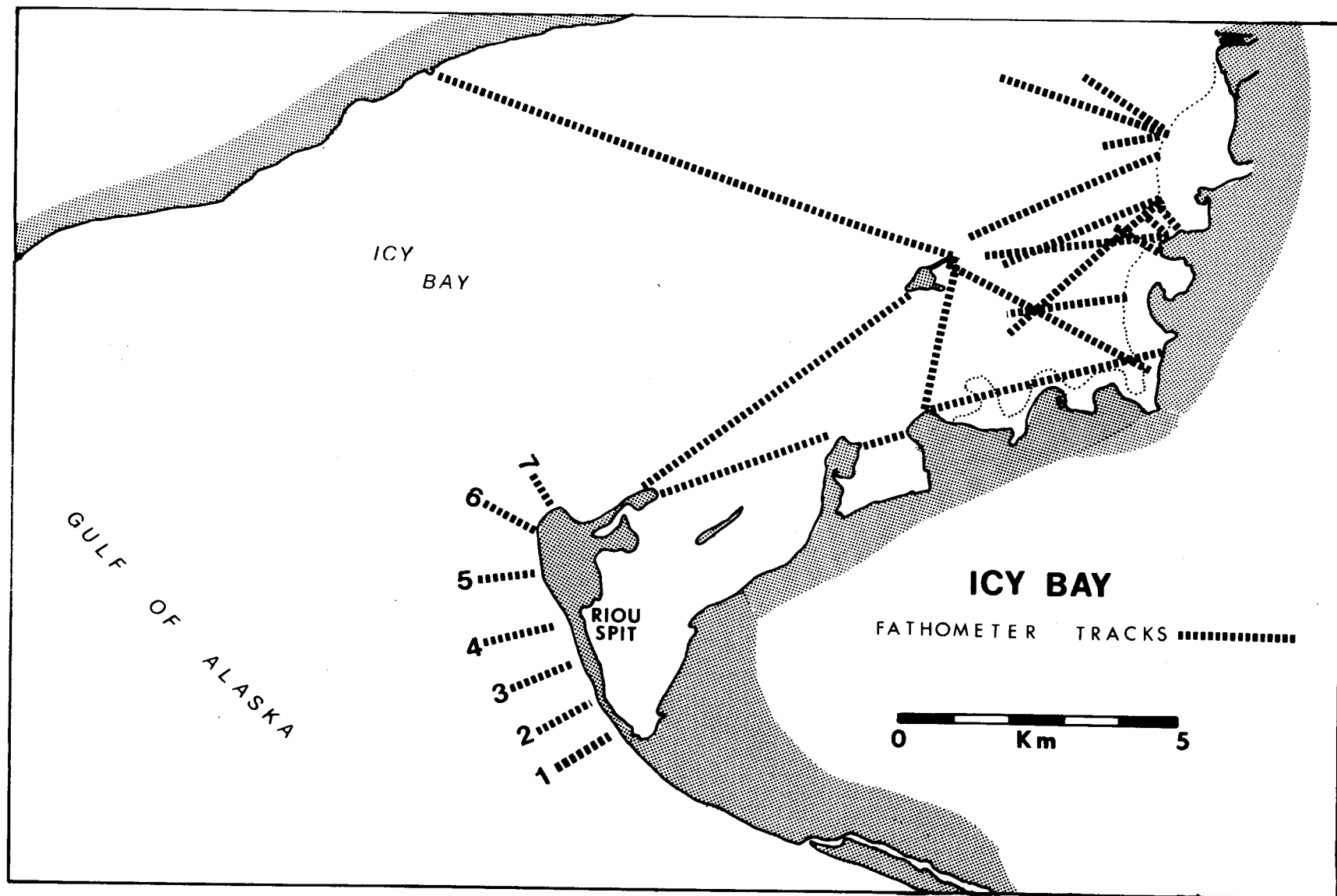


Figure 44. Nearshore fathometer profiles, Riou Spit, Alaska. The location of the profiles, numbered in the upper left corner of each diagram, is shown in Figure 43. The numbers in the lower left corner of each diagram refer to the adjacent beach profiles shown in Figure 46. Note the well developed offshore bar at the spit neck and the rapid increase in nearshore slope towards the west. The one meter oscillations in the traces are largely due to surface waves.

NEARSHORE FATHOMETER PROFILES, RIOU SPIT, ALASKA

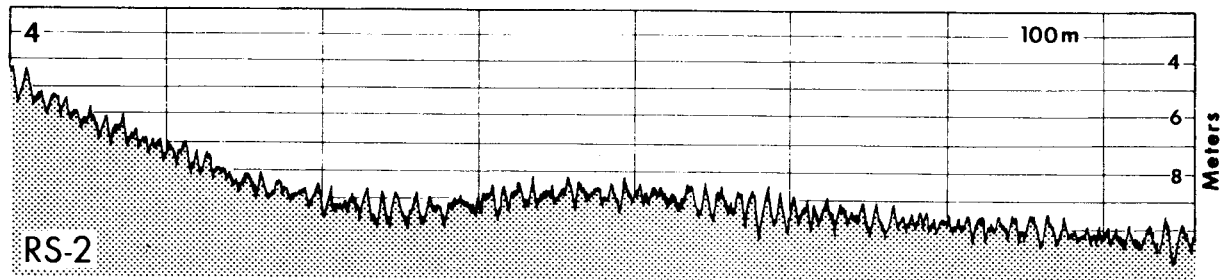
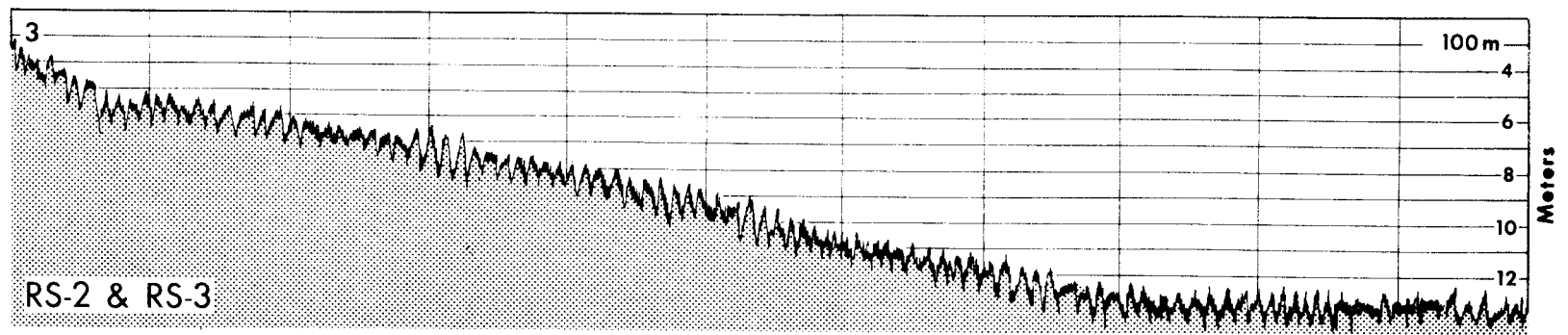
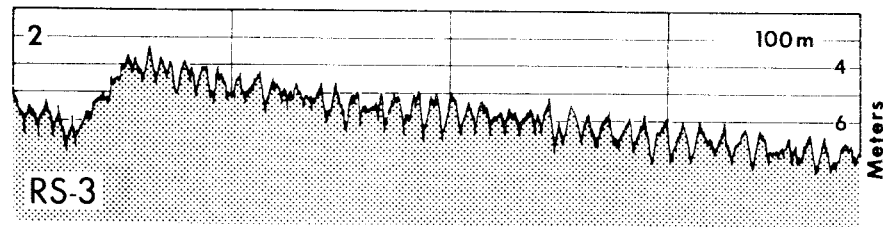
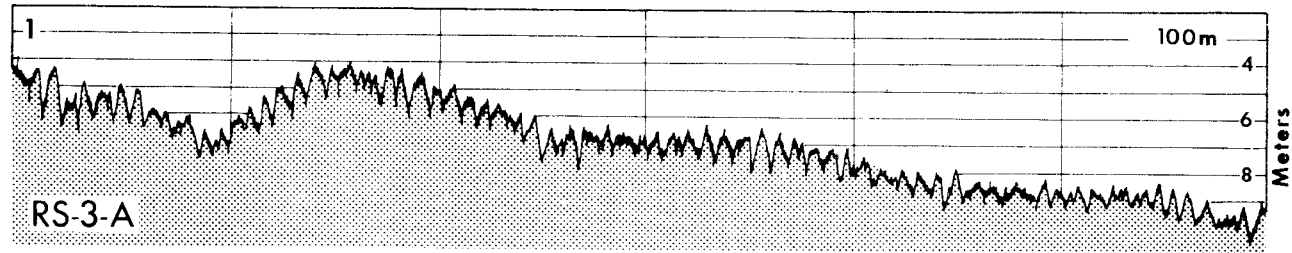


Figure 45. Nearshore fathometer profiles, Riou Spit, Alaska. The location of the profiles (numbered in upper left corner of each diagram) is shown in Figure 43. The numbers in the lower left corner of each diagram refer to the adjoining beach profiles, presented in Figure 46.

A well developed subaqueous platform is present at profile 5. Further west, at the depositional end of the spit, the nearshore slope is extremely steep (profiles 6 and 7).

NEARSHORE FATHOMETER PROFILES, RIOU SPIT, ALASKA

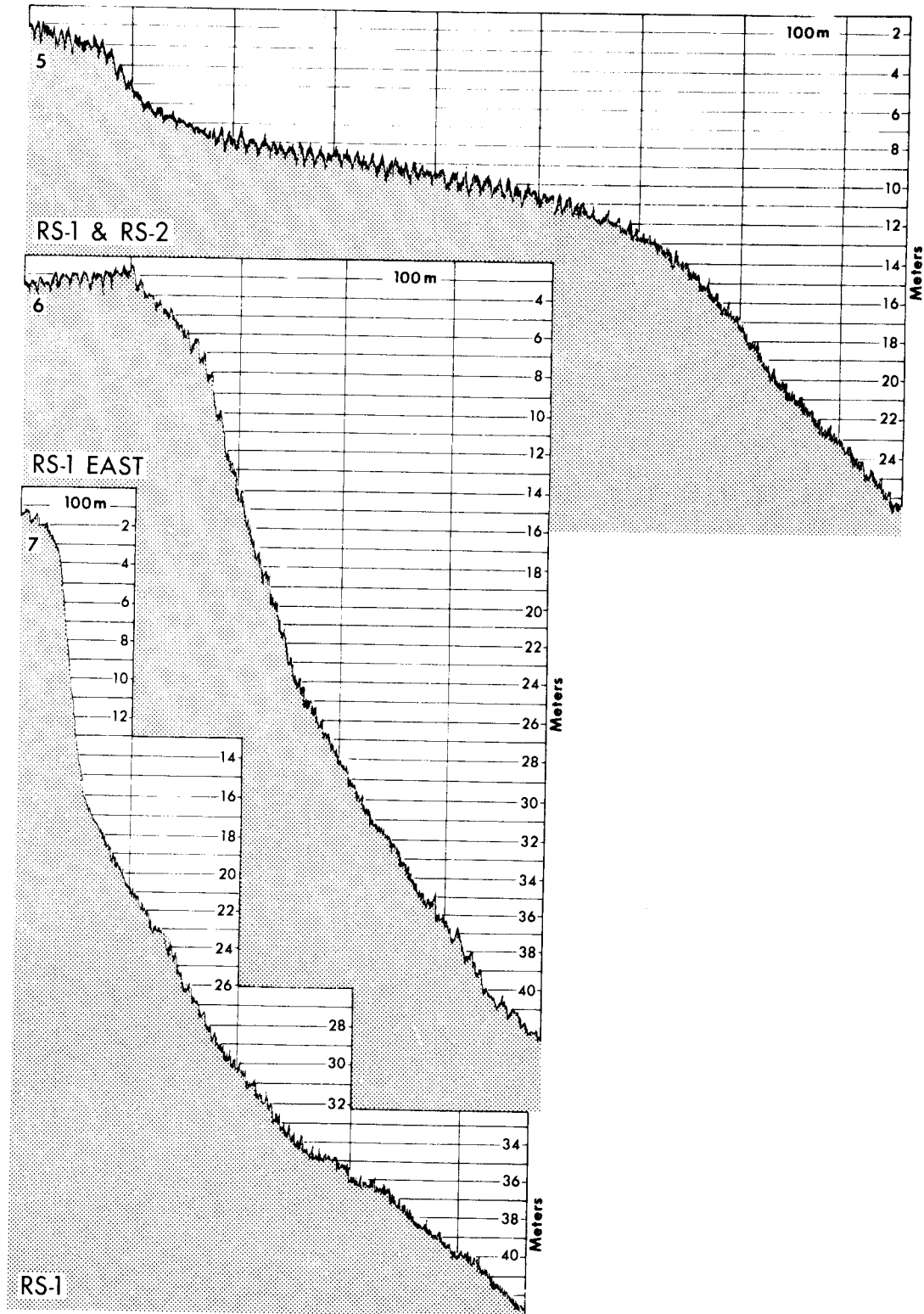
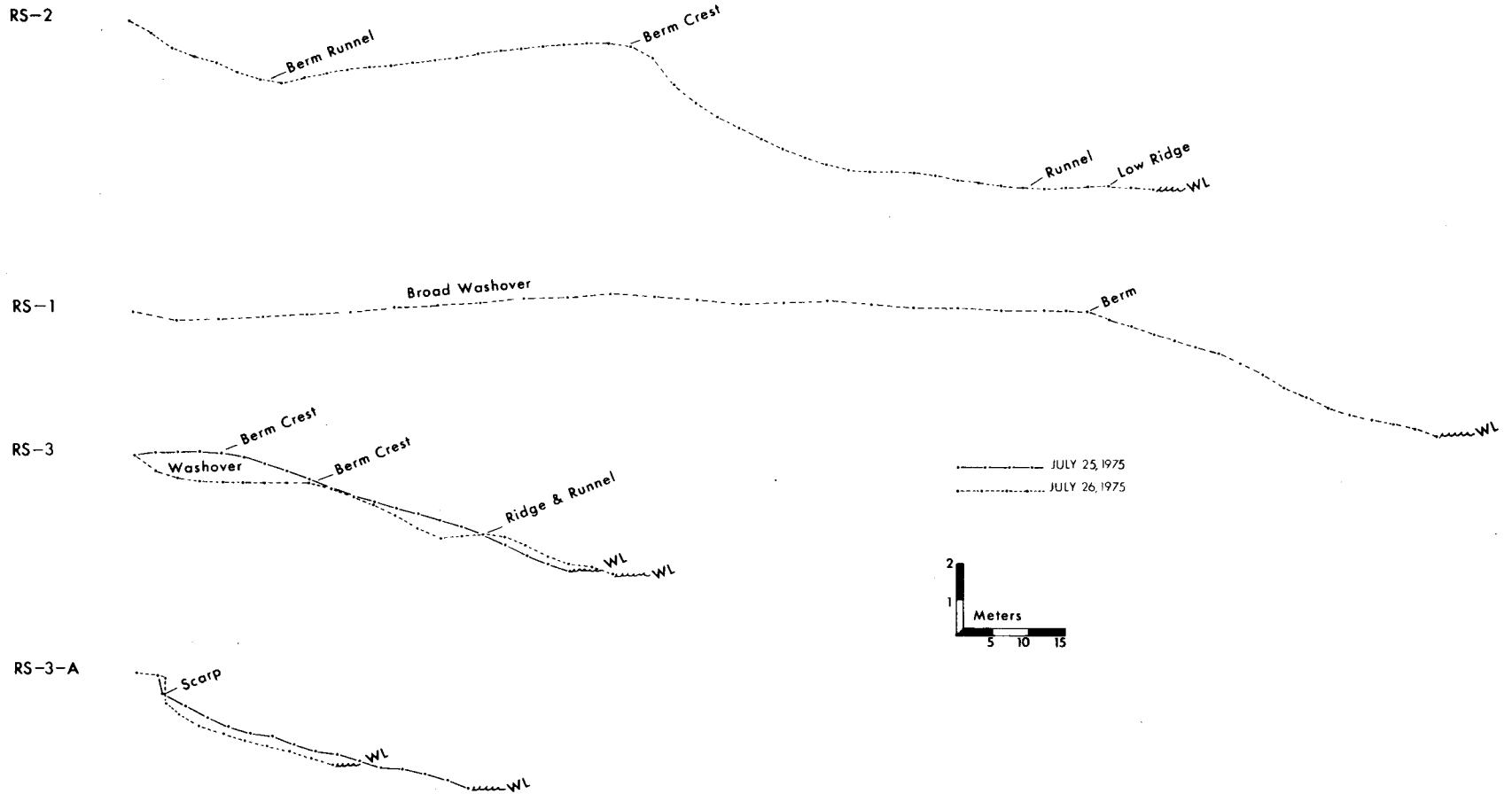


Figure 46. Riou Spit beach profiles, measured on July 25 and 26, 1975. Profile locations are shown on the oblique air photo of Figure 42. The long depositional profiles at the west end of the spit (RS-1, RS-2) adjoin a steep nearshore zone. The short steep erosional profiles at the spit neck (RS-3, RS-3-A) adjoin a gentle nearshore zone with a major bar system.

CONSECUTIVE BEACH PROFILES, RS PROCESS ZONALS



349

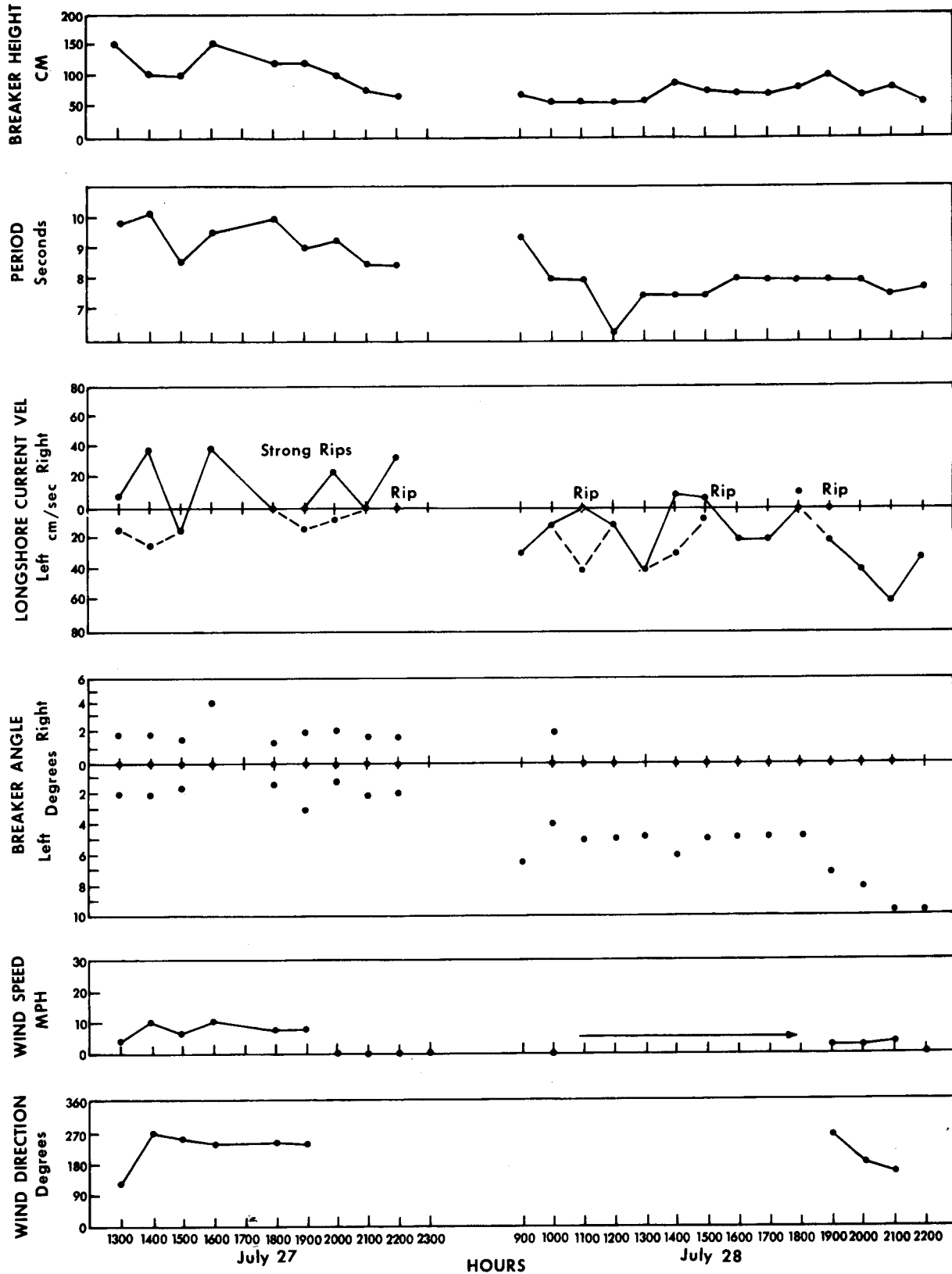
Figure 47. View towards the east at RS-3-A on Riou Spit. Photo was taken on July 26 after three-meter storm waves struck the beach. Note large scarp along the upper beach face. Small storms such as the one documented by the RS process zonal cause severe erosion at Point Riou and at the eastern neck of Riou Spit.

351



Figure 48. Littoral process variables measured at the Alder Stream shoreline (Fig. 28) on July 27 and 28, 1975. The longshore current picture is very confused because of the interference of two apparent wave trains causing alternating westward (right) and eastward (left) oriented energy flux components. Waves arriving straight onto the beach cause strong rip currents.

PROCESS VARIABLES, AS-1, JULY 27-28, 1975



straight onto the beach, producing strong rip currents, especially towards the evening that day.

In calm weather on July 28th, the waves out of the southwest became dominant, causing more consistent longshore currents towards the east (left). About 50 per cent of the waves still arrived straight onto the beach, maintaining a series of rip currents.

These measurements corroborate evidence presented elsewhere in this report, which indicates the frequent occurrence of transport reversals on the Alder Stream shoreline. However, the net transport is directed to the east.

Chirp Island--Several littoral process observations were made at Chirp Island on July 24, 1975. The observations serve to illustrate the low wave energies in the eastern part of Icy Bay (see Figs. 4 and 28 for location) and explain the curious morphology of the island. The results are presented in Table 6; station locations are indicated on Figure 49.

Riou Spit shelters Chirp Island from ocean waves arriving directly from any direction east of southwest. To reach Chirp Island, most oceanic waves have to be significantly refracted in Icy Bay. In addition, all oceanic waves suffer significant energy losses in traversing the submerged moraines at the Icy Bay entrance. Waves causing two to three meter breakers at the exposed beaches on the Malaspina Foreland typically form 50 cm breakers at Chirp Island.

Of great importance inside Icy Bay are the orographic winds which drain into the bay from glaciers in the St. Elias Range. These winds blew consistently at speeds of 10 to 20 miles per hour in late July and August. Local bush pilots indicate that these northerly winds can reach velocities above 100 mph in winter (J. Wells, personal communication, 1975).

TABLE 6

Chirp Island Littoral Processes - July 24, 1975

| Station Number | Breaker Height (cm) | Breaker Angle (degrees) | Wind Speed (mph) | Wind Direction | Littoral Current Velocity (cm/sec) |
|----------------|---|-------------------------|------------------|----------------|------------------------------------|
| 1 | 28 | 0-8 | 10 | NNE | 7 |
| 2 | 28 | 20 | 7 | NNE | 14 |
| 3 | 15 | 30 | 6 | NNE | 0 |
| 4 | 60 | 30 | calm | -- | 10 |
| 5 | 40 | 50 | 7 | NNE | 16 |
| 6 | 10 | 8 | 10 | NNE | 0 |
| 7 | (CI-2) At this station 30 cm chop approached from two directions, causing no resultant longshore current. | | | | |

*Observations were made at various locations along the sinuous western side of the island, thus resulting in the large variation in breaker angle. All wave angles opened to the south.

Figure 49. Morphological sketch map of Chirp Island, Icy Bay. The island is composed of a till and a kame high connected by wave-built spits. The orientation of the spits, the fining sediment trends and the "comet tail" spits at C all demonstrate that waves from the north and northwest control the development of the island.

Sketch Of Chirp Island Morphology

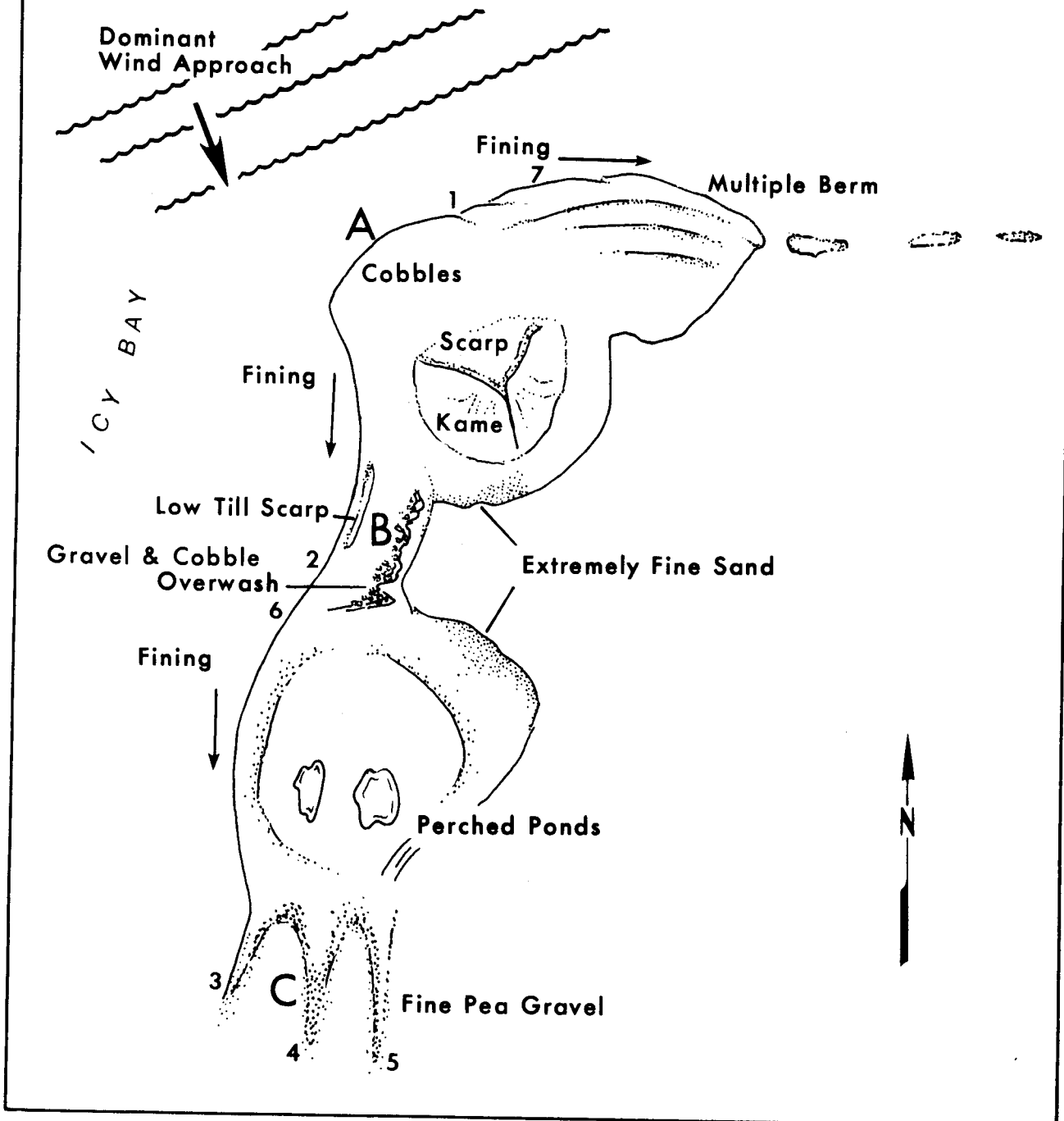
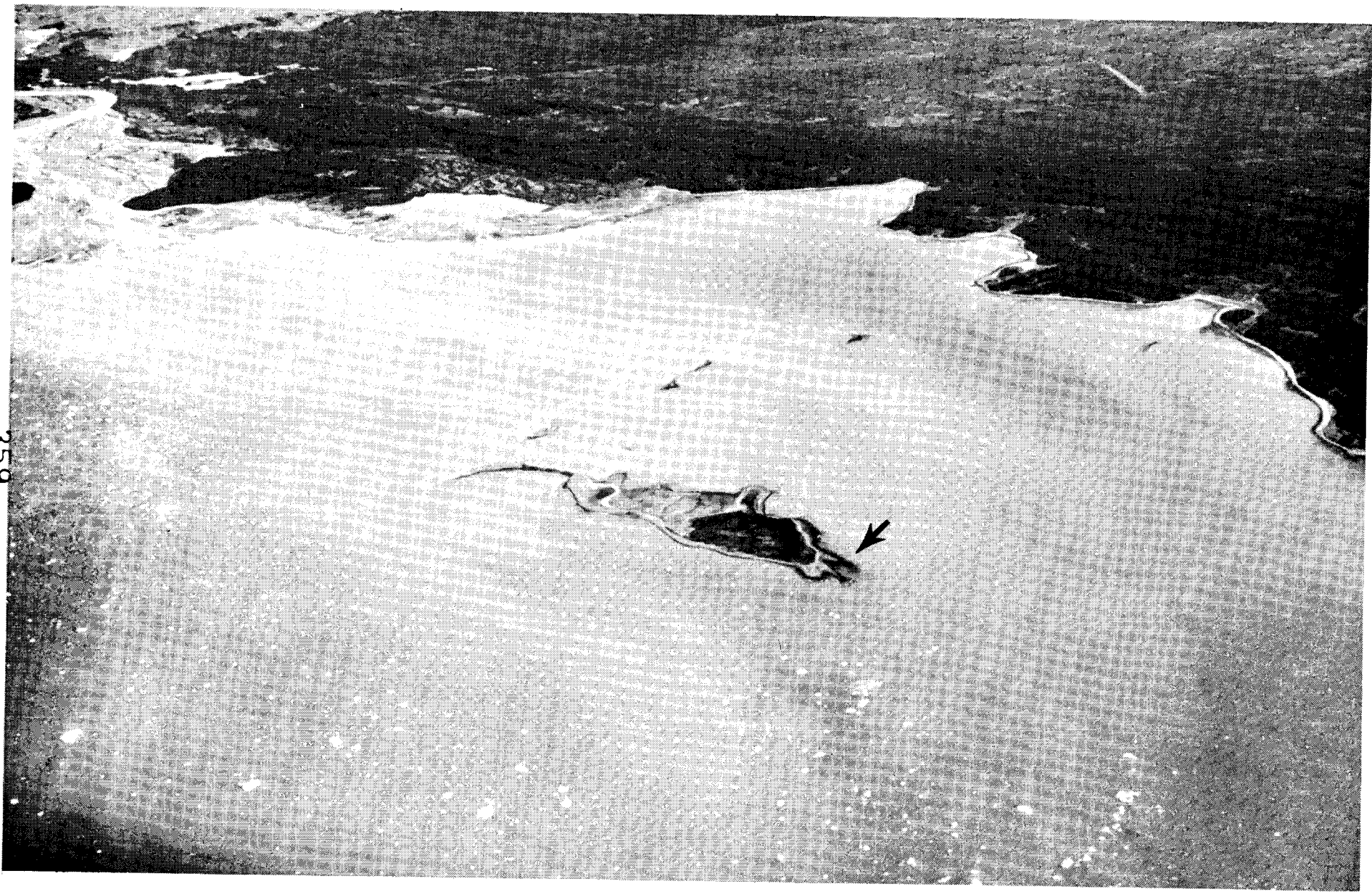


Figure 50. Oblique aerial view of Chirp Island and the east side of Icy Bay. The photo was taken from 8000 feet on August 4, 1975. Note the "comet tails" at the south end of the island (dark arrow). The active deltas of the New Yahtse River are visible in the upper left.

359



The local waves generated by the orographic winds inside Icy Bay seem to exert the dominant influence on Chirp Island morphology. The morphologic map (Fig. 49) and oblique air photo (Fig. 50) show Chirp Island to be composed of a kame and a till high, connected by wave-built spits. Bay waves from the north and northwest move sediment along the shores of Chirp Island away from point A (Fig. 49), forming the recurved spit to the east and the gravel ridge (B) which connects the two topographic highs. This picture is supported by fining sediment trends in both directions away from A. The tri-pronged spit at the southern end of Chirp Island (C) is what King (1972) defines as a "comet tail" spit. These prongs are oriented parallel to the direction of sediment transport responsible for their formation.

The total morphology of Chirp Island demonstrates that waves from the north or northwest control its morphologic development.

Point Riou--A few process observations were made on July 26th at Point Riou at the western margin of the Malaspina Foreland (Figs. 5 and 28). Wave heights of 1.8 to 2 meters were observed at high tide.

The beach at Point Riou is a flat eroded basal till backed by till, sand and clay cliffs up to 30 feet in height (Fig. 51). At high tide, incoming waves strike the base of the cliff. The force exerted by the waves makes the cliffs vibrate during storms.

During the storm of July 24th to 26th, these cliffs were severely eroded. Large mats of fresh sod which hang over the edge of the cliffs (Fig. 51) documented up to 5 feet of cliff retreat as a result of this single storm. Once released from the bluffs, the sediments are eroded by strong currents generated by wave reflection at the cliff face (Fig. 52).

Most of the finer materials are transported directly offshore. The coarse sediments are moved westward along the bar system towards Riou Spit.

The dominant process along Point Riou is sediment bypassing. Because most of the wave energy is reflected, well developed beaches do not occur. The sand is kept in continuous motion on the nearshore bar system.

Summary of Process Variability

Icy Cape and Claybluff Point--Process network measurements indicate that for south and southeasterly deep water waves the largest breakers occur at Icy Cape and Riou Spit. The lowest breakers along the exposed shoreline occur at Manby Point. This pattern correlates well with the predicted wave height distribution (Fig. 25). Longshore currents frequently reverse at Icy Cape, creating a nodal point for sediment transportation. Between Icy Cape and Cape Yakataga, longshore currents and sediment transport are oriented westward (Fig. 53). From Icy Cape to Claybluff Point, longshore currents and sediment transport are directed to the east. Summer field observations indicate that the western side of Icy Bay is dominated by high-angle plunging waves. The beaches at Claybluff Point are also affected by icebergs which are blown out of the inner bay by strong northerly orographic winds.

Chirp Island and Icy Bay--The eastern side of Icy Bay is well sheltered from oceanic waves, leaving the control of Chirp Island morphology to waves of local bay origin. Process observations document that Chirp Island is in a low energy environment compared to the exposed Malaspina Foreland shoreline.

Western Malaspina Foreland--Zonal studies at Old Yahtse Stream demonstrate the occurrence of spilling waves and well developed ridge-and-runnel systems along the western margin of the Malaspina Foreland. Longshore

Figure 51. Till and sand cliffs at Point Riou are exposed to direct wave attack at high tide. During storms large volumes of material are eroded from the cliffs. During the storm of July 24 through 26, three-meter waves eroded up to five feet of the cliff. The large mats of fresh sod and fallen trees are indicative of the rapid rate of cliff retreat.

363



Figure 52. Wave reflection at Point Riou. At high tide, large waves break directly on the till cliffs at Point Riou, thereby reflecting seaward as shown in this picture. Strong currents result and sediments are carried offshore and along shore in the well-developed bar system along this section of coastline.

365

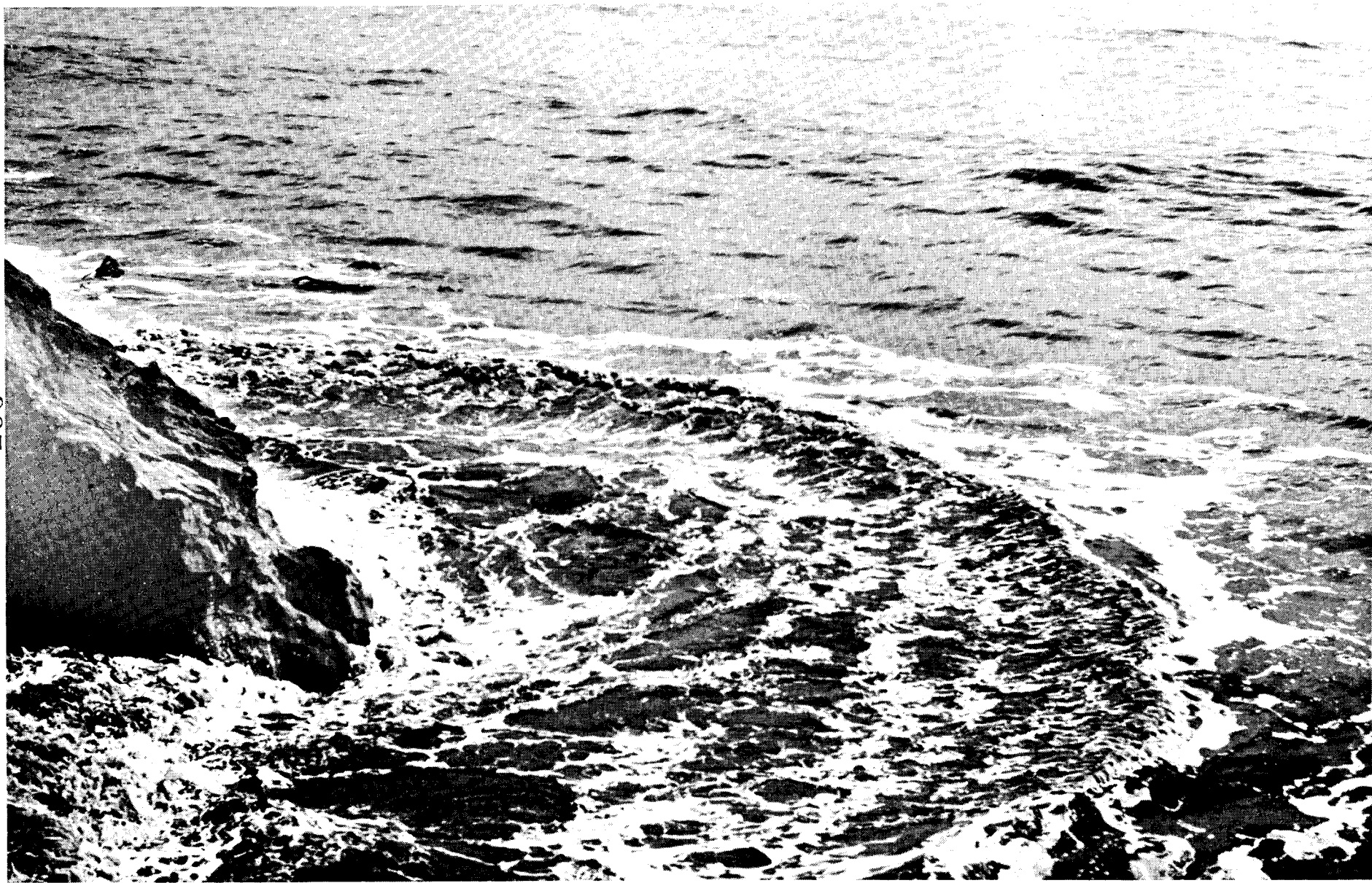


Figure 53. The figure summarizes the sediment transport directions along the shoreline of the northeast Gulf of Alaska from Yakutat Bay to Cape Yakataga. Information is derived from observations of local coastal morphology, longshore current directions, transport patterns on storm generated features like high berms and washover terraces and computations of longshore energy flux directions.

367



- Transport direction inferred from morphology
- Observed longshore current directions
- Transport direction computed from SSMO data
- Storm transport direction- observed

current directions are variable; however, net sediment transport is towards the west (Fig. 53). Till and sand bluffs at Point Riou provide sediment which moves down the beaches of Riou Spit. Fathometer profiles show the existence of a well developed bar 150 m offshore along Point Riou and most of Riou Spit. Towards the west the bar gradually comes to within 50 m of the beach and then disappears as a topographic entity. Beach profiles indicate that sediment is bypassing Riou Point and the eastern narrow neck of Riou Spit. The sediments are then deposited as they move west to the recurved end of the spit.

Process zonal observations at Riou Spit document the rapid increase in wave height which occurs during storm approach. Wave angles up to 30 degrees, wave heights of 380 cm, and longshore currents up to 200 cm/sec were observed.

Eastern Malaspina Foreland--Longshore current directions along the eastern Malaspina Foreland in the vicinity of Alder Stream are highly variable. A combination of criteria indicate a long-term net transport to the east with frequent reversals during major storms (Fig. 53). Rip currents were observed during a storm because of the perpendicular wave approach.

On the western side of Yakutat Bay, a process zonal between Manby Point and Grand Wash Stream showed the predominance of high angle plunging breakers which produced eastward directed longshore currents and net sediment transportation.

CONCLUSIONS

1. The Gulf of Alaska is found to be one of the highest wave energy environments in the world. Winter cyclones generally migrate into the

central Gulf from Pacific polar and arctic fronts to the west. Because of the temperature-induced pressure barrier along the Alaska and St. Elias Ranges cyclones generally remain within the Gulf till their energy is dissipated. This weather situation generates strong winds from the southeast and east along the northeast Gulf coast. Few significant cyclones travel into the Gulf during the summer, as the weather situation at that time is influenced by the North Pacific high.

2. Ship wave and weather observations presented in SSMO tables were used to determine the annual wave energy flux distribution within the coastal zone of the Gulf of Alaska. Resultant energy flux vectors point to the north and northwest between Vancouver and Cordova, and to the east and northeast between Unimak and Prince William Sound. This pattern correlates well with long-term sediment transport directions determined from coastal geomorphic features like spits, headland or inlet offsets, and crescentic bays.

3. Observed process variability and wave height distribution predicted from refraction diagrams on the continental shelf indicate that waves from the south and southeast are high near Cape Suckling, maintain the deep water wave height along the Bering Foreland, decrease between Cape Yakataga and Icy Point, increase again at Icy Point and at the entrance to Icy Bay, are high along the west Malaspina Foreland, and drop off dramatically into Yakutat Bay.

4. Longshore currents and sediment transportation show the following pattern of variation: a net flux to the west between Cape Yakataga and Icy Cape, a nodal point at the Cape, eastward net flux along the bay shore past Claybluff Point, a westward net flux on the west Malaspina Foreland

and Riou Spit, a nodal zone immediately east of Sitkagi Bluffs, and net flux towards the east into Yakutat Bay.

5. The annual average gross longshore sediment transport rate, computed from ship wave observations and shelf refraction diagrams, was found to be about 6.5 million cubic meters. The annual net sediment flux ranges from about 5.8 million cubic meters to the west, between Cape Yakataga and Icy Cape, to about 170,000 cubic meters to the east, between Sitkagi Bluffs and the western shores of Yakutat Bay.

Short-term transport rates computed from littoral process parameters observed in the summer of 1975 show a range in good agreement with the annual rates.

REFERENCES CITED

- Alaska Regional Profiles, Southcentral Region, 1975, L. L. Selkregg (Coordinator), The University of Alaska, 255 p.
- Brown, P. J., 1975, Coastal morphology of South Carolina: M. Sc. Thesis, University of South Carolina, Columbia, 122 p.
- Coastal Engineering Research Center, 1973, Shore Protection Manual, 3 vols.: U. S. Government Printing Office, Washington, D. C.
- Davies, J. L., 1973, Geographical variation in coastal development: Hafner Publ. Co., New York, 204 p.
- Eagleson, P. S., and R. G. Dean, 1966, Small amplitude wave theory: in A. T. Ippen (ed.), Estuary and Coastline Hydrodynamics, p. 1-92, McGraw-Hill Co., New York.
- Hayes, M. O., E. H. Owens, D. K. Hubbard and R. W. Abele, 1973, The investigation of form and processes in the coastal zone: in D. R. Coates (ed.), Coastal Geomorphology, P. 11-41, SUNY Binghamton, New York.
- King, C. A. M., 1972, Beaches and Coasts: St. Martin's Press, New York, 570 p.
- Molnia, B. F., and P. R. Carlson, 1975, Base map of the northern Gulf of Alaska: U. S. Geol. Survey, Open File map 75-506.
- National Oceanic and Atmospheric Administration, Northern Hemisphere synoptic surface charts: National Climatic Center, Asheville, North Carolina.
- Nummedal, D., 1975, Wave climate and littoral sediment transportation on the southeast coast of Iceland: Proc. 9th International Congress on Sedimentology, Nice, France.
- Petterssen, S., 1969, Introduction to meteorology: McGraw-Hill Book Co., New York, 333 p.
- Silvester, R., 1974, Coastal Engineering, II: Elsevier Publ. Co., Amsterdam, 338 p.
- U. S. Naval Weather Service Command, 1970, Summary of synoptic meteorological observations, North American coastal marine areas: National Climatic Center, Asheville, North Carolina.
- U. S. Naval Weather Service Command, Surface marine environmental data survey charts: National Climatic Center, Asheville, North Carolina (no date).
- Walton, T. L., Jr., 1973, Littoral drift computations along the coast of Florida by means of ship wave observations: Coastal and Oceanographic Engineering Laboratory, Univ. of Florida, Tech. Rept. no. 15, 96 p. + figures.

Wiegel, R. L., 1964, Oceanographical engineering: Prentice-Hall, Inc.,
Englewood Cliffs, N. J., 532 p.

ANNUAL REPORT

Contract # 03-5-022-56

Research Unit # 99

Reporting Period 4/1/75-3/31/76

Number of Pages 12

THE ENVIRONMENTAL GEOLOGY AND GEOMORPHOLOGY
OF THE GULF OF ALASKA COASTAL PLAIN

Dr. P. JAN CANNON
Department of Geology
University of Alaska

March 31, 1976

ANNUAL REPORT FOR YEAR ENDING MARCH 31, 1976

Project Title: The Environmental Geology and Geomorphology
of the Gulf of Alaska Coastal Plain

Contract Number: 03-5-022-56

Task Order Number: 6

Principal Investigator: Dr. P. Jan Cannon

I. Task Objectives

- A. To produce three maps of the coastal plain section of the Gulf of Alaska
- B. To produce a report on the application of radar imagery to the environmental geologic mapping of coastal zones
- C. To construct an annotated mosaic of the area from radar imagery.
- D. To indicate the effects (beneficial and adverse) that oil and gas development might have in relation to the geologic setting.

II. Introduction

- A. To produce information which can be used in an environmental assessment of the coastal plain section of the Gulf of Alaska, in relation to possible oil and gas development. To evaluate radar imagery as a major information source for environmental geological mapping.
- B. The following are the objectives of this research:
 1. To produce three maps, with explanations, which will display certain baseline data necessary for an environmental assessment of the coastal plain section of the Gulf of Alaska. The maps will be produced at a scale of 1:250,000. (See Map 1, Map 2, and Map 3 below).

Map 1. Environmental Geologic Hazards and Shoreline Stability

This map will indicate the extent of possible environmental geologic hazards such as storm flooding, seismic sea waves, landslides, ice falls, and outburst flooding. This map will also indicate the relative stability of the shoreline as determined by quantitative data from other projects and landform analysis.

Map 2. Major Coastal Plain Landforms

This map will locate, identify, and describe the various coastal landforms. The explanation will indicate the origin of the particular landform types, the possible lifetime or stability of each particular landform type, and the economic importance of each landform type.

Map 3. Major Beach Materials

This map will indicate the distribution of beach materials that will be important in an environmental assessment of the coastal zone.

2. To produce a report on the application of side-looking airborne radar (SLAR) imagery to the environmental geologic mapping of coastal zones. This report will also contain a comparison of SLAR imagery with aerial photography and satellite imagery. (See Report below.)

Report. Application of Radar Imagery (SLAR) to the Environmental Geologic Mapping of Coastal Zones

This report will demonstrate the capabilities of radar imagery in environmental geologic and geomorphic mapping of coastal zones, and will evaluate other available remote sensing data for their potential to coastal zone mapping.

3. To construct an annotated mosaic of the area from SLAR imagery. The scale of this annotated mosaic is yet to be determined. (See Mosaic below.)

Mosaic. Annotated SLAR Mosaic of Coastal Zone

This annotated mosaic constructed from the radar imagery (SLAR) will be used to present an explanation of the unique view provided by the radar imagery.

- C. The information displayed on the maps will indicate the potential effects of natural hazards in relation to oil and gas development.

III. Current State of Knowledge

The coastal plain of the Gulf of Alaska is a narrow strip of land which is bordered along its upper margin with some of the highest mountains on the North American continent and large glaciers. The area is usually overcast and cold. Obtaining aerial photographs of this area is almost impossible. Due to the geographic location of the Gulf of Alaska on the Earth and the fact that two ranges of the highest mountains on the North American continent lie just to the north of the Gulf of Alaska, the area has a climate that is unusually warm for its latitude. However, this relative warmth is offset by the situation that the same factors that make temperatures warmer also help produce high amounts of precipitation (average 302 cm per year), almost continual overcast conditions, and an impact zone for some of the worst storms created on the entire planet.

IV. Study Area

The coastal plain of the Gulf of Alaska is a narrow strip of land (1 to 40 km wide) which extends some 600 km from Icy Point to the western margin of the Copper River Delta. The upper or inland margin is bordered with the high mountains of the Chugach, St. Elias, and Fairweather Ranges, which extend in elevation from 3,650 to 5,800 metres.

The coastal plain has been described as having a diversified topography carved in Tertiary rocks. The assemblage of landforms in the area is indeed quite diverse which is unlike most coastal plains on this planet. However, this diversity is valuable in constructing a chronology of the geomorphic events which have occurred in the area. The coastal plain is crossed in several places by fiords and active glaciers. The assemblage of landforms includes: morainal belts, dead ice moraines, thermokarst pits, outwash plains, meltwater streams, marine terraces, abandoned beach ridges, active dune fields, blowouts, large tidal flats in shallow bays, and the associated longshore features of bars, spits, and backwater lagoons. The materials of the coastal plain consist of till, gravels, sand, mud, ice, and various mixtures of these materials.

The portion of the coastal plain which will be the most involved with petroleum development is a section 255 km long, from Dry Bay westward to Cape Yakataga. This section, therefore, was the subject of an intense environmental geologic investigation as a part of the overall environmental assessment. The most up-to-date data was needed of the area during the ice-free part of the year. Because the area is usually overcast, obtaining aerial photography of the area is almost impossible. Since radar imagery can be obtained nearly anytime a fully instrumented aircraft can fly, radar imagery was chosen as the principle data source. Therefore, X-band, real aperture radar imagery was obtained of the area at scales of 1:250,000 and 1:500,000.

V. Sources, Methods and Rationale of Data Collection

The following lists sequentially the methods planned to produce each of the products:

Map 1. Environmental Geologic Hazards and Shoreline Stability

1. Evaluate existing literature and correspond with on-going projects in the area.
2. Search for and interpret any existing raw data on erosion and deposition.
3. Comparison of sequential mapping of coastal areas.
4. Identification of major shoreline processes.
5. Evaluation of historical records.
6. Identification of the materials which comprise the shoreline features.
7. Interpretation of the origin or source(s) of the beach materials.
8. Comparison of sequential ERTS imagery.
9. Field observations and measurements of shoreline changes from previous and current studies.
10. Interpretation of the shoreline morphostratigraphy.

Map 2. Major Coastal Plain Landforms

This map will locate, identify, and describe the various coastal landforms. The explanation will indicate the origin of the particular landform types, the possible lifetime or stability of each particular landform type, and the economic importance of each landform type. The explanation will also relate the general wildlife habitat to each particular type of major landform. The information to be displayed on this map will be gathered by the following methods:

1. Use of existing maps.
2. Use of existing aerial photographs.
3. Interpretation of acquired high-altitude aerial photographs (approximately 62,500 feet AGL).

4. Interpretation of acquired side-looking airborne radar imagery (SLAR).
5. Ground reconnaissance of difficult areas.

Map 3. Major Beach Materials

This map will indicate the distribution of beach materials of a certain nature that will be important in an environmental assessment of the Gulf of Alaska coastal zone. This map will indicate the general nature of the beach materials which is related to the information presented in the other two maps. The nature of the beach materials has an extremely important economic value. The information of this map will be obtained by the following methods:

1. Communication with other projects being performed in the area.
2. Photogeologic interpretations.
3. Interpretation of side-looking airborne radar imagery (SLAR).
4. Ground sampling.

VI. Results

- A. Activities such as highway construction and railroad construction would have a net effect that would be beneficial to the Yakutat district (see Discussion below).
- B. Activities such as pipeline construction in the area would not be recommended because of the numerous active faults (lineaments) which cross the area (see Discussion below).
- C. The Malaspina Glacier is retreating (see Discussion below).
- D. The heavy erosion of the headlands along the beach of the Yakataga district is due to natural processes (see Discussion below).
- E. Clear-cut logging of a part of the Yakataga district might have a net result which would be beneficial to the Yakataga district (see Discussion below).
- F. Radar imagery is an excellent tool to use in environmental geologic evaluations (see Discussion and Conclusions below).
- G. Information about radar imagery and coastal studies was collected (see Table 1).

VII. Discussion

Radar imagery was obtained of the Gulf of Alaska coastal plain at the scales of 1:500,000 and 1:250,000. The area was covered with one strip of imagery at the scale of 1:500,000, and with four overlapping strips of imagery at the scale of 1:250,000. The radar imagery was used as the most up-to-date data source and as a mapping base.

The area can be divided into three physiographic zones separated by large fiords: the Yakutat District, the Malaspina District, and the Yakataga District. The Yakutat district is comprised of the coastal plain that extends from Dry Bay and the Alsek River northwestward to Yakutat Bay. The natural environmental geologic units of the Yakutat district are comprised of moraines, outwash deposits, beach deposits, tidal flats, and sand dunes. Abandoned beaches, which make up a chenier plain between Dry Bay and the outwash deposits of Yakutat Glacier indicate that the Alsek River has been a major source of sediments. These sediments have been reworked by longshore processes to form a large portion of the coastal plain between Dry Bay and Phipps Peninsula on Yakutat Bay. This is extremely important environmentally. The flow of sediments from the Alsek River nourishes the coastal plain and maintains it in spite of the poundings by heavy storms. Activities which would reduce the sediment flow from the Alsek River, such as hydroelectric projects, should not be enacted. However, activities which maintain or increase the sediment flow from the Alsek River, such as road construction and mining, should be encouraged as long as there are little adverse effects to the marine life.

Several large lineaments were detected on the radar imagery that extend completely across the coastal plain of the Yakutat District (Fig. 1). These lineaments were discovered to be the traces of active faults which have been offset vertically as much as 2.5 meters within the last 80 years. The activity of these faults has been well documented (Tarr and Martin, 1912). An account of continuous and severe tectonic activity in the nearby Lituya Bay area over a period of 125 years (Miller, 1960) provides conclusive evidence as to the structural instability of the region. The construction of pipelines across the coastal plain should be avoided and the erection of tall buildings on the unconsolidated materials of the coastal plain would not be recommended.

Outburst floods could occur anytime in the area (Post and Mayo, 1971). The radar imagery reveals features that appear to be related to past outburst floods on the Dangerous, Tanis, and Alsek Rivers.

The Malaspina District consists of the Malaspina Glacier and the Malaspina forelands. The Malaspina Glacier is considered to be the largest piedmont glacier in the world, being greater in areal extent than the State of Rhode Island. The Malaspina forelands consist of dead-ice moraine and morainal materials that have been reworked by wave action and meltwater.

There have been some great changes in the last 30 years in the district. The glaciers have ceased to advance and a large lake of approximately 300 square km in area has formed in the southeast part of the district between the glacier's margin and the foreland. The foreland is also crossed with lineaments taken from radar and Landsat imagery.

The Malaspina District is separated on the east from the Yakutat District by the large fiord of Yakutat Bay. It is separated on the west from the Yakataga District by the fiord of Icy Bay. Less than seventy years ago Icy Bay was completely occupied with a large piedmont glacier (Tarr and Martin, 1912). This indicates that the ice front retreated approximately 42 km in less than 50 years.

The Yakataga District is a narrow strip of coastal plain cut by several meltwater streams. The Yakataga District does not exhibit a diverse number of environmental geologic units. It is important to note that in the Yakataga District natural processes are rapidly eroding the coastal plain. The headlands, where the most severe erosion is taking place, are readily discerned on the radar imagery. Based on sequential observations it appears that large portions of the coastal plain will erode away within the next 30 years. However, since this is the result of natural processes, and is not related to man's activities, it should probably not be interfered with. The headlands consist of two promontories, Icy Cape and Umbrella Reef. As the promontories are eroded back, the large trees which cover them fall into the sea. So as to not waste a natural resource it would be pertinent to lumber off a line of the trees with a rate equal to the retreat of the headlands. As the trees fall off the cliff their root systems tear away large chunks of the soil. Clearing off a line of trees might reduce the rate of erosion.

References Cited:

- Cannon, P. J., 1975, The application of radar imagery to specific problems of Interior Alaska: in NASA Earth Resources Survey Symposium, June, 1975, Proceedings, v. 1-B, p. 761-768.
- Miller, D. J., 1960, Giant waves in Lituya Bay, Alaska: U.S. Geol. Survey Prof. Paper 354-C, p. 51-86.
- Post, Austin, and Mayo, L. R., 1971, Glacier dammed lakes and outburst floods in Alaska: U.S. Geol. Survey Hydrologic Investigations Atlas HA-455, 10 p., 3 pl.
- Tarr, R. S., and Martin, Lawrence, 1912, Earthquakes at Yakutat Bay, Alaska, in September, 1899, with a preface by G. K. Gilbert: U.S. Geol. Survey Prof. Paper 64, pt. 1, p. 1-144.

VIII. Conclusions

Radar imagery is an adequate tool to use in the environmental evaluations of diverse types of coasts. There are three important factors to keep in mind when acquiring radar imagery of coasts. One, the look-direction should be towards the landward side of the coast away from the water. Two, the altitude of acquisition should be low in order to maximize the return of radar energy. Three, the depression angles should be small so that the important low relief features of coasts can be enhanced. The amount of information displayed on radar imagery is related to the wavelength of the radar energy used. Usually, the greatest amount of information can be obtained with the shorter wave-lengths. In mapping large regions, radar imagery would be less expensive than photographic coverage of the same area, and it would take less time to map from radar imagery than it would from low- or intermediate-altitude aerial photographs. Aerial photographs must be viewed stereoscopically in order to observe what can be seen with the unaided eye on radar imagery, hence the difference in map compilation time.

X-band, real aperture radar imagery of the Gulf of Alaska coastal plain is adequate both as a mapping base and as a source of important environmental geologic data. It is essential to an environmental assessment of an area that information be as current as possible. In some areas the most current data can be acquired only with the use of radar imagery. The radar imagery of the Gulf of Alaska coastal plain indicates that severe environmental geologic hazards, such as earthquakes, surface movements along active faults, and outburst floods, have occurred recently and will continue to occur with a relatively high frequency.

Analysis of the geomorphic features of the coastal plain indicates that the seaward portion of the Yakutat District is comprised of sediments from the Alsek River. The continued existence of the area depends upon a continual supply of sediments from the Alsek River.

Natural processes are modifying parts of the coastal plain at a relatively rapid rate. These processes include the formation of large lakes by glacial ablation and the erosion of headlands due to changes in the sediment supply from glaciers. It is necessary to emphasize that the changes are natural and not the result of man's activities. In an area like the Gulf of Alaska, radar imagery is the only tool which can be used to adequately monitor the results of natural processes.

IX. Need for Further Study

K- or X-band, real aperture, radar imagery should be acquired immediately of the areas in which this type of study is expected to be extended.

X. Summary of 4th Quarter Operations

- A. Continued interpretative analysis of the radar imagery.
- B. Began preparation of first draft of maps.
- C. Participated in OCSEAP Workshop in Seattle at the request of NOAA.
- D. Revised preliminary draft of report on the application of radar imagery to environmental geologic mapping of coastal zones.
- E. Attended workshop for prospective geological researchers on the Alaskan Coastal zone, in Columbia, South Carolina, at the University of South Carolina, under the approval of the Juneau Project Office.

Table 1. Comparison of radar wavelengths and the information pertinent to coastal studies which is displayed on radar imagery.

| Information Sources | K-Band* | X-Band* | L-Band† |
|----------------------|---------|------------|------------|
| Beach Materials | good | inadequate | inadequate |
| Landforms | good | good | inadequate |
| Land-Water Contact | good | good | marginal |
| Minor-Vegetation | good | marginal | inadequate |
| Major-Vegetation | good | good | inadequate |
| Ice Surface Features | good | good | marginal |
| Ice Structure | good | good | good |
| Cultural Features | good | good | inadequate |

*K- and X-band data from real aperture imagery
 †L-band data from synthetic aperture imagery

Note: For a visual comparison of real aperture imagery with synthetic aperture imagery, see Cannon, 1975, pages 764 through 766.

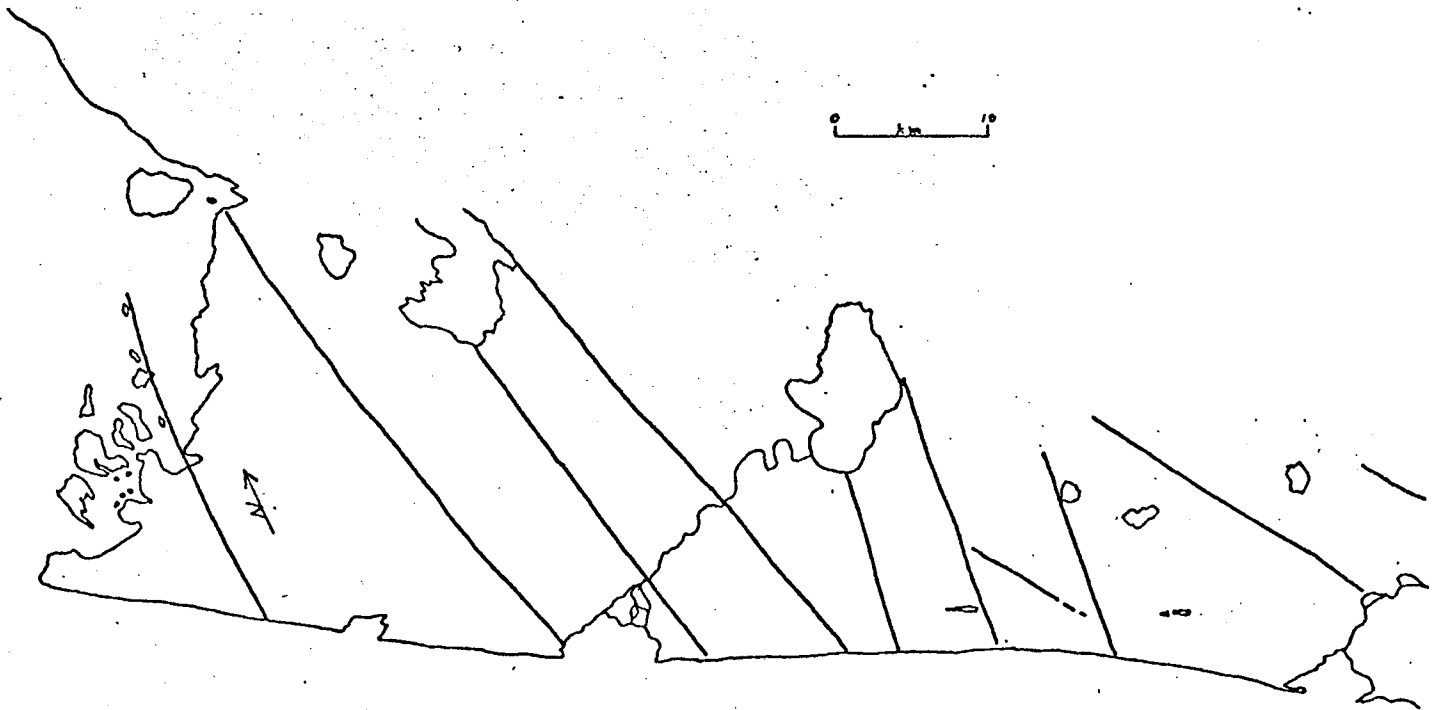


Fig. 1 A map showing the lineaments that cross a portion of the Yakutat district. The lineaments correspond with active faults.

OCS COORDINATION OFFICE

University of Alaska

ENVIRONMENTAL DATA SUBMISSION SCHEDULE

DATE: March 31, 1976

CONTRACT NUMBER: 03-5-022-56 T/O NUMBER: 6 R.U. NUMBER: 99

PRINCIPAL INVESTIGATOR: Dr. P. Jan Cannon

No environmental data are to be taken by this task order as indicated in the Data Management Plan. A schedule of submission is therefore not applicable¹.

NOTE: ¹ Data management plan was submitted to NOAA in draft form on October 9, 1975 and University of Alaska approval given on November 20, 1975. We await formal approval from NOAA.

OCS COORDINATION OFFICE

University of Alaska

ESTIMATE OF FUNDS EXPENDED

DATE: March 31, 1976
 CONTRACT NUMBER: 03-5-022-56
 TASK ORDER NUMBER: 6
 PRINCIPAL INVESTIGATOR: Dr. P. Jan Cannon

Period April 1, 1975 - March 31, 1976* (12 mos)

| | <u>Total Budget</u> | <u>Expended</u> | <u>Remaining</u> |
|------------------|---------------------|------------------|------------------|
| Salaries & Wages | 14,887.00 | 4,936.09 | 9,950.91 |
| Staff Benefits | 2,505.00 | 815.89 | 1,689.11 |
| Equipment | -0- | -0- | -0- |
| Travel | 2,560.00 | 1,488.66 | 1,071.34 |
| Other | <u>1,600.00</u> | <u>382.96</u> | <u>1,217.04</u> |
| Total Direct | <u>21,552.00</u> | <u>7,623.60</u> | <u>13,928.40</u> |
| Indirect | <u>8,515.00</u> | <u>2,823.44</u> | <u>5,691.56</u> |
| Task Order Total | <u>30,067.00</u> | <u>10,447.04</u> | <u>19,619.96</u> |

* Preliminary cost data, not yet fully processed.

Following is part 2 of the quarterly report R.U.# 99 for the period ending December 31, 1975. This was received after the printing of the Quarterly Reports, July - September 1975, therefore is included here.

RECEIVED

JAN 19 1976

OCS COORDINATION OFFICE

University of Alaska

NEGOA

Quarterly Report for Quarter Ending December 31, 1975

Project Title: The Environmental Geology and Geomorphology
of the Gulf of Alaska Coastal Plain

Contract Number: 03-5-022-56

Task Order Number: 6

Principal Investigator: Dr. P. Jan Cannon

Jan Cannon
RH 99

I. Task Objectives

- A. To produce three maps of the coastal plain section of the Gulf of Alaska
- B. To produce a report on the application of radar imagery to the environmental geologic mapping of coastal zones
- C. To construct an annotated mosaic of the area from radar imagery.

II. Activities

Made work copies of SLAR data and constructed a mosaic of the field area of radar imagery at a scale of 1:250,000. Began the interpretative analysis of the radar imagery and the field data. Produced a preliminary draft of report on the application of radar imagery to environmental geologic mapping of coastal zones. Attended a conference on geodesy and remote sensing of coastal areas in order to acquaint myself with the most recent work of other investigators of coastal problems. While at the conference, I presented a paper titled: "Environmental Evaluation of Coasts Using Radar Imagery"

III. Results

Compiled information about the optimum parameters and systems for coastal information from radar imagery. Constructed a table which shows a comparison of radar wave lengths and information displayed on radar imagery concerning coastal zone mapping. This information indicates that radar imagery is an adequate tool to use in the environmental geologic mapping of coasts, and there are three important factors to keep in mind when acquiring radar imagery of coasts. One, the look-direction should be toward the landward side of the coast away from the water. Two, the altitude of acquisition should be low ~~in order~~ to maximize the return of radar energy. Three, the depression angles should be small so that the important

low relief features of coasts can be enhanced. The amount of information displayed on radar imagery is related to the wave lengths. In mapping large regions, radar imagery would be less expensive than photographic coverage of the same area, and it would take less time to map from radar imagery than it would from low or intermediate-altitude aerial photographs. Aerial photographs must be viewed stereoscopically in order to observe what can be seen with the unaided eye on radar imagery hence the difference in map compilation time.

IV. Problems Encountered

Due to computer problems at the EROS data center the listing of LANDSAT scenes up to November, 1975 is not completed. The original scale of the SLAR data is smaller than anticipated which indicates that a final scale for the three maps would be best at 1:250,000. It appears that this scale change will not significantly alter the amount of information presented by the maps.

OCS COORDINATION OFFICE

University of Alaska

ENVIRONMENTAL DATA SUBMISSION SCHEDULE

DATE: December 31, 1975

CONTRACT NUMBER: 03-5-022-56 T/O NUMBER: 6 R.U. NUMBER: 99

PRINCIPAL INVESTIGATOR: Dr. P. Jan Cannon

No environmental data are to be taken by this task order as indicated in the Data Management Plan. A schedule of submission is therefore not applicable⁽¹⁾.

NOTE: (1) Data management plan was submitted to NOAA in draft form on October 9, 1975 and University of Alaska approval given on November 20, 1975. We await formal approval from NOAA.

OCS COORDINATION OFFICE

University of Alaska

ESTIMATE OF FUNDS EXPENDED

DATE: December 31, 1975
CONTRACT NUMBER: 03-5-022-56
TASK ORDER NUMBER: 6
PRINCIPAL INVESTIGATOR: Dr. P. Jan Cannon

Period April 1 - December 31, 1975* (9 mos)

| | <u>Total Budget</u> | <u>Expended</u> | <u>Remaining</u> |
|------------------|---------------------|-----------------|------------------|
| Salaries & Wages | 14,887.00 | 4,936.09 | 9,950.91 |
| Staff Benefits | 2,505.00 | 815.89 | 1,689.11 |
| Equipment | -0- | -0- | -0- |
| Travel | 2,560.00 | 332.06 | 2,227.94 |
| Other | <u>1,600.00</u> | <u>315.02</u> | <u>1,284.98</u> |
| Total Direct | 21,552.00 | 6,399.06 | 15,152.94 |
| Indirect | <u>8,515.00</u> | <u>2,823.44</u> | <u>5,691.56</u> |
| Task Order Total | <u>30,067.00</u> | <u>9,222.50</u> | <u>20,844.50</u> |

* Preliminary cost data, not yet fully processed.



Contract no. - 01-50-22-2313
Research Unit no. - 105
Reporting period - June 1975-
April 1976
Number of pages - 17

DELINEATION AND ENGINEERING CHARACTERISTICS OF
PERMAFROST BENEATH THE BEAUFORT SEA

Principal Investigator:
P.V. Sellmann

Associate Investigators:
R. Berg
J. Brown
S. Blouin
E. Chamberlain
A. Iskandar
H. Ueda

PREFACE

This combined 4th quarter and annual report follows the guidance provided in the 5 February 1976 memo received from the OCS Arctic Project Office. The report was prepared as the mobilization phase for offshore drilling at Prudhoe Bay was being completed. The entire effort to date has involved the planning and mobilization of a drilling and sampling program for the purpose of gathering data on the physical, chemical and thermal properties of permafrost beneath the Beaufort Sea. Therefore, the report deals primarily with activities leading up to the actual data acquisition phase, which is scheduled to commence on or about 1 April 1976.

U.S. Army Cold Regions Research and Engineering Laboratory
Hanover, New Hampshire 03755

1 April 1976

I. TASK OBJECTIVES

The emphasis of the program is on quantifying the engineering characteristics of permafrost beneath the Beaufort Sea, and determining their relation to temperature, sediment type, ice content and chemical composition. These data will be used in conjunction with those from the marine and subsea permafrost projects listed below to develop a map portraying the occurrence and depth of permafrost under the Beaufort Sea. The drilling program will provide subsurface samples and control for the other programs. It is also designed to test drilling, sampling, and in situ measurement techniques in this offshore environmental setting where material types and ice conditions make acquisition of undisturbed samples extremely difficult.

We are actively coordinating our activities with the following OCS projects:

Research Unit #204: Offshore permafrost studies, Beaufort Sea - Peter Barnes and Erk Reimnitz, U.S. Geological Survey.

Research Unit #205: Marine environmental problems in the ice-covered Beaufort Sea Shelf and coastal regions - Peter Barnes, Erk Reimnitz and David Drake, U.S. Geological Survey.

Research Units #253, 255, 256: Offshore permafrost drilling, boundary conditions, properties, processes and models - T.E. Osterkamp and William D. Harrison, University of Alaska.

Research Unit #271: Beaufort seacoast permafrost studies - James C. Rogers, University of Alaska.

Research Unit #407: A study of Beaufort Sea coastal erosion, northern Alaska - Robert Lewellen, Littleton, Colorado.

The USGS annual report (Research Unit 204) contains additional background information on this coordinated OCS subprogram.

II. FIELD OR LABORATORY ACTIVITIES

A. Field Trip Schedule

During the reporting period a series of planning and field meetings were attended. Planning meetings were held at Menlo Park in July and December 1975. During November 1975, Mr. Sellmann visited Prudhoe Bay, Fairbanks and Anchorage to coordinate requirements for the field program.

During the fourth quarter final logistics plans were completed and equipment was transported to the Prudhoe Bay holding area at the V&E facility. This equipment came from several places: Hanover, N.H.; Menlo Park, Calif.; Spokane, Wash., and NARL, Barrow, Alaska. Much of the CRREL equipment from Hanover was transported to Fairbanks at no cost to the project by government-owned C-130 aircraft. All shipments

except the one originating in Barrow were shipped to and centrally organized at the CRREL facilities in Fairbanks in preparation for truck transport to Prudhoe, which took place during the last part of February 1976. Additional logistics coordination was accomplished by Dr. Robert Lewellen between 27 February and 5 March. He inspected the equipment in the Fairbanks area before it was shipped to Prudhoe by truck, and prepared all the equipment in Barrow for rolligon transport to Prudhoe Bay. The Barrow equipment, including a sled-mounted workshop and sled-mounted structure for the drilling equipment and pumps, was transported to Prudhoe during the first week of March by Crowley's rolligons that are based at Prudhoe. This equipment move, covering a one-way distance of 400 km, was carried out without any difficulties. The transport of equipment to Prudhoe was accomplished through a coordinated effort on the part of CRREL personnel in Hanover and Fairbanks, Menlo Park personnel at the USGS, Dr. Robert Lewellen at NARL, and Mr. David Kennedy at the OCS office in Fairbanks.

B. Scientific Party

The initial field crew (Sellmann, Ueda and Delaney) departed from Hanover on 19 March and arrived in Prudhoe on the 20th. Their first objective was to uncrate and assemble the drilling system and to supervise the mounting of the portable field camp and soils lab unit onto their sled. Two additional CRREL personnel were scheduled to arrive at Prudhoe in the last days of March to prepare the soils testing equipment and laboratory. Dr. Jerry Brown and Dr. Alex Iskandar plan a brief site visit in early April to coordinate sampling procedures for the chemical studies.

The following personnel were scheduled to be at Prudhoe by 1 April:

- Mr. Paul V. Sellmann, CRREL - Drilling effort and core logging.
- Mr. Herbert Ueda, CRREL - Drilling effort.
- Mr. Allen Delaney, CRREL - Drilling effort.
- Dr. Peter Barnes, USGS (cooperative) - Field control, positioning of drill sites, and sediment analyses.
- Dr. Robert Lewellen, Arctic consultant (cooperative) - Drilling effort and obtaining thermal data.
- Mr. Edwin Chamberlain, CRREL - Engineering soils testing and analyses.
- Mr. Scott Blouin, CRREL - Engineering soils testing and analyses.

C. Methods

Drilling program

The sampling program will rely on rotary drilling and drive sampling techniques. The equipment for this program has been assembled from a variety of sources. Components of the drilling system are owned by CRREL and ONR (Lewellen's ONR project) with some sampling equipment and drill hole casing having been purchased with OCS project funds. The CRREL and ONR equipment is being provided at no cost to the project. The CRREL drill rig is an Acker Mountaineer with a depth capability of 600 m with NW rod.

Sampling equipment available includes: 1) Two drilling systems and HQ string, manufactured by Longyear, including a 1.2-m core barrel. A Diamond Drill string, N-HR size, including a 1.2-m core barrel, modified to use a spring-loaded inner tube sampler which combines some positive aspects of drive sampling with rotary drilling. 2) Conventional, double-wall sample barrels of the high recovery type (Diamond Drill Company), equipped with both diamond and carbide type cutters (available from the ONR Barrow-based drilling program). 3) A range of drive sampling tools, including split and single tube samplers.

The general range of sample diameters available with the above equipment is between 5 and 7 cm.

A permit (State Miscellaneous Land Use Permit) for this study was obtained from the State of Alaska by the OCS Alaska Project Office.

Field facilities

The facilities available for the field program include three sleds containing the workshop, the drill rig, and the soils lab and housing unit.

Workshop: This small shop unit provides a working area for equipment repair and for storage of much of the drilling equipment, such as bits, sampling tools and some drill pipe and casing.

Drill sled: The drilling equipment, including all necessary components for the drilling operation such as pumps, tanks and mud pit, and parts of the circulation system, are enclosed in this unit. A 10-m mast is also provided for the drill rig.

Living accommodations and soils laboratory: An eight-man sleeper was leased from Crowley at Prudhoe. This unit plus the soils lab and power plant will be mounted on a 12-m-long leased Nabors sled. The laboratory is equipped with drying oven, balance, triaxial testing equipment, and a system for photographically logging the cores.

In situ and field soil measurement

Methods for in situ probing and on-site laboratory strength testing were evaluated. A cone penetrometer probe was designed and fabricated. The essential element of this probe is a 6-cm, 60° cone. The probe can be driven by a 65-kg drop weight or hydraulic ram. Only point resistance will be measured as the skin friction component will be eliminated by the use of a 5-cm-O.D. casing that will be driven with the probe but held fixed when measuring point penetration resistance. The penetration resistance will be measured in the drill holes and at adjacent locations. Equipment was also obtained to conduct quick multi-stage triaxial strength tests on prepared core obtained from the drill holes. As many as possible of these tests will be conducted in the on-site soils laboratory to avoid disturbances due to shipping and temperature fluctuations. Correlations of cone penetration resistance and triaxial shear strength will be obtained upon return from the field.

Chemical characteristics

Chemical analyses of the solution extracted from the thawed permafrost samples and the unfrozen sediments will be performed for correlation with engineering and geologic studies. The extracts will be obtained at

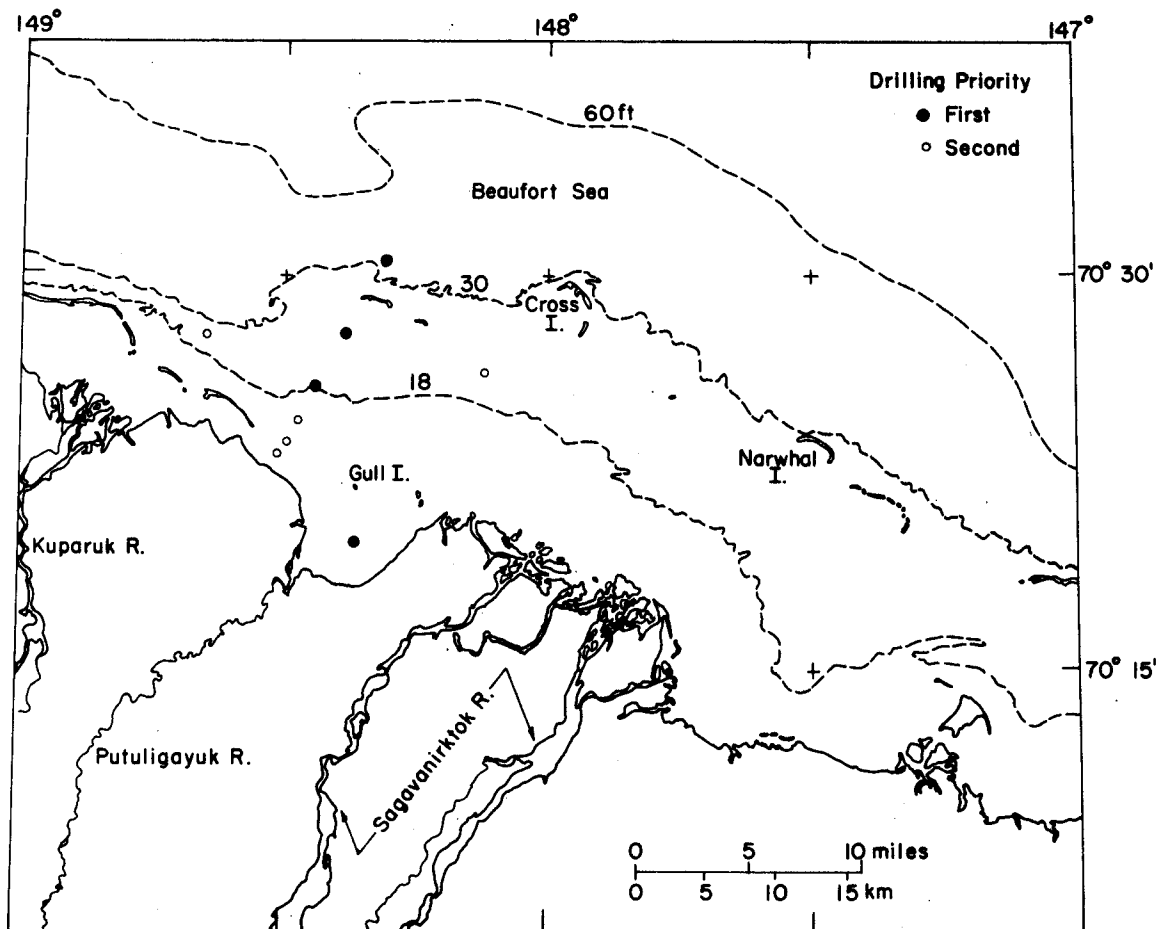


Figure 1. USACRREL-USGS subsea drilling locations, Prudhoe Bay region, Spring 1976.

the CRREL laboratory by centrifuging immediately upon thawing of the frozen samples. In the field, portable electrical conductivity and pH meters will be available to monitor water chemistry. Although we expect chemical contamination of the cores to be minimal, we will attempt to monitor possible contamination of the samples with fluorescent dyes.

D. Sample Localities

Figure 1 shows the primary and secondary sites for spring 1976 drilling. The first hole planned is in Prudhoe Bay in proximity to support facilities. This will allow us to solve operational problems in preparation for drilling at the more distant sites. The Prudhoe hole will provide supplemental data for the spring 1975 sampling and analyses by Osterkamp and Harrison (see Research Units #253, 255, 256). The depth of each hole will depend on local conditions but will not generally exceed 150 meters. The final number of holes will depend on time available on the ice.

E. Data Collected

This section is not applicable since sample collection and analyses will commence on 1 April 1976. However, the preliminary data management plan (App. 1), submitted to the NOAA-OCS Juneau, indicates the type of data that will be available for the project.

III. RESULTS

This section is not applicable since the field studies will commence on 1 April 1976. Appendix 2 contains a preliminary literature search of the Soviet subsea permafrost literature.

IV. PRELIMINARY INTERPRETATION OF RESULTS

This section is not applicable since the field studies will commence on 1 April 1976.

V. PROBLEMS ENCOUNTERED/RECOMMENDED CHANGES

The original proposal called for contracting the drilling equipment and drilling. However, due to cost considerations and scheduling of commercially available equipment it was decided to utilize and upgrade existing equipment and to utilize CRREL personnel and Dr. Lewellen as the drilling crew. This provides a specialized team experienced in offshore, onshore and ice cap drilling which can cope with many of the day-to-day problems and still allow the project to remain within the original cost estimates.

Since the project will still be in the field and only preliminary information will be available at the time second-year renewal proposals are due (17 May 1976), we recommend that the deadline for this project's renewal be extended to 1 June 1976. We anticipate that the second-year continuation proposal will emphasize permafrost conditions in the Beaufort Sea.

VI. ESTIMATE OF FUNDS EXPENDED

As of 29 February 1976, a total of \$137,000 of the total \$330,000 had been obligated.

APPENDIX 1

USACRREL SUBSEA DRILLING DATA

1. Definition of Data Types

A. Field Station Data

- | | |
|---|--------------------------------|
| (1) Project Identification | |
| (2) Station Number | |
| (3) Location | Latitude & Longitude |
| (4) Date | |
| (5) Air Temperature | °C |
| (6) Estimated Wind Speed | km/hr |
| (7) Cloud Cover | % |
| (8) Visibility | km |
| (9) Datum for Elevations | (benchmark, ice surface, etc.) |
| (10) Snow Depth | m |
| (11) Ice Thickness | m |
| (12) Water Depth | m |
| (13) Water Temperature Beneath Ice | °C |
| (14) Water Temperature at Sea Floor | °C |
| (15) Drill Crew Members | |
| (16) Drilling Equipment | |
| (17) Boring Number(s) | |
| (18) Boring Information (casing, etc.) | |

B. Boring Data Within Station

- | | |
|---|----|
| (1) Core Identification | |
| (2) Depth to Top and Bottom of Core | m |
| (3) Sampler Type | |
| (4) Temperature | °C |
| (5) Visual Ice Classification (NRC/ACFEL Ice Class. System) | |
| (6) Color of Core | |
| (7) Visual Texture Class. (Gravel, Sand, Silt, Clay) | |
| (8) Visual Structure Class. (Bonded, Unbonded, Banded, etc.) | |
| (9) Photo Identification Number | |
| (10) Comments (quality of sample, number of pieces, etc.) | |

C. Laboratory Index Property Tests

- | | |
|--------------------|---|
| (1) Core Number | |
| (2) Length | |
| (3) Gravel Content | % |

- (4) Sand Content %
- (5) Silt Content %
- (6) Clay Content %
- (7) Unified Soil Classification
- (8) Water Content %
- (9) Organic Content %
- (10) Liquid Limit %
- (11) Plastic Limit %
- (12) Dry Density g/cm^3
- (13) Saturation %
- (14) Comments

D. Laboratory Chemical Analysis of Soil Water

- (1) Core Number
- (2) Length cm
- (3) pH $\mu\text{mhos/cm}$
- (4) Conductivity ~~$\mu\text{-ohm/cm}$~~ cmhos/cm
- (5) Ca ppm
- (6) Mg ppm
- (7) Na ppm
- (8) K ppm
- (9) Cl ppm
- (10) NO_3 ppm
- (11) HCO_3 ppm
- (12) $\text{PO}_4\text{-P}$ ppm
- (13) Organic -C ppm
- (14) Organic -N ppm
- (15) Water Content %

E. Laboratory Triaxial Strength Data

- (1) Core Number
- (2) Length cm
- (3) Diameter cm
- (4) Temperature $^{\circ}\text{C}$
- (5) Confining Pressure kg/cm^2
- (6) Maximum Deviator Stress kg/cm^2
- (7) Strain at Maximum Deviator Stress %
- (8) Strain Rate $\%/min$
- (9) Comments

F. Laboratory Thaw Consolidation Data

- (1) Core Number
- (2) Length cm
- (3) Diameter cm
- (4) Temperature Frozen $^{\circ}\text{C}$
- (5) Temperature Thawed $^{\circ}\text{C}$

| | |
|-----------------------------|--------------------|
| (6) Axial Pressure | kg/cm ² |
| (7) Strain Frozen | % |
| (8) Strain Thawed | % |
| (9) Dry Unit Weight Frozen | g/cm ³ |
| (10) Dry Unit Weight Thawed | g/cm ³ |
| (11) Comments | |

2. Projected Schedule and Quantity of Data

Punched cards for the field and laboratory data will be submitted within 60 days of completion of the work. It is estimated that the field data will be available by 1 July 1976 and the laboratory data by 30 September 1976.

It is estimated that 1350 data cards will be submitted. See inclosures for data types and quantity distribution.

3. Format and File Type

No appropriate format is provided in the 23 December 1975 file listing. See inclosures for suggested format. It is suggested that this file be designated "Description and Engineering Properties of Subsea Permafrost."

4. Data Documentation and Quality Control Procedures

Core obtained in the field will be logged in bound notebooks on site with a complete description of each core. Each length of core will be assigned a coded identification number indicating the site, hole, and sequence of sampling. Photographs of each core length will be obtained with special core photography equipment using a standardized format for identification and size referencing.

Laboratory studies will be conducted using standardized procedures when available. Soil index property testing will follow procedures outlined in U.S. Army Engineer Manual EM 1110-2-1906. The chemical analysis of the soil water will follow standard methods of testing water and wastewater established by the American Public Health Association. Quality control will be evaluated by testing standards obtained from the EPA.

Unfortunately, no standardized procedures are available for conducting strength and consolidation tests on frozen and thawing soils. This portion of the laboratory program will be conducted relying on expertise developed at CRREL over the past few years. Care will be used to employ calibrated load, pressure and displacement transducers. A standard triaxial compression cell has been modified to accept 2-in.-diameter frozen soil cylinders. Special thaw consolidation equipment presently in use will be available for the thaw consolidation tests. Procedures outlined in EM 1110-2-1906 will be followed when appropriate.

All laboratory tests will be indexed to the core identification data.

SUGGESTED FORMAT FOR A. Field Station Data (Estimated 50 data cards)

| | | | | | | | | | | | | | | | | | | | | | | | | | | | | | | | | | | | | | | | | | | | | | | | | | | | | | | | | | | | | | | | | | | | | | | | | | | | | | | | | |
|---------------------|---|--|-----------|-------------|------------|-----------------|--------------|-------------|-------|--------------|----------------|----|------|---------|----|----|----|----|----|----|----|----|----|----|----|----|----|----|----|----|----|----|----|----|----|----|----|----|----|----|----|----|----|----|----|----|----|----|----|----|----|----|----|----|----|----|----|----|----|----|----|----|----|----|----|----|----|----|----|----|----|----|----|----|----|----|----|----|----|--|
| 1 | 2 | 3 | 4 | 5 | 6 | 7 | 8 | 9 | 10 | 11 | 12 | 13 | 14 | 15 | 16 | 17 | 18 | 19 | 20 | 21 | 22 | 23 | 24 | 25 | 26 | 27 | 28 | 29 | 30 | 31 | 32 | 33 | 34 | 35 | 36 | 37 | 38 | 39 | 40 | 41 | 42 | 43 | 44 | 45 | 46 | 47 | 48 | 49 | 50 | 51 | 52 | 53 | 54 | 55 | 56 | 57 | 58 | 59 | 60 | 61 | 62 | 63 | 64 | 65 | 66 | 67 | 68 | 69 | 70 | 71 | 72 | 73 | 74 | 75 | 76 | 77 | 78 | 79 | 80 | |
| PROJECT: | | CRREL OCS DRILLING PROJECT | | | | | | | | | | | | | | | | | | | | | | | | | | | | | | | | | | | | | | | | | | | | | | | | | | | | | | | | | | | | | | | | | | | | | | | | | | | | | | |
| STATION NO: | | 1 | LOCATION: | | 148-24-33W | 710-18-24N | | DATE: | | 24-25 | APRIL | | 1976 | | | | | | | | | | | | | | | | | | | | | | | | | | | | | | | | | | | | | | | | | | | | | | | | | | | | | | | | | | | | | | | | | | | |
| AIR TEMP: | | -4 | TO | | +8C | EST WIND SPEED: | | 10-15 | KM/HR | | CLOUD COVER: | | 25 | PERCENT | | | | | | | | | | | | | | | | | | | | | | | | | | | | | | | | | | | | | | | | | | | | | | | | | | | | | | | | | | | | | | | | | | |
| VISIBILITY: | | CLEAR | | DATUM: | | ICE SURFACE | | SNOW DEPTH: | | 0.5M | ICE THICKNESS: | | 3.5M | | | | | | | | | | | | | | | | | | | | | | | | | | | | | | | | | | | | | | | | | | | | | | | | | | | | | | | | | | | | | | | | | | | |
| WATER DEPTH: | | 10.3M | | WATER TEMP: | | -0.5C | BENEATH ICE; | | -0.7C | AT SEA FLOOR | | | | | | | | | | | | | | | | | | | | | | | | | | | | | | | | | | | | | | | | | | | | | | | | | | | | | | | | | | | | | | | | | | | | | | |
| DRILL CREW: | | LEWELLEN, SELLMANN, DELANEY, UEDIA | | | | | | | | | | | | | | | | | | | | | | | | | | | | | | | | | | | | | | | | | | | | | | | | | | | | | | | | | | | | | | | | | | | | | | | | | | | | | | |
| DRILLING EQUIPMENT: | | ACKER 119 | | | | | | | | | | | | | | | | | | | | | | | | | | | | | | | | | | | | | | | | | | | | | | | | | | | | | | | | | | | | | | | | | | | | | | | | | | | | | | |
| BORING NO: | | OCS1, OCS2 | | | | | | | | | | | | | | | | | | | | | | | | | | | | | | | | | | | | | | | | | | | | | | | | | | | | | | | | | | | | | | | | | | | | | | | | | | | | | | |
| BORING INFORMATION: | | 30M CASING THRU ICE, 15CM CASING SET 2M INTO SEA FLOOR | | | | | | | | | | | | | | | | | | | | | | | | | | | | | | | | | | | | | | | | | | | | | | | | | | | | | | | | | | | | | | | | | | | | | | | | | | | | | | |

SUGGESTED FORMAT FOR B. Boring Data Within Station (Estimated 600 data sets)

| | | | | | | | | | | | | | | | | | | | | | | | | | | | | | | | | | | | | | | | | | | | | | | | | | | | | | | | | | | | | | | | | | | | | | | | | | | | | | | | | |
|-------------------|---|-------------|---|-----------|---|---------|---|-----------|----|-------|----|--------|----|------|----|----|----|----|----|----|----|----|----|----|----|----|----|----|----|----|----|----|----|----|----|----|----|----|----|----|----|----|----|----|----|----|----|----|----|----|----|----|----|----|----|----|----|----|----|----|----|----|----|----|----|----|----|----|----|----|----|----|----|----|----|----|----|----|----|--|
| 1 | 2 | 3 | 4 | 5 | 6 | 7 | 8 | 9 | 10 | 11 | 12 | 13 | 14 | 15 | 16 | 17 | 18 | 19 | 20 | 21 | 22 | 23 | 24 | 25 | 26 | 27 | 28 | 29 | 30 | 31 | 32 | 33 | 34 | 35 | 36 | 37 | 38 | 39 | 40 | 41 | 42 | 43 | 44 | 45 | 46 | 47 | 48 | 49 | 50 | 51 | 52 | 53 | 54 | 55 | 56 | 57 | 58 | 59 | 60 | 61 | 62 | 63 | 64 | 65 | 66 | 67 | 68 | 69 | 70 | 71 | 72 | 73 | 74 | 75 | 76 | 77 | 78 | 79 | 80 | |
| CORE DESCRIPTIONS | | | | | | | | | | | | | | | | | | | | | | | | | | | | | | | | | | | | | | | | | | | | | | | | | | | | | | | | | | | | | | | | | | | | | | | | | | | | | | | | |
| BORING NO | | OCS-1 | | | | | | | | | | | | | | | | | | | | | | | | | | | | | | | | | | | | | | | | | | | | | | | | | | | | | | | | | | | | | | | | | | | | | | | | | | | | | | |
| CORE DEPTH | | SAMP-TEMP | | ICE COLOR | | TEXTURE | | STRUCTURE | | PHOTO | | | | | | | | | | | | | | | | | | | | | | | | | | | | | | | | | | | | | | | | | | | | | | | | | | | | | | | | | | | | | | | | | | | | | | |
| NO | | M | | LER | | C | | | | ID | | | | | | | | | | | | | | | | | | | | | | | | | | | | | | | | | | | | | | | | | | | | | | | | | | | | | | | | | | | | | | | | | | | | | | |
| OCS1-1 | | 11.05-14.13 | | COR-10.31 | | VX-VS | | BRN | | SAND | | BONDED | | 1-15 | | | | | | | | | | | | | | | | | | | | | | | | | | | | | | | | | | | | | | | | | | | | | | | | | | | | | | | | | | | | | | | | | | |

SUGGESTED FORMAT FOR C. Laboratory Index Property Tests (Estimated 500 data cards)

| 1 | 2 | 3 | 4 | 5 | 6 | 7 | 8 | 9 | 10 | 11 | 12 | 13 | 14 | 15 | 16 | 17 | 18 | 19 | 20 | 21 | 22 | 23 | 24 | 25 | 26 | 27 | 28 | 29 | 30 | 31 | 32 | 33 | 34 | 35 | 36 | 37 | 38 | 39 | 40 | 41 | 42 | 43 | 44 | 45 | 46 | 47 | 48 | 49 | 50 | 51 | 52 | 53 | 54 | 55 | 56 | 57 | 58 | 59 | 60 | 61 | 62 | 63 | 64 | 65 | 66 | 67 | 68 | 69 | 70 | 71 | 72 | 73 | 74 | 75 | 76 | 77 | 78 | 79 | 80 |
|--|------|-----|------|------|-----|----|------|-----|-----|-----|-------|------|----------|----|----|----|----|----|----|----|----|----|----|----|----|----|----|----|----|----|----|----|----|----|----|----|----|----|----|----|----|----|----|----|----|----|----|----|----|----|----|----|----|----|----|----|----|----|----|----|----|----|----|----|----|----|----|----|----|----|----|----|----|----|----|----|----|----|----|
| LABORATORY SOIL INDEX PROPERTY DATA | | | | | | | | | | | | | | | | | | | | | | | | | | | | | | | | | | | | | | | | | | | | | | | | | | | | | | | | | | | | | | | | | | | | | | | | | | | | | | | |
| BORING NO OCS-1 | | | | | | | | | | | | | | | | | | | | | | | | | | | | | | | | | | | | | | | | | | | | | | | | | | | | | | | | | | | | | | | | | | | | | | | | | | | | | | | |
| CORE LENGTH PERCENT US C W O LL PL DRY DENS SAT COMMENTS | | | | | | | | | | | | | | | | | | | | | | | | | | | | | | | | | | | | | | | | | | | | | | | | | | | | | | | | | | | | | | | | | | | | | | | | | | | | | | | |
| NO M GRVL SAND SILT CLAY % % % % GRICC % | | | | | | | | | | | | | | | | | | | | | | | | | | | | | | | | | | | | | | | | | | | | | | | | | | | | | | | | | | | | | | | | | | | | | | | | | | | | | | | |
| OCS1-1 | 3.08 | 0.0 | 50.4 | 42.8 | 6.8 | SM | 43.8 | 3.2 | 0.0 | 0.0 | 2.031 | 99.4 | 4 PIECES | | | | | | | | | | | | | | | | | | | | | | | | | | | | | | | | | | | | | | | | | | | | | | | | | | | | | | | | | | | | | | | | | | |

SUGGESTED FORMAT FOR D. Laboratory Chemical Analysis of Soil Water (Estimated 50 data cards)

| 1 | 2 | 3 | 4 | 5 | 6 | 7 | 8 | 9 | 10 | 11 | 12 | 13 | 14 | 15 | 16 | 17 | 18 | 19 | 20 | 21 | 22 | 23 | 24 | 25 | 26 | 27 | 28 | 29 | 30 | 31 | 32 | 33 | 34 | 35 | 36 | 37 | 38 | 39 | 40 | 41 | 42 | 43 | 44 | 45 | 46 | 47 | 48 | 49 | 50 | 51 | 52 | 53 | 54 | 55 | 56 | 57 | 58 | 59 | 60 | 61 | 62 | 63 | 64 | 65 | 66 | 67 | 68 | 69 | 70 | 71 | 72 | 73 | 74 | 75 | 76 | 77 | 78 | 79 | 80 |
|--|------|-----|---|---|---|---|---|---|----|----|----|----|----|----|----|----|----|----|----|----|----|----|----|----|----|----|----|----|----|----|----|----|----|----|----|----|----|----|----|----|----|----|----|----|----|----|----|----|----|----|----|----|----|----|----|----|----|----|----|----|----|----|----|----|----|----|----|----|----|----|----|----|----|----|----|----|----|----|----|
| LABORATORY SOIL WATER CHEMICAL ANALYSIS | | | | | | | | | | | | | | | | | | | | | | | | | | | | | | | | | | | | | | | | | | | | | | | | | | | | | | | | | | | | | | | | | | | | | | | | | | | | | | | |
| BORING NO: OCS-1 | | | | | | | | | | | | | | | | | | | | | | | | | | | | | | | | | | | | | | | | | | | | | | | | | | | | | | | | | | | | | | | | | | | | | | | | | | | | | | | |
| CORE LENGTH PH CON CA MG NA K CL NO3 HCO3 PO4-P ORGC ORGN WATER | | | | | | | | | | | | | | | | | | | | | | | | | | | | | | | | | | | | | | | | | | | | | | | | | | | | | | | | | | | | | | | | | | | | | | | | | | | | | | | |
| NO M PPM UO4M/CM PPM PPM PPM PPM PPM PPM PPM PPM PPM PPM PPM PPM | | | | | | | | | | | | | | | | | | | | | | | | | | | | | | | | | | | | | | | | | | | | | | | | | | | | | | | | | | | | | | | | | | | | | | | | | | | | | | | |
| OCS1-2 | 2.12 | 6.3 | | | | | | | | | | | | | | | | | | | | | | | | | | | | | | | | | | | | | | | | | | | | | | | | | | | | | | | | | | | | | | | | | | | | | | | | | | | | | |

APPENDIX 2

PRELIMINARY BIBLIOGRAPHY ON SUBSEA PERMAFROST - SOVIET LITERATURE

Compiled by J. Brown

The study of subsea permafrost, particularly in North America, is relatively new. Within the past few years an increasing number of Canadian and U.S. papers and project reports have appeared. The research and field studies have been stimulated by the exploration for oil and gas in the offshore regions of the Beaufort Sea. Several key Soviet references have come to the attention of North American investigators. Unlike the voluminous Soviet literature covering permafrost on land, Soviet publications on offshore permafrost are relatively few. It is our objective to perform an in-depth search of the Soviet literature to determine what information exists on subsea permafrost and related processes. We are confining the citations to post-1950 publications and restricting the related literature to coastal and lacustrine processes of erosion and in some cases the influence of water bodies such as northern lakes on permafrost.

The following bibliography represents our initial effort, and contains many incomplete citations. It relied heavily on a cursory review of the CRREL Bibliography on Cold Regions Science and Technology, several OASIS searches including geology, water resources, oceanic abstract, and engineering index, and a review of the eight translated Soviet volumes of the Second International Permafrost Conference held in Yakutsk in 1973, and several other translations. The most recent translation is the 1966 book by Grigor'yev entitled Perennially Frozen Rocks of the Coastal Zone of Yakutia (CRREL Draft Translation 512). The book was translated as part of CRREL's regular translation program and copies have been distributed to OCS and other permafrost investigators. We are currently reviewing the Bibliography on Cold Regions Science and Technology through the CRREL Library of Congress project, and are requesting several additional OASIS searches.

Comments on the following bibliography are welcomed. After completing the Soviet bibliography we plan to make a compilation of the North American literature.

PRELIMINARY BIBLIOGRAPHY ON SUBSEA PERMAFROST
Recent (post-1950) Soviet Literature*

- Are, F.E. (1964) Role of multiple vein ice in the destruction of beach scarps on the Arctic coast. Thermal Processes in Frozen Rocks, Moscow, Izd-vo Nauka, p. 100-110. (23-1235)
- Are, F.E. (1964) Influence of thermophysical properties of frozen rocks on the destruction of the beaches on the arctic coast. Thermal Processes in Frozen Rocks, Moscow, Izd-vo Nauka, p. 111-116. (23-1236)
- Are, F.E. (1968) The development of the topography of thermal abrasion shores. Izv. AN SSSR, Ser. Geogr., Jan-Feb, no. 1, p. 92-100. (25-5588)
- Are, F.E. (1972) The reworking of shores in the permafrost zone. In International Geography 1972 (W.P. Adams and F.M. Helleiner, Eds.). Proceedings of the 22nd International Geographical Congress, Montreal, Canada, 1972. Toronto and Buffalo: University of Toronto Press, p. 78-79. (28-1579)
- Are, F.E. (1973) Shore erosion in permafrost regions. Second International Conference on Permafrost, Yakutsk, vol. 2, p. 5-10. (28-1030)
- Are, F.E. and E.N. Molochuskin (1965) Speed of arctic shore-cliff destruction in Yakutia by thermal erosion. Heat and Mass Exchange Processes in Frozen Rocks, Moscow, Nauka, p. 130-138. (28-418)
- Averina, I.M. et al. (1962) Northern Yakutia (Physiographic characteristics). Arkticheskii i antarkticheskii Nauchno-Issledovatel'skii Institut, Trudy Leningrad, vol. 236, 280 p. (30-1561)
- Balobaev, V.T., V.N. Deviatkin and I.M. Kutasov (1973) Recent geothermal conditions under which permafrost exists and develops. Second International Conference on Permafrost, Yakutsk, vol. 1, p. 51-52. (28-1015)
- Bogoslovsky, W.A. and A.A. Ogilvy (1974) Detailed electrometric and thermometric observations in offshore areas. Geophysical Prospecting, vol. 22, p. 381.
- Gakkel, Ya.Ya. (1958) Destruction of Semenovskiy Island. Problems of the Arctic. Leningrad, Izd-vo Morskogo Transporta, no. 4.
- Grigor'yev, N.F. (1952) Permafrost-geological characteristics of the northern part of the Yana River Delta in the region of the mouth of the Pravaya distributary. Permafrost Research in the Yakutian Republic. Moscow, Izd-vo AN SSSR, no. 3.
- Grigor'yev, N.F. (1959) Influence of water bodies on geocryological conditions in the coastal lowland of the Ust'-Yanskiy region of the Yakutian ASSR. Materials of the Conference on Permafrost Science. Moscow, Izd-vo AN SSSR.

*Numbers in () refer to CRREL Bibliographic citation.

- Grigor'yev, N.F. (1960) Temperature of perennially frozen rocks in the region of the Lena River Delta. Conditions of Bedding and Properties of Perennially Frozen Rocks in the Territory of the Yakutian ASSR. Trudy svo in-ta Merzlotovedeniya Imeni V.A. Obrucheva AN SSSR, no. 2, Yakutskoye Knizhnoye Izd-vo.
- Grigor'yev, N.F. (1962) Role of cryogenic factors in the formation of the Yakutia shorelines. Moscow Izd. AN SSR, p. 68-78. (23-1305)
- Grigor'yev, N.F. (1962) The role of cryogenic factors in the formation of the marine shorelines of Yakutiya. Permafrost and the Phenomena Accompanying it in the Yakut ASSR. Moscow, Izd-vo AN SSSR.
- Grigor'yev, N.F. (1964) Peculiarities of formation of shores under polar climate conditions. Scientific Communications under the Program of the Twentieth International Geographical Congress. Moscow, Izd-vo Nauka.
- Grigor'yev, N.F. (1966) Perennially frozen rocks of the coastal zone of Yakutia. Moscow, Nauka, 180 p. (25-742) (CRREL Draft Translation 512.)
- Grigor'yev, N.F. (1973) Role of cryogenic factors in the formation of placers in the nearshore zone of the Laptev Sea shelf. Second International Conference on Permafrost, Yakutsk, vol. 3, p. 19-22. (28-1060)
- Gusev, A.M. (1959) Method for the mapping of shores in deltas of rivers of the Polar Basin. Trudy Nauchno-Issled. in-ta Geol. Arktiki, vol. 107, no. 12. Moscow-Leningrad, Izd-vo Glavsevmorputi.
- Kaplina, T.N. (1959) Some peculiarities of the erosion of shores made up of perennially frozen rocks. Trudy Okeanogr. Komissii, Moscow, Izd-vo AN SSSR, vol. 4.
- Klyuyev, Ye.V. (1965) The role of permafrost factors in the dynamics of bottom topography in polar seas. Acad. Sci., USSR, Oceanology 5, p. 78-83.
- Klyuyev, Ye.V. (1966) Thermokarst on the bottom of the Laptev Sea. Problems of the Arctic and Antarctic, vol. 23, p. 26-32.
- Korotkevich, E.S. (1972) Polar deserts. Gidrometeorzdat, Leningrad, 420 p. (27-2642)
- Kuznetsova, T.P. and T.N. Kaplina (1960) Characteristics of the morphology of shore slopes consisting of perennially frozen rocks with vein ice. Trudy svo in-ta Merzlotovedeniya Im.V.A. Obrucheva AN SSSR, no. 2, Yakutsk.
- Kuznetsova, L.O. (1972) Variation of the salinity of water during ice formation in shallow seas. Meteorology and Hydrology, no. 5. (JPRS translation 56595, p. 75-79.) (27-944)
- Lapina, N.N. (1956) Changes in porosity and gas permeability of rocks at a negative temperature. Trudy Nauchno-Issled. in-ta Geol. Arktiki, vol. 89, no. 6, Leningrad, Izd-vo Glavsevmorputi.

- Molochushkin, E.N. (1969) Some data on the salinity and temperature conditions of the water in the coastal zone of the Laptev Sea. The Geography of Yakutia, 5th edition, Yakutsk.
- Molochushkin, E.N. et al. (1970) Thermal properties of bottom deposits in the near-shore zone of the Laptev Sea. Methods of Determining Thermal Properties of Rocks, Moscow, Nauka, p. 154-169. (25-2948)
- Molochushkin, E.N. (1973) The effect of thermal weathering on permafrost temperature in the nearshore zone of the Laptev Sea. Second International Conference on Permafrost, Yakutsk, vol. 2, p. 52-58. (28-1036)
- Molochushkin, Ye.N. and R.I. Gavil'yev (1970) The structure, phase composition and thermal regime of rocks occurring in the bottom of the Laptev Sea nearshore zone. In Severerny Ledovityy Okean I Yego Poberezli'ye v kaynozoye, Paleogeografika severnykh territoriy v pozdvem Kaynozoye, p. 503-508.
- Moscow, AN SSSR (1962) The role of cryogenic factors in the formation of sea shore of Yakutia. In Permafrost and Related Phenomena in the Yakut ASSR, p. 68-78.
- Neizvestnov, Ya.V. et al. (1970) Low temperature waters of the earth. Summary Reports of the All-Union Permafrost Conference 1970. Publ. Moscow State University.
- Neizvestnov, Ia.V. and Iu.P. Semenov (1973) Unfrozen water in the permafrost zone of the continental shelf and islands of the Soviet Arctic. Ground Water in the Cryolithosphere. Second International Conference on Permafrost, Yakutsk, vol. 5, p. 103-106. (28-1131) (CRREL Draft Translation 437).
- Oberman, N.G. et al. (1970) New data on the hydrogeology and thickness of the cryolithic zone on the coast of the Kara Sea. Summary Reports of the All-Union Permafrost Conference 1970. Publ. Moscow State University.
- Oberman, N.G. and N.B. Kakunov (1973) Determining thickness of the rock zone with subzero temperatures on the arctic coast. Second International Conference on Permafrost, Yakutsk, vol. 2, p. 130-137. (28-1054)
- Panov, D.G. (1938) Geomorphological outline of the shores of the Polar Seas of the U.S.S.R. Scientific Notes of Moscow State University, Moscow, Geografiz, no. 19.
- Ponomarev, U.M. (1950) Formation of subterranean waters along the coast of the Northern Sea in the permafrost zone. U.S.S.R. Acad. Sci., Moscow.
- Ponomarev, V.M. (1952) Permafrost and subterranean waters of the Ust'Port area on the Yenisei River. Proceedings of the V.A. Obruchev Institute of Permafrost, U.S.S.R. Acad. Sci., Moscow, vol. 10.
- Romanovskiy, N.N. (1961) Structure of the Yana-Indigirka coastal alluvial plain and conditions for its formation. Permafrost Research, Moscow, Izd-vo MGU, no. 2. (27-1745)

- Romanovskiy, N.N. (1961) Erosional-thermokarst basins in the northern maritime plains of Yakutia and Novosibirskiye Islands. Merzlotnyye Issledovaniya, Moscow, no. 1, p. 124-144. (25-2722)
- Ryabchun, V.K. (1966) The dynamics of the frozen shores of arctic bodies of water. Transactions of the 4th Seminar-type conference on the exchange of information relating to experience in construction operations under severe climatic conditions. Vorkuta, vol. 10.
- Sharbatyan, A.A. (1973) Formulas for the calculating time required for the formation and degradation of the permafrost zone. Second International Conference on Permafrost, Yakutsk, vol. 2, p. 94-98. (28-1029)
- Sharbatyan, A.A. (1974) Extreme estimations in geothermy and geocryology. 140 p. (29-1659) (CRREL Draft Translation 465.)
- Sisko, R.K. (1970) Thermal abrasion of arctic sea shores in Novoya Sibir' Island. Leningrad, Arkticheskii i antarkticheskii nauch.-issled. inst. Trudy, vol. 294, p. 183-194. (25-3739)
- Sokolov, A.V. (1928) Movement of the shoreline in the Siberian Sea. Notes on Hydrology, vol. 60, Leningrad.
- Strelkov, S.A. (1961) Development of the shorelines of arctic seas of the USSR in the Quaternary. Transactions of the Geology Institute of the Estonian SSR, vol. IV.
- Tomirdiario, S.V. (1962) Heating and melting of perennially frozen ground beneath separate basins, water reservoirs and buildings. Krasnoiarsk, Gosstroj, p. 230-244. (25-1393)
- Tomirdiario, S.S. (1972) Permafrost and economic development of uplands and plains in the Magadan region and Yakutia. Magadan, Magadanskoe Knizh izd-vo, 174 p. (28-924)
- Tomirdiario, S.V. (1974) Erosion of ice-saturated shores and reservoirs, p. 53-60. (29-1389)
- Tomirdiario, S.V. et al. (1974) Forecasting the erosion of ice-saturated shores of lakes and water reservoirs in the Anadyr tundra. Lakes of the Siberian Cryolithozone, Novosibirsk, Nauka, p. 53-60. (29-1389)
- Tomirdiario, S.V., V.A. Kirillov and A.D. Golodovkina (1975) Energy cycle in lakes of permafrost regions. Transactions of the Conference on the Study of the Shores of Reservoirs and Drainage Problems under the Conditions Prevailing. Held Sept 1969, Novosibirsk, Nauka, p. 293-299. (30-961)
- Velli, Iu.Ia. and A.A. Karpunina (1973) Saline permafrost as bearing ground for structures. Second International Conference on Permafrost, Yakutsk, vol. 7, p. 49-59. (28-1162) (CRREL Draft Translation 438.)
- Yefimov, A.I. (1964) Permafrost-hydrogeological characteristics of coastal and channel reaches of the Lena River in the Yakutsk area. Geocryological Conditions of Western Siberia, Yakutia and Chukotka, Moscow, Izd-vo, Nauka.

Zenkovich, V.P. (1937) Observations of marine abrasion and physical weathering on the Murmansk Shore. Scientific Notes of Moscow State University, Moscow, Izd-vo MGU, no. 16.

Zhigarev, L.A. (1974) Structure, distribution and formation of submarine permafrost. In Problemy Kriolithologic (A.I. Popov, Ed.), vol. 4, p. 110-114. (29-3310) (Being translated.)

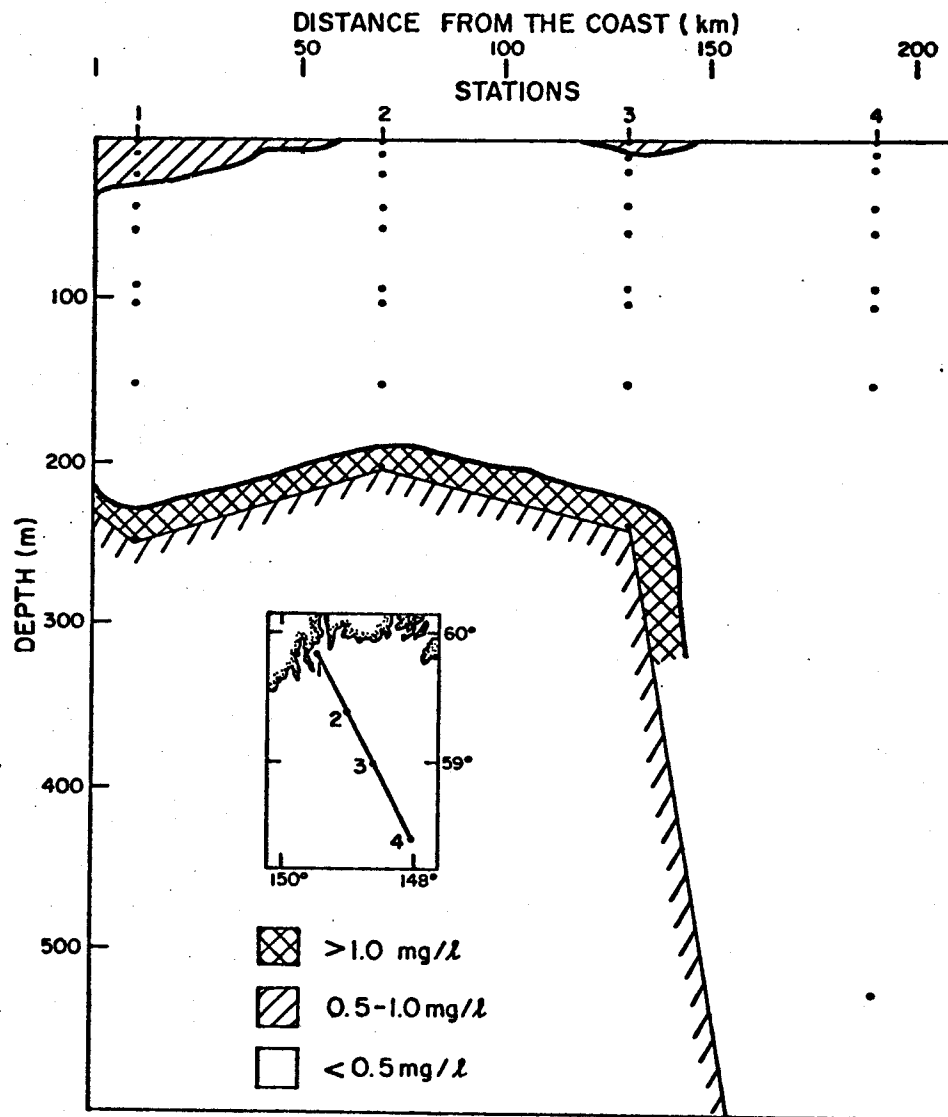


Figure 22. Vertical cross section of the distribution of total suspended matter for stations 1 thru 4 in the north-eastern Gulf of Alaska (Cruise RP-4-Di-75C-I, 21 Oct.-10 Nov., 1975).

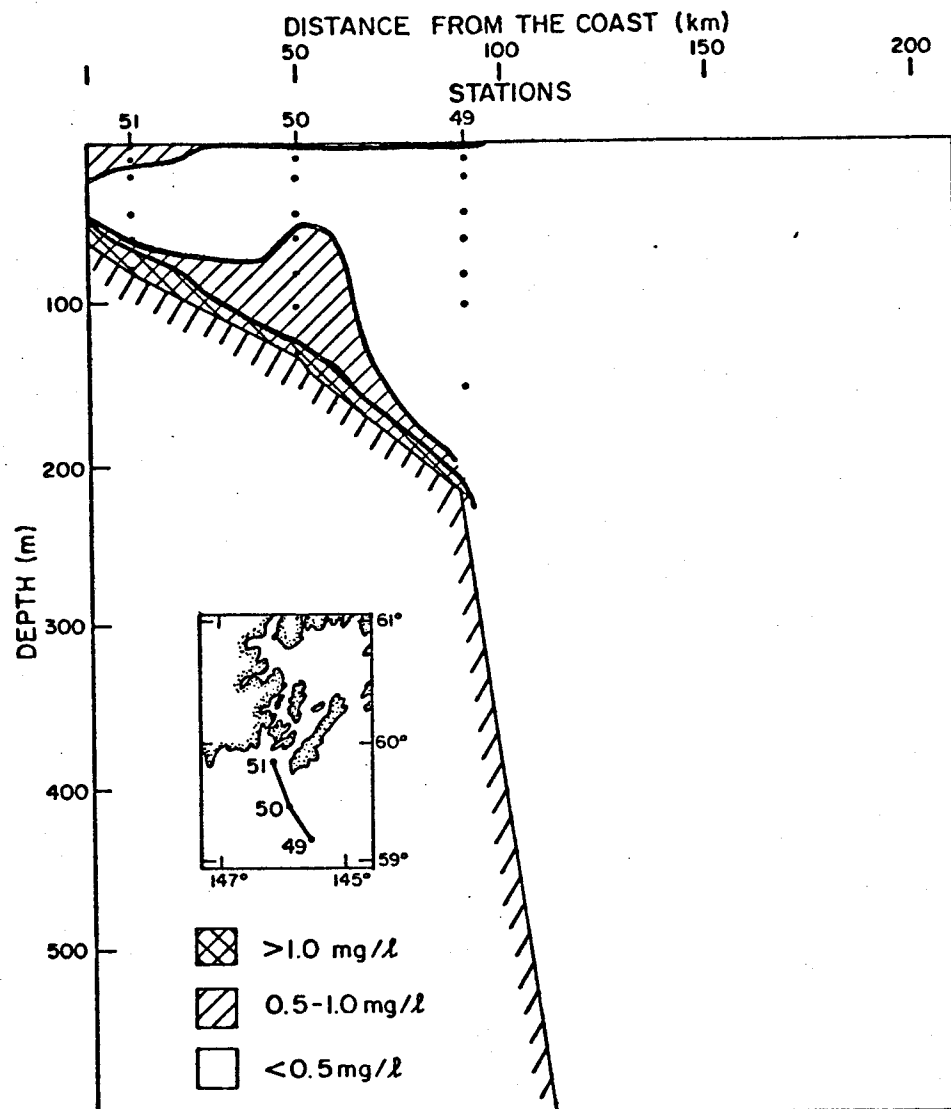


Figure 23. Vertical cross section of the distribution of total suspended matter for stations 49 thru 51 in the northeastern Gulf of Alaska (Cruise RP-4-Di-75C-I, 21 Oct.-10 Nov., 1975).

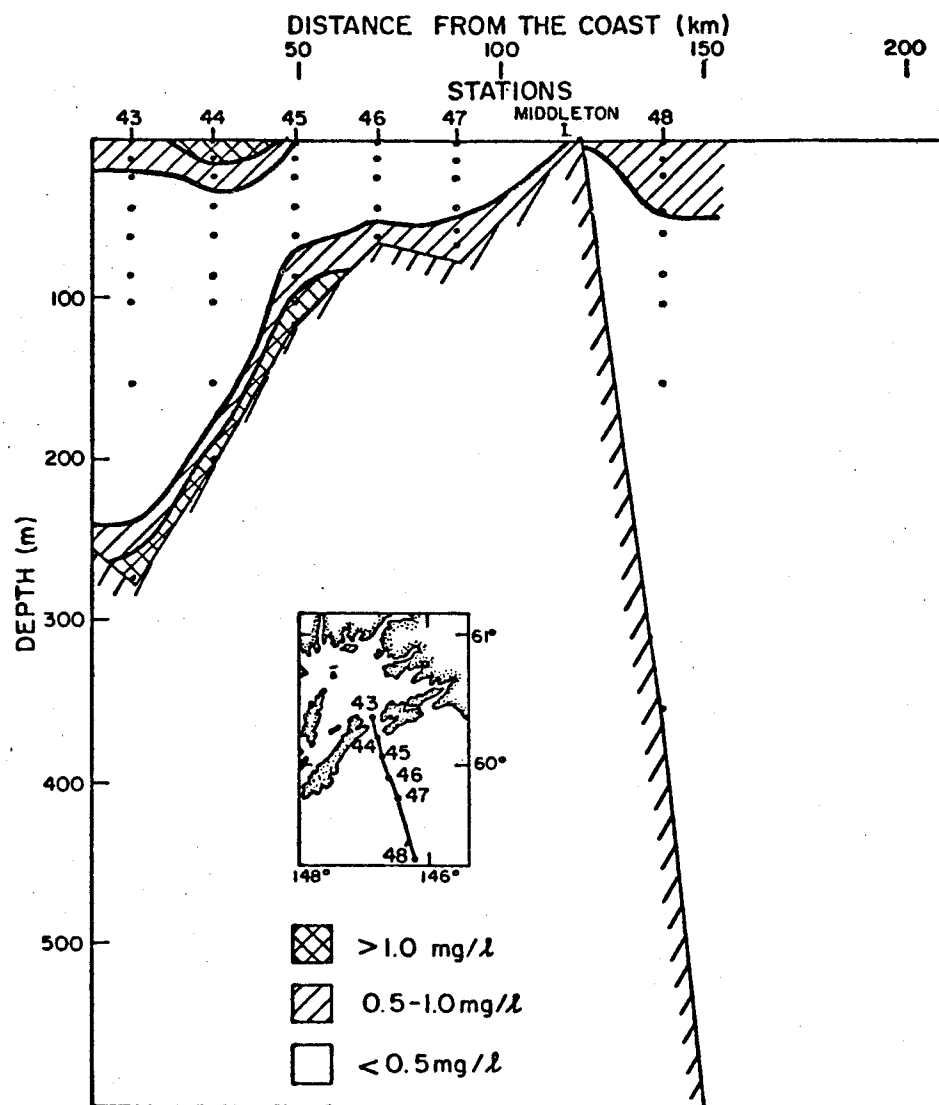


Figure 24. Vertical cross section of the distribution of total suspended matter for stations 43 thru 48 in the northeastern Gulf of Alaska (Cruise RP-4-Di-75C-I, 21 Oct.-10 Nov., 1975).

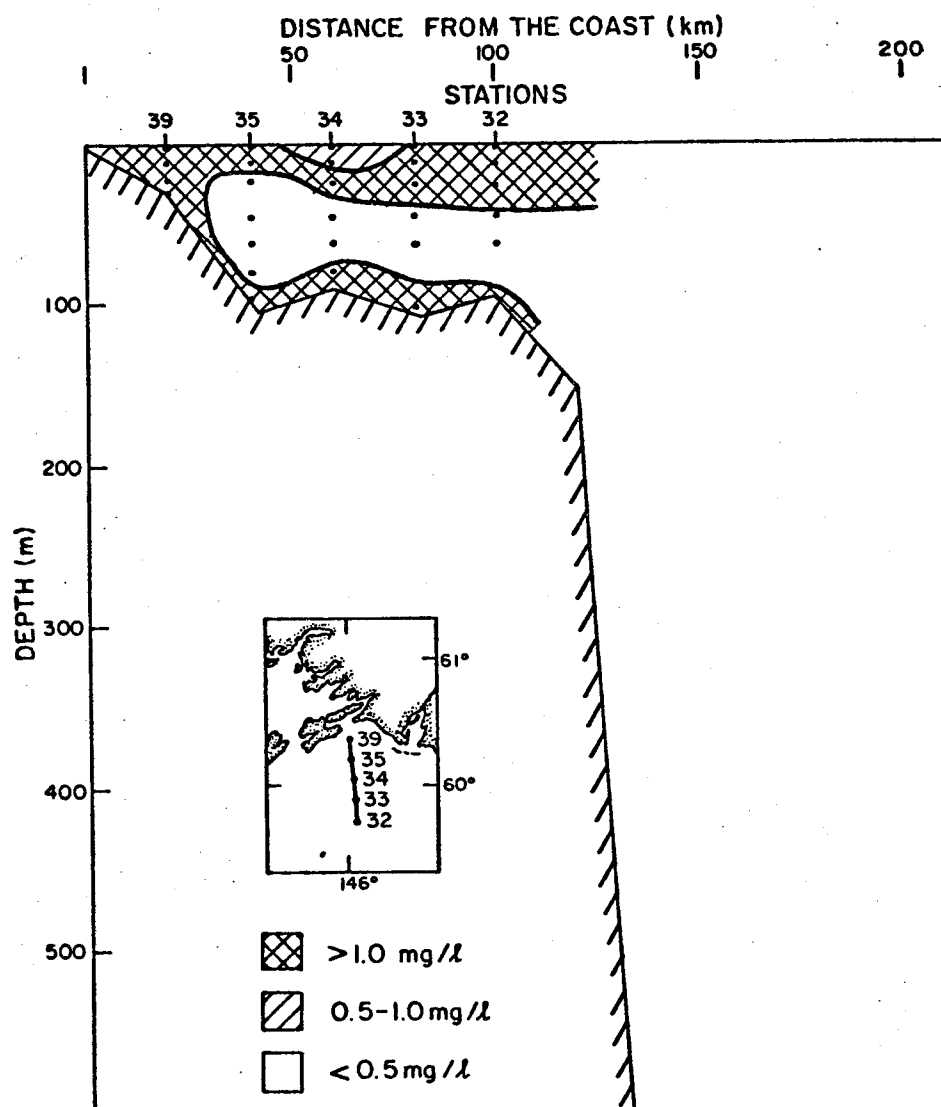


Figure 25. Vertical cross section of the distribution of total suspended matter for stations 32 thru 35 and station 39 in the northeastern Gulf of Alaska (Cruise RP-4-Di-75C-I, 21 Oct.-10 Nov., 1975).

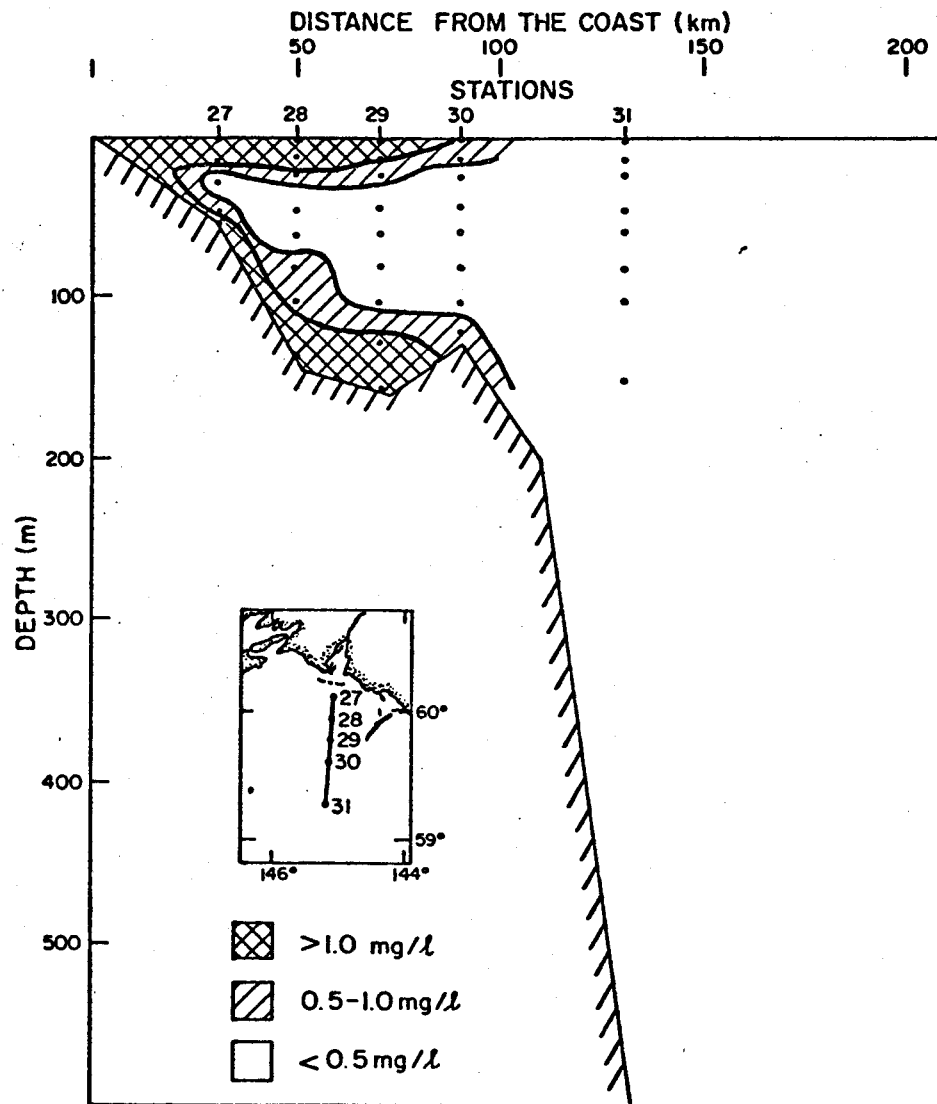


Figure 26. Vertical cross section of the distribution of total suspended matter for stations 27 thru 31 in the northeastern Gulf of Alaska (Cruise RP-4-Di-75C-I, 21 Oct.-10 Nov., 1975).

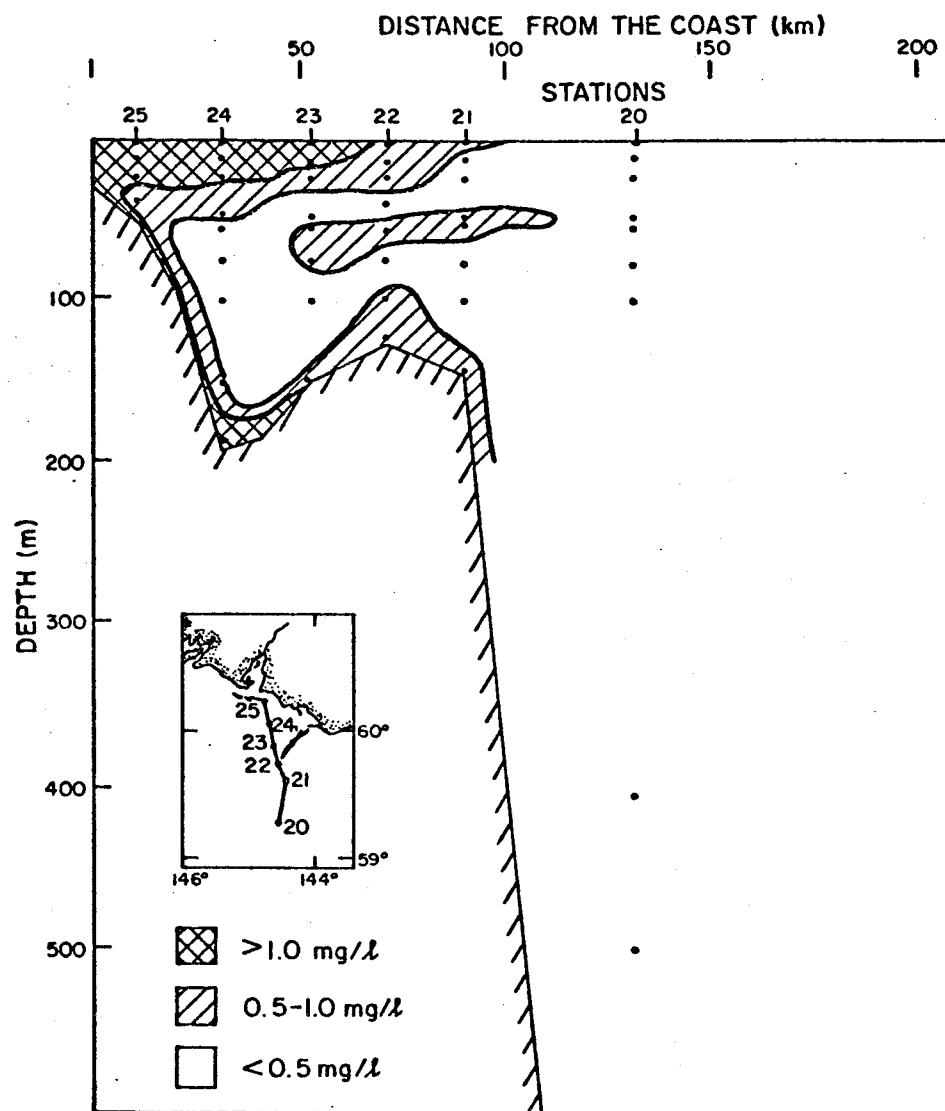


Figure 27. Vertical cross section of the distribution of total suspended matter for stations 20 thru 25 in the northeastern Gulf of Alaska (Cruise RP-4-Di-75C-I, 21 Oct.-10 Nov., 1975).

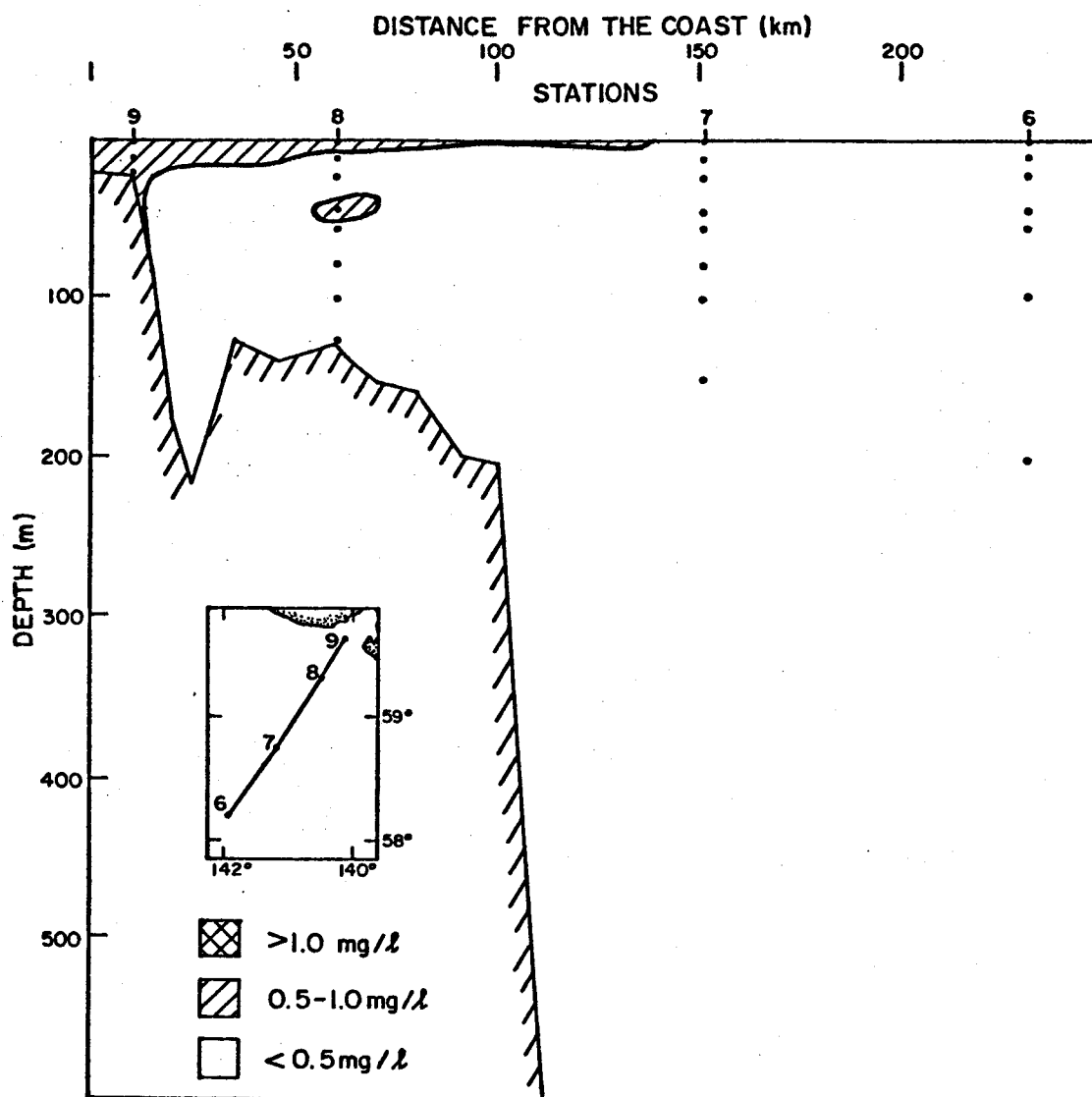


Figure 28. Vertical cross section of the distribution of total suspended matter for stations 6 thru 9 in the north-eastern Gulf of Alaska (Cruise RP-4-Di-75C-I, 21 Oct.-, 10 Nov., 1975).

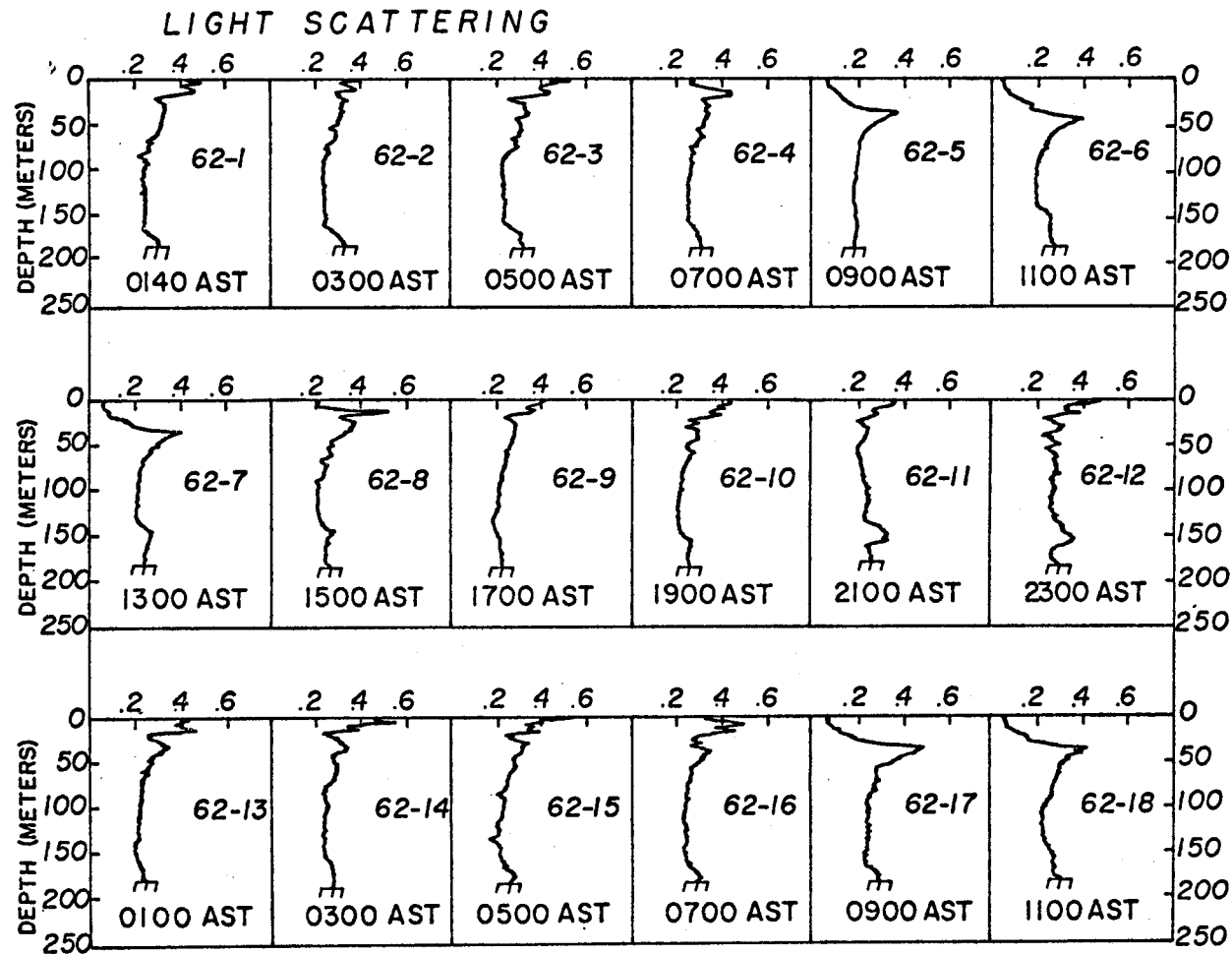


Figure 29. Light scattering profiles for a 36 hour time-series experiment at station 62 in the northeastern Gulf of Alaska (November 5-6, 1975). The light scattering values are reported as a frequency (kHz). However, in order to conserve space, the first two digits of the frequency (14) have been removed from the figure.

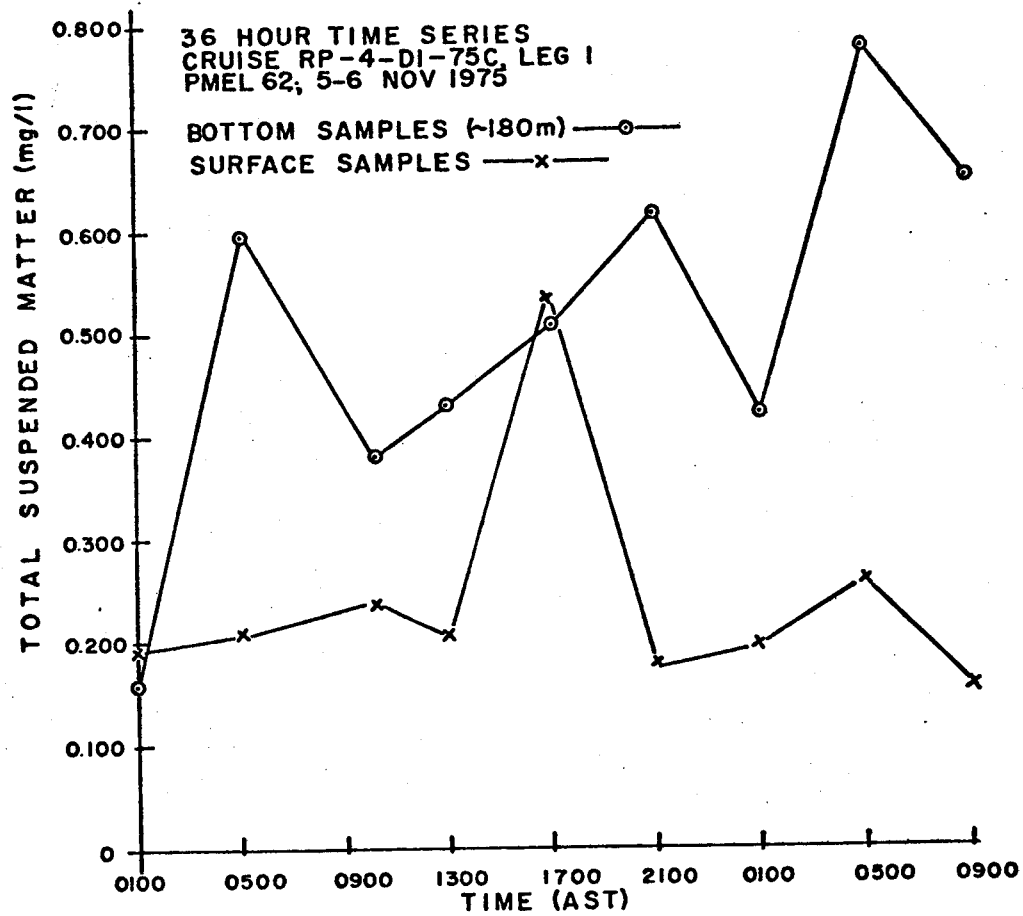


Figure 30. Temporal variability of total suspended matter at the surface and 5 meters above the bottom at station 62 in the northeastern Gulf of Alaska (November 5-6, 1975).

VIII. Conclusions - Southeastern Bering Shelf

Although most of the results of the suspended matter program in the southeastern Bering Shelf are still somewhat preliminary, there are several important conclusions which should be considered to be pertinent to the problems of oil development in the Bristol Bay region. These conclusions are listed below.

1. The surface suspended matter distributions appear to follow the general pattern of circulation in Bristol Bay. Suspended material from the northern rivers is generally carried to the west and southwest by the counterclockwise currents.
2. Large plumes of suspended matter can be seen extending to the southwest from Cape Newenham and to the west from Kuskokwim Bay. Apparently these plumes represent sedimentary material derived from the Kvichak, Nushagak and Kuskokwim Rivers.
3. Suspended material of marine origin is carried into Bristol Bay along the northern coast of the Alaska Peninsula.
4. Sharp increases in suspended matter concentrations near the bottom indicate that resuspension of bottom sediments may be occurring.

Conclusions - Gulf of Alaska

The most significant conclusions of the particulate matter program in the Gulf of Alaska are listed below.

1. The distribution of suspended matter at the surface appears to follow the general pattern of circulation in the Gulf of Alaska. East of Kayak Island sedimentary material, which

is discharged along the coast, is quickly deflected to the west by the westward flowing currents. This material is carried to the west along the coast until it reaches Kayak Island where it is deflected to the southwest and is trapped by a seasonal clockwise gyre.

2. Sedimentary material from the Copper River is carried to the northwest along the coast until it reaches Hinchinbrook Island where a portion of the material passes into Prince William Sound and the remaining material is carried to the southwest along the southwestern coast of Montague Island.
3. A bottom nepheloid layer is present throughout most of the Gulf. The height of the bottom nepheloid layer appears to be dependent upon the bottom topography and the currents.
4. Studies of the temporal variability of suspended matter near the bottom indicate that resuspension processes may be occurring.
5. There is a significant bottom nepheloid layer in Prince William Sound. The top of the nepheloid layer is at about the same depth as the sill depth of Hinchinbrook Entrance. The presence of this nepheloid layer might be related to bottom water renewal in the Sound.

IX. Needs for Further Study - Southeastern Bering Shelf

The following recommendations for future studies with respect to the suspended matter program in the southeastern Bering Shelf are presented below.

1. The suspended matter distributions studies should be extended into the area northwest of Nunivak Island. This will provide information about the fate of the sedimentary material that is discharged into Bristol Bay from the northern rivers.
2. Studies of the processes that control sediment resuspension and redistribution should be emphasized. However, these studies should be integrated with the physical oceanography program in such a manner that the effect of waves, storms, tides and permanent currents can be evaluated.
3. Studies of the interaction of oil with suspended matter from the Bristol Bay area should be initiated. This should include studies of the nature and quantity of oil that is adsorbed onto the surfaces of the suspended particles, their sedimentation characteristics and dissolution processes.

Needs for Further Study - Gulf of Alaska

The following recommendations for future studies with respect to the suspended matter program in the Gulf of Alaska are presented below.

1. The area between Kayak Island and Montague Islands needs further study. The circulation patterns are not well understood and seasonal variations may be significant. There is

some evidence from ERTS imagery and this report that a large clockwise gyre is located southwest of Kayak Island.

This gyre appears to trap suspended matter from either side of Kayak Island and carry it to the west. At present, we do not know to what extent this is a seasonal feature in the Gulf. Nor can we determine to what extent the gyre is able to concentrate suspended matter in the region west of Kayak Island. We need to have a higher density of sampling stations in the region west of Kayak Island in order to fully understand the processes of sediment transport by the gyre.

2. The regions on either side of Tarr Bank (Kayak Trough and Hinchinbrook Sea Valley) show evidence for relatively broad bottom nepheloid layers (Figs. 23 and 26). These regions are also areas of maximum sediment accumulation (Bruce Molnia, personal communication, 1976). Apparently there is a relationship between the formation of a broad bottom nepheloid layer and the sedimentation process. This would be an ideal location to study the dynamics of sedimentation.
3. Studies of the processes that control sediment resuspension and redistribution should be emphasized. However, these studies should be integrated with physical oceanography programs in such a manner that the effects of waves, storms, tide and permanent currents can be evaluated.

4. Studies of the interaction of oil with suspended matter from the Gulf of Alaska should be initiated. This should include studies of the nature and quantity of oil that is adsorbed onto the surfaces of the suspended particles, their sedimentation characteristics and dissolution processes.

X. Summary of 4th Quarter Operations

A. Task Objectives

The primary objective of the particulate matter program in the Gulf of Alaska and Bering Sea is to determine the seasonal variations in the distribution, composition and transport of suspended matter. Other objectives include: (1) the high frequency (hourly) variability in the distribution of suspended matter and (2) an investigation of the role of resuspension processes as a mechanism for redistribution of materials.

B. Field Activities from January 1 - April 1, 1976

No field activities were conducted during the fourth quarter.

C. Laboratory Activities from January 1 - April 1, 1976

During the fourth quarter, most of our laboratory work has been concerned with the analysis of the samples from the first two cruises. We have completed the weight determinations from the samples from both cruises. We have also completed the particulate carbon and nitrogen analyses from the first cruise (Bristol Bay) and work is proceeding on the samples from the second cruise (Gulf of Alaska). The completed data are presently being compiled according to the format designed by EDS/NODC and will be submitted to the project office by the end of the next quarter.

Since we received our X-ray fluorescence equipment in our laboratory only two months ago, most of our efforts have been devoted to the setup and calibration of the equipment. Consequently, very little information about the major and trace element composition of the particulate matter is available at this time.

D. Laboratory Procedures

The major (Mg, Al, Si, K, Ca, Ti, and Fe) and trace (Cr, Mn, Cu, Zn, and Pb) inorganic elemental chemistry of the particulate matter is being determined by X-ray fluorescence. This technique has been used successfully for the determination of the major inorganic elements in particulate matter in coastal and deep water environments and the methods are fairly well established (Cann and Winter, 1971, and Baker and Piper, 1975). Recent advances in this field have lowered the minimum detectable limits to such an extent that many trace elements in particulate matter can be analyzed routinely.

In order to obtain standards with similar compositions as the samples, Baker and Piper (1975) chose the USGS standard rocks W-I, AGV-I and BCR-I to calibrate their X-ray fluorescence system to determine the major element composition of suspended matter from the Washington Continental Shelf. We have adopted their basic techniques to analyze the major element composition of suspended matter from the Gulf of Alaska and southeastern Bering Shelf. Although the details of the techniques have been described adequately elsewhere, a brief description will be presented below.

Radiation from a silver X-ray tube is used to obtain a monochromatic source of X-rays from a secondary target. Baker and Piper (op. cit.) used the K_{α} X-ray of S to analyze the light elements (Na, Mg, Al and Si) and the continuum from the X-ray tube to analyze for the heavier elements. We will use a combination of secondary targets

(S, Ge, Zr, and Mo) to analyze the particulate matter for both major and trace elements. The samples will be calibrated against the USGS standard rocks for major elements and the NBS glass standards (612 and 614) for trace elements.

The organic carbon and nitrogen content of suspended particulate matter has been shown to be a valuable indicator of terrestrial and marine sources of organic matter in the coastal waters of Alaska (Loder, 1971). Specifically, Loder and Hood (1972) have used the C/N ratio of particulate matter to distinguish between terrestrial, glacial, estuarine and marine-derived sources of organic matter.

Particulate organic carbon and nitrogen are being analyzed by the micro-Dumas combustion method, employing a Hewlett-Packard® Model 185B C-H-N analyzer (Sharp, 1974). Particulate matter has been separated from seawater by vacuum filtration (precombusted 0.4 μm silver filters [Sharp, 1974; Gordon and Sutcliffe, 1974]) and the carbon and nitrogen combusted to CO_2 and N_2 . After separation by standard gas-solid chromatography (GS), the gases are quantitatively determined by thermal conductivity (TC). Sample analysis time is about 10 minutes.

Standardization will be effected with cyclohexanone-2, 4-dinitrophenylhydrozone, acetanilide (Sharp, 1974) and L-cystine; the latter two are NBS standards. These results will be corroborated by direct GC analysis of CO_2 and N_2 .

E. Sampling Protocol

No field samples were taken during the fourth quarter.

F. Data Analysis

The data from the first two cruises are being reduced and compiled according to the format designed by EDS/NODC. These data will be submitted to the project office by the end of the next quarter.

G. Results

The results of our field activities during the first two cruises are graphically displayed and summarized in section VI of this report and will not be reproduced here.

References

- Baker, E. T. and D. Z. Piper, Suspended Particulate Matter: Collection by pressure filtration and elemental analysis by thin film X-ray fluorescence, submitted to Deep Sea Research (1975).
- Banse, K., On the interpretation of data for the carbon to nitrogen ratio of phytoplankton. Limnology and Oceanography, 19 (4), 695-699 (1974)
- Bogdanov, Y. A., Suspended organic matter in the Pacific. Oceanology 5(2): 77-85 (1955).
- ✓ Burbank, D. C., Suspended sediment transport and deposition in Alaskan coastal waters. M.S. Thesis, University of Alaska, Fairbanks, Alaska (1974).
- Cann, J. R. and C. K. Winter, X-ray fluorescence analysis of suspended sediment in seawater, Marine Geology 11: M33-M37 (1971).
- Carlson, P. R., T. J. Conomos, J. Janda, and D. H. Peterson, Principal sources and dispersal patterns of suspended particulate matter in nearshore surface water of the northeast Pacific Ocean, U.S.G.S. Final Report to the Goddard Space Flight Center (1975).
- El Wardani, S. A., Total and organic phosphorus in waters of the Bering Sea, Aleutian Trench and Gulf of Alaska, Deep Sea Research, 7: 201-207 (1960).
- Feely, R. A., Chemical characterization of the particulate matter in the near bottom nepheloid layer of the Gulf of Mexico, Dept. of Oceanography, Texas A&M Univ. Ref. 74-4-T (1974).

- Feely, R. A., Major element composition of the particulate matter in the near bottom nepheloid layer of the Gulf of Mexico, Mar. Chem., 3: 121-156 (1975).
- ✓ Galt, J. A. and T. C. Royer, Physical oceanography and dynamics of the NE Gulf of Alaska. Submitted for publication (1976).
- Gordon, D. D. Jr., and W. H. Sutcliffe, Jr., Filtration of seawater using silver filters for particulate nitrogen and carbon analysis, Limnology and Oceanography, 19(6): 989-993 (1974).
- Hebard, J. F., Currents in southeastern Bering Sea and possible effects upon king crab larvae. U.S. Fish and Wildlife Service Special Report No. 293. Washington, D.C. (1959).
- Krauskopf, K. B., Introduction to Geochemistry. McGraw-Hill, New York, N.Y., 721 pp (1965).
- Loder, T. C. and D. W. Hood, Distribution of organic carbon in a glacial estuary in Alaska, Limnology and Oceanography, 17(3), 349-355 (1972).
- ✓ Loder, T. C., III, Distribution of dissolved and particulate organic carbon in Alaskan polar, subpolar and estuarine waters. Ph.D. Thesis Inst. Mar. Sci., University of Alaska, 1971.
- Menzel, D. W. and R. F. Vaccaro, The measurement of dissolved organic and particulate carbon in seawater, Limnology and Oceanography 9: 138-142 (1964).
- Meyers, P. A. and J. G. Quinn, Association of hydrocarbons and mineral particles in saline solution, Nature, 224: 23-24 (1973).

- Muench, R. D., The circulation of Prince William Sound. ERTS Project 110-1, Final Report to NASA, 13 Mar 1974. Inst. Mar. Sci., University of Alaska, Fairbanks, Alaska (1974).
- Muench, R. D. and C. M. Schmidt, Variations in the Hydrographic Structure of Prince William Sound. Sea Grant Report R75-1, Institute of Marine Science, University of Alaska, Fairbanks, Alaska (1975).
- Nelson, C. H., Late holocene sediment dispersal in northeastern Bering Sea. In U.S. Geological Survey Alaska Program, 1974. (Circ. 700) (C. Carter, Ed.), U.S. Geol. Survey, Reston, Virginia (1974).
- Price, N. B. and S. E. Calvert. A study of the geochemistry of suspended particulate matter in coastal waters. Mar. Chem, 1: 169-189 (1973).
- Reimnitz, E., Late Quaternary history and sedimentation of the Copper River Delta and vicinity, Alaska (unpublished dissertation).
Univ. Calif., La Jolla, 225 pp.
- Riley, G. A., Particulate organic matter in seawater. In: R. S. Russel and M. Young (Editors), Advances in Marine Biology. Academic Press, New York, N.Y., pp 1-118 (1970).
- Sharma, G. D., Graded sedimentation on the Bering Shelf. 24th IGC. Section 8 (1972).
- Sharma, G. D., F. F. Wright, J. J. Burns and D. C. Burbank, Sea surface circulation, sediment transport, and marine mammal distribution, Alaska Continental Shelf, Report prepared for the National Aeronautics and Space Administration (1974).
- Sharma, G. D., Contemporary depositional environment of the eastern Bering Sea. In Oceanography of the Bering Sea (D. W. Hood and E. J. Kelley, eds.), Institute of Marine Science Occasional Publication No. 2, Univ. of Alaska, Fairbanks, Alaska, pp 517-552 (1974).

- Sharp, J. H., Improved analysis for "particulate" organic carbon and nitrogen from seawater, Limnology and Oceanography, 19(6): 984-989 (1974).
- Spencer, D. W. and P. L. Sachs, Some aspects of the distribution, chemistry and mineralogy of suspended matter in the Gulf of Maine. Marine Geol., 9, 117-136 (1970).
- Sternberg, R. W., E. T. Baker, D. A. McManus, S. Smith, and D. R. Morrison, An integrating nephelometer for measuring particle concentrations in the deep sea, Deep Sea Research, 21: 887-892 (1974).
- Tsunogai, Y., M. Nozaki, M. Minagawa, and S. Yamamoto, Dynamics of particulate material in the ocean, pp. 175-189. In "Oceanography of the Bering Sea", edited by D. W. Hood and E. J. Kelley, Institute of Marine Science, University of Alaska, Fairbanks, Alaska (1974).

47 mm diameter 0.4 μm Nuclepore[®] filters. The results are presented in Table 3. The average relative standard deviation for the replicate studies is 7.8%. Since the precision of our weighing techniques (based on replicate studies of standard reference filters) is less than 1%, most of the variability in the data appears to be due to the inhomogeneity of particulate matter in the water sample. This suggests that one must be extremely careful when comparing small differences in the suspended matter distributions. For the Gulf of Alaska, only differences greater than ± 0.13 mg/L are considered to be significant at the 95% confidence level.

In order to obtain some information about the high frequency (hourly) time variations in the distribution of suspended matter, two 36-hour time series experiments were conducted at stations 46 and 62. Water samples were collected every 4 hours from the surface and 5 meters above the bottom. The results of these experiments are also given in Table 3. The relative standard deviations of the data from the two time-series stations are significantly higher than the relative standard deviations from the replicate studies. This suggests that high frequency time variations, which may be due to the action of waves, tides and local variations in productivity, are highly significant and must be carefully considered if seasonal particulate matter distribution maps are to have any significance. Using a mean value of 1.02 mg/L for total suspended matter at

431

Cont from p. 4⁵¹~~40~~

the surface and the maximum relative standard deviation of 47.6% from the time series at station 62 a value of ± 0.77 mg/L is significant at the 95% confidence level for seasonal variations. For these reasons, the contour intervals on the suspended matter distribution maps have been limited to ± 1.0 mg/L.

36-Hour Time Series

In order to obtain some information about the processes that control resuspension and redistribution of bottom sediments along the shelf, a 36-hour time series was conducted at station 62 on November 5 - 6, 1975. Station 62 is located southeast of Icy Bay and has been used as the site for extensive measurements of bottom currents by the physical oceanographers at PMEL.

Light scattering profiles were obtained every two hours and water samples at the surface and 5 meters above the bottom were collected and filtered for suspended matter every four hours. Figure 29 shows the light scattering profiles and Figure 30 shows the suspended matter distributions for the 36-hour experiment. Although this experiment was only intended to be a preliminary investigation prior to the long-term time series which is to be carried out in April of this year, some of the preliminary data have proved to be quite interesting. The near-bottom suspended matter distributions show maxima that are roughly repeated every twelve hours. The light scattering profiles also show a corresponding pattern of increasing concentrations near the bottom which

appears to have the same general periodicity. At their maximum intensification, the profiles begin to increase at about 20-30 meters above the bottom. Presumably, the increase in light scattering and suspended matter concentrations near the bottom are due to resuspension of bottom sediments by bottom currents. At station 62, the Alaskan Stream comes in contact with the sea floor and tends to follow the bathymetry and moves in a northwesterly direction. The major axis of the tidal ellipse at station 62 is also in a northwest-southeast direction (J. Schumacher, personal communication, 1975). One possible explanation of the data from the time series may be that when the northwesterly component of the tides is superimposed on the Alaskan Stream the combined effect of the two currents is just sufficient to erode bottom sediments. This would suggest that resuspended sediments might have a net transport to the northwest.

At this point, these conclusions must be considered to be preliminary at best. We are in the process of deploying a current meter nephelometer array at station 62 which, hopefully, will provide approximately two months of data on the temporal variability of suspended matter near the bottom.

B. Elemental Chemistry of the Particulate Matter

Since we received our X-ray fluorescence equipment in our laboratory only two months ago, most of our efforts have been devoted to the setup and calibration of the equipment. Consequently, little information about the major and trace element composition of the particulates from the Gulf of Alaska is available at this time. Therefore, the analytical results will be presented in a future report.

Table 3. Comparison of replicate samples collected in 10-liter Top-Drop Niskin[®] bottles and filtered through 47 mm diameter, 0.4 μ m Nuclepore[®] filters with samples collected every four hours during a 36-hour time series experiment.

| Station | Depth | Number of Replicates | TSM Mean (mg/L) | Std. Dev. | Rel. Std. Dev. |
|-----------------------------|-------|----------------------|-----------------|-----------|----------------|
| PMEL 1 | sfc | 4 | 0.510 | 0.029 | 0.057 |
| PMEL 5 | sfc | 4 | 0.495 | 0.089 | 0.179 |
| PMEL 9 | sfc | 3 | 1.241 | 0.099 | 0.079 |
| PMEL 10 | sfc | 4 | 2.728 | 0.162 | 0.059 |
| PMEL 16 | sfc | 3 | 0.635 | 0.023 | 0.036 |
| PMEL 17 | sfc | 4 | 2.211 | 0.044 | 0.020 |
| PMEL 39 | sfc | 4 | 3.482 | 0.123 | 0.035 |
| PMEL 51 | sfc | 4 | 0.465 | 0.075 | 0.161 |
| <u>TIME-SERIES STATIONS</u> | | | | | |
| PMEL 46 | sfc | 9 | 0.333 | 0.066 | 0.199 |
| PMEL 62 | sfc | 9 | 0.238 | 0.113 | 0.476 |
| PMEL 46 | 60 m | 9 | 0.512 | 0.119 | 0.232 |
| PMEL 62 | 184 m | 9 | 0.504 | 0.181 | 0.359 |

435

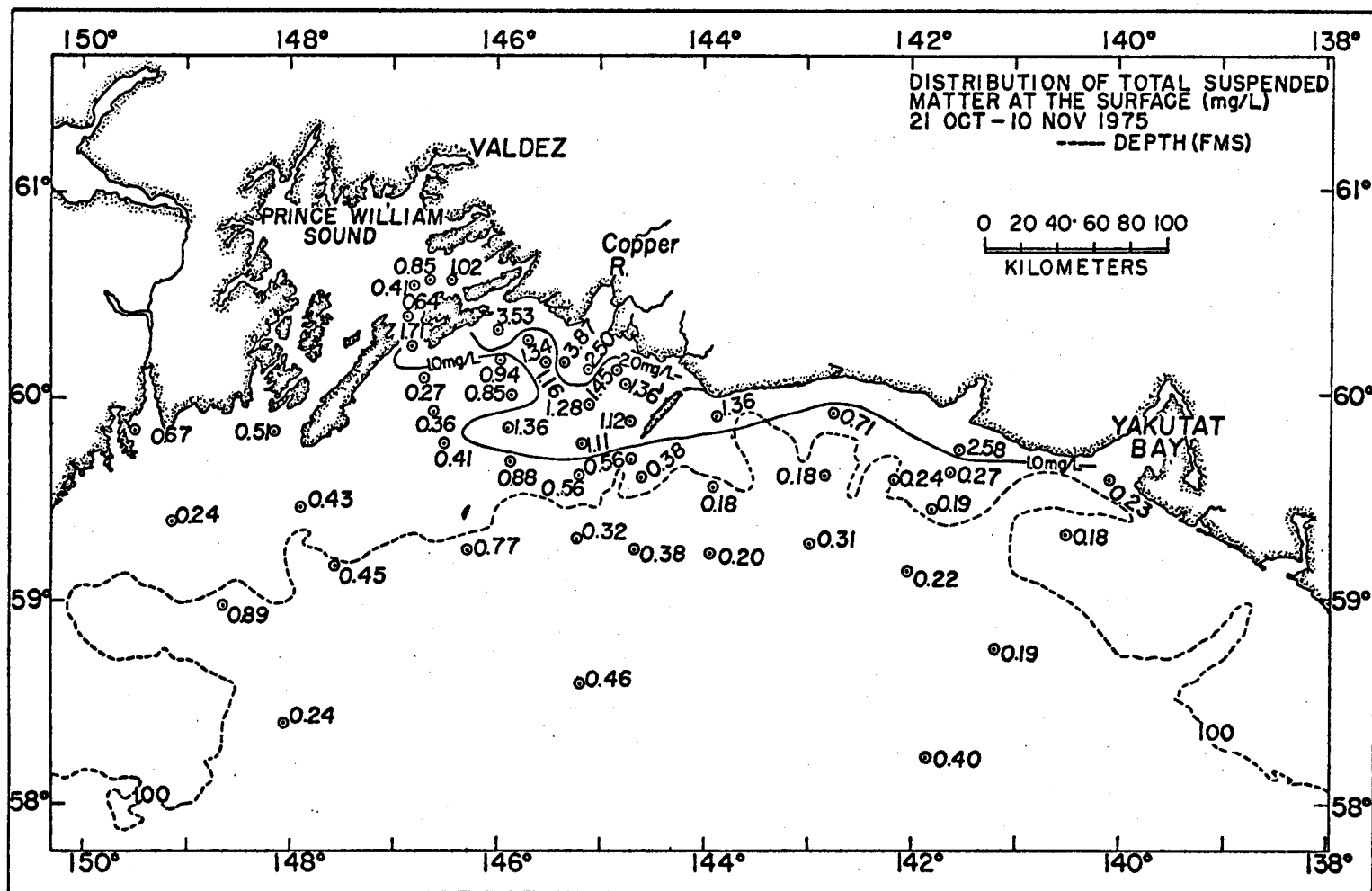


Figure 15. Distribution of total suspended matter at the surface in the northeastern Gulf of Alaska (Cruise RP-4-Di-75C-I, 21 Oct.-10 Nov., 1975).

436

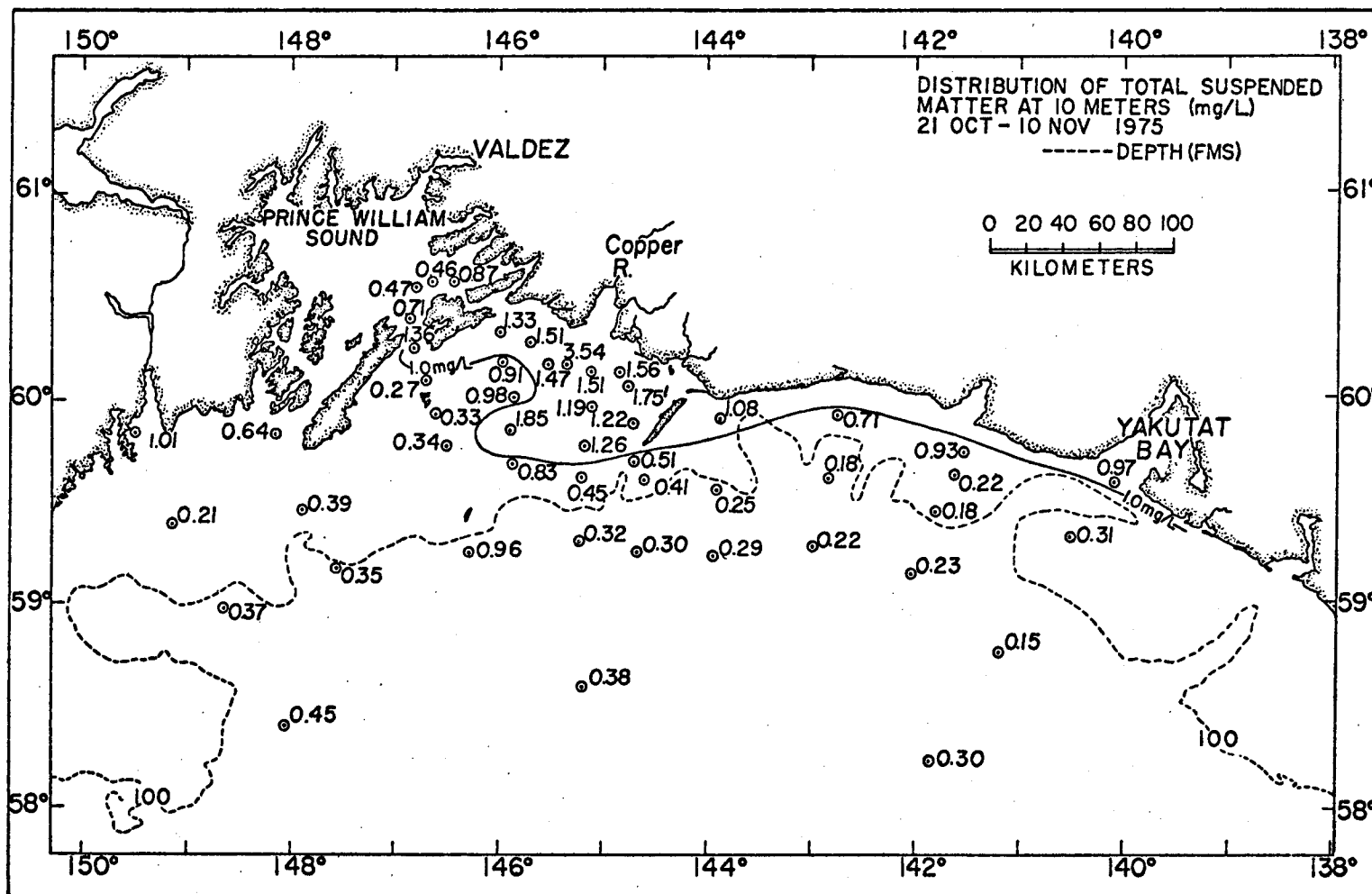


Figure 16. Distribution of total suspended matter at 10 meters in the northeastern Gulf of Alaska (Cruise RP-4-Di-75C-I, 21 Oct.-10 Nov., 1975).

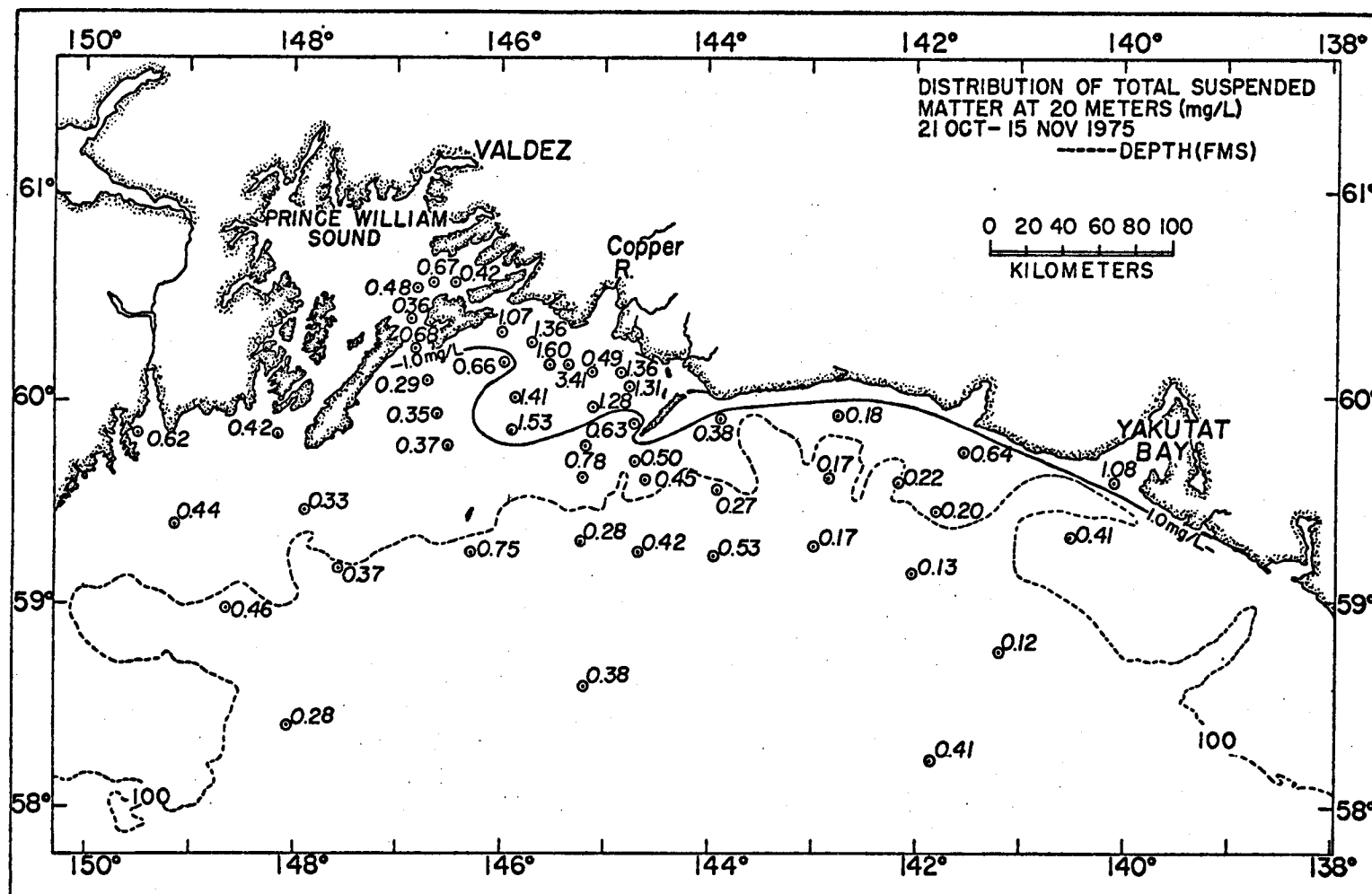


Figure 17. Distribution of total suspended matter at 20 meters in the northeastern Gulf of Alaska (Cruise RP-4-Di-75C-I, 21 Oct.-10 Nov., 1975).

438

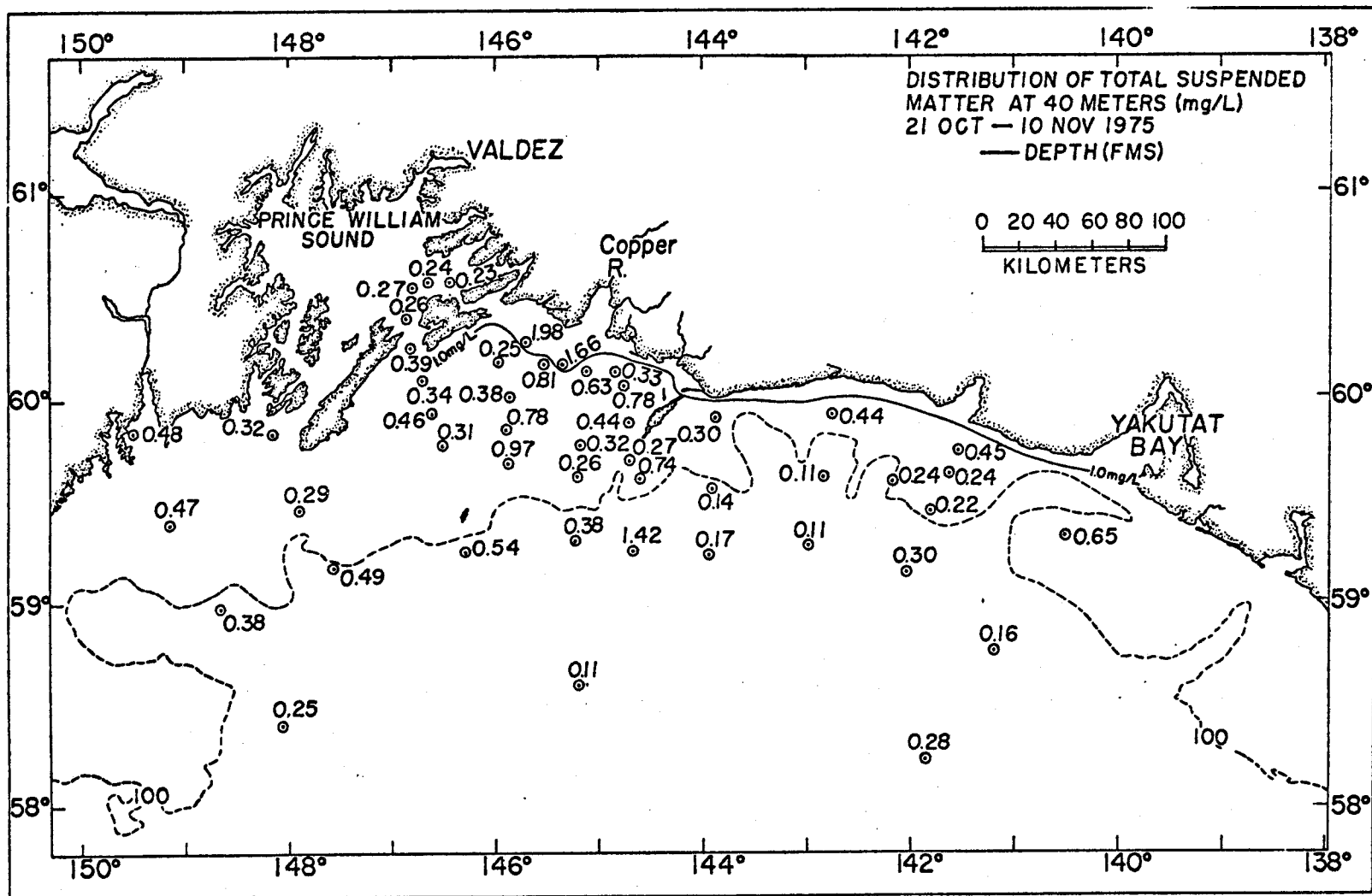


Figure 18. Distribution of total suspended matter at 40 meters in the northeastern Gulf of Alaska (Cruise RP-4-Di-75C-I, 21 Oct.-10 Nov., 1975).

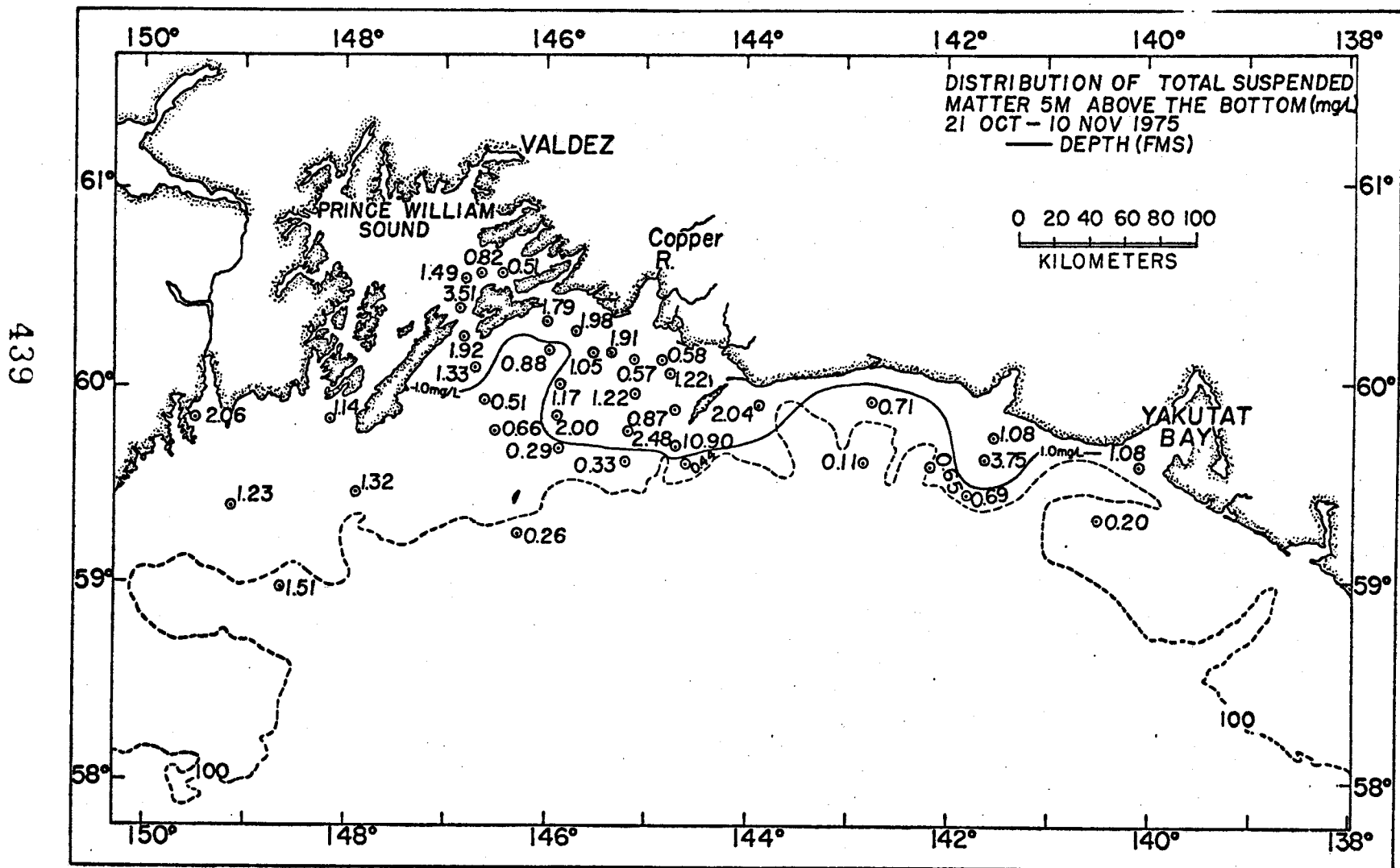


Figure 19. Distribution of total suspended matter at 5 meters above the bottom in the northeastern Gulf of Alaska. (Cruise RP-4-Di-75C-I, 21 Oct.-10 Nov., 1975).



Figure 20. ERTS-I image of the region between Montague Island and Kayak Island showing the large clockwise gyre southwest of Kayak Island. The image was obtained on August 14, 1973.

LIGHT SCATTERING PROFILES - GULF OF ALASKA CONTINENTAL SHELF

STATIONS 42-47 NEPHELOMETER SCALE #1 --- TEMPERATURE °C — LIGHT SCATTERING

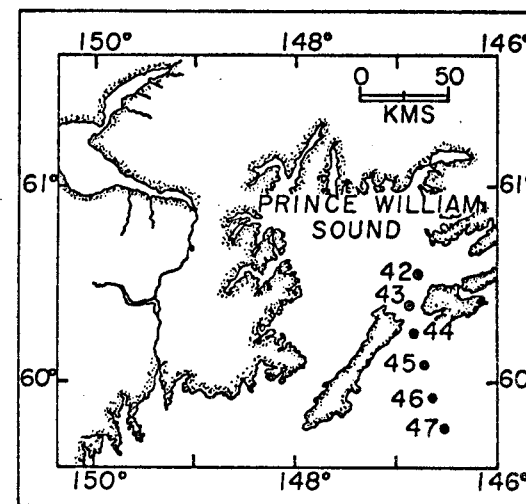
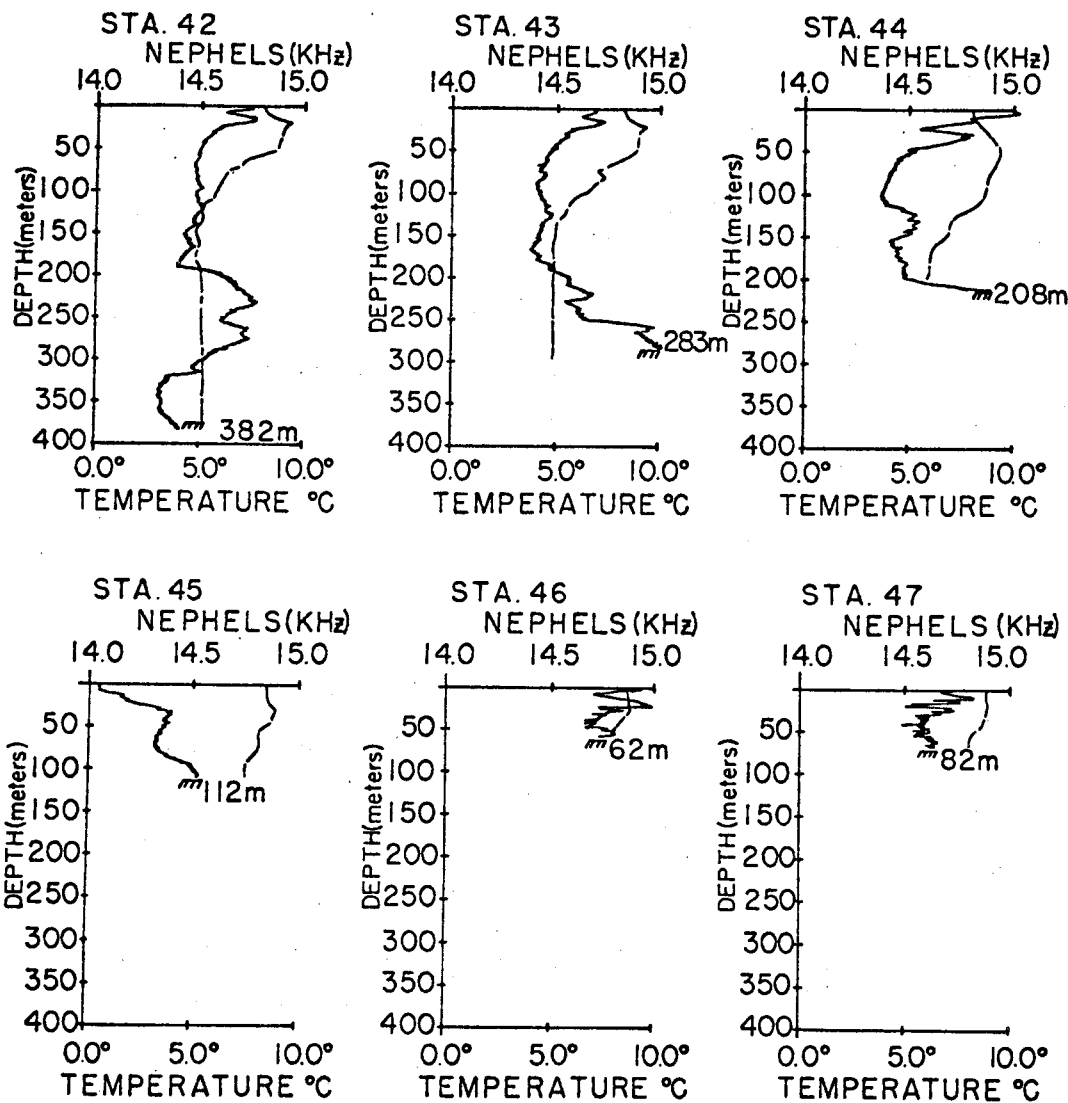


Figure 21. Light scattering and temperature profiles for a line of stations from Prince William Sound to Middleton Island.

Cont on p. 409

441

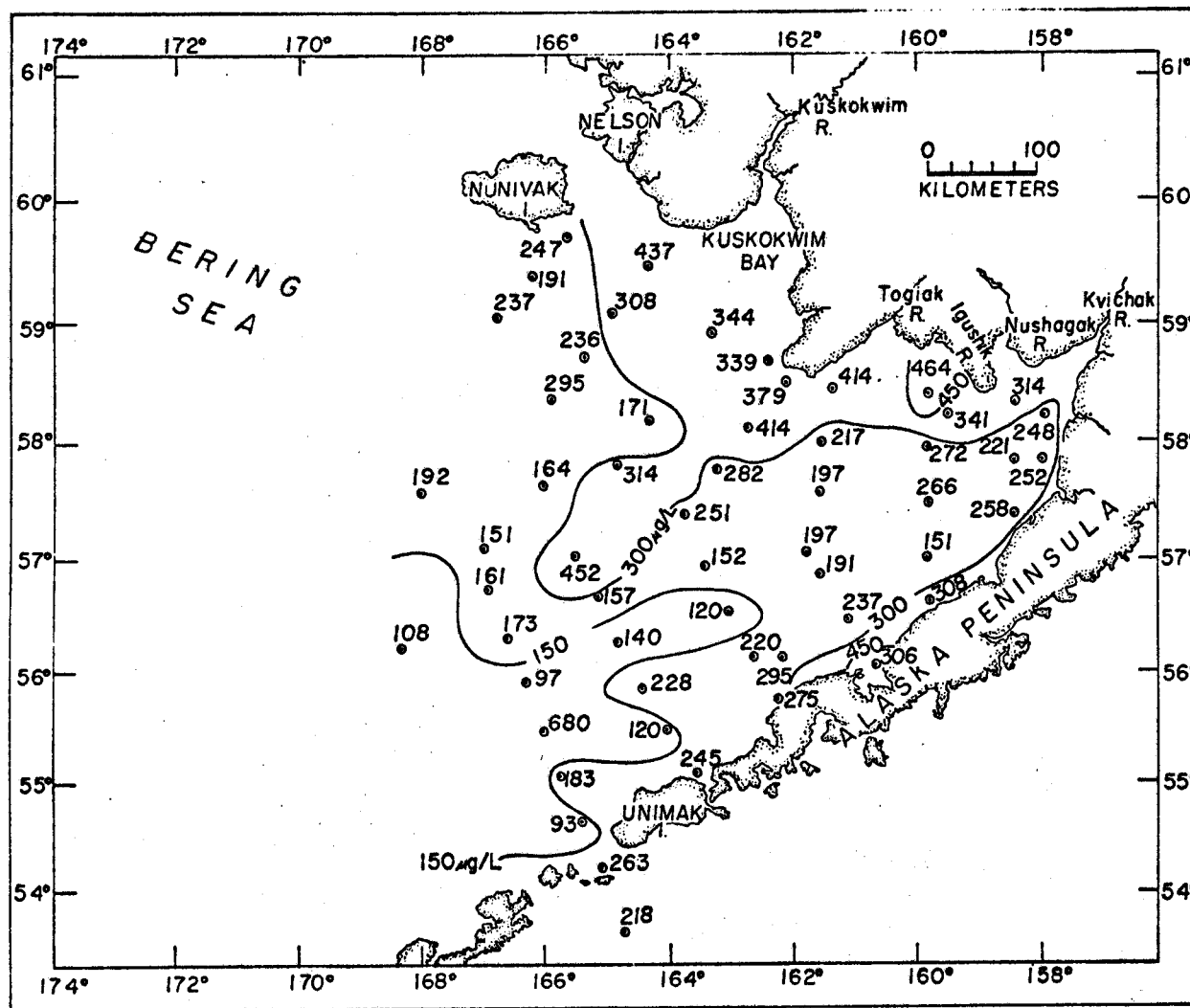


Figure 10. Distribution of particulate carbon at the surface in the southeastern Bering Shelf (Cruise RP-4-Di-75B-III, 12 Sept.-5 Oct., 1975).

Chart from 466
442

443

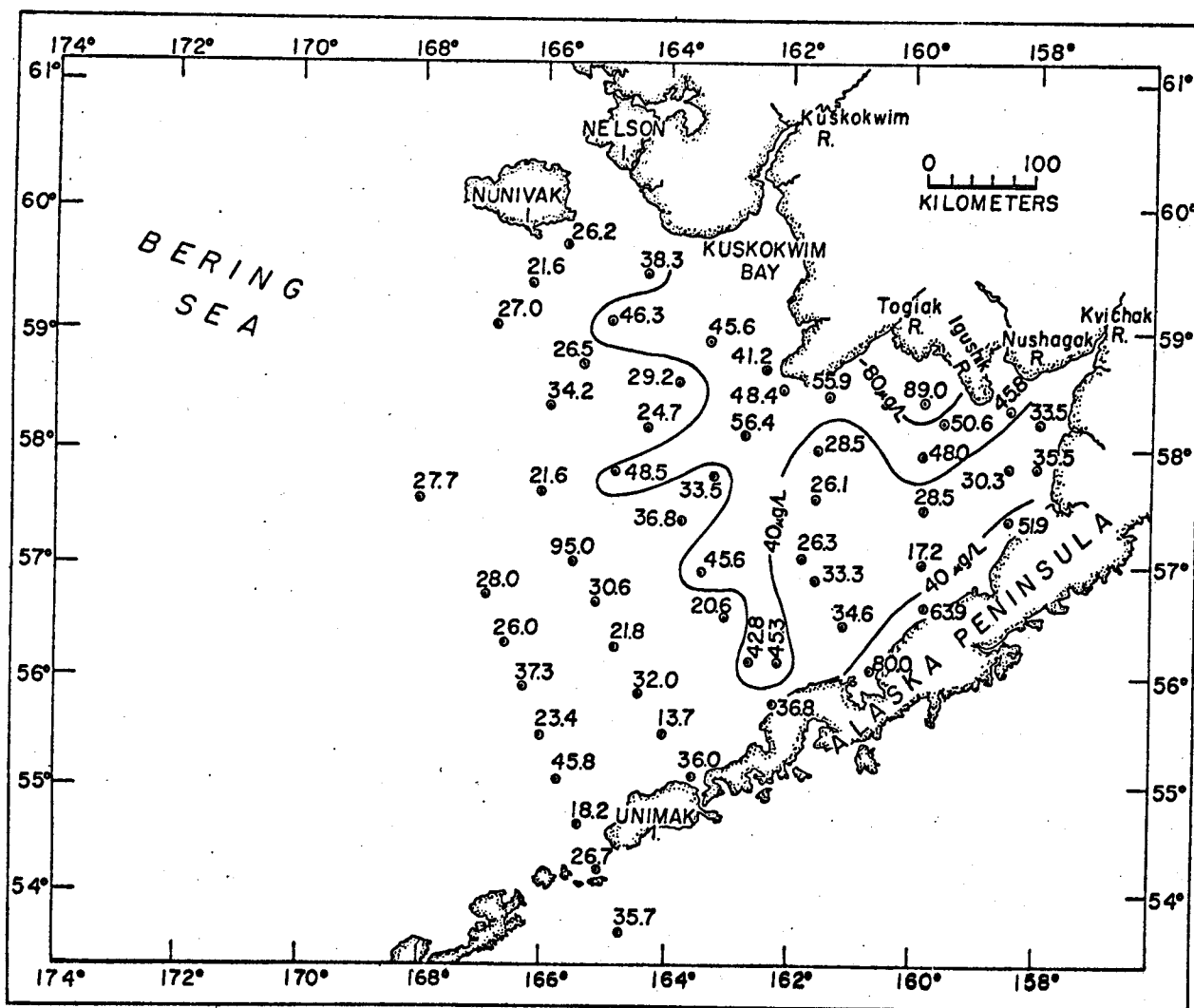


Figure 11. Distribution of particulate nitrogen at the surface in the southeastern Bering Shelf (Cruise RP-4-Di-75B-III, 2 Sept.-5 Oct., 1975)

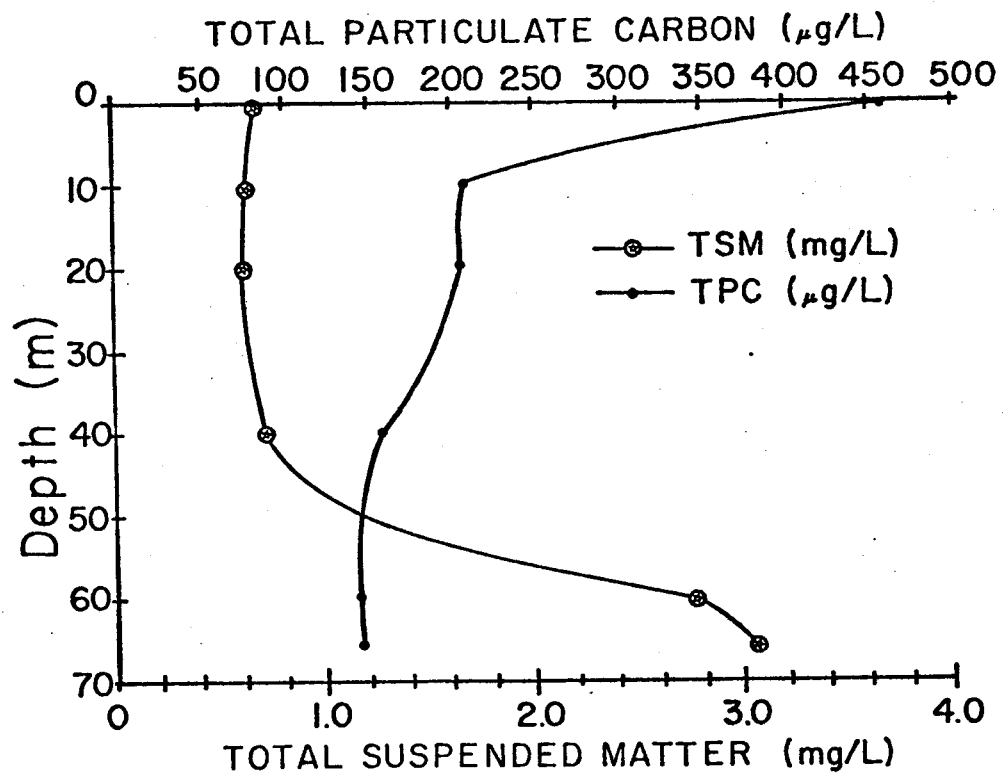


Figure 12. Vertical distribution of total suspended matter and particulate carbon at station 40 in the southeastern Bering Shelf (Cruise RP-4-Di-75B-III, 12 Sept.-5 Oct., 1975).

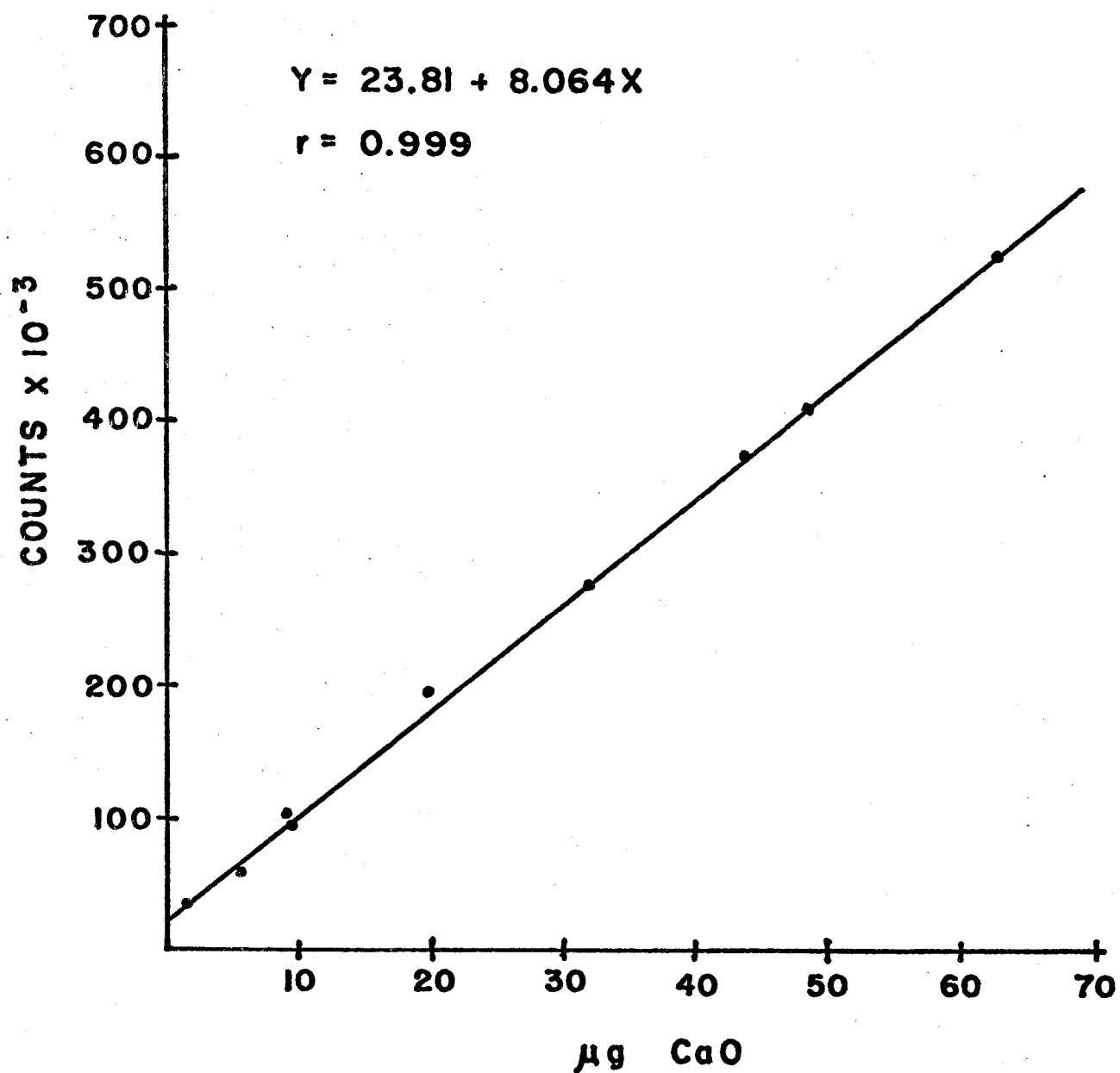


Figure 13. Calibration curve for CaO using a finely ground USGS W-I rock as the standard reference material.

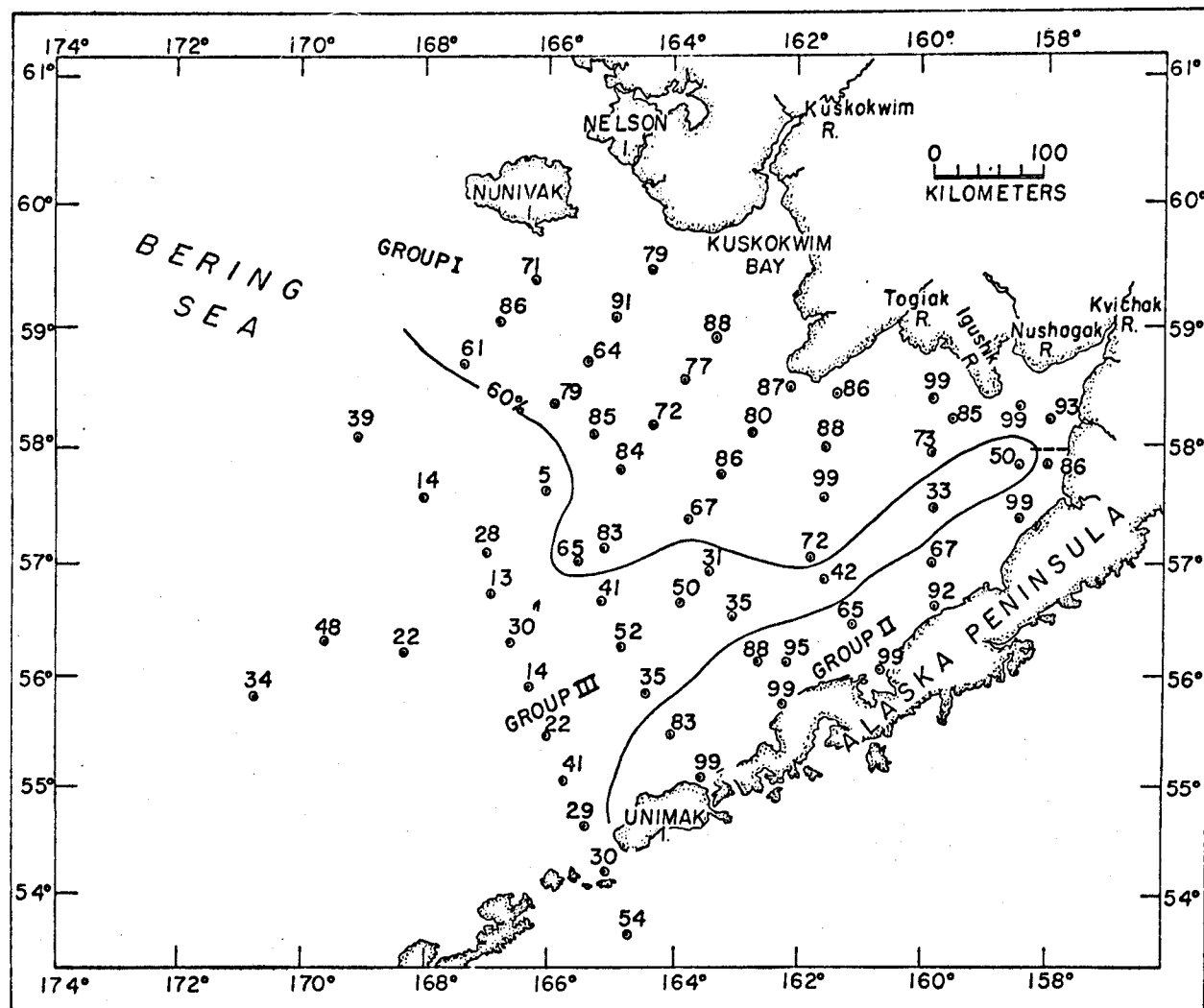


Figure 14. Map of the surface distribution of the percentage of total suspended matter that is due to the sum of the major inorganic elements expressed as oxides (Cruise RP-4-Di-75B-III, 12 Sept.-5 Oct., 1975).

Northeastern Gulf of Alaska

A. Particulate Matter Distributions

Figures 15 through 19 show the distribution of total suspended matter in the northeastern Gulf of Alaska. East of Kayak Island the surface particulate matter distributions (Fig. 15) are dominated by the discharge of sedimentary material from the coastal streams which drain the Bering, Guyot and Malaspina Glaciers. As this material is discharged into the Gulf, the westward flowing currents quickly deflect this material to the west along the coast. Comprehensive analyses of ERTS imagery for this region (Sharma et al. 1974; Burbank, 1974; and Carlson et al., 1975) have indicated that most of the material that is discharged from the rivers east of Kayak Island remains relatively close to the coast (within 40 km) until it reaches Kayak Island where it is deflected to the southwest. The surface suspended matter distributions for the October-November cruise follow this same general pattern. Along the transects southeast of Icy Bay (stations 10-13), particulate matter concentrations decrease from 2.58 mg/L near the coast to 0.25 mg/L approximately 40 km off the coast. However, a few eddies containing highly turbid water have been observed in the area south of Malaspina Glacier which appear to be capable of transporting sedimentary material offshore (Burbank, 1974). Since these eddies appear to be transient they are probably associated with local wind patterns.

Near Kayak Island a plume of turbid water (>1.0 mg/L) extends to the southwest from the eastern coast of the island. From an analysis of ERTS imagery taken on August 14, 1973 (Fig. 20), Sharma et al. (op. cit.) postulate

that as this material is carried to the west around the southwestern tip of Kayak Island, it is trapped by a seasonal clockwise gyre. Our data from the October-November cruise appear to support this hypothesis. A plume of turbid water (>1.0 mg/L) extends to the west from Kayak Island as far as station 33. To the north and south of station 33, particulate matter concentrations drop below 1.0 mg/L. This suggests that the plume originates from the east rather than the north. Similar distributions are observed at 10 meters (Fig. 16). Preliminary chemical analysis of the particulate matter from the plume indicates that it is predominantly of terrestrial origin ($> 70\%$ inorganic). Apparently, particulate material originating from the east side of Kayak Island is trapped by the gyre and carried to the west. However, since the number of stations located west of Kayak Island is too few for fine scale resolution of the suspended matter distributions at the surface, it is not possible, at this time, to determine whether or not the suspended matter is deflected to the north as would be expected from the ERTS imagery.

As stated previously, the major source of sedimentary material to the Gulf of Alaska is the Copper River. Although the fall cruise occurred at a time when the Copper River was approaching the period of minimum discharge, plumes of highly turbid water (>2.0 mg/L) extend out as far as 30 km from the coast. Once discharged into the Gulf, the sedimentary material from the Copper River is carried to the northwest

along the coast until it reaches Hinchinbrook Island, where a portion of the material passes into Prince William Sound and the remaining material is carried to the southwest along the southeastern coast of Montague Island.

From an analysis of ERTS imagery, suspended load distributions and sediment distributions, Sharma et al. (1974) and Burbank (1974) have concluded that the Copper River provides the major source of sediments to Prince William Sound. Copper River sediments enter Prince William Sound through channels on either side of Hinchinbrook Island. However, the channel on the northeast side of the island is quite shallow and probably accounts for a small fraction of the total sediment input. The major sediment input is through Hinchinbrook Entrance. Burbank (1974) states that upon entering Prince William Sound the Copper River sediment disperses and settles to the bottom.

In general, our data support the conclusions of these authors. Surface particulate matter concentrations near Hinchinbrook Entrance are relatively high (1.71 mg/L at station 44). Just inside the Entrance, surface concentrations decrease rapidly, indicating rapid dispersal and settling. However, careful analysis of vertical profiles of light scattering and total suspended matter indicates that other processes may be affecting the distribution of suspended matter within Prince William Sound. Figure 21 shows light scattering and temperature profiles for a number of stations across Hinchinbrook Entrance and into Prince

William Sound. The light scattering profiles within the Sound show an increase just below the sill depth of the Entrance. The maxima in light scattering below the sill correlates very well with the suspended matter concentrations which are highest in this region (1.48 mg/L at 230 m for station 42 and 3.51 mg/L at 272 m for station 43). The temperature of the bottom water in the Sound is approximately the same as the bottom water immediately south of the Entrance at about 180 meters. Muench and Schmidt (1975) state that bottom water renewal in the Sound is most likely to occur in October and November by inflow of water over the sill. Thus, near-bottom transport of suspended matter across the sill may be contributing a significant amount of sediments into the Sound.

In general, concentrations of suspended matter in the Gulf of Alaska are high at the surface with an average concentration of 1.02 mg/L. Beneath the surface concentrations generally decrease with depth until the sea floor is approached. Close to the sea floor suspended matter concentrations begin to increase sharply and the highest concentrations of suspended matter are found within 5 meters of the seawater-sediment interface (Fig. 19). In general, a bottom turbidity layer can be found throughout most of the Gulf. The height of the bottom nepheloid layer appears to be dependent upon the bottom topography and the currents. Figures 22 through 27 show vertical cross sections of suspended ds

(in mg/L) for several north-south transects in the Gulf. Near topographic highs such as the transects across Tarr Bank (Figs. 24 and 25), the light scattering and suspended matter profiles increase sharply very close to the bottom. In these regions, the bottom nepheloid layer is quite thin (<20 m). Resuspension and transport of bottom materials can be expected to dominate these areas.

In contrast, transects along topographic depressions such as the transect along Kayak Trough (Fig. 26) show light scattering profiles and suspended matter distributions which increase gradually to the bottom. Here, the bottom nepheloid layer is quite thick (>50 m) and rapid sedimentation can be expected to occur in this region.

In some cases, highly turbid plumes of suspended matter can be observed at midwater depths. This is usually due to advective transport of suspended material over or around some topographic feature. Figure 27 shows an example of this situation. The midwater maximum in suspended loads is due to the transport of highly turbid water around the southeastern tip of Kayak Island.

Replicate Studies

In order to evaluate the reproducibility of the measurements for total suspended matter, a number of replicate experiments were conducted during the fall cruise in the Gulf. Surface samples were collected in 10-liter Top Drop Niskin[®] bottles and simultaneously filtered through

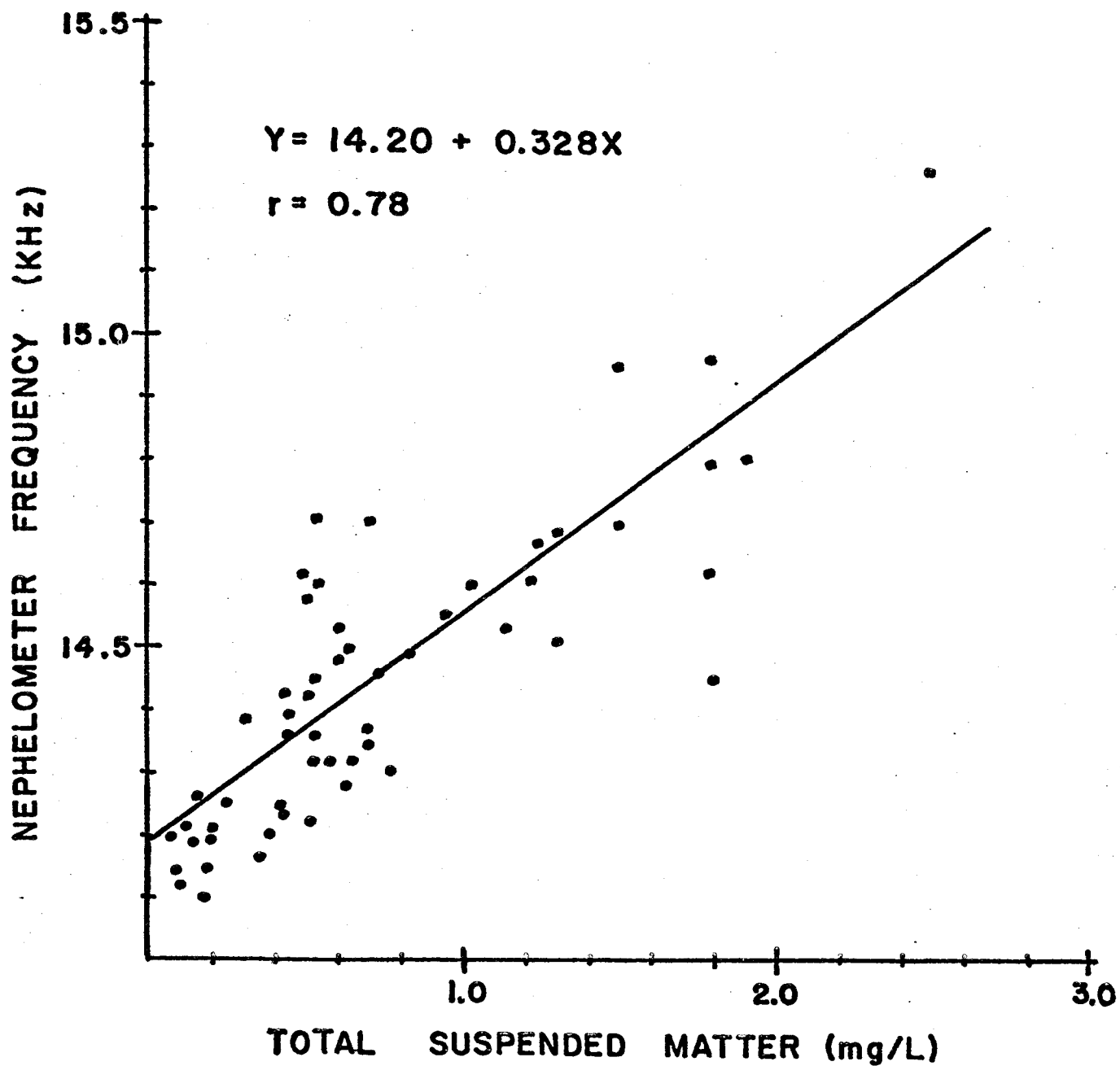


Figure 5. Scatter plot of the frequency output of the nephelometer versus total suspended matter for 55 near bottom samples from the northeastern Gulf of Alaska.

VI. Results and Discussion

To date, we have completed two of the five cruises scheduled during the present fiscal year for the Gulf of Alaska and southeastern Bering Shelf. The first cruise, RP-4-Di-75B Leg III of the NOAA ship DISCOVERER, was conducted in the southeastern Bering Shelf during the fall of 1975 (12 September - 5 October). The second cruise, RP-4-Di-75C Leg I, was conducted in the northeastern Gulf of Alaska during late fall of the same year (21 October - 10 November). Since the two regions should be considered independently, I will discuss the results in chronological order of the cruises.

Southeastern Bering Shelf

A. Particulate Matter Distributions

Figures 6 through 9 show the distribution of suspended matter at selected depths in the southeastern Bering Shelf. The surface particulate matter distributions (Fig. 6) are dominated by the discharge of suspended material from the northern rivers. A large plume of suspended matter extends to the southwest from Cape Newenham. Similar suspended matter distributions were found by Sharma et al. (1974) from samples collected during June-July 1973. The authors suggested that suspended material originating from the Kvichak and Nushagak Rivers moves generally to the west until it reaches Cape Newenham where it combines with a portion

of the material discharged from the Kuskokwim River and is deflected to the southwest. Preliminary chemical analysis of the particulate matter suggests that the material is essentially of terrestrial origin (>70% inorganic²).

A second plume extends to the southwest from Kuskokwim Bay. High concentrations of suspended matter extend as far west as Nunivak Island. This material is also predominantly inorganic and is probably derived from the Kuskokwim River.

Along the Alaska Peninsula surface concentrations decrease rapidly away from the coast. In some locations surface concentrations are as low as 0.31 mg/L within 40 km of the coastline. Since there are no significant rivers discharging into Bristol Bay from the Alaska Peninsula, it is not surprising that suspended matter concentrations decrease rapidly away from the coast. However, the surface concentrations south of Unimak Pass are nearly the same (~ 0.5 mg/L) as the surface concentrations north of the Alaska Peninsula. Furthermore, the chemical analysis of the suspended matter from both regions indicates that the suspended material is predominantly of marine origin (<50% inorganic). As the Pacific Ocean water passes through Unimak Pass and is deflected to the northeast along the coast of the Alaska Peninsula, suspended matter of marine origin is carried into Bristol Bay. When the Pacific

² For the purpose of this report, the inorganic particulate matter is defined as the percentage of total particulate matter that is due to terrigenous and skeletal debris. This value is determined by calculating the sum (in mg/L) of the major inorganic elements expressed as oxides and presenting it as a percentage of total suspended matter.

Ocean surface water mixes with the Shelf water, the highly turbid Shelf water is diluted by the relatively clear Pacific Ocean water producing the sharp gradients in the suspended matter distributions near the coast.

Beneath the surface, the particulate matter distributions follow the same general pattern as at the surface. This suggests that the semi-permanent counterclockwise currents in Bristol Bay appear to be controlling the distribution of suspended matter throughout the water column. However, suspended matter concentrations increase sharply near the bottom indicating possible resuspension of bottom sediments. Since Bristol Bay is a relatively shallow embayment, it is entirely possible that waves and tides play an active role in the resuspension of sediments. Preliminary chemical analysis of the suspended matter near the bottom indicates that this material is predominantly of terrestrial origin (>70% inorganic).

Sharma et al. (1972) have presented evidence from grain size distributions of Bristol Bay sediments to show that wave energy on the bottom plays a predominant role in the redistribution of sediments. The authors state that the distribution of sedimentary particles coarser than 2ϕ is primarily controlled by wave energy and bottom relief. Whereas, the distribution of particles finer than 2ϕ is controlled by the action of currents, waves and tides.

We are presently conducting a number of experiments designed to delineate some of the processes controlling the resuspension of bottom sediments. Some preliminary results of these experiments will be presented later in this report.

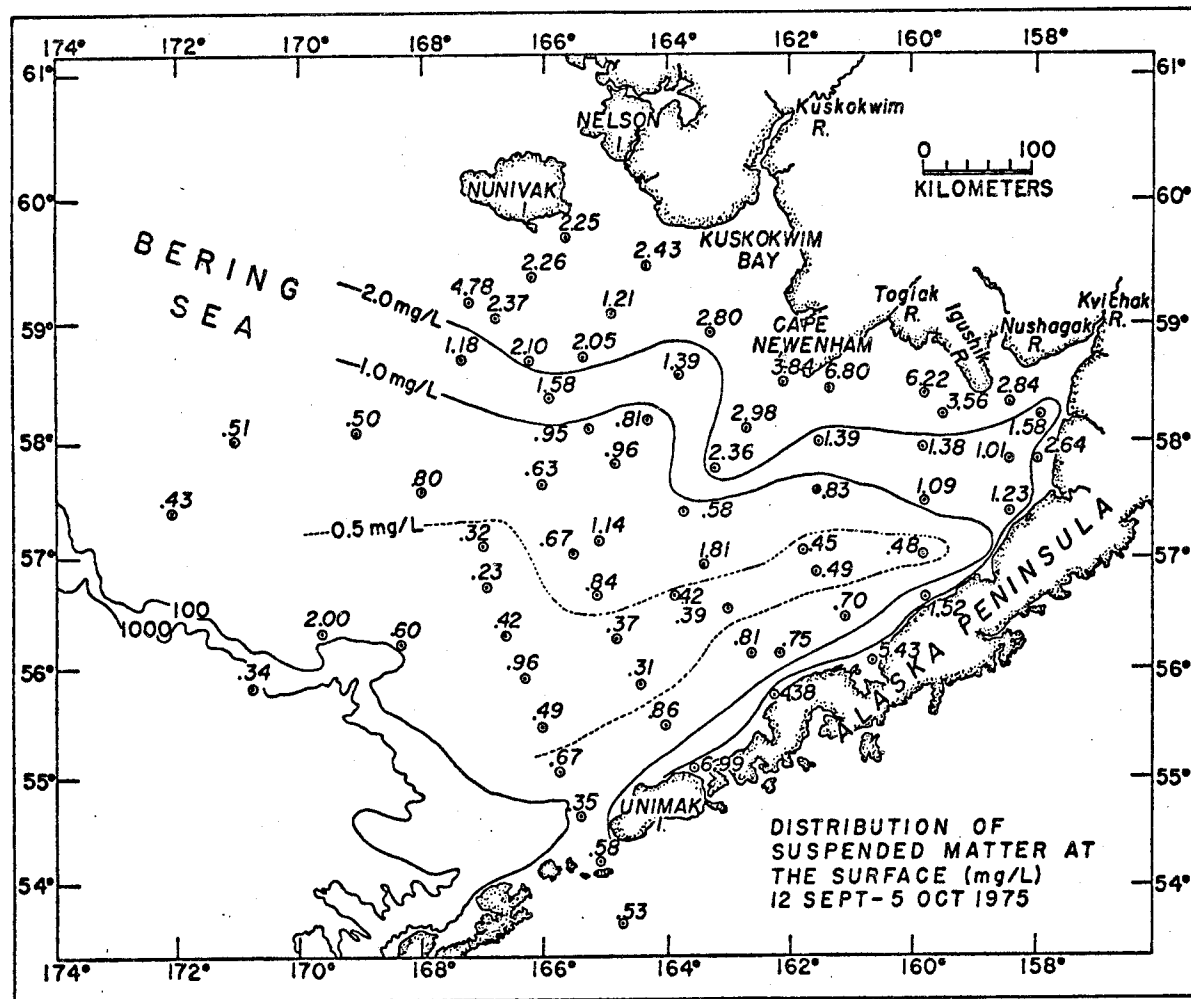


Figure 6. Distribution of total suspended matter at the surface in the southeastern Bering Shelf (Cruise RP-4-Di-75B-III, 12 Sept.-5 Oct., 1975).

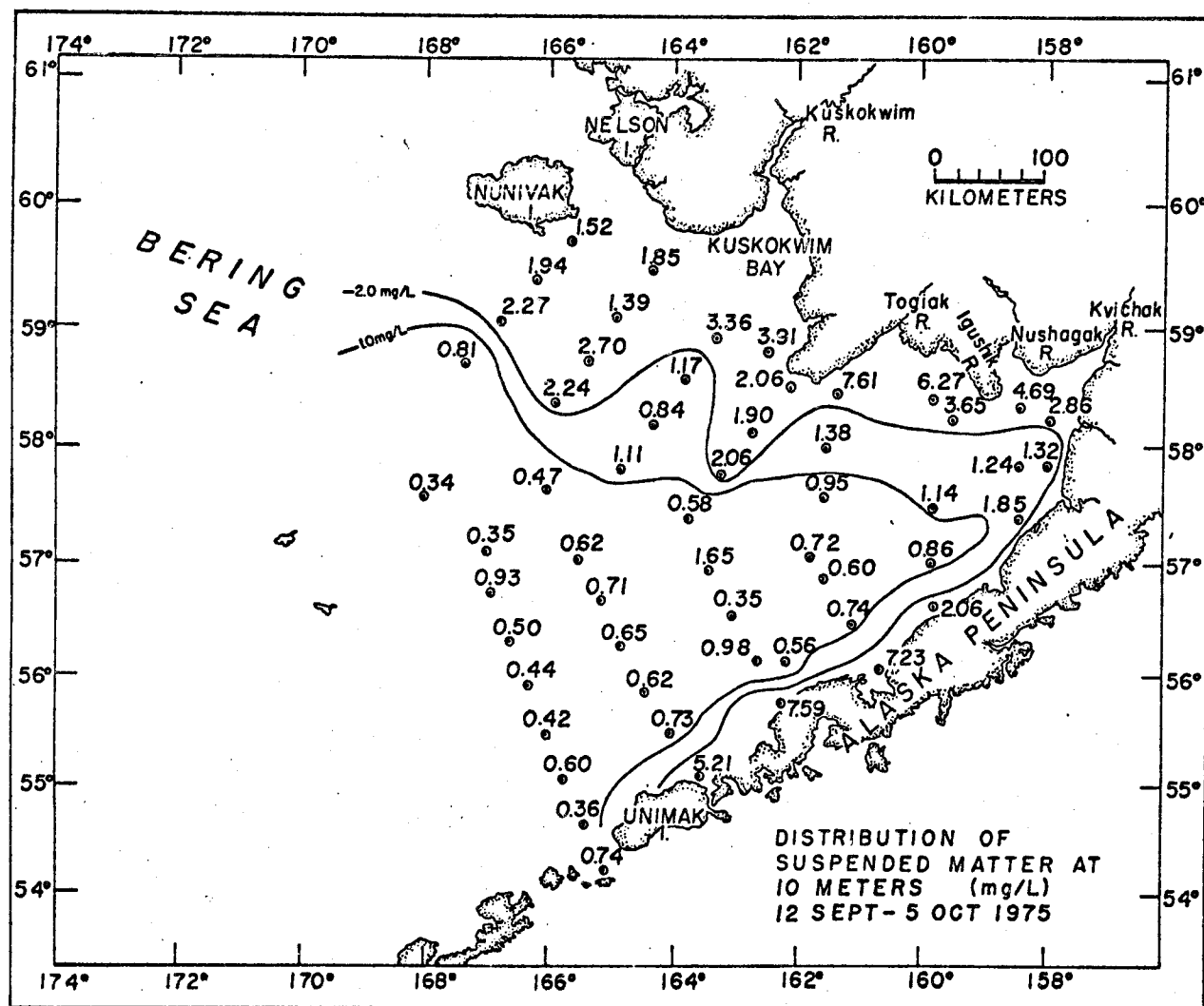


Figure 7. Distribution of total suspended matter at 10 meters in the south-eastern Bering Shelf (Cruise RP-4-Di-75B-III, 12 Sept.-5 Oct., 1975).

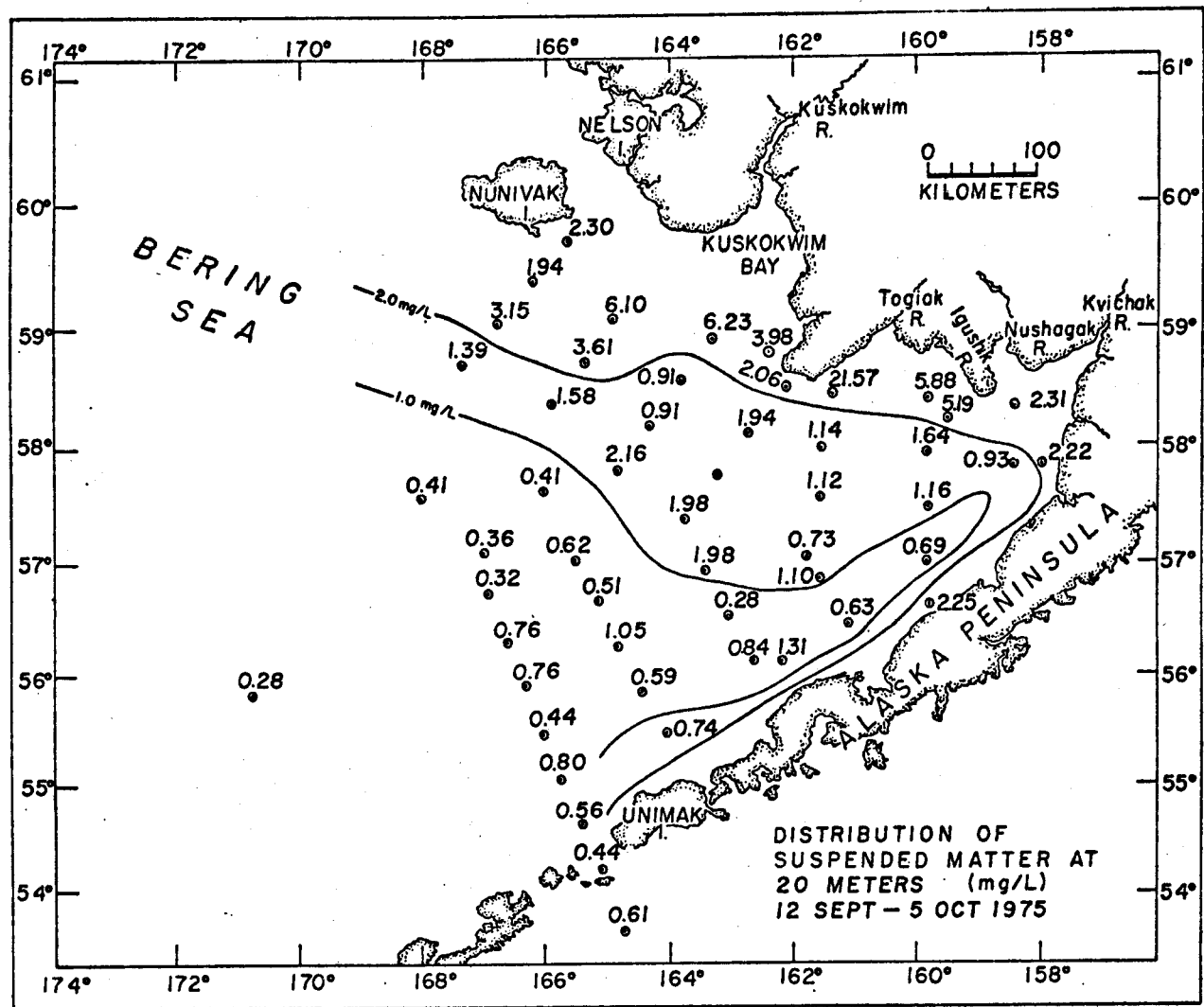


Figure 8. Distribution of total suspended matter at 20 meters in the southeastern Bering Shelf (Cruise RP-4-Di-75B-III, 12 Sept.-5 Oct., 1975).

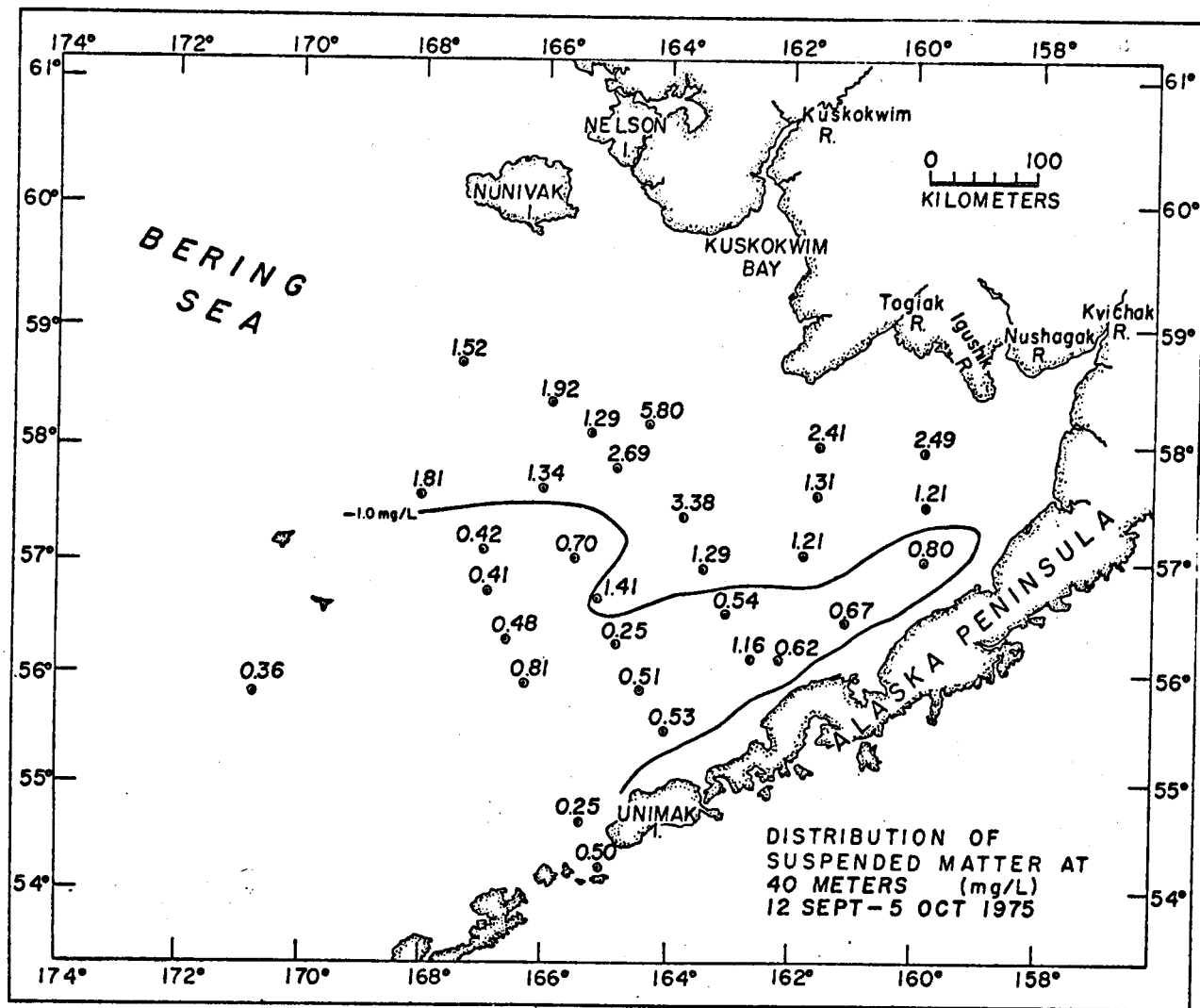


Figure 9. Distribution of total suspended matter at 40 meters in the southeastern Bering Shelf (Cruise RP-4-Di-75B-III, 12 Sept.-5 Oct., 1975).

B. Elemental Chemistry of the Particulate Matter

At this point, the data on the elemental composition of the particulate matter in the southeastern Bering Shelf are incomplete. We have completed most of the particulate carbon and nitrogen analyses and some preliminary results are presented below. Our analyses of the major and trace element compositions of the particulate matter have just been started and little data can be presented at this time.

Since the early work of Menzel and Vaccaro (1964), many investigators have used particulate carbon as a tracer of particulate organic matter in the oceans. Riley (1970) suggested that a factor of 2.0 be used to estimate concentrations of particulate organic matter from particulate carbon. Recent investigators have used the carbon to nitrogen ratios in particulate matter to distinguish between terrestrial and marine sources of organic matter (Loder and Hood, 1972). The authors found that riverborne organic matter have C:N ratios which range between 15-22. In contrast, ratios for marine organic matter range between 5-15.

The distribution of particulate carbon and nitrogen at the surface in the southeastern Shelf are presented in Figures 10 and 11. Generally speaking, the surface distributions follow the same pattern as total suspended matter. High concentrations of particulate carbon and nitrogen are found along the coast with concentration gradients decreasing slowly in a seaward direction from the northern coast and rapidly from the coast of the Alaska Peninsula. A plume of turbid water

containing high concentrations of particulate carbon and nitrogen extends to the southwest from Kuskokwim Bay. Apparently, the semi-permanent counterclockwise currents which appear to be controlling the distributions of total particulate matter at the surface also control the distribution of particulate carbon and nitrogen.

The carbon to nitrogen ratios in the particulate matter at the surface indicate that the organic matter is of marine origin. Ratios range from 0.7 to 29.4 with a mean 7.2. Although the ratios increase slightly from south to north, studies of the variability of C:N ratios in marine phytoplankton indicate that these small differences are probably not significant (Banse, 1974).

Near the bottom, particulate carbon and nitrogen distributions tend to be more localized and appear to follow the bathymetry. Figure 12 shows a vertical profile of total suspended matter and total particulate carbon for station 40 in central Bristol Bay. Concentrations of total particulate carbon are high at the surface (450 $\mu\text{gC/L}$). Beneath the surface, concentrations of particulate carbon decrease rapidly until a constant level of about 150 $\mu\text{gC/L}$ is reached below 40 meters. In contrast, total suspended matter concentrations are relatively low and constant in the top 40 meters. Below 40 meters, concentrations of total particulate matter increase sharply near the bottom indicating possible resuspension of bottom sediments. Apparently, resuspension of bottom sediments has little or no effect on the distribution of particulate organic matter near the bottom.

Since we received our X-ray fluorescence equipment in our laboratory only two months ago, most of our efforts have been devoted to the set-up and calibration of the equipment. Consequently, very little information about the major and trace element composition of the particulate matter is available at this time.

In order to obtain standards with similar compositions as the samples, Baker and Piper (1975) chose the USGS standard rocks W-I, AGV-I and BCR-I to calibrate their X-ray fluorescence system to determine the major element composition of suspended matter from the Washington Continental Shelf. We have adopted their basic techniques to analyze the major element composition of suspended matter from the Gulf of Alaska and southeastern Bering Shelf. Although the details of the techniques have been described adequately elsewhere, a brief description will be presented below.

Radiation from a silver X-ray tube is used to obtain a monochromatic source of X-rays from a secondary target. Baker and Piper (op. cit.) used the K_{α} X-ray of S to analyze the light elements (Na, Mg, Al and Si) and the continuum from the X-ray tube to analyze for the heavier elements. We will use a combination of secondary targets (S, Ge, Zr and Mo) to analyze the particulate matter for both major and trace elements. The samples will be calibrated against the USGS standard rocks for major elements and the NBS glass standards (612 and 614) for trace elements.

Preliminary calibrations of our system using the USGS rock standards for major elements are quite good. Figure 13 shows a typical calibration curve for CaO using the USGS W-I rock as the reference material. Similar calibration curves have been prepared for each element by plotting the characteristic X-ray intensity against the known concentration of the element. The results indicate that for sample loadings between 50 and 300 $\mu\text{g cm}^{-2}$ the calibration curves are linear. Baker and Piper (op. cit.) state that for sample loading greater than 300 $\mu\text{g cm}^{-2}$ there is a significant loss of X-ray intensity due to self-absorption and the thin film criteria is no longer valid. Fortunately, most of our samples have loadings well below this upper limit.

As stated previously, we have made some preliminary analyses of the surface samples from the southwestern Bering Shelf for major elements. Table 1 summarizes the data we have obtained thus far. In order to simplify the data, I have arranged the surface samples into three groups. Group I contains all the northern stations in which the sum of the major inorganic element concentrations (expressed as oxides) is greater than 60% of the total weight of material on the filter. Group II contains all the southern stations in which the sum of the major inorganic element concentrations is also greater than 60% of the total weight. Group III contains all the stations in between

in which the sum is less than 60% of the total suspended load. Figure 14 shows the percentage of total suspended matter that is due to the sum of the major inorganic elements (expressed as oxides) for each station. The 60% isopleth divides the stations into their respective groups.

As shown in Table 1, Groups I and II are very similar. Within the statistical limits of the measurements, the major element composition of the suspended matter is very nearly the same for both groups. Group III, on the other hand, shows an elemental composition which is quite different from Groups I and II. The major element composition of the suspended matter from Groups I and II appear to be dominated by the supply of terrigenous material from the Kuskokwim, Nushagak and Kvichak Rivers to the north (for Group I) and the coastal streams and lagoons to the south (for group II). Several authors have suggested that since K, Mg, Al, and Ti are almost exclusively associated with aluminosilicate minerals, the presence of these elements in suspended matter is indicative of terrestrial input (Spencer and Sachs, 1970; Price and Calvert, 1973; and Feely, 1975). The high concentrations of these elements in the samples from Groups I and II indicate that aluminosilicate minerals are the most dominant solid phase in the particulate matter. The data from Table 1 shows that for Groups I and II approximately 44-50% of the particulate matter is aluminosilicate material of terrestrial origin. In contrast, the particulate matter samples from Group III only contain about 20% aluminosilicate material.³

³ The aluminosilicate content of suspended matter can be estimated by multiplying the aluminum content by a factor of 10 (Feely, 1975).

Price and Calvert (1973) used the elemental ratios of the major elements to aluminum to help identify the particular sources of the suspended matter. Table 2 shows the variation in the Mg/Al, Si/Al, K/Al, Ca/Al, Ti/Al and Fe/Al ratios for the particulate matter from the three groups. The Fe/Al, Ti/Al and K/Al ratios for the particulate matter from Groups I and II are similar to values for average shales (Krauskopf, 1967) and probably represent the elemental composition of the suspended material discharged from the rivers. However, the Si/Al ratio is considerably elevated over what would be expected from average sedimentary rocks (7.1 for Group I vs. 3.0 for average shales, Krauskopf, 1967). This is probably due to the presence of diatom frustules and fine grain quartz in the suspended matter.

The particulate matter samples from Group III contain significantly lower concentrations of the major inorganic elements. As stated previously, only about 20% of the particulate matter from this region is estimated to be aluminosilicate material. The remaining 80% appears to be biogenic in nature (primarily consisting of organic matter and skeletal fragments).

Table 1. Summary of the major element composition of the surface samples from the Southeastern Bering Shelf.

| Region | # of Samples | MgO | | Al ₂ O ₃ | | SiO ₂ | | K ₂ O | | CaO | | TiO | | Fe | |
|-----------|--------------|-----------|---|--------------------------------|---|------------------|---|------------------|---|-----------|---|-----------|---|-----------|---|
| | | Wt % | % | Wt % | % | Wt % | % | Wt % | % | Wt % | % | Wt % | % | Wt % | % |
| Group I | 23 | 2.52±0.98 | | 8.27±2.7 | | 67.1±11 | | .699±0.20 | | .178±0.07 | | .378±0.12 | | 2.26±0.86 | |
| Group II | 9 | 2.50±1.00 | | 9.37±4.9 | | 74.0±12 | | .527±0.23 | | .294±0.31 | | .418±0.29 | | 2.31±1.90 | |
| Group III | 23 | 0.96±0.77 | | 4.03±3.2 | | 21.8±12 | | .228±0.14 | | .131±0.22 | | .186±0.13 | | 0.78±0.62 | |

Table 2. Elemental ratios to aluminum for the surface samples from the Southeastern Bering Shelf.

| Region | # of Samples | Mg/Al | Si/Al | K/Al | Ca/Al | Ti/Al | Fe/Al |
|-----------|--------------|-------|-------|-------|-------|-------|-------|
| Group I | 23 | 0.347 | 7.146 | 0.132 | 0.028 | 0.051 | 0.517 |
| Group II | 9 | 0.302 | 6.950 | 0.088 | 0.042 | 0.050 | 0.465 |
| Group III | 23 | 0.253 | 4.788 | 0.088 | 0.043 | 0.052 | 0.366 |

466
cont on p. ~~43~~442

First Annual Report

Research Unit #152/154
Reporting Period 7-1-75/4-1-76
Number of pages 76

Distribution, Composition and Transport of Suspended
Particulate Matter in the Gulf of Alaska and Southeastern
Bering Shelf

Principal Investigators: Richard A. Feely, Oceanographer
Joel D. Cline, Oceanographer

Pacific Marine Environmental Laboratory
3711 15th Avenue N.E., Seattle, Washington 98105

I. Summary - The Southeastern Bering Shelf

The surface distribution of suspended matter in the southeastern Bering Shelf is controlled by the discharge of sedimentary material from the coastal rivers and the semi-permanent counterclockwise currents which dominate the water circulation in Bristol Bay. A large plume of suspended matter extends to the southwest from Cape Newenham. Suspended matter originating from the Kvichak and Nushagak Rivers is carried to the west until it reaches Cape Newenham where it combines with a portion of the material discharged from the Kuskokwim River and is deflected to the southwest. Preliminary chemical analysis of the particulate material from this plume indicates that it is essentially of terrestrial origin.

A second plume extends to the southwest from Kuskokwim Bay. High concentrations of suspended matter extend as far west as Nunivak Island. This material is probably derived from the Kuskokwim River.

Along the Alaska Peninsula surface suspended matter concentrations decrease rapidly away from the coast. As the Pacific Ocean water passes through Unimak Pass and is deflected to the northeast along the coast of the Alaska Peninsula, suspended matter of marine origin is carried into Bristol Bay. When this water mixes with the highly turbid Shelf water, the Shelf water is diluted by the relatively clear Pacific Ocean water producing the sharp gradients in the suspended matter distributions near the coast.

Below the surface, the particulate matter distributions follow the same general pattern as at the surface. However, suspended matter concentrations increase sharply near the bottom indicating possible resuspension of bottom sediments.

Summary - Gulf of Alaska

The distribution of suspended matter in the northeastern Gulf of Alaska is affected by a number of parameters which combine to form a unique distribution pattern. East of Kayak Island the surface particulate matter distributions are dominated by the discharge of sedimentary material from the coastal streams which drain the Bering, Guyot and Malaspina Glaciers. As this material is discharged into the Gulf, the westward flowing currents quickly deflect this material to the west along the coast until it reaches Kayak Island where it is deflected to the southwest and is trapped by a seasonal clockwise gyre.

The major source of sedimentary material to the Gulf of Alaska is the Copper River. Once discharged into the Gulf, the Copper River sediment is carried to the northwest along the coast until it reaches Hinchinbrook Island where a portion of the material passes into Prince William Sound and the remaining material is carried to the southwest along the southwestern coast of Montague Island.

In general, concentrations of suspended matter in the Gulf of Alaska are high at the surface with an average concentration of 1.02 mg/L. Beneath the surface concentrations generally decrease with depth until the seafloor is approached. Close to the seafloor suspended matter concentrations increase sharply and the highest concentrations are found within 5 meters of the seawater-sediment interface. Studies of the temporal variability of suspended matter near the bottom indicate that resuspension of bottom sediments might be occurring.

II. Introduction

Particles suspended in seawater play a major role in regulating the chemical forms, distributions and ultimate deposition of many marine pollutants. Some toxic substances in particulate form are transported to the oceans where they are desorbed at the freshwater-seawater interface. Other substances (particularly petroleum hydrocarbons) are adsorbed onto the surface of suspended particles and are removed to the sediments as the particles settle.

In areas where the bottom environment is especially dynamic, near-bottom processes such as resuspension and transport of sediments may affect the ultimate deposition of pollutants. An understanding of the processes controlling the distribution, composition, and transport of suspended particulate matter is essential to the assessment of the fate of toxic pollutants in the marine environment.

The major objective of the particulate matter program in the Gulf of Alaska and southeastern Bering Shelf is to determine the seasonal variations in the distribution, composition, and transport of suspended matter. Other objectives include: (1) the high frequency (hourly) variability in the distribution of suspended matter, and (2) an investigation of the role of resuspension processes as a mechanism for redistribution of sedimentary materials.

III. Current State of Knowledge - Southeastern Bering Shelf

There is very little published information about the distribution and composition of suspended particulate matter in the southeastern Bering Shelf.

Sharma et al. (1974) compared some particulate matter distributions taken during June-July 1973 in the southern Bering Sea and Bristol Bay region with ERTS multispectral scanner images of the same area which were obtained on October 2, 1972. The surface contours of suspended load distributions indicate several regions of relatively turbid water which originate from a variety of sources. These turbid regions include:

- (1) A region of turbid water which is north of the Aleutian Islands. This is probably due to the high level of primary productivity that is the result of the mixing of nutrient-rich deep water with the Alaskan Stream which flows into the Bering Sea from the south.
- (2) A region of turbid water which extends south from Kuskokwim Bay and west from northern Bristol Bay. This plume probably represents suspended sediments derived from the Kuskokwim River from the north and the Kvichak and Nushagak Rivers from the east.
- (3) A region of slightly turbid water extending to the southwest from Bristol Bay which probably represents suspended matter derived from the Kvichak and Nushagak Rivers.

The ERTS imagery indicates that the Nushagak River is a major source for particulate matter in the Bristol Bay area. The suspended particles from the Kvichak and Nushagak Rivers are carried to the west by the

prevailing counterclockwise current. Sharma et al. (op. cit.) state that although the river plumes remain close to shore, offshore transport of material in suspension is probably brought about by tidal currents.

There is only a small amount of information about the chemical composition of the suspended matter in the southeastern Bering Shelf. Loder (1971) studied the distribution of particulate organic carbon (POC) north of Unimak Pass and found high POC concentrations (221-811 $\mu\text{gC/L}$) north in the thermally stabilized upwelled water north of Unalaska Island. Lower POC concentrations were found north of Unimak Island and west Akutan Pass which presumably were due to current mixing.

Tsunogai et al. (1974) studied the distribution and composition of particulate matter from six stations in the south central and southeastern Bering Sea. They found the highest concentrations of particulate matter occurred at 20 to 30 meters depth which appeared to be due to the high productivity and the slow decomposition of organic matter just below the surface. The organic portion of the suspended matter was about 67 percent for the samples from the Bering Sea and 80 percent for the samples south of the Aleutian Islands in the northern North Pacific.

Current State of Knowledge - Gulf of Alaska

Reimnitz (1966) studied the sedimentation history and lithology of sediments from the Copper River Delta. He estimated the particulate matter supply of the Copper River to be 107×10^6 tons/yr which mostly consists of fine grain sands and silts.

Sharma et al. (1974) compared some surface particulate matter distributions taken during February 24-28, 1973 between Kenai Peninsula and Kayak Island with ERTS multispectral scanner images of the same region which were obtained on October 12, 1972 and August 14, 1973. The ERTS images show that the Copper River and Bering Glacier provide most of the sediment load to this region. The westward flowing current deflects a portion of the Copper River plume to the west. The suspended matter moves along the coast with some material entering Prince William Sound through the passages on either side of Hinchinbrook Island and the remaining material is carried along the southeast shore of Montague Island.

Carlson et al. (1975) used ERTS imagery to study the transport of suspended material in nearshore surface waters of the Gulf of Alaska. During the late summer and early fall months large quantities of fine grain silt and clay sized material from the Bering, Guyot and Malaspina Glaciers are discharged into the Gulf between Kayak Island and Yakutat Bay. This material is carried to the west by the Alaska Current until it reaches Kayak Island where it is deflected to the south.

El Wardani (1960) studied the distribution of organic phosphorus in the Bering Sea, Aleutian trench and the Gulf of Alaska. He demonstrated that organic phosphorus in the upper 200 m of the water column bears an inverse relationship to inorganic phosphorus. Below 200 m no detectable organic phosphorus was found.

IV. The Study Area - Southeastern Bering Shelf

The southeastern Bering Shelf (Fig. 1) is a relatively shallow embayment which is bounded by the Kilbuk Mountains to the north and east, and the Alaska Peninsula to the south. Except for some small depressions near the Alaska Peninsula, the Shelf floor is extremely smooth with an average slope of about 0.0003 (Sharma, 1974).

The region receives sedimentary material from the Kuskokwim, Kvichak, and Nushagak Rivers. The largest river, the Kuskokwim, discharges approximately 4.0×10^6 tons of sediments annually (Nelson, 1974). Figure 2 shows the range and mean values of the monthly mean discharge of the Kuskokwim for the period of record (Water Supply Papers, U.S. Geological Survey). The maximum discharge occurs during the months of May through September.

A counterclockwise movement generally dominates the water motion in the Bristol Bay region. Pacific Ocean water enters the Bering Sea through the Aleutian Island passes and flows to the northeast along the coast of the Alaska Peninsula. The water moves along the northern coastline by tidal and wind driven currents until it reaches Nunivak Island where it is turned to the north.

The permanent currents in the southeastern Bering Shelf appear to be somewhat sluggish. Current velocities ranging from 2.0-5.0 cm/sec have been observed north of the Alaska Peninsula (Hebard, 1959). However, tidal currents are dominant in northeastern Bristol Bay where tidal velocities of up to 125 cm/sec have been observed in Nushagak Bay (U.S. National Ocean Survey, 1973).

The Study Area - Gulf of Alaska

The northeastern Gulf of Alaska (Fig. 3) is bordered by a rugged mountainous coastline containing numerous glaciers which deliver large quantities of suspended material to the Gulf during the summer months when maximum discharge occurs. The major sediment discharge is from the Copper River. Reimnitz (1966) estimates that approximately 107×10^6 tons of fine grain material are delivered annually to the Gulf by way of the Copper River system. Figure 4 shows the range and mean values of the monthly mean discharge of the Copper River for the period of record (Water Supply Papers, U.S. Geological Survey). The maximum discharge of the Copper River occurs during the months of June through September.

Additional inputs into the Gulf occur along the coastline east of Kayak Island where coastal streams containing high sediment concentrations drain the Bering, Guyot and Malaspina Glaciers. Since there are no permanent gauging stations on these streams, there is no information about the quantities of materials that are discharged into the Gulf from these sources.

The current systems in the Gulf are dominated by the large counter-clockwise gyre of the Alaskan Stream. It is usually characterized by a core of relatively warm (5.5° - 6.2°C) water at about 130 meters (Galt and Royer, 1976). The Alaskan Stream comes in contact with the shelf just east of Icy Bay where it is turned to the west and appears to follow the 150 m isobath.

West of Cape St. Elias the Alaskan Stream is deflected to the southwest leaving the large shelf area between Middleton Island and the Copper River Delta relatively free of its influence. In this region the circulation is affected by seasonal wind patterns. In the summer, the winds are predominantly from the southwest. This produces an Ekman drift of surface waters offshore. During the winter, the winds are from the southeast which results in an Ekman drift onshore and downwelling in subsurface waters.

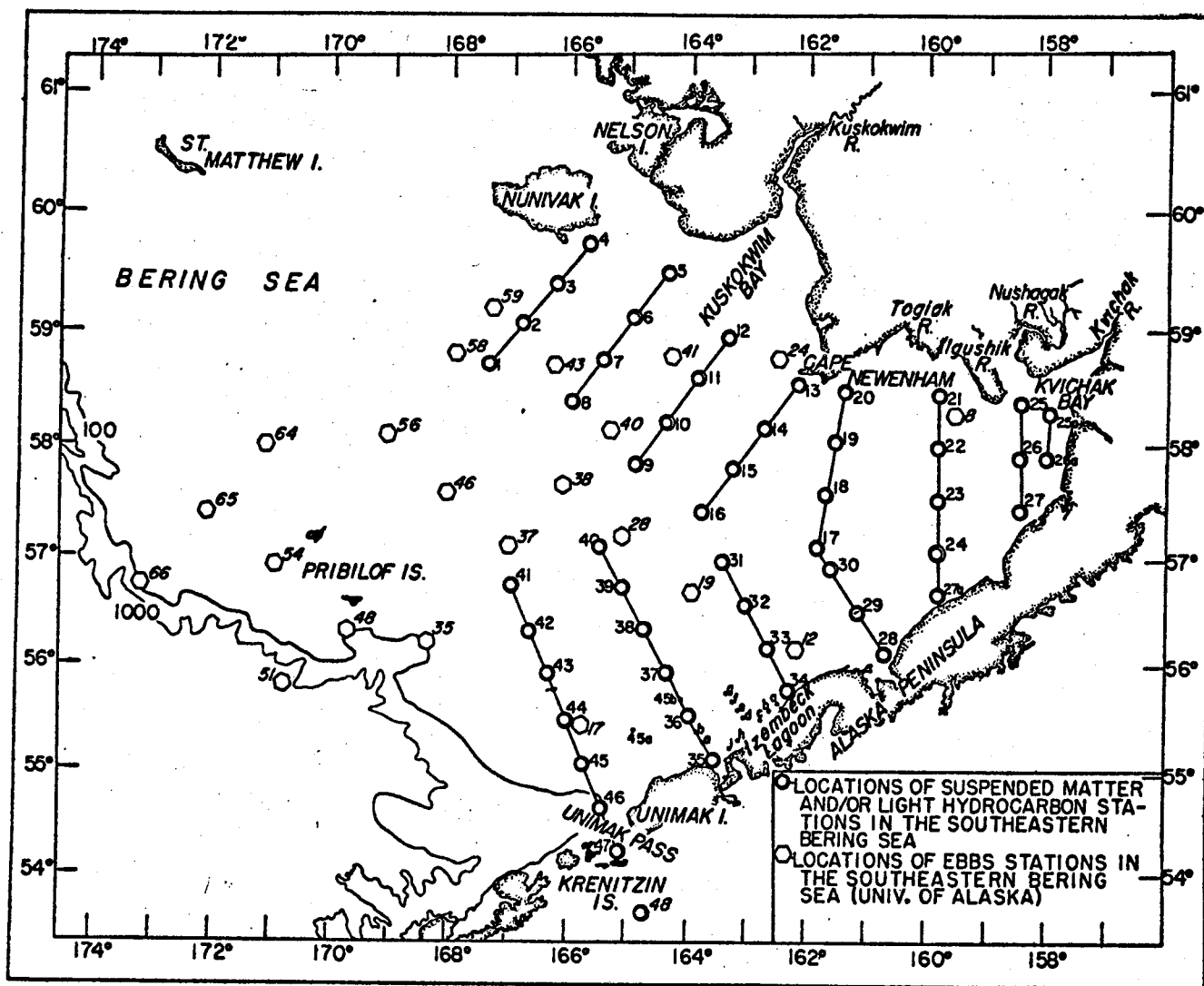


Figure 1. Locations of suspended matter stations in the southeastern Bering Shelf (Cruise RP-4-Di-75B-III, 12 Sept.-6 Oct., 1975).

478

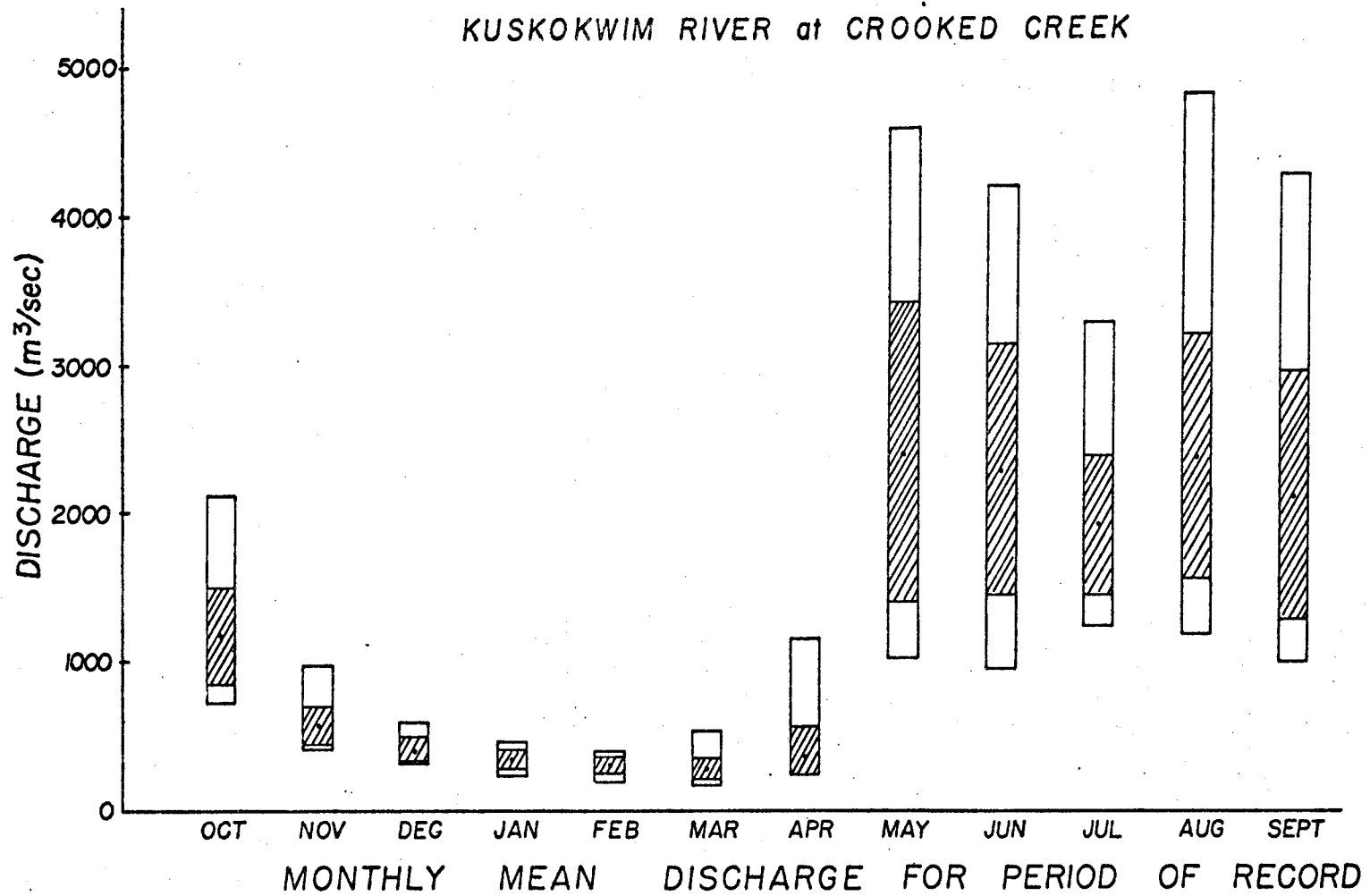


Figure 2. Range, mean and standard deviation of the monthly mean discharge of the Kuskokwim River at Crooked Creek for the period of record through 1974 (Water Supply Papers, U.S. Geological Survey).

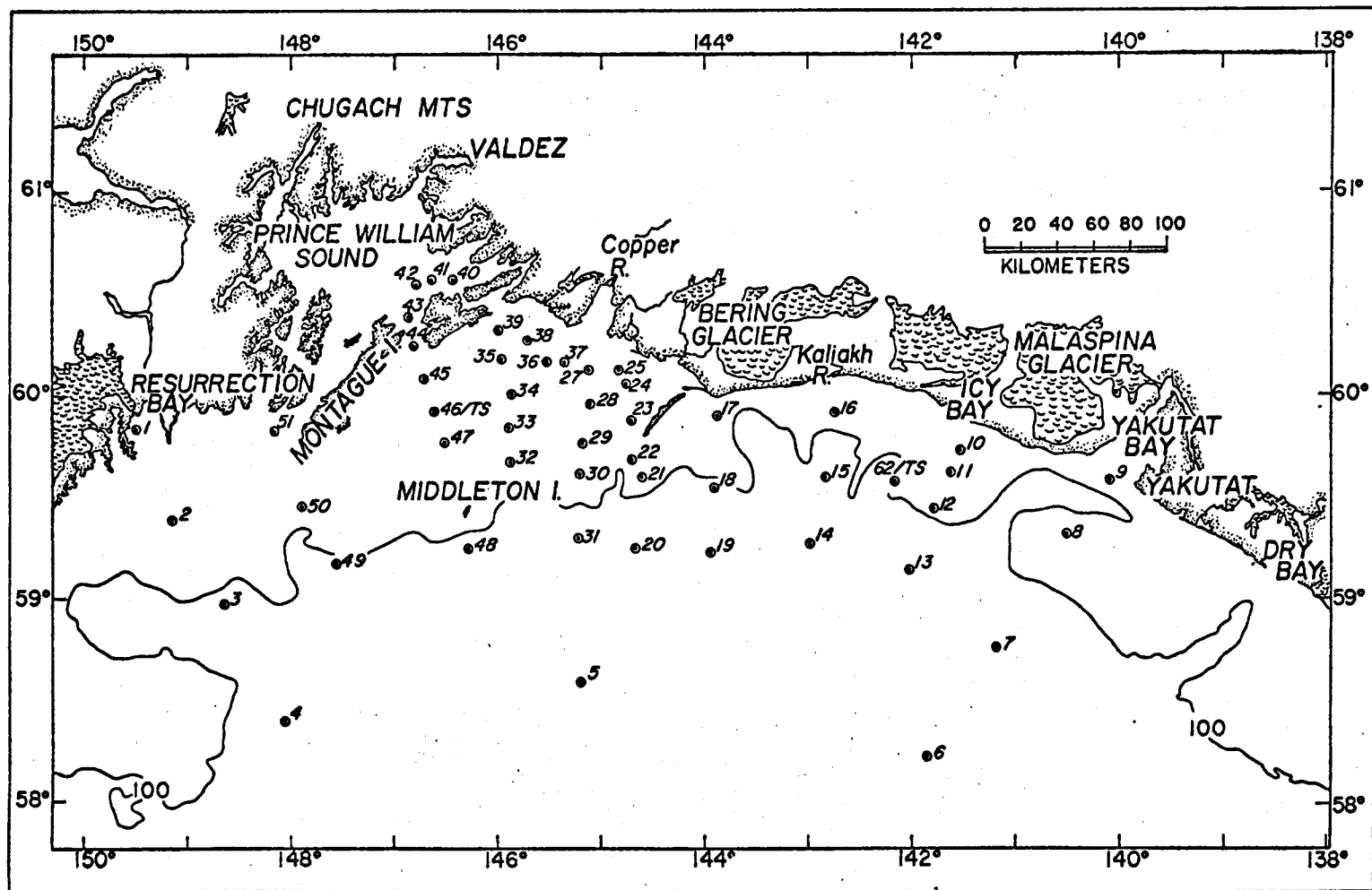


Figure 3. Locations of suspended matter stations in the northeastern Gulf of Alaska (Cruise RP-4-Di-75C-I, 21 Oct.-10 Nov., 1975).

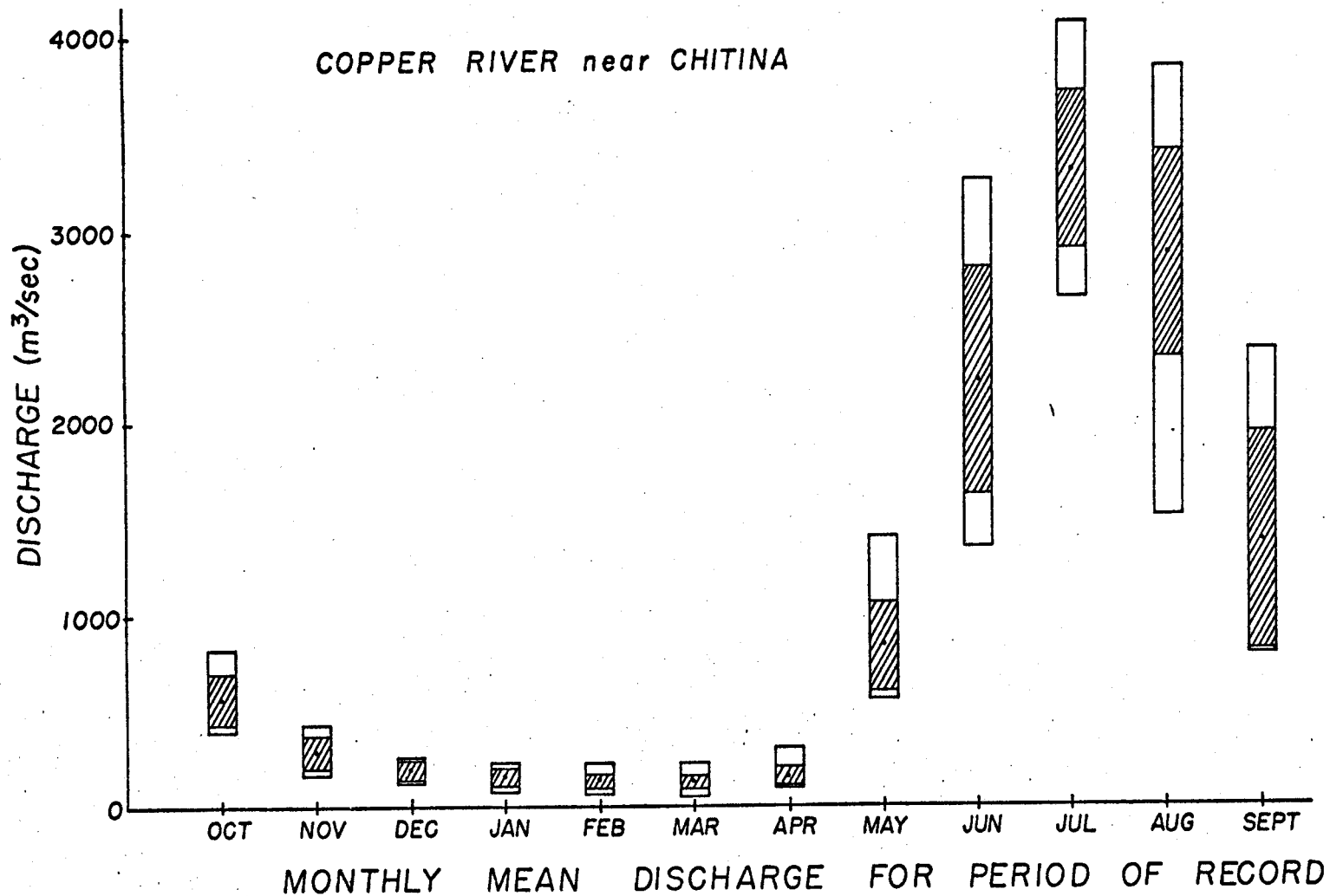


Figure 4. Range, mean and standard deviation of the monthly mean discharge of the Copper River near Chitina for the period of record through 1974 (Water Supply Papers, U.S. Geological Survey).

V. Sources, Methods, and Rationale of Data Collection

In order to obtain information about the seasonal variations of the distribution and composition of suspended matter we have planned three cruises in the Gulf of Alaska and two cruises in the Bering Sea during the present fiscal year. The field program has been integrated with the physical, geological and biological programs so that concomitant information about water mass transport, primary productivity and recent sedimentation can be obtained.

In addition to the seasonal distributions, we have planned a number of high frequency (hourly) time series studies at selected locations. This will provide valuable information about the variability in the distribution of suspended matter that may be due to waves, tides, and the "patchiness" of primary productivity in surface waters and resuspension of sediments in near-bottom waters.

A second aspect of the suspended matter program will be concerned with the process of sediment resuspension and redeposition. Observations of light scattering profiles from the Gulf of Alaska have indicated evidence of near bottom turbidity layers which may be due to resuspension of bottom sediments. The erosion and transport of bottom sediments are expected to be related to the action of near bottom currents. These currents are presumably influenced mainly by the actions of waves, tides and storms.

To determine how these processes affect the near bottom distribution of particulate matter we are deploying a small mooring in the eastern Gulf at approximately 200 meters. The mooring will contain an

Aanderaa current meters and a nephelometer located within 3 meters of the bottom. The mooring will be maintained for approximately two months and recovered under the direction of J. Schumacher of PMEL.

Sampling Methods

Sample collection has occurred concurrently with STD-nephelometer hydrocasts so that the particulate matter distributions can be related to the hydrography. Water samples were collected in 10-liter PVC Model 1070 Drop-top Niskin[®] bottles and filtered through preweighed 0.40 μm Nuclepore[®] filters. The filters were washed with three 10-ml aliquots of deionized filtered water, dried in a desiccator, stored in plastic petri dishes, and returned to the laboratory. At the laboratory, the filters were reweighed on a seven-place Cahn[®] Model 4700 Electrobalance. Additional water samples were filtered through appropriate filters for the determination of organic carbon and nitrogen.

Analytical Methods

The major (Mg, Al, Si, K, Ca, Ti, and Fe) and trace (Cr, Mn, Cu, Zn, and Pb) inorganic elemental chemistry of the particulate matter is being determined by X-ray fluorescence. This technique has been used successfully for the determination of the major inorganic elements in particulate matter in coastal and deep water environments and the methods are fairly well established (Cann and Winter, 1971, and Baker and Piper, 1975). Recent advances in this field have lowered the minimum detectable limits to such an extent that many trace elements in particulate matter can be analyzed routinely.

The organic carbon and nitrogen content of suspended particulate matter has been shown to be a valuable indicator of terrestrial and marine sources of organic matter in the coastal waters of Alaska (Loder, 1971). Specifically, Loder and Hood (1972) have used the C/N ratio of particulate matter to distinguish between terrestrial, glacial, estuarine and marine-derived sources of organic matter.

Particulate organic carbon and nitrogen are being analyzed by the micro-Dumas combustion method, employing a Hewlett Packard[®] Model 185B C-H-N analyzer (Sharp, 1974). Particulate matter has been separated from seawater by vacuum filtration (precombusted 0.4 μm silver filters [Sharp, 1974; Gordon and Sutcliffe, 1974]) and the carbon and nitrogen combusted to CO_2 and N_2 . After separation by standard gas-solid chromatography (GC), the gases are quantitatively determined by thermal conductivity (TC). Sample analysis time is about 10 minutes.

Standardization will be effected with cyclohexanone-2, 4-dinitrophenylhydrozone, acetanilide (Sharp, 1974) and L-cystine; the latter two are NBS standards. These results will be corroborated by direct GC analysis of CO_2 and N_2 .

Nephelometry

The vertical distribution of suspended particulate matter will be determined using a continuously recording integrating nephelometer (Sternberg *et al.*, 1974). The nephelometer consists of a flashing light source, a scattered light detection system, a data transmission system, and Ni-Cd batteries mounted in a self-contained, easily portable, deep sea housing.

The instrument has been interfaced into the Plessey CTD system using the sound velocity channel (14-16 kHz) such that real time measurements of forward light scattering can be obtained. Since the light scattering measurements are relative, the instrument must be calibrated against discrete samples for a given area. Figure 5 shows the relationship between total suspended matter and light scattering (reported as a frequency) for 55 near bottom samples from the Gulf of Alaska¹ using the PMEL nephelometer under uniform operating conditions. The figure indicates that the relationship between light scattering and total suspended matter is linear to some degree. This suggests that the light scattering profiles may be used to estimate suspended matter concentrations near the bottom.

¹ Since the nephelometer is adversely affected by ambient light in the near surface waters, the light scattering data will only be used to provide information about near bottom processes where ambient light levels are well below the 1% level.

484
go to p. 452

ANNUAL REPORT

Contract No. RK6-6074
Research Unit #204
Reporting period -
30 May 1975 - April 1976

Pages

Offshore Permafrost Studies, Beaufort Sea

Investigators

Peter Barnes
David Carter
David Drake
David Hopkins
Arthur Lachenbruch
Robert Nelson
Erk Reimnitz

U.S. Geological Survey
Menlo Park, California

In cooperation with

Paul Sellmann
Richard Berg
Jerry Brown
Edwin Chamberlain
Alex Iskandar
George Swinzow
Herbert Ueda

U.S. Army CRREL
Hanover, New Hampshire

Robert Lewellen
Boulder, Colorado

1 April 1976

1) What is the present distribution of temperature beneath the sea bed and;

2) What is the distribution of fluid there whose freezing point is below its ambient temperature?

In the absence of appreciable heat transfer by moving interstitial fluids, the temperature distribution in the outer one-kilometer layer of the solid earth is determined uniquely from a knowledge of:

1) The heat flow from below,

2) The temperature distribution (and its history) at the earth's solid surface, and

3) The distribution of thermal properties (including water content) in the layer of interest.

Our present knowledge of 1) is probably adequate for the present purpose. Our knowledge of 2) is poor, but it can be refined by better estimates of the shoreline and climate history over the past 10^4 to 10^5 years, and by studies of the present mean temperature of the sea floor. Our fragmentary information on 3) can be augmented by various geological and geophysical studies.

The mean annual temperature on the land surface near the Arctic Coast is -8°C to -10°C , and up until a century ago it was lower by 2° or 3°C (Lachenbruch and Brewer, 1959; Lachenbruch et al., 1962; Gold and Lachenbruch, 1973; Lachenbruch and Marshall, 1969). The mean annual temperature of the shallow sea bed, where ice does not rest on the bottom, is probably $-1 \pm 0.8^{\circ}\text{C}$ (Gold and Lachenbruch, 1973). Steady heat loss from the earth's interior at the rate of 30 to 40 $\text{cal}/\text{cm}^2 \text{ yr}$ results in a

thermal conductivity of the material. Thus, in a region where the long-term mean was -9°C and the steady-state gradient was $15^{\circ}\text{C}/\text{km}$ (rather like the land near Prudhoe Bay today) negative centigrade temperatures ("permafrost") would extend to a depth of about 600 m. Under steady conditions at a point a few kilometers offshore, a steady sea bottom temperature of -1.5°C would result in negative temperatures to a depth of 50 to 100 m depending on the thermal conductivity. If the point on land was transformed into the point offshore by a rapid transgression of the shoreline, we should like to know how long it would take for the steady offshore condition to prevail. The answer is that it would take only a few thousand years (Lachenbruch, 1957a) if the ice content of permafrost were negligible and several tens of thousands of years if it were high (Mackay, 1972). In both cases the permafrost would, of course, thin from below. For the high ice-content case the gradient in the permafrost would fall rapidly, and heat transfer at the sea floor would soon become unimportant. Heat entering from below could melt about 1/2 cm of solid ice per year. If the ice content were 40% by volume, as it probably is near Prudhoe Bay today (Gold and Lachenbruch, 1973), permafrost would thin from below on the order of 1 cm/yr. Thus, 20,000 years after transgression the sea would, in this case, be underlain by 400 m of ice-rich permafrost. This extreme example serves to illustrate the important roles played by ice content and shoreline history and to underscore the need for direct observations to constrain theoretical estimates. The transition of permafrost thickness from the offshore to onshore conditions and near islands and shoals is easily estimated by theoretical or numerical techniques once the basic information

on ice content and surface temperature is available (Lachenbruch, 1957a, 1957b; Lachenbruch et al., 1966).

Geologic Studies

Regional uplift and tilting have also played a role in determining changes in the position of the shoreline. The recent, unpublished studies of D. M. Hopkins and L. D. Carter show that coastal areas southwest of Barrow are undergoing slow uplift, and suggest that the lower Colville River region is also rising slowly. When quantified, these observations will be useful in determining the position of the shoreline at various moments in the past. The character of Holocene crustal movement in the Prudhoe Bay area is uncertain.

Studies of fossil pollen and marine microfossils now underway by the U.S.G.S. will provide information on past air and sea temperatures and on the snow cover of the past. These data will be needed in order to quantify temperature history for use in predictive geothermal models.

Barnes and Reimnitz (1974) discuss the distribution of sediments on the shelf in a process oriented study. Apparently, distinctive sedimentary structures and facies changes related to wave, current, and ice influence occur in zones across the shelf and may be used to interpret sedimentary environments in a vertical section. Reimnitz and Barnes (1974) are particularly concerned with the interaction of ice at the sea floor, as are Kovacs (1972), Kovacs and Mellor (1974), Reimnitz and others (1972), Pelletier and Shearer (1972), and Barnes and Reimnitz (1974).

Important to the interpretation of sea level history is the influx of coarse clastic material from an apparent easterly source. These materials have been considered by Leffingwell (1919), MacCarthy (1958), Naidu and Mowatt (1973), Mowatt and Naidu (1974), and Rodeick (1974) as relict gravels and boulders. Mowatt and Naidu (1974) look to Ellesmere Island as a main source of this ice rafted material with the Coronation Gulf in the Canadian Archipelago as a possible subordinate source, while Rodeick (in preparation) suggests most of the material has been ice rafted from the Amundsen Gulf region, a western extension of Coronation Gulf. These exotic gravels and boulders extend onshore into the Quaternary Gubik Formation (Rodeick, 1974). On the upper continental slope they overlie deposits dated at 15,000 B.P. Thus, evidence for two transgressive phases of ice rafted material are seen and the interfingering of these deposits may be crucial in the interpretation of sea level history.

Holocene sediments on the Beaufort Sea shelf are thin or lacking in most places (Reimnitz and others, 1972; Short, 1973; Reimnitz and Barnes, 1974; Barnes and Reimnitz, 1974; Reimnitz and others, in press), and consequently early Holocene sediments are found at the surface. These older sediments are highly consolidated compared to the modern marine sediments. Thus, much of the Beaufort shelf is apparently an area of non-deposition or is being subject to erosion by currents and ice.

Offshore Permafrost

Until the present, the controversial problem of the extent and distribution of offshore permafrost has been treated theoretically or extrapolated from land based data (Lachenbruch, 1957a; Mackey, 1972a; Judge, 1974), studied by small boat seismic refraction methods (Hunter, 1973; Rogers, RU #271), and to a very limited extent by drilling (Lewellen, 1974, Mackey, 1972a, 1972b; Osterkamp and Harrison, RU #253, 255, 256). It is the general consensus of most arctic investigators that drilling and sampling the continental shelf sediments is essential for determining offshore permafrost characteristics and distribution. This is predicated on the fact that permafrost distribution is related to past thermal and depositional histories and to the material properties of the sediments which can only be determined through direct measurement.

A knowledge of the distribution of deep ice-rich permafrost is, of course, fundamental to engineering problems related to offshore drilling and oil production and to the interpretation of seismic data for resource studies. However, for the many problems relating to foundations of sea-bed structures such as pipelines, drill rigs, and docking facilities, the distribution of ice in the upper 10 to 50 m is of primary importance. (The near-freezing temperature of sub-sea permafrost makes it vulnerable to engineering disruption like permafrost in the subarctic (Lachenbruch, 1970)). This is a problem that can be investigated directly with temperature and properties information from relatively few shallow boreholes. The

information so obtained can be extended theoretically with the aid of surface investigations of the thermal regime of the bottom water and information on the sediment characteristics throughout the area of interest.

Several corollary problems are related to this study. Furthermore they must be examined prior to offshore development and are a logical outgrowth of any drilling and sampling program:

1. Engineering properties: Permafrost has a marked influence on the engineering properties of soils, and probably of marine sediments. Ice gouging of the sea floor commonly exposes semi-consolidated sediments and creates metastable gouge ridges (Reimnitz and Barnes, 1974). Thus, the engineering properties of surface and subsurface shelf sediment need to be assessed, so that potential hazard to offshore construction may be determined.

2. Construction material. Sand and gravel are essential construction materials for drill pads, air strips, roads and offshore islands. In the Prudhoe Bay area, materials are now obtained from the river channels and from the offshore islands, where the gravel has apparently been reconcentrated from the Gubik Formation. In the vicinity of Barrow the Gubik Formation has little gravel and this building material is in short supply (LaBelle, 1973). As a result, the potential for the offshore sand and gravel resources needs to be evaluated.

3. Stratigraphic studies. In a study of offshore permafrost a knowledge of the last transgression is of prime importance. The

probability of dissimilar tectonic histories makes it dangerous to extrapolate sea level histories from one area to another. Hopkins (1967, 1973) has delineated the sea level history of the eastern Bering Sea. This data is closest to the proposed study area. From his field observations Hopkins states, "I have long been convinced that sea level rose to within a few tens of meters of its present position during a middle Wisconsin interstadial warming about 30,000 yr. B.P.". Hopkins (1973) shows the mid-Wisconsin transgression in the Bering Sea reached the -20 meter contour. Curray (1964) suggested the highest position of the sea during the mid-Wisconsin transgression was several meters below its present level, while Morner (1971) has expressed doubts that enough continental ice melted to permit such an extensive middle Wisconsin transgression. MacCarthy (1958) suggested a minimum of 8 meters of uplift on the Arctic Coast, based on the distribution of ice-rafted boulders. Sellman and Brown (1973) describe beach ridges at an elevation of +7 meters near Point Barrow, data 25,000 - 40,000 B.P. From the previous discussion it is clear that a sea level history for the Beaufort Sea must be established through stratigraphic and paleoclimatologic investigations in the area itself.

4. Marine environmental data. Data on geologic and oceanographic conditions during the winter months is almost non-existent for arctic shelves. Thus, the processes operating during the major part of the year are poorly known. It has been hypothesized that the ice regime, in particular the ice in the stamukhi zone, significantly

interacts with the sediments during this period probably influencing the thermal regime where grounded (Kovacs and Mellor, 1974; Barnes and Reimnitz, 1974; Reimnitz and Barnes, 1974; Reimnitz and others, in press). Therefore, quantification of the current and tide regimes, water and sediment temperatures, and suspended sediment both inside and outside of the stamukhi would aid significantly in defining the active processes during the ice-covered season.

IV. Study Area

The primary study area is located in Stefansson Sound, between Pt. McIntyre and Reindeer Island (Fig. 1). The ice regime in this area consists almost exclusively of bottom fast ice and floating fast ice (Reimnitz and other, in prep.). The most seaward of the proposed drilling holes (Fig. 1) is located only approximately as the location will be predicated on the character of the stamukhi zone which runs close inshore along this section of the coast. Two rivers flank the study area; the Sagavanirktok river is located to the east, and the Kuparuk empties into Gwydr Bay to the west. Neither river has a direct influence on the thermal regime of the study area either during the period of floor or during the open water season. Stefansson Sound is characterized by a thin covering of recent sediments (Reimnitz and others, 1972) composed of silts and fine sands (Barnes and Reimnitz, 1974). Examination of historical photos of the coastline would indicate the shore is relatively stable at this time. Reindeer Island is a constructional feature on a pre-Holocene surface and is apparently frozen only in the upper part as reflection seismic lines do

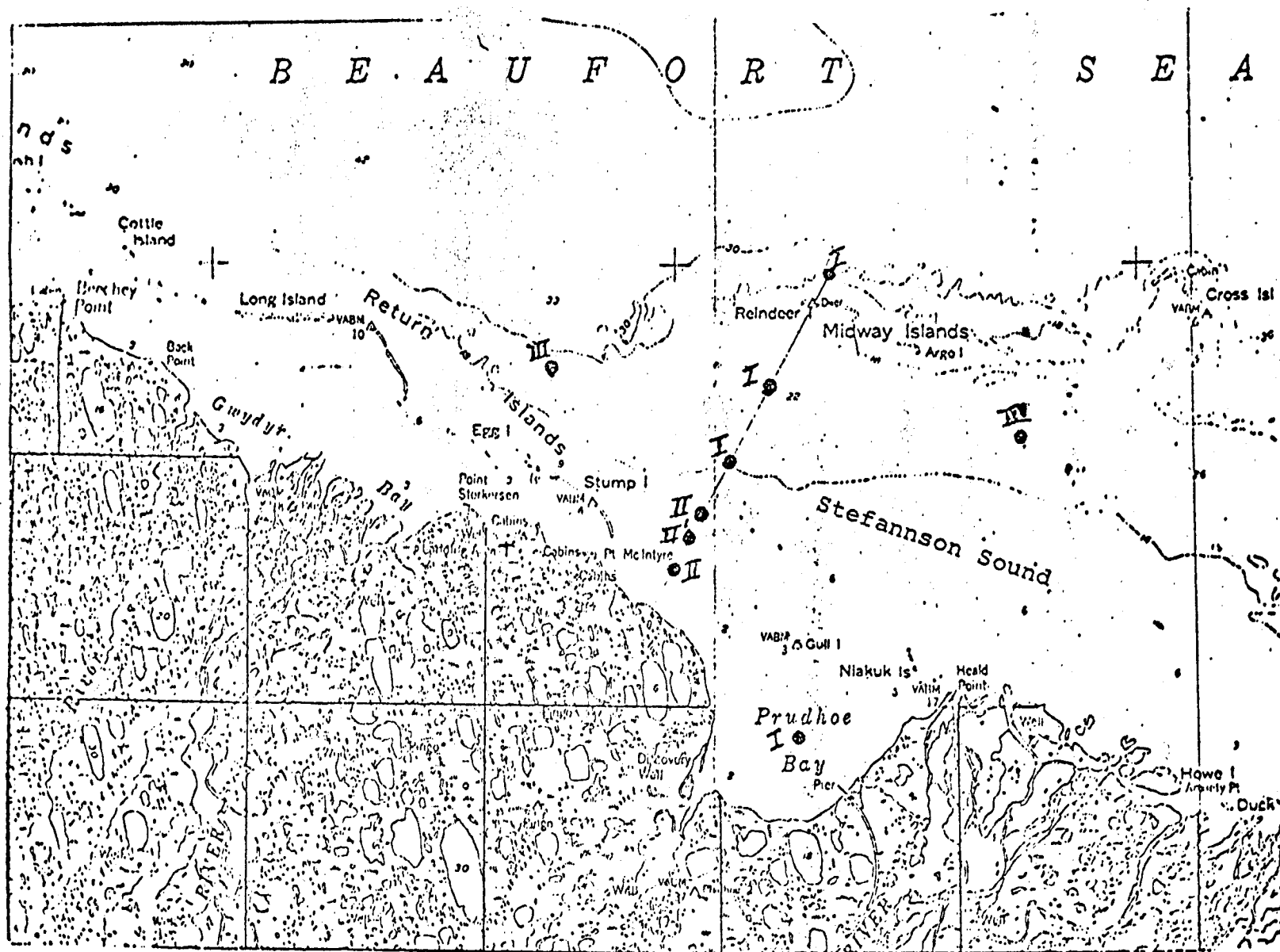
not show an increased velocity under the island as one would anticipate with frozen material. The oceanography, permafrost history, stratigraphy, and biology of Stefansson Sound are essentially unknown.

V. Sources, methods and rationale of data collection.

We are proposing to examine the above problems by sampling and in situ measurements of a series of holes drilled to a maximum depth of 150 m using the sea ice as a stable platform during April 1976. The effort is designed to test drilling techniques, methods of sample recovery, and to establish routine methods of data collection as well as to develop a subsurface geothermal geologic framework. Holes will be drilled at strategically located sites to augment nearly 2000 kilometers of high resolution seismic profiles already acquired by the U. S. Geological Survey (Reimnitz and others, 1972; Reimnitz and Barnes, 1974).

The proposed first year field work includes the drilling of four to seven holes during a four week period. Work during this first season will be restricted to the Prudhoe Bay area. The close proximity to the only major logistics support center will minimize down time resulting from any potential mechanical problems. It is also the most likely location of initial OCS exploitation by industry.

Figure 1 shows the primary and secondary drill sites. The transect lies approximately normal to the coastline, was chosen to connect holes existing onshore and Reindeer Island.



Proposed 1976 drill sites - I, primary sites; II, secondary sites; III, tertiary sites. Site in Prudhoe Bay will be an equipment testing site.

In addition this transect parallels the refraction line occupied by J. Rogers (RU #271). The inner 3 km of this line has been drilled to 50 m by Osterkam and Harrison under RU# 253, 255, 256. The southernmost end of the transect has a hole which has been monitored for a number of years. A traverse normal to the present coast will also enable us to estimate rates of transgression. Sites of secondary priority represent a tie with Osterkamp and Harrison's work and the existing onland hole. Tertiary sites have the potential for lateral extrapolation of data and will be drilled if time and funds permit.

A coordinated program is underway involving seismic refraction by the University of Alaska (J. Roger, RU #271) to aid in extrapolating the hole information to a regional area.

The proposed research consists of 4 scientific studies plus the drilling program as discussed below and outlined in Figure 2 and 3. One of the field logging sheets is shown in Figure 4.

PART I Geothermal

In the holes to be drilled in the present investigation, we propose to log temperatures to millidegree accuracy over a period of two or three weeks until enough information is obtained to calculate the undisturbed equilibrium temperatures (Lachenbruch and Brewer, 1959). Samples will be obtained for thermal conductivity measurements and for determination of the abundance and freezing characteristics of the interstitial fluid. An attempt will be made to combine these data with regional information shoreline and climatic history, sea-bed temperature, distribution of sediments, and onshore geothermal information to provide an interim model of

PROGRAM SEQUENCE

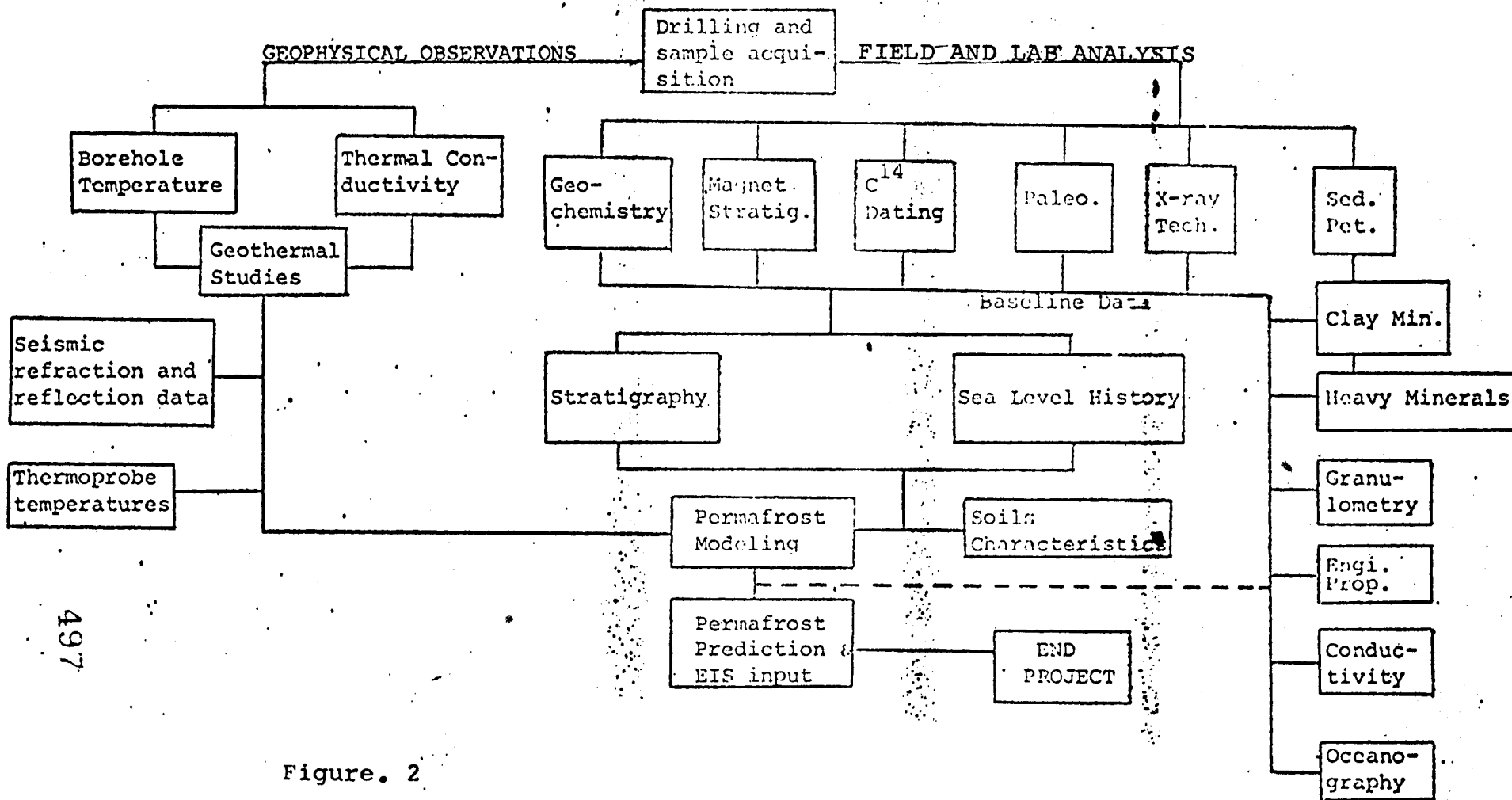


Figure. 2

497

SAMPLE HANDLING SCHEME

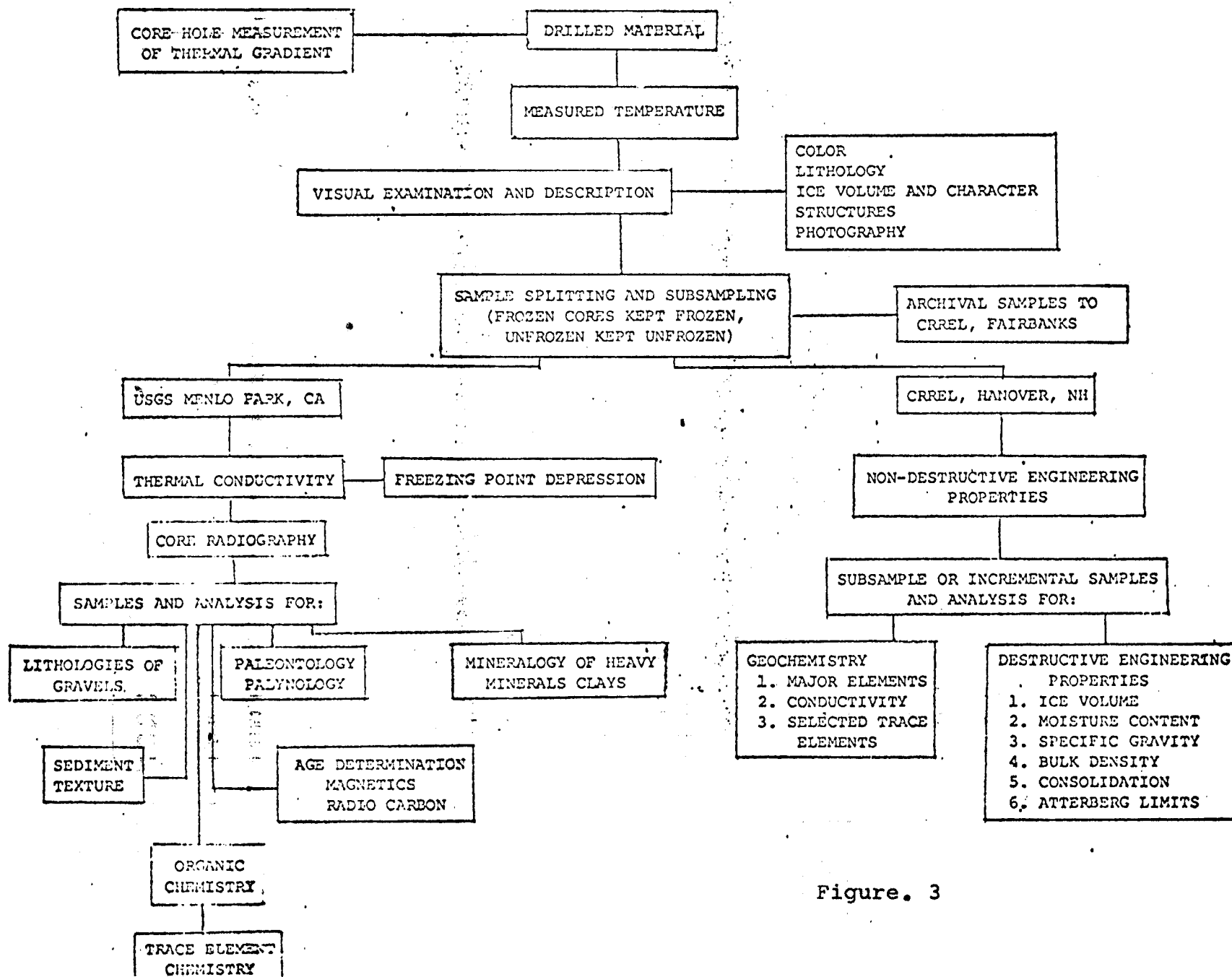


Figure. 3

the thermal regime of the sub-bottom sediments and the likely distribution of ice within them.

Part II Geology

Examination of core samples obtained from drilling will yield information on stratigraphy, lithologies, and geochemistry of the shelf sediments. Standard granulometric methods and sedimentary petrologic techniques, such as grain size analysis, heavy mineral studies, radiography of cores, and organic and total carbon analysis will be used to determine the depositional environments represented in the stratigraphic section. Paleontologic and palynologic investigations will also be undertaken. These studies will allow us to evaluate the depositional environments and paleoclimate throughout the section and to determine the source and distance of transport of the sediments.

Barnes and Reimnitz (1974) have shown zonation of various sedimentary structures attributable to ice gouging, may be used to estimate paleo-depths. Radiography of core samples will enable this work to be extended into the past, allowing a quantitative estimate of the effect of ice as a geologic agent.

The examination of coarse clastic materials will enable us to estimate the importance of ice-rafted sediment input (Leffingwell, 1919; MacCarthy, 1958; Naidu and Mowatt, 1973; Mowatt, 1974; Rodeick, 1974). Data for this phase may be taken from undisturbed core samples, or from disturbed drive samples.

Part III Sedimentologic Processes

Certain oceanographic measurements will be attempted during the spring. These investigations will include tide, current, suspended sediment, transmissivity, temperature and salinity measurements. Current velocities will be recorded and factory processed into a final computer output format. Temperature and salinity data will be determined by portable equipment, while suspended sediment samples will be filtered from water samples obtained at each site, and correlated with transmissometer data. Attempts will be made to record tides and currents inside and outside of the stamukhi (10 to 30 m depth), for the duration of the field program, and possibly extending into the following summer.

Part IV Technical Aspects

Drilling expenses comprise the largest part of the projected spending. This is probably understandable when one examines the objectives, the drilling and sampling techniques necessary, and the technical problems one might expect to encounter on such a venture. This part of the program is being managed by Paul Sellman of CRREL and by Robert Lewellen.

REFERENCES AND SELECTED BIBLIOGRAPHY

- Baranov, I. Ya., 1959, Geographical distribution of seasonally frozen ground and permafrost. Translated from the Russian by A. Nurklik. National Research Council, Canada, TT-1121, 1964. Principles of Geocryology, Part 1, Chapter VII, Academy of Sciences of the U.S.S.R., Fig. 24.
- Barnes, P. W., and Reimnitz, E., 1974, Observations of arctic shelf processes from marine geologic studies conducted off the northern coast of Alaska. In J.C. Reed, J. E. Sater, The Coast and Shelf of the Beaufort Sea, Arctic Institute of North America, Arlington, Va., p. 439-476.
- Birch, F., 1948, The effects of Pleistocene climatic variations upon geothermal gradients. American Journal of Science, V. 246, pp. 729-760.
- Black, C. A., D. D. Evans, J. L. White, L. E. Endminger, and F. E. Clark, 1965, Methods of Soil Analysis. Agronomy, No. 9, Part 1, American Society of Agronomy, Madison, Wisconsin, 770 p.
- Broecker, W. S., and Van Donk, J., 1970, Insolation changes, ice volumes and the O^{18} record in deep-sea cores. Reviews of Geophysics and Space Physics, V. 8, pp. 169-198.
- Brown, J., 1968, Ionci concentration gradients in permafrost, Barrow, Alaska. USA CRREL Technical Note., 31 p.
- Burrell, D. C., Kinney, P. J., Hadley, R.S., and Arhelger, M.E., 1970, Beaufort Sea environmental data; 1968-1969. Report No. R70-20, Inst. Marine Science, Univ. of Alaska, 274 p.
- Carsola, A. J., 1954, Recent marine sediments from Alaskan and northwest Canadian Arctic. bull. Am. Assoc. Petrol. Geologists, V. 38, pp. 1552-1586.
- Curray, J. R., 1964, Transgressions and Regressions. In Papers in Marine Geology, Shepard Commemorative Volume, R. Miller [Ed.], pp. 175-203.
- Gerasimov, I. P. and K. K. Markov, 1939, Permafrost and ancient glaciation. Translated from the Russian by E. R. Hope, Defense Research Board (Canada), T 499 R, 1968, pp. 11-19. The Ice Age in the U.S.S.R., Tr. Inst. Geog. Acad. Sc., U.S.S.R. 33, pp. 35-44.

- Gold, L. W., and Lachenbruch, A. H., 1973, Thermal conditions in permafrost -- A review of North American literature, in Permafrost--North American Contribution, Second Internat. Conf., Yakutsk, USSR, July 1973: Natl. Acad. Sci., Washington, p. 3-25.
- Govorukha, L. S., 1968, Ya. Ya. Gakkel on Arctis. In Problems of polar geography, Belov [Ed.], Translated from the Russian by N. Kaner, Arctic and Antarctic Research Institute, Leningrad. Trudy 285, pp. 37-51.
- Grigorev, N. F., 1962, Role of cryogenic factors in the formation of the Yakutia Sea Shores. Moscow, Izd. AN SSR, pp. 68-78.
- Hopkins, D. M., 1967, Quaternary marine transgressions in Alaska. In The Bering Land Bridge. D. M. Hopkins [Ed.], Stanford Univ. Press., Stanford, California, pp. 47-91.
- Hopkins, D. M., 1973, Sea level history in Beringia during the past 250,000 years. Jour. Quaternary Research, V. 3, No. 4, pp. 521-540.
- Hunter, J. A. M., 1973, The application of shallow seismic methods to mapping of frozen surficial materials. In Permafrost: Proceedings of Second International Conference. National Academy of Sciences, Washington, D. C., pp. 527-535.
- Judge, A., 1974, The occurrence of offshore permafrost in northern Canada. [abst.], Program of Symposium on Beaufort Sea Coastal and Shelf Research. San Francisco.
- Kinney, P. J., Schell, D. M., Dygas, J., Nenahlo, R., and Hall, G.E., 1972, Nearshore currents. In Baseline data study of the Alaskan arctic aquatic environment, Inst. Marine Science, Univ. of Alaska, Report No. 72-3, pp. 29-48.
- Kovacs, A., 1972, Ice scoring marks on the floor of the Arctic Shelf. The Oil and Gas Journal, Oct. 23, 1972, pp. 92-106.
- Kovacs, A. and Mellor, M. E., 1974, Sea ice morphology and ice as a geologic agent in the southern Beaufort Sea: In J.C. Reed, J.E. Sater The Coast and Shelf of the Beaufort Sea, Arctic Institute of North America, Arlington, Va., p. 113-162.
- La Belle, J. C., 1973, Fill materials and aggregate near Barrow, Naval Petroleum Reserve No. 4, Alaska: Arctic Institute of North America, ONPR Report Contract NOD-9915 (72-2) 146 p.

- Lachenbruch, A. H., 1957a, Thermal effects of the ocean on permafrost: Geol. Soc. America Bull., V. 68, p. 1515-1530.
- Lachenbruch, A. H., 1957b, Three-dimensional heat conduction in permafrost beneath heated buildings: U.S. Geol. Survey Bull. 1052-B, p. 51-69.
- Lachenbruch, A. H., and Brewer, M. C., 1959, Dissipation of the temperature effect of drilling a well in Arctic Alaska: U. S. Geol. Survey Bull. 1083-C, p. 73-109.
- Lachenbruch, A. H., Brewer, M. C., Greene, G. W., and Marshall, B.V., 1962, Temperatures in permafrost in Temperature, its measurement and control in science and industry: Reinhold Pub. Co., V. 3, pt. 1, p. 791-803.
- Lachenbruch, A. H., Greene, G. W., and Marshall, B. V., 1966, Permafrost and the geothermal regimes. In Environment of the Cape Thompson Region, Alaska. USAEC Division of Technical Information pp. 149-165.
- Lachenbruch, A. H. Greene, G. W., and Marshall, B. V., 1966, Permafrost and the geothermal regimes, in Wilimovsky, N. J., and Wolfe, J. N., eds., Environment of the Cape Thompson region, Alaska: U.S. Atomic Energy Comm., Div. Tech. Inf., p. 149-163.
- Lachenbruch, A. H., and Marshall, B. V., 1969, Heat flow in the Arctic. Arctic, V. 22, No. 3, pp. 300-312.
- Lachenbruch, A. H., 1970, Some estimates of the thermal effects of a heated pipeline in permafrost: U.S. Geol Survey Circular 632, 23 p.
- Leffingwell, Ernest deK., 1919, The Canning River region, Northern Alaska. U. S. Geol. Survey Prof. Paper 109, 251 p.
- Lewellen, R. I., 1973, The occurrence and characteristics of near-shore permafrost, Northern Alaska. In Permafrost: Proceedings of Second International Conference. National Academy of Sciences, Washington, D. C. pp. 131-136.
- Lewellen, R. I., 1974, Offshore permafrost, Beaufort Sea, Alaska. In Program of Symposium on Beaufort Sea Coastal and Shelf Research, San Francisco (abst.).
- Loder, T. C., 1971, Distribution of dissolved and particulate organic carbon in Alaskan polar and subpolar estuarine waters. Ph.D. Dissertation, Inst. Marine Science, Univ. of Alaska, Report No. R71-15, 236 p.

- MacCarthy, G. R., 1958, Glacial boulders on the Arctic Coast of Alaska. *Arctic*, V. 11, No. 2, pp. 79-85.
- Mackay, J. R., 1972a, The world of underground ice. *Ann. Assoc. Am. Geogr.*, V. 62, pp. 1-22.
- Mackay, J. R. 1972b, Offshore permafrost and ground ice, southern Beaufort Sea, Canada. *Canadian Jour. of Earth Sciences*, V. 9, No. 11, pp. 1550-1561.
- Melnikov, P., 1966, Geocryologic map of the Yakut A.S.S.R. Academy of Sciences, U.S.S.R. Scale 1:5,000,000.
- Morner, N. A., 1971, The position of the ocean level during the interstadial at about 30,000 B. P. - a discussion from a climatic-geologic point of view. *Canadian Jour. of Earth Sciences*, V.8, pp. 132-143.
- Mowatt, T. C., and Naidu, A. S., 1974, Detailed clay mineralogy of The Colville River and Delta, northern Arctic Alaska. Alaskan Division of Geological and Geophysical Survey. Open File Report 45, Fairbanks.
- Naidu, A. S., 1971, Geochemical studies on the bottom sediments of the Beaufort Sea, Arctic Ocean. Report No. R71-12, Inst. of Marine Science, Univ. of Alaska, pp. 113-120.
- Naidu, A. S., 1972, Clay mineralogy and heavy-metal geochemistry of deltaic sediments of the Colville and adjacent rivers. In Baseline data study of the Alaskan arctic aquatic environment. Report No. R72-3, Inst. Marine Science, Univ. of Alaska, pp. 123-138.
- Naidu, A. S., and Sharma, G. D., 1972, Texture, mineralogy and chemistry of Arctic Ocean sediments. Report No. R-72-12, Inst. Marine Science, Univ. of Alaska, 31 p.
- Naidu, A. S. and Mowatt, T. C., 1974 (in press), Aspects of size distributions, mineralogy, and geochemistry of deltaic and adjacent shallow marine sediment, north Arctic Alaska. U.S. Coast Guard; Oceanographic Report No. CG 373-64, p. 238-268.
- National Academy of Sciences, 1974, Priorities for Basic research on Permafrost, Nat. ACD-SC, Washington, D. C., 54 p.
- Pelletier, B. R., and Shearer, J. M., 1972, Sea bottom scouring in the Beaufort Sea of the Arctic Ocean. 24th IGC, Section 8, pp. 251-261.

- Reimnitz, E., Barnes, P. W., Forgatsch, T., and Rodeick, C., 1972, Influence of grounding ice on the arctic shelf of Alaska. *Mar. Geol.*, V. 13, pp. 323-334.
- Reimnitz, E., Wolf, S. C., and Rodeick, C., A., 1972, Preliminary interpretation of seismic profiles in the Prudhoe Bay area, Beaufort Sea, Alaska. U.S. Geol. Survey Open File Report 548.
- Reimnitz, E., and Barnes, P. W., 1974, Sea ice as a geologic agent on the Beaufort Sea shelf of Alaska. In J.C. Reed, J. E. Sater, The Coast and Shelf of the Beaufort Sea, Arctic Institute of North America, Arlington, Va., p. 113-162.
- Rodeick, C. A., 1974, Origin, distribution, and depositional history of gravel deposits on the Beaufort Sea continental shelf, Alaska. In Proceedings of the Symposium on Beaufort Sea Coastal and Shelf Research, A.I.N.A.
- Samson, L., and Tordon, F., 1969, Experience with engineering site investigations in Northern Quebec and northern Baffin Island. In Proceedings of the Third Canadian Conference on Permafrost. Tech. Mem. 96, pp. 21-39.
- Sellmann, P. V., Brown, J., 1973, Stratigraphy and diagenesis of perennially frozen sediments in the Barrow, Alaska Region. In Permafrost: Proceedings of the Second International Conference. National Academy of Sciences, Washington, D.C., pp. 171-185.
- Short, A. D., 1973, Beach dynamics and nearshore morphology of the Alaskan Arctic Coast. Louisiana State University, Dept. of Marine Science Doctoral dissertation, 140 p.
- Werenskiold, W., 1953, The extent of frozen ground under the sea bottom and glacier beds. *Jour. of Glaciology*, V. , pp. 197-200.
- Yorath, C. J., Shearer, J., and Havard, C., 1971, Seismic and sediment studies in the Beaufort Sea. Geol. Survey of Canada, Paper 71-1A, pp. 242-244.

VI. Results

The field effort is planned for April, 1976, thus no results are available at the present time.

Activity has been aimed at preparing for the field study. Instrument development to log temperatures and measure thermal conductivities in situ has progressed to near completion. This equipment will allow us to obtain near-surface (4 meters) sediment temperatures and thermal conductivity which will allow us to explore the transient nature of shallow temperatures.

VII. Discussion - N/A

VIII. Conclusions - N/A

IX. Needs for further study

In light of the planning and logistics preparation that has gone into the drilling program this year and in view of the uncertainties that have arisen from the studies of J. Rogers' (RU #271) and Osterkamp and Harrison's (RU #253, 255, 256) offshore permafrost programs; an additional year of drilling would prove to be scientifically and economically advantageous in defining the problems associated with offshore permafrost. In particular two areas will need further definition: 1) the lateral extent will be incompletely defined, even if the tertiary objectives are accomplished, 2) the bottom of the permafrost will be only poorly understood as it will likely lie below the drilling depths of this years program.

X. Summary of 4th quarter operations

1. Field Schedule -

The drilling program and ancillary field activities are scheduled for 20 March thru April 1976. The operation will be staged out of Prudhoe Bay using a leased camp and CRREL and ONR drilling equipment. Some work will also be accomplished from the Oliktok DEW site. Support will be provided by project personnel and equipment and NOAA supplied Rollington and helicopter.

2. Scientific party -

Peter Barnes - USGS
David Carter - USGS
David Drake - USGS
David Hopkins - USGS
Vaughn Marshall - USGS

Paul Sellmann - CRREL
Ed Chamberlain - CRREL
Allen Delaney - CRREL
Richard Berg - CRREL
Herbert Ueda - CRREL
Robert Lewellen - Arctic Research

3. Methods -

A detailed discussion of the methods used in this study are presented in V above.

The U.S. Army Cold Regions Research and Engineering Laboratory (CRREL) and the U.S.G.S. will drill a series of holes on a profile offshore from Prudhoe Bay, Alaska. These holes will be drilled to a depth of about 150 m during the late winter and early spring, 1976, using the sea ice as a platform. In the holes to be drilled, temperatures will be logged to millidegree accuracy and thereby determine the undisturbed equilibrium temperatures. Samples will be obtained from thermal conducti-

vity measurements and for determination of the abundance and freezing characteristics of the interstitial fluid. An attempt will be made to combine these data with regional information on shoreline and climatic history, sea-bed temperature, distribution of sediments and onshore geothermal information to provide an interim model for the thermal regime of the sub-bottom sediments and the likely distribution of ice within them. Near surface thermoprobe observations will be obtained at sites adjacent to the drill holes. Cores samples and cuttings will be examined for stratigraphy, lithology, geochemistry and engineering properties. Standard sedimentological techniques will be used to determine the depositional environments represented in the stratigraphic section. In order to make maximum use of the boreholes, the drill cores or cuttings will be sampled for their fossil content, especially mollusks, foraminifers, ostracodes, and pollen.

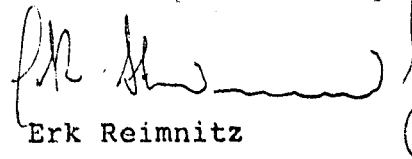
4. Sample localities/sip or aircraft tracklines (see attached chartlet).

5. Data collected or analyzed -

No data or samples have been collected during this report period.

Note:

Section C : " Evaluation of the Prudhoe Bay channel by fast ice" could not be included at this time. This section presents our interpretation of data collected for ARCO in 1969. Clearance to report on this data should be forthcoming any day, we were told, and we should be able to send the report shortly.



Erk Reimnitz

March 30, 1976.

ANNUAL REPORT

Contract #RK6-6074
Research Unit #205
Reporting period -
May 1975 - April 1976

Pages

Marine environmental problems in the ice covered
Beaufort Sea shelf and coastal regions

Principal Investigators:

Peter Barnes
Erk Reimnitz
David Drake

1 April 1976

TABLE OF CONTENTS

| | | |
|-------|---|----|
| I. | Summary of objectives, conclusions and implications with respect to OCS oil and gas development | 1 |
| II. | Introduction | 3 |
| | A. General nature and scope of study | |
| | B. Specific objectives | |
| | C. Relevance to problems of petroleum development | |
| III. | Current state of knowledge | 7 |
| IV. | Study area | 8 |
| V. | Sources, methods and rationale of data collection | 8 |
| VI. | Results (For section VI, VII, VIII refer to attachments A thru K) | 10 |
| VII. | Discussion (For section VI, VII, VIII refer to attachments A thru K) | 10 |
| VIII. | Conclusions (For section VI, VII, VIII refer to attachments A thru K) | 10 |
| XI. | Needs for further study (see section IIB) | |
| X. | Summary of 4th quarter operations | 11 |

I. Summary of objectives, conclusions and implications with respect to OCS oil and gas development

The marine environment of the Arctic shelf poses special problems to offshore development. Faulting, tectonic activity, and sea floor instability are environmentally of lower concern. When compared to unique Arctic processes and phenomena related to cold temperatures and the predominant influence of sea ice. Five years of study have provided a basic understanding of the unique factors, but many of their important aspects have yet to be addressed. For example, a major process to be understood is that of ice gouging, in particular maximum scour depth, recurrence rate, depth distribution, and the relation to ice regime. Another is the spring flooding of the fast ice with river water, a hazard to operations and a process that could greatly affect dispersal of pollutants. The growth of the fast ice and its vertical fluctuation with tides and surges, sets up currents that not only influence sedimentary processes but also the dispersal of pollutants. The interaction of the stamukhi with the continental margin, its effects on oceanographic circulation, sediment dispersal, and shelf profile, must be understood. The stamukhi is a formidable barrier to offshore development, and shipping, and appears to be an important key to an understanding of the shelf ecosystem.

The first year of field studies aboard the R/V KARLUK and subsequent laboratory and office work has resulted in the following tentative conclusions regarding the arctic nearshore environment.

1. Ice gouging and other ice related processes are important

factors in the nearshore environment, at least as far south as Kotzebue Sound, although the influence of currents, related to flow through the Bering Straits and the longer open water period are more pronounced.

2. Several precisely controlled, side scan sonar survey lines established in 1973 and resurveyed in 1975 establish without a doubt that ice gouge patterns to a depth of 20 m can change substantially within a two-year period.

3. The pronounced linear topographic highs on the inner shelf between Prudhoe Bay and Harrison Bay appear to control shear zone dynamics and stamukhi development. Accurate bathymetry by the U.S.C. and G.S. from 1949-51, was resurveyed in 1975 with excellent navigational control and precision fathometer. These shoals were found to have survived 25 years of ice interaction, but all have shifted landward for distances of 100 to 400 m. We believe this shift is related to shear zone processes and stamukhi. This is the first solid evidence for a relationship between anomalies in the overall profile of an Arctic shelf and boundary processes of the Beaufort Gyre pack ice. These findings have extremely important implications for offshore development in the Arctic especially concerning the construction of artificial islands. We can now make certain predictions regarding the longevity of such structures and on how they will interact with pack ice. It even seems feasible to make the inner shelf ice environment less hostile for man's endeavors by the proper placement of such structures,

4. The presence of unique, anomalous subbottom seismic reflections in Harrison Bay, noted prior to our study, was confirmed. We are spec-

ulating on possible causes related to gas pockets or shallow permafrost.

5. A system of ancient filled river valleys (?) on the shelf between Prudhoe Bay and Harrison Bay was surveyed in reconnaissance fashion, using high resolution seismic techniques. The presence of a major river system in this area, combining the Colville and several drainage basins to the east, has been suggested by others from observations on land.

6. A comparison of temperature, salinity and turbidity observation from the 1972 and 1975 field season indicates that the area northwest of Oliktok is consistently a zone of upwelling of higher salinity and lower temperature, clear waters. Colville river water appears to move offshore to the west. It remains to be determined whether the source of the upwelled waters is at greater depths off the shelf seaward or from local sources, perhaps related to brine formation from ice during the winter. We postulate that this area is a zone of potentially high biologic productivity.

II. Introduction

A. General nature and scope of study

Investigation of the marine geology and sedimentary processes of the continental shelf and shores of the Chukchi and Beaufort Seas in northern Alaska were initiated in 1970. Many aspects have been cooperative efforts with federal and state agencies and universities. The primary goal of the program has been to understand the processes that are unique to Arctic shelves and their sedimentary environment, where sea ice plays an important role. Our specific objectives have included: 1) a definition

of the character of the bottom materials, including permafrost; 2) a study of the present sediment transport and depositional mechanisms; and 3) studies of the Holocene and Pleistocene geologic record.

Our results to date have clearly established drifting ice as a major factor in the marine geologic and sedimentologic environment of Arctic shelves (best summarized in Reimnitz and Barnes, 1974; and Barnes and Reimnitz, 1974). A rudimentary framework for the processes and related sedimentologic record over the entire shelf width has been established. Utilizing this framework a conceptual model has been developed which relates the relative importance of ice and water as dynamic agents to depth and distance from the coast. It is believed that the two areas of most intense sedimentologic activity occur along the coast and in the stamukhi zone between the coastal ice and the arctic pack ice. Ice deforms and stirs bottom sediments, permits conductive thermal transfer between the atmosphere and the seafloor where grounded, inhibits free discharge of river water during spring, resuspends sediments and transports sediments by bulldozing and rafting.

Processes related to the fast-ice flooding by rivers during the late spring flood, have a strong influence on the inner shelf sedimentary environment of the Beaufort Sea shelf. It is during this event that pollutants accumulated during wintertime would be remobilized and redistributed. Drainage through strudel and subsequent underflow scour and reshape the bottom in the region off arctic deltas. However, little sediment is transported at this time and conditions for ice rafting sediments great distances of the inner shelf are unfavorable. Seismic studies have shown

only a thin layer of Holocene sediments manteling the entire width of the continental shelf, thus the scarcity of modern deltaic sediments near Arctic River mouths remains an enigma. These same studies show that the Holocene sedimentary section is reworked by ice, currents, and strudel scour, obliterating most of the bedding features.

B. Specific objectives

Many questions have been raised on the basis of our past investigations, and apparently hold the key to an understanding of the seasonal cycle in the marine environment. It is these tasks that we address in our current research.

1) Processes of ice gouging - in particular the repetitive rates of gouging and the extent to which it occurs outside the area of our past investigations. Repetitive side scan sonar surveys with precise navigational control, direct diving observations, and a deep-tow package with underwater television and a high frequency subbottom profiler, will be used. For the outer shelf studies a manned submersible must be chartered.

2) Shelf sediment transport regime - including ice rafting, river effluents and bottom reworking and resuspension by ice and benthos.

3) The fast-ice zone, and its influence on nearshore current circulation, bedforms, sediment transport, permafrost, and on river discharge.

4) The stamukhi between the coastal ice and the offshore pack ice, and its influence and/or relationship to bathymetry, thermal effects on the sea floor, ice gouging, and winter current regime, tides, and sediment

transport. Some of the studies on this topic can be done during summer operations, but winter operations utilizing record and remote sensing are also required.

5) An estimation of coastal erosion and its relationship to the formation of offshore islands and the stability of the coastal marine environment.

6) Shelf oceanography, related to the sedimentary environment. This includes upwelling in the coastal zone, the dispersal of highly saline (60 o/oo) and cold (-5°C) water generated in shallow embayments, lagoons, and river mouths during the winter, and possibility of anchor ice formation as a factor in the sedimentary environment. Much of the necessary data must be gathered through instrument packages which record data throughout the winter.

7) The apparent lack of deltaic sedimentation near river mouths in the Arctic, and the unique marine aspects of Arctic rivers in general. Seismic reflection surveys will be extended up into the major river channels. Instrument packages, including current-, temperature-, salinity-, turbidity-, and tide-sensors shall be used to monitor specific nearshore locations throughout the winter.

8) Pleistocene stratigraphy and geologic history, from a combined analysis of available sediment and seismic data, the expected drill hole data, and 2-m long vibro-corer samples.

9) Offshore sand and gravel resources, in the Barrow area from shipboard studies, in the Prudhoe Bay area from correlation of available seismic reflection records with permafrost drill hole data.

C. Relevance to problems of petroleum development

The character of the arctic continental shelf and coastal area, with its permafrost, faces the developer with many special problems. Any structure which is to be connected to the ocean floor requires data concerning the strength and character of the ocean floor. In addition, the offshore drilling operation may encounter permafrost which would be substantially altered during the process of pumping hot oil up to the sea floor or along the sea floor in gathering and transportation pipelines. The interaction of the arctic shelf with the arctic pack ice takes the form of ice gouging and the formation of a large stamukhi zone each winter. These factors are of utmost importance to the designers and operators of offshore terminals and pipelines.

Because oil drilling and production during the next several years will probably not extend seaward of the seasonal fast-ice zone, and because existing data in this area are sparse, the summer operations focus on the shelf region shoreward of the stamukhi zone (10-30 m).

A similar emphasis has been taken by the Canadian Beaufort Sea Project in their more advanced state of knowledge and readiness to lease their outer continental shelf lands (Milne and Smiley, 1976).

III. Current state of knowledge

The current state of general knowledge has been excellently summarized in the Arctic Institute of North America's 1974 publication: The Coast and Shelf of the Beaufort Sea. The bulk of background geologic material for the Alaskan Beaufort shelf have been summarized in two articles by Reimnitz and Barnes, in this same volume. References to more

recent material may be found in the Results and Discussion sections below and in the appended reports.

IV. Study area

Since oil drilling and production during the next several years probably will not extend seaward beyond the seasonal fast-ice zone, and since existing data in this area is sparse, our summer operations will focus on the shelf region from the stamukhi zone (10-30 m) shoreward to the coast. The Geological Survey utilizes a shallow draft research vessel, especially adapted to independent operations on the inner shelf.

During the summer of 1975, this vessel (R/V KARLUK) commenced working in the Kotzebue area (Chukchi Sea) by mid-July, followed the retreating ice around Barrow, accomplishing some reconnaissance observations enroute. After working during September from Harrison Bay to Flaxman Island, it was winterized at Prudhoe Bay.

V. Sources, methods and rationale of data collection

Equipment operated routinely from the KARLUK includes bottom sampling and coring gear, water salinity, -temperature, and -turbidity sensors, fathometers, a high resolution seismic system, underwater television, and a side-scan sonar. Precision navigation is maintained to 3 m accuracy with range-range system. Near Barrow and Prudhoe Bay, a seismic refraction system is being used (in cooperation with the Institute of Geophysics of the University of Alaska) to search for high-velocity layers that may be related to permafrost.

Topical problems listed earlier will be investigated using current meters implanted on the open shelf, and on the inner shelf near Prudhoe and just off the Colville River. Special techniques include (a) repetitive sonar and fathometer surveys of ice gouges, (b) diving observations and bottom photography, (c) measurements of sediment thicknesses within ice gouges by combined use of narrow beam echo sounder, and (d) a near-bottom tow package incorporating sub-bottom profiler and television, and (e) near surface stratigraphic studies using a vibrocorer capable of obtaining two meter long cores. River delta sediments will also be examined with cores and sediment profiler.

ATTACHMENTS

- A. Preliminary Cruise Report and Tracklines (Beaufort Sea)
- B. Preliminary Cruise Report and Tracklines (Chukchi Sea)
- C. Evaluation of the Prudhoe Bay channel restriction by fast ice
- D. Cross Island Changes in Morphology from 1949 to 1975 and their implications
- E. A study of the repetitive rate of ice gouging in Harrison Bay, Beaufort Sea
- F. Shoal migration under the influence of ice: A comparison study 1950-1975
- G. This 1:80,000 chart of the bathymetry between 147°45' and 145°35'
- H. Surface current observations - Beaufort Sea, 1972
- I. Distribution and character of icings in northeastern Alaska
- J. A Herringbone pattern of possible Taylor-Gortler-type flow origin seen in sonographs
- K. Heavy-mineral trends in the Beaufort Sea

X. Summary of 4th quarter operations

A. Ship or Laboratory Activities

1. Operations

a) After having completed marine environmental studies of the inner shelves and coast of both the eastern Chukchi and southern Beaufort Seas, the U.S.G.S. R/V KARLUK was winterized at Prudhoe Bay during the freeze-up in late September, 1975. Since that time a continuing program of redesign and updating of the vessel's operational and surveying systems has been undertaken, in preparation of planned summer, 1976 activities. No ship operations were conducted during the 4th quarter covered by this report.

b) An ice-based field operation is presently in progress, under the direction of Peter Barnes and David Drake, to recover two continuously recording temperature-, salinity-, and current direction and velocity meters placed on the inner shelf in September 1975. After their recovery, the two instruments packages will be re-deployed through holes in the ice at locations selected on a real-time base, dependent on ice- and weather conditions. Another instrument package, consisting of two current meters, a tide gage, and nephelometer will be deployed in Harrison Bay at a depth of 10 to 15 meters. Still another system, including temperature-, salinity-, tide-, and current-recording capability will be deployed north of Argo Island, at a depth of about 30 meters. Furthermore, the ice-based operations will attempt to obtain real-time measurements through the ice of temperature, salinity and water flow in regions of

tidal inlets and/or channels, where the intensification of flow due to constriction of an ice cover is suspected. Suspended sediment samples will be obtained along with the above measurements.

General observations of ice morphology, particularly the location and spacial distribution of grounded pressure ridge systems along the inner shelf, will also be made during the present field operation.

2) Scientific personnel involved in analysis, interpretation, and compilation of data included in 4th quarter activities:

| | | | | | |
|-----------------|------------------------|-----------------------------------|---|---|--|
| Peter Barnes | Project Chief | Office of Marine Geology- USGS | | | |
| Erk Reimnitz | Principal Investigator | " | " | " | |
| Dave Drake | " | " | " | " | |
| Larry Toimil | Co-Investigator | " | " | " | |
| John Melchoir | Assistant | " | " | " | |
| Graig Smith | " | " | " | " | |
| Gretchen Luepke | Co-Investigator | " | " | " | |
| Deborah Harden | " | " | " | " | |

3) Methods

Because oil drilling and production in the next several years will likely not extend seaward of the seasonal fast-ice zone, and because existing data is sparse, summer 1975 field operations aboard the U.S.G.S. R/V KARLUK were concentrated on the shelf shoreward of the winter shear-zone (10-30 m water depths). Data collected and systems routinely run during the summer included: bottom sediment samples obtained using both a Van Veen type and underway sampler; suspended sediment samples of

surface waters; water salinity, temperature and turbidity measurements; bathymetry using both 30 and 200 kHz fathometers; sub-bottom profiles using 7 kHz and high resolution seismic-reflection systems; underwater television observations; and side-scan sonar recording of seabed morphology. A range-range precision navigation system was utilized in detailed bathymetric and repetivity side-scan sonar surveys. Direct observations of the seafloor at a number of selected sites were carried out by divers using Scuba. The temporal and spacial scheme of samples obtained was often dictated by day-to-day changes in ice conditions, while others were selected on the basis of side-scan sonar, seismic profiles and underwater television observations.

4. Sample localities/ship or aircraft tracklines

a) Figure 4a shows the locations of salinity, temperature, tide and current monitors to be established during 4th quarter field operations now in progress. The locations are tentative and dependent on favorable ice and weather conditions. Also shown in the figure are sites at which salinity, temperature, turbidity and current measurements along with suspended sediment samples are to be obtained through the fast-ice.

5. Data collected or analyzed:

| <u>Data Type</u> | <u>Trackline miles/or # samples analyzed during 4th quarter operations</u> |
|----------------------------------|--|
| High resolution seismic profiles | 150 line miles |
| 7 kHz sub-bottom profiles | 90 line miles |
| side-scan sonar profiles | 50 " " |
| 200 kHz bathymetric profiles | 175 " " |

5. Data collected or analyzed (cont'd)

| | |
|---|----------------|
| Underwater T.V. video tape | 1.5 line miles |
| Bottom sediment samples (Van Veen and gravity core) | 150 samples |
| Suspended sediment samples | 98 samples |
| Temperature, salinity and water turbidity measurements | 275 stations |
| Recovered drift cards (4200 released) | 75 stations |

U.S. Hydrographic survey charts #7754, 7757, 7758, 7851 and 7852.

REFERENCES CITED

- Barnes, P. W., and Reimnitz, E., 1974, Sedimentary processes observed on arctic shelves off the northern coast of Alaska, in Coast and Shelf of the Beaufort Sea, J. C. Reed and J. E. Sater, ed., Arctic Institute of North America, Washington, D. C., p. 439-476.
- Reimnitz, E., and Barnes, P. W., 1974, Ice as a geologic agent on the Beaufort Sea shelf of Alaska, in Coast and Shelf of the Beaufort Sea, J. C. Reed and J. E. Sater, ed., Arctic Institute of North America, Washington, D. C., p. 301-353.
- Milne, A. R., and Smiley, B. D., Offshore drilling for oil in the Beaufort Sea: a preliminary environmental assessment; Beaufort Sea Project, Tech. Rept. No. 39, Department of the Environment, Victoria, B. C., 43 p.

10
15

SELECTED BIBLIOGRAPHY OF PERTINENT PUBLISHED USGS REPORTS
(not inclusive of reports "in press" - see attachments)

- Barnes, P., and G. Richard, Surface Current Observations-Beaufort Sea,
1972. U.S.G.S. Open File Report #75-619, 4 p.
- _____, K. Leong, C. Gustafson, 1974, Maps showing distribution of
copper, lead, zinc, mercury, and arsenic in the sediments off
of northern Alaska, U.S. Geological Survey Misc. Field Studies,
Map. MF-614.
- _____, Erk Reimnitz, 1974, Sedimentary processes on Arctic Shelves off
northern coast of Alaska; in The coast and shelf of the Beaufort
Sea. Proceedings of the Arctic Institute of North American
Symposium on Beaufort Sea Coast and Shelf Research. Arlington,
Va., Arctic Institute of North America.
- _____, Preliminary results of Marine Geologic Studies off the northern
coast of Alaska; in An Ecological Survey in the Beaufort Sea;
U.S. Coast Guard, Oceanographic Unit, Report #C.B. 373-64.
- _____, Erk Reimnitz, Alaska Natural Gas Transportation System: Draft
Environmental Impact Statement, Part VI, Alternatives. U.S.
Department of the Interior, v. 2.
- Reimnitz, E., and K. F. Bruder, 1972, River discharge into an ice
covered ocean and related sediment dispersal, Beaufort Sea,
Coast of Alaska, Geological Society of America Bulletin,
83: 861-866.

Reimnitz, E., P. W. Barnes, T. Forgatsch, and C. Rodeick, 1972,

Influence of grounding ice on the arctic shelf of Alaska.

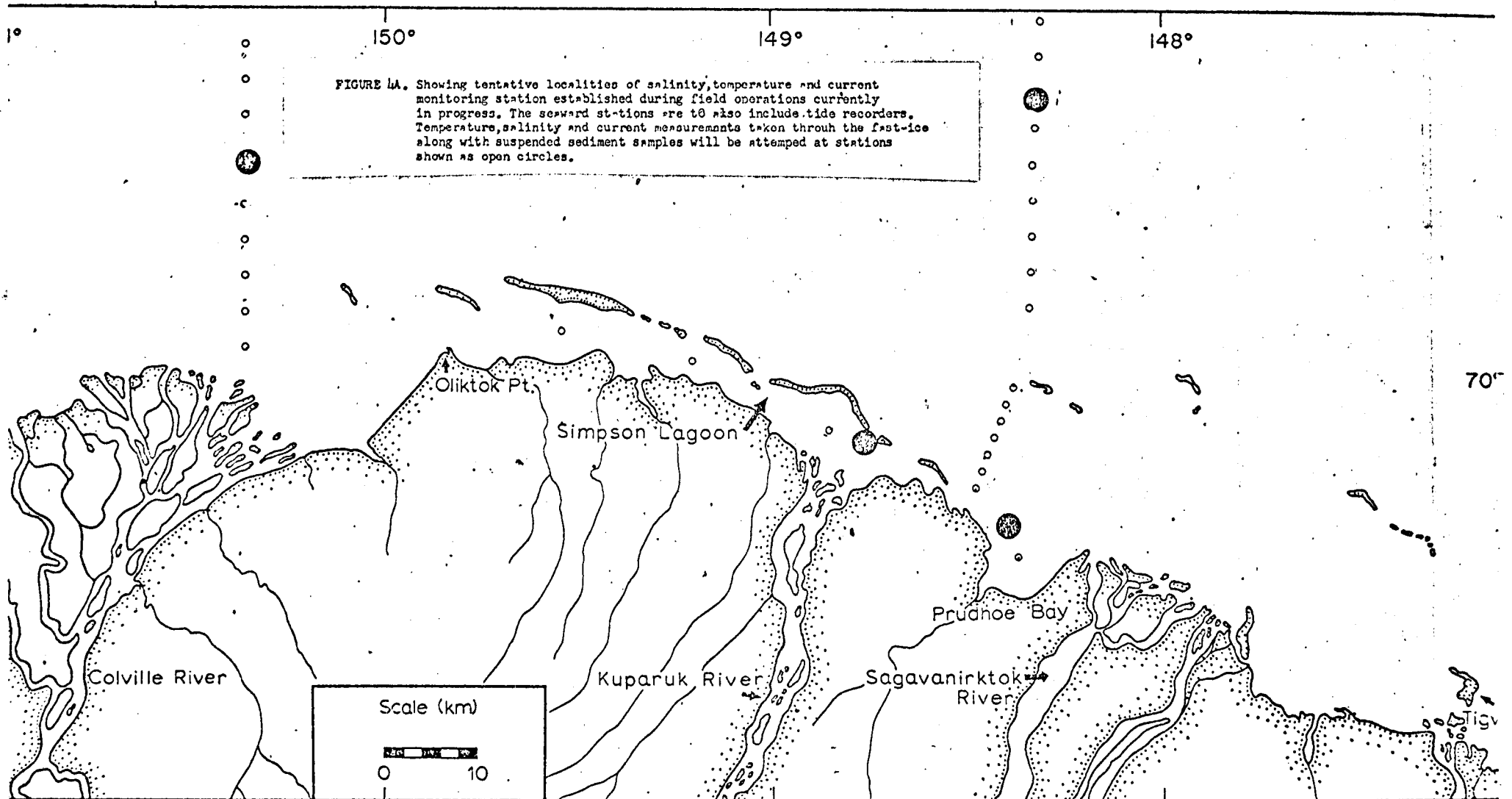
U.S. Geological Survey Misc. Field Studies Map, MF-532.

_____, S. C. Wolf, and C. A. Rodeick, 1972, Preliminary interpretation of seismic profiles in the Prudhoe Bay area, Beaufort Sea, Alaska, U.S. Geological Survey open file report, 11 pp.

_____, P. W. Barnes, and T. R. Alpha, 1973, Bottom features and processes related to drifting ice on the arctic shelf, Alaska, U.S. Geological Survey Misc. Field Studies Map, MF-532.

_____, C. A. Rodeick, and S. C. Wolf, 1974, Strudel scours: a unique arctic marine geologic phenomenon. *Journal of Sedimentary Petrology*, v. 44, p. 409-420.

_____, P. W. Barnes, 1974, Sea ice as a geologic agent on the Beaufort Sea shelf of Alaska; in *The coast and shelf of the Beaufort Sea. Proceedings of the Arctic Institute of North American Symposium on Beaufort Sea Coast and Shelf Research.* Arlington, Va., Arctic Institute of North America, pp. 301-353.



PRELIMINARY CRUISE
REPORT

ARCS 75 KE
Area Yr ID

AREA: Chukchi & Beaufort Sea

DATE: 20 Sept '75

I CRUISE DATES (INCLUDING PORT STOPS)

Aug 31, 1975 Sept 23, 1975

II CRUISE PERSONNEL

L. Toimil

E. Remitz - chief scientist

H. Hill

B. Clague

III TYPES OF DATA collected (with # Line miles OR # Samples)

Side Scan Sonar \approx 196 N. Miles suspended sediment sample

High Resolution Seismis (Unibcom) \approx 156 N. Miles \downarrow
30 sample

7.5Kj \approx 288 N. Miles

Underwater TV 6 Hrs operations, 2 $\frac{1}{2}$ tapes

Videotapes 2 $\frac{1}{2}$ tapes

temp/salinity profiles \approx 196 readings

current meter 2 emplaced for a period of one year

diving observation 2 $\frac{1}{2}$ hours (1 hr/tape)

transmissivity \approx 196 readings

seismic refraction (40" airgun) \approx 40 N. miles 532

FINAL EDITED SEARCH

SHIP-KARLUK

CRUISE LOCATOR ARCS-75-KE
AREA-YR-ID

CHIEF
SCIENTIST-REIMNITZ

ARCHIVE NUMBER

OPTIONAL

| JUL. TIME | DATUM | SUB- SEQNC | SPLIT START DISPO- | STATION | LATITUDE | LONGITUDE | POS. |
|-----------|-------|-------------------|--------------------|---------|----------|-----------|------|
| DAY | GMT | TYPE TYPE STN NO. | NO. END SITION | DATA | DEG MIN | DEG MIN | CODE |

TRACKLINES (VKNT)-

| | | | | | | | |
|---------|--------|-----------|----|---|-------------------|--|---|
| 244 | 730.0 | VK - NT - | 1 | S | LINE 1 ST | | |
| 244 | 930.0 | VK - NT - | 1 | E | LINE 1 END | | |
| 245 | 1235.0 | VK - NT - | 2 | S | LINE 2 ST | | |
| 245 | 1820.0 | VK - NT - | 2 | E | LINE 2 END | | |
| 248 | 1155.0 | VK - NT - | 3 | S | LINE 3 ST | | |
| 248 | 1730.0 | VK - NT - | 3 | E | LINE 3 END | | |
| 248 | 1750.0 | VK - NT - | 4 | S | LINE 4 START | | M |
| 248 | 20 0.0 | VK - NT - | 4 | E | LINE 4 END | | |
| 250 | 11 0.0 | VK - NT - | 4A | S | LINE 4A START | | R |
| 250 | 1135.0 | VK - NT - | 4A | E | END LINE 4A | | |
| 250 | 1230.0 | VK - NT - | 5 | S | ST LINE 5 | | |
| 250 | 14 8.0 | VK - NT - | 5 | E | END LINE 5 | | |
| 250 | 1445.0 | VK - NT - | 6 | S | ST LINE 6 | | M |
| 250 | 1530.0 | VK - NT - | 6 | E | LINE 6 END | | |
| 251 | 1230.0 | VK - NT - | 7 | S | LINE 7 START | | |
| 533 251 | 1350.0 | VK - NT - | 7 | E | LINE 7 END | | |
| 254 | 11 0.0 | VK - NT - | 8 | S | LINE 8 START | | |
| 254 | 1455.0 | VK - NT - | 8 | E | LINE 8 END | | |
| 255 | 1848.0 | VK - NT - | 9 | S | LINE 9 START | | |
| 255 | 2022.0 | VK - NT - | 9 | E | LINE 9 END | | |
| 256 | 1018.0 | VK - NT - | 10 | S | ST LINE 10 | | M |
| 256 | 17 7.0 | VK - NT - | 10 | E | END LINE 10 | | |
| 257 | 1228.0 | VK - NT - | 11 | S | START LINE 11 | | M |
| 257 | 1428.0 | VK - NT - | 11 | E | END LINE 11 | | |
| 258 | 1028.0 | VK - NT - | 12 | S | LINE 12 START | | M |
| 258 | 1752.0 | VK - NT - | 12 | E | END LINE 12 | | |
| 259 | 1314.0 | VK - NT - | 13 | S | TEST LINE SPY IS. | | M |
| 259 | 1534.0 | VK - NT - | 13 | E | LINE 13 END | | |
| 259 | 17 7.0 | VK - NT - | 14 | S | ST LINE 14 | | |
| 259 | 19 2.0 | VK - NT - | 14 | E | LINE 14 END | | |
| 260 | 1132.0 | VK - NT - | 15 | S | START LINE 15 | | |
| 260 | 1830.0 | VK - NT - | 15 | E | LINE 15 END | | |

SHIP-KARLUK

CRUISE LOCATOR ARCS-75-KE
AREA-YR-IDCHIEF
SCIENTIST-REIMNITZ

ARCHIVE NUMBER

OPTIONAL

| JUL. TIME | DATUM | SUB- | SEQUENCE, | SPLIT | START | DISPG- | STATION | LATITUDE | LONGITUDE | POS. | |
|----------------------------|--------|--------|-----------|--------|-------|--------|-------------|----------|-----------------|-------------|------|
| DAY - GMT | TYPE | TYPE | STN NO. | NO. | END | SITION | DESCRIPTION | DATA | DEG MIN | DEG MIN | CODE |
| 200 KHZ BATHYMETRY (XABT)- | | | | | | | | | | | |
| 244 | 730.0 | XA | - BT - | 9 | | S | UGS | | ROLL 9 | 7KH BATH | STRT |
| 244 | 930.0 | XA | - BT - | | R | E | | | 7 KH BATH | OFF | |
| 248 | 1155.0 | XA | - BT - | | R | S | | | ROLL 9 | 7 KH BATH | ON |
| 248 | 1910.0 | XA | - BT - | 9 | | E | UGS | | 7 KH BATHY | ROLL 9 | ED |
| 248 | 1915.0 | XA | - BT - | 10 | | S | UGS | | 7 KH BATHY | ROLL 10 | ST |
| 248 | 2000.0 | XA | - BT - | | R | E | | | 7 KH BATHY | ROLL 10 | UP |
| 250 | 1100.0 | XA | - BT - | | R | S | | | 7 KH BATHY | ROLL 10 | UN |
| 250 | 1135.0 | XA | - BT - | | R | E | | | 7 KH BATHY | OFF | |
| 250 | 1235.0 | XA | - BT - | | R | S | | | 200 KH BATHY | ON | |
| 250 | 1408.0 | XA | - BT - | | R | E | | | 200 KH BATHY | OFF | |
| 250 | 1445.0 | XA | - BT - | | R | S | | | 200 KH BATHY | ON | |
| 250 | 1530.0 | XA | - BT - | | R | E | | | 7 KH BATHY | OFF | |
| 251 | 1235.0 | XA | - BT - | | R | S | | | 7 KH BATHY | ON | |
| 251 | 1350.0 | XA | - BT - | 10 | | E | UGS | | 7 KH BATH | ROLL 10 | ED |
| 254 | 1115.0 | XA | - BT - | 11 | | S | UGS | | 7 KH BATH | ROLL 11 | ST |
| 534 | 254 | 1455.0 | XA | - BT - | | R | E | | 7 KH BATHY | OFF | |
| | 255 | 1848.0 | XA | - BT - | | R | S | | 200 KHZ BATHY | ON | |
| | 255 | 2022.0 | XA | - BT - | 11 | | E | UGS | 200 KHZ BATHY | 11 | ED |
| 256 | 1018.0 | XA | - BT - | 12 | | S | UGS | | ROLL 12 | START BATHY | |
| 256 | 1306.0 | XA | - BT - | 12 | | E | UGS | | END ROLL 12 | BATHY | |
| 256 | 1314.0 | XA | - BT - | 13 | | S | UGS | | START ROLL 13 | BATHY | |
| 256 | 1612.0 | XA | - BT - | 13 | | E | UGS | | END ROLL 13 | BATHY | |
| 256 | 1620.0 | XA | - BT - | 14 | | S | UGS | | START ROLL 14 | BATHY | |
| 257 | 1228.0 | XA | - BT - | | R | S | | | 7 KH BATHY | ON | |
| 257 | 1428.0 | XA | - BT - | | R | E | | | 7 KH BATHY | OFF | |
| 258 | 1028.0 | XA | - BT - | | R | S | | | 7 KH BATHY | ON | |
| 258 | 1335.0 | XA | - BT - | 14 | | E | UGS | | END 7KH BATHY | | |
| 258 | 1400.0 | XA | - BT - | 15 | | S | UGS | | START 7KH BATHY | | |
| 258 | 1610.0 | XA | - BT - | | R | E | | | 7 KH BATHY | OFF | |
| 259 | 1314.0 | XA | - BT - | | R | S | | | 7KH BATHY | ON | |
| 259 | 1534.0 | XA | - BT - | | R | E | | | 7 KH BATHY | OFF | |
| 259 | 1707.0 | XA | - BT - | | R | S | | | 7 KH BATHY | ON | |

SHIP-KARLUK

CRUISE LOCATOR ARCS-75-KE
AREA-YR-ID

CHIEF
SCIENTIST-REIMNITZ

ARCHIVE NUMBER

OPTIONAL

| JUL. DAY | TIME GMT | DATUM TYPE | SUB-TYPE | SEQUENCE STN NO. | SPLIT NO. | START END | DISPE-SITION | DESCRIPTION | STATION DATA | LATITUDE DEG MIN | LONGITUDE DEG MIN | PUS. CODE |
|----------|----------|------------|----------|------------------|-----------|-----------|--------------|-------------|--------------|------------------|-------------------|-----------|
|----------|----------|------------|----------|------------------|-----------|-----------|--------------|-------------|--------------|------------------|-------------------|-----------|

200 KHZ BATHYMETRY (XABT)-

| | | | | | | | | | | | | |
|-----|--------|----|--------|----|---|---|-----|-----------------------|--|--|--|--|
| 259 | 1740.0 | XA | - BT - | 15 | | E | UGS | END ROLL 15 BATHY | | | | |
| 259 | 1745.0 | XA | - BT - | 16 | | S | UGS | START ROLL 16 BATHY | | | | |
| 259 | 1745.0 | XA | - BT - | | R | E | | 7 KH BATHY OFF | | | | |
| 260 | 1132.0 | XA | - BT - | | R | S | | 7 KH BATHY ON | | | | |
| 260 | 16 0.0 | XA | - BT - | 16 | | E | UGS | END 7KH BATHY ROLL 16 | | | | |
| 260 | 16 0.0 | XA | - BT - | 17 | | S | UGS | ST 7KH BATHY ROLL 17 | | | | |
| 260 | 1830.0 | XA | - BT - | 17 | | E | UGS | END BATHY ROLL 17 | | | | |

SHIP-KARLUK

CRUISE LOCATOR ARCS-75-KE
AREA-YR-IDCHIEF
SCIENTIST-REIMNITZ

ARCHIVE NUMBER

OPTIONAL

| JUL. TIME | DATUM | SUB- | SEQNCE, | SPLIT | START | DISPO- | STATION | LATITUDE | LONGITUDE | POS. | |
|-----------------|--------|-----------|---------|-------|-------|--------|----------------------|----------|-----------|---------|------|
| DAY | GMT | TYPE | STN NO. | NO. | END | SITION | DESCRIPTION | DATA | DEG MIN | DEG MIN | CODE |
| UNIBOOM (XAHU)- | | | | | | | | | | | |
| 244 | 743.0 | XA - HU - | 11 | | S | UGS | ROLL 11 UNIBOOM STRT | | | | |
| 244 | 930.0 | XA - HU - | | R | E | | ROLL 11 UNIBOOM OFF | | | | |
| 248 | 1155.0 | XA - HU - | | R | S | | ROLL 11 UNIBOOM ON | | | | |
| 248 | 20 0.0 | XA - HU - | | R | E | | ROLL 11 UNIBOOM OFF | | | | |
| 250 | 1235.0 | XA - HU - | | R | S | | UNIBOOM ROLL 11 ON | | | | |
| 250 | 14 8.0 | XA - HU - | | R | E | | UNIBOOM OFF | | | | |
| 250 | 1445.0 | XA - HU - | | R | S | | UNIBOOM ROLL 11 ON | | | | |
| 250 | 1530.0 | XA - HU - | 11 | | E | UGS | UNIBOOM ROLL11 END | | | | |
| 257 | 1410.0 | XA - HU - | 12 | | S | UGS | UNIBOOM ROLL12 START | | | | |
| 257 | 1428.0 | XA - HU - | | R | E | | UNIBOOM OFF | | | | |
| 258 | 1028.0 | XA - HU - | | R | S | | UNIBOOM ON | | | | |
| 258 | 1610.0 | XA - HU - | 12 | | E | UGS | UNIBOOM ROLL 12 END | | | | |
| 258 | 1730.0 | XA - HU - | 13 | | S | UGS | 12KHZ BATHY ROLL13 S | | | | |
| 258 | 1752.0 | XA - HU - | | R | E | | 12KHZ BATHY OFF | | | | |
| 259 | 1314.0 | XA - HU - | | R | S | | UNIBOOM ON | | | | |
| 259 | 1534.0 | XA - HU - | | R | E | | UNIBOOM OFF | | | | |
| 259 | 17 7.0 | XA - HU - | | R | S | | UNIBOOM ON | | | | |
| 259 | 1745.0 | XA - HU - | | R | E | | UNIBOOM OFF | | | | |
| 260 | 1132.0 | XA - HU - | | R | S | | UNIBOOM ON | | | | |
| 260 | 1425.0 | XA - HU - | 13 | | E | UGS | END UNIBOOM ROLL 13 | | | | |
| 260 | 1430.0 | XA - HU - | 14 | | S | UGS | ST UNIBOOM ROLL 14 | | | | |
| 260 | 1830.0 | XA - HU - | 14 | | E | UGS | END UNIBOOM ROLL 14 | | | | |

536

SHIP-KARLUK

CRUISE LOCATOR ARCS-75-KE
AREA-YR-10CHIEF
SCIENTIST-REIMNITZ

ARCHIVE NUMBER

OPTIONAL

| JUL. DAY | TIME GMT | DATUM TYPE | SUB-TYPE | SEQNCE, STN NO. | SPLIT NO. | START END | DISPO- SITION | DESCRIPTION | STATION DATA | LATITUDE DEG MIN | LONGITUDE DEG MIN | POS. CODE |
|----------|----------|------------|----------|-----------------|-----------|-----------|---------------|-------------|--------------|------------------|-------------------|-----------|
|----------|----------|------------|----------|-----------------|-----------|-----------|---------------|-------------|--------------|------------------|-------------------|-----------|

SIDESCAN (XAHS)-

| | | | | | | | | | | | | |
|-----|--------|----|------|------|--|---|-----|----------------------|--|--|--|--|
| 244 | 8 0.0 | XA | - HS | - 11 | | S | UGS | ROLL 11 S/SCAN START | | | | |
| 244 | 930.0 | XA | - HS | - | | R | E | ROLL 11 S/SCAN OFF | | | | |
| 248 | 1155.0 | XA | - HS | - | | R | S | ROLL 11 S/SCAN ON | | | | |
| 248 | 17 0.0 | XA | - HS | - 11 | | E | UGS | S/SCAN ROLL 11 END | | | | |
| 248 | 1710.0 | XA | - HS | - 12 | | S | UGS | S/SCAN ROLL 12 START | | | | |
| 248 | 20 0.0 | XA | - HS | - | | R | E | ROLL 12 S/SCAN OFF | | | | |
| 250 | 1245.0 | XA | - HS | - | | R | S | S/SCAN ROLL 12 ON | | | | |
| 250 | 14 8.0 | XA | - HS | - | | R | E | S/SCAN OFF | | | | |
| 250 | 1445.0 | XA | - HS | - | | R | S | S/SCAN ROLL 12 ON | | | | |
| 250 | 1530.0 | XA | - HS | - 12 | | E | UGS | S/SCAN ROLL 12 END | | | | |
| 251 | 1235.0 | XA | - HS | - 13 | | S | UGS | S/SCAN ROLL 13 START | | | | |
| 251 | 1350.0 | XA | - HS | - | | R | E | S/SCAN OFF | | | | |
| 254 | 11 3.0 | XA | - HS | - | | R | S | S/SCAN ON | | | | |
| 254 | 1455.0 | XA | - HS | - | | R | E | S/SCAN OFF | | | | |
| 257 | 1230.0 | XA | - HS | - | | R | S | S/SCAN ON | | | | |
| 257 | 1348.0 | XA | - HS | - 13 | | E | UGS | END S/SCAN ROLL 13 | | | | |
| 257 | 1348.0 | XA | - HS | - 14 | | S | UGS | ST. S/SCAN ROLL 14 | | | | |
| 257 | 1428.0 | XA | - HS | - | | R | E | S/SCAN OFF | | | | |
| 258 | 1028.0 | XA | - HS | - | | R | S | S/SCAN ON | | | | |
| 258 | 1630.0 | XA | - HS | - 14 | | E | UGS | END S/SCAN ROLL 14 | | | | |
| 259 | 1314.0 | XA | - HS | - 15 | | S | UGS | ST S/SCAN ROLL 15 | | | | |
| 259 | 1534.0 | XA | - HS | - | | R | E | S/SCAN OFF | | | | |
| 259 | 17 7.0 | XA | - HS | - | | R | S | S/SCAN ON | | | | |
| 259 | 1745.0 | XA | - HS | - | | R | E | S/SCAN OFF | | | | |
| 260 | 1132.0 | XA | - HS | - | | R | S | S/SCAN ON | | | | |
| 260 | 1355.0 | XA | - HS | - 15 | | E | UGS | END ROLL 15 S/SCAN | | | | |
| 260 | 1356.0 | XA | - HS | - 16 | | S | UGS | START ROLL 16 S/SCAN | | | | |
| 260 | 1830.0 | XA | - HS | - 16 | | E | UGS | END S/SCAN ROLL 16 | | | | |

537

SHIP-KARLUK

CRUISE LOCATOR ARCS-75-KE
AREA-YR-IDCHIEF
SCIENTIST-PEIMNITZ

ARCHIVE NUMBER

OPTIONAL

| JUL. TIME | DAY | CMT | DATUM | SUB- TYPE | SEQUENCE, STN NO. | SPLIT NO. | START END | DISPC- SITION | DESCRIPTION | STATION DATA | LATITUDE DEG MIN | LONGITUDE DEG MIN | POS. CODE |
|---|-----|------|-------|--------------|----------------------|--------------|--------------|------------------|-----------------|-----------------|---------------------|----------------------|--------------|
| BECKMAN SALINITY/TEMP/CONDUCTIVITY/DENSITY (HVS)- | | | | | | | | | | | | | |
| 244 | 8 | 5.0 | HV | - SB | - | R | S | | SALTEMP ON | | | | |
| 244 | 9 | 30.0 | HV | - SB | - | R | E | | SAL/TEMP OFF | | | | |
| 245 | 12 | 35.0 | HV | - SB | - | R | S | | SAL/TEMP ON | | | | |
| 245 | 18 | 20.0 | HV | - SB | - | R | E | | SAL/TEMP OFF | | | | |
| 248 | 11 | 55.0 | HV | - SB | - | R | S | | SAL/TEMP ON | | | | |
| 248 | 20 | 0.0 | HV | - SB | - | R | E | | SAL/TEMP OFF | | | | |
| 250 | 12 | 45.0 | HV | - SB | - | R | S | | SAL TEMP ON | | | | |
| 250 | 14 | 8.0 | HV | - SB | - | R | E | | SAL TEMP OFF | | | | |
| 250 | 14 | 45.0 | HV | - SB | - | R | S | | SAL/TEMP ON | | | | |
| 250 | 15 | 30.0 | HV | - SB | - | R | E | | SAL TEMP OFF | | | | |
| 252 | 17 | 50.0 | HV | - SB | - | | | | SAL/TEMP RECORD | | | | |
| 257 | 12 | 35.0 | HV | - SB | - | R | S | | SAL/TEMP ON | | | | |
| 257 | 14 | 28.0 | HV | - SB | - | R | E | | SAL/TEMP OFF | | | | |
| 258 | 10 | 28.0 | HV | - SB | - | R | S | | SAL/TEMP ON | | | | |
| 258 | 16 | 10.0 | HV | - SB | - | R | E | | SAL/TEMP OFF | | | | |
| 259 | 13 | 14.0 | HV | - SB | - | R | S | | SAL/TEMP ON | | | | |
| 538 | 259 | 15 | 34.0 | HV | - SB | - | R | E | SAL/TEMP OFF | | | | |
| 259 | 17 | 7.0 | HV | - SB | - | R | S | | SAL/TEMP ON | | | | |
| 259 | 17 | 45.0 | HV | - SB | - | R | E | | SAL/TEMP OFF | | | | |
| 260 | 11 | 32.0 | HV | - SB | - | R | S | | SAL/TEMP ON | | | | |
| 260 | 18 | 30.0 | HV | - SB | - | R | E | | SAL/TEMP OFF | | | | |

SHIP-KARLUK

CRUISE LOCATOR ARCS-75-KE
AREA-YR-IDCHIEF
SCIENTIST-REIMNITZ

ARCHIVE NUMBER

OPTIONAL

| JUL. TIME | DATUM | SUB- | SEQNCE, | SPLIT | START | DISPU- | OPTIONAL | LATITUDE | LONGITUDE | POS. | | |
|-----------|-------|------|---------|---------|-------|--------|----------|-------------|-----------|---------|---------|------|
| DAY | GMT | TYPE | TYPE | STN NO. | NO. | END | SITUN | DESCRIPTION | DATA | DEG MIN | DEG MIN | CODE |

TURBIDITY TRANSMISSOMETER (HVT)-

| | | | | | | | | | | | | |
|-----|--------|----|------|---|---|---|--|----------------|-------|--|--|--|
| 248 | 1155.0 | HV | - TT | - | R | S | | TRANSMISSIVITY | ON | | | |
| 248 | 20 0.0 | HV | - TT | - | R | E | | TRANSMISSIVITY | OFF | | | |
| 250 | 1245.0 | HV | - TT | - | R | S | | TRANSMISSIVITY | ON | | | |
| 250 | 14 8.0 | HV | - TT | - | R | E | | TRANSMISSIVITY | OFF | | | |
| 252 | 1750.0 | HV | - TT | - | | | | TRANSMISSIVITY | RECOR | | | |
| 258 | 1028.0 | HV | - TT | - | R | S | | TRANSMISSIVITY | ON | | | |
| 258 | 1610.0 | HV | - TT | - | R | E | | TRANSMISSIVITY | OFF | | | |
| 259 | 1314.0 | HV | - TT | - | R | S | | TRANSMISSIVITY | ON | | | |
| 259 | 1534.0 | HV | - TT | - | R | E | | TRANSMISSIVITY | OFF | | | |
| 259 | 17 7.0 | HV | - TT | - | R | S | | TRANSMISSIVITY | ON | | | |
| 259 | 1745.0 | HV | - TT | - | R | E | | TRANSMISSIVITY | | | | |
| 260 | 1132.0 | HV | - TT | - | R | S | | TRANSMISSIVITY | ON | | | |
| 260 | 1830.0 | HV | - TT | - | R | E | | TRANSMISSIVITY | OFF | | | |

SHIP-KARLUK

CRUISE LOCATOR ARCS-75-KE
AREA-YR-ID

CHIEF
SCIENTIST-REIMNITZ

ARCHIVE NUMBER

OPTIONAL

| JUL. TIME | DATUM | SUB- | SEQNCE, | SPLIT | START | DISPO- | STATION | LATITUDE | LONGITUDE | POS. | | |
|-----------|-------|------|---------|---------|-------|--------|---------|-------------|-----------|---------|---------|------|
| DAY | GMT | TYPE | TYPE | STN NO. | NO. | END | SITON | DESCRIPTION | DATA | DEG MIN | DEG MIN | CODE |

AGGAR CURRENT METER (HPCG)-

| | | | | | | | | | | | | | |
|-----|--------|-----|----|----|----|---|---|---|--|--------|-------|-----|-----|
| 252 | 15 | 0.0 | HP | - | CG | - | 1 | S | | DEPLOY | CURNT | MET | 1YR |
| 252 | 1750.0 | HP | - | CG | - | 2 | S | | | DEPLOY | CURNT | MET | 1YR |

540

SHIP-KARLUK

CRUISE LOCATOR ARCS-75-KE
AREA-YR-IDCHIEF
SCIENTIST-REIMNITZ

ARCHIVE NUMBER

OPTIONAL

| JUL. TIME | DATUM | SUB- | SEQNCE, | SPLIT | START | DISPU- | STATION | LATITUDE | LONGITUDE | POS. | | |
|-----------|-------|------|---------|---------|-------|--------|---------|-------------|-----------|---------|---------|------|
| DAY | GMT | TYPE | TYPE | STN NO. | NO. | END | SITION | DESCRIPTION | DATA | DEG MIN | DEG MIN | CODE |

VIDEO TAPE RECORDER (GTQI)-

| | | | | | | | | | | | | |
|-----|--------|----|---|----|---|---|---|-----|----------------------|--|--|---|
| 248 | 1355.0 | GT | - | QI | - | 1 | S | UGS | VIDEO TAPE ROLL 1 ST | | | |
| 248 | 1425.0 | GT | - | QI | - | | R | E | VIDEO TAPE OFF | | | |
| 248 | 1535.0 | GT | - | QI | - | | R | S | VIDEO TAPE ON | | | |
| 248 | 1615.0 | GT | - | QI | - | | R | E | VIDEO TAPE OFF | | | |
| 250 | 11 0.0 | GT | - | QI | - | | R | S | VIDEO TAPE ON | | | |
| 250 | 1135.0 | GT | - | QI | - | 1 | E | UGS | VIDEO TAPE 1 OFF | | | M |
| 250 | 1328.0 | GT | - | QI | - | 2 | S | UGS | VIDEO TAPE 2 ON | | | |
| 250 | 14 8.0 | GT | - | QI | - | 2 | E | UGS | VIDEO TAPE 2 OFF | | | |
| 254 | 1155.0 | GT | - | QI | - | 3 | S | UGS | VIDEO TAPE 3 START | | | |
| 254 | 1337.0 | GT | - | QI | - | 3 | E | UGS | VIDEO TAPE 3 END | | | |
| 258 | 1630.0 | GT | - | QI | - | 4 | S | UGS | VIDEO TAPE 4 START | | | |
| 258 | 1730.0 | GT | - | QI | - | 4 | E | UGS | VIDEO TAPE END | | | |

541

SHIP-KARLUK

CRUISE LOCATOR ARCS-75-KE
AREA-YR-ID

CHIEF
SCIENTIST-PEIMNITZ

ARCHIVE NUMBER

OPTIONAL

| JUL. TIME | DATUM | SUB- SOURCE, | SPLIT START DISPO- | STATION | LATITUDE | LONGITUDE | POS. |
|-----------|-------|-------------------|--------------------|------------------|----------|-----------|------|
| DAY | GMT | TYPE TYPE STN NO. | NO. END SITION | DESCRIPTION DATA | DEG MIN | DEG MIN | CODE |

SCIENTIFIC EQUIPMENT STATUS (X R)-

| | | | | | | | |
|-----|--------|-----------|---|---|-------------|--|--|
| 245 | 1235.0 | XX - TA - | R | S | AIR GUN CN | | |
| 245 | 1820.0 | XX - TA - | R | E | AIR GUN OFF | | |

542

PRELIMINARY CRUISE
REPORT

ARCS 75 KB
Area Yr ID

AREA: CHUKCHI SEA

DATE: 26 Sept 75

I CRUISE DATES (INCLUDING PORT STOPS)

25 JULY KOTARBUE

30 AUG BARROW

II CRUISE PERSONNEL

P. Barnes - chief sci

L. Jirmil

H. Hill

B. CLIQUE

J. ROGER ^{Univ} ALASK (23-30 AUG)

III TYPES OF DATA collected (with # Linemiles or # Samples)

Strode

High Res Seismic (\approx #00 km)

Side scan Sonar "

7 kHz Seismic "

Temp/sal "

TV - 10 Stations

24 channel Seismic refraction (100 km)

Suspended sediment

Transmissometer

Current Drogues (LSU)

FINAL EDITED SEARCH

SHIP-KARLUK

CRUISE LOCATOR ARCS-75-KR
AREA-YR-ID

CHIEF
SCIENTIST-BARNES

| | | ARCHIVE NUMBER | | | | OPTIONAL | | | | | | |
|--------------------|------------|----------------|----------|----------------|-----------|-----------|---------------|-------------------------|--------------|------------------|-------------------|-----------|
| JUL. DAY | TIME GMT | DATUM TYPE | SUB-TYPE | SEQNCE STN NO. | SPLIT NO. | START END | DISPO- SITION | DESCRIPTION | STATION DATA | LATITUDE DEG MIN | LONGITUDE DEG MIN | POS. CODE |
| TRACKLINES (VKNT)- | | | | | | | | | | | | |
| | 209 1540.0 | VK | - NT | - 1 | | S | | START TEST LINE 01 | | | | P |
| | 209 1755.0 | VK | - NT | - 1 | | F | | END LINE TEST 1 | | | | |
| | 210 930.0 | VK | - NT | - 2 | | S | | ST LINE 2 | | | | P |
| | 210 15 0.0 | VK | - NT | - 2 | | F | | END LINE 2 | | | | |
| | 210 15 1.0 | VK | - NT | - 3 | | S | | ST. TRACK LINE 3 | | | | |
| | 210 17 0.0 | VK | - NT | - 3 | | F | | END LINE 03 | | | | |
| | 211 1150.0 | VK | - NT | - 4 | | S | | ST. TRACK LINE 4 | | | | |
| | 211 13 1.0 | VK | - NT | - 4 | | F | | END TRACK LINE 4 | | | | |
| | 212 1353.0 | VK | - NT | - 5 | | S | | ST LINE 05 (PT. HOPE) | | | | M |
| | 212 1730.0 | VK | - NT | - 5 | | F | | END LINE 5 | | | | |
| | 214 1110.0 | VK | - NT | - 6 | | S | | START LINE 06 | | | | P |
| | 214 1412.0 | VK | - NT | - 6 | | F | | END LINE 6 | | | | |
| | 215 12 5.0 | VK | - NT | - 7 | | S | | ST. LINE 7 | | | | M |
| | 215 1515.0 | VK | - NT | - 7 | | F | | END LINE 07 | | | | |
| | 216 6 0.0 | VK | - NT | - 8 | | S | | ST. HYDROGRAPHIC LINE 8 | | | | P |
| | 216 14 0.0 | VK | - NT | - 8 | | F | | END LINE 8 | | | | |
| | 217 8 0.0 | VK | - NT | - 9 | | S | | ST. LINE 9 | | | | |
| | 217 1250.0 | VK | - NT | - 9 | | F | | END LINE 9 | | | | |
| | 218 1345.0 | VK | - NT | - 10 | | S | | START LINE 10 | | | | M |
| | 218 1810.0 | VK | - NT | - 10 | | F | | END LINE 10 | | | | |
| | 222 1135.0 | VK | - NT | - 11 | | S | | ST. LINE 11 | | | | M |
| | 222 1642.0 | VK | - NT | - 11 | | F | | END LINE 11 | | | | |
| | 225 815.0 | VK | - NT | - 12 | | S | | START LINE 12 | | | | M |
| | 225 11 0.0 | VK | - NT | - 12 | | F | | END LINE 12 | | | | |
| | 225 1140.0 | VK | - NT | - 13 | | S | | START LINE 13 | | | | M |
| | 225 15 5.0 | VK | - NT | - 13 | | F | | END LINE 13 | | | | |
| | 227 0 7.1 | VK | - NT | - 14 | | S | | START LINE 14 | | | | R |
| | 227 011.5 | VK | - NT | - 14 | | F | | END LINE 14 | | | | |
| | 227 014.0 | VK | - NT | - 15 | | S | | START LINE 15 | | | | |
| | 227 17 5.0 | VK | - NT | - 15 | | F | | END LINE 15 | | | | |
| | 229 1150.0 | VK | - NT | - 16 | | S | | START LINE 16 | | | | R |
| | 229 1515.0 | VK | - NT | - 16 | | F | | END LINE 16 | | | | |

574

SHIP-KARLUK

CRUISE LOCATOR ARCS-75-KR
AREA-YR-IDCHIEF
SCIENTIST-BARNES

| ARCHIVE NUMBER | | | | | OPTIONAL | | | | | | |
|----------------|-------|------|--------------|-------|----------|--------|-------------|----------|-----------|---------|------|
| JUL. TIME | DATUM | SUB- | SEQNCE, | SPLIT | START | DISPO- | STATION | LATITUDE | LONGITUDE | POS. | |
| DAY | GMT | TYPE | TYPE STN NO. | NO. | END | SITION | DESCRIPTION | DATA | DEG MIN | DEG MIN | CODE |

TRACKLINES (VKNT)-

| | | | | | | | | | | | |
|-----|--------|----|--------|----|--|---|---------------|--|--|--|---|
| 231 | 1430.0 | VK | - NT - | 17 | | S | START LINE 17 | | | | P |
| 231 | 1545.0 | VK | - NT - | 17 | | F | END LINE 17 | | | | |
| 233 | 8 0.0 | VK | - NT - | 18 | | S | ST. LINE 18 | | | | |
| 233 | 1030.0 | VK | - NT - | 18 | | E | END LINE 18 | | | | |
| 233 | 1140.0 | VK | - NT - | 19 | | S | START LINE 19 | | | | M |
| 233 | 1210.0 | VK | - NT - | 19 | | F | END LINE 19 | | | | |
| 237 | 1030.0 | VK | - NT - | 20 | | S | START LINE 20 | | | | |
| 237 | 1415.0 | VK | - NT - | 20 | | E | END LINE 20 | | | | |
| 241 | 740.0 | VK | - NT - | 21 | | S | START LINE 21 | | | | P |
| 241 | 955.0 | VK | - NT - | 21 | | E | END LINE 21 | | | | |
| 241 | 1010.0 | VK | - NT - | 22 | | S | START LINE 22 | | | | P |
| 241 | 13 0.0 | VK | - NT - | 22 | | E | END LINE 22 | | | | |
| 241 | 13 5.0 | VK | - NT - | 23 | | S | START LINE 23 | | | | P |
| 241 | 1550.0 | VK | - NT - | 23 | | E | END LINE 23 | | | | |
| 242 | 1730.0 | VK | - NT - | 24 | | S | ST LINE 24 | | | | |
| 242 | 2030.0 | VK | - NT - | 24 | | F | END LINE 24 | | | | |

545

SHIP-KARLUK

CRUISE LOCATOR ARCS-75-KR
AREA-YR-IDCHIEF
SCIENTIST-BARNES

ARCHIVE NUMBER

OPTIONAL

| JUL. TIME | DATUM | SUB- | SEQNCE, | SPLIT | START | DISPO- | STATION | LATITUDE | LONGITUDE | POS. | | |
|-----------------|--------|------|---------|---------|-------|--------|----------|----------------------|-----------|---------|---------|------|
| DAY | GMT | TYPE | TYPE | STN NO. | NO. | END | SITATION | DESCRIPTION | DATA | DEG MIN | DEG MIN | CODE |
| UNIBOOM (XAHU)- | | | | | | | | | | | | |
| 209 | 1540.0 | XA | HU | 1 | | S | UGS | UNIBOOM ON | ROLL 1 | | | |
| 209 | 1750.0 | XA | HU | | | R | E | SHUT DOWN UNIBOOM | | | | |
| 210 | 030.0 | XA | HU | | | R | S | UNIBOOM ON | | | | |
| 210 | 1240.0 | XA | HU | 1 | | F | UGS | END ROLL 1 UNIBOOM | | | | |
| 210 | 1245.0 | XA | HU | 2 | | S | UGS | ST UNI.ROLL 2 | | | | |
| 210 | 1350.0 | XA | HU | | | R | F | LOST UNI PWR CABLE | | | | |
| 210 | 1510.0 | XA | HU | | | R | S | UNI. ON & FIXED | | | | |
| 210 | 17 0.0 | XA | HU | | | R | E | UNI OFF | | | | |
| 211 | 1151.0 | XA | HU | | | R | S | UNIBOOM ON | | | | |
| 211 | 13 0.0 | XA | HU | | | R | F | UNIBOOM OFF | | | | |
| 214 | 1112.0 | XA | HU | | | R | S | UNIBOOM ON | | | | |
| 214 | 1320.0 | XA | HU | 2 | | F | UGS | END UNIBOOM ROLL 2 | | | | |
| 214 | 1325.0 | XA | HU | 3 | | S | UGS | ST. UNIBOOM ROLL 3 | | | | |
| 214 | 14 0.0 | XA | HU | | | R | E | UNIBOOM SHUT DOWN | | | | |
| 215 | 1215.0 | YA | HU | | | P | S | UNIBOOM ON | | | | |
| 215 | 1516.0 | XA | HU | | | R | F | UNIBOOM OFF | | | | |
| 217 | 8 0.0 | XA | HU | | | R | S | UNIBOOM ON | | | | |
| 217 | 10 0.0 | XA | HU | 3 | | E | UGS | END ROLL 3 UNIBOOM | | | | |
| 217 | 10 5.0 | XA | HU | 4 | | S | UGS | ST UNIBOOM ROLL 4 | | | | |
| 217 | 1245.0 | XA | HU | 4 | | E | UGS | END UNIBOOM ROLL 4 | | | | |
| 218 | 1345.0 | XA | HU | 5 | | S | UGS | UNIBOOM ROLL # 5 ST | | | | |
| 218 | 18 0.0 | XA | HU | | | R | F | UNIBOOM OFF | | | | |
| 222 | 1135.0 | XA | HU | | | R | S | UNIBOOM START | | | | |
| 222 | 1410.0 | XA | HU | 5 | | F | UGS | END ROLL 5 UNIBOOM | | | | M |
| 222 | 1411.0 | XA | HU | 6 | | S | UGS | ST. ROLL 6 UNIBOOM | | | | |
| 222 | 1525.0 | XA | HU | | | R | F | UNIBOOM OFF | | | | |
| 225 | 815.0 | XA | HU | | | R | S | UNIBOOM START | | | | |
| 225 | 11 0.0 | XA | HU | | | R | F | UNIBOOM OFF | | | | |
| 225 | 1140.0 | XA | HU | | | R | S | UNIBOOM START | | | | |
| 225 | 15 5.0 | XA | HU | 6 | | F | UGS | END UNIBOOM ROLL #6 | | | | |
| 227 | 0 7.2 | XA | HU | 7 | | S | UGS | UNIBOOM ON ST ROLL 7 | | | | R |
| 227 | 011.5 | XA | HU | | | R | E | UNIBOOM OFF | | | | |

546

SIIP-KARLUK

CRUISE LOCATOR APC5-75-KR
AREA-YR-IDCHIEF
SCIENTIST-BARNES

ARCHIVE NUMBER

OPTIONAL

| JUL. TIME | DATUM | SUB- | SEQNC, | SPLIT | START | DISPO- | OPTIONAL | LATITUDE | LONGITUDE | POS. | | |
|-----------------|--------|------|--------|---------|-------|--------|----------|---------------|-----------|---------|---------|------|
| DAY | GMT | TYPE | TYPE | STN NO. | NO. | END | SITON | DESCRIPTION | DATA | DEG MIN | DEG MIN | CODE |
| UNIBOOM (XAHU)- | | | | | | | | | | | | |
| 227 | 014.0 | XA | HU | - | | R | S | UNIBOOM ON | | | | |
| 227 | 17 5.0 | XA | HU | - | 7 | | F | UGS, | | | | |
| 231 | 1430.0 | XA | HU | - | 8 | | S | UGS | | | | |
| 231 | 1545.0 | XA | HU | - | | R | F | UNIBOOM OFF | | | | |
| 233 | 845.0 | XA | HU | - | | R | S | UNIBOOM START | | | | |
| 233 | 1030.0 | XA | HU | - | | R | E | UNIBOOM OFF | | | | |
| 233 | 1140.0 | XA | HU | - | | R | S | UNIBOOM START | | | | |
| 233 | 1310.0 | XA | HU | - | | R | E | UNIBOOM OFF | | | | |
| 237 | 1030.0 | XA | HU | - | | R | S | UNIBOOM START | | | | |
| 237 | 1415.0 | XA | HU | - | 8 | | F | UGS | | | | |
| 241 | 740.0 | XA | HU | - | 9 | | S | UGS | | | | |
| 241 | 955.0 | XA | HU | - | | R | E | UNIBOOM OFF | | | | |
| 241 | 10 5.0 | XA | HU | - | | R | S | UNIBOOM START | | | | |
| 241 | 1550.0 | XA | HU | - | 9 | | F | UGS | | | | |
| 242 | 1730.0 | XA | HU | - | 10 | | S | UGS | | | | |
| 242 | 2030.0 | XA | HU | - | 10 | | E | UGS | | | | R |

547

SHIP-KARI,UK

CRUISE LOCATOR ARCS-75-KB
AREA-YR-IDCHIEF
SCIENTIST-BARNES

ARCHIVE NUMBER

OPTIONAL

| JUL. TIME | DATUM | SUB- SEONCE, | SPLIT START DISPO- | OPTIONAL | STATION | LATITUDE | LONGITUDE | POS. |
|------------------|-------|--------------|--------------------|-------------|---------|----------|-----------|------|
| DAY GMT | TYPE | TYPE STN NO. | NO. END SITION | DESCRIPTION | DATA | DEG MIN | DEG MIN | CODE |
| SIDESCAN (XAHS)- | | | | | | | | |
| 209 16 0.0 | XA | - HS - | 1 | S | UGS | | | |
| 209 1730.0 | XA | - HS - | | R | F | | | |
| 210 930.0 | XA | - HS - | | R | S | | | |
| 210 1210.0 | XA | - HS - | 1 | F | UGS | | | |
| 210 1215.0 | XA | - HS - | 2 | S | UGS | | | |
| 210 17 0.0 | XA | - HS - | | R | F | | | |
| 211 1151.0 | XA | - HS - | | R | S | | | |
| 211 13 0.0 | XA | - HS - | 2 | F | UGS | | | |
| 212 1353.0 | XA | - HS - | 3 | S | UGS | | | |
| 212 1445.0 | XA | - HS - | | R | F | | | |
| 214 1119.0 | XA | - HS - | | R | S | | | |
| 214 14 7.0 | XA | - HS - | 3 | F | UGS | | | |
| 215 1315.0 | XA | - HS - | 4 | S | UGS | | | |
| 215 1515.0 | XA | - HS - | | R | F | | | |
| 217 8 0.0 | XA | - HS - | | R | S | | | |
| 217 10 6.0 | XA | - HS - | 4 | F | UGS | | | |
| 217 1011.0 | XA | - HS - | 5 | S | UGS | | | |
| 217 1245.0 | XA | - HS - | | R | F | | | R |
| 218 1345.0 | XA | - HS - | | R | S | | | |
| 218 1645.0 | XA | - HS - | 5 | F | UGS | | | |
| 218 1645.0 | XA | - HS - | 6 | S | UGS | | | |
| 218 18 0.0 | XA | - HS - | | R | F | | | |
| 222 1140.0 | XA | - HS - | | R | S | | | |
| 222 1650.0 | XA | - HS - | 6 | F | UGS | | | |
| 225 816.0 | XA | - HS - | 7 | S | UGS | | | |
| 225 11 0.0 | XA | - HS - | | P | F | | | |
| 225 1141.0 | XA | - HS - | | R | S | | | |
| 225 1412.0 | XA | - HS - | 7 | F | UGS | | | |
| 225 1423.0 | XA | - HS - | 8 | S | UGS | | | |
| 225 15 5.0 | XA | - HS - | | R | F | | | |
| 227 0 7.2 | XA | - HS - | | R | S | | | P |
| 227 011.5 | XA | - HS - | | R | F | | | |

548

SHIP-KARLUK

CRUISE LOCATOR APC5-75-KB

CHIFF

AREA-YR-ID

SCIENTIST-BARNES

ARCHIVE NUMBER

OPTIONAL

| JUL. TIME | DATUM | SUB- | SEQNCE, | SPLIT | START | DISPO- | OPTIONAL | LATITUDE | LONGITUDE | POS. |
|------------------|--------|------|---------|---------|-------|--------|----------|----------|-----------|------|
| DAY | GMT | TYPE | TYPE | STN NO. | NO. | END | STATION | DEG MIN | DEG MIN | CODE |
| SIDESCAN (XAHS)- | | | | | | | | | | |
| 227 | 014.0 | XA | - HS | - | | R | S | | | |
| 227 | 16 0.0 | XA | - HS | - | 8 | | E | UGS | | |
| 231 | 1430.0 | XA | - HS | - | 9 | | S | UGS | | P |
| 231 | 1440.0 | XA | - HS | - | | R | E | | | |
| 231 | 1455.0 | XA | - HS | - | | R | S | | | P |
| 231 | 1545.0 | XA | - HS | - | | R | E | | | |
| 233 | 845.0 | XA | - HS | - | | R | S | | | |
| 233 | 1030.0 | XA | - HS | - | | R | E | | | |
| 233 | 1140.0 | XA | - HS | - | | R | S | | | |
| 233 | 1310.0 | XA | - HS | - | | R | E | | | |
| 241 | 740.0 | XA | - HS | - | | R | S | | | |
| 241 | 920.0 | XA | - HS | - | 9 | | F | UGS | | |
| 241 | 935.0 | XA | - HS | - | 10 | | S | UGS | | |
| 241 | 955.0 | XA | - HS | - | | R | E | | | |
| 241 | 10 5.0 | XA | - HS | - | | R | S | | | |
| 241 | 1550.0 | XA | - HS | - | 10 | | E | UGS | | |

549

SHIP-KARLUK

CRUISE LOCATOR ARCS-75-KB

CHIEF
SCIENTIST-BARNES

AREA-YR-ID

ARCHIVE NUMBER

OPTIONAL

| JUL. TIME | DATUM | SUB- SOURCE, | SPLIT START DISPO- | OPTIONAL | LATITUDE | LONGITUDE | POS. |
|-----------|-------|-------------------|--------------------|--------------------------|----------|-----------|------|
| DAY | GMT | TYPE TYPE STN NO. | NO. END SITION | STATION DESCRIPTION DATA | DEG MIN | DEG MIN | CODE |

200 KHZ BATHYMETRY (XART)-

550

| | | | | | | | |
|-----|--------|-------------|---|---|---|-----|----------------------|
| 209 | 1540.0 | XA - BT - | 1 | | S | UGS | 200 & 7KHZ ONROLL 7 |
| 209 | 1752.0 | XA - BT - | | R | E | | SHUT DOWN 200&7KHZ |
| 210 | 930.0 | XA - BT - | | R | S | | 200 & 7 KH BAYTH. ST |
| 210 | 15 0.0 | XA - BT - | 1 | | F | UGS | END ROLL 01 BATHY |
| 210 | 15 1.0 | XA - BT - | 2 | | S | UGS | ST. BATHY ROLL 2 |
| 210 | 17 0.0 | XA - BT - | | R | F | | BATHY + 200 KHZ OFF |
| 211 | 1151.0 | XA - BT - | | R | S | | START 200 & 7 KHZ |
| 211 | 13 0.0 | XA - BT - | | R | F | | 200 & 7 KHZ OFF |
| 212 | 1353.0 | XA - BT - | | R | S | | ST. BAYTHEON 200&7 |
| 212 | 1445.0 | XA - BT - | | R | F | | END BAYTHEON 200&7KH |
| 212 | 15 0.0 | XA - BT - | | P | S | | 200KH TRNDOP W/TV |
| 212 | 16 0.0 | XA - BT - | | R | F | | ED 200KH TRNDOP W/TV |
| 212 | 1630.0 | XA - BT - | | R | S | | ST 200KH TRNDOP W/TV |
| 212 | 1730.0 | XA - BT - | | R | E | | ED 200KH TRNDOP W/TV |
| 214 | 1112.0 | XA - BT - | | R | S | | 200 & 7KH BAYTH. ON |
| 214 | 14 7.0 | XA - BT - | 2 | | F | UGS | ED 200 & 7KH ROLL 2 |
| 215 | 1210.0 | XA - BT - S | 1 | | S | UGS | 7KHZ ON EPC ROLL 1 |
| 215 | 1210.0 | XA - BT - | 3 | | S | UGS | ST 200 & 7KH ROLL #3 |
| 215 | 1358.0 | XA - BT - S | 1 | | F | UGS | END ROLL 01 7KHZ EPC |
| 215 | 1515.0 | XA - BT - | | R | E | | 200 & 7KH BATHY OFF |
| 217 | 8 0.0 | XA - BT - | | R | S | | 200 BAYTHEON ON |
| 217 | 8 0.0 | XA - BT - S | 2 | | S | UGS | 7 KHZ ST ROLL 2 EPC |
| 217 | 830.0 | XA - BT - S | 2 | | F | UGS | END 7KH EPC ROLL 2 |
| 217 | 1245.0 | XA - BT - | | R | F | | 200 & 7KH BAYTH OFF |
| 218 | 1345.0 | XA - BT - | | R | S | | 200 & 7KH BAYTH. ON |
| 218 | 1630.0 | XA - BT - | 3 | | F | UGS | ED 200 & 7KH ROLL 3 |
| 218 | 1645.0 | XA - BT - | 4 | | S | UGS | ST 200 & 7KH ROLL 4 |
| 218 | 18 0.0 | XA - BT - | | R | E | | 200 & 7KH BATHY OFF |
| 222 | 1135.0 | XA - BT - | | R | S | | 200 & 7KH BATHY ON |
| 222 | 1525.0 | XA - BT - | | R | E | | END BAYTHEON 200&7 |
| 225 | 820.0 | XA - BT - | | R | S | | 200 & 7KH BATHY ON |
| 225 | 11 0.0 | XA - BT - | 4 | | F | UGS | ED 200KHZ ROLL #4 |

SHIP-KARLUK

CRUISE LOCATOR ARCS-75-KB
AREA-YR-IDCHIEF
SCIENTIST-BARNES

ARCHIVE NUMBER

OPTIONAL

| JUL. TIME | DATUM | SUB- | SEQNCF, | SPLIT | START | DISPO- | OPTIONAL | LATITUDE | LONGITUDE | POS. | | |
|-----------|-------|------|---------|---------|-------|--------|----------|-------------|-----------|---------|---------|------|
| DAY | GMT | TYPE | TYPE | STN NO. | NO. | END | SITON | DESCRIPTION | DATA | DEG MIN | DEG MIN | CODE |

200 KHZ BATHYMETRY (XABT)-

| | | | | | | | | | | | | |
|-----|--------|----|---|----|---|---|---|---|-----|----------------------|--|---|
| 225 | 1141.0 | XA | - | BT | - | 5 | | S | UGS | ST 200KHZ ROLL #5 | | |
| 225 | 15 5.0 | XA | - | BT | - | | R | F | | 200KHZ OFF | | |
| 227 | 0 7.2 | XA | - | BT | - | | R | S | | RAYTH. 200 & 7KH ON | | |
| 227 | 011.5 | XA | - | BT | - | | R | E | | RAYTH 200 & 7KH OFF | | |
| 227 | 014.0 | XA | - | BT | - | | R | S | | RAYTH 200 & 7KH ON | | |
| 227 | 17 5.0 | XA | - | BT | - | 5 | | F | UGS | END 200 & 7KH ROLL 5 | | |
| 229 | 1220.0 | XA | - | BT | - | 6 | | S | UGS | ST BATHY ROLL #6 | | |
| 229 | 1530.0 | XA | - | BT | - | | R | F | | BATHY OFF | | |
| 231 | 1430.0 | XA | - | BT | - | | R | S | | RAYTH 200 & 7KH ON | | |
| 231 | 1545.0 | XA | - | BT | - | | R | F | | RAYTH 200 & 7KH OFF | | |
| 233 | 845.0 | XA | - | BT | - | | R | S | | RAYTH 200 & 7KH ON | | |
| 233 | 1030.0 | XA | - | BT | - | | R | F | | RAYTH 200 & 7KH OFF | | |
| 233 | 1140.0 | XA | - | BT | - | | R | S | | RAYTH 200 & 7KH ON | | |
| 233 | 1310.0 | XA | - | BT | - | | P | E | | RAYTH 200 & 7KH OFF | | |
| 237 | 1030.0 | XA | - | BT | - | | R | S | | 200 & 7KH RAYTH ON | | M |
| 237 | 1415.0 | XA | - | BT | - | | P | E | | 200 & 7KH RAYTH OFF | | |
| 241 | 740.0 | XA | - | BT | - | | R | S | | RAYTH 200 & 7KH ON | | |
| 241 | 740.0 | XA | - | BT | - | 6 | | F | UGS | END 200 & 7KH ROLL 6 | | |
| 241 | 740.0 | XA | - | BT | - | 7 | | S | UGS | ST 200 & 7KH ROLL 7 | | |
| 241 | 955.0 | XA | - | BT | - | | R | F | | 200 & 7KH RAYTH OFF | | |
| 241 | 10 5.0 | XA | - | BT | - | | R | S | | 200 & 7KH RAYTH ON | | |
| 241 | 1550.0 | XA | - | BT | - | 7 | | F | UGS | ED 200 & 7KH ROLL 7 | | |
| 242 | 1730.0 | XA | - | BT | - | 8 | | S | UGS | ST 200 & 7KH ROLL 8 | | |
| 242 | 2030.0 | XA | - | BT | - | 8 | | F | UGS | 200 & 7KH RAYTH OFF | | |

551

SHIP-KARLUK

CRUISE LOCATOR ARCS-75-KR
AREA-YR-IDCHIEF
SCIENTIST-BARNES

ARCHIVE NUMBER

OPTIONAL

| JUL. TIME | DATUM | SUR- | SEQNCE, | SPLIT | START | DISPO- | STATION | LATITUDE | LONGITUDE | POS. | |
|-----------|-------|------|---------------|-------|-------|--------|-------------|----------|-----------|---------|------|
| DAY | GMT | TYPE | TYPE- STN NO. | NO. | END | SITION | DESCRIPTION | DATA | DEG MIN | DEG MIN | CODE |

BECKMAN SALINITY/TEMP/CONDUCTIVITY/DENSITY (HVS^R)

| | | | | |
|------------|---------------|-----|-----------------|-----|
| 210 1023.0 | HV - SB - 13A | UGS | TEMP/SALIN/COND | M |
| 210 1045.0 | HV - SB - 14 | UGS | TEMP/SALIN/COND | |
| 210 1115.0 | HV - SB - 15 | UGS | TEMP/SALIN/COND | |
| 210 1130.0 | HV - SB - 16 | UGS | TEMP/SALIN/COND | |
| 210 12 0.0 | HV - SB - 17 | UGS | TEMP/SALIN/COND | |
| 210 1230.0 | HV - SB - 18 | UGS | TEMP/SALIN/COND | |
| 210 1245.0 | HV - SB - 19 | UGS | TEMP/SALIN/COND | |
| 210 13 0.0 | HV - SB - 20 | UGS | TEMP/SALIN/COND | |
| 210 1315.0 | HV - SB - 21 | UGS | TEMP/SALIN/COND | |
| 210 1330.0 | HV - SB - 22 | UGS | TEMP/SALIN/COND | |
| 210 1345.0 | HV - SB - 23 | UGS | TEMP/SALIN/COND | |
| 210 1415.0 | HV - SB - 24 | UGS | TEMP/SALIN/COND | |
| 210 1430.0 | HV - SB - 25 | UGS | TEMP/SALIN/COND | |
| 210 1445.0 | HV - SB - 26 | UGS | TEMP/SALIN/COND | |
| 210 1515.0 | HV - SB - 27 | UGS | TEMP/SALIN/COND | |
| 210 1530.0 | HV - SB - 29 | UGS | TEMP/SALIN/COND | |
| 210 1545.0 | HV - SB - 31 | UGS | TEMP/SALIN/COND | |
| 210 16 0.0 | HV - SB - 33 | UGS | TEMP/SALIN/COND | |
| 210 1615.0 | HV - SB - 35 | UGS | TEMP/SALIN/COND | |
| 210 1630.0 | HV - SB - 37 | UGS | TEMP/SALIN/COND | |
| 210 1645.0 | HV - SB - 39 | UGS | TEMP/SALIN/COND | |
| 210 17 0.0 | HV - SB - 41 | UGS | TEMP/SAL/COND | |
| 211 1149.0 | HV - SB - 43 | UGS | TEMP/SALT/COND | 10M |
| 211 12 0.0 | HV - SB - 45 | UGS | TEM/SAL/COND | |
| 211 1215.0 | HV - SB - 47 | UGS | TEM/SAL/COND | |
| 211 1230.0 | HV - SB - 49 | UGS | TEM/SAL/COND | |
| 211 1245.0 | HV - SB - 51 | UGS | TEM/SAL/COND | |
| 214 1130.0 | HV - SB - 53 | UGS | TEM/SAL/COND | |
| 214 1145.0 | HV - SB - 54 | UGS | TEM/SAL/COND | |
| 214 12 0.0 | HV - SB - 55 | UGS | TEM/SAL/COND | |
| 214 1215.0 | HV - SB - 56 | UGS | TEM/SAL/COND | |
| 214 1233.0 | HV - SB - 57 | UGS | TEM/SAL/COND | |

52

SHIP-KARLUK

CRUISE LOCATOR ARCS-75-KR
ARFA-YR-IDCHIEF
SCIENTIST-BARNES

ARCHIVE NUMBER

OPTIONAL

| JUL. TIME | DATUM | SUB- | SOURCE, | SPLIT | START | DISPO- | OPTIONAL | LATITUDE | LONGITUDE | POS. |
|-----------|-------|------|---------|-------|-------|--------|-------------|----------|-----------|------|
| DAY | GMT | TYPE | STN NO. | NO. | END | SITION | STATION | DEG MIN | DEG MIN | CODE |
| | | | | | | | DESCRIPTION | DATA | | |

BECKMAN SALINITY/TEMP/CONDUCTIVITY/DENSITY (HVSF)-

| | | | | | | | | | | |
|------------|----|---|----|---|----|--|-----|-----------------|-------|--|
| 214 1245.0 | HV | - | SB | - | 58 | | UGS | TEMP/SAL/COND | | |
| 214 1315.0 | HV | - | SB | - | 59 | | UGS | TEMP/SAL/COND | | |
| 214 1330.0 | HV | - | SB | - | 60 | | UGS | TEMP/SAL/COND | | |
| 214 1346.0 | HV | - | SB | - | 61 | | UGS | TEMP/SAL/COND | | |
| 214 14 0.0 | HV | - | SB | - | 62 | | UGS | TEMP/SAL/COND | | |
| 215 14 0.0 | HV | - | SB | - | 63 | | UGS | TEMP/SAL/COND | | |
| 215 1530.0 | HV | - | SB | - | 64 | | UGS | TEMP/SAL/COND | | |
| 216 750.0 | HV | - | SB | - | 65 | | UGS | TEMP/SALINITY | 0.0M | |
| 216 752.0 | HV | - | SB | - | 67 | | UGS | TEMP/SALINITY | 10.0M | |
| 216 915.0 | HV | - | SB | - | 68 | | UGS | TEMP/SALINITY | 0.0M | |
| 216 917.0 | HV | - | SB | - | 70 | | UGS | TEMP/SALINITY | 10.0M | |
| 216 1030.0 | HV | - | SB | - | 71 | | UGS | TEMP/SALINITY | 0.0M | |
| 216 1032.0 | HV | - | SB | - | 73 | | UGS | TEMP/SALINITY | 10.0M | |
| 216 12 4.0 | HV | - | SB | - | 74 | | UGS | TEMP/SALINITY | 0.0M | |
| 216 12 6.0 | HV | - | SB | - | 76 | | UGS | TEMP/SALINITY | 10.0M | |
| 216 1255.0 | HV | - | SB | - | 77 | | UGS | TEMP/SALINITY | 0.0M | |
| 216 1257.0 | HV | - | SB | - | 79 | | UGS | TEMP/SALINITY | 10.0M | |
| 216 1355.0 | HV | - | SB | - | 80 | | UGS | TEMP/SALINITY | 0.0M | |
| 216 1357.0 | HV | - | SB | - | 82 | | UGS | TEMP/SALINITY | 10.0M | |
| 217 815.0 | HV | - | SB | - | 83 | | UGS | TEMP/SALIN/COND | | |
| 217 820.0 | HV | - | SB | - | 84 | | UGS | TEMP/SALIN/COND | | |
| 217 845.0 | HV | - | SB | - | 85 | | UGS | TEMP/SALIN/COND | | |
| 217 9 0.0 | HV | - | SB | - | 86 | | UGS | TEMP/SALIN/COND | | |
| 217 915.0 | HV | - | SB | - | 87 | | UGS | TEMP/SALIN/COND | | |
| 217 930.0 | HV | - | SB | - | 88 | | UGS | TEMP/SALIN/COND | | |
| 217 946.0 | HV | - | SB | - | 89 | | UGS | TEMP/SALIN/COND | | |
| 217 10 0.0 | HV | - | SB | - | 90 | | UGS | TEMP/SALIN/COND | | |
| 217 1030.0 | HV | - | SB | - | 91 | | UGS | TEMP/SALIN/COND | | |
| 217 1045.0 | HV | - | SB | - | 92 | | UGS | TEMP/SALIN/COND | | |
| 222 12 0.0 | HV | - | SB | - | 93 | | UGS | TEMP/SALIN/COND | | |
| 222 1215.0 | HV | - | SB | - | 94 | | UGS | TEMP/SALIN/COND | | |
| 222 1232.0 | HV | - | SB | - | 95 | | UGS | TEMP/SALIN/COND | | |

53

SHIP-KARLUK

CRUISE LOCATOR ARCS-75-KR

CHIEF

AREA-YR-ID

SCIENTIST-BARNES

ARCHIVE NUMBER

OPTIONAL

| JUL. TIME | DATUM | SUR- | SEQNCE, | SPLIT | START | DISPO- | STATION | LATITUDE | LONGITUDE | POS. | | |
|---|--------|------|---------|---------|-------|--------|---------|-----------------|-----------|---------|---------|------|
| DAY | GMT | TYPE | TYPE | STN NO. | NO. | END | SITION | DESCRIPTION | DATA | DEG MIN | DEG MIN | CODE |
| ----- | | | | | | | | | | | | |
| BECKMAN SALINITY/TEMP/CONDUCTIVITY/DENSITY (HVS B)- | | | | | | | | | | | | |
| 222 | 1250.0 | HV | - SR | - | 96 | | UGS | TEMP/SALIN/COND | | | | |
| 222 | 1310.0 | HV | - SB | - | 97 | | UGS | TEMP/SALIN/COND | | | | |
| 222 | 1330.0 | HV | - SB | - | 98 | | UGS | TEMP/SALIN/COND | | | | |
| 222 | 14 0.0 | HV | - SB | - | 99 | | UGS | TEMP/SALIN/COND | | | | |
| 222 | 1415.0 | HV | - SB | - | 100 | | UGS | TEMP/SALIN/COND | | | | |
| 222 | 1430.0 | HV | - SB | - | 101 | | UGS | TEMP/SALIN/COND | | | | |
| 222 | 1445.0 | HV | - SB | - | 102 | | UGS | TEMP/SALIN/COND | | | | |
| 225 | 830.0 | HV | - SB | - | 103 | | UGS | TEMP/SALIN/COND | | | | |
| 225 | 846.0 | HV | - SB | - | 105 | | UGS | TEMP/SALIN/COND | | | | |
| 225 | 9 0.0 | HV | - SB | - | 107 | | UGS | TEMP/SALIN/COND | | | | |
| 225 | 915.0 | HV | - SB | - | 109 | | UGS | TEMP/SALIN/COND | | | | |
| 225 | 928.0 | HV | - SB | - | 111 | | UGS | TEMP/SALIN/COND | | | | |
| 225 | 945.0 | HV | - SB | - | 113 | | UGS | TEMP/SALIN/COND | | | | |
| 225 | 10 0.0 | HV | - SB | - | 115 | | UGS | TEMP/SALIN/COND | | | | |
| 225 | 1015.0 | HV | - SB | - | 117 | | UGS | TEMP/SALIN/COND | | | | |
| 225 | 1030.0 | HV | - SB | - | 119 | | UGS | TEMP/SALIN/COND | | | | |
| 225 | 1045.0 | HV | - SB | - | 121 | | UGS | TEMP/SALIN/COND | | | | |
| 225 | 1150.0 | HV | - SB | - | 123 | | UGS | TEMP/SALIN/COND | | | | |
| 225 | 12 0.0 | HV | - SB | - | 125 | | UGS | TEMP/SALIN/COND | | | | |
| 225 | 1215.0 | HV | - SB | - | 127 | | UGS | TEMP/SALIN/COND | | | | |
| 225 | 1230.0 | HV | - SB | - | 129 | | UGS | TEMP/SALIN/COND | | | | |
| 225 | 1245.0 | HV | - SB | - | 131 | | UGS | TEMP/SALIN/COND | | | | |
| 225 | 1255.0 | HV | - SB | - | 133 | | UGS | TEMP/SALIN/COND | | | | |
| 225 | 1315.0 | HV | - SB | - | 135 | | UGS | TEMP/SALIN/COND | | | | |
| 225 | 1330.0 | HV | - SB | - | 137 | | UGS | TEMP/SALIN/COND | | | | |
| 225 | 1346.0 | HV | - SB | - | 139 | | UGS | TEMP/SALIN/COND | | | | |
| 225 | 14 0.0 | HV | - SB | - | 141 | | UGS | TEMP/SALIN/COND | | | | |
| 225 | 1425.0 | HV | - SB | - | 143 | | UGS | TEMP/SALIN/COND | | | | |
| 225 | 1445.0 | HV | - SB | - | 145 | | UGS | TEMP/SALIN/COND | | | | |
| 227 | 730.0 | HV | - SB | - | 147 | | UGS | TEMP/SALIN/COND | | | | |
| 227 | 745.0 | HV | - SB | - | 149 | | UGS | TEMP/SALIN/COND | | | | |
| 227 | 8 0.0 | HV | - SB | - | 151 | | UGS | TEMP/SALIN/COND | | | | |

SS4

SHIP-KARLUK

CRUISE LOCATOR ARCS-75-KR
AREA-YR-IDCHIEF
SCIENTIST-BARNES

ARCHIVE NUMBER

OPTIONAL

| JUL. TIME | DATUM | SUB- | SEQNCE, | SPLIT | START | DISPO- | STATION | LATITUDE | LONGITUDE | POS. | | |
|-----------|-------|------|---------|---------|-------|--------|---------|-------------|-----------|---------|---------|------|
| DAY | GMT | TYPE | TYPE | STN NO. | NO. | END | SITIOIN | DESCRIPTION | DATA | DEG MIN | DEG MIN | CODE |

BECKMAN SALINITY/TEMP/CONDUCTIVITY/DENSITY (HVSF)-

| | | | | | | | | | | | | |
|-----|--------|--------|----|----|----|-----|-----|-----------------|-----------------|--|--|--|
| 227 | 830.0 | HV | - | SB | - | 153 | UGS | TEMP/SALIN/COND | | | | |
| 227 | 852.0 | HV | - | SB | - | 155 | UGS | TEMP/SALIN/COND | | | | |
| 227 | 9 0.0 | HV | - | SB | - | 157 | UGS | TEMP/SALIN/COND | | | | |
| 227 | 915.0 | HV | - | SB | - | 159 | UGS | TEMP/SALIN/COND | | | | |
| 227 | 920.0 | HV | - | SB | - | 161 | UGS | TEMP/SALIN/COND | | | | |
| 227 | 945.0 | HV | - | SB | - | 163 | UGS | TEMP/SALIN/COND | | | | |
| 227 | 10 0.0 | HV | - | SB | - | 165 | UGS | TEMP/SALIN/COND | | | | |
| 227 | 1015.0 | HV | - | SB | - | 167 | UGS | TEMP/SALIN/COND | | | | |
| 227 | 11 0.0 | HV | - | SB | - | 169 | UGS | TEMP/SALIN/COND | | | | |
| 227 | 1115.0 | HV | - | SB | - | 171 | UGS | TEMP/SALIN/COND | | | | |
| 227 | 1130.0 | HV | - | SB | - | 173 | UGS | TEMP/SALIN/COND | | | | |
| 227 | 1145.0 | HV | - | SB | - | 175 | UGS | TEMP/SALIN/COND | | | | |
| 227 | 1415.0 | HV | - | SB | - | 176 | UGS | TEMP/SALIN/COND | | | | |
| 227 | 1430.0 | HV | - | SB | - | 178 | UGS | TEMP/SALIN/COND | | | | |
| 227 | 1447.0 | HV | - | SB | - | 180 | UGS | TEMP/SALIN/COND | | | | |
| 555 | 227 | 1515.0 | HV | - | SB | - | 182 | UGS | TEMP/SALIN/COND | | | |
| 555 | 227 | 1530.0 | HV | - | SB | - | 184 | UGS | TEMP/SALIN/COND | | | |
| 555 | 227 | 1546.0 | HV | - | SB | - | 186 | UGS | TEMP/SALIN/COND | | | |
| 227 | 16 2.0 | HV | - | SB | - | 188 | UGS | TEMP/SALIN/COND | | | | |
| 227 | 1620.0 | HV | - | SB | - | 190 | UGS | TEMP/SALIN/COND | | | | |
| 227 | 1630.0 | HV | - | SB | - | 192 | UGS | TEMP/SALIN/COND | | | | |
| 227 | 1645.0 | HV | - | SB | - | 194 | UGS | TEMP/SALIN/COND | | | | |
| 227 | 17 0.0 | HV | - | SB | - | 196 | UGS | TEMP/SALIN/COND | | | | |
| 232 | 1445.0 | HV | - | SB | - | 198 | UGS | TEMP/SALIN/COND | | | | |
| 232 | 15 0.0 | HV | - | SB | - | 200 | UGS | TEMP/SALIN/COND | | | | |
| 232 | 1515.0 | HV | - | SB | - | 202 | UGS | TEMP/SALIN/COND | | | | |
| 232 | 1530.0 | HV | - | SB | - | 204 | UGS | TEMP/SALIN/COND | | | | |
| 233 | 750.0 | HV | - | SB | - | 206 | UGS | TEMP/SALIN/CON | 0.0M | | | |
| 233 | 8 0.0 | HV | - | SB | - | 208 | UGS | TEMP/SALIN/CON | 2.0M | | | |
| 233 | 8 0.0 | HV | - | SB | - | 209 | UGS | TEMP/SALIN/CON | 1.0M | | | |
| 233 | 8 0.0 | HV | - | SB | - | 210 | UGS | TEMP/SALIN/CON | 2.5M | | | |
| 233 | 9 0.0 | HV | - | SB | - | 211 | UGS | TEMP/SALIN/CON | 0.0M | | | |

SHIP-KARLUK

CRUISE LOCATOR ARCS-75-KB
AREA-YR-IDCHIEF
SCIENTIST-BARNES

| JUL. TIME | | ARCHIVE NUMBER | | OPTIONAL | | LATITUDE | LONGITUDE | POS. |
|-----------|-----|----------------|----------|----------|-------------|----------|-----------|------|
| DAY | GMT | DATUM | SUB-TYPE | STATION | DESCRIPTION | | | |

BECKMAN SALINITY/TEMP/CONDUCTIVITY/DENSITY (HVS8)-

| | | | | | | | | |
|-----|---------|----|--------|-----|-----|-----------------|------|--|
| 233 | 9 0.0 | HV | - SR - | 213 | UGS | TEMP/SALIN/CON | 1.0M | |
| 233 | 9 0.0 | HV | - SR - | 214 | UGS | TEMP/SALIN/CON | 2.0M | |
| 233 | 9 0.0 | HV | - SR - | 215 | UGS | TEMP/SALIN/CON | 3.0M | |
| 233 | 9 30.0 | HV | - SR - | 216 | UGS | TEMP/SALIN/CON | 0.0M | |
| 233 | 9 30.0 | HV | - SR - | 218 | UGS | TEMP/SALIN/CON | 1.0M | |
| 233 | 9 30.0 | HV | - SR - | 219 | UGS | TEMP/SALIN/COND | 2.0M | |
| 233 | 9 30.0 | HV | - SR - | 220 | UGS | TEMP/SALIN/COND | 3.0M | |
| 233 | 10 0.0 | HV | - SR - | 221 | UGS | TEMP/SALIN/COND | 0.0M | |
| 233 | 10 0.0 | HV | - SR - | 223 | UGS | TEMP/SALIN/COND | 1.0M | |
| 233 | 10 0.0 | HV | - SR - | 224 | UGS | TEMP/SALIN/COND | 2.0M | |
| 233 | 10 0.0 | HV | - SR - | 225 | UGS | TEMP/SALIN/COND | 3.0M | |
| 233 | 10 0.0 | HV | - SR - | 226 | UGS | TEMP/SALIN/COND | 4.0M | |
| 233 | 10 30.0 | HV | - SR - | 227 | UGS | TEMP/SALIN/COND | 0.0M | |
| 233 | 10 30.0 | HV | - SR - | 229 | UGS | TEMP/SALIN/COND | 1.0M | |
| 233 | 10 30.0 | HV | - SR - | 230 | UGS | TEMP/SALIN/COND | 2.0M | |
| 233 | 10 30.0 | HV | - SR - | 231 | UGS | TEMP/SALIN/COND | 3.0M | |
| 233 | 11 9.0 | HV | - SR - | 232 | UGS | TEMP/SALIN/COND | 0.0M | |
| 233 | 11 9.0 | HV | - SR - | 234 | UGS | TEMP/SALIN/COND | 1.0M | |
| 233 | 11 9.0 | HV | - SB - | 235 | UGS | TEMP/SALIN/COND | 2.0M | |
| 233 | 11 9.0 | HV | - SP - | 236 | UGS | TEMP/SALIN/COND | 4.0M | |
| 233 | 11 9.0 | HV | - SB - | 237 | UGS | TEMP/SALIN/COND | 6.0M | |
| 233 | 11 9.0 | HV | - SB - | 238 | UGS | TEMP/SALIN/COND | 8.0M | |
| 233 | 13 18.0 | HV | - SB - | 239 | UGS | TEMP/SALIN/COND | 0.0M | |
| 233 | 13 18.0 | HV | - SR - | 240 | UGS | TEMP/SALIN/COND | 1.0M | |
| 233 | 13 18.0 | HV | - SP - | 241 | UGS | TEMP/SALIN/COND | 2.0M | |
| 233 | 13 18.0 | HV | - SR - | 242 | UGS | TEMP/SALIN/COND | 3.0M | |
| 233 | 19 19.0 | HV | - SB - | 1A | UGS | TEMP/SALIN/COND | 0.0M | |
| 233 | 19 19.0 | HV | - SB - | 1B | UGS | TEMP/SALIN/COND | 1.0M | |
| 233 | 19 19.0 | HV | - SB - | 1C | UGS | TEMP/SALIN/COND | 1.5M | |
| 233 | 19 19.0 | HV | - SB - | 1D | UGS | TEMP/SALIN/COND | 2.0M | |
| 233 | 19 19.0 | HV | - SB - | 1E | UGS | TEMP/SALIN/COND | 2.5M | |
| 233 | 19 31.0 | HV | - SB - | 2A | UGS | TEMP/SALIN/COND | 0.0M | |

556

SHIP-KARLUK

CRUISE LOCATOR ARCS-75-KR
AREA-YR-IDCHIEF
SCIENTIST-BARNES

| | | ARCHIVE NUMBER | | | | OPTIONAL | | LATITUDE | LONGITUDE | POS. |
|--|------------|----------------|----------|----------------|-----------|------------------|--------------------|----------|-----------|------|
| JUL. DAY | TIME GMT | DATUM TYPE | SUB-TYPE | SEQNCE STN NO. | SPLIT NO. | START END SITION | DISPO- DESCRIPTION | DEG MIN | DEG MIN | CODE |
| BECKMAN SALINITY/TEMP/CONDUCTIVITY/DENSITY (HVS8)- | | | | | | | | | | |
| | 233 1931.0 | HV | - SB - | 2B | | UGS | TEMP/SALIN/COND | 1.0M | | |
| | 233 1931.0 | HV | - SB - | 2C | | UGS | TEMP/SALIN/COND | 2.0M | | |
| | 233 1931.0 | HV | - SB - | 2D | | UGS | TEMP/SALIN/COND | 3.0M | | |
| | 233 1947.0 | HV | - SB - | 3A | | UGS | TEMP/SALIN/COND | 0.0M | | |
| | 233 1947.0 | HV | - SB - | 3B | | UGS | TEMP/SALIN/COND | 1.0M | | |
| | 233 1947.0 | HV | - SB - | 3C | | UGS | TEMP/SALIN/COND | 2.0M | | |
| | 233 1947.0 | HV | - SB - | 3D | | UGS | TEMP/SALIN/COND | 2.5M | | |
| | 233 1955.0 | HV | - SB - | 4A | | UGS | TEMP/SALIN/COND | 0.0M | | |
| | 233 1955.0 | HV | - SB - | 4B | | UGS | TEMP/SALIN/COND | 1.0M | | |
| | 233 1955.0 | HV | - SB - | 4C | | UGS | TEMP/SALIN/COND | 2.0M | | |
| | 233 1955.0 | HV | - SB - | 4D | | UGS | TEMP/SALIN/COND | 2.5M | | |
| | 233 20 9.0 | HV | - SB - | 6A | | UGS | TEMP/SALIN/COND | 0.0M | | |
| | 233 2010.0 | HV | - SB - | 6B | | UGS | TEMP/SALIN/COND | 1.0M | | |
| | 233 2017.0 | HV | - SB - | 5A | | UGS | TEMP/SALIN/COND | 0.0M | | |
| | 233 2017.0 | HV | - SB - | 5B | | UGS | TEMP/SALIN/COND | 1.0M | | |
| | 233 2017.0 | HV | - SB - | 5C | | UGS | TEMP/SALIN/COND | 2.0M | | |
| | 233 2019.0 | HV | - SB - | 5D | | UGS | TEMP/SALIN/COND | 2.5M | | |
| 5 | 233 2030.0 | HV | - SB - | 7A | | UGS | TEMP/SALIN/COND | 0.0M | | |
| 7 | 233 2030.0 | HV | - SB - | 7B | | UGS | TEMP/SALIN/COND | 1.0M | | |
| | 233 2032.0 | HV | - SB - | 7C | | UGS | TEMP/SALIN/COND | 2.0M | | |
| | 233 2040.0 | HV | - SB - | 8A | | UGS | TEMP/SALIN/COND | 0.0M | | |
| | 233 2040.0 | HV | - SB - | 8B | | UGS | TEMP/SALIN/COND | 1.0M | | |
| | 233 2042.0 | HV | - SB - | 8C | | UGS | TEMP/SALIN/COND | 2.0M | | |
| | 233 2049.0 | HV | - SB - | 9A | | UGS | TEMP/SALIN/COND | 0.0M | | |
| | 233 2049.0 | HV | - SB - | 9B | | UGS | TEMP/SALIN/COND | 1.0M | | |
| | 233 2049.0 | HV | - SB - | 9C | | UGS | TEMP/SALIN/COND | 2.0M | | |
| | 233 2059.0 | HV | - SB - | 10A | | UGS | TEMP/SALIN/COND | 0.0M | | |
| | 233 2059.0 | HV | - SB - | 10B | | UGS | TEMP/SALIN/COND | 1.0M | | |
| | 233 2059.0 | HV | - SB - | 10C | | UGS | TEMP/SALIN/COND | 2.0M | | |
| | 233 2110.0 | HV | - SB - | 11 | | UGS | TEMP/SALIN/COND | 0.5M | | |
| | 233 2136.0 | HV | - SB - | 12A | | UGS | TEMP/SALIN/COND | 0.0M | | |
| | 233 2136.0 | HV | - SB - | 12B | | UGS | TEMP/SALIN/COND | 1.0M | | |

SHIP-KARLUK

CRUISE LOCATOR ARCS-75-KB
AREA-YR-ID

CHIEF
SCIENTIST-BARNES

ARCHIVE NUMBER

OPTIONAL

| JUL. TIME | DATUM | SUB- | SEQNC | SPLIT | START | DISPO- | STATION | LATITUDE | LONGITUDE | POS. | | |
|-----------|-------|------|-------|---------|-------|--------|---------|-------------|-----------|---------|---------|------|
| DAY | GMT | TYPE | TYPE | STN NO. | NO. | END | SITION | DESCRIPTION | DATA | DEG MIN | DEG MIN | CODE |

BECKMAN SALINITY/TEMP/CONDUCTIVITY/DENSITY (HVSF)-

| | | | | | | | | | | | | |
|-----|--------|----|---|----|---|-----|-----|-----------------|------|--|--|--|
| 233 | 2136.0 | HV | - | SB | - | 120 | UGS | TEMP/SALIN/COND | 1.5M | | | |
|-----|--------|----|---|----|---|-----|-----|-----------------|------|--|--|--|

SHIP-KARLUK

CRUISE LOCATOR ARCS-75-KR

CHIEF
SCIENTIST-BARNES

AREA-YP-ID

ARCHIVE NUMBER

OPTIONAL

| JUL. TIME | DATUM | SUB- | SEONCE, | SPLIT | START | DISPO- | OPTIONAL | LATITUDE | LONGITUDE | POS. |
|-----------|-------|------|---------|---------|-------|--------|-------------|----------|-----------|------|
| DAY | GMT | TYPE | TYPE | STN NO. | NO. | END | STATION | DEG MIN | DEG MIN | CODE |
| | | | | | | | DESCRIPTION | DATA | | |

TURBIDITY TRANSMISSOMETER (HVTT)-

| | | | | | | | | | | |
|-----|--------|----|------|---|-----|--|-----|--|--|---------------------|
| 210 | 1515.0 | HV | - TT | - | 28 | | UGS | | | TRANSMISSIVITY |
| 210 | 1530.0 | HV | - TT | - | 30 | | UGS | | | TRANSMISS. |
| 210 | 1545.0 | HV | - TT | - | 32 | | UGS | | | TRANSMISS. |
| 210 | 16 0.0 | HV | - TT | - | 34 | | UGS | | | TRANSMISS. |
| 210 | 1615.0 | HV | - TT | - | 36 | | UGS | | | TRANSMISS. |
| 210 | 1630.0 | HV | - TT | - | 38 | | UGS | | | TRANSMISS. |
| 210 | 1645.0 | HV | - TT | - | 40 | | UGS | | | TRANSMISS. |
| 210 | 17 0.0 | HV | - TT | - | 42 | | UGS | | | TRANSMISS. |
| 211 | 1149.0 | HV | - TT | - | 44 | | UGS | | | TRANS. RECORDED 10M |
| 211 | 12 0.0 | HV | - TT | - | 46 | | UGS | | | TRANSMISSIVITY |
| 211 | 1215.0 | HV | - TT | - | 48 | | UGS | | | TRANSMISSIVITY |
| 211 | 1230.0 | HV | - TT | - | 50 | | UGS | | | TRANSMISSIVITY |
| 211 | 1245.0 | HV | - TT | - | 52 | | UGS | | | TRANSMISSIVITY |
| 216 | 750.0 | HV | - TT | - | 66 | | UGS | | | TRANSMISSIVITY 0.0M |
| 216 | 915.0 | HV | - TT | - | 69 | | UGS | | | TRANSMISSIVITY 0.0M |
| 216 | 1030.0 | HV | - TT | - | 72 | | UGS | | | TRANSMISSIVITY 0.0M |
| 216 | 12 6.0 | HV | - TT | - | 75 | | UGS | | | TRANSMISSIVITY 0.0M |
| 216 | 1255.0 | HV | - TT | - | 78 | | UGS | | | TRANSMISSIVITY 0.0M |
| 216 | 1355.0 | HV | - TT | - | 81 | | UGS | | | TRANSMISSIVITY 0.0M |
| 225 | 830.0 | HV | - TT | - | 104 | | UGS | | | TRANSMISSIVITY |
| 225 | 846.0 | HV | - TT | - | 106 | | UGS | | | TRANSMISSIVITY |
| 225 | 9 0.0 | HV | - TT | - | 108 | | UGS | | | TRANSMISSIVITY |
| 225 | 915.0 | HV | - TT | - | 110 | | UGS | | | TRANSMISSIVITY |
| 225 | 928.0 | HV | - TT | - | 112 | | UGS | | | TRANSMISSIVITY |
| 225 | 945.0 | HV | - TT | - | 114 | | UGS | | | TRANSMISSIVITY |
| 225 | 10 0.0 | HV | - TT | - | 116 | | UGS | | | TRANSMISSIVITY |
| 225 | 1015.0 | HV | - TT | - | 118 | | UGS | | | TRANSMISSIVITY |
| 225 | 1030.0 | HV | - TT | - | 120 | | UGS | | | TRANSMISSIVITY |
| 225 | 1045.0 | HV | - TT | - | 122 | | UGS | | | TRANSMISSIVITY |
| 225 | 1150.0 | HV | - TT | - | 124 | | UGS | | | TRANSMISSIVITY |
| 225 | 12 0.0 | HV | - TT | - | 126 | | UGS | | | TRANSMISSIVITY |
| 225 | 1215.0 | HV | - TT | - | 128 | | UGS | | | TRANSMISSIVITY |

559

SHIP-KARLUK

CRUISE LOCATOR APCS-75-KP
AREA-YR-IDCHIEF
SCIENTIST-PARNES

ARCHIVE NUMBER

OPTIONAL

| JUL. TIME | DATUM | SUB- | SEQNC | SPLIT | START | DISPO- | OPTIONAL | LATITUDE | LONGITUDE | POS. |
|-----------|-------|------|-------|---------|-------|--------|-------------|----------|-----------|------|
| DAY | GMT | TYPE | TYPE | STN NO. | NO. | END | STATION | DEG MIN | DEG MIN | CODE |
| | | | | | | | DESCRIPTION | DATA | | |

TURBIDITY TRANSMISSOMETER (HVTT)-

| | | | | | | | | | | |
|-----|--------|----|------|---|-----|--|-----|--|--|--------------|
| 225 | 1230.0 | HV | - TT | - | 130 | | UGS | | | TRANSMISSIV. |
| 225 | 1245.0 | HV | - TT | - | 132 | | UGS | | | TRANSMISSIV. |
| 225 | 1255.0 | HV | - TT | - | 134 | | UGS | | | TRANSMISSIV. |
| 225 | 1315.0 | HV | - TT | - | 136 | | UGS | | | TRANSMISSIV. |
| 225 | 1330.0 | HV | - TT | - | 138 | | UGS | | | TRANSMISSIV. |
| 225 | 1346.0 | HV | - TT | - | 140 | | UGS | | | TRANSMISSIV. |
| 225 | 14 0.0 | HV | - TT | - | 142 | | UGS | | | TRANSMISSIV. |
| 225 | 1425.0 | HV | - TT | - | 144 | | UGS | | | TRANSMISSIV. |
| 225 | 1445.0 | HV | - TT | - | 146 | | UGS | | | TRANSMISSIV. |
| 227 | 730.0 | HV | - TT | - | 148 | | UGS | | | TRANSMISSIV. |
| 227 | 745.0 | HV | - TT | - | 150 | | UGS | | | TRANSMISSIV. |
| 227 | 8 0.0 | HV | - TT | - | 152 | | UGS | | | TRANSMISSIV. |
| 227 | 820.0 | HV | - TT | - | 154 | | UGS | | | TRANSMISSIV. |
| 227 | 852.0 | HV | - TT | - | 156 | | UGS | | | TRANSMISSIV. |
| 227 | 9 0.0 | HV | - TT | - | 158 | | UGS | | | TRANSMISSIV. |
| 227 | 915.0 | HV | - TT | - | 160 | | UGS | | | TRANSMISSIV. |
| 227 | 930.0 | HV | - TT | - | 162 | | UGS | | | TRANSMISSIV. |
| 227 | 945.0 | HV | - TT | - | 164 | | UGS | | | TRANSMISSIV. |
| 227 | 10 0.0 | HV | - TT | - | 166 | | UGS | | | TRANSMISSIV. |
| 227 | 1015.0 | HV | - TT | - | 168 | | UGS | | | TRANSMISSIV. |
| 227 | 11 0.0 | HV | - TT | - | 170 | | UGS | | | TRANSMISSIV. |
| 227 | 1115.0 | HV | - TT | - | 172 | | UGS | | | TRANSMISSIV. |
| 227 | 1415.0 | HV | - TT | - | 177 | | UGS | | | TRANSMISSIV. |
| 227 | 1430.0 | HV | - TT | - | 179 | | UGS | | | TRANSMISSIV. |
| 227 | 1447.0 | HV | - TT | - | 181 | | UGS | | | TRANSMISSIV. |
| 227 | 1515.0 | HV | - TT | - | 183 | | UGS | | | TRANSMISSIV. |
| 227 | 1530.0 | HV | - TT | - | 185 | | UGS | | | TRANSMISSIV. |
| 227 | 1546.0 | HV | - TT | - | 187 | | UGS | | | TRANSMISSIV. |
| 227 | 16 2.0 | HV | - TT | - | 189 | | UGS | | | TRANSMISSIV. |
| 227 | 1620.0 | HV | - TT | - | 191 | | UGS | | | TRANSMISSIV. |
| 227 | 1630.0 | HV | - TT | - | 193 | | UGS | | | TRANSMISSIV. |
| 227 | 1645.0 | HV | - TT | - | 195 | | UGS | | | TRANSMISSIV. |

OBS

SHIP-KAPLUK

CRUISE LOCATOR ARCS-75-KB
AREA-YR-ID

CHIEF
SCIENTIST-BARNES

ARCHIVE NUMBER

OPTIONAL

| JUL. TIME | DATUM | SUB- | SEANCE, | SPLIT | START | DISPO- | STATION | LATITUDE | LONGITUDE | POS. | | |
|-----------|-------|------|---------|---------|-------|--------|---------|-------------|-----------|---------|---------|------|
| DAY | GMT | TYPE | TYPE | STN NO. | NO. | END | SITON | DESCRIPTION | DATA | DEG MIN | DEG MIN | CODE |

TURBIDITY TRANSMISSOMETER (HVTT)-

| | | | | | | | | | | | | | | |
|-----|----|------|----|---|----|---|-----|--|--|--|--|--|-----|--------------|
| 227 | 17 | 0.0 | HV | - | TT | - | 197 | | | | | | UGS | TRANSMISSIV. |
| 232 | 14 | 45.0 | HV | - | TT | - | 199 | | | | | | UGS | TRANSMISSIV. |
| 232 | 15 | 0.0 | HV | - | TT | - | 201 | | | | | | UGS | TRANSMISSIV. |
| 232 | 15 | 15.0 | HV | - | TT | - | 203 | | | | | | UGS | TRANSMISSIV. |
| 232 | 15 | 30.0 | HV | - | TT | - | 205 | | | | | | UGS | TRANSMISSIV. |
| 233 | 7 | 50.0 | HV | - | TT | - | 207 | | | | | | UGS | TRANSMISSIV. |
| 233 | 9 | 0.0 | HV | - | TT | - | 212 | | | | | | UGS | TRANSMISSIV. |
| 233 | 9 | 30.0 | HV | - | TT | - | 217 | | | | | | UGS | TRANSMISSIV. |
| 233 | 10 | 0.0 | HV | - | TT | - | 222 | | | | | | UGS | TRANSMISSIV. |
| 233 | 10 | 30.0 | HV | - | TT | - | 228 | | | | | | UGS | TRANSMISSIV. |
| 233 | 11 | 9.0 | HV | - | TT | - | 233 | | | | | | UGS | TRANSMISSIV. |

561

SHIP-KARLUK

CRUISE LOCATOR ARCS-75-KB

CHIEF

AREA-YR-ID

SCIENTIST-BARNES

ARCHIVE NUMBER

OPTIONAL

| JUL. TIME | DATUM | SUB- SEONCE, | SPLIT START DISPO- | OPTIONAL | LATITUDE | LONGITUDE | POS. |
|-----------|-------|-------------------|--------------------|--------------|----------|-----------|------|
| DAY | GMT | TYPE TYPE STN NO. | NO. END SITION | STATION DATA | DEG MIN | DEG MIN | CODE |

SUSPENDED SEDIMENT (HSTS)-

| | | | | | | | |
|-----|--------|-----------|--|---|---|--|----------------------|
| 216 | 750.0 | HS - TS - | | P | S | | SUSP.SED.LINE START. |
| 216 | 14 0.0 | HS - TS - | | R | F | | SUSP.SED.LINE END |
| 225 | 1150.0 | HS - TS - | | P | S | | SUSP.SED.LINE START |
| 225 | 15 5.0 | HS - TS - | | R | F | | SUSP.SED.LINE END |
| 227 | 0 7.2 | HS - TS - | | R | S | | SUSP.SED.LINE START |
| 227 | 011.5 | HS - TS - | | R | F | | SUSP.SED.LINE END |
| 227 | 014.0 | HS - TS - | | R | S | | SUSP.SED.LINE START |
| 227 | 1615.0 | HS - TS - | | R | E | | SUSP.SED.LINE END |
| 233 | 930.0 | HS - TS - | | R | S | | SUSP.SED.LINE START |
| 233 | 1030.0 | HS - TS - | | R | F | | SUSP.SED.LINE END |
| 233 | 1140.0 | HS - TS - | | R | S | | SUSP.SED.LINE START |
| 233 | 1215.0 | HS - TS - | | R | E | | SUSP.SED.LINE END |

562

SHIP-KARLUK

CRUISE LOCATOR APCS-75-KR
AREA-YR-ID

CHIEF

SCIENTIST-BARNES

ARCHIVE NUMBER

OPTIONAL

| JUL. TIME | DATUM | SUB- | SEQNCE, | SPLIT | START | DISPO- | STATION | LATITUDE | LONGITUDE | POS. | | |
|-----------------------------|--------|-----------|-----------|---------|-------|--------|---------|-------------|-----------|---------|---------|---------------------|
| DAY | GMT | TYPE | TYPE | STN NO. | NÓ. | END | SITTON | DESCRIPTION | DATA | DEG MIN | DEG MIN | CODE |
| VIDEO TAPE RECORDER (GTOT)- | | | | | | | | | | | | |
| 212 | 15 | 0.0 | GT - QI - | 1 | | | S | UGS | | | | TV RUN ROLL 1 |
| 212 | 16 | 0.0 | GT - QI - | | | | R | E | | | | END TV RUN 1 LINE 5 |
| 212 | 1630.0 | GT - QI - | | | | | R | S | | | | TV LINE 2 START |
| 212 | 1730.0 | GT - QI - | | | | | R | E | | | | TV LINE 2 STOP |
| 222 | 1525.0 | GT - QI - | | | | | R | S | | | | ST TV RUN ON TAPE 1 |
| 222 | 1640.0 | GT - QI - | | | | | R | E | | | | END TV RUN |
| 229 | 1150.0 | GT - QI - | | | | | R | S | | | | STRT TV & VIDEO TPE |
| 229 | 12 0.0 | GT - QI - | | 1 | | | E | UGS | | | | END VIDEO TAPE #1 |
| 229 | 12 5.0 | GT - QI - | | 2 | | | S | UGS | | | | ST. VIDEO TAPE #2 |
| 229 | 1330.0 | GT - QI - | | 2 | | | E | UGS | | | | END VIDEO TAPE #2 |
| 229 | 1410.0 | GT - QI - | | 3 | | | S | UGS | | | | ST. VIDEO TAPE #3 |
| 229 | 1515.0 | GT - QI - | | | | | R | E | | | | VIDEO TAPE OFF |

563

SHIP-KARLUK

CRUISE LOCATOR APC5-75-KB

CHIEF
SCIENTIST-BARNES

AREA-YR-ID

ARCHIVE NUMBER

OPTIONAL

| JUL. TIME | DATUM | SUB- | SEONCE, | SPLIT | START | DISPO- | STATION | LATITUDE | LONGITUDE | POS. | | |
|-----------|-------|------|---------|---------|-------|--------|---------|-------------|-----------|---------|---------|------|
| DAY | GMT | TYPE | TYPE | STN NO. | NO. | END | SITION | DESCRIPTION | DATA | DEG MIN | DEG MIN | CODE |

VANVEEN GRAB (GSKV)-

| | | | | | | | | | | | | |
|-----|----|------|----|---|----|---|----|-----|--|--|--|---------------------|
| 233 | 8 | 5.0 | GS | - | KV | - | 9 | UGS | | | | VAN VEEN STATION #9 |
| 233 | 9 | 0.0 | GS | - | KV | - | 10 | UGS | | | | VAN VEEN STATION#10 |
| 233 | 9 | 20.0 | GS | - | KV | - | 11 | UGS | | | | VAN VEEN STATION#11 |
| 233 | 10 | 0.0 | GS | - | KV | - | 12 | UGS | | | | V/VEEN SAMPLE # 12 |
| 233 | 10 | 30.0 | GS | - | KV | - | 13 | UGS | | | | V/VEEN SAMPLE # 13 |

SHIP-KARLUK

CRUISE LOCATOR ARCS-75-KR
AREA-YR-ID

CHIEF
SCIENTIST-BARNES

ARCHIVE NUMBER

OPTIONAL

| JUL. TIME | DATUM | SUR- | SEQNCE, | SPLIT | START | DISPO- | DESCRIPTION | STATION | LATITUDE | LONGITUDE | POS. |
|-----------|-------|------|---------|---------|-------|--------|-------------|---------|----------|-----------|------|
| DAY | GMT | TYPE | TYPE | STN NO. | NO. | END | SITION | DATA | DEG MIN | DEG MIN | CODE |

SCIENTIFIC EQUIPMENT STATUS (X R)-

| | | | | | | | | | | | |
|-----|--------|----|--------|--|---|---|-----|--|-----------------|--|---|
| 237 | 1030.0 | XX | - TA - | | R | S | IMS | | AIR GUN LINE | | |
| 237 | 1415.0 | XX | - TA - | | R | E | IMS | | AIR GUN OFF | | |
| 241 | 740.0 | XX | - TA - | | R | S | IMS | | AIR GUN LINE ON | | M |
| 241 | 955.0 | XX | - TA - | | R | F | IMS | | AIR GUN OFF | | |
| 241 | 10 5.0 | XX | - TA - | | R | S | IMS | | AIR GUN ON | | |
| 241 | 1550.0 | XX | - TA - | | P | E | IMS | | AIR GUN OFF | | |
| 242 | 1730.0 | XX | - TA - | | R | S | | | AIR GUN ON | | |
| 242 | 2030.0 | XX | - TA - | | R | E | IMS | | AIR GUN OFF | | |

565

SHIP-KARLUK

CRUISE LOCATOR ARCS-75-KB
AREA-YR-ID

CHIEF
SCIENTIST-BARNES

| JUL. TIME DAY | TIME GMT | ARCHIVE NUMBER | | | | SPLIT NO. | START END | DISPO- SITION | DESCRIPTION | OPTIONAL | LATITUDE DEG MIN | LONGITUDE DEG MIN | POS. CODE |
|------------------|-------------|----------------|--------------|----------------------|-----------------|--------------|--------------|------------------|-------------|----------|---------------------|----------------------|--------------|
| | | DATUM TYPE | SUB- TYPE | SEQUENCE, STN NO. | STATION DATA | | | | | | | | |

COMMENTS (U)-

216 750.1 U - -

TAKEN EVERY 15 MIN.

CROSS ISLAND CHANGES IN MORPHOLOGY FROM
1949 to 1975 AND THEIR IMPLICATIONS

The location of the early-winter shearzone off Prudhoe Bay is controlled by Cross Island, located approximately 12 miles north of the Sagavanirktok River delta. Considering the energy expended by the moving ice field on the island, and the action of storm waves, changes in the island might be expected over several decades. An attempt was made to document the changes in the morphology and position of the island using aerial photos, both vertical and oblique, photos from the ground, and published navigational charts. The changes in morphology over the years were measured using characteristic embayment, lake and ridge patterns of the island as the stable bases for alignment of photos and charts. The series of drawings in Figure 1 show how the island appeared on the earliest (1914?) map by Leffingwell up to the present day. The Leffingwell drawing could not be keyed into the other drawings accurately, because of the lack of identifying features used to match the scales between pictures. It is shown only to give the general impression of the earliest recorded view of the island.

The information gathered for the comparison of the island's shape and position consisted of 1) vertical B&W photo taken in July 1949 from 10,000 feet altitude, 2) vertical B&W photo taken in July 1955 from 25,000 feet altitude, 3) U-2 color photo taken in June 1974 from 65,000 feet altitude, 4) April 1955 edition of NOAA chart #9472 with coastal revisions updated to June 1973, and 5) U.S. Hydrographic Survey Chart #7761 from 1950.

Cross Island as seen on the NOAA chart appears to have been taken from the 1949 photo, and matches nearly perfectly. This chart was used to determine changes in overall position. The Hydrographic Survey chart was only used to study changes in position relative to the mainland, since the island was drawn too crudely to give details of morphologic changes. The 1949, 1955 and 1974 photos were brought to common scale, with all the details of stream, lake and topography that could be unambiguously identified. These patterns remained stable through the years and enabled us to measure the shoreline changes. Close examination of vertical photos, oblique photos taken by Reimnitz from the air in August 1970 and June 1971, and photos from the top of a RACON tower on the island in 1973 confirm the stability of these land-locked features. A small wooden cabin approximately 30 years old, that is located on a high point of the island, was also used as an artificial "benchmark" to confirm positions seen in the photos (see photo A). The two linear depressions on either side of the cabin, and the lake seen in the far left of the photo can be precisely located on all the photos. In Figure 1 in the 1949 photo the cabin and RACON tower positions are shown.

The 1974 U-2 photo shows Cross Island surrounded by ice which partially obscures the shoreline. For this reason, the 1974 shore is not as accurately represented as in 1949 and 1955. However, the personal observations by Reimnitz of the shore area during periods of ice cover, and examination of the photos taken from the RACON tower, which show the width of the island between the north shore and the lagoon

during the summer (see photo B) indicate that for the north shore the U-2 photo coastline is accurate to within 20 meters. The southern (inner) beaches have gentle slopes. With fast ice and snow drifts lapping onto this shore, an accurate determination of the shore is nearly impossible. Dashed lines in Figure 1 indicated where shoreline positions are in doubt and are roughly drawn in from photographic contrast changes seen in the U-2 photo.

The attempt to document the large scale movement of the island by comparing its position to mainland based features was not successful because the comparison between the Mercator projections of the NOAA and Hydrographic survey charts and the planimetrically photographed U-2 image was not possible within the accuracy needed. Leffingwell's map of the area was considered too inaccurate to use in a comparison since the method of fixing the island's position must have involved numerous extended surveys far out onto the ice to reach the island, introducing errors fatal to the accuracy desired for a comparison.

RESULTS OF MEASUREMENTS

The north shore beach retreat measured between 1949 and 1955, is slightly less than 50 meters in 6 years at the point of greatest change. The new shore is approximately parallel to the old shoreline, indicating an average retreat of about 40 meters. The measurements from the 1974 photo gives an average retreat of 150 meters from the 1949 position, with the largest value of 170 meters near the point of maximum curvature of the north beach. This gives an average of 7 meters a year from 1949 to 1955 and 6 meters a year from 1949 to 1974. Extrapolating this back

to the position Leffingwell gives for Cross Island, the 1914 location should be 245 meters seaward. His map puts the island 2000 meters to the northeast of the 1949 position. For this reason, we chose to disregard his location, and blame lack of adequate survey control for the error. Figure 1 suggests that sediment eroded from the northern shore is transported to and deposited on both ends of the island, but movement of beach material seems to be mainly toward the west. On the west end of the island a recurved spit is being formed, that eventually may become similar in shape and morphology to the spits that enclose the two shallow embayments on the landward side of the islands. This would form a third embayment. The embayments enclosed by recurved spits record the migration of the island. The two existing embayments indicate northwesterly migration, the presently forming embayment seems to indicate a shift in migration direction to westerly. A westward migration of Cross Island is in agreement with the migration direction of other barrier islands along this section of the Beaufort Sea coast.

DISCUSSION AND CONCLUSION

Sand and gravel is in high demand on the northslope as construction material. Most of the barrier islands including Cross Island, are composed of sand and gravel. Some of the islands near Prudhoe Bay have already been mined. It is anticipated that others will be soon. For this reason it is important to know the gravel sources that supply the islands with new material, and to know how erosion and deposition change the shapes and locations of the islands.

From 1949 to 1974, Cross Island has lost 6 to 7 meters a year on the seaward side. It is becoming narrower, because the landward side is not accreting at the same rate. Possibly most of the eroded material can be accounted for by spit accretion, mainly on the west end. Various types of evidence indicate that Cross Island presently is not receiving gravel from an outside source. It represents a lag deposit of sand and gravel, and should not be mined, especially since it is one of the more important Eider duck nesting grounds in the area.

A manuscript under preparation shows that Cross Island is the focal point for the early winter shear lines in the sea ice. Major ridges form close to the island, and ice shove commonly affects the beaches. Other islands in the area, protected from shear zone dynamics, are little affected by ice shove. Ice shove brings cobbles and pebbles, found by diving near the beach at 15 to 20 ft depth, up onto the beach face. This ice shove may be one of the reasons why Cross Island is 4 to 5 ft higher than the characteristic barrier islands along Simpson Lagoon. The bottom off Cross Island also slopes much steeper than off other islands that are protected from shear zone dynamics, as shown in the above report (Fig. 2). Grounded ridges off the island commonly remain stationary throughout the summer. Therefore, the north side is almost completely protected from wave action during the average year. Photos A and B were taken during an unusually ice-free summer.

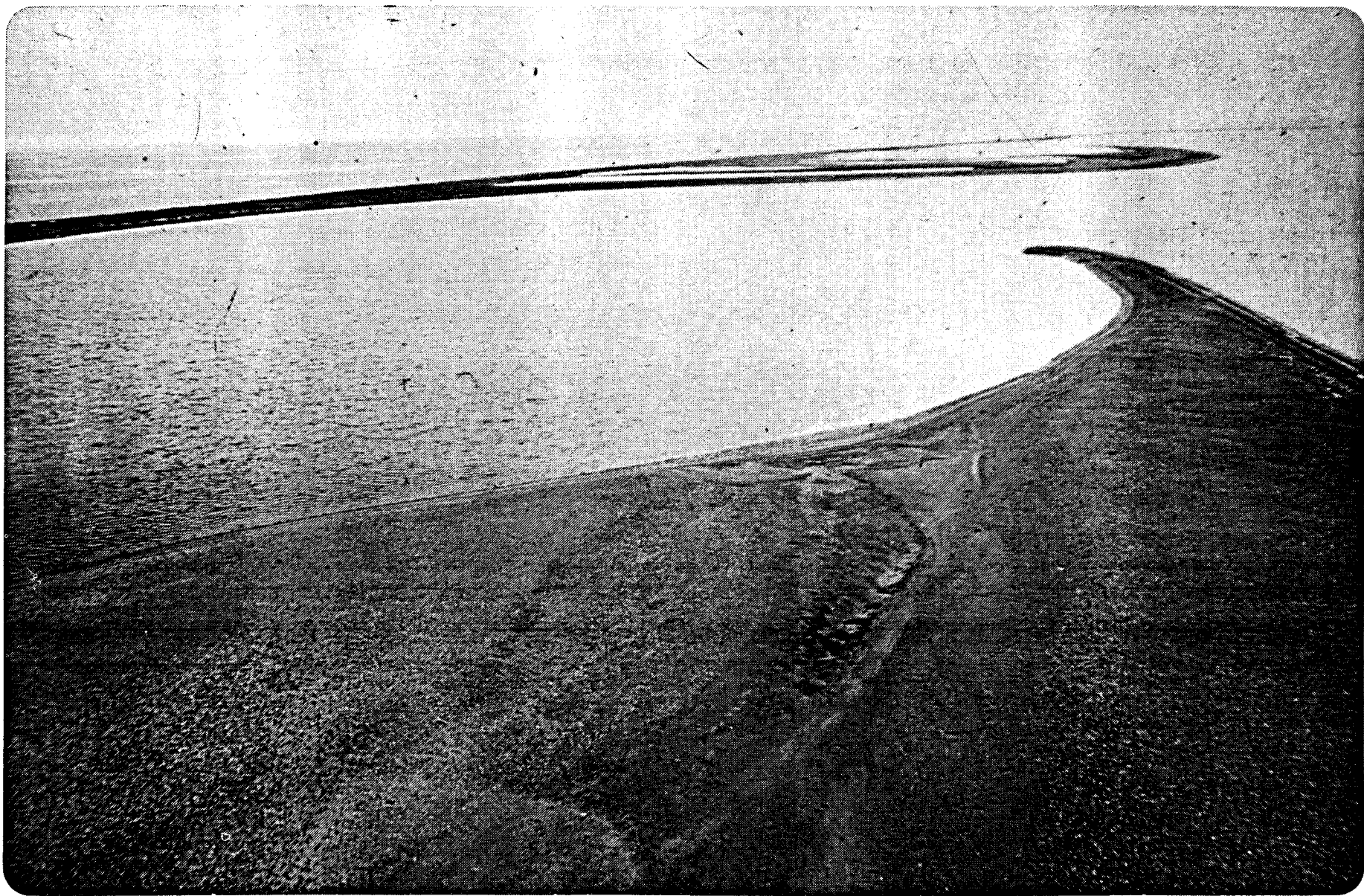
The above observations on Cross Island may have certain implications for offshore development and construction by man, because of some similarities between the island and artificial drilling islands used

elsewhere in the Arctic. It lies further offshore, and in deeper water than those, and is exposed to pack ice drift. In fact, Cross Island controls the pack ice drift, and the extent of the relatively undeformed fast ice. Further studies of ice dynamics in relationship to the island may provide information on the feasibility of modifying the ice zonation off Prudhoe Bay.

573



574



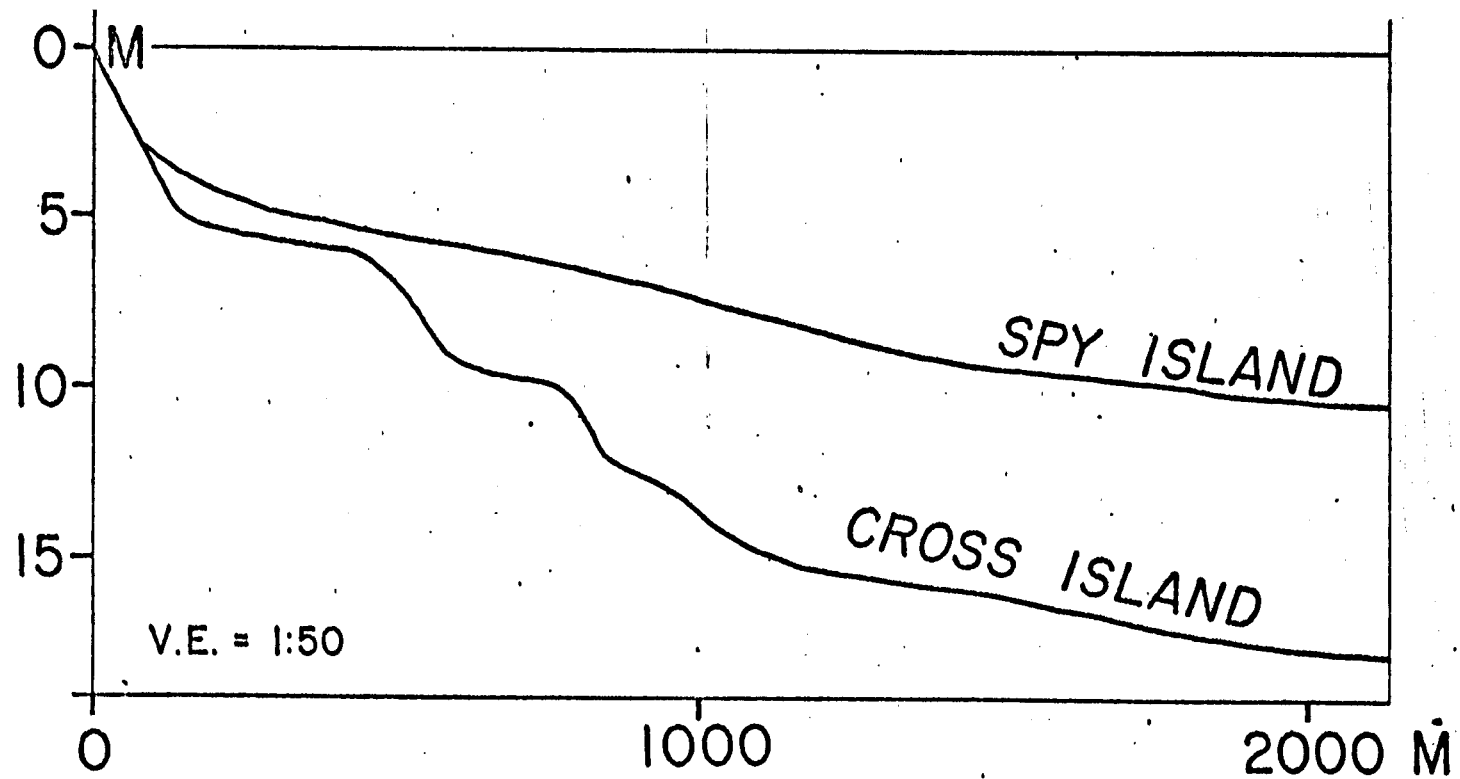


Figure 2 Nearshore bottom profiles, comparing Cross Island, where the Shear zone impinges on the coast, and spy island, where the zone lies offshore and is localized by shoals.

A study of the repetitive rate of ice gouging
in Harrison Bay, Beaufort Sea

Knowledge of the repetitive rates and depth of ice gouging on the continental shelf of the Beaufort Sea is important for several reasons: 1) it provides an indirect method of determining the maximum ice-keel depth distribution, important for pressure ridge studies, 2) it provides insights on the rates at which bottom sediments and benthic communities are being reworked and disrupted by the physical action of ice, important for the marine geologist and biologist, 3) it may serve as a guide in the planning and design of offshore pipelines and other bottom mounted installations.

In 1973 a precise range-range navigation system was available for the first time for our Beaufort Sea studies. Using this navigation system, we surveyed three particular tracks between Prudhoe Bay and Harrison Bay, which we plan to resurvey occasionally with side-scan sonar, in order to determine the repetitive rates of ice gouging on the shelf. The three track lines of 1973 were resurveyed in 1975. Unfortunately, ice during these two years has prevented us from extending these survey lines from the coast far enough offshore to study the entire zone of predominantly grounded ice (stamukhi zone). Also, the quality of the sonar records obtained during the two surveys is not equal, making a comparison of bottom features difficult. However, the results from the comparison of one of these three transects, Harrison Bay, are significant, and are reported below.

METHODS AND RESULTS

A group of 3 side-scan sonar survey lines from 1973 were resurveyed in 1975 to study the changes in ice gouging patterns within the 2 year period. Line 1 from 1973 and line 14 from 1975 extend to the northwest from Thetis Island. Line 2 from 1973 and line 13 from 1975 extend directly north from Spy Island. Line 3 from 1973 and line 7 from 1975 extend northward from near Argo Island of Prudhoe Bay. Still earlier sonar records (from 1972), lines 17 and 20, ran transverse to lines 2 and 13 and were used to check the instrument resolution stability between 1973 and 1975 by running over the same bottom 3 times with the same equipment. The 1972 and 1975 records were able to resolve features of similar relief with equal clarity, while the 1973 records lack sharp resolution, giving the impression of viewing a rather featureless bottom. Lines 2 and 3 from 1973 could not be compared to their 1974 counterparts because of this lack of resolution. Only line 1 showed enough detail to make a comparison with its 1975 counterpart, Line 14 (Fig. 1).

By steering the vessel on a range of two landmarks - a cabin on Thetis Island and the tower at the Oliktok DEW site - the two tracks matched almost precisely along the southeastern two thirds of the line. Further seaward visuals were lost, but using the range-range navigation system we were able to steer the boat within a 50-m distance of the previous survey, done by the same method. Thus, gouges on the seafloor with certain characteristics could be identified in the surveys separated by a two-year period, as will be shown later.

On cursory inspection of the two years' records, the 1973 data indicated a nearly featureless bottom with a few subdued gouges, while the bottom in 1975 was criss-crossed by numerous crisp appearing gouges. This difference at first was interpreted to represent a dominantly wave- and current reworked bottom in 1973, and a great increase in new gouges since then. However, close examination and matching of the two record sets showed a large number of faint gouges in the 1973 data, that could be clearly identified as the same features seen again in the 1975 data, but with much better resolution and crispness. The 1975 record also showed many gouges that were clearly post-dating the older survey. These new gouges commonly were still crisper in appearance, indicating steeper relief, than the older gouges identified on the 1973 records. Still, a large number of old gouges had to be dated by noting when a positively identified 1973 or older gouge had cut through them. In this way many fainter gouges could be identified on the 1975 record which could not be seen on the 1973 record.

The next step in our analysis was the preparation of trace overlays that distinguishes the 1973 and older gouges from those post-dating the 1973 survey. This was done as described below.

All gouges visible on the 1973 records of relatively low quality were traced on overlays. Those that had easily distinguished features, such as unusual patterns, intersections of gouges with characteristic angles, and notable curves and bends, commonly could be identified again on the 1975 records. These gouges were used to accurately match the 1973 records to the 1975 records. As a next step an overlay of the 1975 records

was prepared, with all gouges seen in the 1973 records traced as dashed lines (Fig. 2). On this overlay we also traced in solid lines all of the 1975 gouges that were clearly more pronounced (giving stronger reflections) than those shown as dashed lines. The gouges represented by solid lines were formed between 1973 and 1975. If these pronounced gouges had been present during the 1973 survey, we certainly would have detected them.

In summary, figure 2 shows as dashed lines the gouges seen in both the 1973 and 1975 records, and as solid lines the post-1973 gouges. But all small gouges below the limits of resolution in the 1973 records are deleted. The number of 2 year or younger gouges shown therefore give a conservative value for the rate of ice gouging along this particular transect.

In order to determine the rate at which the sediments along the survey track are being reworked by ice gouging, the fathograms recorded along with the sonographs were analyzed. The fathograms show the cross-sectional relief of ice gouges directly below the vessel. The width of new gouge incisions below the general level of the sea floor were used to give a conservative estimate of the ratio of the area gouged within two years to the total area along the track. The fathogram used for this determination represented 10 km of survey track, of which .65 km was gouged within two years. Assuming that no area is gouged more than once, the total area would be reworked by ice within 30 years. The .65 km value is conservative, because it does not include the very small gouges, and because it assumes that the gouge incisions were produced by efficient cutting tools. ^{Actually} The area of bottom disturbed by a blunt ice-keel is greater

than the measured width of the gouge.

If the present sea level has been constant (within a few meters) over the last 8,000 years, the sedimentation rate along the survey track can be estimated from the thickness of the Holocene marine sediments seen in sub-bottom profiles recorded simultaneously. The average thickness of Holocene sediments is 5 meters.. The sedimentation rate, therefore, is estimated to be 6.3 cm/100 years for the last 8,000 years. The average gouge depth, also measured off the fathogram, is approximately 30 cm. Within the 30 years that the entire bottom is gouged to an average depth of 30 cm, only 2 cm of sediment will be deposited. Thus, the stratigraphic column should be completely reworked before any sediment is buried deep enough to escape the action of the ice.

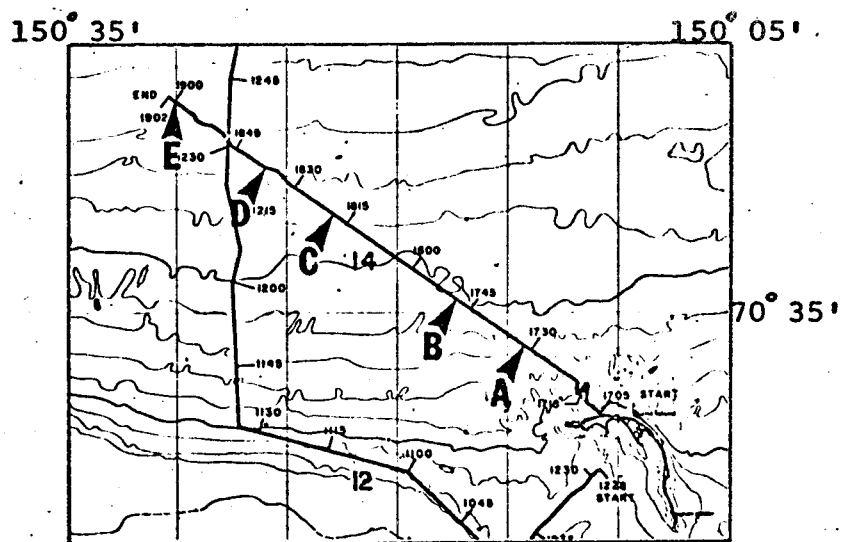


FIG. 1

Trackline for line 14 in 1975 which was rerun over line 1 from 1973. The lines match so closely only line 14 is shown here for clarity. The letter guides given are for reference in location in figure 2. Gouge rates were calculated from times 1745 to 1900 along the trackline.

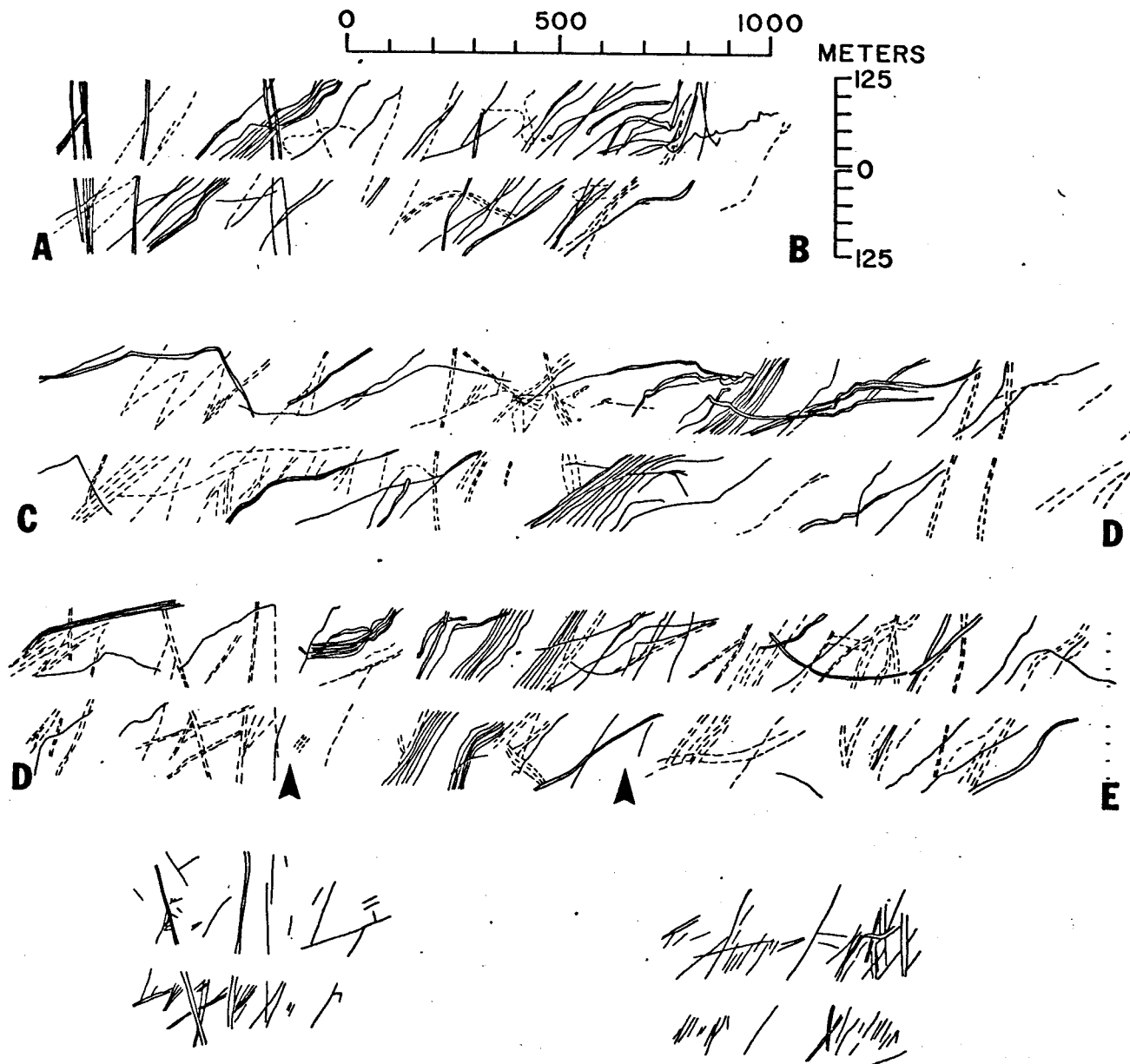


FIG. 2 The upper three lines were taken from the 1975 sonograph, showing the 1973 and older gouges as dashed and the post-1973 gouges as solid lines. The bottom line was taken from the 1973 record and shows how the 1973 and 1975 sonograph records can be matched using characteristic gouge patterns seen in both.

SHOAL MIGRATION UNDER THE INFLUENCE OF ICE:
A COMPARISON STUDY 1950-1975

During the course of our summer operations with small boats, which began in 1970, we have commonly noted the existence of grounded ice on offshore shoals. This grounded ice generally appears to be of pressure ridge origin, with a sail 5 to 8 m high, a keel of at least 10 m, and in plain view much longer (the order of kms), parallel to depth contours than wide. Pack ice fragments and floes frequently accumulate along the seaward side of these grounded ridges, which act as fences. In many cases the grounded ridges mark a distinct boundary between the scattered ice on the inner shelf and tightly packed ice on the central shelf. Figure 1 is an example of such a boundary.

The areal distribution of such grounded ridge systems was determined for the area between Cross Island and Cape Halkett from ERTS-1 satellite imagery of early July, 1973. Systems of well developed pressure ridges, shear ridges, and linear hummock fields corresponding to major shear events between the polar pack ice and shorefast ice from the previous winter were recorded in the imagery as pronounced lineations within the ice of the inner shelf.

A striking correlation between the areal distribution of linear ridge systems and charted shoal, can be seen in Figure 2. This winter relationship along with summer observations led us to suspect an interaction between ice dynamics and shoals found along the inner Arctic.

The inner shelf bathymetry between Long Island and Oliktok Point is shown in Figure 3. It is based on a dense pattern of accurately

controlled sounding lines run by the U.S. Coast and Geodetic Survey from 1949 through 1951. Using all original data from U.S. Coast and Geodetic Survey smooth sheets, the bathymetry was contoured at 1 m intervals.

During the summer of 1975, the U.S.G.S. R/V KARLUK completed bathymetric surveys across a number of the shoals seen in Figure 3. With a Del Norte Trisponder system and shore control stations at the established bench marks indicated by triangles in Figure 3, the navigational control for the surveys was accurate to within + 5 meters. From the 1949/51 and 1975 surveys a comparison of certain shoal cross sections and their locations was made. These are presented in Figure 4, with individual profiles keyed to Figure 3 by letters A through H. The 1949/51 bottom configuration is represented by the dashed line, the new configuration by a solid line, which also shows micro-relief due to ice gouging.

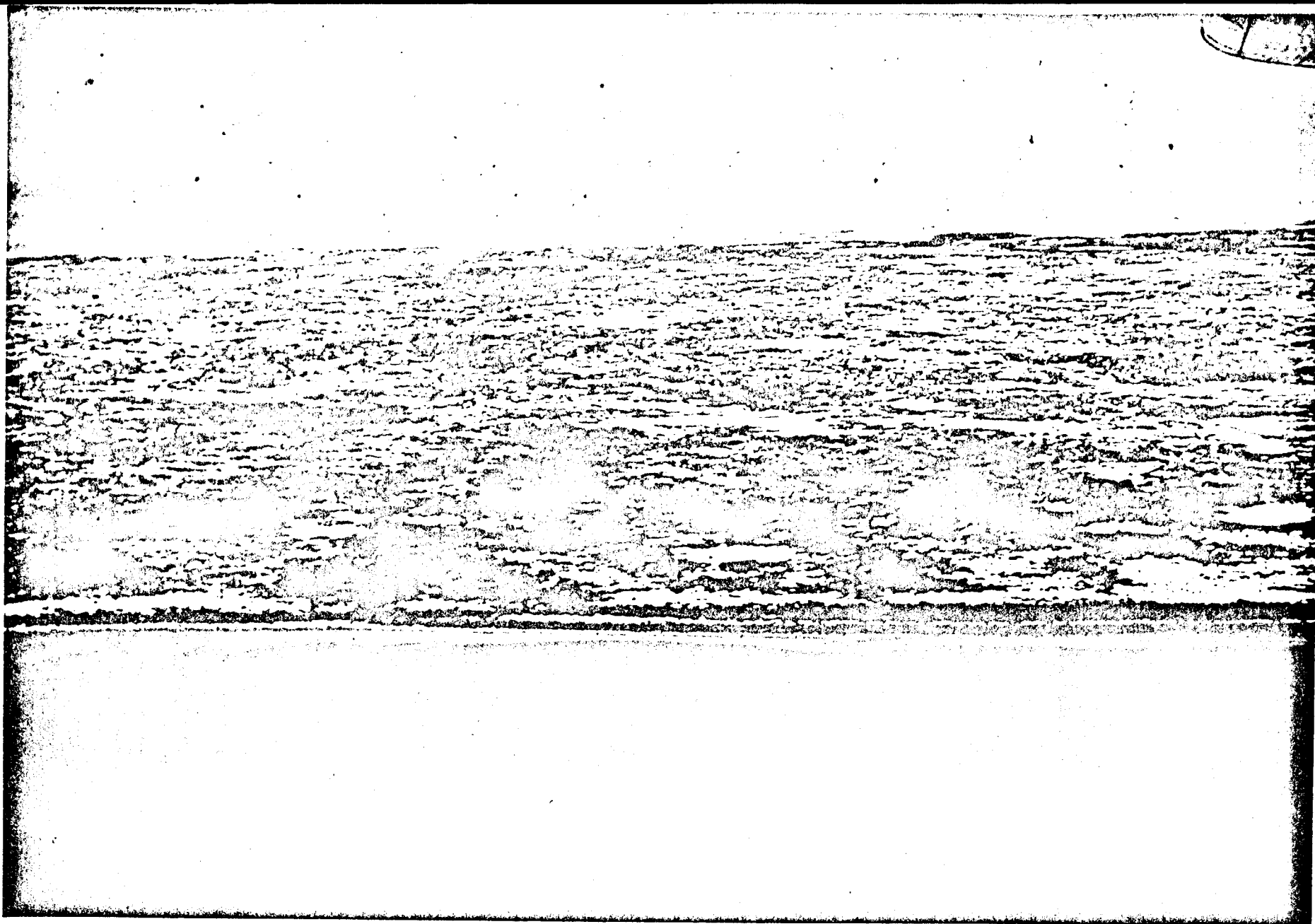
The shoals are very subtle features, considering that the vertical exaggeration is about 1:30. The seaward one (A) has shifted landward by about 200 m, retaining its shape, while the landward one (B) shifted only 120 m, but increased in size. Among the shoals north of Cottle Island, C is closest to shore. Considering that the dashed line represents an average drawn through a number of data points on the contour chart, while the solid line was traced directly from the fathogram with all detail, the two profiles are remarkably similar. Ridge cross sections D through H, located farther offshore, show pronounced changes. All ^{but one} have migrated landward through distances of 100 to 400 meters (avg. +200 m), and all but D have undergone considerable changes in shape. In general, the offshore shoals most exposed to dynamic forces within the shear zone,

have changed more than those further inshore.

The offshore shoals between Harrison Bay and Cross Island have also been studied with various seismic profiling techniques. The Holocene marine sediments in this region generally are only several meters thick on a flat-lying sub-bottom reflector. The shoals correspond to a thickening marine section, indicating that they are constructional features post-dating the last transgression. The shoals and the modern barrier island are rather similar in cross-sectional view. However, the shoals are composed of well sorted sand with a trace of individual pebbles, while the barrier islands consist of sandy gravel to gravelly sand. The shoals, therefore, do not appear to represent drowned barrier islands. One to 3-m high nearshore bars are known to be migrating under the influence of summer waves and currents. The larger shoals under discussion clearly are not formed by similar nearshore processes.

All available evidence leads to the conclusion that the shoals under discussion are not hydraulic bedforms related to open-water conditions, but that they were formed, and presently are migrating, under influence of ice-related processes. Future studies will have to show whether such shoals form by a) the bulldozing action of ice during one or several major events, b) the cumulative effects of several thousand years of ice push by grounded ridges along the edge of the Pacific Gyre rubbing against the continent, c) winter currents intensified along major grounded ridge systems to concentrate available sediments into sand ridges, or whether d) several of these processes act together to form the shoals.

The findings presented here are the first solid evidence for a relationship between anomalies in the overall profile of an Arctic shelf and boundary processes of the Beaufort Gyre Pack ice. These findings have extremely important implications for offshore development in the Arctic especially concerning the construction of artificial islands.



587

Figure 1. Oblique aerial photograph taken northeast of Pt. Barrow on August 13, 1975. Grounded ridges occur along lines paralleling isobaths (upper fourth of photo) marking a distinct boundary between scattered ice on the inner shelf (central portion of photo) and tightly packed ice on central shelf.

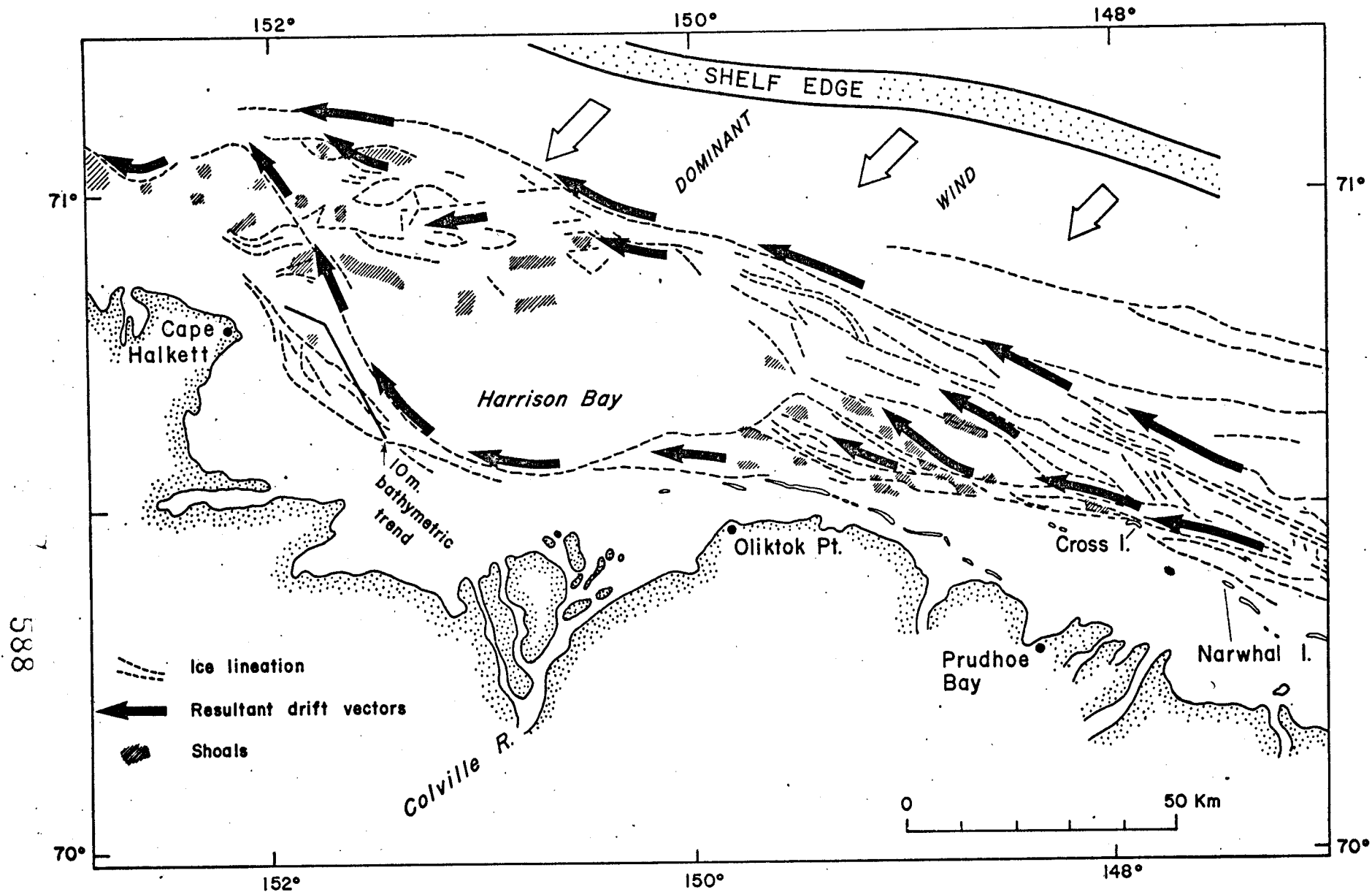


Figure 2. Generalized model of ice drift within area of detailed study, indicating movement of pack ice along well defined shearlines, dominant wind direction and location of charted shoals (hatched areas). A striking correlation is seen between distribution of shoals and major ice lineations seen in ERTS-1 images which represent shear ridges, pressure ridges, and linear hummock fields.

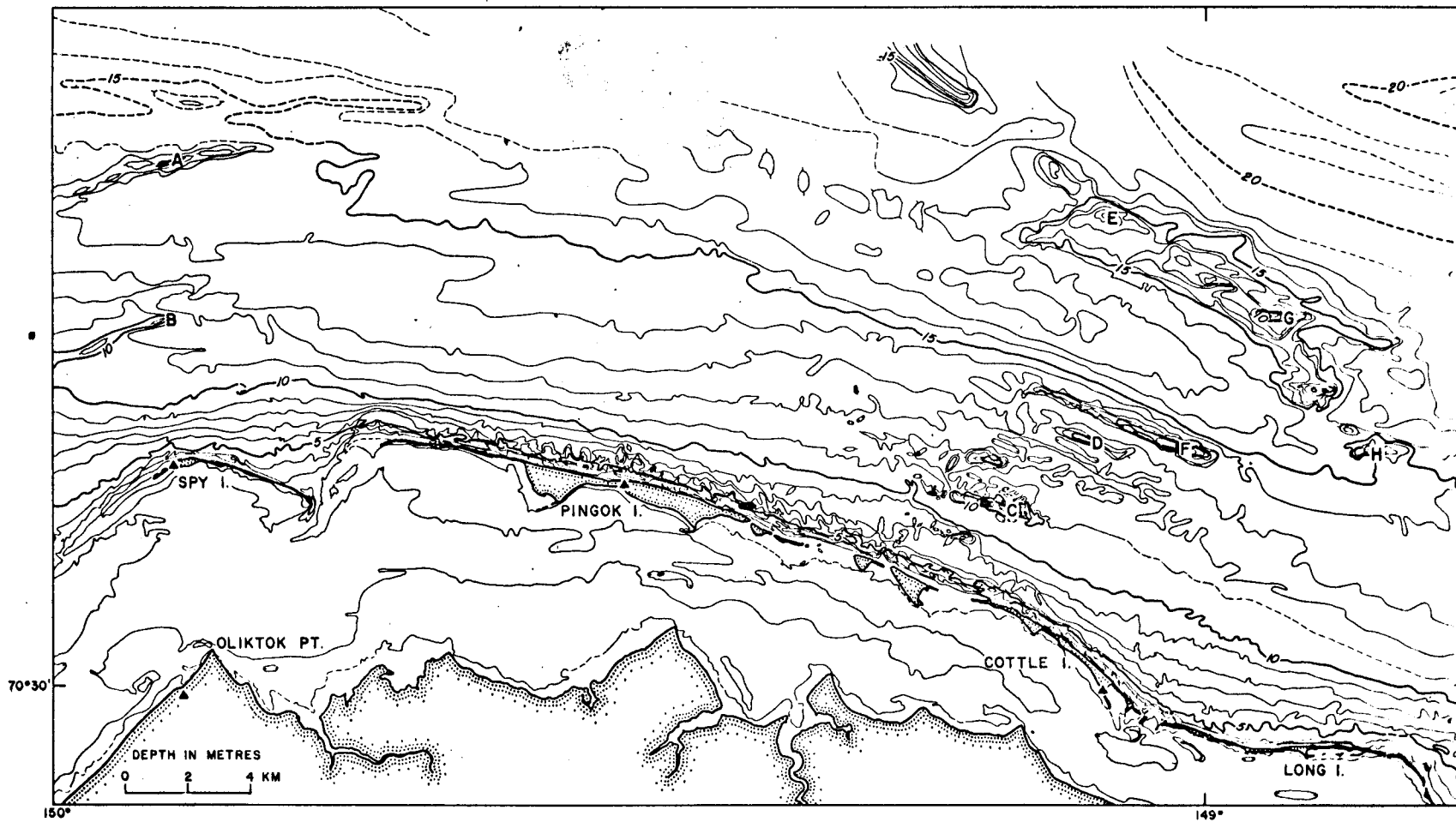


Figure 3. Bathymetry of inner shelf, within central portion of study area. The contours are based on 1949 through 1951 soundings, taken from U.S. Coast and Geodetic Survey smooth sheets. The location of individual shoal cross sections shown in Figure 4 are keyed in alphabetic order. Benchmarks used for the 1975 survey are shown by triangles.

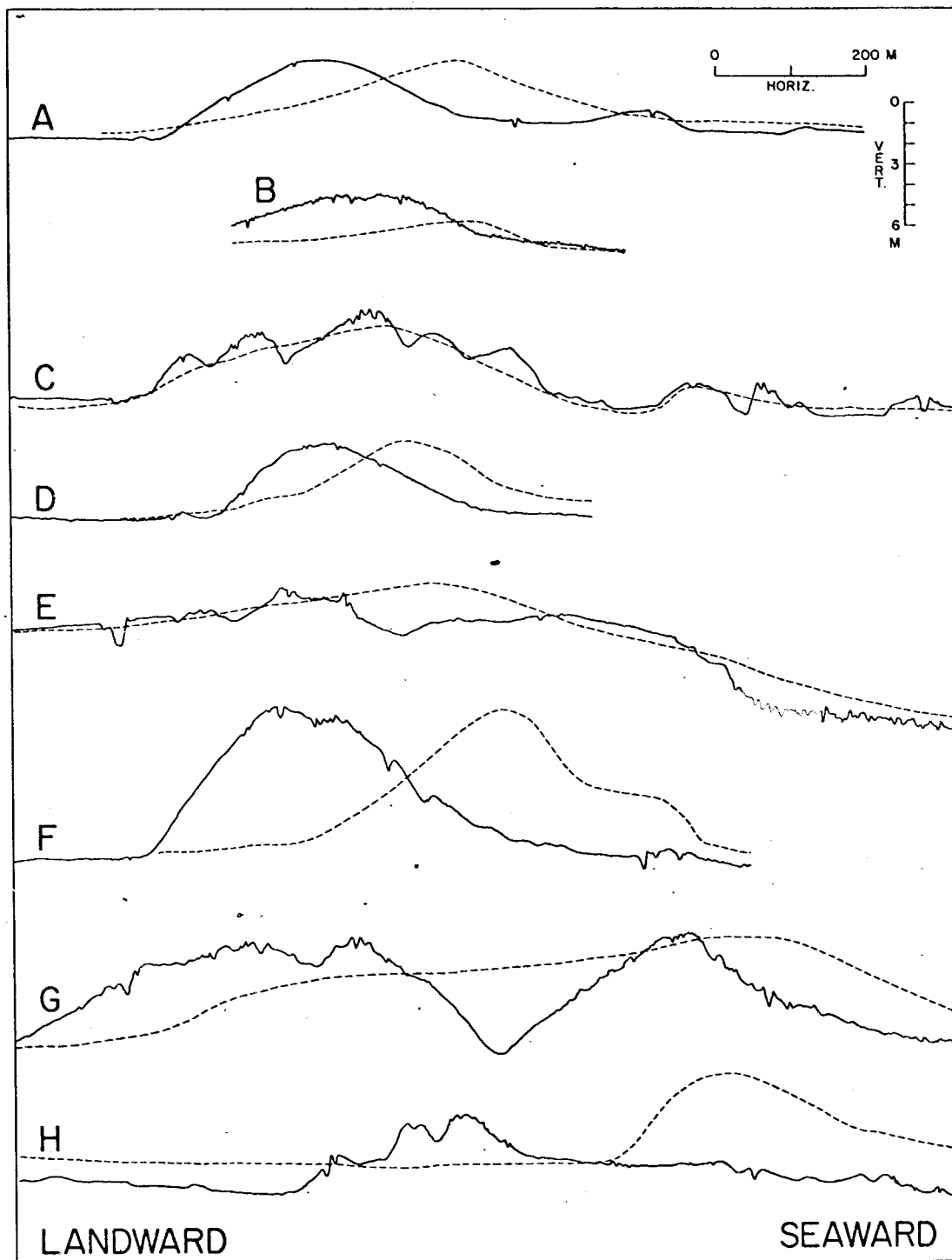


Figure 4. Comparison of shoal locations and cross sectional profiles from 1949/51 (dashed line) and 1975 (solid line) surveys. All the shoals but one have migrated landward through distances of 100 to 400 meters.

H

SURFACE CURRENT OBSERVATIONS - BEAUFORT SEA, 1972

By

Peter Barnes and Richard Garlow

U. S. Geological Survey

OPEN FILE REPORT

75-619

This report is preliminary and has not been edited or reviewed for conformity with Geological Survey standards

SURFACE CURRENT OBSERVATIONS - BEAUFORT SEA, 1972

by Peter Barnes and Richard Garlow

Sediment transport via water and ice in the Beaufort Sea off northern Alaska is related to the movement of the surficial waters. As development proceeds along the north slope of Alaska, a knowledge of the potential drift trajectories of water, ice, sediment and pollutants will be needed. In an attempt to better define the probable paths and rates of transport, 4200 surface drift cards were dropped during the U. S. Coast Guard WEBSEC cruise of August and September, 1972 (Hufford and others, 1974). The results of this release are the subject of this report. Because the data presented here will be used primarily by those interested in solving problems of transport, the emphasis has been placed on data presentation rather than a detailed analysis of the circulation.

The drifter used in this study consisted of a 10 by 15 cm printed orange card encased in a 6 mil clear plastic envelope (Figure 1). A 1/2 inch steel washer was sealed in the bottom of the drifter as ballast. In order to reduce the direct effect of wind on the cards, the air trapped in the envelope was adjusted prior to sealing such that less than 2 cm of freeboard existed. Problems were encountered in achieving an adequate seal and an estimated 5 percent drifters sank when launched. Others have been quite sturdy; surviving several arctic winters with more than 20% of the returns being found in 1975.

Drifter release and recovery data are summarized in Table 1. The low rate of return (1.8%) is expected in this remote area. The 1970 population of the North Slope Borough was 3,385. With the additional installations

Sender LT. WILLIAM WADE

Address FPO BOX 33

SEATTLE, WASH 98790

Zip Code

POSTAGE AND FEES PAID
U.S. DEPARTMENT OF THE INTERIOR

INT 413



POSTAGE WILL BE PAID BY —

OFFICE OF MARINE GEOLOGY

United States Geological Survey
345 Middlefield Road, Menlo Park,
California 94025

Attention: Dr. P. W. Barnes

4908

ТЕКУЩИЕ ИССЛЕДОВАНИЯ ОКЕАНА

OCEAN CURRENT SURVEY 4909

LOCATION WHERE CARD WAS FOUND: 70-10.4N 146-48W

DATE FOUND: JULY 17 1973
Month Day Year

CARD WAS FOUND: On Beach In Water
In or On Ice

REMARKS: LOCATED WELL
BELOW HIGH WATER LINE.
ICE WAS APPROX 10 MILES
OFF SHORE

Your assistance will help us determine the movement of ocean currents along the north coast of Alaska. Thank You

MARK CARD LOCATION ON MAP

0 40 80 MILES

GPO 701-095

Figure 1. Reproduction of drift card used in this survey. Post Paid card was placed in 6 mil plastic envelope with 1/2 inch washer and heat sealed.

at Prudhoe Bay, the present population is estimated near 5,000. More cards were returned (5.2%) from the nearshore releases; a situation common to surveys of this type (Kolpack, 1971; Conomos and others, 1971). In view of the sparse population of the north slope of Alaska and the short season when beaches are not snow and ice covered the recovery rate is considered very good. Recoveries have come predominately from the existing population centers; Barrow, Prudhoe Bay, Barter Island and the DEW line sites. The late summer (September) release of many of the drifters limited the time for transit to the beaches prior to freezeup when surface water motion ceases and the drifters could have been incorporated into the coastal ice or the polar pack. Although cards have been found and returned for three consecutive summers, there is no data suggesting drifters were not already ashore before freezeup in 1972.

The direction of drifter movement as summarized in Table 2 and on Figure 2, shows a dominance (79%) of westerly movement. About half of the recovery points were essentially onshore from their release points (distance to shore \geq half distances traveled parallel to shore). If the onshore movements are not considered as part of the directional data, the ratio of west to east drifters remains about the same with about 80% of the drifters moving west.

Velocity data are sparse, with only 9 useable recoveries occurring prior to freezeup in 1972 (Table 3). Rates of drift range from less than 1 cm/sec to almost 38 cm/sec. The lowest velocities were seen in those two cards which drifted essentially onshore. Drifters traveled westerly at the highest velocities with an average drift rate of 18 cm/sec (1/3 knot).

The one rate of drift calculated for an easterly direction (7.5 cm/sec) was less than 1/2 the average westerly rate.

Discussion

Although the data are limited and do not justify a detailed analysis, several general observations are in order. The surface currents are reportedly variable (U. S. Hydrographic Office, 1968). East of the Sagavanirktok River the drifters predominately moved eastward while all recoveries west of the Sagavanirktok invariably were to the west of their respective release points (Figure 2). Thus it would appear that a divergence in surface current drift existed in 1972 on the inner shelf off the Sagavanirktok River delta. The onshore surface water east of the delta flow toward Barter Island and water west of the delta flowed toward Barrow.

Curiously, the oceanographic values reported by Hufford and others (1974) show a change in character in this same area. Located off the Sagavanirktok are the salinity and temperature minimums and ice and dissolved oxygen maximums (Hufford and others, 1974). East of 146° upwelling is evident (Hufford and others, 1974). To the west an intrusion of Bering sea water is postulated along the shelf break with a compensating westerly flow on the inner shelf (Mountain, 1974).

In a more intensive study of surface currents in the Canadian Beaufort Sea, using much more elaborate drifters, MacNeill and Garrett (1974) found surface currents generally moving at about 5% of the wind speed and within 45° to the right of the wind direction. The drifter velocities that these workers reported are similar to the velocities that we observed (Table 3). However, velocities reported in Table 3 are not based on a sufficient number of data to warrant comparisons with wind data.

REFERENCES

- Conomos, T. J., McCulloch, D. S., Peterson, D. H., and Carlson, P. R.,
1971, Drift of surface and near-bottom waters of the San Francisco
Bay system, California: March 1970 through April 1971; U. S.
Geological Survey, Misc. Field Studies Map MF-33.
- Hufford, G. S., Fortier, S. H., Wolfe, D. E., Doster, J. F., Nobel, D. L.,
1974, Physical Oceanography of the Western Beaufort Sea, in WEBSEC
71-72, An Ecological Survey in the Beaufort Sea, U. S. Coast Guard
Oceanographic Report No. CG 373-64. pl-176.
- Kolpack, R. L., 1971, Oceanography of the Santa Barbara Channel, in
Biological and Oceanographical Survey of the Santa Barbara Channel
Oil Spill 1969-1970, R. L. Kolpack (ed.), v. II, pp. 90-180.
- MacNeill, Margaret, and Garrett, John, 1974, Open water surface currents;
Interim report of Beaufort Sea Project, Study D3, Beaufort Sea Project,
Federal Building, Victoria, B. C., 50 pp.
- Mountain, D. G., 1974, Preliminary analysis of Beaufort shelf circulation
in summer, in The Coast and Shelf of the Beaufort Sea, J. C. Reed
and J. E. Sater (eds.), Arctic Inst. of North Am., Arlington, Va.,
pp. 27-48.
- U. S. Navy Hydrographic Office, 1968, Oceanographic Atlas for the Polar
Seas - Part II Arctic: H. O. Pub. No. 705, 149 pp.

Table 1. Drifter release and recovery data

| <u>Date released</u> | <u>Number released</u> | <u>Number recovered</u> | <u>Percent recovered</u> |
|----------------------------|---|-------------------------|--------------------------|
| 8 August - 11 September | 2925 (released from ice breaker in waters <u>deeper</u> than 20 meters) | 9 | 0.3% |
| 21 August - 6 September | 1275 (released from coastal vessel in water depths less than 20 meters) | 66 | 5.2% |
| TOTALS | 4200 | 75 | 1.8% |

Table 2. Summary of drifter movements

| Direction of movement | number | percent |
|-----------------------|--------|----------|
| Easterly | 16 | 21 |
| Westerly | 59 | 79 |
| ----- | | |
| East along coast | 8 | 11 (22%) |
| Onshore | 38 | 50 (-) |
| West along coast | 29 | 39 (78%) |

Table 3. Drifter speed comparison and data 1972

| <u>Release Date</u> | <u>Recovery Date</u> | <u>Days adrift</u> | <u>Distance (miles)</u> | <u>Rate (mi/day)</u> | <u>Rate (cm/sec)</u> | <u>Direction</u> | <u>Recovery Location</u> |
|---------------------|----------------------|--------------------|-------------------------|----------------------|----------------------|--------------------|--------------------------|
| 21 Aug | 22 Aug | 1+ | 15 | 15+ | 32.0+ | West | Lagoon |
| 21 Aug | 27 Aug | 6 | 17.5 | 2.9 | 6.3 | West | Lagoon |
| 21 Aug | 27 Aug | 6 | 24 | 4 | 8.6 | West | Oliktok |
| 23 Aug | 26 Aug | 3 | 17 | 5.7 | 12.0 | West | Kup. R. |
| 23 Aug | 28 Aug | 5 | 8 | 0.62 | 1.3 | South (onshore) | Prudhoe Bay |
| 23 Aug | 9 Sept | 16 | 7 | 0.44 | 0.9 | South (onshore) | Prudhoe Bay |
| 29 Aug | 19 Sept | 21 | 73 | 3.5 | 7.5 | East | Barter |
| 3 Sept | 11 Sept | 8 | 107 | 13.3 | 29.0 | West | Cape Simpson |
| 6 Sept | 9 Sept | 3 | 53 | 17.7 | 38.0 | West | Barrow |

I

DISTRIBUTION AND CHARACTER OF ICINGS IN
NORTHEASTERN ALASKA

Deborah Harden

Peter Barnes

Erk Reimnitz

Form of publication: 1) ERTS final report
2) Journal - Arctic

Abstract

An examination of the distribution of river icings seen ⁱⁿERTS-1 satellite imagery and high- and low-altitude aerial photography of Alaska's North Slope indicates these features are numerous and widespread east of the Colville River and rare to the west. Where icings occur, stream channels are wide and often form braided channels. Their distribution can be related to changes in stream gradient and to the occurrence of springs. Large icings, such as on the Kongakut River, often remain through the summer melt season to form the nucleus of icings in the succeeding winter. Major icings also are likely to have a profound influence on the nature of permafrost. The map of river icings may serve as a guide to the occurrence year-round flowing water, a sparse commodity in the area.

Introduction

Repetitive ERTS-1 imagery can be used for seasonal observations of river icings on a regional scale. Although the existence of icings on the North Slope of Alaska (Fig. 1) has been known for sometime (Leffingwell, 1919), regional mapping and seasonal monitoring have not been attempted. Here we present a study of the distribution, longevity and character of arctic river icings, and speculate on the causes, effects, and their importance to man's development in the region.

Icing refers to the process of progressive ice growth or accretion on a pre-existing ice surface. It is an imprecise term in that it is also used to designate many other phenomena of the Arctic. In reference to arctic rivers, it is used both as designating the processes of ice build up and for the actual body of ice thus formed. Equivalent terms are the Russian "naled" and the German "aufeis", both of which mean on or upon ice.

The type of icing we are concerned with here develops when water repeatedly or continuously emerges onto the land or ice surface during the winter at subfreezing temperatures, freezing in successive layers. Commonly this water may seep from the ground, a river or from a spring (Carey, 1973; Anisimova, 1973). Thus, icings may be classified genetically as ground-, river-, or spring-icings.

Russian studies (Anisimova, 1973) have shown that in some river basins in Northeastern Siberia icings (naleds) accumulate up to 25-30% of the annual volume or river flow and up to 60-80% of the subsurface drainage. Icings commonly year after year in the same locations, and

generally have the same morphologic character. River floodplains often are widened as spring flood waters are forced to flow around the periphery of the icing mounds. The size and location of icings is a function of 1) source discharge (stream, groundwater, or spring), 2) hydrostatic head, and 3) geologic setting.

Icings which appear to grow throughout the winter indicate perennial fresh water sources which might be used by man. Considering the present rapid development of the region, knowledge of the distribution and character of icings could have important implications. In addition, construction projects such as roads are effected by icings which are either naturally occurring or are induced by the construction activity (Anderson and others, 1973). Potentially, any alteration of a balanced hydrologic-permafrost-geologic regime may induce the formation of icing. In areas where icing areas extend to the coast, as in the Icy Reef area (Fig. 2), icings have a definite influence on the deltaic and coastal/marine processes.

BACKGROUND INFORMATION

The Northslope of Alaska falls into three major physiographic provinces (Wahrhaftig, 1965, and Figure 1): 1) the Arctic Coastal Plain, 2) the Arctic Foothills Province, and 3) the Brooks Range. The coastal plain is a broad, low-relief tundra surface with numerous lakes, that includes the deltas and meandering streams draining the higher terrain to the south. The Foothills Province is characterized by rolling terrain with some bluffs along the river courses. Most of the known springs occur in this province, and it is marked by an abrupt decrease in river gradients.

Both the Arctic Coastal Plain and the Foothills province narrow toward the east, where the Brooks Range approaches the coast near the Canadian boundary. The Brooks Range is the source for all of the northward flowing rivers.

The seasonal freeze-thaw cycle controls the development and dissipation of river ice in northern Alaska. All of the rivers of the north slope flow in the zone of continuous permafrost. River ice forms during mid- to late-September, after mean temperatures fall below freezing. By late December, when mean temperatures are below -20°C , river ice is commonly more than one meter thick. Ice continues to thicken to a maximum of about two meters until May, when temperatures rise above freezing and the melt season begins. During late May and early June, thawing proceeds rapidly, flow begins on top of river and sea ice, and eventually most of the river ice breaks up and flows downstream (Walker, 1974). During summer, temperatures are above freezing and streamflow is unimpeded by ice.

Two conditions must be met before an icing forms. First, there must be a source for water flowing beneath the initially frozen surface. Secondly, there must be a barrier to the flow of water which forces it to the surface. These barriers are commonly provided by the total freezing of the river cross section, permafrost formation, reduction in aquifer permeability due to permafrost, or outcrops of impermeable strata (Sokolov, 1973; Carey, 1973).

River icings develop after the formation of the seasonal ice cover (Carey, 1973). If water remains unfrozen below the ice cover - in the

stream channel or in an alluvial layer above the permafrost or bedrock - it will continue to flow as long as water is supplied to the system. If flow is sufficiently restricted, as by a sudden change in stream gradient, or by a decrease in the permeability or thickness of the channel fill, water will be forced upward over the river ice. Continuing or subsequent overflows will build sheets of fresh ice over the original icing. The total thickness may reach 5 to 6 meters under such conditions (Pewe, 1973; Williams, 1953, 1970). Icings can occur at several points along a river or only at isolated points.

METHODS

Imagery from the multi-spectral scanner (MSS) of the Earth Resources Technology Satellite - 1 (ERTS-1) was used to delineate icings on the North Slope of Alaska and adjacent areas of Canada. Our satellite coverage extends from the coast to about 200 km inland. Imagery was received from late July 1972 through the fall of 1973 except during the polar night (mid-October through late February). Thus, it was possible to monitor one seasonal cycle of river icing and to compare the extent of icing remnants during August and September of 1972 with those of 1973.

Successive coverage of the study area occurred at 18 day intervals. Overlap of successive images often provided three days of continuous coverage of a given location. However, since delineation of ground features is dependent on the absence of cloud cover, the frequency of our observations was often limited by weather conditions.

Each image covers an area approximately 100 nautical miles square at a scale of about 1:1,000,000. This scale enables us to clearly identify

icing patches larger than about 300 meters square. Smaller icings are discernable when high contrast of ice-tundra or water-snow scenes are imaged.

The scanner operates in four spectral bands: band 4, 500-600 nm (green), band 5, 600-700 nm (red), band 6, 700-800 nm (visible-near IR), and band 7, 800-1100 nm (near IR). One image is taken in each band for every satellite pass.

During the summer months, bands 4 and 5 show the greatest contrast between the icings, the unfrozen channels, and the surrounding tundra. On these images, icings appear white, channels and deltas are light-toned, and the higher ground a darker shade (Figs. 6a, d). During the winter, MSS band 7 shows the greatest contrast between the icings and the snow covered tundra and stream channels (Fig. 6b). In these images fresh ice or water appear dark, while the surrounding terrain is white, except where relief is sufficient to produce shadows.

Additional information was available from a high altitude U-2 flight of 21 June, 1974 (NASA Flight No. 74-101). This flight utilized a RC-10 camera with color infrared film at a flight altitude of 65,000 ft (19.9 km) on flight lines north and south over the Sagavaniktok River and east and west across the middle of the Arctic Coastal Plain.

DISTRIBUTION OF ICINGS

River icings detectable on ERTS-1 imagery during late winter are shown in Figure 2. The Colville River is the largest of the rivers in the study area. In a cursory analysis of imagery of rivers west of, and including the lower Colville, almost no icings were identified, with the

exception of a distinct icing along the Ikpikpuk River ($\sim 155^{\circ}$ W long.), about 40 km from the coast.

East of the Colville River, most of the larger streams between the Anaktuvuk and Firth Rivers show icings in the foothills province. The larger deltas also commonly show icings. Fewest icings occur in the reaches between the foothills and the river mouths.

The downstream ends of icings are more diffuse and feather-like, presumably because surface flow continues downstream for varying distances after initial overflow. These downstream tails may extend for considerable distances and connect icing patches. For instance, the Canning River shows almost continuous icing from the Brooks Range to within about 10 km of its mouth (Figs. 2 and 3).

The distribution of icings shows good correlation with that of the shallow reaches of braided streams (Figs. 1 and 2). However, whether icings are the cause or the result of the braiding is not clear. During summer, the elevated surfaces of icing remnants may be obstacles to stream flow, causing diversion of channels around ice patches. On the other hand, low altitude aerial photos show channels dissecting icing patches during spring flooding (Fig. 4).

A comparison of known perennial springs (Childers et al., 1973) with the sites of river icings shows that all of the springs correspond with locations of icing deposits (Figs. 1 and 2). Icings may indicate other unmapped springs, especially in areas with no apparent upstream water sources (Williams and Van Everdingen, 1973). Presumably, perennially flowing springs would exist at or upstream from such icings.

DEVELOPMENT OF ICINGS

ERTS imagery from mid-September to the shut-off of the cameras for the arctic night in late October 1972, does not show new icing development. Many rivers were still flowing at this time indicating that the basic requirements for an initial ice cover and water flow barrier had not yet been met.

During the period from the first 1973 imagery in early March until spring break-up in June, many icings increased in size. However, some were apparently unchanged throughout this part of winter, indicating that their water sources may have been cut off or frozen prior to March.

During the first week of August, 1973, weather conditions permitted continuous coverage of most of the study area. At this time, remnants of most of the larger icings are visible (for example .1376-21112, 1378-21164, 3 & 5 August). There are considerably less extensive than the winter icings, and some undoubtedly melted before autumn freeze-up. The largest icings of the previous winter, such as on the Kongakut-Sagayaniktok and Canning Rivers, still had remnants in September (for example 1410-20533, 1414-21162). It is probable that these large icings do remain for more than one season under favorable conditions. Perennial icing should promote a perturbation in the permafrost regime by lowering summer temperature. This would seemingly promote the development of icings in the following winter. In this sense long-lived icings may be self-perpetuating.

ICINGS ON THE KONGAKUT RIVER

The delta of the Kongakut River (Kangikat on some charts) located in

the Arctic Wildlife Refuge (Fig. 2), repeatedly came to our attention as we studied icings. Icings on this river are particularly spectacular and long lived. The delta ice buildup commonly extends into the lagoon seaward of the delta front and out to Icy Reef. This interaction of river icings with the marine environment and delta front is unique along the Alaskan coastline.

Icy Reef was named by the Franklin expedition in August 1826, when heavy ice outside the reef necessitated dragging boats over the mudflats at the mouth of the Kongakut River to Beaufort Lagoon (Leffingwell, 1919). Leffingwell's description thus indicates that the name did not result from the extension of icings afeis into the lagoon.

Icings on the delta were present throughout the year of our ERTS-image coverage (Figs. 5 and 6). During the winter of 1972/73 the icings increased in size (Fig. 5c & d) starting sometime after September and continuing through March, 1973, (April and May imagery were cloudy). With the start of the thaw season in late May and continuing to late August the icings decreased in size, undergoing about a 10 fold change in areal extent (Figs. 5e, f, g, h, and 6c & d). It appears that the extent of the icing was essentially unchanged from mid-August to mid-September, 1973 (Figs. 5a, b, h, i).

During the winter of 1973 the icing extended into the lagoon in front of the delta (Figs. 5c & d; 6b). An image obtained about two weeks after the initiation of river flow (Figs. 5e and 6c), indicates that icing deposits remained in the lagoon through the flooding period. Field observations during August 1972 and September 1973 as well as the ERTS

imagery shown in Figures 5g, h, i and 6a, d reveal no ice present in the lagoon during these periods. However, during field operations in late August of 1971 we observed ice in the lagoon behind Icy Reef and according to the Coast Pilot (1964) ice is commonly present in the lagoon behind Icy Reef throughout the summer.

In trying to explain the lagoon ice seen in 1971 and reported in the Coast Pilot, we considered that the coastline may have retreated very recently off the Kongakut River, and that permafrost may be near the surface in the lagoon, thereby enhancing the summer occurrence of ice by lowering the water temperature regime in the lagoon. A comparison of Leffingwell's (1919) map of the coastline, which is quite accurate in most areas, with the modern maps, suggested such a drastic retreat of the coastline over a period of about 35 years. However, further investigations of aerial photography taken during the past 20 years and modern coverage reveal that the early maps are in error and that the coastline is rather stable.

It has become apparent from the study of ERTS imagery that the river icing process is an important factor influencing the marine processes along the delta front of the Kongakut River. A comparison of 1972 and 1973 imagery in mid-August and early September shows little difference in the size of the Kongakut River icing, although channel patterns through it are somewhat different (Figs. 5a, b; 6h, i). In following years of favorable icing formation, the lagoon in front of the delta remains ice covered through the summer. The fact that icings on the delta last through the summer make them the logical loci for the formation of icing of the succeeding winter.

CLIMATE AND ICINGS

In order to assess the effect of weather conditions on the size of icings, monthly rainfall and snow accumulation data for the nearest weather station (Barter Island) were analyzed for 1971, 1972 and 1973 (U.S. Dept. Commerce, 1971-1973).

Heavy summer precipitation would presumably favor icing development during the following winter by creating an abundant ground water supply. In contrast, the insulating effect of heavy snowfall during the early winter would decrease the growth rate of river ice cover, thus producing unfavorable icing conditions. Heavy snow cover late in the winter may extend the period of icing activity by preserving lower temperatures in the ground, but according to Carey (1973), this insulating effect is less important than rain and snow conditions during the preceding summer and early winter.

During the two seasons studied, the influence of varied summer precipitation was apparently balanced by differing with snowfall conditions. Precipitation was much greater than average during the summer of 1971 and below average for the following summer season. Groundwater conditions would therefore have been more favorable for icing development during the winter of 1971-72 than in the following winter. On the other hand, snowfall was heavier during early winter 1971 than during the same period of 1972, which would insulate the ground and lead to less favorable icing conditions in 1971-72. Opposing this effect is the fact that snowfall during late winter was greater in 1972 than in 1973, a condition that is more favorable to 1971-72 icing.

Due to the contrasting and balancing climatic influences during 1971-1973, it is not possible to evaluate the impact of climate on icing growth with our present information. Our data suggest that there appears to be no significant difference in the amount of icings during the two summers of ERTS observations (Figs. 5b, i; 6a, d). In order to assess the variability in weather and icing conditions, several more seasons would have to be studied.

DISCUSSION AND CONCLUSIONS

Icings on the North Slope of Alaska are widespread, but are concentrated east of the Colville River, at the heads of deltas, and where streams leave confined mountain channels. The Colville River has few icings and virtually none along the lower two thirds of its course. One might assume that there is continuous flow along the channel under the ice with the flow discharging into the sea. The work of Walker and others (Arhborg and others, 1966; Walker, 1974) has shown that there probably is a sub-ice channel that extends to the sea, even at the maximum ice growth. However, Walker's work also shows that highly saline water occurs below the ice covering along the channel thalweg from the delta front upstream for 60 km. This would suggest that either there is no continuous source of water in the drainage basin of this large system, or that the river flow is so greatly reduced in volume and force that it can be accommodated in a thin layer between the ice and the intruding salt water wedge. The lack of springs along this river (Fig. 1) suggest that there may be virtually no winter fresh water flow in the Colville River system. This would be significant in any search for a year round water supply.

In pumping from a river with little or no winter recharge, the fresh water in the stream could easily be depleted to a point where salt water is encountered. Pumping for the Prudhoe Bay Complex on the Sagavaniktok River, which has numerous icings (Fig. 2), indicating year-round water recharge, has already forced overwintering river fish to retreat to isolated pockets within the river bed.

Icings influence the ground temperature and permafrost in such a way as to encourage the repeated development of icings in the same locations. The presence of icings into the long summer days when ground temperatures are revised and surficial thaw layer is formed, would cause a change in the albedo of the icing area, reflecting much of the incoming solar energy. Therefore, ground temperatures would be lower and/or the active layer above the permafrost thinner. This in turn would enhance an icing development in the same area during the following freeze season, as a permafrost barrier would tend to form at these locations first.

The morphology of the stream where icings occur in some instances may be shaped by icings. Under some conditions major portions of the spring-flood waters initially are forced to detour around icings, widening the stream banks in icing areas. Thus most of the braided sections of streams and rivers shown in Figures 1 and 2 are probably the location of recent or present day icings.

Icing on the deltas appear to be readily dissected by the seasonal river flow (Fig. 4). There appears to be sufficient depth in the flood, to overtop the icing, such that the water flow seeks low areas within the icing, which then form the forerunners of the channels dissections.

Icings which extend into the lagoon off the delta of the Kongakut River are bounded on the seaward side by Icy Reef, a barrier beach (Figs. 5 and 6). The new lagoon ice is floating at the beginning of the winter. It is depressed by the load of icing tails to where it rests on the bottom. Subsequently, there must be a mound of ice covering the delta and lagoon. During the flooding of the river, water flowing over this mound will bypass the delta and lagoon to beyond the barrier island. Since most of the river sediment load is carried at this time (Walker, 1974) the sediments will also bypass the delta and lagoon.

During the glacial episodes along the arctic coast of Alaska, the icing environment must have been quite different. The climate was colder and dryer (Hopkins, 1967), thus less surface water would be available, the flow season would be shorter, and the depth of winter freeze more severe. Icings of the type seen in the Arctic today would probably be more widespread at lower latitudes. However, icings along the arctic coast would be concentrated in areas where thermal springs are found today. River icings along the Alaskan Arctic coast would probably be more widespread due to the shorter thaw season and the greater probability that icings would last from one year to the next.

The map of icings (Fig. 2) also is a map of fresh water sources for potential utilization by man. The map may also serve as a guide in the planning of future construction activities, which might interact with the hydrologic regime to create potential problems. To the biologist icing locations are overwinterizing sites for some fish species (Childers and others, 1973). The relative absence of icings west of the Colville River

is a phenomena that suggests limited water resources or extensive un-
impeded groundwater flow. Considering the importance of a water supply
in the arctic this should be investigated.

CONCLUSIONS

1. Icings on the North Slope of Alaska are widespread, but are concentrated east of the Colville River, primarily at the heads of deltas, and where the streams leave the confined mountain channels.
2. Some of the larger icings can last through the summer melt season, to form the nucleus of the following years icing growth, although channels may dissect the icings.
3. It appears that the summer flow of the streams, in forming shallow braided channels and delta head distributaries, are forerunners to the formation of icings in these areas.
4. Some icings are, and others may be, the loci of groundwater discharge in the form of springs. They are thus potential sources of year-round fresh water for man's activities.
5. Precipitation patterns should have an effect on icing patterns; however, the major controlling climatic factors tended to cancel each other in the two years studied and the influence is, as yet, unknown.

REFERENCES .

- Anderson, D. M., H. L. McKin, W. K. Crowder, R. K. Haugen,
L. W. Gatton, and T. L. Marljar, 1973, Applications of ERTS-1
imagery to terrestrial and marine environmental analysis in
Alaska; in Third ERTS-1 Symposium, v. 1 Section B, NASA,
Goddard Space Flight Center, Washington, D. C., p. 1575-1605.
- Anisimova, N. P. and others, 1973, Ground water in the cryolitho-
sphere; Akademiya Nauk SSSR Sektisiya Nauk o Zemle, Sibirskoye,
II Mezhdunarodnaya Konferentsiya po Merzlotovedeniyu (USSR
Academy of Sciences, Earth Sciences section, Siberian Branch,
Second International Conference on Permafrost), Lectures and
Reports, No. 5, Yakutsk Book Publishing Co., Yakutsk, USSR,
172 p.
- Arnborg, Lennart, Walker, H. J., Peippo, Johan, 1966, Water discharge
in the Colville River Alaska, 1962, Geografiska Annaler,
v. 48, ser. A, p. 195-210.
- Carey, K. L., 1973, Icings developed from surface water and ground
water; Cold Regions Science and Engineering Monography III-D3,
U.S. Army Cold Regions Research and Engineering Laboratory,
Hanover, New Hampshire, 65 p.
- Childers, J. M., C. E. Sloan, and J. P. Meckel, 1973, Hydrologic
reconnaissance of streams and springs in eastern Brooks Range,
Alaska - July 1972; U.S. Geological Survey, Water Resources
Division, Basin-Data Report, Anchorage, Alaska, 25 p.

- Hopkins, D. M., 1967, The Cenozoic History of Beringia - A synthesis; in D. M. Hopkins, ed., The Bering Land Bridge; Stanford University Press, Stanford, CA. p. 451-484.
- Leffingwell, E. DeK., 1919, The Canning River region, northern Alaska, U.S. Geological Survey Prof. Paper 109, 251 p.
- Lewis, C. R., 1962, Icing mound on the Sadlerochit River, Alaska; Arctic, v. 15, p. 145-150.
- Pewe, T. L., 1973, Permafrost conference in Siberia; Geotimes, v. 18, no. 12, December, p. 23-26.
- Sokolov, B. L., 1973, Regime of Naleds; in Anisimova, N.P., Ground water in the cryolithosphere; p. 98-106.
- Wahrhaftig, Clyde, 1965, Physiographic divisions of Alaska: U.S. Geological Survey, Prof. Paper 482, 52 p.
- Walker, H. J., 1974, The Colville River and the Beaufort Sea: some interactions; in The Coast and Shelf of the Beaufort Sea, Reed, J. C., and Sater, J. E., eds., Arctic Institute of North America, Arlington, Virginia, p. 513-540.
- Williams, J. R., 1953, Icings in Alaska, 1949-1950; Engineering Intelligence Division, Engineering Notes No. 32, 23 p.
- Williams, J. R., 1970, Groundwater in permafrost regions of Alaska; U.S. Geological Survey Prof. Paper 696.
- Williams, J. R., and van Everdingen, R. O., 1973, Groundwater investigations in permafrost regions of North America; a review, in North American contribution, Permafrost, Second International Conference, National Academy of Sciences, Washington, D.C., p. 435-446.

U.S. Department of Commerce, 1964, United States Coast Pilot 9, Pacific and Arctic coasts, Alaska, Cape Spencer to Beaufort Sea,

U.S. Government Printing Office, p. 285.

U.S. Department of Commerce, 1971, 1972, 1973, Local Climatological Data, Annual Summary, Barter Island, Alaska, U.S. Department of Commerce, National Climatic Center, Asheville, N.C., 4 p.

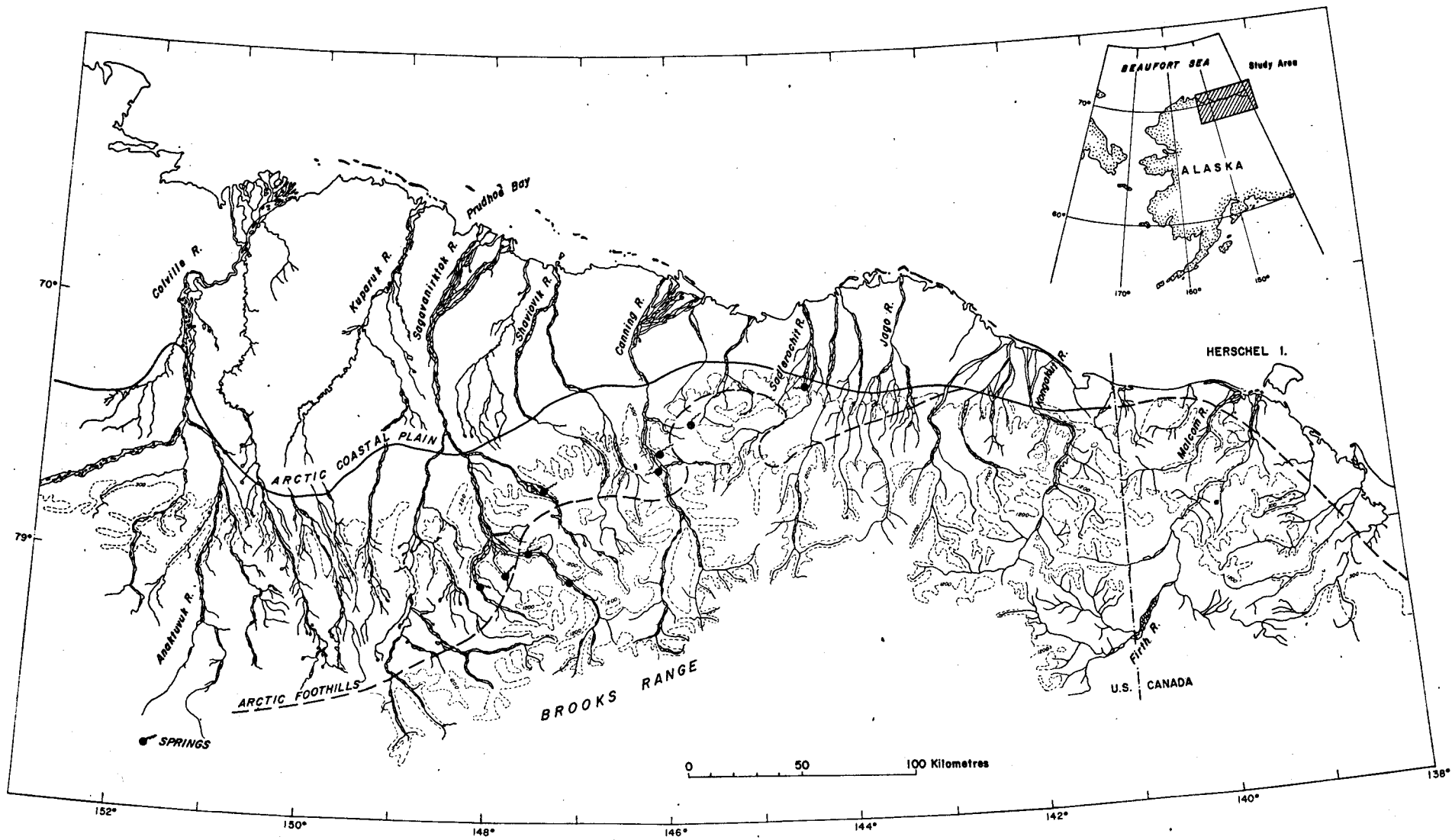


Figure 1. Location map showing physiographic provinces and stream patterns.

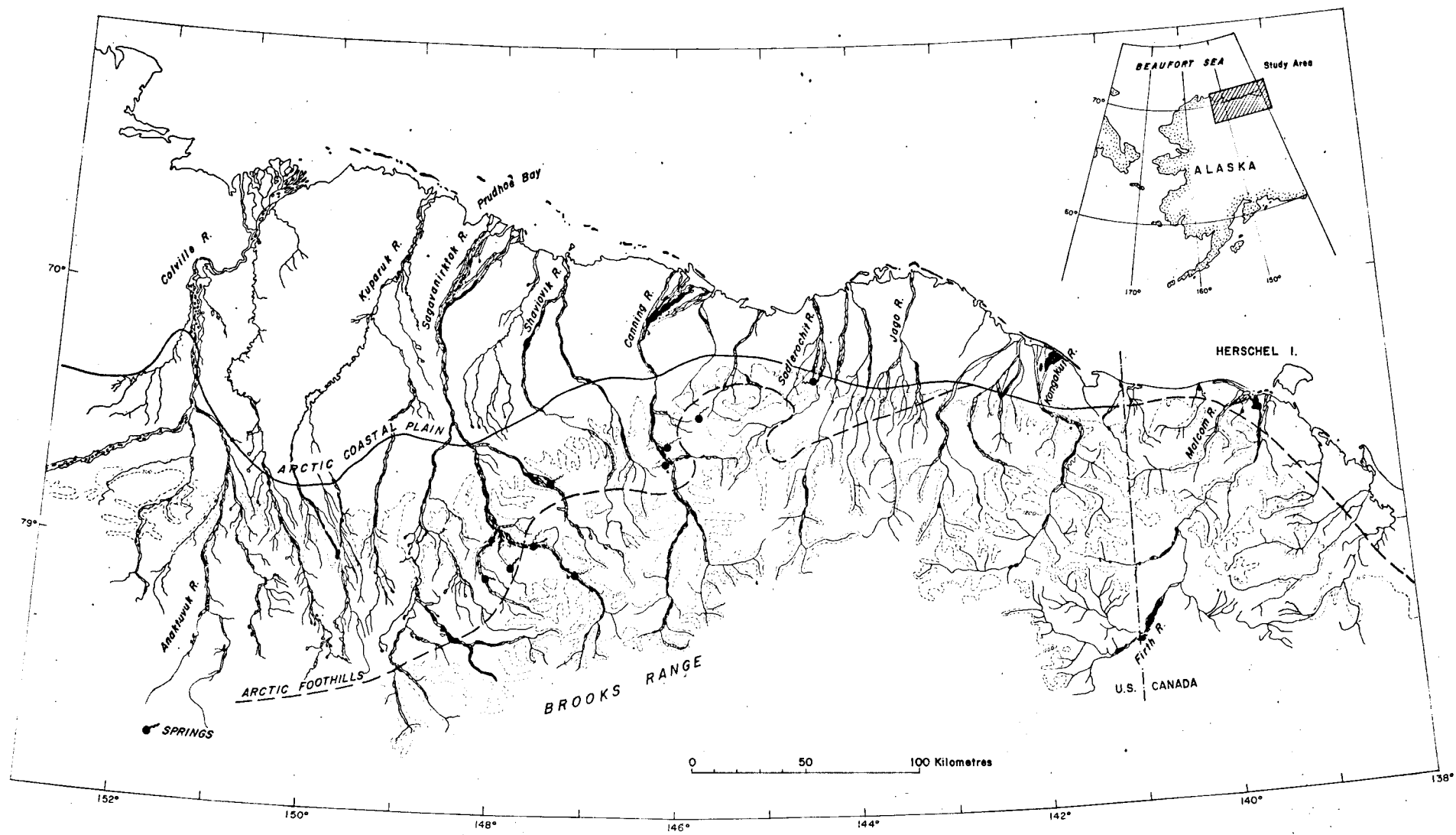


Figure 2. Distribution of icings in northeastern Alaska from ERTS

imagery.

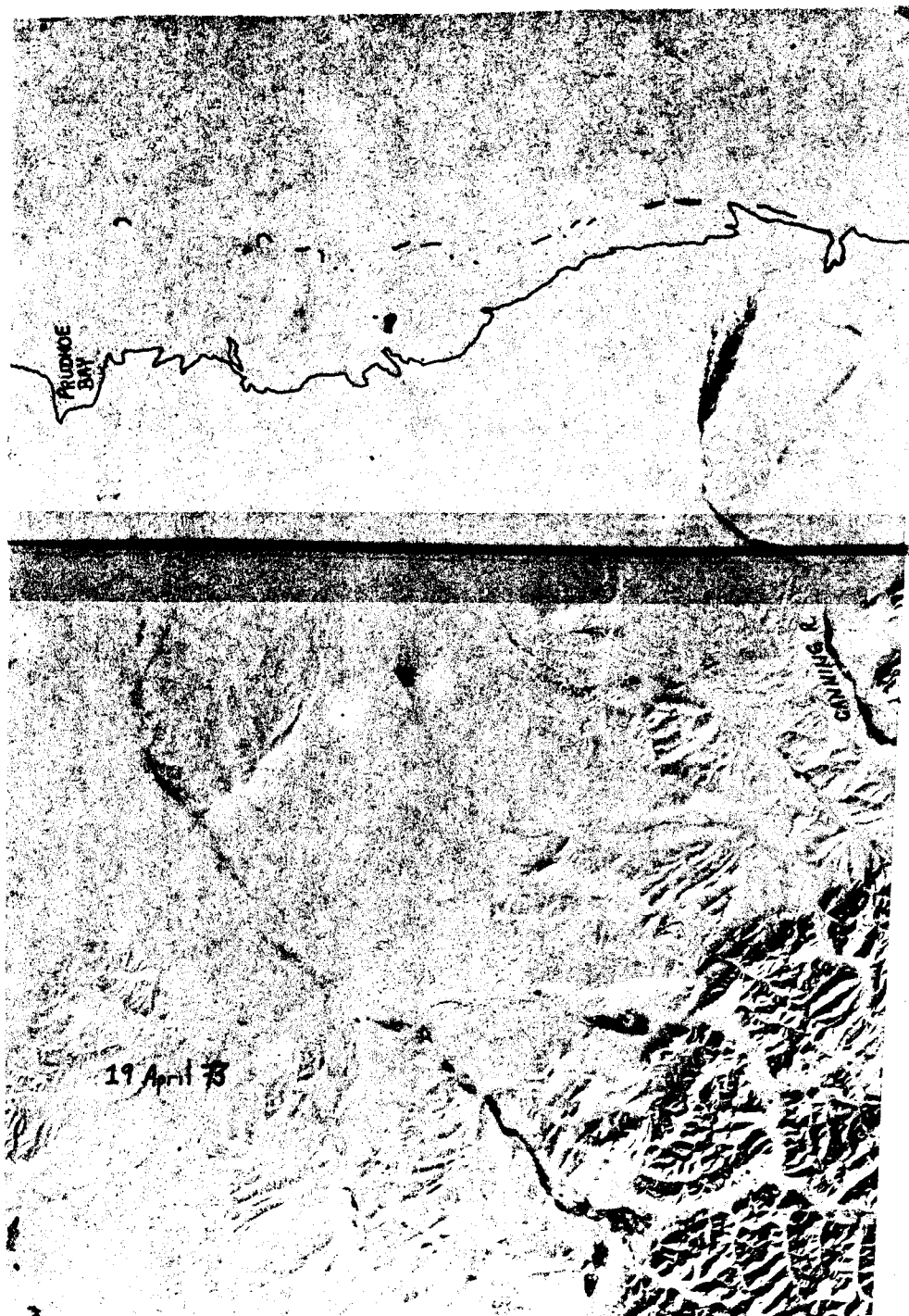


Figure 3. Icings on lower Canning and Sagavanirktok Rivers on April 19, 1973. ERTS imagery ID nos. 1270-21175 and 1270-21181. 622

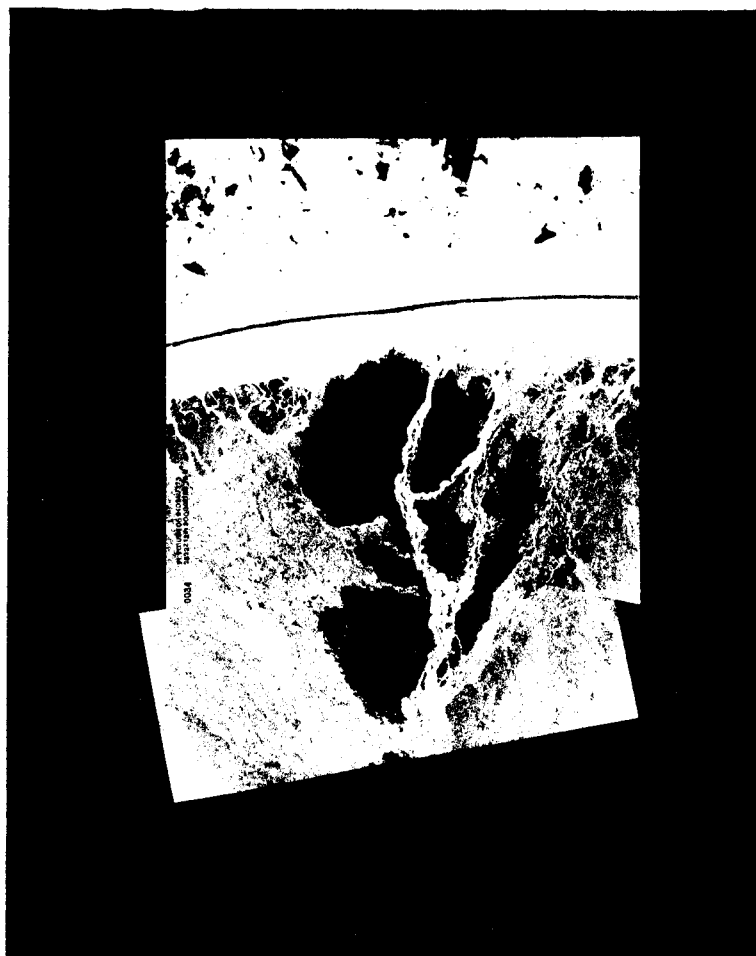


Figure 4. Icing on Kongakut River Delta, near Canadian/Alaskan boundary (Fig. 5). The name "Icy Reef" may be related to the fact that the lagoon in some summers remains ice covered. (Photo courtesy by Andrew Short, L.S.U., Inst. of Coastal Studies).

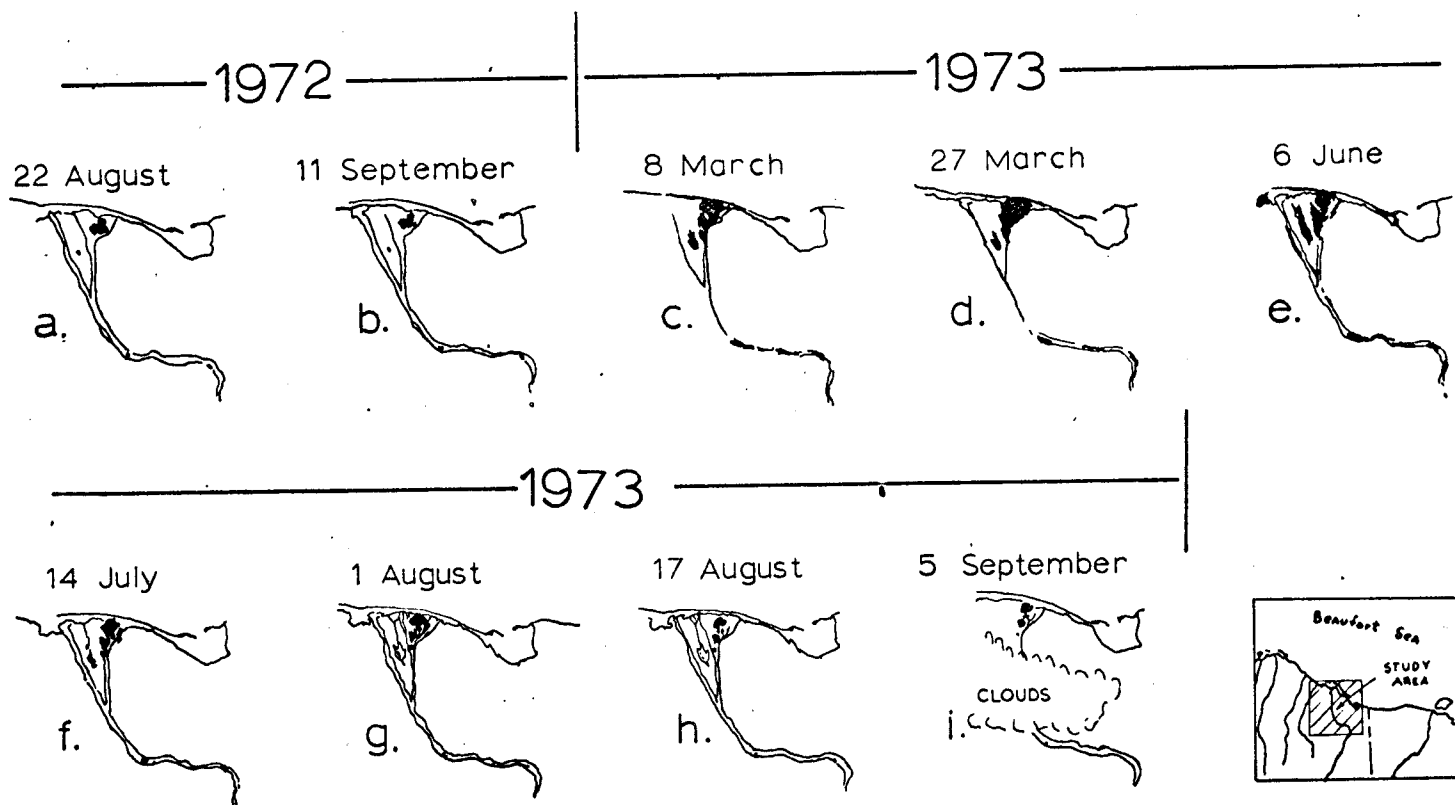


Figure 5. Development and decay of the delta and lagoon icing on the Kongakut River Delta. Data from ERTS imagery ID nos.:
 .1038-20424, 1050-20541, 1228-20435, 1247-20493, 1318-20426,
 1356-20542, 1374-20541, 1390-20423, 1409-20475.

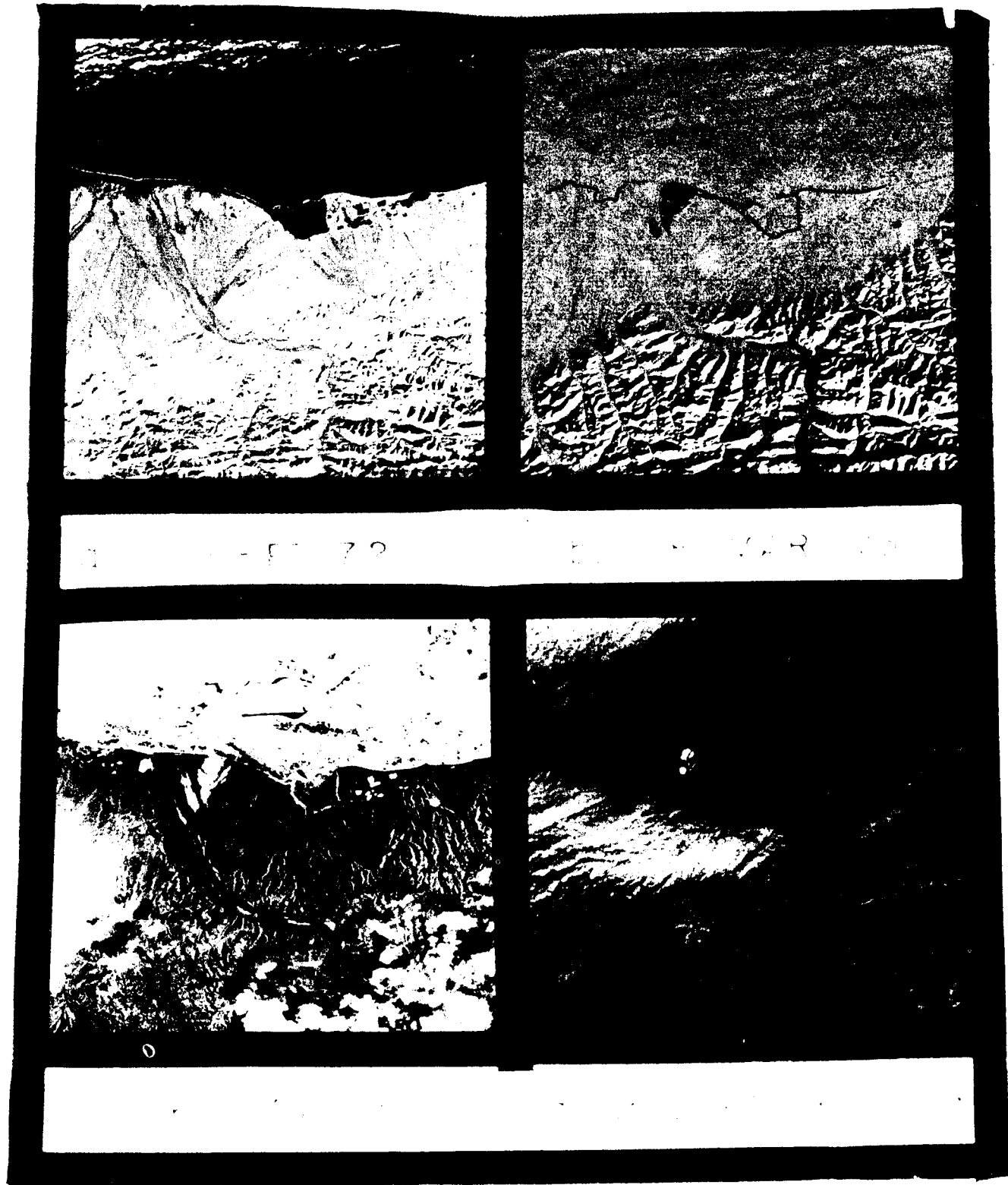


Figure 6. Comparative ERTS imagery of the icing on the Kongakut River Delta, September 1972 through September 1973.

ERTS Imagery nos. 1050-20541, 1078-20435, 1318-20476,
1409-20475.

J

A "HERRING-BONE" PATTERN OF POSSIBLE
TAYLOR-GÖRTER-TYPE FLOW ORIGIN SEEN IN SONOGRAPHS

by

Lawrence J. Toimil and Erk Reimnitz, U.S. Geological Survey,
345 Middlefield Road, Menlo Park, California 94025

ABSTRACT

The potential usefulness of side-scan sonar in detailed studies of helical flow phenomena is indicated by records obtained within a shallow Arctic lagoon. The records reveal a "herring-bone" - like pattern of current aligned linear reflectors with branching diagonals. Major longitudinal reflectors have no detectable relief and are believed to represent current-aligned, winnowed zones of the lagoon's silty fine sand. The winnowing processes are interpreted to occur along regions of helical cell divergence, suggesting a three-dimensional Taylor-Görter flow origin.

INTRODUCTION

Large scale "herring-bone" patterns were observed with side-scan sonar on the floor of a shallow, Arctic lagoon. The patterns strongly suggest an origin by a helical flow system of the Taylor-Görter type. Such three-dimensional flow also referred to as Langmuir circulation, has been described by Allen (1968) as consisting of an array of pairs of oppositely rotating helical spiral vortices, whose axes lie parallel to the direction of primary (net) flow. Depositional features ascribed to such flow have been observed in subaerial, intertidal and abyssal environments, but apparently not in lagoonal environments at such scale or definition as observed in our sonographs.

REGIONAL SETTING

The pattern was found in the shallow eastern part of "Leffingwell Lagoon", here named in honor of E. de K. Leffingwell, a pioneer geologist who studied this part of Arctic Alaska. The lagoon is located 90 km east of Prudhoe Bay, and is separated from the Beaufort Sea by Flaxman Island (Fig. 1).

The island is a remnant of the inundated coastal plain, and is marked by tundra capped bluffs up to 7 m in height. Both the island and the mainland shore are retreating by erosion (Lewellen, 1970) except near the very eastern end of the lagoon, where a small distributary of the Canning River is discharging, building extensive shoals (Fig. 1). Bathymetric contours shown in Figure 1 are based on U.S. Coast and Geodetic Survey smooth sheets nos. 7851 and 7852. A major inlet east of the island connects the lagoon and the open sea. The only analyzed

sediment sample collected in the shallow eastern part of the lagoon, consists of silty fine sand (mean dia. 0.125 mm).

Ice plays a dominant role in the lagoon's environment. It starts forming in late September, attains a maximum thickness of 2 m by April-May, and breaks up in late June. The ice canopy rises and falls throughout the winter. These fluctuations are related to small astronomical tides (< .5 m) and to more significant meteorologic tides, which during westerly summer storms can exceed +3 m (Reimnitz et al., 1972), and with easterly winds reach -1 m. Such fluctuations cause cracking of the ice and periodic adfreezing of sediments to the underside of the ice landward of the 2 m depth contour, as described by Barnes and Reimnitz (1974). They also suggested that flow constriction during the late stages of ice growth results in intensified currents landward of the 2 m isobath, possibly resulting in winnowing and transport of sediments to beyond the 2 m depth contour.

ERTS-1 satellite imagery of June 12, 1973 indicates that the Canning River flooded the lagoon ice as far west as the central part of Flaxman Island. This arctic phenomenon and associated processes and results have been described by Reimnitz and Bruder (1972), Reimnitz et al., (1974), Walker (1974), Barnes and Reimnitz (1974) and Reimnitz and Barnes (1974). The flooding proceeds to its maximum extent within about 2 days. Initially, the floodwaters depress the floating portion of the ice canopy seaward of the 2 m depth contour, rapidly displacing large volumes of water below. The river water subsequently drains at holes and cracks, i.e. strudel (Reimnitz and Bruder, 1972), and flows seaward

under the floating ice. During this period the cross section for flow is greatly reduced by the presence of ice in the shallow lagoon.

Starting about mid-July, the lagoon is ice free and its sediments subjected to reworking by wind generated waves and currents. Fetch is limited for all but westerly winds, which generally result in a raised sea level. Eight days prior to our survey of September 5, 1975, westerly winds of more than 20 m/sec were recorded at Barter Island, located 42 km east of the study area (N.O.A.A. Climatological Data, v. 61, no. 7). Winds remained westerly for the next six days with average speeds less than 6 m/sec. Light northerly winds were recorded during the survey.

METHODS

Side-scan sonar and precision fathometer records were obtained concurrently along the track lines shown in Figure 1. The survey was carried out aboard the U.S. Geological Survey's R/V KARLUK. The side-scan sonar transmits short bursts of high frequency (105 kHz) sound in fan-shaped beams on each side of the survey track. The return echoes, when processed and graphically recorded, produce an acoustic picture (sonograph) of the seabed, detailing morphology and spatial distributions not delineated by fathometers (Belderson et al., 1972). In the sonographs the distance parallel to the ship's track (length) is dependent on ship's speed and rate of paper advance. Across the record (width) the scale is fixed for a given scan angle. In the records shown (Figs. 2 and 4a) the width scale is exaggerated relative to the length scale by a factor of 2.0.

The fathometer employed an 8°-cone-angle, 200-kHz transducer capable of resolving bottom relief of about 20 cm. Direct observations of the seabed were made by underwater TV with video tape recorder. Navigation during the survey was based on radar ranges and considered accurate to within 200 m.

DESCRIPTION OF RESULTS

Alternating light and dark, irregular, roughly parallel bands were observed on the sonographs in water shallower than 2.5 m in the eastern part of the lagoon (Fig. 2). The dark lineations represent zones where seafloor reflections are strong relative to those from the intervening bottom. The zones lie approximately parallel to 85° - 265° T and trend toward 50° - 230° T near the lagoon's eastern inlet (Fig. 1). No detectable relief was associated with the lineations on either the side-scan sonar or fathometer records. The vertical line across the right hand portion of Figure 2 marks a 70° easterly course change. During the turn individual lineations can be followed into a more complex pattern revealed in sonographs along a course more nearly parallel to their dominant trend (Fig. 4a). Viewed from this course the spacing of bands is slightly expanded relative to that of the oblique crossing due to scale (width) exaggeration. In this orientation one can clearly discern that minor reflectors, spaced 1 to 3 m apart, branch off from the major longitudinal reflectors, which are spaced between 6 and 8 m apart at angles between 35° and 50° forming a herring-bone pattern. One can also see that the major longitudinal reflectors commonly bifurcated forming 30° to 48° angles opening to the east.

By lowering a TV camera from the vessel while it was drifting in this area (Fig. 1) we saw symmetric sand ripples, too small to show on the sonographs. The ripple crests trend north-south, with wave lengths of 6 to 8 cm and heights of 1 to 2 cm. The ripples were considerably disturbed by bioturbation and contained some organic debris in the troughs. Perhaps, 0.5 cm, thick, suspension layer locally covered the entire sea floor. Bottom sediment collected during these observations consisted of silty fine sand. Figure 1 [Figure 1] illustrates representative orientation^s of the small scale ripple crests along the track surveyed.

DISCUSSION AND CONCLUSIONS

Comparing the sonographs with the TV images and with the fathograms, we find that the herring-bone pattern has no detectable (< 20 cm) relief. Newton and Stefanon (1975) have shown that subtle differences in sediment grain sizes (between muddy and washed sand) with no associated relief were clearly defined in sonographs obtained with a system identical to that used in our survey. We suggest that the dark linear reflectors in our sonographs similarly represent coarse fractions winnowed from the fine silty sand covering the lagoon floor. The fact that winnowed zones were not observed with the TV camera may be due to their being partly masked by suspended matter, and^{also} due to inadequate resolution with this tool.

The direction of primary flow in the study area, inferred from the configuration of the lagoon and the location of the tidal inlet and river input are plotted in figure 1 and are found to be nearly parallel to representative orientations of the major lineations.

Current aligned bedform patterns similar to those seen in our sonographs have been attributed to secondary Taylor-Görtler type flow (Karcz, 1967; Houbolt, 1968; Hanna, 1969; and Hollister et al., 1974). Secondary flow of this type has been described by Karcz (1967) as "flow which has been split into a series of longitudinal vortex tubes with an alternating sense of rotation. The individual flow filaments advance helically, and the kinematic picture of the flow is that of a system of arrays of spiral flow threads" (Fig. 3). Bedforms resulting from such flow characteristically exhibit current parallel lineations which commonly bifurcate in the up-current direction, forming tuning fork junctions similar to those seen in our sonographs (Fig. 4a) (Folk, 1971). It has also been shown that the major longitudinal bedforms frequently have superimposed small-scale ripples trending transverse to the direction of primary flow (van Straaten, 1951; Karcz, 1967). In some cases, secondary current produced bedforms branch obliquely from major longitudinal features in herring-bone patterns, as observed by Hollister (1974) and Folk (1971). These secondary bedforms apparently lie transverse to the skin-friction lines of the flow system, as illustrated by Allen (1968) and shown in Figure 3.

The characteristic bedform patterns attributed to three-dimensional helical flow regimes discussed above are strikingly similar to those seen in our sonographs. Using the pattern from figure 4a as a base, and assuming that (1) the major longitudinal lineations represent erosional zones corresponding with flow divergence at the sea floor;

(2) the minor diagonal lineations lie transverse to the skin-friction lines of a secondary flow system (Fig. 3); and (3) the tuning fork junctions open upcurrent, a near-bottom flow regime may be interpreted. Such an interpretation is shown in Figure 4b. We pointed out that assumption (2) implies that the minor diagonal lineations are associated with some relief, which we did not detect. An alternative possibility is that they represent winnowed zones parallel to the skin-friction lines of the secondary flow system and result from a tertiary flow regime. Such a tertiary regime would imply a more complex flow pattern than previously thought.

While the interpretation of the minor diagonal lineations remains questionable, we believe it is reasonable to assume that Taylor-Görtler type flow is responsible for the formation of the pattern observed in our study. The factors producing the flow itself are still unanswered. Sonographs obtained in 1973 indicate a similar pattern in the same areas and depths, which implies a permanence or recurrence of the pattern. It may be significant that the pattern is only apparent in areas shallow than 2.5 m, where the constriction and intensification of flow by an ice cover can be expected [~~under several different conditions~~]. However, it must be noted that the strong westerly winds recorded prior to our survey are likely to have generated waves and currents capable of considerable reworking of the surficial sediments and it may be that the helical flow was produced by such currents in an ice-free lagoon.

One of the alternative routes for a proposed gas line to Canada crosses the study area. The possibility that under-ice processes, so

poorly known in the shallow lagoons of the Arctic, re-distribute sediments, points to the need for detailed studies in this environment. We feel that the spacial distributions resolvable using side-scan sonar will prove useful in these studies and future studies of bedforms and sediment distribution patterns of helical flow origin.

ACKNOWLEDGMENTS

We wish to thank A. Sallenger who was very helpful in formulating our thoughts for this report and R. Hunter and H. E. Clifton of the U. S. Geological Survey for reviewing the manuscript.

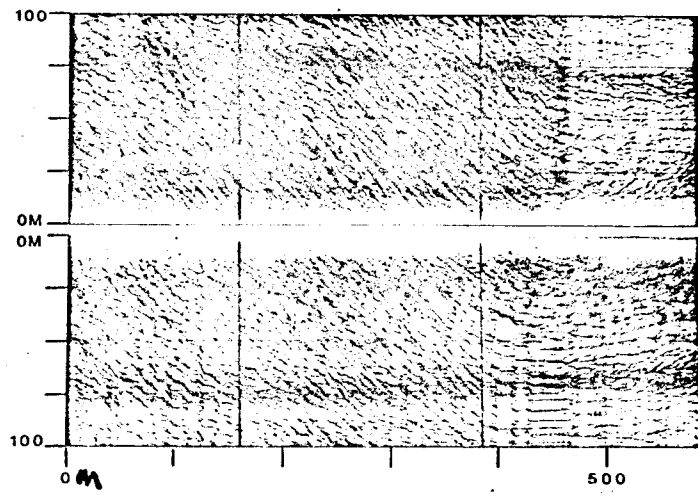
FIGURE CAPTIONS

- Figure 1. Chart of Leffingwell Lagoon showing track lines, inferred trend of primary flow, and representative orientations of major lineations and small scale ripple crests.
- Figure 2. Side-scan sonar record obtained oblique to trend of major lineations. The dark bands paralleling the ship's track near the outer margin of each channel of the sonographs presented are reflections from the ship's wake. Individual reflectors may be traced through a 70° course change marked by vertical line on the right.
- Figure 3. Vortices of Taylor-Görtler type flow and skin-friction vectors associated with such flow, modified from Allen (1968). Regions of helical cell convergence and divergence are indicated respectively by broken and solid black bands.
- Figure 4. A. Side-scan sonar record taken on a course nearly parallel to trend of major lineations revealing "Herring-Bone" pattern and "Tuning-fork" junctions.
B. Line drawing of major and minor lineations seen in figure 4a showing interpreted secondary flow vectors and zones of implied helical cell divergence (solid black bands) and convergence (broken black bands).

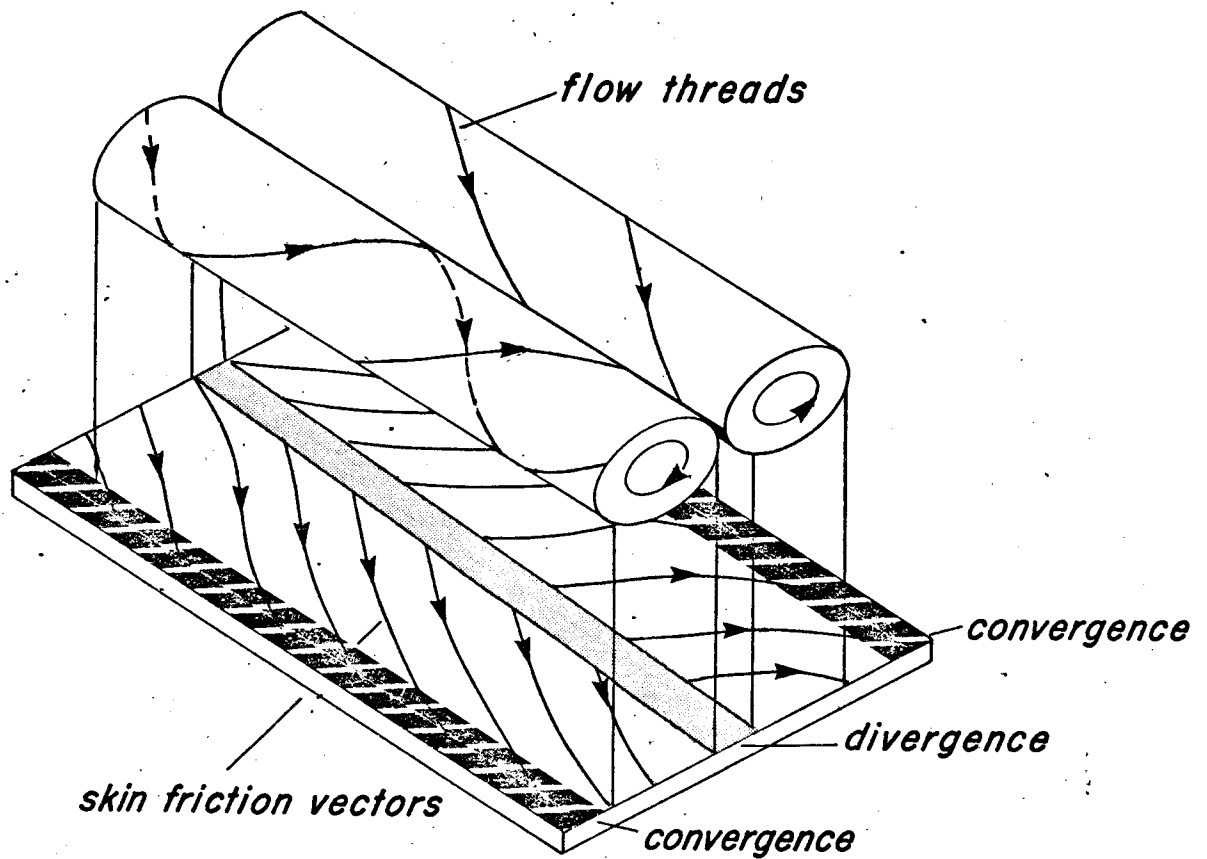
REFERENCES CITED

- Allen, J. R. L., 1968, The nature and origin of bedform hierarchies, sedimentology; Elsevier Publishing Company, Amsterdam in the Netherlands (10) 1968, pp. 161-182.
- Barnes, P. W., and Reimnitz, Erk, 1974, Sedimentary processes on Arctic Shelves off the northern coast of Alaska; in the coast and shelf of the Beaufort Sea. Proceedings of the Arctic Institute of North American Symposium on Beaufort Sea Coast and Shelf Research. Arlington, Va., Arctic Institute of North America.
- Belderson, R. H., Kenyon, N. H., Stride, A. H., and Stubbs, A. R., 1972, Sonographs of the Sea Floor: A Picture Atlas, Elsevier Publishing Company, New York.
- Folk, R. L., 1971, Genesis of Longitudinal and Oghurd Dunes Elucidated by ^oRelling upon Grease, Geol. Soc. of America Bulletin, v. 82. p. 245-273.
- Hanna, S. R., 1969, The formation of longitudinal sand dunes by large helical eddies in the atmosphere: Jour. Applied Meterology, v. 8, p. 874-883.
- Houbolt, J. J. H. C., 1968, Recent sediments of the southern bight of the North Sea; Geologie en Mijnbouw, v. 47, p. 245-273.
- Hollister, D. C., Flood, R. D., Johnson, D. A., Lonsdale, P., and Southard, J. B., 1974, Abyssal furrows and hyberbolic echo traces on the Bahama Outer Ridge, Geology, v. 2, no. 8, p. 395-400.
- Karcz, Iaakov, 1967, Harrow marks, current aligned sedimentary structures, Jour. Geol., v. 76, p. 113-121.

- Lewellen, R. I., 1970, Permafrost erosion along the Beaufort Sea Coast, Private Publication, Geography and geology Dept., University of Denver, Denver, Colorado, 25 p.
- Newton, R. S., and Stefanon, A., 1975, Application of side-scan sonar in Marine Biology, Marine Biology by Springer-Verlag, 1975, v. 31, pp. 287-291.
- Reimnitz, E., and Bruder, K. F., 1972, River discharge into an ice covered ocean and related sediment dispersal, Beaufort Sea, Coast of Alaska: Geol. Soc. America Bull., v. 83, no. 3, p. 861-866.
- _____, Rodeick, C. A., and Wolf, S. C., 1974, Strudel Scour: A unique Arctic marine geologic phenomenon, Jour. of Sed. Petro., v. 44, no. 2, pp. 409-420.
- _____, and Barnes, P. W., 1974, Sea ice as a geologic agent on the Beaufort Sea shelf of Alaska, in The coast and shelf of the Beaufort Sea. Proceedings of the Arctic Institute of North American Symposium on Beaufort Sea Coast and Shelf Research. Arlington, V., Arctic Institute of North America, pp. 301-353.
- von Straaten, L. M. J. V., 1951, Longitudinal ripple marks in mud and sand, Jour. of Sedimentary Petrology, v. 21, no. 1, pp. 47-54.
- Walker, H. J., 1974, The Colville River and the Beaufort Sea: some interactions; in The coast and shelf of the Beaufort Sea. Proceedings of the Arctic Institute of North American Symposium on Beaufort Sea Coast and Shelf Research. Arlington, Va., Arctic Institute of North America; pp. 513-540.

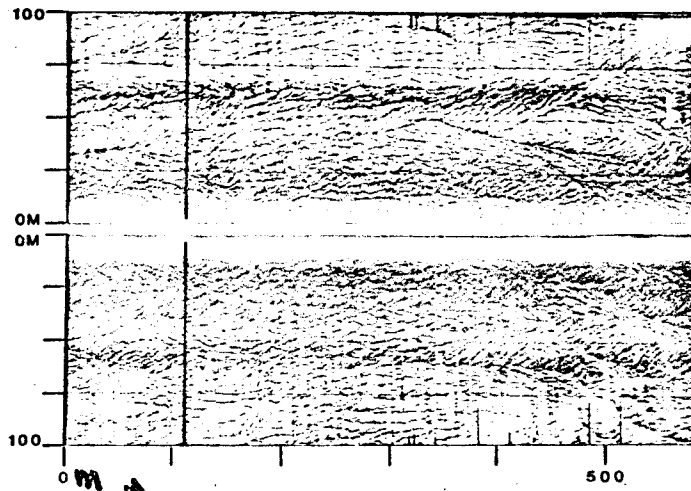


2

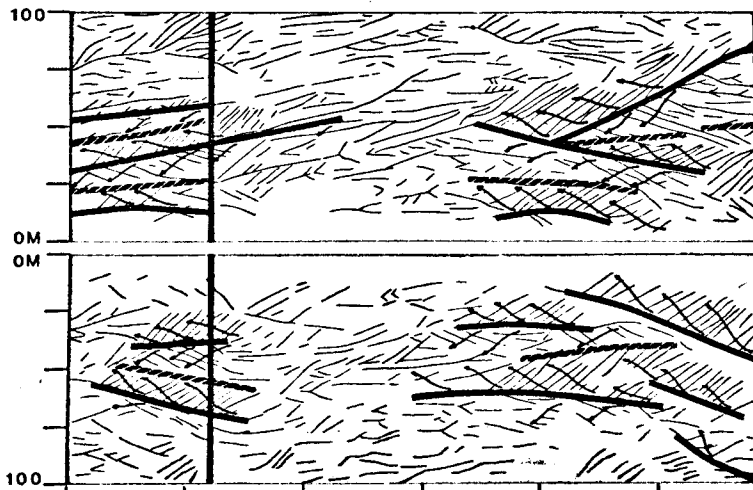


PAIRED VORTICES OF
TAYLOR-GÖRTER HELICAL FLOW

FIG 3



0m
4a



4b

K

HEAVY-MINERAL TRENDS IN THE BEAUFORT SEA

By

Gretchen Luepke

75-667

Open-file report
1975

This report is preliminary
and has not been edited or
reviewed for conformity with
Geological Survey standards

HEAVY-MINERAL TRENDS IN THE BEAUFORT SEA

Gretchen Luepke

Abstract

Sediments of the Beaufort Sea, off the North Slope of Alaska contain a great variety of heavy minerals. These include garnet, chrome spinel, augite, pigeonite, diopside, hornblende, enstatite, hypersthene, epidote, clinozoisite, zoisite, apatite, tourmaline, chloritoid, sphene, zircon, and opaque minerals. Much rarer constituents are glaucophane, lamprobolite, rutile, kyanite, staurolite, and riebeckite.

The heavy-mineral fractions that were not treated with hydrochloric acid contain "iron-stained aggregates", grains of unidentifiable material encrusted with limonite. Samples containing relatively high percentages of iron-stained aggregates and altered opaque minerals occur in depths less than 10 m and within 16 km from shore.

Garnet increases in abundance from east to west, which corresponds to a similar increase in garnet abundance in coastal outcrops of the Gubik Formation sands. Only garnet and iron-stained aggregates appear to have source-related distribution patterns. The other heavy minerals lack distinct distributive provinces, reflecting an environment dominated by intense mixing by ice-gouging and bioturbation and a homogenous source area. Waves and currents are not strong enough to sort sediments at depths greater than 10 m except during summer storms.

The source of the Beaufort Sea heavy minerals is dominated by contributions from the Alaskan North Slope deposits of Tertiary and younger age. The Colville River, largest in the region, is probably the most influential in transporting sediments, but because of wave and current-mixing of sediments on the shelf, exact contributions from each river drainage cannot be ascertained. Coastal erosion of the Gubik Formation is probably at least as important as the Colville River in supplying heavy minerals to the Beaufort Sea.

HEAVY-MINERAL TRENDS IN THE BEAUFORT SEA

Introduction

Purpose. As part of the environmental-baseline studies of the offshore North Slope of Alaska, a study was made of the heavy minerals in the Beaufort Sea to ascertain the source areas and transport routes of sediments on the continental shelf.

Setting. The Beaufort Sea lies north of Alaska from Point Barrow eastward to the islands of the Canadian Arctic Archipelago (fig. 1). The present study area extends from Point Barrow to Barter Island, off the Alaska coast.

Two geomorphic provinces dominate the North Slope of Alaska. The arctic coastal plain is a gently-sloping surface of low relief extending from the coast to the arctic foothills. The Gubik Formation, a dominantly marine unit of Pleistocene age, blankets the entire coastal area immediately adjacent to the Beaufort Sea (Payne and others, 1951). Thickness averages about 20 metres. The Gubik unconformably overlies the Sagavanirktok Formation (Early Tertiary) and the formations of the Colville and Nanushuk groups (Cretaceous) (see fig. 2).

Pack ice covers the shelf for nine months of the year, eliminating waves and mitigating the effects of wind-driven currents and storm tides. During the open-water period, the most common waves observed have periods of 2 to 3 seconds and heights of 20-30 cm. Surface currents nearshore are wind-driven. Meteorological tides are of larger amplitude than astronomical tides in the arctic coastal zone (Wiseman, Suhayda and Hsu, 1974, p. 51-59).

Eighty percent of the North Slope (see fig. 1) drains into the Beaufort Sea (Walker, 1974, p. 517). The 600-km Colville River and its massive tributary system drain seventy-eight percent. Rivers such as the Kuparuk and Sagavanirktok are comparatively short and empty into lagoons bounded by offshore bars and barrier islands (Walker, 1974, p. 537).

Barnes and Reimnitz (1974, p. 444) measured currents below the ice cover that show an overall westward movement of near-bottom water on the inner shelf at 2 cm/sec parallel to the coastline. Mountain (1974, p. 27) notes an eastward flow of surface water on the outer shelf. Hufford (1974, p. 569) states that subsurface currents appear to behave independently and often opposite of surface currents; 1971 and 1972 measurements showed bottom currents flowing eastward at speeds less than 15 cm/sec.

Subsurface currents may change directions from season to season. But long-range sediment transport along the coast appears to be westerly. Documentation of this westerly transport is multifaceted: Barrier islands migrate westward (Wiseman and others, 1973, p. 161; Reed and Sater, 1974, p. 563); sediment plumes from rivers, seen on ERTS-1 imagery, veer westward (Barnes and Reimnitz, 1974, p. 444); ice moves dominantly westward under the influence of the Pacific Gyre off northern Alaska (Reimnitz and Barnes 1974, p. 301).

Previous studies show that weight percentages of heavy minerals in different size fractions in the Beaufort Sea are unrelated to grain size. Table 1 lists the specific areas studied and the size-fractions in which weight-percentages of heavy minerals were determined.

TABLE 1. Studies of heavy-mineral weight-percentages in the Beaufort Sea.

| <u>Reference</u> | <u>Area/Sediment type</u> | <u>Size-fractions compared</u> |
|---|--|--|
| Naidu & Sharma 1972, p. 7-8 | Point Barrow to Barter Is. Offshore sediments | 0.75-0.25 mm 0.25-0.125 mm 0.125-0.062 mm |
| Dygas, Tucker & Burrell 1972, p. 112 | Colville River sands; coastal & barrier-beach sands | 0.25-0.125 mm 0.125-0.062 mm 0.062-0.038 mm |
| Burrell, Dygas & Tucker 1974, p. 125-126 | Simpson Lagoon, btw. Oliktok & Beechey points offshore sediments | 0.500-0.250 mm 0.250-0.125 mm 0.125-0.062 mm |
| This report | Point Barrow to Barter Is. Offshore Sediments | 2.00-0.062 mm |

The percent of heavy minerals in the areas studied by the above authors averages about 5%; only rarely do fractions contain percentages of heavy minerals greater than 10%. The beach and river sands contain higher overall percentages of heavy minerals than do the offshore sands.

Naidu and Mowatt (1974) discuss relative heavy-mineral weight-percents in deltaic and shallow-water Beaufort Sea sediments, noting a more normal grain-size relationship (i.e., higher heavy-mineral percents with decreasing grain-size) in the deltaic sediments.

Studies of heavy-mineral distribution patterns have been made in other shelf seas bordering the Arctic Ocean. Holmes (1967) did not find enough significant differences in heavy-mineral assemblages of the Laptev Sea (fig. 1) to attempt any interpretation. General uniformity of mineral composition in the East Siberian Sea was also noted by Naugler (1967). However, he found garnet decreases uniformly toward the center of the study area from the west, and orthopyroxene dominates the eastern regions. Silverberg (1972) studied heavy-mineral distributions in both the Laptev and East Siberian seas and identified three heavy-mineral provinces: clinopyroxene-garnet (west); amphibole-clinopyroxene-epidote central; and clinopyroxene-epidote-amphibole-opaque minerals (east).

Carsola (1954, p. 1570) examined Beaufort Sea sediment with a binocular microscope and noted that heavy minerals appeared to constitute a varied assemblage. The present study, the first to study in detail heavy-mineral species in Beaufort Sea sediment, confirms this impression.

Methods. Heavy-minerals were separated in tetrabromoethane (S.G. = 2.96), from microsplits of the sand-size fractions (2.0-0.062 mm) of 153 samples (Table 2). Three surface samples were taken at the mouth of the Colville and Sagavanirktok, rivers and 20 km upstream in the Kuparuk River; all other samples were taken in offshore areas (fig. 1). The weight of the splits ranged from 3.5 to 28.0 grams (average = 14 g).

TABLE 2. Weight-percentages of heavy minerals the sand-size fraction (2.0-0.062 mm).
 For sample locations refer to Figure 1. Percentages marked with asterisk (*)
 are an average of two.

| <u>SAMPLE</u> | <u>% HEAVY-MINERALS</u> | <u>SAMPLE</u> | <u>% HEAVY-MINERALS</u> | <u>SAMPLE</u> | <u>% HEAVY-MINERALS</u> | <u>SAMPLE</u> | <u>% HEAVY-MINERALS</u> |
|---------------|-------------------------|---------------|-------------------------|---------------|-------------------------|---------------|-------------------------|
| 1. | 0.79 | 38. | 1.7 | 76. | 1.9 | 113. | 0.57 |
| 2. | 2.0 | 39. | 2.8 | 77. | 4.6 | 114. | 0.62 |
| 3. | 0.84 | 40. | 0.40 | 78. | 1.8 | 115. | 0.93 |
| 4. | 1.7 | 41. | 0.15 | 79. | 2.1 | 116. | 0.97 |
| 5. | 1.3 | 42. | 1.5 | 80. | 2.3 | 117. | 1.3 |
| 6. | 1.6 | 43. | 2.9 | 81. | 2.4 | 118. | 0.59 |
| 7. | 1.5 | 44. | 1.5 | 82. | 2.6 | 119. | 0.60 |
| 8. | 2.0 | 45. | 2.8 | 83. | 0.92 | 120. | 1.0 |
| 9. | 0.10 | 46. | 2.1 | 84. | 0.96 | 121. | 0.35 |
| 10. | 2.5 | 47. | 0.14 | 85. | 2.7 | 122. | 0.15 |
| 11. | 4.7 | 48. | 0.38 | 86. | 1.2 | 123. | 0.77 |
| 12. | 1.1 | 49. | 1.5 | 87. | 1.8 | 124. | 1.3 |
| 13. | 1.2 | 50. | 1.9 | 88. | 3.8 | 125. | 1.3 |
| 14. | 1.2 | 51. | 1.2 | 89. | 0.77 | 126. | 1.4 |
| 15. | 2.4 | 52. | 0.77* | 90. | 0.17 | 127. | 0.47 |
| 16. | 3.4 | 53. | 1.4 | 91. | 1.5 | 128. | 1.4 |
| 17. | 1.8 | 54. | 0.76 | 92. | 0.22 | 129. | 1.0 |
| 18. | 1.3 | 55. | 0.48 | 93. | 0.49 | 130. | 1.1 |
| 19. | 1.7 | 56. | 0.59 | 94. | 0.86 | 131. | 0.64 |
| 20. | 2.8 | 57. | 0.76 | 95. | 3.6 | 132. | 0.79 |
| 21. | 2.4 | 58. | 1.2 | 96. | 2.0 | 133. | 1.6 |
| 22. | 1.3 | 59. | 0.79 | 97. | 0.93 | 134. | 0.41 |
| 23. | 0.50 | 60. | 0.78 | 98. | 0.90 | 135. | 0.77 |
| 24. | 0.54 | 61. | 0.65 | 99. | 1.2 | 136. | 0.81 |
| 25. | 1.0 | 62. | 0.27 | 100. | 0.56 | 137. | 0.44 |
| 26. | 1.1 | 63. | 0.25 | 101. | 0.90 | 138. | 0.70 |
| 27. | 4.3 | 64. | 0.30* | 102. | 1.1 | 139. | 0.70 |
| 28. | 2.1 | 65. | 0.45 | 103. | 1.2 | 140. | 0.69 |
| 29. | 1.3 | 66. | 0.29 | 104. | 0.41 | 141. | 0.91 |
| 30. | 1.8 | 67. | 0.30 | 105. | 0.43* | 142. | 0.79 |
| 31. | 1.0* | 68. | 0.69 | 106. | 0.42 | 143. | 0.40 |
| 32. | 2.0 | 69. | 0.56 | 107. | 0.60 | 144. | 1.2 |
| 33. | 2.1 | 70. | 0.79 | 108. | 0.69* | 145. | 1.05 |
| 34. | 1.9 | 71. | 0.52 | 109. | 0.94 | 146. | 0.66 |
| 35. | 1.8 | 72. | 0.38 | 110. | 0.33 | 147. | 1.1 |
| 36. | 1.4 | 73. | 0.93 | 111. | 0.11 | 148. | 1.9 |
| 37. | 2.2 | 74. | 1.9 | 112. | 0.93 | 149. | 1.9 |
| | | 75. | 1.8 | | | 150. | 1.3 |
| | | | | | | 151. | 1.4 |
| | | | | | | 152. | 0.80 |
| | | | | | | 153. | 0.75 |

Table 2.

648

The heavy-mineral concentrates were sieved and grains were mounted in Lakeside 70 (n = 1.56). Some of the concentrates prepared early in the study were not microsplit. Comparisons of slides prepared with and without splitting revealed no major differences in mineral frequencies. Point-counts were made of 42 selected samples (see Table 3; fig. 1 for locations) in the 0.25 - 0.062 mm size range; for seven of these samples the 0.25 - 0.125 mm size range; for seven of these samples the 0.25 - 0.125 mm size range was also point-counted, to determine if size-related differences in mineralogy occurred. No significant differences were detected.

Heavy minerals were identified and counted following a line in the grain mount where the cross-hairs touched a grain. To help insure a random count, half the total number of grains were counted in east-west sweeps, the other half in north-south sweeps. Care was taken that the two areas did not overlap.

This method actually gives only number frequency, which gives a sample bias, in that a larger grain is more likely to be encountered during the analysis than a smaller one. The discrepancy is minimized by counting a limited size range (Galehouse, 1969, p. 814). Grains were identified as to mineralogic species when possible. The opaque minerals and aggregates were separated into iron-stained and unstained groups (see Table 3).

To insure the preservation of apatite, no samples were initially treated with HCl. Later, microsplits of five selected heavy-mineral concentrates were heated in concentrated HCl over low heat for 30-45 min. The results were compared with the respective nontreated microsplits.

TABLE 3. Mineralogic composition of joint-counted samples from the Braufort Sea. Data only for 4 ϕ grain-sizes (0.125-0.062 mm) not treated with hydrochloric acid. Data for 3 ϕ sizes (0.25-0.125 mm) are not significantly different. Sample depths from Barnes, Reimnitz, Gustafson and Larsen, 1973.

| SAMPLE | DEPTH m | STAINING Aggreg. | RATIO Unag. | OPALITES | UNSTAINED AGGREGATES | HYDROLYZED ACALCINATES | GARNEY | CHROMIUM SPINEL | CLINOPIPYXENE | ORTHOPIYXENE | NIORIBLENDE | EPIDOTE GROUP | ALVITE | TOURMALINE | SPHENE | ZIRCON | CHLORITOID | RUETILE | LAMPROBOLITE | GLAUCOPHANE | OTHER | UNKNOWN | TOTAL POINT COUNT |
|--------|------------|---------------------|----------------|----------|-------------------------|---------------------------|--------|--------------------|---------------|--------------|-------------|------------------|--------|------------|--------|--------|------------|---------|--------------|-------------|-------------------|---------|----------------------|
| | | | | | | | | | | | | | | | | | | | | | | | |
| 1 | 22 | 0.54 | 0.20 | 14.0 | 19.0 | 10.3 | 7.3 | 5.7 | 16.3 | * | * | * | * | * | * | * | * | * | * | * | 27.3 1) | - | 300 |
| 2 | 78 | 0.58 | 0.13 | 24.8 | 16.0 | 9.3 | 11.0 | 2.2 | 13.2 | 3.8 | 6.7 | 7.2 | 0.7 | 0.7 | 0.2 | 2.0 | 0.3 | * 0.5 | * | * 2) | 1.5 | 600 | |
| 3 | 31 | 0.88 | 0.30 | 11.7 | 19.3 | 17.0 | 3.0 | 5.7 | 19.7 | * | * | * | * | * | * | * | * | * | * | * | 23.7 1) | - | 300 |
| 4 | 48 | 0.56 | 0.74 | 11.0 | 20.3 | 11.3 | 5.0 | 2.3 | 24.3 | * | * | * | * | * | * | * | * | * | * | * | 25.7 1) | - | 300 |
| 5 | 28 | 0.53 | 0.86 | 13.0 | 24.0 | 12.7 | 4.0 | 2.3 | 24.3 | * | * | * | * | * | * | * | * | * | * | * | 19.7 1) | - | 300 |
| 6 | 100 | 1.21 | 0.20 | 20.0 | 8.0 | 9.7 | 8.0 | 4.3 | 19.3 | 5.0 | 14.7 | 6.3 | 1.3 | 0.3 | 0.3 | 2.0 | * | * | * | * | - | 0.7 | 300 |
| 7 | 21 | 0.71 | 0.32 | 13.7 | 22.7 | 16.0 | 5.3 | 2.0 | 21.7 | * | * | * | * | * | * | * | * | * | * | * | 18.7 1) | - | 300 |
| 8 | 48 | 1.00 | 0.21 | 32.3 | 6.7 | 6.7 | 5.0 | 4.7 | 21.7 | 4.0 | 10.7 | 5.3 | 0.7 | - | 1.0 | 1.0 | - | 0.3 | - | - | - | - | 300 |
| 9 | 21 | 1.51 | 0.78 | 12.2 | 18.7 | 28.2 | 2.0 | 4.7 | 20.3 | * 3.8 | * | * | * | * | * | * | * | * | * | * | 10.2 1) 3), 4) | - | 600 |
| 10 | 7.2 | 2.35 | 1.25 | 21.0 | 8.7 | 20.3 | 1.0 | 16.7 | 16.0 | 1.3 | 10.7 | 3.3 | 1.0 | * | * | - | - | - | - | - | - | - | 300 |
| 11 | 4.5 | 4.68 | 7.50 | 13.1 | 10.5 | 49.2 | 0.8 | 7.9 | 8.7 | 0.5 | 5.6 | 2.1 | 0.5 | 0.3 | - | 0.5 | - | - | - | 0.3 | - | - | 390 |
| 12 | 140 | 0.92 | 0.28 | 10.7 | 12.0 | 11.0 | 8.3 | 1.7 | 34.7 | * 7.7 | * | * | * | * | * | * | * | * | * | * | 14.0 1) 3) | * | 300 |
| 13 | 20 | 1.20 | 4.00 | 6.7 | 23.0 | 27.7 | 1.7 | 4.3 | 19.3 | * | * | * | * | * | - | - | * | * | - | - | 17.3 1) | - | 300 |
| 14 | 2.0 | 4.26 | 1.71 | 6.3 | 13.0 | 55.3 | - | 3.3 | 12.7 | 1.7 | 4.0 | 1.7 | 1.7 | - | - | - | * | - | - | 0.3 | - | - | 300 |
| 15 | 1.7 | 2.92 | 4.80 | 9.7 | 15.7 | 45.7 | 1.0 | 6.3 | 7.3 | 2.0 | 4.7 | 2.7 | 1.0 | 0.3 | 0.3 | 0.7 | * | * | * | * | - | 2.7 | 300 |
| 16 | 17 | 1.14 | 1.64 | 29.0 | 12.3 | 14.0 | 3.3 | 7.0 | 19.7 | 1.0 | 8.0 | 3.7 | 0.3 | 0.3 | * | * | 1.0 | 0.3 | - | - | - | - | 300 |
| 17 | 18 | 1.72 | 3.19 | 29.3 | 10.0 | 17.7 | 1.7 | 2.3 | 21.3 | 2.7 | 6.3 | 5.0 | 0.7 | 1.0 | - | 0.7 | 0.3 | 0.3 | - | - | - | 0.7 | 300 |
| 18 | 63 | 0.83 | 0.33 | 6.7 | 23.3 | 19.3 | 2.7 | 2.3 | 22.3 | * | * | * | * | * | * | - | * | * | - | - | 23.3 1) | - | 300 |
| 19 | 48 | 1.28 | 0.17 | 16.3 | 16.3 | 21.0 | 2.0 | 2.7 | 16.7 | 6.3 | 7.0 | 6.3 | 0.7 | 0.7 | - | 1.3 | - | 0.3 | - | * 2) | 2.3 | 300 | |
| 20 | 23 | 1.30 | 0.37 | 21.0 | 12.3 | 16.0 | 1.0 | 2.7 | 24.3 | 2.0 | 10.3 | 7.0 | 0.3 | 0.3 | - | 0.7 | 0.3 | - | - | - | - | 1.7 | 300 |
| 21 | 10.5 | 1.06 | 0.57 | 25.7 | 18.0 | 19.0 | 3.0 | 8.3 | 11.3 | 1.7 | 2.0 | 6.3 | 0.7 | 0.7 | * | 1.7 | - | - | - | - | - | 1.7 | 300 |
| 22 | 4.6 | 2.82 | 2.43 | 8.0 | 18.3 | 51.7 | 0.3 | 8.0 | 1.3 | 0.3 | 2.3 | 8.3 | 0.3 | 1.3 | * | * | * | * | * | * | * 2) | - | 300 |
| 23 | 1.7 | 2.05 | 5.33 | 6.3 | 21.7 | 44.3 | 0.7 | 1.0 | 10.3 | * 2.7 | * | * | * | * | * | * | * | * | * | * | 13.0 1) | - | 300 |
| 24 | 1.0 | 1.20 | 1.08 | 9.0 | 30.0 | 36.0 | 0.7 | 5.0 | 6.3 | * 2.3 | * | * | * | * | * | * | * | * | * | * | 10.7 1) | - | 300 |
| 25 | 93 | 1.12 | 0.36 | 20.0 | 18.3 | 16.3 | 1.3 | 2.7 | 19.3 | 4.3 | 5.0 | 8.3 | 1.3 | 1.0 | 0.7 | - | - | 0.3 | * | 0.3 3) | 0.7 | 300 | |
| 26 | 33 | 0.93 | 0.43 | 22.0 | 15.0 | 14.0 | 3.7 | 5.0 | 14.3 | 3.0 | 9.7 | 6.3 | 1.3 | 1.3 | 1.0 | 1.3 | - | 0.3 | - | 0.3 2) | 1.3 | 300 | |
| 27 | 22 | 1.10 | 0.23 | 28.3 | 10.0 | 11.0 | 3.7 | 8.3 | 19.7 | 4.3 | 6.7 | 3.7 | 1.0 | 1.0 | 0.3 | 1.0 | - | 0.3 | - | - | - | 0.7 | 300 |
| 28 | 4.6 | 1.61 | 1.12 | 12.0 | 23.3 | 37.7 | 1.3 | 5.3 | 2.7 | 1.0 | 3.7 | 7.3 | 0.3 | 1.3 | - | 2.0 | - | 0.3 | - | - | - | 1.7 | 300 |
| 29 | 0.9 | 2.29 | 2.36 | 28.0 | 16.0 | 36.7 | * | 3.0 | 5.3 | 0.7 | 1.3 | 3.7 | 0.7 | 1.3 | 0.3 | 1.7 | - | 0.7 | - | 0.3 4) | 0.3 | 300 | |
| 30 | 6.1 | 0.46 | 0.61 | 23.0 | 31.7 | 14.7 | 2.3 | 6.3 | 1.3 | 1.0 | 1.3 | 8.7 | 2.0 | 1.0 | 2.0 | 3.7 | * | * | * | * 2) | 1.0 | 300 | |
| 31 | 8.5 | 2.24 | 1.40 | 12.0 | 20.5 | 45.8 | 0.7 | 5.5 | 4.5 | 0.5 | 3.2 | 6.2 | 0.3 | * | - | 0.5 | * 0.2 | - | - | - | - | 0.2 | 600 |
| 32 | 29 | 0.88 | 1.08 | 8.3 | 26.0 | 23.0 | 1.0 | 3.7 | 20.7 | * | * | * | * | * | - | * | - | * | - | * | 17.3 1) | - | 300 |
| 33 | 46 | 0.81 | 0.60 | 10.7 | 23.3 | 19.0 | 2.3 | 1.7 | 25.7 | * | * | * | * | * | * | - | * | - | * | - | 17.3 2) | - | 300 |
| 34 | 81 | 0.79 | 0.45 | 14.0 | 15.7 | 12.3 | 4.7 | 2.3 | 26.7 | 3.3 | 15.0 | 4.3 | - | 0.7 | 0.3 | - | - | - | - | - | - | 0.7 | 300 |
| 35 | 33 | 0.81 | 0.85 | 16.7 | 15.7 | 12.7 | 1.3 | 10.0 | 14.0 | 2.7 | 17.0 | 6.7 | 0.3 | 1.0 | - | 0.3 | - | - | - | - | - | 1.7 | 300 |
| 36 | 2.0 | 1.92 | 1.69 | 11.7 | 24.3 | 46.7 | 0.3 | 2.3 | 7.3 | - | 2.7 | 2.3 | 0.7 | 0.3 | - | 0.3 | - | - | - | - | - | 1.0 | 300 |
| 37 | 16 | 0.95 | 1.42 | 21.0 | 12.7 | 12.0 | 1.3 | 7.0 | 15.7 | 2.3 | 18.0 | 6.3 | * | 2.3 | 0.3 | 1.0 | - | - | - | - | - | - | 300 |
| 38 | 26 | 0.84 | 0.69 | 15.7 | 23.7 | 19.8 | 1.1 | 2.7 | 11.7 | 2.2 | 11.5 | 8.4 | 0.4 | 0.5 | - | 0.2 | - | - | - | * | - | 2.0 | 549 |
| 39 | 44 | 0.65 | 0.12 | 28.7 | 13.3 | 8.7 | 2.0 | 2.0 | 26.3 | 4.0 | 10.3 | 3.3 | - | 0.3 | - | * | - | - | - | - | - | 1.0 | 300 |
| 40 | sfc | 5.06 | 7.57 | 20.0 | 11.7 | 59.0 | 0.7 | 3.3 | 0.7 | - | 0.3 | 1.0 | 1.3 | * | 0.3 | 0.7 | 0.3 | 0.3 | - | - | - | 0.3 | 300 |
| 41 | sfc | 3.18 | 3.08 | 32.7 | 12.7 | 40.3 | 0.7 | 2.3 | 1.3 | 0.3 | 2.0 | 4.3 | 1.3 | 0.7 | * | * | 0.7 | 0.7 | - | * 4) 5) | - | 300 | |
| 42 | sfc | 2.38 | 2.00 | 9.0 | 18.3 | 43.7 | 1.3 | 2.3 | 15.7 | 0.7 | 3.7 | 2.3 | 1.3 | 0.3 | 0.3 | * | 0.7 | - | * | 0.3 | - | - | 300 |

* mineral seen but not counted sfc= surface sample
 1) total percent of all "species; complete species counts were not made for the sample
 2) staurolite
 3) ryanite
 4) riebeckite
 5) lawsonite

Micas and carbonate grains were noted in most samples, particularly those taken close to shore. Because of their wide specific-gravity range (2.7 - 3.1 for the micas, 2.7-2.9 for calcite and dolomite; from Allman and Lawrence, 1972, p. 181, Table 28), they are not considered true "heavy minerals" and are therefore omitted from the point-counting.

Description of Heavy Minerals

A great variety of heavy minerals were identified: opaque minerals, garnet, chrome spinel, augite, diopside, pigeonite, hornblende, enstatite, hypersthene, epidote, clinozoisite, zoisite, apatite, tourmaline, chloritoid, sphene, and zircon. Extremely rare, but positively identified, were glaucophane, lamprobolite, rutile, kyanite, staurolite, and riebeckite. One grain of lawsonite was seen in the acid-treated microsplit of the Kuparuk River heavy-mineral concentrate.

Opaque minerals. Opaque minerals compose an average of 17% of the heavy minerals counted, with extremes at 6% and 35%. Magnetite is present (detected with a horseshoe magnet) in virtually all samples. Where magnetite was not detected, the percent of heavy minerals was consistently less than 1%, and the weight of the heavy-mineral fraction less than 0.1 g. The lack of magnetite in these samples is probably a function of either the small heavy-mineral fraction or of sorting. Ilmenite is probably also present, although opaque grains with a whitish (leucoxene?) alteration were rare. Pyrite (authigenic) was seen in the 0.25 - 0.125 mm fraction of sample 70ABP-1.

The forms of the opaque grains ranges from crystalline to well-rounded. Some grains were surficially altered to iron-oxide. This will be discussed later.

Treatment in hydrochloric acid did not systematically change the percents of opaque minerals. Usually the counts remained within + 5%, but in one sample the percentage decreased 24%.

Chrome spinel. Chrome spinel composes between 1 and 8 percent of the heavy minerals in all samples. This mineral is usually partially translucent and isotropic. The grains show very high relief and forms varying from crystalline to well-rounded. Conchoidal fractures may be present. Translucent beer-bottle-brown-colored grains are probably picotite (Morris, 1952). Similar translucent to nearly opaque grains are blood-red, an anomalous color for picotite.

Garnet. Percentages of garnet ranged from 1 to 11%. Samples containing greater than 5% garnet all lay west of Cape Halkett (fig. 3). East of Cape Halkett the distribution is uniformly low. Colorless and pink garnet occurs in all samples. The colorless variety generally is more numerous and more etched than the pink variety. In samples taken west of Cape Halkett, garnets with yellowish hues were seen; this was the rarest variety noted. All garnets were rounded to some degree and many contained inclusions. No systematic attempt was made to identify these inclusions, although in one sample they were clearly rutile.

Clinopyroxene. As a group, clinopyroxenes constitute a range of 11 to 26% of all samples, with a maximum of 35%. HCl-treatment, while not necessarily rendering species more identifiable, invariably increased the percentage of identifiable clinopyroxene grains by at least 7% and as much as 18%. The sample from the Colville River contained 34% clinopyroxene after acid treatment, compared to 16% before treatment.

These differences did not alter the overall distribution of clinopyroxenes. The percentages of this group ranged from 1 to 16% within 18 km of the coast and from 13 to 35% beyond 18 km.

Augite, diopside, and pigeonite were identified, but it was frequently impossible to identify a clinopyroxene as to species, even where the sample was acid-treated. Because of this difficulty, the clinopyroxene were grouped together for correlation purposes.

Augite, the most abundant clinopyroxene, had many colors: green, brown, colorless, occasionally purplish. Form ranged from prismatic to well-rounded. Saw-toothed etching of grains was occasionally noted.

Diopside, the most difficult clinopyroxene to positively identify, had a very high birefringence and a characteristic extinction angle (about 39°). Where identified, diopside and pigeonite occurred in roughly equal amounts, always less than 5% of the heavy mineral fraction.

Hornblende. Hornblende, with its characteristic extinction angle ($12 - 30^{\circ}$) and pleochroism, constitutes 1 to 18% of all samples, usually less than 11%. HCl-treatment did not systematically alter the percentages of hornblende identified. However, lamprobolite grains

were more likely to be found in acid-treated samples, possibly because they were masked by limonitic alteration in untreated samples.

Overall hornblende percentages tend to increase with distance from shore.

The blue-green and green varieties of hornblende occur in about equal proportions. The brown varieties, if present, are less abundant than either green or blue-green varieties. Lamprobolite (basaltic hornblende) was seen in 14 samples but it is extremely rare, always composing less than 1% of the heavy-mineral fraction. It is distinguished from ordinary brown hornblende by its much smaller extinction angle ($0-12^{\circ}$) and red-brown color.

Orthopyroxene. Enstatite and hypersthene rarely exceed 4% of the heavy-mineral fraction. Enstatite occurs slightly more frequently than hypersthene. Enstatite may occur as prismatic or rounded grains; hypersthene more commonly is prismatic.

The pleochroism of the hypersthene is in general extremely faint, indicating that the variety may be ferrohpersthene (Naugler, 1967, p. 42). True hypersthene, with its intense pleochroism, is not as common as ferrohpersthene in these sediments. In some cases hypersthene could only be distinguished from enstatite is by its optic sign.

Epidote group. In the Beaufort Sea sediments, the epidote groups constitutes an average of 6% of the heavy-mineral fraction, with extremes at 2% and 9%. Acid-treatment slightly increased the number of identifiable epidote grains.

Epidote (pistacite) is the most common mineral of this group. It is optically negative and characteristically yellow-green but occasionally colorless. Epidote aggregates (yellow-green grains which do not go extinct) are common, sometimes exceeding the number of single-crystal grains.

Clinozoisite and zoisite are generally less common than epidote; together they may equal the amount of epidote. Zoisite appears to be the more common of the two, though these minerals may be hard to distinguish. Both ferrian (normal interference colors) and non-ferrian (anomalous deep-blue interference colors) varieties of zoisite are present.

Apatite. Apatite constitutes about 1% of the heavy-mineral fraction of all samples mostly in small, equidimensional to elongate, rounded grains. The mineral occasionally occurs in prismatic grains. Apatite was not seen in acid-treated samples.

Apatite is a uniaxial mineral, but sometimes grains may show a pseudo-biaxial figure (Milner, 1940, p. 243). In the Beaufort Sea sediments, pseudo-biaxial figures were seen most commonly in thick grains (birefringence in first-order yellow). Such grains can be confused with zoisite, although this mineral is optically positive in contrast to apatite.

Tourmaline. Tourmaline is ubiquitous but generally composes less than 1% of the heavy-mineral fraction. Although an acid-treated microsplit from the Kuparuk River contains 3%, acid-treatment did not in general increase the amount of identifiable tourmaline.

Both brown and blue-gray varieties of tourmaline are present, although the brown variety is by far more common. Grain-form ranges from prismatic to well-rounded. Overgrowths are rare.

Chloritoid. Chloritoid usually constitutes less than 1% of the heavy-mineral fraction. The largest amount (3%) of chloritoid was seen in the acid-treated sample from the Kuparuk River. It occurs as small, platy grains.

Sphene. Except for one sample containing 2% sphene, this mineral invariably makes up less than 1% of the heavy-mineral fraction. The grains are colorless to yellow-brown and rounded.

Zircon. Zircon, though rare, is present in nearly all samples. Several varieties were seen: euhedral, colorless, unzoned crystals; colorless to slightly yellow, rounded, ovoid grains; pinkish, zoned crystals.

Some grains identified as zircon showed very small extinction angles. The interference figures of such grains appeared to be uniaxial positive but could also have been biaxial positive with a low 2V. It is therefore possible that such grains are monazite, a mineral difficult to distinguish from zircon.

Other minerals. Glauco-phane, kyanite, staurolite, riebeckite, and lawsonite occurred too sporadically to be significant. Glauco-phane, however, was identified consistently in samples from the Colville River and its delta. Rutile, though extremely rare, was identified in samples near the mouths of the Sagavanirktok and Kuparuk rivers and in many samples west of the Sagavanirktok.

Aggregates. The term "aggregate" refers here to a grain containing one or more minerals identifiable in varied degrees. Two categories of aggregates were point-counted.

The first group, called here "unstained aggregates", is made up of grains consisting of two or more minerals (for example, an opaque mineral and a clinopyroxene), or an unidentifiable grain which did not go extinct.

The second category consists of "iron-stained aggregates". Such grains are not mineralogically identifiable but are encrusted with a yellow-orange iron-oxide material, probably limonite. Treatment with HCl does not render these grains identifiable, but does destroy the limonite, leaving the grains white.

Both categories of aggregates combined generally compose 20 to 50% but could, in a few samples, constitute as much as 71% of the heavy-mineral fraction. Samples containing more than 60% aggregates occur invariably within 16 Km of the coast. Of the five acid-treated samples, the percentages of aggregates remained about the same in two and decreased in the others.

Discussion

Distribution. The heavy minerals never composed more than 5% the sand-size fraction (see Table 2). No significant relationship was apparent between percent of heavy minerals and either mean grain-size or depth of sample. The patterns of concentration were quite random, though percentages greater than 1% seemed to lie in a belt beyond the barred islands and generally shoreward of the shelf break. Percentages are comparable to those obtained by other workers (Burrell, Dygas and Tucker, 1974; Dygas, Tucker and Burrell, 1972; Naidu and Mowatt, 1974; Naidu and Sharma, 1972). Of all the heavy-mineral species, only garnet and iron-stained aggregates show any definite distribution patterns in the Beaufort Sea. Both of these patterns may well be source-dependent.

Six samples of the Gubik Formation taken near Point Barrow contain an average of 8.5% garnet, a maximum of 15%. On the other hand, samples of the Gubik taken at six different localities east of the Colville River, between Simpson Lagoon and Prudhoe Bay, contain less than 1% garnet.

The higher percentages of garnet in marine sediments west of Cape Halkett (fig. 3) would seem to suggest either a westward direction for sediment transport or little transport from the source rocks. Currents effectively keep the garnet supplied from the Gubik Formation moving westward.

In samples containing high percentages of iron-stained aggregates, the opaque minerals present commonly show iron-oxide alteration. For both groups the staining ratio, the ratio of the frequency of iron-stained to unstained grains, was calculated.

As seen in Figure 4b the staining ratio for opaque minerals is generally less than 1.0. Only close to the mouths of the major rivers does the ratio exceed 2.0. The staining ratios for aggregates (fig. 4a) follow a similar pattern. Only one sample at the mouth of the Sagavanirtok contains relatively few iron-stained aggregates. This same sample also contains few iron-stained opaques (see also Table 3).

The percentage of iron-stained grains (opaque minerals + aggregates) diminishes rapidly with increasing depth to about 20 m, beyond which the percentage remains on the order of 19.5%, never exceeding 27% (fig. 5).

The prevalence of iron-stained aggregates at lesser depths close to shore probably results from proximity to source. These aggregates occur in the Pleistocene Gubik Formation, which forms seacliffs bordering the coastline. The widespread Cretaceous formations of the region are commonly oxidized at the surface (David M. Hopkins, oral commun., 1975). The low clinopyroxene percentages within 18 km of the coast are probably an artifact resulting from extensive iron-staining of grains in samples from this area.

Table 4. Minerals of the Beaufort Sea grouped as to average specific gravity.

| | |
|------------------------|---|
| Avg. S.G. = 3.0 - 3.49 | Apatite Augite Clinzoisite Diopside Enstatite Epidote Glaucophane Hypersthene Lamprobolite Lawsonite Pigeonite Riebeckite Tourmaline Zoisite |
| Avg. S.G. = 3.5 - 4.49 | Chloritoid Chrome spinel Garnet Hornblende Kyanite Limonite Rutile Sphene Staurolite |
| Avg. S.G. = 4.5 - 5.5 | Opaque minerals Zircon |

Data from Allman and Lawrence 1972, Table 28, p. 181, supplemented where necessary with data from Milner, 1940.

Closely associated samples, particularly in shallow water, tend to show distinctive differences in mineralogy; percentages of opaque minerals, for example, may differ by 10-15%. To examine possible reasons for these differences, all identified minerals were divided into three specific-gravity groups (Table 4). The percent of minerals in the "low" specific-gravity range (3.0-3.49) is dominated by the amount of pyroxene; the "medium" range (3.5-4.5) by iron-stained aggregates (limonite S.G. = 3.6-4.0); and the "high" range (greater than 4.5) by opaque minerals. Because the distribution of iron-stained aggregates appears to be controlled by proximity to the shoreline, the ratio of minerals in the high range to that of the low range was used. This quantity is defined as the density ratio.

$$\text{Density Ratio (D.R.)} = \frac{\% \text{ minerals of S.G. } > 4.5}{\% \text{ minerals of S.G. } = 3.0-3.49}$$

Density ratios for 32 samples were plotted against depth (fig. 6). In depths greater than 20 m, D.R. never exceeds 1.1. In water shallower than 20 m, several samples have D.R. greater than 1.1, and two near the mouth of the Sagavanirktok exceed 1.8. Although some samples from water depths less than 20 m have low density ratios, the highest values occur only in shallow water.

Although the number of samples from this study with very high density ratios is too small to be statistically significant, it is interesting to speculate on the origin of the apparent decrease in density-ratio range with depth where source is not a factor. A wide range of density ratios in closely-spaced samples suggests hydraulic sorting. A narrow range of density ratios would suggest mixing.

Hydraulic sorting. Waves in the Beaufort Sea normally range from 2 to 3-second periods and 20 to 30 cm height. A storm of Pingok Island (see fig. 1) in 1972 produced swells of 9 to 10-second periods and 1.5 to 2.5 m height. The storm lasted several days and produced longshore currents with velocities as much as 50 cm/sec. (Wiseman, Syhayda and Hsu, 1974, p. 51).

Threshold orbital velocities (u_m) which would act to sort sediments may be calculated for the typical and extreme wave regimes noted above from the equations of Komar and Miller (1974).

Table 5 shows u_m as calculated for waves of given period (T) height (H), and water depth (h).

TABLE 5. Representative threshold orbital velocities for specific waves.

| <u>T, sec.</u> | <u>H, cm</u> | <u>h, m</u> | <u>u_m, cm/sec</u> | <u>sed.grain-size moved</u> |
|----------------|--------------|-------------|---------------------------------|-----------------------------|
| 3 | 30 | 4 | 9.8 | 0.085 mm |
| 10 | 250 | 10 | 107 | 11.93 mm |
| 10 | 250 | 15 | 80 | 6.05 mm |
| 10 | 250 | 20 | 63 | 3.47 mm |
| 10 | 250 | 30 | 43 | 1.42 mm |
| 10 | 250 | 50 | 20 | 0.22 mm |

Table 6. Non-opaque minerals and formations of Alaska North Slope where identified (Brosge, Whittington and Morris, 1966; Keller, Morris and DeHerman, 1961; Morris, 1952; Patton and Tailleur, 1964, Payne and others, 1951; and this paper)

| FORMATION | Beaufort Sea Sediments | Gubik/Meade Unit | Sagavanirktok | Prince Creek/Tuluvak Tongue | Schrader Bluff | Seabee | Chandler | Ninuluk | Grandstand | Topagoruk | Tuktu | Fortress Mt. | Torok | Okpikruak | Tiglukupuk | Kingak | Shublik |
|---------------|------------------------|------------------|---------------|-----------------------------|----------------|--------|----------|---------|------------|-----------|-------|--------------|-------|-----------|------------|--------|---------|
| MINERAL | | | | | | | | | | | | | | | | | |
| Garnet | x | x | x | x | x | x | x | x | x | | | | x | | x | x | |
| Chrome spinel | x | x | | x | x | x | x | x | x | | x | | | | | | |
| Augite | x | x | | | | | | | | | | x | x | x | x | x | |
| Hornblende | x | x | | x | x | 2 | x | 1 | 1 | | | x | x | x | x | | |
| Epidote | x | x | | | | | | | | | | x | | x | x | | |
| Zoisite | x | x | | | | | | | | | | | | x | | | |
| Clinozoisite | x | x | | | | | | | | | | | | | | | |
| Tourmaline | x | x | x | x | x | x | x | x | x | | x | x | x | | | x | x |
| Apatite | x | x | | x | x | x | x | x | | | | | x | | | | |
| Glaucophane | x | x | | x | x | x | | x | x | | | x | | | | | |
| Hypersthene | x | x | | | | | | | | | | | | | | | |
| Chloritoid | x | x | | x | x | x | x | x | x | | | | | | | | |
| Zircon | x | x | x | x | x | | 3 | 4 | 3 | 3 | 3 | 3 | 3 | | 3 | x | 5 |
| Rutile | x | | | | 6 | | | | | | | | | | | | |
| Sphene | x | x | | | | | | | | | | | | x | | | |
| Kyanite | x | | x | | | | | | | | | | | | | | |
| Staurolite | x | | | | | | | | | | | | x | | | | |

1) blue-green
2) green
3) zoned

4) clear prisms
5) ovoid
6) seen only in Sentinel Hill Member

A certain threshold orbital velocity is required to initiate transport of a given sediment-grain-size. Thus a wave of T=10 sec and $u_{max} = 20$ cm/sec will move 0.20 mm (medium-grained) sand at depths of 50 m. But a wave of T=3 sec and $u_{max} = 9.8$ cm/sec will not move 0.125 mm (fine-grained) sand at a depth of 4 m (Komar and Miller, 1974, p. 772, fig. 7).

Therefore, during the three-month summer period of normal waves in the Beaufort Sea, sands are influenced by waves only in the shallowest depths, probably less than 5 m, and wave-generated currents are not likely to be significant for sorting. Waves from storm such as that observed in 1972 would be strong enough to sort sediments over most of the shelf. In winter, waves are unimportant, due to ice-cover.

At shallow depths off river mouths, the bottom is dotted with strudel scours (Reimnitz, Rodeick and Wolf, 1974, p. 418, fig. 11), depressions caused by water pouring through drain holes in the ice cover during the spring ice-breakup (Reimnitz and Bruder, 1972, p. 162). These depressions could serve as concentrating areas for heavy minerals. The scouring process itself is potentially a sorting mechanism. For grains of a given size, the minerals with higher specific gravities are more likely to resist further transport once deposited, especially in a depression (Brady and Jobson, 1973, p. 26).

In depths greater than 15 m, ice-gouging of the seafloor is most pronounced in winter (Barnes and Reimnitz, 1974, p. 464, fig. 19) in winter. Sediments within areas of strong ice-gouging are probably deeply disturbed. Thicknesses of Recent sediments are 5 m or less, well within the range of the deepest modern gouges (Reimnitz and Barnes, 1974, p. 302). In heavily-gouged areas, older material may be mixed in with surface sediments (Reimnitz and Barnes, 1974, p. 346).

Both bioturbation and ice-gouging are undoubtedly at work in waters deeper than 15 m. During summer, the potential for ice-gouging is present in shallow water but decreases with increasing depth because of fewer ice keels with drafts sufficient to reach the bottom (Barnes and Reimnitz, 1974, p. 463). Seasonal effects of bioturbation are unknown at present. The random pattern of mineral distribution reflects this mixing process.

Source area. A series of six samples from the Meade Unit of the Gubik Formation were collected from the 2.5 m interval of an ice cellar at 9 m depth, at the Naval Arctic Research Laboratory near Point Barrow. Most of the minerals identified in the Beaufort sediments, including iron-stained aggregates, are represented in the Meade Unit samples. The Gubik Formation characteristically contains rounded grains (Morris, 1952). The Meade Unit however, also contains many prismatic grains; hypersthene is almost exclusively prismatic. Beaufort Sea sediments contain both rounded and prismatic grains.

Kyanite has been identified in the Sagavanirktok Formation (Payne and others, 1951). Sphene is present in trace amounts in the Okpikruak Formation (Keller, Morris and Detterman, 1961), as well as the Gubik Formation Meade Unit (this paper). Staurolite was tentatively identified by Keller in the Killik-Itillik region (Tailleur, oral commun., 1975). The mineral identified in earlier works by Morris as andalusite was found to be apatite (Patton and Tailleur 1964, p. 72). The present study confirms this identification.

A summary table (Table 6) lists non-opaque minerals identified in the Beaufort Sea and the formation onshore in which they have been found. Minerals not previously identified in either the Beaufort Sea sediments on the Alaska North Slope are diopside, pigeonite, enstatite, lamprobolite, riebeckite, and lawsonite. These minerals are, however, sufficiently uncommon that they were probably not encountered at the time.

Because there are no distinctive exotic heavy minerals described in the Beaufort Sea sediments, ice-rafting does not appear to be significant.

Sediment is probably shed directly from the coastal cliffs as well as transported as bed-load by major rivers and small, local streams. Also, much of the sediment may be relict.

It seems reasonable to say that the source of the Beaufort Sea sediments is the Alaskan North Slope and dominantly the Gubik Formation. Because of the extensive mixing of the sediment and lack of distinctive mineral assemblages, the contribution of each major drainage to the Beaufort Sea is masked.

Conclusions

In sediments of the Beaufort Sea, heavy minerals never composed over 5% of the sand-size fraction. Twenty-four heavy-mineral species have been identified. This great variety attests to the mineralogic immaturity of the sediments and to the heterogeneity of the source area.

Except for garnet and iron-stained aggregates, the heavy minerals lack distinct distribution provinces. The iron-stained aggregates occur in highest percentages in samples within 16 km of shore. They are probably derived from the sea cliffs bordering the Beaufort. The garnet occurs in greatest amounts west of Cape Halkett, reflecting a higher percent of garnet in the Gubik formation west of the Colville River compared to east of the river. Higher percentages of garnet may also be a reflection of the dominant westward transport of sediments in the area.

Waves and currents in the Beaufort Sea are not strong enough to sort sands at depths greater than 5 m except during summer storms. Therefore, the overall uniformity of heavy-mineral distribution suggests an environment dominated by mixing processes. Bioturbation and ice-gouging are believed to be the most significant. Sorting processes seem to occur only in depths of 1-15 m. Strudel scours may serve as concentration areas for heavy minerals.

ACKNOWLEDGMENTS

Peter W. Barnes and H. Edward Clifton reviewed the manuscript and offered many helpful discussions and encouragement throughout this project. Gloria Harris made a number of heavy-mineral grain-mounts. C. W. Gustafson collected the samples from the Meade Unit of the Gubik Formation, and L. David Carter provided Gubik Formation samples from localities between Simpson Lagoon and Prudhoe Bay. Norma Jeanne Jackson drafted the illustrations used in this report.

Robert H. Morris, U.S. Geological Survey, Denver, clarified questions concerning the identification of the mineral picotite. Irwin Tailleux provided helpful discussions about the onshore geology of Alaska's North Slope.

REFERENCES CITED

- Allman, Michael and Lawrence, D. F., 1972, Geological Laboratory techniques: Arco Publ. Co., Inc., New York, 335 p.
- Arnborg, Lennart, Walker, H. J., and Peippo, Johan, 1967, Suspended load in the Colville River, Alaska, 1962: Geografiska Annaler, v. 49, series A., p. 131-144.
- Barnes, P. W., 1974, Preliminary results of marine geologic studies off the northern coast of Alaska; p. 184-227, In: An ecological survey of the Beaufort Sea, U.S. Coast Guard Oceano. Rept. CG 373-64.
- Barnes, P. W., and Reimnitz, Erk, 1974, Sedimentary processes on Arctic shelves off the northern coast of Alaska, p. 439-476 (with discussion), In: The coast and shelf of the Beaufort Sea, J. C. Reed and J. E. Sater, eds., Arctic Inst. North America.
- Barnes, P. W., Reimnitz, Erk, Gustafson, C. W., and Larsen, B. R., 1973, U.S.G.S. marine geologic studies in the Beaufort Sea off northern Alaska, 1970-1972, location and type of data: U.S.G.S. Open file rept. 561, 11 p.
- Brady, L. L. and Jobson, H. E., 1973, An experimental study of heavy-mineral segregations under alluvial-flow conditions: U.S. Geol. Survey 562-K. 38 p.
- Brosge, W. P., Whittington, C. L. and Morris, R. H., 1966, Geology of the Umiat-Maybe Creek region, Alaska: U.S. Geological Survey Prof. Paper 303-H, p. 501-638.
- Burrell, D. C., Dygas, J. A., and Tucker, R. W., 1974, Beach morphology and sedimentology of Simpson Lagoon, p. 45-143, In: Environmental studies of an arctic estuarine system-final report, V. Alexander and others, Univ. of Alaska Institute Marine Sci. Report 74-1 (Sea Grant Rept. 73-16).
- Carsola, A. J., 1954, Recent marine sediments from Alaska and Northwest Canadian Arctic: Amer. Assoc. Petroleum Geologists Bull., v. 38, n. 7, p. 1552-1586.
- Chapman, R. M., and Sable, E. G., 1960, Geology of the Utukok-Corwin region, northwestern Alaska: U.S. Geol. Survey Prof. Paper 303-C, p. 47-167.
- Collins, F. R. and Bergquist, H. R., 1958a, Test wells, Topagoruk area, Alaska: U.S. Geol. Survey Prof. Paper 305-D, p. 265-316.
- Collins, F. R., and Bergquist, H. R., 1958b, Test wells, Meade and Kaolak areas, Alaska: U.S. Geol. Survey Prof. Paper 305-F, p. 341-376.

- Collins, F. R., and Bergquist, H. R., 1959, Test wells, Square Lake and Wolf Creek areas, Alaska: U.S. Geol. Survey Prof. Paper 305-H, p. 423-484.
- Collins, F. R., and Brewer, M. C., 1961, Core tests and test wells, Barrow area, Alaska: U.S. Geol. Survey Prof. Paper 305-K, p. 569-644.
- Collins, F. R., and Brewer, M. C., 1964, Core tests, Simpson area, Alaska: U.S. Geol. Survey Prof. Paper 305-L, p. 645-730.
- Collins, F. R., and others, 1958, Tests wells, Umiat area, Alaska: U.S. Geol. Survey Prof. Paper 305-B, p. 71-206.
- Dygas, J. A., Tucker, Robert, and Burrell, D. C., 1972, Geologic report of the heavy minerals, sediment transport and shoreline changes of the barrier islands and coast between Oliktok Point and Beechey Point, p. 61-121: In: Kinney, P. J. and others, Baseline data study of the Alaskan Arctic aquatic environment, Univ. Alaska Inst. Marine Sci. Rept. R72-3.
- Galehouse, J. S., 1969, Counting grain mounts - number percentage vs. number frequency: Jour. Sed. Petrology, v. 39, n. 2, p. 812-815.
- Gryc, George and others, 1956, Mesozoic sequence in Colville River region, northern Alaska: Amer. Assoc. Petroleum Geologists Bull., v. 40, no. 2, p. 209-254.
- Holmes, M. L., 1967, Late Pleistocene and Holocene history of the Laptev Sea: Unpubl. M. S. thesis, Univ. of Washington, 99 p.
- Hufford, G. L., 1974, Dissolved oxygen and nutrients along the North Alaskan shelf, pp. 567-588 (with discussion), In: The coast and shelf of the Beaufort Sea, J. C. Reed, and J. E. Sater, eds., Arctic Institute of North America.
- Keller, A. S., Morris, R. H., and Detterman, R. L., 1961, Geology of the Shavirovik and Sagavanirktok Rivers region, Alaska: U.S. Geol. Survey Prof. Paper 303-D, p. 169-222.
- Komar, P. D., and Miller, M. C., 1974, Sediment threshold under oscillatory waves: 14th Conf. Coastal Engineering Proc., Amer. Soc. Civil Engineers, p. 756-775.

- Milner, H. B., 1940, Sedimentary petrography, 3rd ed.: Thomas Murby and Co., London, 666 p.
- Mountain, D. G., 1974, Preliminary analysis of Beaufort Sea shelf circulation in summer, p. 27-42, In: The coast and shelf of the Beaufort Sea, J. C. Reef, and J. E. Sater, eds., Arctic Inst. North America.
- Morris, R. H., 1952, Heavy mineral analysis of sedimentary rocks of northern Alaska: U.S. Geol. Survey Open-File Rept. 68 p.
- Naidu, A. S., and Mowatt, T. C., 1974, Aspects of size distribution, mineralogy and geochemistry of deltaic and ancient shallow marine sediments, North Arctic Alaska: Univ. Alaska Inst. Marine Science Rept. 74-1, p. 145-207. (also p. 238-268, In: An ecological survey of the Beaufort Sea, U.S. Coast Guard Oceano. Rept. CG 373-64.
- Naidu, A. S., and Sharma, G. D., 1972, Texture, mineralogy, and chemistry of Arctic Ocean sediments: Inst. Marine Science, Univ. of Alaska, Rept. R72-12, 31 p.
- Naugler, F. P., 1967, Recent sediments of the East Siberian Sea: Unpubl. M.S. thesis, Univ. of Washington, 71 p.
- Patton, W. W., Jr., and Tailleur, I. L., 1964, Geology of the Killik-Itkillik region, Alaska: U.S. Geol. Survey Prof. Paper 303-G, p. 409-500.
- Payne, T. G., and others, 1952, Geology of the Arctic slope of Alaska: U.S. Geol. Survey Oil and Gas Invest. Map OM-126, 3 sheets.
- Reed, J. C., and Sater, J. E., eds., 1974, The coast and shelf of the Beaufort Sea: Arctic Institute of North America, Arlington, Virginia, 750 p.
- Reimnitz, Erk and Barnes, P. W., 1974, Sea ice as a geologic agent on the Beaufort Sea shelf of Alaska, p. 301-353 (with discussion), In: The coast and shelf of the Beaufort Sea, J. C. Reed and J. E. Sater eds., Arctic Inst. North America.
- Reimnitz, Erk and Bruder, K. F., 1972, River discharge into an ice-covered ocean and related sediment dispersal, Beaufort Sea, coast of Alaska: Geol. Soc. America Bull., v. 83, no. 3, p. 861-866.
- Reimnitz, Erk, Rodeick, C. A., and Wolf, S. C., 1974, Strudel scour - a unique Arctic marine geologic phenomenon: Jour. Sed. Petrology, v. 44, no. 2, p. 409-420.

- Robinson, F. M., 1956, Core tests and test wells, Oumalik area, Alaska: U.S. Geol. Survey Prof. Paper 305-A, p. 1-70.
- Robinson, F. M., 1958a, Test wells, Gubik area, Alaska: U.S. Geol. Survey Prof. Paper 305-C, p. 207-264.
- Robinson, F. M., 1958b, Test wells, Grandstand area, Alaska: U.S. Geol. Survey Prof. Paper 305-E, p. 317-339.
- Robinson, F. M., and Bergquist, H. R., 1959, Test wells, Titaluk and Knifeblade areas, Alaska: U.S. Geol. Survey Prof. Paper 305-G, p. 377-422.
- Robinson, F. M., and Collins, F. R., 1959, Core test, Sentinel Hill area and test well, Fish Creek area, Alaska: U.S. Geol. Survey Prof. Paper 305-I, p. 485-521.
- Robinson, F. M., and Yuster, S. T., 1959, Test wells, Simpson area, Alaska: U.S. Geol. Survey Prof. Paper 305-J, p. 523-568.
- Silverberg, Norman, 1972, Sedimentology of the surface sediment of the East Siberian and Laptev Seas: Unpubl. Ph.D. thesis, University of Washington, 134 p.
- Walker, H. J., 1974, The Colville River and the Beaufort Sea-some interactions, p. 513-540 (with discussion), In: The coast and shelf of the Beaufort Sea, J. C. Reed and J. E. Sater, eds., Arctic Inst. of North America.
- Wiseman, W. J., Jr., Suhayda, J. N., and Hsu, S. A., 1974, Characteristics of nearshore oceanographic environment of Arctic Alaska, p. 49-64, In: The coast and shelf of the Beaufort Sea, J. C. Reed and J. E. Sater, eds., Arctic Inst. of North America.
- Wiseman, W. J., Jr., and others, 1973, Alaska Arctic coastal processes and morphology: Louisiana State Univer. Coastal Studies Inst. Tech. Rept. 149. 171 p.

List of Figures

- Figure 1. Index map showing study area in the Beaufort Sea.
- Figure 2. Generalized stratigraphic column of Cenozoic and Mesozoic rocks of Alaska's North Slope (Colville River region).
- Figure 3. Distribution of garnet in the Beaufort Sea.
- Figure 4a. Staining ratios for aggregates in the Beaufort Sea.
- Figure 4b. Staining ratios for opaque minerals in the Beaufort Sea.
- Figure 5. Relationship of percent of iron stained grains (aggregates of opaque minerals) to sample depth.
- Figure 6. Relationship of density ratio to sample depth.

| | | | | | | |
|------------|-------------------------|----------------|------------------------|--|----------------------|---------------------|
| QUATERNARY | Gubik Formation | | | | | |
| TERTIARY | Sagavanirktok Formation | | | | | |
| | ← south | | north → | | | |
| CRETACEOUS | UPPER | Colville Group | Prince Creek Formation | Schrader Bluff Formation | | |
| | | | Seabee Formation | | | |
| | LOWER & UPPER | absent | Nanushuk Group | Chandler Formation | | |
| | | | | | Ninuluk Formation | Nanushuk Group |
| | | | | | Grandstand Formation | |
| | | | | ? | Tuktuk Formation | Topagoruk Formation |
| | | | | Fortress Mountain Formation | Torok Formation | Oumalik Formation |
| | LOWER | | Okpikruak Formation | undifferentiated L. Cretaceous (?) & U. Jurassic (?) rocks | | |
| | JURASSIC | | Tiglukpuk Formation | Kingak Formation | | |
| | | | absent | | | |
| TRIASSIC | Shublik Formation | | | | | |

Figure 2. Generalized stratigraphic column of Cenozoic and Mesozoic rocks of Alaska's North Slope (Colville River region). (After Gryc and others, 1956, p. 212, fig. 2).

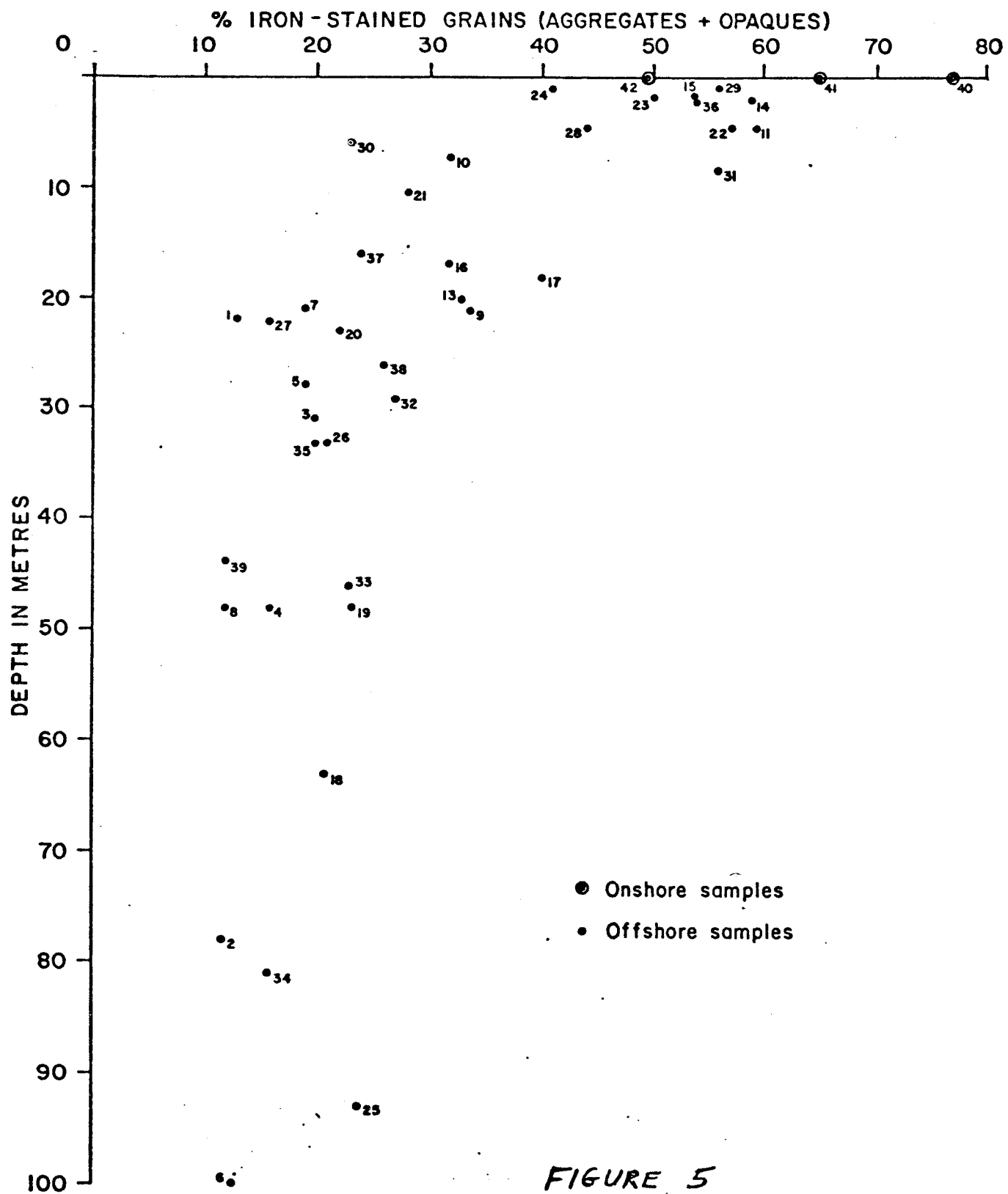


FIGURE 5

FIGURE 6.

